ARTICLE IN PRESS Available online http://jopr.mpob.gov.my/category/article-in-press/

Journal of Oil Palm Research

Vol. 37 (3) • September 2025

REVIEW ARTICLES

- Discovering the Global Landscape of Wood Preservatives
- Enhancing Corrosion Resistance in Biodiesel Distribution and Terminal Operations: A Comprehensive Materials Compatibility Review

eISSN 2811-4701

MPOB

JOURNAL OF OIL PALM RESEARCH (formerly known as ELAEIS)

JOURNAL OF OIL PALM RESEARCH (JOPR), an international refereed journal, carries full-length original research papers, short communications and scientific review papers on various aspects of oil palm and palm oil and other palms. JOPR is published four times per year, *i.e.* March, June, September and December.

Impact Factor:
1.2
data from *2024 Journal Citation Report*® Science Edition
– A Clarivate Analytics product.

For more information on advertisement for the JOPR, please write to:

Editor-in-Chief
Journal of Oil Palm Research
Malaysian Palm Oil Board
6, Persiaran Institusi, Bandar Baru Bangi
43000 Kajang, Selangor, Malaysia

Tel: *+603-8769 4400*
E-mail: *jopr.admin@mpob.gov.my*
Website: *jopr.mpob.gov.my*

DISCLAIMER
Views of writers expressed in this publication are not necessarily endorsed by or represent the views of MPOB.

MPOB Press
Malaysian Palm Oil Board
6, Persiaran Institusi, Bandar Baru Bangi
43000 Kajang, Selangor, Malaysia
Tel: +603-8769 4400 | Fax: +603-8925 9446
E-mail: *jopr.admin@mpob.gov.my*

JOURNAL OF OIL PALM RESEARCH

Vol. 37 (3) September 2025

CONTENTS

Cover picture:

1. Application of oil palm wood vinegar as a natural wood preservative to enhance durability and fungal resistance.
2. Polymeric coating applied for corrosion protection and reinforcement in biodiesel distribution facilities.

EDITORIAL BOARD

(1 January 2024 – 31 December 2025)

PUBLICATION COMMITTEE

Celebrating 25 Years of Research and Development at MPOB

The oil palm industry is one of Malaysia's strongest economic pillars, contributing to national income and the livelihoods of millions. It is an industry built on resilience, research and development (R&D), innovation, and foresight. As we mark the 25th anniversary of the Malaysian Palm Oil Board (MPOB), it is timely to reflect on how the R&D have carried the industry forward and where they will take us next.

MPOB was established with a mandate to strengthen the industry through science and technology. A quarter of a century later, it is evident that research under MPOB spanning from agronomy and biotechnology to engineering, food safety, oleochemicals, and climate change mitigation, has reshaped oil palm into one of the world's most dynamic and competitive commodities.

Our central R&D has been the drive to raise productivity while safeguarding sustainability. Over the years, technologies ranging from breeding, innovative fertiliser formulations to nutrient recycling strategies have helped growers optimise yields. Geospatial platforms now allow plantations to map soils, assess peatland, and diseases monitoring more precisely than ever before. At the same time, pest and disease management has advanced from conventional approaches to highly targeted solutions. The deployment of beneficial plants, pheromone traps, and biological agents delivered by drones or helicopters are no longer ideas on the horizon but practical tools in the field. For challenges such as *Ganoderma*, MPOB has introduced integrated management systems and even established a National Biosecurity Plan, securing the future of plantations against one of their most persistent threats.

Sustainability has never been an afterthought as the global call to act on climate change has been addressed through efforts such as quantification of greenhouse gas emissions, the development of drought-tolerant palms and the restoration of riparian zones. Malaysia's commitments on the international stage ensures the long-term viability of the crop.

MPOB has steered oil palm breeding into the genomics era. The Palm Series varieties have provided the industry with compact palms, thin-shelled *tenera* and vitamin E-rich options. Among them, PS1.1 has stood out as a commercial favourite, combining high yields with manageable growth to extend plantation lifespans. Clonal propagation has also transformed the industry, enabling higher and more consistent yields across plantations. The risks of abnormal fruiting, once a major limitation, are now reduced through DNA diagnostics such as the SureSawit™ kits, the first of their kind in the world. By building genomic platforms and pioneering molecular breeding, MPOB has positioned Malaysia at the forefront of oil palm biotechnology.

Looking ahead, transgenic and genome-edited palms are already within sight. These technologies promise to accelerate the development of palms with improved nutritional traits and stronger disease resistance, without the long timelines of conventional breeding. They mark the beginning of a new era in which oil palm science can respond faster and more precisely to industry needs.

Beyond the plantation and the laboratory, research has also shaped how oil palm is seen by consumers worldwide. The recognition of palm-based tocotrienol-rich fraction as a functional nutrient opened opportunities for palm-derived health products, adding its value as more than just a cooking oil. At the same time, MPOB's leadership in addressing food safety challenges has been critical. By tackling contaminants such as 3-MCPD esters and glycidyl esters through advanced refining and testing methods, Malaysia has secured consumer trust and ensured compliance with international food safety standards.

Engineering innovations have likewise redefined palm oil processing. The introduction of continuous sterilisation systems for fresh fruit bunches brought safer, more efficient, and higher-quality outcomes. In product innovation, the development of red palm oil stands out. By retaining natural nutrients such as carotenoids and tocotrienols, this technology has created a new functional food now available in markets nationwide, earning recognition both locally and internationally.

The oleochemical frontier tells yet another story of diversification. Over the past 25 years, MPOB has developed more than 170 technologies that have expanded palm oil applications into cosmetics, surfactants, lubricants, polyurethanes, and into transformer oils, which serve as a renewable substitute for mineral oil in electrical power transformers. These advances highlight palm oil's versatility and strengthen Malaysia's position as a global leader in the non-food sector.

As I reflect on these achievements, I am reminded that they are not merely milestones on paper but lived realities for the planters, millers, researchers, and policy makers who shape this industry daily. Many of these innovations have been reported in the pages of JOPR, and I believe it is this ongoing dialogue between research and practice that gives our journal its enduring value.

The challenges confronting the oil palm industry today such as climate change, certification pressures, shifting trade dynamics, and evolving consumer expectations, are undeniably complex. Yet the past 25 years have shown that when science and innovation align with industry needs, challenges can be turned into opportunities. The next frontier will demand faster translation of research into practice, greater integration of digital agriculture and artificial intelligence, and stronger emphasis on circular economy models.

As we celebrate this milestone, let us reaffirm a shared commitment to keep oil palm research bold, relevant, and impactful. The coming decades will demand nothing less than the same spirit of innovation, collaboration, and vision that has carried us thus far.

And in that pursuit, JOPR will continue to play its role; documenting, disseminating, and debating the science that sustains an industry, and through it, sustains a nation.

Here's to the next 25 years of discovery and impact.

Ahmad Parveez Ghulam Kadir (PJN, Ph.D, FASc)
Editor-in-Chief
Journal of Oil Palm Research (JOPR)

REVIEW ARTICLES

Journal of Oil Palm Research Vol. 37 (3) September 2025 p. 377-396
DOI: https://doi.org/10.21894/jopr.2024.0018

DISCOVERING THE GLOBAL LANDSCAPE OF WOOD PRESERVATIVES

NUR AZREENA, I[1]*; ZAWAWI, I[1] and NOORSHAMSIANA, A W[1]

ABSTRACT

Wood is a precious natural resource used in many human activities, including construction and furnishing of building interiors. However, wood decomposes due to a variety of wood decay fungi species, including brown rot, white rot or soft rot fungi, inorganic elements, moisture and weathering. Therefore, a variety of wood preservation techniques have been developed to lengthen the service life of wood, lowering replacement costs and enabling wood to be used more effectively in numerous applications. A bibliometric analysis of 4,153 Scopus articles on wood preservatives, including biocide use of wood vinegar and oil palm wood vinegar, was conducted. The data was visualised using VOSviewer, analysed using Harzing's Publish or Perish and evaluated in Microsoft Excel for frequency of occurrences. This article analysed wood preservative research and development over time by categorising article by title, country of origin, publishing institution, and publication citation patterns. This review highlighted the most important research participants and suggested that wood preservatives are extensively used and have had a significant impact on the number of articles published in regions such as Europe and Asia. These findings extend to emerging patterns and issues in terms of publication frequency, journal impact factor, collaborative patterns and research components, which supplement the scarce global wood preservative trends literature.

Keywords: bibliometric, decay, VOSviewer, wood, wood preservatives.

Received: 9 August 2023; **Accepted:** 29 December 2023; **Published online:** 21 February 2024.

INTRODUCTION

Wood is a significant biomaterial due to its durability and versatility (Pędzik *et al*., 2021). Its flexibility has resulted in its widespread use in fields as diverse as architecture, interior design, transportation and decoration. Its adaptability has led to its extensive use in a wide variety of structural, architectural, aesthetic, and decorative applications, as well as in automobiles and ships (Lazim *et al*., 2020). This has led to a rise in demand for its consumption, which is largely attributable to the increase in global population, despite resulting in a corresponding decline in forest-covered regions around the world (Chen *et al*., 2020).

According to the wood products global market report, 2022 forecasts, the value of the global wood products market will increase from USD696.78 billion in 2022 to USD748.01 billion in 2023, at a compound annual growth rate (CAGR) of 7.4%. In addition, the Russia-Ukraine war affected the chances of the global economy recovering from the COVID-19 pandemic. The war between these two nations has resulted in economic sanctions on multiple nations, a spike in commodity prices, and supply chain disruptions, resulting in inflation across goods and services and affecting many global markets. Despite that, the wood products market is projected to reach USD964.41 billion by 2027 at a CAGR of 6.6% (The Business Research Company, 2022).

In contrast to plastics, wood has significant limitations such as dimensional instability and lack of durability due to high carbohydrate content in parenchymal cells (Mohamad Amini *et al*., 2019; Zhang *et al*., 2018). Furthermore, since wood contains cell walls, porous and hygroscopic by nature, it is extremely vulnerable to biological degradation by termites, fungi and insects (Sun *et al*., 2022; Yan *et al*., 2021). As a result, there will be economic losses and negative effects on the environment. Biodegradable

[1] Malaysian Palm Oil Board,
6, Persiaran Institusi, Bandar Baru Bangi,
43000 Kajang, Selangor, Malaysia.

* *Corresponding author e-mail: azreena@mpob.gov.my*

wood, an engineered wood product manufactured from natural wood fibres and biodegradable resins has a low carbon footprint and is recyclable besides its biodegradability properties (Cai *et al.*, 2020). Wood-plastic composites (WPCs) are a greener option to traditional wood products like lumber and plywood, which have a negative effect on the environment and contribute to deforestation (Lee *et al.*, 2020). One of the main advantages of biodegradable wood in the furniture industry is its longevity. Due to its strength and resistance to deterioration, it is an ideal furniture as it will not be damaged by moisture, fungus, or insects (Pour *et al.*, 2021).

The cell wall components of wood are composed of hemicelluloses, cellulose, and lignin. Meanwhile, parenchyma cells serve primarily as storage organelles for macromolecules like starch, pectin, simple sugars, fatty acids, and proteins. They are responsible for the structural qualities of wood, but microorganisms, particularly fungi and bacteria, can rapidly degrade them (Martín & López, 2023). Under certain environmental circumstances, such as moisture content above 20%, oxygen availability and a temperature range of 15°C-45°C, wood becomes susceptible to fungal infestation (Broda, 2020). Traditionally, wood-decay fungi have been classified into three main groups; white-rot, brown-rot and soft-rot fungi. The white-rot basidiomycetes are capable of breaking down the cell wall (polysaccharides and lignin). It can either degrade all wood components at once or specialise in degrading either lignin or polysaccharides. One of the most harmful types of wood-decay is caused by the brown-rot fungi, which is also a basidiomycete, the second category of wood-decaying organisms that can metabolise cell wall polysaccharides. Additionally, the third category of wood-rotting fungi consists of the ascomycete soft-rot fungi, which can degrade both cell wall polysaccharides and lignin (Nadali *et al.*, 2021). Therefore, it is necessary to lessen wood's hygroscopicity, enhance its dimensional stability and avoid attacks from biological organisms that cause decay by using wood preservatives.

Wood preservatives are chemical substances used in various wood preservation treatments to protect wood from insects and fungi. The different types of preservatives, such as oil-borne, water-borne and organic solvent-borne preservatives, can be identified by the solvents in which they are dissolved. Different characteristics and chemical properties distinguish each preservative (Teng *et al.*, 2018). Oil-borne preservatives, which include pentachlorophenol (PCP) and creosote, are generally referred to as heavy-duty organic preservatives. These preservatives can withstand high temperatures and chemicals without breaking down, and they are also resistant to leaching since they are insoluble in water (Khademibami & Bobadilha, 2022). However, these oil-based preservatives make the treated wood appear dark brown and produce a strong odour. They typically cause harm to both people and the environment. Thus, oil-borne preservatives are often only used in outdoor applications, such as poles and train lines where there is no risk to human contact and limited effects on the environment (Ahmed *et al.*, 2020).

Typically, water-borne preservatives are among the least expensive options available to consumers, and this may be their greatest advantage. Nevertheless, their biggest drawback is that they frequently cause the treated wood to swell if it is already porous, as the water in the preservatives is absorbed into the wood. Many water-based preservatives, such as chromated copper arsenate (CCA), alkaline copper quaternary and copper azole, have copper or a copper-based molecule as their primary active ingredient (Liu *et al.*, 2021). The primary chemical compound used in producing a water-borne preservative is CCA. However, many of them have been restricted from use due to environmental and health concerns due to the presence of arsenic in CCA, which is toxic to aquatic life and can cause cancer in humans due to their being easily absorbed by the human body (Lin *et al.*, 2009), necessitating the development of substitute wood protection agents and techniques based on non-toxic natural products. Despite their effectiveness as fungicides, it was recently discovered that these chemical compounds are carcinogenic and contain immunotoxins that can cause skin cancer (Smith, 2020).

Despite their usefulness in extending the life of wood products, wood preservatives can have various environmental impacts. Certain wood preservatives can leach into the soil and water, causing contamination. Both aquatic and terrestrial ecosystems may be harmed by this contamination (Chang *et al.*, 2015). Wood preservatives can potentially seep into groundwater, thereby having a harmful effect on both human health and aquatic life. They may also be introduced into nearby streams, rivers, and other water bodies, which can be toxic to aquatic life, harming fish, insects and other organisms in the ecosystem (Engwall *et al.*, 1999). In addition, airborne particles and volatile organic compounds (VOCs) may be generated while applying wood preservatives, which could have an impact on air quality, have implications for human health and may contribute to smog formation (Bahmani & Schmidt, 2018).

A study was conducted by Lebow *et al.* (2002) to determine the CCA, ammoniacal copper zinc arsenate (ACZA), ammoniacal copper quat (ACQ-B) and copper dimethyldithiocarbamate (CDDC) treated wood leaching into surrounding water and soil, as well as their effects to the environment. Based on their study, the soil and sediments in the

wetland areas were contaminated by these four different types of treated wood. In general, higher concentrations were found in soil due to the greater mobility of these leached components compared to sediments. Meanwhile, the levels of preservative components found in sediments did not appear to have any negative effects on the number or variety of aquatic invertebrates. Furthermore, in Brazil, traditional treatments based on CCA and chromated copper borate (CCB) are the most utilised. Even though this type of treatment causes undesirable wood colour changes, and presents risks to the environment and human health, they have a significantly better performance from wood treated with alternative copper-based preservatives than that of CCA-treated wood (Hingston *et al.*, 2001).

Despite its purpose in preserving wood products, the usage of wood preservatives raises various safety concerns. Many wood preservatives contain toxic chemicals, such as arsenic, creosote, PCP and CCA (Bayatkashkoli *et al.*, 2017). Workers involved in the manufacturing, application, or disposal of treated wood may be exposed to these toxic chemicals, and prolonged or high-level exposure can lead to serious health issues. Additionally, wood preservatives can cause skin and eye irritation when they come in contact. Skin contact with these substances over time may cause dermatitis and other skin problems. Redness, discomfort, and even permanent damage to the eyes can happen from accidental eye contact (Broda, 2020).

Furthermore, breathing in dust and VOCs while applying wood preservatives can irritate the respiratory system and cause breathing problems. This could lead to mild respiratory symptoms like coughing or more serious cases like wheezing (Aguayo *et al.*, 2022). Chemicals used as wood preservatives can be toxic and, in extreme situations, cause poisoning if consumed or inhaled. It is essential to follow safety protocols and use appropriate protective gear and ventilation to reduce the risk of exposure (Jin *et al.*, 2020). Besides, they must educate and remain up-to-date on pertinent rules and guidelines to maintain regulatory compliance and reduce safety risks. They must also adhere to disposal regulations and utilise approved disposal methods for treated wood products (Adhikari & Ozarska, 2018). Moreover, there are health and safety concerns associated with the final disposal of treated wood products. Improper disposal techniques for the treated wood may lead to groundwater contamination while burning it will emit dangerous chemicals into the atmosphere. Therefore, to reduce these risks, proper disposal procedures are required. Rules and regulations aimed at safeguarding the environment and public health may apply to the use of specific wood preservatives (Meena, 2022). To address these safety concerns, the use of proper personal protective equipment (PPE) is crucial when handling wood preservatives (Bernard Effah, 2015).

Future directions in wood preservatives will likely be affected by environmental concerns, regulatory changes, and technological advances (Freeman *et al.*, 2003). To increase the efficiency of wood preservatives, nanoscale additives and coatings are being developed. These advances in technology can improve the effectiveness of wood preservatives, making them more resistant to decay and insect infestations (Pařil *et al.*, 2017). Alternative wood preservation techniques like heat treatment, acetylation, and furfurylation are all being investigated by researchers. These treatments modify the wood's properties to make it naturally resistant to decay and insects. By altering its natural characteristics, these treatments provide resistance against insects and rot (Sandberg *et al.*, 2017). This will encourage the industry to develop and implement more environmentally friendly solutions. Technological advancements in testing methodologies will enable manufacturers to better analyse the durability of treated wood, resulting in the development of more effective preservation systems. The trend of procuring wood in a sustainable and accountable manner will continue to increase. This includes encouraging the use of recycled wood and utilising only certified wood from sustainably managed forests. As consumers become more aware of the impact of their decisions on the environment, there will be a greater emphasis on educating the public about the advantages of using preserved wood and the proper disposal of treated wood products. These trends reflect ongoing efforts to maintain a balance between the preservation of wood products and environmental and safety concerns. It is crucial for the wood preservation industry to adapt and innovate in response to these changing trends.

Various efforts, including the use of alternative, eco-friendly wood preservatives, improved application and disposal techniques, and the establishment of treated wood recycling programmes, can be implemented to minimise these environmental impacts (Cai *et al.*, 2020). To eliminate the use of toxic metallic preservatives, organic solvent-borne preservatives like triazoles and pyrethroids have been developed. These types of preservatives are non-volatile, odourless, non-toxic and hypoallergenic; thus, they are utilised for indoor applications (Petrič *et al.*, 2000). Combining antioxidants and metal chelators with organic solvent-borne preservatives can increase the efficacy and water dispensability of the biocides. However, the relatively high price of organic solvents and emulsifiers restricts their use, so the majority of relevant industrial facilities continue to support water-based formulations (Broda, 2020).

Currently, a wide range of techniques are being researched in depth for eco-friendly wood protection that are naturally formed, such as wood extractives, plant extracts, or biomass (Teacă *et al*., 2019). Since wood-degrading fungi can only grow in the presence of water, it is best to prevent their growth by keeping the wood dry with hydrophobic materials like plant oils and natural resins (Calegari *et al*., 2017). Wood can be preserved in another way by embedding organic substances with biocidal properties into its structure. The more cutting-edge approach uses biological control agents, which are microscopic organisms such as other fungi and bacteria that compete with wood-decaying fungi (Barbero-lópez *et al*., 2021).

Additionally, wood vinegar (WV) is a liquid by-product of biomass pyrolysis used to produce biofuels and biochar through the downstream processes of condensation and gas/vapour separation. WV typically consists of over 80% water and a wide variety of organic compounds, including acids, phenols and alcohols. Its organic components have been found to affect microbial activities, making it useful as an antibacterial agent, pesticide, and antioxidant (Zhang *et al*., 2019). For instance, Desvita *et al.* (2022) aimed to determine the antimicrobial activity of cocoa pod shell-derived WV. WV was found to be effective in preventing the spread of two potentially harmful microorganisms, *Candida albicans* and *Aspergillus niger*. The diameter of the microbial growth inhibition zone increased with WV concentration, suggesting that WV made from cocoa pod shells has antimicrobial characteristics. Jung *et al.* (2016) investigated the fungal inhibitory effect of wood blocks with WV. According to the findings, a concentration of 0.30 g/mL of WV protected the wood against white rot and brown rot fungi. Since WV inhibited the growth and spread of mycelia, it preserved the wood from deterioration by preventing cell wall erosion and thinning. Furthermore, the degree of weight loss reflected how effectively the body repelled the fungal infection.

Oil palm WV, produced by carbonising oil palm lignocellulosic materials (*e.g*., oil palm trunk and oil palm kernel shell), primarily comprises phenolic and acetic acid compounds that exhibit significant antifungal properties (Ariffin *et al*., 2017). For years, special attention has been given to this biomass pyrolysis product to increase the economic viability while contributing to the reduction of the environmental pollution arising from oil palm lignocellulosic by-product accumulation and open field burning (Oramahi *et al*., 2019). Lee *et al*. (2022) proved that WV which is also known as pyroligneous acid could be used as a wood preservative for the renewable timber species that are currently in demand despite their lower durability against biodegradation. In the study, rubberwood was protected from decay and mould when treated with 50% rubberwood wood vinegar (RWWV) and 30% oil palm trunk wood vinegar (OPTWV). Consequently, OPTWV indicated better biological durability compared to RWWV. Therefore, additional research confirming the new role of WV as an antibiological wood preservative will elevate the green value and serviceability of one of the woods.

Despite the increasing popularity of sustainable wood preservatives and a wide range of potential uses, there is a significant research gap in the form of insufficient systematic and quantitative analyses. Thus, our primary objective is to bridge this gap by conducting a comprehensive bibliometric analysis, which will provide a holistic view of the wood preservatives research landscape. Bibliometric analysis is extensively used since it permits precise measurement and analysis of the articles indexed in an investigative database (Donthu *et al*., 2021; Moral-muñoz *et al*., 2020). Earlier, Li *et al*. (2022) conducted a bibliometric review entitled "Wood decay fungi: An analysis of worldwide research" by using the Web of Science (WOS) Core Collection to perform a literature review. This study summarised the current research landscape, highlighted leading research centres, journals, authors and academic communities and elucidated the most imperative research questions search from 1913-2020. This review presented the current state of research, identified significant institutions, journals, authors and academic communities and elucidated the most relevant areas of current research. Since then, research on wood preservatives has advanced substantially, and it is essential to stay updated on the most recent literary developments. This study conducted a bibliometric analysis of published wood preservatives research from 1909-2024 to determine the breadth and depth of scholarly work on wood preservatives. Additionally, three fundamental research questions were addressed. First, how is the study of wood preservatives evolving and progressing? Second, what are the most prevalent research topics concerning wood preservatives? Third, who and what are the leading researchers and institutions in terms of wood preservative publication output?

In the next sections of this study, the research methods, evolution, and distribution of published studies per year, sources, document categories and document languages were detailed. Keyword frequency and co-occurrences, among the most prominent subjects of interest to scholars, were also emphasised.

MATERIALS AND METHODS

In this work, the assessment of wood preservatives in wood deterioration research was the centre of the research complement with WV and oil palm

WV as the applicable wood preservatives. These bibliometric study materials were analysed using the Scopus database (Muhuri *et al.*, 2019). There was more than 27,100 active titles in Scopus, 7,000 publishers, 84 million documents, 17.6 million author profiles, 249,000 books, 80,000 institutional profiles and 1.8 billion citations. This database was chosen because of its comprehensive coverage of scientific research around the world and its status as one of the most important data repositories in the field (Mansour *et al.*, 2022). Scopus is therefore recommended as a good database for extracting content relating to the topic of this study.

Keywords were used to identify the relevant documents. 'Wood preservatives', 'wood vinegar' and 'oil palm wood vinegar' were used as keywords to locate article titles and abstracts in the Scopus database. This search was conducted on 17 March 2023, using specified documents published from 1909 until 2024. A total of 4,162 new articles appeared as a result. After the documents were further screened, and nine types of erratum documents were omitted, the final number of Scopus-retrieved documents was down to 4,153. In addition, the standard protocol of the Preferred Reporting Items for Systematic Reviews and Meta-analyses (PRISMA) statement was applied to the review of articles, as depicted in a flowchart (*Figure 1*). Thus, this review gained conformance by adhering to the PRISMA protocol's detailed procedures (Maier, 2021).

The number of publications indexed by the repository was determined and analysed through bibliometric analysis for this study (Moral-muñoz *et al.*, 2020). This analysis, which is based on statistical data, is used in archives and records to identify publication trends within a particular field or body of literature (Van Eck & Waltman, 2010). To provide comprehensive answers to the research questions, a number of methods were used to collect data. The frequency and percentage of each publication were calculated using Microsoft Excel 2019 along with the necessary graphs and charts. The bibliometric linkages and visualisation were generated using VOSviewer (version 1.6.18), and the citation metrics were calculated using Harzing's Publish and Perish software version 8.6.4198.8332.

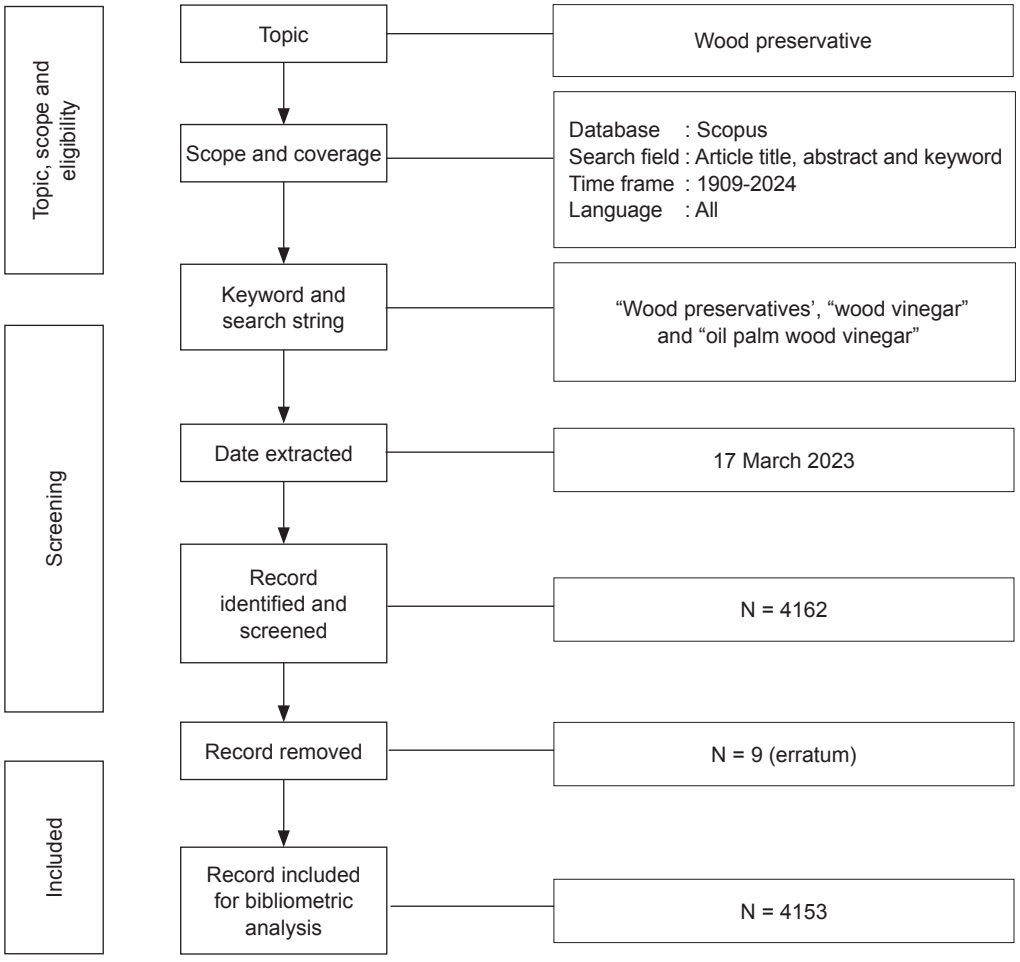

Figure 1. Schematic in accordance with the PRISMA declaration.

RESULTS AND DISCUSSION

The Advancement and Development of Wood Preservatives Research

To respond to the first research question (How the study of wood preservatives is developing and moving forward?), the following discussions were included: (a) Annual number of published studies; (b) document types; (c) source types; and (d) document languages.

Annual number of published studies. Detailed statistics on annual publications of wood preservatives (from 1909 to 2024), wood vinegar (from 1993-2023) and oil palm wood vinegar (from 2017-2023) research are shown in *Figure 2*. The highest number of publications was received for 2020 (161, wood preservatives), 2022 (60, wood vinegar) and 2023 (3, oil palm wood vinegar). Less than 100 articles on wood preservatives were documented in the Scopus database for articles published between 1929 and 2004, while all articles on wood vinegar and oil palm wood vinegar were less than 100. The number of publications varied from 2005-2022, due to the increased interest in wood preservatives. This analysis was done immediately at the end of March 2023, even though there were only 30 articles up to that time of the year. The total quantity of documents for the year had yet to be disclosed. The Scopus database also noted that a journal had publications arranged up to 2024 and the number of documents released in prior years 1909-1971 was less than 20. Total publications were rising, although with a fluctuating tendency. The annual total document revealed the language of documents published in wood preservative publications, the types of documents, the most popular source titles, and the sources for wood preservative research.

Document types. The document types were differentiated into 12 different categories (*Table 1*). More than half of the publications from those three titles (wood preservative, wood vinegar and oil palm wood vinegar) were categorised as articles, accounting for 2,943, 378 and 5 (79.18%, 88.11% and 55.56%), conference papers 374, 35 and 3 (10.06%, 8.16% and 33.33%), and reviews accounting 206, 8 and 0 (5.54%, 1.86% and 0.00%). Other forms of publications, such as book chapters, notes, books, short surveys, letters, conference reviews and reports made up less than 5% of the total publications. The least frequent document type, accounting for 1 document, was notes and conference reviews for the wood vinegar title.

Sources types. Research articles were classified into seven primary source types, with journal documents comprised of 3,043, 383, and six documents (81.87%, 89.28% and 66.67%) being the largest source type, while conference proceedings with 237, 27 and 3 documents, respectively (6.38%, 6.29% and 33.33%) coming in second. Trade journals, which accounted for 5.38% and 0.70% (200 and 3 articles) of all publications, also contributed significantly (*Table 2*). Articles that made up less than 5.00% of total publications were books (n = 115 and 3, 3.09% and 0.70%), book series (n = 109 and 12, 2.93% and 2.80%), reports (n = 11, 0.30%), and undefined (n = 2 and

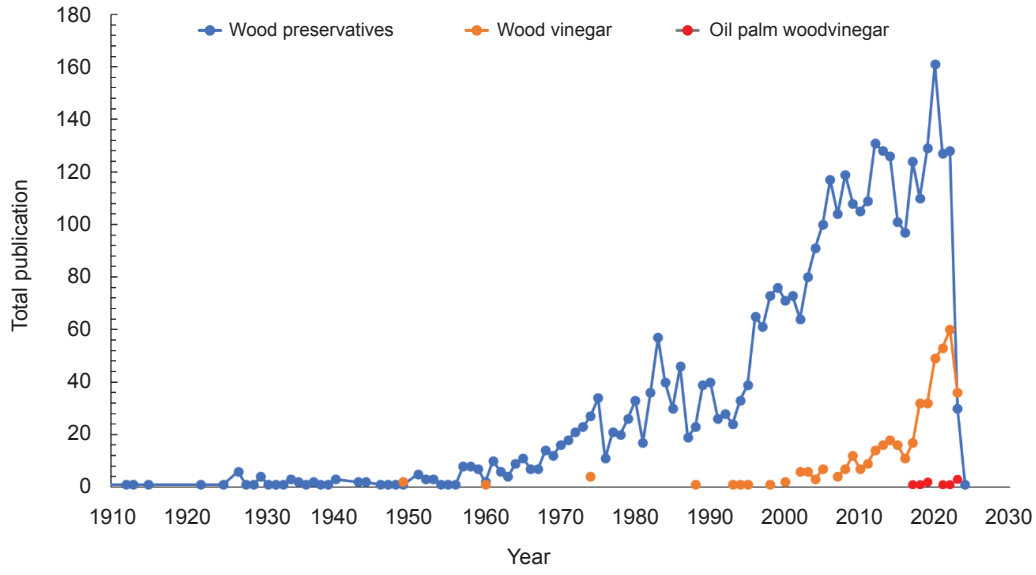

Figure 2. Annual totals for publications.

TABLE 1. TYPES OF DOCUMENTS

Types of documents	Total publications			(%)		
	1	2	3	1	2	3
Articles	2,943	378	5	79.18	88.11	55.56
Conference papers	374	35	3	10.06	8.16	33.33
Reviews	206	8	0	5.54	1.86	0
Book chapters	108	3	0	2.91	0.7	0
Notes	22	1	0	0.59	0.23	0
Books	14	0	0	0.38	0	0
Short surveys	12	0	0	0.32	0	0
Letters	11	0	0	0.30	0	0
Conference reviews	10	1	0	0.27	0.23	0
Reports	9	0	0	0.24	0	0
Erratum	5	3	1	0.13	0.70	11.11
Editorial	3	14	0	0.08	0	0

Note: 1 - wood preservative; 2 - wood vinegar; 3 - oil palm wood vinegar.

TABLE 2. SOURCES TYPE

Sources types	Total publication			(%)		
	1	2	3	1	2	3
Journals	3,043	383	6	81.87	89.28	66.67
Conference proceedings	237	27	3	6.38	6.29	33.33
Trade journals	200	3	0	5.38	0.7	0.00
Books	115	3	0	3.09	0.7	0.00
Book series	109	12	0	2.93	2.8	0.00
Reports	11	0	0	0.30	0.00	0.00
Undefined	2	1	0	0.05	0.23	0.00

Note: 1 - wood preservative; 2 - wood vinegar; 3 - oil palm wood vinegar.

1.0, 0.05% and 0.23%). Once the document and source types were established, the most frequently published language was analysed to determine its prevalence.

Languages of documents. Wood preservatives, WV and oil palm WV research articles were produced in a total of 25, six and single languages, respectively, with English being the most prominent (82.00%-100.00%) followed by Chinese (15.12%) and German (5.78%) (*Figure 3*). The remainder of the materials were translated into other languages namely Portuguese, Japanese, Korean, Spanish, French, Turkish, Polish, Russian, Finnish, Croatian, Dutch, Italian, Danish, Estonian, Moldavian, Moldovan, Persian, Romanian, Serbian, Slovak, Swedish and Ukrainian. After determining the current language trends, the subject area was the final identifier of the present trend.

Key areas of wood preservative research. The second research question was to identify the most prevalent themes in wood preservatives research in terms of (a) major subject areas, and (b) keyword frequency.

Subject area. Documents were categorised according to their subject area (*Table 3*) in which it was found that materials science accounted for more than 37.07% (n = 1,378) of the total articles, and agricultural and biological Sciences accounted for a considerable proportion (n = 1362; 36.64%) while less than 30.00% of all publications were in the fields of chemical engineering, chemistry, engineering, and environmental science. Meanwhile, biochemistry, computer science, earth and planetary sciences, energy, immunology and microbiology, medicine, pharmacology, toxicology and pharmaceutics, physics and astronomy, and social sciences, accounted for less than 10.00% of total publications. Arts and humanities, business, management and accounting, decision sciences, dentistry, economics, econometrics and finance, health professions, mathematics, multidisciplinary, neuroscience, nursing, psychology and veterinary accounted for less than 1.00% of the total publications. After ascertaining the trend and influence of publications in wood preservatives research, the most frequently used keywords in wood preservatives studies were analysed.

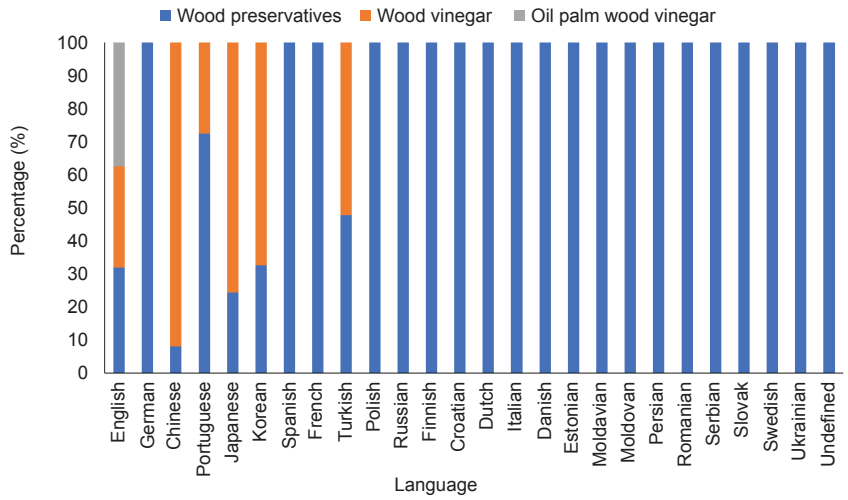

Figure 3. Languages used for publications.

TABLE 3. SUBJECT AREA

Subject areas	Total publications			(%)		
	1	2	3	1	2	3
Agricultural and biological sciences	1,362	170	2	36.64	39.63	22.22
Arts and humanities	23	0	0	0.62	0.00	0.00
Biochemistry, genetics and molecular biology	195	49	1	5.25	11.42	11.11
Business, management and accounting	34	4	0	0.91	0.93	0.00
Chemical engineering	401	0	0	10.79	0.00	0.00
Chemistry	506	54	0	13.61	12.59	0.00
Computer science	37	9	0	1.00	2.10	0.00
Decision sciences	1	0	0	0.03	0.00	0.00
Dentistry	2	0	0	0.05	0.00	0.00
Earth and planetary sciences	79	22	1	2.13	5.13	11.11
Economics, econometrics and finance	12	2	0	0.32	0.47	0.00
Energy	85	78	0	2.29	0.00	0.00
Engineering	767	62	1	20.63	0.00	11.11
Environmental sciences	890	119	2	23.94	0.00	22.22
Health professions	7	2	0	0.19	0.47	0.00
Immunology and microbiology	169	0	0	4.55	0.00	0.00
Materials science	1,378	34	2	37.07	7.93	22.22
Mathematics	17	3	0	0.46	0.70	0.00
Medicine	306	22	0	8.23	5.13	0.00
Multidisciplinary	36	13	2	0.97	3.03	22.22
Neuroscience	6	1	0	0.16	0.232	0.00
Nursing	4	2	0	0.11	0.47	0.00
Pharmacology, toxicology and pharmaceutics	125	0	0	3.36	0.00	0.00
Physics and astronomy	146	0	1	3.93	0.00	11.11
Psychology	1	0	0	0.03	0.00	0.00
Social sciences	38	7	0	1.02	1.63	0.00
Veterinary	16	11	0	0.43	2.56	0.00
Undefined	2	0	0	0.05	0.00	0.00

Note: 1- wood preservative; 2 - wood vinegar; 3 - oil palm wood vinegar.

Frequency of keywords. The fundamental concept of keyword analysis is that the author's keywords adequately reflect the article's subject area (Donthu *et al*., 2021). *Table 4* summarises 20 of the most frequently used keywords in wood preservatives, WV and oil palm WV studies. The data further revealed that wood preservation was the keyword most associated with wood preservatives (n = 1,071; 28.81%) followed by wood with 1,005 of total publications (27.04%). Other keywords that appeared more than 100 times were wood preservatives, article, protective coatings, copper, fungi, leaching, nonhuman, wood products, human, wood protecting agent, decay (organic), controlled study, timber, pentachlorophenol, priority journal, preservative, arsenic, chromated copper arsenate, chromium. After conducting a keywords analysis, the analysis on the title was made to further understand the prevalent themes.

Meanwhile, for WV and oil palm WV, there were the same keywords such as wood vinegar (257 and 5), acetic acid (163 and 2) and pyrolysis (100 and 2) were found in both search titles. This is speculated due to limited research and countries involved in oil palm wood vinegar production. *Figure 4* is a network visualisation of the most frequently used words and phrases. When two related keywords appear in the same article, it suggests that the two subjects are related (Nordin *et al*., 2022). To address the second research question, the keyword and co-occurrence analysis features of VOSviewer were utilised. VOSviewer is a software application for constructing and visualising bibliometric networks and mapping each article's assigned keywords. The colour, circle size, font size, and line thickness of connecting lines signify associations between other terms (Van Eck & Waltman, 2010).

Keywords that are frequently assigned the same colour are frequently clustered together. Based on the authors' keywords, 10 clusters including 323 items in the wood preservatives research were generated. The figure indicated that wood preservatives, PCP, biodegradation PCDD, indoor air, biocide, pesticide and nanotechnology have similar colours, indicating that these terms are closely related and frequently appear together. The primary keywords supplied in the search query were wood preservatives, article, protective coatings, copper and fungi were among the most often occurring (>10%) terms.

TABLE 4. TOP 20 KEYWORDS

No.	Keywords					
	Wood preservatives		**WV**		**Oil palm WV**	
1	Wood preservation	1,071	Wood vinegar	257	Wood vinegar	5
2	Wood	1,005	Acetic acid	163	Palm oil	3
3	Wood preservatives	643	Wood	133	Acetic acid	2
4	Article	577	Wood Vinegars	102	Pyrolysis	2
5	Protective coatings	576	Pyrolysis	100	Pyrolysis temperature	2
6	Copper	475	Vinegar	78	Agriculture	1
7	Fungi	420	Article	61	Anti Termites	1
8	Leaching	311	Biomass	60	Anti-fungal activity	1
9	Nonhuman	262	Charcoal	53	Antifungal activity	1
10	Wood Products	262	Nonhuman	44	Antioxidant enzymes	1
11	Human	232	Biochar	43	Antitermite activity	1
12	Wood protecting agent	231	Phenols	37	Bioactive compounds	1
13	Decay (Organic)	222	Unclassified drug	37	Biofilm	1
14	Controlled study	204	PH	36	Biological tests	1
15	Timber	201	Pyroligneous acid	35	Biostimulants	1
16	Pentachlorophenol	197	Controlled study	32	Carbendazim	1
17	Priority journal	197	Methanol	32	Central composite designs	1
18	Preservative	189	Carbonisation	28	Compost	1
19	Arsenic	188	Ketones	27	*Coptotermes formosanus*	1
20	Chromated copper arsenate	178	Animals	24	Drought stress	1

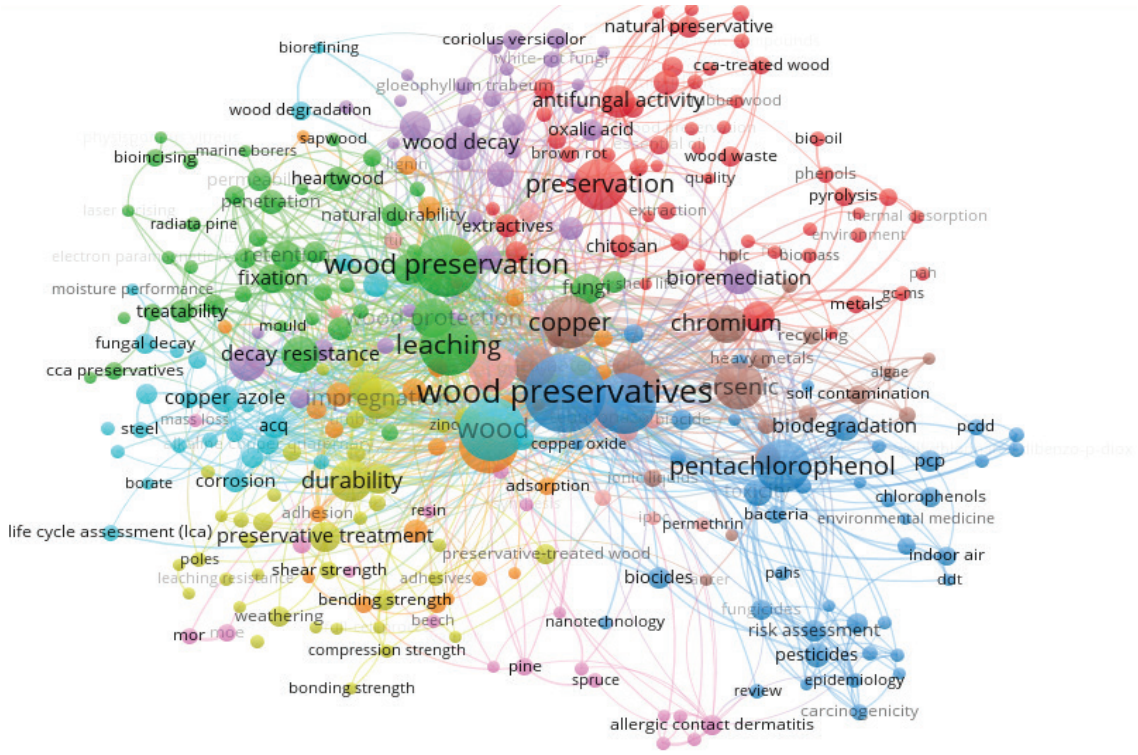

Figure 4. Network visualisation map of author's keywords.

Major Players and Research Collaborations

This section analysed the literature to answer the third research question, which aimed to assess international collaboration in the field of wood preservatives by looking at (a) publication counts by country, (b) the most prolific research institutions, (c) authorship patterns and (d) citation frequencies.

Publication by countries. *Figure 5* provides a summary of the publications on wood preservatives for the top 20 countries. There were 822 research publications in the USA on the topic of wood preservatives, followed by Germany (307), China (233) and Canada (218). Less than 200 publications were scattered over the globe, including Japan, the United Kingdom, Australia, Turkey, Brazil, India, Sweden, Finland, France, Poland, South Korea, Slovenia, New Zealand, Spain, Indonesia, Italy and Malaysia. Evidently, wood preservatives are essential across multiple continents, including North America, Europe, Asia, Oceania, and South America.

Although Canada ranked fourth in terms of total publications, it is imperative to emphasise that the country has higher total citations (n = 5,384) compared to Germany (n = 4,069) and China (n = 2,703) with higher total publications (*Figure 5*). The number of publications in Asia, including China, Japan, India, South Korea, Indonesia and Malaysia, was competitive, with China in the lead.

Main institutions. Analyses were conducted on the current status of the leading wood preservatives research centres. The top 20 most prolific institutions and their total number of publications are shown in *Table 5*. USA Forest Products Laboratory was ranked first in terms of publication volume, followed by Mississippi State University and Oregon State University. The top 10 institutes conducting wood preservatives research included five in the United States, two each in Canada, New Zealand, and Germany, as well as one each in Slovenia, Japan, Australia, Brazil, Hong Kong, China and Turkey.

Authorship analysis. In addition to analysing the current state of collaboration, this section also elucidated the most productive authors writing about wood preservatives. Twenty one of the prominent authors with at least 18 publications in the area of wood processing were Morrell, J J; Humar, M; Nicholas, D D; Cooper, P A; Zelinka, S L; Kartal, S N; Anon Schultz, TP; Pizzi, A; Imamura, Y; Pohleven, F; Ruddick, J N R; Barnes, H M; Militz, H; Kamdem, D P; Schwarze, F W M R.; Gjovik, L R; Lesar, B; Paes, J B; Clausen, C A and Tascioglu, C (*Table 6*). Six of the authors were from the United States, indicating that the country produced productive authors in the field of wood preservatives research. In terms of the number of total citations, Pizzi, A was rated first with 1,039 citations followed by Clausen, C A (774) and Nicholas, D D (733). There was a total of 154 authors contributing more than 3,719 articles on wood preservative.

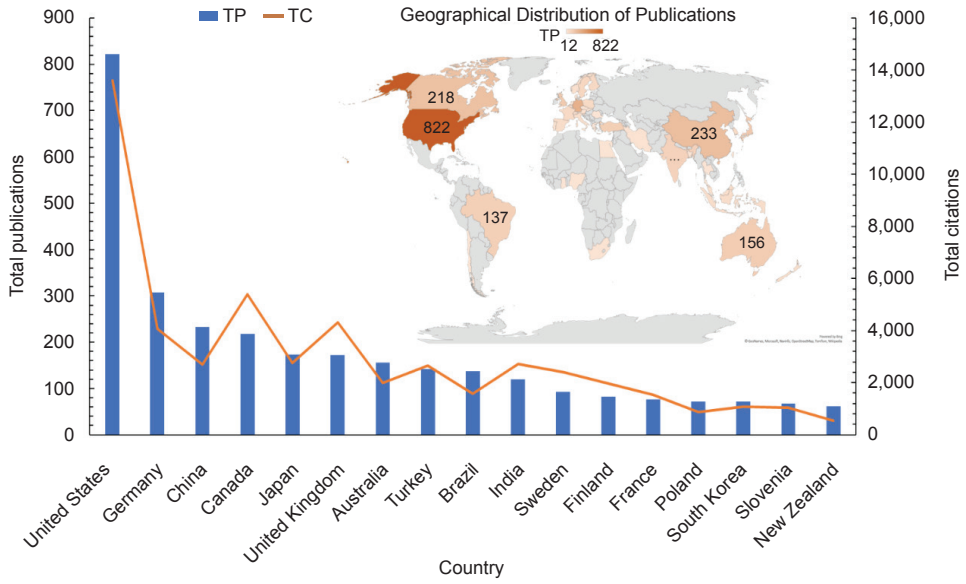

Figure 5. Total publications and total citations based on geographical location.

TABLE 5. MOST ACTIVE INSTITUTIONS

Institution	TP	%	Country	NCP	TC	C/P	C/CP	h	g
USDA Forest Products Laboratory	172	4.63	US	158	2,962	17.22	18.75	30	48
Mississippi State University	86	2.31	US	8	56	0.65	7.00	5	7
Oregon State University	85	2.29	US	9	80	0.94	8.89	6	8
USDA forest service	75	2.02	US	9	59	0.79	6.56	4	7
Univerza v Ljubljani	63	1.69	Slovenia	59	788	12.51	13.36	17	24
United States Department of Agriculture	50	1.35	US	44	767	15.34	17.43	15	26
Kyoto University	44	1.18	Japan	41	835	18.98	20.37	18	27
Commonwealth Scientific and Industrial Research Organization	44	1.18	Australia	42	442	10.05	10.52	12	19
The University of British Columbia	41	1.10	Canada	40	900	21.95	22.50	17	29
University of Toronto	41	1.10	Canada	39	465	11.34	11.92	13	18
SCION	38	1.02	New Zealand	31	321	8.45	10.35	10	17
Bundesforschungsanstalt fur Forst Und Holzwirtschaft	37	1.00	Germany	29	342	9.24	11.79	11	17
Federal Institute for Materials Research and Testing Berlin	37	1.00	Germany	31	286	7.73	9.23	8	15
Universidade de São Paulo	35	0.94	Brazil	28	240	6.86	8.57	8	14
University of Florida	34	0.91	Hong Kong	31	977	28.74	31.52	19	31
College of Forest Resources	34	0.91	New Zealand	31	543	15.97	17.52	12	22
Northeast Forestry University	33	0.89	China	24	192	5.82	8.00	9	12
Michigan State University	32	0.86	US	30	491	15.34	16.37	13	21
Sveriges lantbruksuniversitet	30	0.81	Sweden	30	658	21.93	21.93	15	25
Karadeniz Technical University	28	0.75	Turkey	26	824	29.43	31.69	17	26
Michigan Technological University	27	0.73	US	23	600	22.22	26.09	11	23

Note: TP - total number of publications; NCP - number of cited publications; TC - total citations; C/P - average citations per publication; C/CP - average citations per cited publication; h - h-index; g - g-index.

The current study employed VOSviewer for co-author analysis to further examine the authors' collaboration. The study was based on the fact that significant numbers of authors were cited at least once in a single article about wood preservatives and were calculated using the fractional counting method. Specific qualities such as colour, circle size, text size and thickness enhanced the writers' relationship. Associated authors were listed sequentially, as shown by the same colour. For example, the figure suggested that Nicholas, D D; Schultz, T P; Barnes, H M and Zelinka, S L; Xue, W; Kennepohl, P and Ruddick worked closely together. In addition, Nicholas, D D; Schultz, T P; Barnes, H M appeared to have had an equivalent strong collaboration with colleagues from other regions in the world, including Canada and Slovenia.

Figure 6 depicts the network visualisation map of the associated nation of the authors. Only countries with multiple articles cited were considered. The data suggested that the United States played a crucial role in international collaboration with tight connections to China, Japan and Germany; whereas Uruguay had links with Turkey, France and Japan. Next, the third research question emphasised the topic of citation.

Citation analysis. *Table 7* gives an overview of references to research on wood preservatives from the Scopus database. A total of 5,389 citations were recorded for 3,717 publications published during 115 years (1909-2024), which equates to an average of 485.87 citations per year.

Table 8 presents an overview of the 10 most often cited research articles on the subject of wood preservatives, ranked by the number of times each document was cited. "Wood Modification: Chemical, Thermal and Other Processes" by C.A.S. Hill was the most cited publication with 1,361 citations (Hill, 2006). The second and third publications, which were both released in 2011 and 2005, were research articles entitled "Plant growth promoting rhizobacteria and endophytes accelerate phytoremediation of metalliferous soils," written by Ma *et al.* (2011) and totalling 776 citations while Holley and Patel (2005) articles entitled "Improvement of shelf-life and safety of perishable foods by plant essential oils and smoke antimicrobials" with 761 citations.

Sources Titles

Additionally, studies on wood preservatives have been published in a number of journals, conferences, and books. *Table 9* indicates that the most active source title was considered based on the total number of articles published under each source title. "Forest Products Journal" had the most significant (242) followed by "Holzforschung" (193). Although "International Biodeterioration and Biodegradation" had fewer total publications (n = 80), it proved to be one of the leaders in total citations (n = 2,057). Other top sources titles included Holz Als Roh Und Werkstoff, Bioresources, International Biodeterioration and Biodegradation, Wood Science and Technology, Chemosphere, Holz Als Roh Und Werkstoff European Journal of Wood and Wood Industries, Wood and Fiber Science, European Journal of Wood and Wood Products.

Figure 7 depicts a visualisation of a term co-occurrence network, based on the title and abstract fields, with at least 15 items. The width of the node shows the item's weight, while the thickness of the connecting line reflects the item's connection strength. When words are displayed in the same colour, they are more likely to appear together. Framework, efficacy, competency, substance, perspective, policy and implementation, for instance, were tightly related and regularly co-occur in the diagram, as were other terms represented in red.

In recent years, there has been a proliferation of research on wood preservatives, with WV serving as one of the bio-wood preservatives, across a wide range of disciplines. The research on oil palm WV, on the other hand, has only recently begun to emerge after making its debut in 2017 with one article and currently three articles in 2023. The purpose of this review was to integrate and assess all current studies, to explain the identified contradictions in the literature, and to provide directions for capacity-related subjects. The data indicated that research on the topic has increased in the past 18 years. More articles published showed that the research stream was not stagnant, as it followed a route of evaluation and incorporated new approaches.

Studies on WV and oil palm WV are currently taking place not just in North America, China and Indonesia but also in many other parts of the world due to their special qualities, and they have been translated into more than 20 different languages. Thus, a 115- year bibliometric analysis of the Scopus-indexed literature on wood preservatives published from 1909 to 17 March 2023 was conducted.

The data collected in response to these inquiries was analysed using several key frameworks. In response to the first research question, two studies found that in 1909, publications on wood preservatives began, and by 1912, "A new wood preservative" was published in Industrial and Engineering Chemistry. For WV, the studies began in 1949 with 'On the Utilisation of Furfural obtained from Cooking of Bamboo stalks with

TABLE 6. AUTHORSHIP ANALYSIS

Author name	TP	%	Affiliation	Country	NCP	TC	C/P	C/CP	h	g
Morrell, J. J.	77	2.07	University of the Sunshine Coast, Sippy Downs, Australia	Australia	66	418	5.43	6.33	11	15
Humar, M.	55	1.48	Univerza v Ljubljani, Department of Wood Science and Technology, Ljubljana, Slovenia	Slovenia	51	594	10.80	11.65	15	21
Nicholas, D. D.	37	1.00	Mississippi State University, Department of Sustainable Bioproducts, Mississippi State, United States	United States	34	733	19.81	21.56	12	26
Cooper, P. A.	35	0.94	University of Toronto, Faculty of Forestry, Toronto, Canada	Canada	34	359	10.26	10.56	12	16
Zelinka, S. L.	30	0.81	USDA Forest Products Laboratory, Building and Fire Sciences, Madison, United States	United States	23	287	9.57	12.48	11	16
Kartal, S. N.	29	0.78	Istanbul University-Cerrahpasa, Istanbul, Turkey	Turkey	28	654	22.55	23.36	14	25
Anon	27	0.73	No affiliation available	-	2	7	0.26	3.50	1	2
Schultz, T. P.	27	0.73	Silvaware, Inc., Starkville, United States	United States	25	642	23.78	25.68	12	25
Pizzi, A.	26	0.70	Université de Lorraine, Nancy, France	France	25	1,039	38.48	41.56	18	25
Imamura, Y.	23	0.62	Research Institute for Sustainable Humanosphere, Uji, Japan	Japan	22	467	20.30	21.23	12	21
Pohleven, F.	23	0.62	Univerza v Ljubljani, Department of Wood Science and Technology, Ljubljana, Slovenia	Slovenia	23	425	18.48	18.48	12	20
Ruddick, J. N. R.	23	0.62	Mychem Wood Protection Consultants Ltd., Vancouver, Canada	Canada	21	228	9.91	10.86	10	14
Barnes, H. M.	22	0.59	College of Forest Resources, College of Forest Resources, Mississippi State, United States	United States	19	278	12.64	14.63	7	16
Militz, H.	22	0.59	Georg-August-Universität Göttingen, Gottingen, Germany	Germany	19	543	24.68	28.58	10	19
Kamdem, D. P.	20	0.54	Michigan State University, East Lansing, United States	United States	18	195	9.75	10.83	9	13
Schwarze, F. W. M. R.	20	0.54	EMPA - Swiss Federal Laboratories for Materials Science and Technology, Laboratory for Cellulose & Wood Materials, Dubendorf, Switzerland	Switzerland	19	431	21.55	22.68	12	19
Gjovik, L. R.	19	0.51	USDA Forest Products Laboratory, Madison, United States	United States	8	35	1.84	4.38	3	5
Lesar, B.	19	0.51	Univerza v Ljubljani, Department of Wood Science and Technology, Ljubljana, Slovenia	Slovenia	17	200	10.53	11.76	8	13
Paes, J. B.	19	0.51	Federal University of Espirito Santo, Vitória, Brazil	Brazil	15	138	7.26	9.20	6	11
Clausen, C. A.	18	0.48	USDA Forest Service, Washington, D.C., United States	United States	18	744	41.33	41.33	12	18
Tascioglu, C.	18	0.48	Düzce Üniversitesi, Department of Forest Products Engineering, Duzce, Turkey	Turkey	18	422	23.44	23.44	11	18

Note: TP - total number of publications; NCP - number of cited publications; TC - total citations; C/P - average citations per publication; C/CP - average citations per cited publication; h - h-index; g - g-index.

TABLE 7. WOOD PRESERVATIVES RESEARCH CITATIONS METRICS

Item	Metric
Total articles	3,717
Total citations	55,389
Number of years	115
Citations per year	485.87
Citations per articles	14.9
Authors per articles	3.29
h-index	84
g-index	142

TABLE 8. MOST CITED PUBLICATIONS

No.	Authors	Title	Year	TC	C/Y
1	Hill, C. A. S. (Hill, 2006)	Wood modification: Chemical, thermal and other processes	2006	1,362	80.12
2.	Ma, Y., Prasad, M. N. V., Rajkumar, M., Freitas, H. (Ma *et al*., 2011)	Plant growth promoting rhizobacteria and endophytes accelerate phytoremediation of metalliferous soils	2011	776	64.67
3	Holley, R. A., Patel, D. (Holley & Patel, 2005)	Improvement of shelf-life and safety of perishable foods by plant essential oils and smoke antimicrobials	2005	761	42.28
4	Pointing, S. B. (Pointing, 2001)	Feasibility of bioremediation by white-rot fungi	2001	698	31.73
5	Baldrian, P. (Baldrian, 2003)	Interactions of heavy metals with white-rot fungi	2003	555	27.75
6	Sophia A., C., Lima, E. C. (Sophia A & Lima, 2018)	Removal of emerging contaminants from the environment by adsorption	2018	512	102.4
7	Barceloux, D. G. (Barceloux, 1999)	Chromium	1999	505	21.04
8	Wang, S., Mulligan, C. N. (Wang & Mulligan, 2006)	Occurrence of arsenic contamination in Canada: Sources, behaviour and distribution	2006	485	28.53
9	Seidler, A., Hellenbrand, W., Robra, B. P., Vieregge, P., Nischan, P., Joerg, J., Oertel, W. H., Ulm, G., Schneider, E. (Seidler *et al*., 1996)	Possible environmental, occupational and other etiologic factors for Parkinson's disease: A case-control study in Germany	1996	403	14.93
10	Hingston, J. A., Collins, C. D., Murphy, R. J., Lester, J. N. (Hingston *et al*., 2001)	Leaching of chromated copper arsenate wood preservatives: A review	2001	293	13.32

Note: TC - total citations; C/Y - citations per year.

TABLE 9. MOST ACTIVE SOURCE TITLES

Sources title	TP	TC
Forest Products Journal	242	2,610
Holzforschung	193	2,966
Holz Als Roh Und Werkstoff	104	749
Bioresources	84	1,043
International Biodeterioration and Biodegradation	80	2,057
Wood Science and Technology	68	1,230
Chemosphere	54	1,491
Holz Als Roh Und Werkstoff European Journal of Wood and Wood Industries	47	171
Wood and Fibre Science	45	465
European Journal of Wood and Wood Products	44	515

Note: TP - total number of publications; TC - total citations.

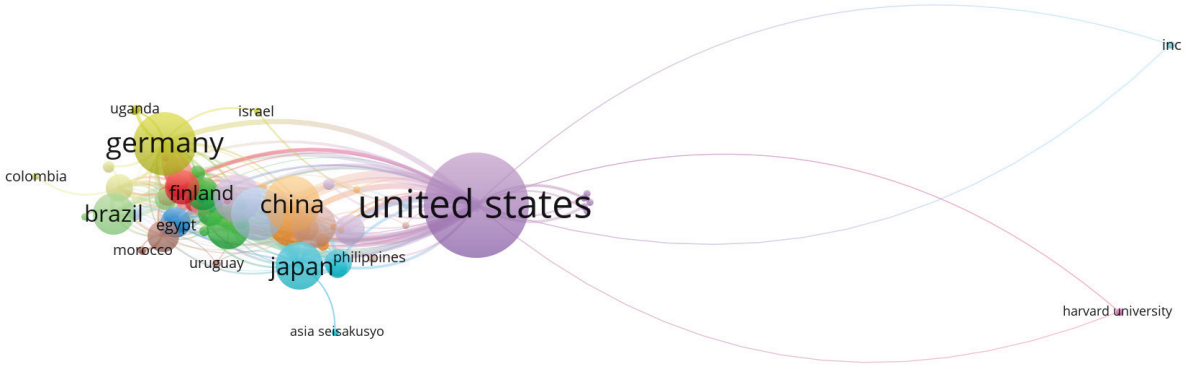

Figure 6. Network visualisation map of the co-authors by country for wood preservatives research.

Wood Vinegar' published in Nihon Ringakkai Shi/ Journal of the Japanese Forestry Society and 'On the pulp-making process of bamboo by the wood vinegar and paper-making tests of these pulps in The Journal of the Japanese Forestry Society. The studies on oil palm WV were only conducted in a few nations which included Indonesia, Malaysia, Ghana, Japan and Thailand, because these nations are the main producers of palm oil. In addition, Japan has a comprehensive plan for the utilisation of biomass for energy production through its Biomass Nippon Plan Policy, which was adopted in 2002 and encompasses the use of palm kernel shells (PKS). Moreover, Japan also has numerous research collaborations with South East Asian countries (Pambudi *et al.*, 2017). The first article published in 2017 appeared in the Indian Journal of Experimental Biology, entitled 'Optimisation of pyroligneous acid production from palm kernel shell and its potential antibacterial and antibiofilm activities'.

From 1968 to 2018, the number of articles on wood preservatives and WV has steadily increased. The growth may be attributable to the publication entitled "The chemical analysis of copper, chromium, and arsenic preservative-treated wood" which detailed the introduction of chemical controls such as copper, chromium and arsenic as wood preservatives. This revealed that experts from the United States recognised wood preservatives early on in their development. In contrast, the increasing interest in WV can be traced back to a study published in 2018 entitled "Combining biochar, zeolite, and wood vinegar for composting of pig manure: The effect on greenhouse gas emission and nitrogen conservation". This study examined the impact of varying concentrations of WV, mixed with biochar and zeolite, on GHG emissions, nitrogen loss and compost maturity, which is increasingly important as the need for sustainable development goals (SDG). Despite the late start of research into oil palm WV, an article entitled "Antifungal and antitermitic activities of wood vinegar from oil palm trunk" (Oramahi *et al.*, 2018) received the most citations in 2018 (46). This demonstrates that interest in oil palm WV is encouraging given that eliminating biological damage is one of the key objectives of the wood protection industry and oil palm WV has benefits as a low-impact technology.

More than 60 articles were published in 1996, probably because wood preservatives began to attract significant attention outside the United States. It was first available in European countries such as Germany, Austria, Sweden, Finland and the United Kingdom. However, there was a significant decrease in overall citations between 2021 and 2022 (from 1,279 to 203). The decrease could be attributed to the rise in publications that focused on environmentally friendly and sustainable wood preservation methods. Compared to other forms of literature, wood preservatives, WV and oil palm WV were most frequently discovered in journal articles. Top-ranking journals from prominent English-language publishers, including Forest Products Society, Springer Nature, North Carolina University, Walter de Gruyter and Elsevier, published the three most popular source titles. All of these publishers had a distinguished history and track record in the publishing industry. The wood preservatives documentations were likewise mostly written in English, despite being also published in other languages.

This article aimed to clarify the most often discussed wood preservatives topics among academics. From the VOSviewer results, it is possible to see the conclusions from the analysis of the keywords, titles, and abstracts. The most common keywords used by researchers were "wood preservation," "wood," "wood preservatives," "wood protection," and "antifungal activity," which denoted the primary subject areas. These terminologies were closely related to one another in the field of wood protectives, showing that they served a vital purpose and might act as a solid starting point for more investigations in this field.

Figure 7. VOSviewer visualisation of a term co-occurrence network based on title and abstract fields.

Wood preservation being the main keyword, is consistent with other findings in this study, such as the most cited articles (*Table 8*) and the most active source titles (*Table 9*). These publications were on wood degradation, wood treated with chemicals like zinc oxide, and the removal of pollutants such as copper, chromium, and arsenic from CCA treated wood.

Chemicals assessment was, in fact, the most frequently cited source in wood preservatives study. This may help other researchers determine the prevalent keyword in the wood preservatives study, which corresponds to the significance of this topic in the wood preservatives domain. In response to the third research question, an examination of countries, institutions, authors, and citations suggested that there was a reasonable amount of scientific collaboration on wood preservatives research worldwide. Although the wood preservatives industry was established in the United States, scientific articles have been widely spread in South America, Europe, Oceania and Asia. Consequently, despite its beginnings in the United States, the framework has global applicability. This study found that most papers on wood preservatives were published in the United States, indicating that it was at the forefront of wood preservatives research at the time. This may be because the United States began research and publication on wood preservatives in 1913. In addition, the majority were in English, German, Chinese, Portuguese, Japanese, Korean, Spanish and French. Based on the variety of languages used and the situations in which they were employed, it was anticipated that the publication rate would also increase. The reputations of the three American institutions including among the most active research institutions in the field of wood preservatives were also indicated.

Wood treatment is the main focus of wood preservatives after an extensive analysis of the industry's major players, including leading researchers and institutions. Publications on wood treatment generated a lot of attention and citations from other academics, and their impact has grown. It is necessary to analyse research collaboration to comprehend how academics work together. This can give insight into clustered research among authors from a given region, which can subsequently be used to rationalise and stimulate new researchers among authors from deprived areas. This study could determine the countries with the most active research collaborations through co-authorship analyses. These included the United States, India, Australia, South Korea, Japan, and Indonesia. However, collaboration in wood preservatives research across Africa was limited.

CONCLUSION

Study on wood preservatives was analysed in terms of its publication history, citation structure, and central themes, and recommendations for future studies are provided. The increase in the number of publications outside the United States, such as in Europe, Oceania and Asia, indicated that researches on wood preservatives were widely spread and had a substantial effect. A bibliometric approach was used in this study to present the data obtained from the Scopus database, which included quantity, quality, and structural map (*i.e.*, the number of publications by year, document types, languages, keyword analysis, most active source titles, countries with the most contributions towards wood preservatives research, most active institutions, number of citations and citation metrics). It should be noted that the research was restricted to the Scopus database and was based on the desired keywords used in the titles of the documents. Other significant and comprehensive databases that covered wood preservatives, such as the Web of Science, Google Scholar, and EBSCO Hosts, were not taken into account in this study. Thus, the overall results of the wood preservatives publishing patterns could be limited. In the future, researchers may use a variety of databases to search, sift through,

and compare search results using a variety of keyword terms to determine how research on wood preservatives varied by study theme. This study summarises the current state of knowledge on wood preservatives and provides information on rising journal performance trends, collaborative patterns, and research features that support in understanding. Each characteristic contributed to the expansion of this field of study, which could result in new possibilities for expanding wood technology systems. In addition, this will aid young researchers in gaining a wider view of this topic. This study contributes further by applying the bibliometric method to enhance academics' understanding of the literature on wood preservatives. The bibliometric method will continue to be a vital tool for detecting gaps in any subject or field. As a result, researchers can employ the method when reviewing literature on a particular subject. The results of this study will help researchers comprehend the reasons behind the widespread use of wood preservatives in the fields of materials science, agriculture, and biological science. They will also provide ideas for further research. Due to its widespread use in wood treatment across the globe and that it is now well-liked among European nations like Germany, Sweden, Finland, France, Poland, Slovenia, Spain, and Italy, which are actively producing publications related to wood preservatives, wood preservatives are predicted to continue to be relevant for the next 10 years. This shows that its appeal is expanding and that it is being used more frequently globally.

ACKNOWLEDGEMENT

The authors thank the Director-General of MPOB for permission to publish this work.

REFERENCES

Adhikari, S., & Ozarska, B. (2018). Minimizing environmental impacts of timber products through the production process "From Sawmill to Final Products." *Environmental Systems Research*, *7*(1). https://doi.org/10.1186/s40068-018-0109-x

Aguayo, M. G., Erazo, O., Montero, C., Reyes, L., Gacitúa, W., Gómez, L., & Torres, H. (2022). Analyses of impregnation quality and mechanical properties of radiata pine wood treated with copper nanoparticle- and micronized-copper-based wood preservatives. *Forests*, *13*(10), 1636. https://doi.org/10.3390/f13101636

Ahmed, S., Fatima, R., & Hassan, B. (2020). Evaluation of different plant derived oils as wood preservatives against subterranean termite *Odontotermes obesus*. *Maderas. Ciencia Y Tecnología*, *22*(1), 109–120.

Ariffin, S. J., Yahayu, M., El-Enshasy, H., Malek, R. A., Aziz, A. A., Hashim, N. M., & Zakaria, Z. A. (2017). Optimization of pyroligneous acid production from palm kernel shell and its potential antibacterial and antibiofilm activities. *Indian Journal of Experimental Biology*, *55*(7), 427–435.

Bahmani, M., & Schmidt, O. (2018). Plant essential oils for environment-friendly protection of wood objects against fungi. *Maderas, Ciencia Y Tecnología*, *20*(3), 325–332.

Baldrian, P. (2003). Interactions of heavy metals with white-rot fungi. *Enzyme and Microbial Technology*, *32*(1), 78–91. https://doi.org/10.1016/s0141-0229(02)00245-4

Barbero-López, A., Akkanen, J., Lappalainen, R., Peräniemi, S., & Haapala, A. (2020). Bio-based wood preservatives: Their efficiency, leaching and ecotoxicity compared to a commercial wood preservative. *The Science of the Total Environment*, *753*, 142013. https://doi.org/10.1016/j.scitotenv.2020.142013

Barceloux, D. G. (1999). Chromium. *Journal of Toxicology Clinical Toxicology*, *37*(2), 173–194. https://doi.org/10.1081/clt-100102418

Bayatkashkoli, A., Kameshki, B., Ravan, S., & Shamsian, M. (2017). Comparing of performance of treated particleboard with alkaline copper quat, boron-fluorine-chromium-arsenic and Chlorotalonil against *Microcerotermes diversus* and *Anacanthotermes vagans* termite. *International Biodeterioration & Biodegradation*, *120*, 186–191. https://doi.org/10.1016/j.ibiod.2017.03.003

Bernard Effah, S. A. G. A. (2015). Safety measures in wood processing: An important component for the entrepreneur – The case of a local furniture industry in Ghana. *International Journal of Innovative Research in Science Engineering and Technology*, *04*(05), 2677–2686. https://doi.org/10.15680/ijirset.2015.0405004

Broda, M. (2020). Natural compounds for wood protection against fungi – A review. *Molecules*, *25*(15), 3538. https://doi.org/10.3390/molecules25153538

Cai, L., Lim, H., Kim, Y., & Jeremic, D. (2020). β-Cyclodextrin-allyl isothiocyanate complex as a natural preservative for strand-based wood

composites. *Composites Part B Engineering*, *193*, 108037. https://doi.org/10.1016/j.compositesb.2020.108037

Calegari, E. P., Porto, J. S., Nejeliski, D. M., Da Cunha Duarte, L., & De Oliveira, B. F. (2017). Experimental study on waterproofing MDF with castor oil-based vegetal polyurethane. *Matéria (Rio De Janeiro)*, *22*(3). https://doi.org/10.1590/s1517-707620170003.0211

Chang, H., Tu, K., Wang, X., and Liu, J. (2015). Facile preparation of stable superhydrophobic coatings on wood surfaces using silica-polymer nanocomposites. *BioResources. 10*(2), 2585-2596.

Chen, C., Chen, J., Zhang, S., Cao, J., & Wang, W. (2020). Forming textured hydrophobic surface coatings via mixed wax emulsion impregnation and drying of poplar wood. *Wood Science and Technology*, *54*(2), 421–439. https://doi.org/10.1007/s00226-020-01156-7

Desvita, H., Faisal, M., Mahidin, N., & Suhendrayatna, N. (2022). Antimicrobial potential of wood vinegar from cocoa pod shells (*Theobroma cacao* L.) against *Candida albicans* and *Aspergillus niger*. *Materials Today Proceedings*, *63*, S210–S213. https://doi.org/10.1016/j.matpr.2022.02.410

Donthu, N., Kumar, S., Mukherjee, D., Pandey, N., & Lim, W. M. (2021). How to conduct a bibliometric analysis: An overview and guidelines. *Journal of Business Research*, *133*, 285–296. https://doi.org/10.1016/j.jbusres.2021.04.070

Engwall, M. A., Pignatello, J. J., & Grasso, D. (1999). Degradation and detoxification of the wood preservatives creosote and pentachlorophenol in water by the photo-Fenton reaction. *Water Research*, *33*(5), 1151–1158. https://doi.org/10.1016/s0043-1354(98)00323-6

Freeman, M. H., Shupe, T. F., Vlosky, R. P., & Barnes, H. M. (2003). Past, present, and future of the wood preservation industry. *Forest Products Journal, 53*(10), 8–15.

Hill, C. A. S. (2006). *Wood modification: Chemical, thermal and other processes*. John Wiley and Sons, Ltd.

Hingston, J., Collins, C., Murphy, R., & Lester, J. (2001). Leaching of chromated copper arsenate wood preservatives: A review. *Environmental Pollution*, *111*(1), 53–66. https://doi.org/10.1016/s0269-7491(00)00030-0

Holley, R. A., & Patel, D. (2005). Improvement in shelf-life and safety of perishable foods by plant essential oils and smoke antimicrobials. *Food Microbiology*, *22*(4), 273–292. https://doi.org/10.1016/j.fm.2004.08.006

Jin, W., Pastor-Pérez, L., Yu, J., Odriozola, J., Gu, S., & Reina, T. (2020). Cost-effective routes for catalytic biomass upgrading. *Current Opinion in Green and Sustainable Chemistry*, *23*, 1–9. https://doi.org/10.1016/j.cogsc.2019.12.008

Jung, M., Hong, J., Lee, K., Jo, C., Kim, Y., & Choi, J. (2016). Fungal inhibitory effect of *Pinus densiflora* and *Zelkova serrata* woods with wood-vinegar. *Journal of Korea Technical Association of the Pulp and Paper Industry*, *48*(5), 13–21. https://doi.org/10.7584/jktappi.2016.10.48.5.13

Khademibami, L., & Bobadilha, G. S. (2022). Recent developments studies on wood protection research in academia: A review. *Frontiers in Forests and Global Change*, *5*. https://doi.org/10.3389/ffgc.2022.793177

Lazim, A. M., Azfaralariff, A., Azman, I., Arip, M. N. M., Zubairi, S., Kaus, N. M., Nazir, N., Mohamad, M., Kamil, A., Azzahari, A. D., Abdullah, A., & Ariff, A. Z. (2020). Improving wood durability against *G. Trabeum* and *C. versicolor* using starch based antifungal coating from *Dioscorea hispida* sp. *Journal of the Taiwan Institute of Chemical Engineers*, *115*, 242–250. https://doi.org/10.1016/j.jtice.2020.10.002

Lebow, S., Brooks, K., & Simonsen, J. (2002). *Environmental impact of treated wood in service*. U.S. Department of Agriculture, Forest Service, Forest Products Laboratory. https://www.fpl.fs.usda.gov/documnts/pdf2002/lebow02a.pdf

Lee, C. L., Chin, K. L., Khoo, P. S., Hafizuddin, M. S., & H'ng, P. S. (2022). Production and potential application of pyroligneous acids from rubberwood and oil palm trunk as wood preservatives through vacuum-pressure impregnation treatment. *Polymers*, *14*(18), 3863. https://doi.org/10.3390/polym14183863

Lee, S. H., Zaidon, A., Rasdianah, D., Lum, W. C., & Aisyah, H. A. (2020). Alteration in colour and fungal resistance of thermally treated oil palm trunk and rubberwood particleboard using palm oil. *Journal of Oil Palm Research, 32*(1), 83–89. https://doi.org/10.21894/jopr.2020.0009

Li, T., Cui, L., Song, X., Cui, X., Wei, Y., Tang, L., Mu, Y., & Xu, Z. (2022). Wood decay fungi: An analysis of worldwide research. *Journal of Soils*

and Sediments, *22*(6), 1688–1702. https://doi.org/10.1007/s11368-022-03225-9

Lin, L., Chen, Y., Wang, S., & Tsai, M. (2009). Leachability, metal corrosion, and termite resistance of wood treated with copper-based preservative. *International Biodeterioration & Biodegradation*, *63*(4), 533–538. https://doi.org/10.1016/j.ibiod.2008.07.012

Liu, X., Zhan, Y., Li, X., Li, Y., Feng, X., Bagavathiannan, M., Zhang, C., Qu, M., & Yu, J. (2021). The use of wood vinegar as a non-synthetic herbicide for control of broadleaf weeds. *Industrial Crops and Products*, *173*, 114105. https://doi.org/10.1016/j.indcrop.2021.114105

Ma, Y., Prasad, M., Rajkumar, M., & Freitas, H. (2011). Plant growth promoting rhizobacteria and endophytes accelerate phytoremediation of metalliferous soils. *Biotechnology Advances*, *29*(2), 248–258. https://doi.org/10.1016/j.biotechadv.2010.12.001

Maier, D. (2021). Building materials made of wood waste a solution to achieve the sustainable development goals. *Materials*, *14*(24), 7638. https://doi.org/10.3390/ma14247638

Mansour, A. Z., Ahmi, A., Popoola, O. M. J., & Znaimat, A. (2022). Discovering the global landscape of fraud detection studies: A bibliometric review. *Journal of Financial Crime*, *29*(2), 701–720. https://doi.org/10.1108/jfc-03-2021-0052

Martín, J. A., & López, R. (2023). Biological deterioration and natural durability of wood in Europe. *Forests*, *14*(2), 283. https://doi.org/10.3390/f14020283

Meena, R. K. (2022). Hazardous effect of chemical wood preservatives on environmental conditions, ecological biodiversity and human being and its alternatives through different botanicals: A review. *Environment and Ecology*, *40*(3), 1137–1143.

Mohamad Amini, M. H. M., Hashim, R., & Sulaiman, N. S. (2019). Formaldehyde-free wood composite fabricated using oil palm starch modified with glutardialdehyde as the binder. *International Journal of Chemical Engineering*, *2019*, 1–9. https://doi.org/10.1155/2019/5357890

Moral-Muñoz, J. A., Herrera-Viedma, E., Santisteban-Espejo, A., & Cobo, M. J. (2020). Software tools for conducting bibliometric analysis in science: An up-to-date review. *El Profesional De La Informacion*, *29*(1). https://doi.org/10.3145/epi.2020.ene.03

Muhuri, P. K., Shukla, A. K., & Abraham, A. (2019). Industry 4.0: A bibliometric analysis and detailed overview. *Engineering Applications of Artificial Intelligence*, *78*, 218–235. https://doi.org/10.1016/j.engappai.2018.11.007

Nadali, E., Tajvidi, M., & Naghdi, R. (2021). Effects of fungal biodegradation on structure-property relationships of medium density fibre board and hybrid polypropylene composite made from sugar-cane residue. *International Wood Products Journal*, *12*(3), 152–163. https://doi.org/10.1080/20426445.2021.1910169

Nordin, N., Khatibi, A., & Azam, S. M. F. (2022). Nonprofit capacity and social performance: Mapping the field and future directions. *Management Review Quarterly*, *74*(1), 171–225. https://doi.org/10.1007/s11301-022-00297-2

Oramahi, H. A., Wardoyo, E. R. P., & Kustiati, N. (2019). Optimization of pyrolysis condition for bioactive compounds of wood vinegar from oil palm empty bunches using response surface methodology (RSM). *IOP Conference Series Materials Science and Engineering*, *633*(1), 012058. https://doi.org/10.1088/1757-899x/633/1/012058

Oramahi, H. A., Yoshimura, T., Diba, F., Setyawati, D., & Nurhaida, N. (2018). Antifungal and antitermitic activities of wood vinegar from oil palm trunk. *Journal of Wood Science*, *64*(3), 311–317. https://doi.org/10.1007/s10086-018-1703-2

Pambudi, N. A., Itaoka, K., Chapman, A., Hoa, N. D., & Yamakawa, N. (2017). Biomass energy in Japan: Current status and future potential. *International Journal of Smart Grid and Clean Energy*, *6*(2), 119–126. https://doi.org/10.12720/sgce.6.2.119-126

Pařil, P., Baar, J., Čermák, P., Rademacher, P., Prucek, R., Sivera, M., & Panáček, A. (2017). Antifungal effects of copper and silver nanoparticles against white and brown-rot fungi. *Journal of Materials Science*, *52*(5), 2720–2729. https://doi.org/10.1007/s10853-016-0565-5

Pędzik, M., Janiszewska, D., & Rogoziński, T. (2021). Alternative lignocellulosic raw materials in particleboard production: A review. *Industrial Crops and Products*, *174*, 114162. https://doi.org/10.1016/j.indcrop.2021.114162

Petrič, M., Murphy, R. J., & Morris, I. (2000). Microdistribution of some copper and zinc containing waterborne and organic solvent wood preservatives in spruce wood cell walls. *Holzforschung*, *54*(1), 23–26. https://doi.org/10.1515/hf.2000.004

Pointing, S. B. (2001). Feasibility of bioremediation by white-rot fungi. *Applied Microbiology and Biotechnology*, *57*(1–2), 20–33. https://doi.org/10.1007/s002530100745

Pour, M. F., Mehdinia, M., Kiamahalleh, M. V., Hoseini, K. D., Hatefnia, H., & Dorieh, A. (2021). Biological durability of particleboard: Fungicidal properties of Ag and Cu nanoparticles against *Trametes versicolor* white-rot fungus. *Wood Material Science and Engineering*, *17*(6), 929–936. https://doi.org/10.1080/17480272.2021.1977996

Sandberg, D., Kutnar, A., & Mantanis, G. (2017). Wood modification technologies – A review. *iForest – Biogeosciences and Forestry*, *10*(6), 895–908. https://doi.org/10.3832/ifor2380-010

Seidler, A., Hellenbrand, W., Robra, B., Vieregge, P., Nischan, P., Joerg, J., Oertel, W. H., Ulm, G., & Schneider, E. (1996). Possible environmental, occupational, and other etiologic factors for Parkinson's disease. *Neurology*, *46*(5), 1275. https://doi.org/10.1212/wnl.46.5.1275

Smith, S. T. (2020). Water-borne wood preservation and end-of-life removal history and projection. *Engineering*, *12*(02), 117–139. https://doi.org/10.4236/eng.2020.122011

Sophia, A. C., & Lima, E. C. (2018). Removal of emerging contaminants from the environment by adsorption. *Ecotoxicology and Environmental Safety*, *150*, 1–17. https://doi.org/10.1016/j.ecoenv.2017.12.026

Sun, W., Tajvidi, M., Hunt, C. G., Cole, B. J., Howell, C., Gardner, D. J., & Wang, J. (2022). Fungal and enzymatic pretreatments in hot-pressed lignocellulosic bio-composites: A critical review. *Journal of Cleaner Production*, *353*, 131659. https://doi.org/10.1016/j.jclepro.2022.131659

Teaca, C.-A., Roşu, D., Mustaţă, F., Rusu, T., Roşu, L., Roşca, I., & Varganici, C. D. (2019). Natural bio-based products for wood coating and protection against degradation: A Review. *BioResources*, *14*(2), 4873–4901.

Teng, T.-J., Mat Arip, M. N., Sudesh, K., Nemoikina, A., Jalaludin, Z., Ng, E.-P., & Lee, H.-L. (2018). Conventional technology and nanotechnology in wood preservation: A Review. *BioResources*, *13*(4), 9220–9252.

The Business Research Company. (2022). *Wood products global market report 2022*. Retrieved June 9, 2023, from https://www.thebusinessresearchcompany.com/report/wood-products-market

Van Eck, N. J., & Waltman, L. (2010). Software survey: VOSviewer, a computer program for bibliometric mapping. *Scientometrics*, *84*(2), 523–538. https://doi.org/10.1007/s11192-009-0146-3

Wang, S., & Mulligan, C. N. (2006). Occurrence of arsenic contamination in Canada: Sources, behavior and distribution. *The Science of the Total Environment*, *366*(2–3), 701–721. https://doi.org/10.1016/j.scitotenv.2005.09.005

Yan, L., Zeng, F., Chen, Z., Chen, S., & Lei, Y. (2020). Improvement of wood decay resistance by salicylic acid/silica microcapsule: Effects on the salicylic leaching, microscopic structure and decay resistance. *International Biodeterioration & Biodegradation*, *156*, 105134. https://doi.org/10.1016/j.ibiod.2020.105134

Zhang, F., Shao, J., Yang, H., Guo, D., Chen, Z., Zhang, S., & Chen, H. (2019). Effects of biomass pyrolysis derived wood vinegar on microbial activity and communities of activated sludge. *Bioresource Technology*, *279*, 252–261. https://doi.org/10.1016/j.biortech.2019.01.133

Zhang, W., Sun, H., Zhu, C., Wan, K., Zhang, Y., Fang, Z., & Ai, Z. (2018). Mechanical and water-resistant properties of rice straw fiberboard bonded with chemically-modified soy protein adhesive. *RSC Advances*, *8*(27), 15188–15195. https://doi.org/10.1039/c7ra12875d

Journal of Oil Palm Research Vol. 37 (3) September 2025 p. 397-420
DOI: https://doi.org/10.21894/jopr.2024.0033

ENHANCING CORROSION RESISTANCE IN BIODIESEL DISTRIBUTION AND TERMINAL OPERATIONS: A COMPREHENSIVE MATERIALS COMPATIBILITY REVIEW

NUR NAQIUDDIN MDD NORDIN[1]*; MOHD NASHRUL MOHD ZUBIR[1]*; SALIM NEWAZ KAZI[1] and NURIN WAHIDAH MOHD ZULKIFLI[1]

ABSTRACT

The viability of integrating biodiesel as a renewable energy source in land and maritime transport systems is promising, given its compatibility with extant fossil fuel infrastructures. However, the corrosivity of biodiesel towards metallic components in fuel distribution and storage facilities has emerged as a critical concern. This study conducts a comprehensive evaluation of the corrosion behaviour of metals in contact with biodiesel, elucidating the underlying mechanisms driving this phenomenon from the perspective of biodiesel processing and storage facilities. It further assesses methodologies for corrosion quantification and investigates the comparative corrosiveness of biodiesel relative to traditional diesel. Contributing factors such as biodiesel's affinity for moisture, the presence of oxygen, the potential for microbial proliferation and the production of corrosive by-products through auto-oxidation are critically analysed. This article aims to provide a comprehensive overview of the current state of research concerning the compatibility of biodiesel with its processing and storage infrastructure, emphasising the role of fibre-reinforced polymer (FRP) as both a corrosion barrier and a means of mechanical reinforcement.

Keywords: biofuel, biodiesel corrosion, fuel distribution, polymeric materials, terminal operations.

Received: 9 November 2023**; Accepted:** 7 March 2024**; Published online:** 27 May 2024.

INTRODUCTION

The rapid depletion of fossil fuel reserves, driven by population growth, poses a significant challenge to the transportation and utility sectors, impacting energy demand. This situation, coupled with the fact that the transportation industry alone contributes 20% of global energy supply in the form of greenhouse gas (GHG) emissions (Chandran, 2020), presents a grave environmental threat. Stricter emission standards have been implemented, but their effectiveness is offset by the growing global vehicle traffic. Moreover, the refining of fossil fuels contributes to air quality degradation. As industrialisation and population growth continue, the energy demand will escalate, further deteriorating air quality. Considering these pressing concerns, researchers have explored alternative fuels that can coexist with sustainable development, energy conversion, efficiency and environmental preservation. Among the viable options, biodiesel stands out as a promising fuel that fulfils all the requirements. The Malaysian government, represented by the Malaysian Palm Oil Board (MPOB), has reaffirmed its dedication to achieving carbon neutrality by 2050. A crucial aspect of this effort will be the prominent role played by biodiesel. In a study conducted by Parveez *et al.* (2021), it was revealed that in 2020, Malaysia boasted a total of 20 operational oleochemical plants and 19 biodiesel plants. These facilities showcased impressive processing capacities, with the oleochemical plants capable of handling 2.63 million tonnes, and the biodiesel plants with a capacity of 2.23 million tonnes. To provide an overview, *Table 1* presents a

[1] Department of Mechanical Engineering, Faculty of Engineering, University of Malaya, 50603 Kuala Lumpur, Malaysia.

* *Corresponding author e-mail: s2151766@siswa.um.edu.my; nashrul@um.edu.my*

comparison of biofuel implementation, future targets and the relevant standards. Additionally, *Table 2* highlights conventional fuel and its biofuel counterparts.

The EURO emissions standards, implemented to reduce harmful pollutants from vehicles, particularly diesel engines in the transportation industry, have set limits for nitrogen oxides (NO_x), particulate matter (PM) and hydrocarbons (HC) emissions to reduce PM emissions, diesel particulate filters (DPF) were also required. EURO 6, which became mandatory for new vehicles in September 2014, is an even stricter standard that limits NO_x and PM emissions even further. Furthermore, EURO 6 mandated real-world emission testing to better reflect the actual emissions of vehicles on the road. These emissions standards have been implemented globally, with many countries requiring new vehicles sold within their borders to meet these standards. The implementation of EURO 5 and EURO 6 has resulted in significant improvements in air quality in many cities, particularly those with high levels of diesel engine usage. The standards, however, have been criticised, with some claiming that they do not go far enough to address the issue of air pollution. Concerns have also been expressed about the accuracy of real-world testing and manufacturers' ability to manipulate test results. *Figure 1* depicts the changes in sulphur content requirements over time because of different implementations of EURO standards. The comparison of biofuel implementation, its future goal, and the implementation standard is presented in *Table 1*. Biodiesel can be derived from various feedstocks, including vegetable oils and animal fats, and is typically categorised as mono-alkyl esters of long-chain fatty acids. These mono-alkyl esters endow biodiesel with diesel-like properties. Biodiesel has the potential to be utilised in contemporary diesel engines, either in its undiluted state as B100 or in combination with petroleum diesel, thereby creating a blend known as a diesel-biodiesel mixture (Fazal *et al*., 2011). The transesterification process, converting vegetable or animal oil into biodiesel, has emerged as a viable renewable fuel option for diesel-powered vehicles. Numerous studies have proposed physical models to optimise the biodiesel transesterification process. The distinct advantages of biodiesel over conventional diesel, including its seamless adoption without significant engine modifications and its versatility in utilising a wide range of feedstocks, have positioned biodiesel as an appealing alternative. Corrosion and degradation issues continue to plague biodiesel utilisation. Biodiesel has a lower storage stability due to its sensitivity to oxygen. Several derivatives are formed during biodiesel oxidation due to degradation, which may be emitted (Fazal *et al*., 2011).

Biodiesel is widely recognised for its higher corrosiveness compared to fossil-based automotive diesel fuel. While studies have been conducted to investigate biodiesel corrosion and degradation in automotive diesel engine parts, research exploring biodiesel's corrosion behaviour in fuel distribution and terminal operations (DTO) remains limited. Additionally, the potential use of nonmetallic materials, whether fully nonmetallic or metallic structures with nonmetallic coatings or linings, to enhance corrosion resistance and serve as reinforcement layers in these structures and components has not been thoroughly explored. The objective of this article is to conduct a literature review on the compatibility of various metallic and nonmetallic materials in biodiesel distribution and terminal operations, emphasising their potential to improve corrosion resistance.

Extensive research has been conducted on the utilisation of biodiesel as a substitute for traditional diesel fuel, resulting in a thorough comprehension of its merits and drawbacks (Aatola *et al*., 2009; Chevron Coorporation, 2007; Fazal *et al*., 2012; Gunstone, 2004; Samuel & Gulum, 2019). Biodiesel offers the potential to reduce crude oil imports, and its use can lead to sulphur deficiency and lower CO_2 emissions throughout its life cycle. Biodiesel offers several superior properties compared to diesel fuel, including a higher cetane number, flash point, lubricity and oxygen content, facilitating cleaner combustion. Furthermore, it is biodegradable, non-toxic and environmentally friendly when combined with petroleum diesel fuel. However, biodiesel's degradation-prone nature renders it more corrosive than traditional diesel, leading to material failure and the formation of sludge and microbial growth. Despite these benefits, challenges hinder the widespread adoption of biodiesel. The high cost, concerns regarding food competition, deforestation for oil crop plantations, and issues such as clogged fuel filters and injector fouling pose significant obstacles. Additionally, biodiesel exhibits lower oxidative stability, resulting in increased vulnerability to fuel oxidation. Its lower heating value translates to reduced torque and power, while oxidative instability, poor low-temperature properties, and solvent-like characteristics further contribute to its unfavourable properties. This article aims to conduct a comprehensive literature review on the compatibility of metallic and nonmetallic materials in biodiesel distribution and terminal operations, with a focus on improving corrosion resistance. The urgency of sustainable energy solutions is discussed in the light of fossil fuel depletion and greenhouse gas emissions. The focus is placed on biodiesel as a viable alternative. Its production, properties, and the challenges associated with its use, particularly regarding material compatibility

and corrosion, are examined. The aim of this article is to provide a comprehensive review of the literature on the suitability of various materials in biodiesel environments. This review encompasses both metallic and nonmetallic materials, emphasising the enhancement of corrosion resistance and sustainability in biodiesel-powered systems.

OVERVIEW OF THE FUEL DISTRIBUTION AND TERMINAL OPERATIONS

Biodiesel fuel is transported from production facilities to end-users through various means, including trucks, marine vessels, and pipelines. The transportation of biodiesel fuel presents unique challenges due to the potential for contamination, especially when transporting higher blends of biodiesel. Biodiesel is hygroscopic, enabling water absorption from the air, which, in turn, creates an environment for microorganisms to thrive and cause biodiesel degradation. In fuel DTO, biodiesel encounters a wide array of materials, categorised as metallic and nonmetallic. Metallic materials can corrode when exposed to biodiesel due to chemical and electrochemical factors. The primary objective of this review article is to investigate the corrosion and degradation phenomena of nonmetallic materials in biodiesel blending systems. Among the various nonmetallic materials, polymers have been frequently utilised and have been observed to undergo degradation when exposed to biodiesel. The article provides a comprehensive review of corrosion and degradation mechanisms involving various materials in biodiesel blending systems. The study also examines the effectiveness of various protective measures aimed at mitigating corrosion and degradation in biodiesel blending systems. Through a detailed analysis of the available literature, this article aims to provide valuable insights into the challenges associated with the use of nonmetallic materials in biodiesel blending systems and to inform future research aimed at enhancing the compatibility of nonmetallic materials with biodiesel. *Figure 2* illustrate the overall automotive diesel oil (ADO) and palm oil methyl ester (PME) distribution and terminal operation from the feedstock until the fueling station.

During storage, biodiesel fuel must be kept in tanks that are free of water, which can lead to the development of microbial growth and the formation of corrosive byproducts. The microbiologically induced corrosion (MIC) of storage tanks and associated equipment is a serious issue in the biodiesel industry that can lead to equipment failure, product loss, and safety hazards. Effective corrosion mitigation strategies are critical for ensuring the safe and reliable storage and distribution of biodiesel fuel. These strategies can include the use of corrosion-resistant materials, protective coatings, and biocides. The use of fibre-reinforced polymer (FRP) materials has emerged as a promising solution to mitigate corrosion in biodiesel storage tanks. Among the various FRP materials, glass fibre reinforced

TABLE 1. THE COMPARISON OF BIOFUEL IMPLEMENTATION, FUTURE TARGET AND THE STANDARD USED IN THE IMPLEMENTATION

Nations	Main source	Current utilisation	Future target	Standard
United States	Corn, soybean	E10, B5-B20	E20	Renewable Fuel Standard (RFS)
Brazil	Sugarcane	E27, B8	B10	National Program for the Production and Use of Biodiesel (PNPB)
Indonesia	Palm oil	B30	B40	National Energy Policy (NEP)
India	Sugarcane	E10	E20	National Biofuel Policy (NBP)
European Union	Rapeseed	E10, B5.75	B10	EN16709
China		E10		Blended Gasoline: GB 18351-2017 and Bioethanol: GB/T 22030-2008
Malaysia	Palm oil	B7, B10	B20	Blended Gasoil: MS 123-5:2020 and Biodiesel: MS 2008:2014

Source: Chandran (2020).

TABLE 2. THE CONVENTIONAL FUEL AND ITS BIOFUEL COUNTERPARTS

Conventional Fuel	Biofuel	Main source	Maximum utilisation
Petrol	Bioethanol	Corn, soybean	E20
Diesel	Biodiesel	Sugarcane, palm oil	B30
Kerosene	Sustainable Aviation Fuel (SAF)	Palm oil	SAF50

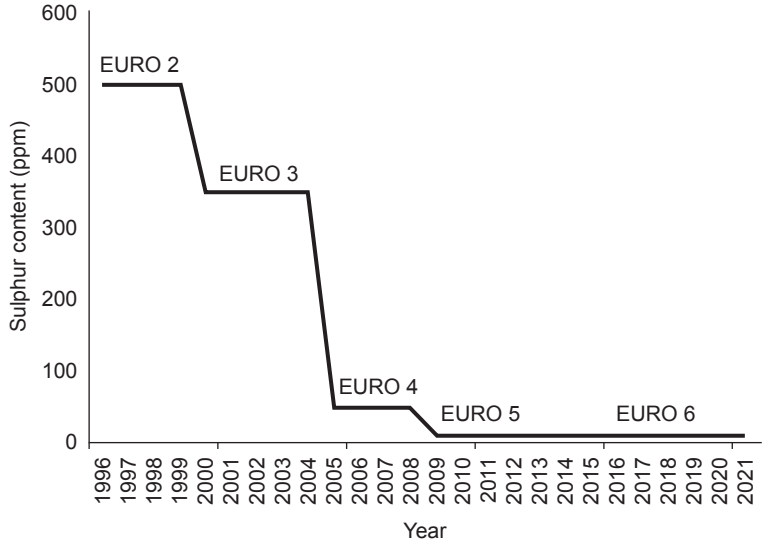

Figure 1. Requirement of sulphur content for diesel – EURO.

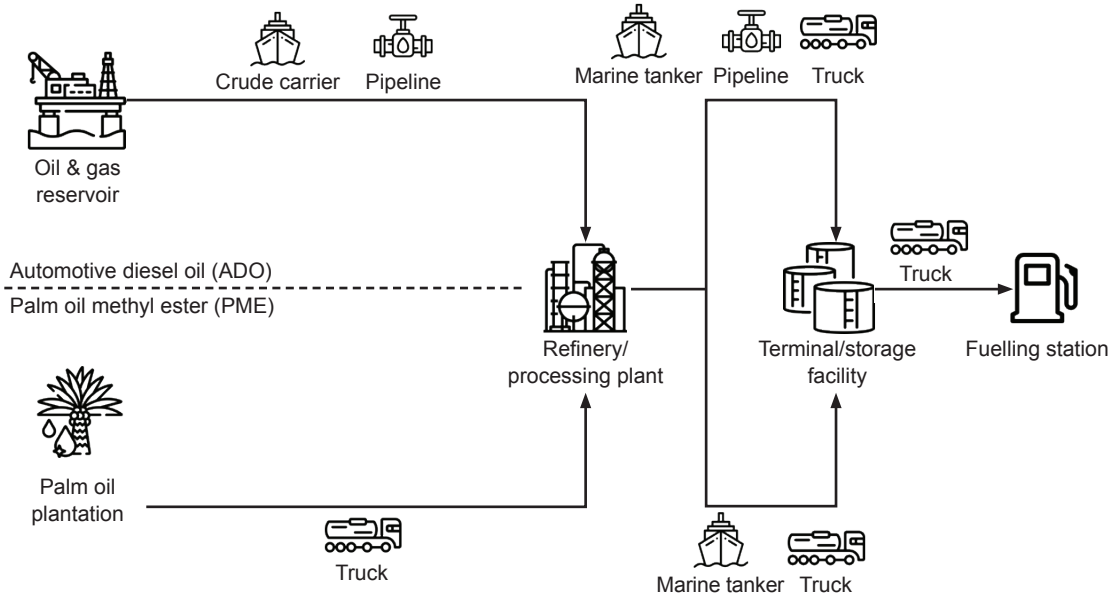

Figure 2. The overview of automotive diesel oil (ADO) and palm oil methyl ester (PME) distribution and terminal operations.

polymer (GFRP) has gained widespread popularity due to its excellent mechanical strength and resistance to corrosion. GFRP has been shown to be particularly effective in resisting the aggressive corrosion mechanisms prevalent in biodiesel storage systems, which can cause significant damage and failure of conventional metallic materials. In addition to the challenges associated with transportation and storage, blending biodiesel with petroleum diesel also presents unique challenges due to differences in physical and chemical properties. Biodiesel blends can be used in conventional diesel engines without modification, but higher blends may require engine modifications or the use of special fuel systems. Overall, the distribution of biodiesel fuel involves several stages, including transportation, storage, blending, and terminal operations. Effective corrosion mitigation strategies are critical for ensuring the safety of reliable storage and distribution of biodiesel fuel and for addressing the challenges associated with microbiologically induced corrosion.

FUEL CHEMISTRY

Biodiesel fuel serves as a renewable alternative to petroleum diesel, produced from diverse feedstocks like vegetable oils, animal fats and used cooking oils. Palm oil is a commonly used feedstock, undergoing transesterification to convert it into a chemical compound known as methyl ester.

Methyl esters consist of a glycerol backbone and three fatty acid chains, including saturated and unsaturated fatty acids such as palmitic acid, oleic acid and linoleic acid. The chemical structure of palm oil methyl ester (PME) closely resembles that of petroleum diesel, with both molecules having long carbon chains typically ranging from 12-18 carbon atoms. The distinction lies in the ester structure of biodiesel. It is referred to as "fatty acid methyl ester" or FAME, denoting the methyl ester's presence beyond the oxygen atom. Biodiesel exhibits reduced viscosity and burns efficiently in diesel engines. Its ester-bound oxygen renders it less toxic and more biodegradable. Notably, the corrosion, oxidation and polymerisation characteristics of biodiesel are influenced by the ester-bound oxygen molecule.

Different feedstock oils may exhibit varying properties. Biodiesel differs from diesel in terms of raw materials and production processes (Fazal *et al*., 2012), as biodiesel is derived from renewable resources such as vegetable oils, waste cooking oil, and animal fats, whereas diesel is derived from crude oil. The production process of diesel involves three processes: Separation, upgrading and conversion, while biodiesel is produced through a single process called transesterification. The products and compositions of diesel and biodiesel are different (Gunstone, 2004). Diesel is mainly composed of carbon and hydrogen, with 81.0% saturated (paraffin and naphthenic) and 18.9% unsaturated (aromatics). On the other hand, biodiesel contains carbon, hydrogen, and oxygen, with varying compositions depending on the feedstock used. For instance, palm biodiesel comprises 81.0% saturated (palmitic and stearic) and 18.9% unsaturated (oleic, linoleic and linolenic) fatty acids, whereas rapeseed and soy biodiesel have a higher percentage of unsaturated fatty acids. These compositional differences between diesel and biodiesel can impact engine performance and emissions. Biodiesel typically exhibits a higher cetane number, flash point, and lubricity compared to diesel, resulting in cleaner combustion and reduced emissions of hydrocarbons and carbon monoxide. However, biodiesel's lower heating value can lead to decreased torque and power. Regarding environmental impact, biodiesel presents both advantages and disadvantages compared to diesel (Fazal *et al*., 2018). It utilises renewable resources, potentially lowering CO_2 emissions over its life cycle and reducing dependence on imported crude oil. It is also biodegradable, non-toxic and environmental-friendly when used with petroleum diesel fuel. Additionally, biodiesel is more prone to degradation, making it more corrosive than conventional diesel, which can lead to material failure, sludge formation, microbial growth and clogging of fuel filters and injectors. *Figure 3* demonstrates the molecular comparison between typical biodiesel and diesel molecules.

Despite the aforementioned benefits, important chemical composition disparities exist between biodiesel fuel and petroleum diesel. Biodiesel boasts a higher oxygen content and a lower carbon-to-hydrogen ratio, influencing combustion properties and emissions. It also exhibits a higher flash point, signifying the temperature at which the fuel ignites in the presence of an ignition source, compared to petroleum diesel. The production of palm oil biodiesel typically involves transesterification, wherein triglycerides in the oil react with an alcohol (*e.g*., methanol) in the presence of a catalyst (*e.g*., sodium hydroxide or potassium hydroxide). This reaction generates glycerol and FAME which are subsequently separated and purified. The process flowchart for PME production is outlined in the European Standard EN 14214:2012, which stipulates specifications for biodiesel fuel quality,

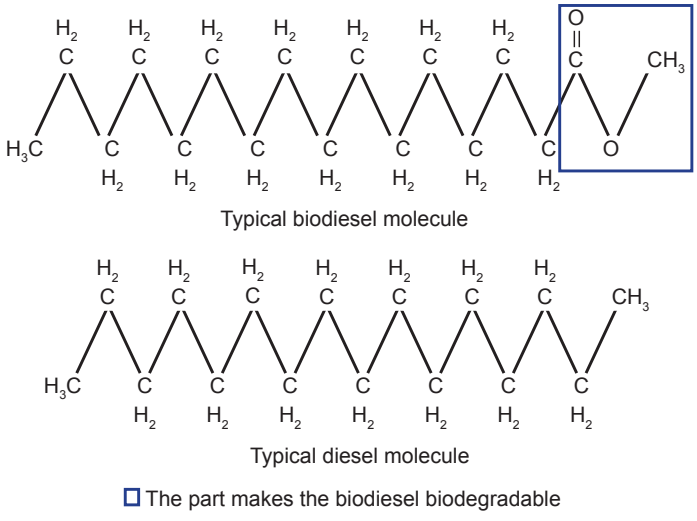

Figure 3. The molecular comparison between typical biodiesel and diesel molecules.

encompassing chemical composition, physical properties and performance characteristics such as flash point, viscosity and acid value. Biodiesel possesses advantages and disadvantages compared to petroleum diesel in terms of properties and processes. While biodiesel offers a renewable fuel source capable of reducing greenhouse gas emissions and diminishing reliance on petroleum-based fuels, it may entail higher costs and necessitate engine modifications or specialised fuel systems to accommodate its distinct properties.

Table 3 presents a comprehensive comparison of key properties between ultra-low sulphur diesel and soy biodiesel, following the standards set by the American Society for Testing and Materials (ASTM) (Fazal *et al*., 2012). *Table 4* illustrates the comparison of limit and codes quality tests of conventional ADO and the B100 PME. These properties play a crucial role in determining the performance of these fuels in various applications. Oxidation stability, for instance, influences the fuel's resistance to degradation over time. The higher heating value is a vital factor that determines the fuel's energy content, thereby affecting its efficiency in engines. Flash point, on the other hand, indicates the lowest temperature at which the fuel can vaporise and ignite in the presence of an ignition source, making it essential for safety considerations. Density at 15°C and viscosity at 40°C determine the fluidity of the fuel and its suitability for different applications. Sulphur content is a critical property, as it contributes to the formation of sulphur oxides during combustion, which have adverse effects on the environment and human health. Ultra-low sulphur diesel adheres to the ASTM D975 specification, containing less than 15 parts per million (ppm) of sulphur, while soy biodiesel complies with the ASTM D6751 specification, containing less than 10 ppm of sulphur. The cetane number, which measures the fuel's ignition quality and ability to start and run smoothly in diesel engines, is also provided. This table serves as a valuable resource, offering insightful information on the essential properties of ultra-low sulphur diesel and soy biodiesel, aiding researchers and industry professionals in making informed decisions regarding fuel choices and applications. *Figure 4* illustrates the typical process flowchart of PME in accordance with EN 14214:2012.

The quality of biodiesel stored in tanks made of carbon steel may be significantly impacted by corrosion of this material. As carbon steel corrodes, it can release iron oxide particles into the biodiesel, which can lead to the formation of insoluble sediments. These sediments can cause filter blockages, reduce fuel flow and lead to engine problems (Milano *et al*., 2021). Furthermore, corrosion can also promote the growth of microorganisms such as bacteria and fungi, which can degrade the quality of the biodiesel by breaking down the fatty acid chains that make up the fuel. Microbial-mediated hydrolysis of fatty acid chains has been identified as a significant process leading to the liberation of free fatty acids (FFA) within the biodiesel matrix. The present

TABLE 3. TYPICAL PROPERTIES OF ULTRA-LOW SULPHUR DIESEL (ASTM D975) AND SOY BIODIESEL (ASTM D6751)

Property	Ultra-low sulphur diesel (ASTM D975)	Soy biodiesel (ASTM D6751)
Oxidation stability (hr)	>40	<10
Higher heating value (kJ/kg)	42.7	40.6
Flash point (°C)	60	130
Density at 15°C (kg/m^3)	0.85	0.88
Viscosity at 40°C (mm^2/s)	2.6	6
Sulphur content	<15	<15
Cetane number	44	55

Source: Chevron Coorporation (2007).

TABLE 4. THE COMPARISON OF LIMIT AND CODES QUALITY TESTS OF AUTOMOTIVE DIESEL OIL (ADO) AND PALM OIL METHYL ESTER (PME)

Test	ADO	PME
Total acid number (mg KOH/g)	Max 0.25 ASTM D974	Max 0.5 EN 14104
Sulphated ash content (%)	Max 0.01 ASTM D482	Max 0.02 ISO 3987
Viscosity @ 40 mm^2/s	2.0-4.5 ASTM D445	3.5-5.0 ISO 3104
Flash point (°C)	Min 60 ASTM D93	Min 120 ISO 3679
Sulphur content (ppm)	Max 10 ASTM D5453	Max 10 ISO 20846
Water content (ppm)	Max 500 ASTM D95	Max 400 ISO 12937
Cetane number	Min 49 ASTM D4737	Min 51 ISO 5165
Copper corrosion	Max 1 3H @ 100 ASTM D130	Min 1 3H @ 50 ISO 2160
Density @ 15 kg/m^3	810-845 ASTM D4052	860-900 ISO 12185

study examines the potential reactivity of FFA with water, leading to the formation of carboxylic acids, thereby elucidating the consequent impact on the acidity levels of biodiesel. Additionally, the presence of iron oxide particles released by corroding carbon steel can also catalyse this reaction and further increase the acidity of the biodiesel. This can lead to increase acidity, viscosity, and oxidation, which can negatively impact engine performance and lifespan (Borugadda & Goud, 2012).

The detrimental effects of corrosion extend beyond the degradation of biodiesel quality, encompassing the potential for consequential harm to storage tanks and associated equipment. Such corrosion-induced damage can result in the occurrence of leaks and spills, posing significant risks to both the environment and human well-being. Therefore, effective corrosion mitigation strategies are necessary to ensure the quality and safety of biodiesel fuel in storage and distribution. Overall, the chemistry and production of biodiesel fuel, including PME, involves a complex series of chemical reactions and purification steps. Understanding the chemical properties and production processes of biodiesel is important for developing effective strategies for its distribution, storage and use as an alternative fuel source. *Figure 5* illustrates the research flowchart to characterise the biodiesel corrosion behaviour.

BIODIESEL CORROSION BEHAVIOUR ON METALLIC STRUCTURES

As previously mentioned, biodiesel comprising FAME can provide a source of nutrients for microorganisms such as bacteria, fungi, and algae. These microorganisms can grow in fuel storage systems and can form biofilms, which are communities of microorganisms that adhere to surfaces and produce a protective slime layer. Biofilms can promote the corrosion of carbon steel and other metals by producing acidic and corrosive metabolic byproducts, such as hydrogen sulphide, acetic acid and carbon dioxide. The presence of

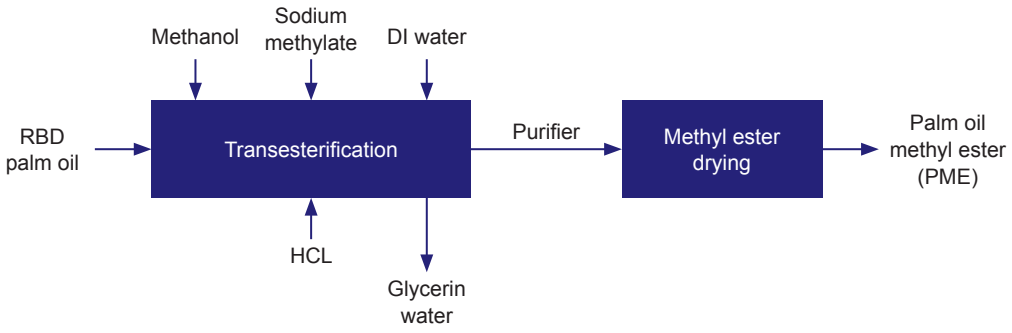

Figure 4. Process flowchart of Palm-oil methyl ester (PME) in accordance with EN 14214:2012.

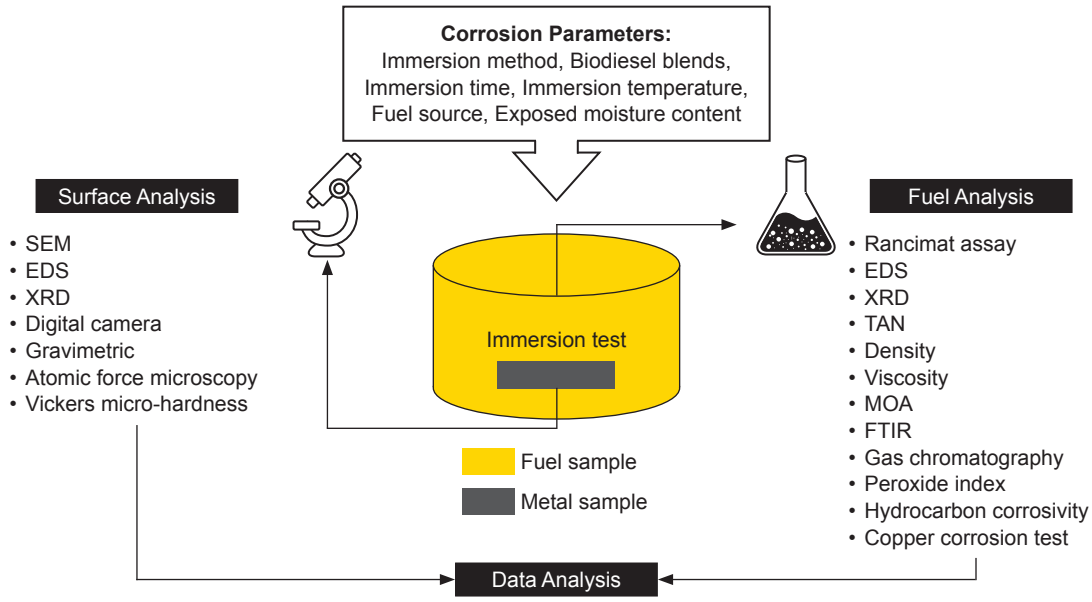

Figure 5. The research flowchart to characterise the biodiesel corrosion behaviour.

water in fuel storage systems, which can result from condensation or leaks, can also increase the growth of microorganisms and promote MIC. Several studies have investigated the corrosive effects of biodiesel on various metals commonly used in processing plants and storage facilities. It is imperative to acknowledge that the corrosive impacts of biodiesel may exhibit variability contingent upon the precise composition of the fuel, alongside the circumstances governing its storage and utilisation. Additionally, if the biodiesel is stored at high temperatures or exposed to air, this can also increase its corrosiveness. Several methods have been proposed to reduce the corrosive effects of biodiesel on processing plants and storage facilities. One method is to use corrosion-resistant materials in the construction of these facilities. Another method is to implement proper storage and handling practices, such as keeping the fuel dry and at cool temperatures. Additionally, using additives to the fuel can also reduce the corrosive effects. Understanding the general corrosion behaviour of biodiesel on metals leads us to examine more closely the interaction between biodiesel and specific metals, such as copper and its alloys, carbon steel, stainless steel, aluminium and its alloys and terne steel which play a crucial role in biodiesel processing. *Table 5* offers a comprehensive summary of research studies investigating the impact of biodiesel on metal corrosion.

Copper and Its Alloy

In biodiesel processing, copper is commonly used as a material in several pieces of equipment due to its high thermal and electrical conductivity, strength, and resistance to corrosion. Some of the equipment that require copper in biodiesel processing include heat exchangers, pipelines, pumps, valves and electrical components. Copper is also used in catalysts for chemical reactions during the biodiesel production process. The specific use of copper in each piece of equipment will depend on the specific requirements of the equipment, such as temperature, pressure and chemical resistance. Nevertheless, it is crucial to consider the potential ramifications of biodiesel on copper corrosion and select the suitable grade and form of copper to guarantee its enduring efficacy and sustainability in the process of biodiesel production. *Figure 6* shows the reported studies on copper corrosion in B100 biodiesel while *Figure 7* compares the studies on copper corrosion in various biodiesel blends. Samuel and Gulum (2019) investigated the effects of waste sunflower oil biodiesel-diesel fuel blends on the mechanical and corrosion properties of brass. The study found that the exposure of brass to the fuel blend resulted in a decrease in the mechanical properties of the brass, but also improved its corrosion resistance. The use of waste sunflower oil biodiesel-diesel fuel blends had a detrimental effect on the mechanical properties of brass, but the improvement in its corrosion resistance could be utilised in certain applications where corrosion resistance was more important than mechanical strength. The statement is supported by the research conducted by Fazal *et al.* (2012) which examined the degradation of automotive materials, copper, brass, aluminium and cast iron, in palm biodiesel. This study presented a comprehensive investigation of the impact of palm biodiesel on the degradation of automotive materials. The results demonstrated that the selection of the appropriate material for vehicle components was critical to ensure the long-term reliability and performance of vehicles powered by biodiesel. The findings revealed that copper, brass, aluminium, and cast iron were susceptible to degradation when exposed to palm biodiesel. The order of degradation for different metals followed the sequence of copper > brass > aluminium > cast iron. The variation in the degradation behaviour of different materials can be attributed to their differing total surface energy. The higher the total surface energy, the greater the affinity for biodiesel, and therefore, the more significant the degradation. These results highlighted the importance of considering material properties, including total surface energy, when selecting materials for use in vehicles that operate on biodiesel. The degradation of automotive materials in palm biodiesel highlighted the importance of careful consideration of the materials used in vehicles powered by biodiesel-based fuels to ensure their long-term performance and sustainability.

In a study conducted by Haseeb *et al*. (2010) copper corrosion was investigated under various fuel conditions, including pure diesel fuel (B0), a blend of 50% biodiesel and 50% diesel (B50), and pure palm biodiesel (B100). The corrosion tests were performed at room temperature for 2,640 hr at 60°C without stirring for 840 hr. The authors observed that the corrosion rate of copper in B100 at room temperature was 0.042 mpy, which increased to 0.053 mpy at 60°C. However, the use of oxidised B100 resulted in a higher corrosion rate of approximately 0.080 mpy. These findings highlight the importance of using biodiesel within specified quality parameters to mitigate the corrosion of incompatible metallic materials. Fazal *et al.* (2012) conducted a similar investigation on copper corrosion in B100 over a period of 2,880 hr at room temperature. The study revealed that copper corrosion rates were higher in contact with palm biodiesel compared to other materials. The authors also noted variations in the degradation of automotive materials in

TABLE 5. REPORTED STUDIES ON THE EFFECTS OF BIODIESEL TOWARDS METAL CORROSION

Metal	Fuel	Experimental conditions	Corrosion rate (mpy)		Observations	Ref.
Copper	B0 (ULSD), B50, B75, B100 (rapeseed)	Immersion, 80°C, 600 hr	B0 B50 B75 B100	0.35 0.62 0.80 0.92	Higher corrosion rate as biodiesel concentration in diesel increases.	Norouzi *et al.* (2012)
Piston metal	B100	Immersion, 26°C, 7,200 hr	*Jatropha curcas* *Karanja* *Madhuca indica* *Salvadora oleides*	0.0117 0.0058 0.0058 0.1236	Corrosion rate varies when exposed to biodiesel made from different feedstock.	Kaul *et al.* (2007)
Aluminium Brass Cast iron Copper	B100 (palm)	Immersion, 26°C, 2,880 hr	Aluminium Brass Cast iron Copper	0.173055 0.209898 0.112232 0.39278	Different metals have different corrosion rates.	Fazal *et al.* (2012)
Mild steel	B100 (palm)	Immersion, 26°C, 50°C, 80°C, 1,200 hr	26°C 50°C 80°C	0.052 0.056 0.059	At higher fuel temperatures, the corrosion rate increases.	Fazal *et al.* (2011)
Copper	B100	Immersion, 26°C, 55°C, 120 hr	26°C 50°C	0.174 0.020	Lower corrosion rate as fuel temperature rises.	Aquino *et al.* (2012)
Copper	B100 (palm)	Immersion, 26°C, 200, 300, 600, 1,200 and 2,880 hr	200 hr 300 hr 600 hr 1,200 hr 2,880 hr	0.295 0.433 0.591 0.709 0.571	Higher corrosion rate with longer immersion time.	Fazal *et al.* (2013)
Low carbon steel	B100 (soy), B100 (soy) with 1% water	Immersion, 2,016 hr	B100 B100 + 1% water	0.591 0.709	Water encourages corrosion.	Grainawi (2009)
Copper	B100 (palm), Oxidised B100 (palm)	Immersion, 60°C, 840 hr	B100 Oxidised B100	0.053 0.084	Corrosion rate is higher in oxidised biodiesel than in non-oxidised biodiesel.	Haseeb *et al.* (2010)
Terne steel	B1, B3, B5	Immersion, 80°C, 1,000 hr Fuel replaced every 250 hr, supplied fresh air once per day.	Initial TAN (mg KOH/g) / Final metal concentration (ppm)		Higher corrosion rate as total acid number increases.	Tsuchiya *et al.* (2006)

	Initial TAN (mg KOH/g)	Final metal concentration (ppm)	
		Pb	Sn
B1	0.05	8	1>
B3	0.06	40	1>
B5	0.07	1,800	12

TABLE 5. REPORTED STUDIES ON THE EFFECTS OF BIODIESEL TOWARDS METAL CORROSION (continued)

Metal	Fuel	Experimental conditions	Corrosion rate (mpy)			Observations	Ref.
Brass, Carbon steel, Copper	B100 (*Jatropha curcas*)	Immersion, 100 hr Linear polarisation resistance (LPR), measured every 24 hr		Immersion	LPR	Lower instantaneous corrosion rate than duration averaged corrosion rate.	Anand *et al.* (2011)
			Brass	0.4875	0.1346		
			Carbon steel	0.1290	0.1483		
			Copper	1.1206	0.1416		
Copper	B100 (*Pongamia pinnata*)	Immersion, 100 hr Rotating cage, 500 rpm	Immersion		0.219	Fuel flow encourages corrosion.	Parameswaran *et al.* (2013)
			Rotating		2.704		
Carbon steel, Copper	B100 (*Jatropha curcas*) B99 (*Jatropha curcas* + 1% NaCl)	Immersion, 100 hr		Carbon steel initial conductivity (µΩ)	Corrosion rate (mpy)	Carbon steel corrodes more quickly in fuel with a higher conductivity value. Lower copper corrosion rate in fuel with higher conductivity value.	Anand *et al.* (2011)
			B100	0.12	0.762		
			B99	0.32	1.339		
				Copper initial conductivity (µΩ)	Corrosion rate (mpy)		
			B100	0.68	0.243		
			B99	0.68	0.085		

palm biodiesel, with some metals experiencing higher levels of degradation than others. The degradation process in palm biodiesel primarily arises from the formation of FFA and glycerol during oxidation, which accelerates the corrosion of metallic materials. These findings underscore the importance of carefully selecting materials for vehicles powered by biodiesel-based fuels to ensure long-term performance and sustainability. The conductivity value, a crucial quality parameter indicating biodiesel deterioration level, can also expedite the ion exchange process during metal corrosion, particularly when biodiesel feedstocks vary (Chandran *et al*., 2016).

Fazal *et al*. (2018) conducted a study to examine the impact of copper on the stability and corrosiveness of palm biodiesel and its blends. The results revealed that the presence of copper in palm biodiesel and its blends significantly reduced their stability and increased their corrosiveness. The authors noted that the use of contaminated feedstock and storage facilities could lead to the presence of copper in biodiesel and its blends, affecting their stability and performance. The findings of this study emphasised the importance of proper storage and handling practices to maintain the quality and sustainability of biodiesel. Chandran *et al*. (2019) evaluated the sustainability of water in diesel emulsion fuel and its impact on the corrosion of copper. The study found that the presence of water in diesel emulsion fuels could significantly increase the corrosion of copper. The corrosion rate increased with the increasing water content. The authors highlighted that the choice of emulsifiers, fuel-water ratio and other factors were crucial for ensuring the long-term sustainability and performance of equipment that came in contact with diesel emulsion fuels. Rocha *et al*. (2019) investigated the impact of biodiesel properties on the corrosion of metallic copper. The study found that the composition of FAME in biodiesel, as well as the acid value and water content, could significantly influence the corrosion of copper. The results revealed that higher acid values and water contents in biodiesel could lead to increase corrosion rates of copper, while the composition of FAME could also have a direct impact on the corrosion behaviour of copper. The authors concluded that the study highlighted the importance of considering the properties of biodiesel in the design and operation of equipment that came in contact with biodiesel to ensure the long-term performance and sustainability of copper-based materials. Overall, these studies emphasise the need for proper storage and handling practices and the consideration of fuel properties in the design and operation of equipment that comes in contact with biodiesel to ensure the long-term performance and sustainability of materials.

In summary, the use of copper in biodiesel processing is common due to its properties such as high thermal and electrical conductivity, strength, and resistance to corrosion. Copper is used in equipment such as heat exchangers, pipelines, pumps, valves and electrical components and in catalysts for chemical reactions during biodiesel production. Ergo, different grades and forms of copper may be chosen based on the specific requirements of the equipment. The degradation of copper can be influenced by factors such as the type of feedstock used in biodiesel production, the conductivity value, the composition of FAME, the acid value and the water content. The presence of copper in biodiesel and its blends can negatively impact their stability and sustainability and highlight the need for proper storage and handling practices. The results emphasise the importance of considering the impact of biodiesel on the corrosion of copper and choosing the appropriate materials for biodiesel processing to ensure their long-term performance and sustainability.

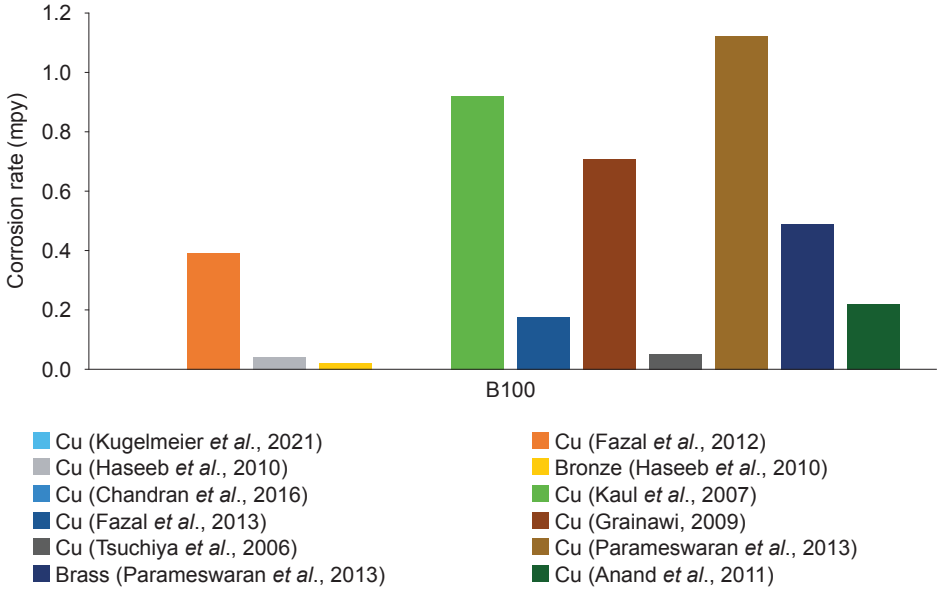

Figure 6. The reported studies on copper corrosion in B100 biodiesel.

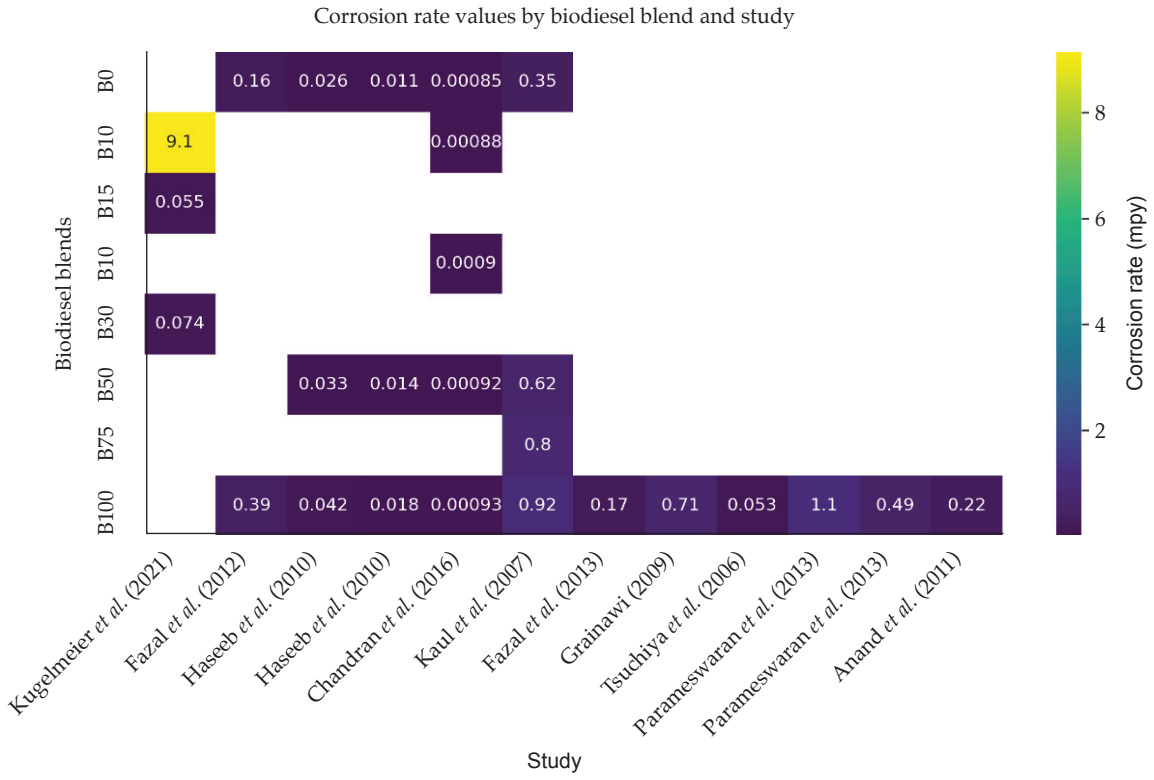

Figure 7. The reported studies on copper corrosion in varying biodiesel blends.

Carbon Steel

As copper is common to high thermal and electrical conductivity applications, carbon steel is a common material used for structures, pipelines, valves, pressure vessel and storage tanks, as it is relatively cheap, strong, and durable. However, biodiesel can be corrosive to carbon steel and cause significant damage to the equipment, leading to increased maintenance costs and reduced operational efficiency. The corrosion phenomenon under consideration is attributed to a confluence of multiple factors, encompassing the intricate interplay between the chemical characteristics inherent to biodiesel, the existence of water, and the proliferation of microorganisms. The presence of elevated concentrations of FFA in biodiesel has been identified as a potential catalyst for corrosion upon interaction with carbon steel. The presence of FFA in the vicinity of metal surfaces can initiate a chemical reaction resulting in the formation of a corrosive layer. This layer, upon accumulation, can induce the degradation of the underlying steel material, ultimately leading to structural failure. Moreover, it is noteworthy to mention that biodiesel exhibits hygroscopic properties, indicating its propensity to readily assimilate moisture from the surrounding environment. The potential impact of water content on corrosion in biodiesel is a subject of concern due to its role as a conducive environment for the proliferation of microorganisms, including bacteria and fungi.

Pusparizkita *et al*. (2020) examined the effect of *Bacillus megaterium* on carbon steel corrosion in biodiesel and diesel oil mixtures. The results showed that the presence of *B. megaterium* led to higher rates of corrosion in the carbon steel. The study concluded that the bacterial strain had a significant impact on the corrosion of carbon steel in biodiesel and diesel oil mixtures. Similar finding was found by Fernandes *et al*. (2019) that presented the carbon steel corrosion behaviour when exposed to *Moringa oleifera* Lam biodiesel. Among the two carbon steels (CS1015 and CS4140), the CS4140 was more compatible with the biodiesel type as there was no iron detected while 8 μg/g of iron was detected in biodiesel exposed with CS1015. CS4140 having higher carbon content and better mechanical properties than CS1015. Subsequent investigations into the effects of MIC, specifically caused by *B. licheniformis*, on ST-37 carbon steel in diesel tanks with varying biodiesel blends, revealed that the microbial activity of *B. licheniformis* notably exacerbated corrosion rates in the B15 biodiesel mixture. However, it was observed that in blends with biodiesel concentrations of B20 or higher, the corrosion rates were reduced, likely due to the formation of a thicker and more uniform biofilm by the bacteria (Pusparizkita *et al*., 2023). The authors found that the biodiesel had a corrosive effect on the carbon steel and concluded that further research is needed to understand the mechanisms involved and determine appropriate measures to prevent corrosion in biodiesel storage systems. In their study, Deshpande *et al*. (2019) investigated the corrosion behaviour of nodular cast iron when exposed to biodiesel blends. The researchers employed a suitable heat treatment technique and immersed the cast iron samples in various biodiesel blends to gain a deeper understanding of the underlying mechanisms at play. The present study investigates the influence of microstructural modifications on the corrosion resistance of metals, specifically in the context of biodiesel applications. The authors have observed that alterations in the fundamental microstructure of metal can lead to an enhanced resistance against corrosion. This phenomenon is attributed to the alteration in the metal phase, which subsequently affects the long-term performance and sustainability of materials utilised in biodiesel applications. In a study conducted by Cursaru *et al*. (2018), an additional factor contributing to biodiesel corrosion was examined. In this study, the researchers examined the influence of moisture on the corrosion behaviour of copper and mild carbon steel when exposed to corn biodiesel. The findings indicated that the corrosion behaviour of both metals in corn biodiesel was notably influenced by moisture content. The experimental investigation conducted herein examines the influence of moisture on the corrosion rates of two distinct metals, namely mild carbon steel and copper. The objective of this study was to ascertain the relative corrosion rates of these metals when exposed to a moist environment. The findings of this investigation revealed that both metals exhibited an increase in corrosion rates in the presence of moisture. Notably, the corrosion rate of mild carbon steel was observed to be higher than that of copper under these conditions. According to the findings above, proper storage conditions and the use of corrosion inhibitors were required to reduce corrosion in biodiesel processing and storage facilities. Batista *et al*. (2019) investigated the ester composition of biodiesel made from Macauba kernel oil in direct contact with carbon steel and galvanised carbon steel. The goal was to track changes in ester composition caused by potential corrosion from contact with metal materials. The results revealed that the composition of esters changed when they came into contact with both types of metal materials, with the changes being more pronounced when they came into contact with carbon steel. The study emphasises the importance of taking metal corrosion into account in biodiesel processing and storage facilities.

In a study by Serqueira *et al.* (2021) the authors proposed the consideration of antioxidants to improve the oxidative stability and corrosivity of biodiesel, thereby enhancing carbon steel corrosion resistance. The oxidative stability and corrosivity of biodiesel, derived from residual cooking oil, were evaluated under simulated storage conditions while exposed to copper and carbon steel. The results demonstrated that antioxidants effectively reduced the corrosivity of biodiesel, thereby improving the long-term performance and sustainability of materials utilised in biodiesel applications. This finding emphasised the significance of considering biodiesel properties and their impact on material corrosion during the design and operation of biodiesel equipment. The study investigated the dual effect of antioxidants on biodiesel stability and corrosivity. The results showed that adding antioxidants to biodiesel affected its oxidative stability and corrosivity. The impact varies depending on the type of antioxidant and the metal to which it was exposed. Martins *et al*. (2020) presented a promising study focusing on the synthesis of a new phenolic-Schiff base molecule as an antioxidant in soybean biodiesel and as a corrosion inhibitor in AISI 1020 carbon steel. The study demonstrated that the new molecule enhanced the oxidative stability of soybean biodiesel and reduced the corrosion rate of AISI 1020 carbon steel. These findings highlighted the potential for reducing biodiesel corrosion through the utilisation of innovative corrosion inhibitors and antioxidants. In summary, preventing biodiesel corrosion necessitates careful consideration of factors such as bacteria-induced corrosion, carbon content, metal phase, biodiesel type, environmental moisture and ester composition. Further research is needed to fully comprehend the effects of biodiesel on non-metal materials and to develop effective strategies for mitigating corrosion. It is advisable to implement proper storage and handling procedures which includes maintaining proper temperature and humidity levels, using appropriate materials for biodiesel processing and storage equipment, and regularly monitoring and cleaning the equipment.

Stainless Steel

Unlike carbon steel, stainless steel is often preferred for specialty services, such as food-grade feedstock storage, transesterification process, methanol recover, glycerol separation and purification in biodiesel service due to its resistance to corrosion caused by the chemical properties of biodiesel. Regular carbon steel is susceptible to corrosion when in contact with biodiesel, which can lead to leaks and failure of the system. On the other hand, stainless steel, specifically type 316 or type 304, has a higher resistance to corrosion and can better withstand the corrosive effects of biodiesel. Additionally, stainless steel has a longer service life, which results in lower maintenance costs and a reduced need for replacement of parts. Stainless steel is more corrosion-resistant and may be a better choice for long-term storage, especially in environments where the biodiesel blend is highly corrosive. Ultimately, the choice of material depends on the specific requirements and conditions of the biodiesel production process.

Alves *et al*. (2019) conducted an investigation on the effect of stainless-steel corrosion on biodiesel oxidation during storage. The study involved immersing samples in a controlled environment of low air turnover and darkness. The results showed that the presence of metal ions released during stainless steel corrosion promoted oxidation of the biodiesel, leading to changes in its composition, quality and a decrease in its overall oxidative stability. Interestingly, the study found that the type of ester used (methyl or ethyl) had little effect on metal degradation, indicating that both routes had a low corrosion rate despite the presence of surface micro-pitting. Kugelmeier *et al*. (2021) conducted a study on the corrosion behaviour of different materials (carbon steel, stainless steel, aluminium and copper) when exposed to a biodiesel/petrodiesel blend. The results indicated that stainless steel exhibited the highest corrosion resistance among the materials tested, outperforming the others. Chandran *et al*. (2023) assessed the corrosion effects on stainless steel and galvanised steel when exposed to water-emulsified diesel, diesel and palm biodiesel, revealing that stainless steel's corrosion rate was 1.1 times higher in emulsified diesel than in diesel, and 0.5 times lower than in biodiesel, while galvanised steel's corrosion rate was 8.5 times higher in emulsified diesel than in diesel and 3.5 times higher than in biodiesel. Additionally, Komariah *et al*. (2021) investigated the corrosion behaviour of different tank materials (stainless steel, galvanised steel and carbon steel) after contact with palm-based biodiesel, focusing on corrosion type and behaviour in different zones within the fuel tank made of various coating elements. The results revealed that different protective layers exhibited diverse corrosion types, with localised corrosion observed in stainless steel tanks but widespread corrosion in galvanised and carbon steel tanks. The contamination level of oil in stainless steel tanks was lower compared to galvanised and carbon steel tanks, and the corrosion type varied across different zones within the tank's interior. Leaks were more likely to occur at the base of the tank than on the walls and roof (Komariah *et al*., 2023). In their study, Yung *et al.* (2018) explored the compatibility of palm biodiesel blends, specifically B7, B10 and

B15, with automotive fuel tank materials, with a particular emphasis on terne sheet. Their research uncovered that when utilising high-quality fuels, the palm biodiesel blends did not induce corrosion or present compatibility concerns with terne sheet. This conclusion was substantiated by scanning electron microscopy analysis and the absence of heavy metal leaching, as documented in the study. These studies provide valuable insights into the corrosion behaviour of different materials when exposed to biodiesel blends, highlighting the importance of considering the type of material and its protective coatings to ensure the long-term sustainability and performance of biodiesel storage and handling equipment.

Aluminium and Its Alloy

In contrast to the above metals, aluminium and its alloys are relatively less common in the biodiesel processing and storage facilities. Aluminium is typically used in the biodiesel equipment that require human handling for ergonomic reason such as transfer hose, drip tray, sampling can and loading arms. However, they are common in the automotive parts due to their lightweight and corrosion-resistant properties, focusing on improving alloy resistance to biodiesel's acidity to ensure component durability and system efficiency, especially for piston material. Kaul *et al*. (2007) performed a long-duration static immersion assessment on piston metals and liners over a consistent ambient temperature span of 15°C-40°C for nearly a full year. The research revealed that Mahua and Karanja biodiesel fuels did not cause corrosion in the piston metals and liners, whereas Salvadora biodiesel did, likely owing to its elevated sulphur levels of 1,200 ppm. Jatropha biodiesel had a minor impact on the piston liner. Following the testing period, all biodiesel variants experienced substantial degradation. The acid number (AN) showed a significant increase for Jatropha, Mahua, and Karanja biodiesels, rising from 0.40 mg of KOH/g to a range of 11.00-19.00 mg of KOH/g. In the case of Salvadora biodiesel, the AN also rose, from 0.45 mg KOH/g to between 2.30 and 2.50 mg KOH/g. Aside from comparing the different biodiesel sources, Fazal *et al*. (2012) assessed the corrosion resistance of aluminium when exposed to pure palm methyl ester biodiesel (B100) at a temperature of 26°C over a span of 2,880 hr, juxtaposing its performance against other metals. The findings revealed that aluminium's corrosion rate stood at 0.17 mils per year (mpy), which outperformed brass and copper. However, it did not surpass cast iron in corrosion resistance. Nonetheless, the reduced weight of aluminium offers a significant advantage over cast iron, making it a compelling choice for applications where fuel efficiency and weight reduction are priorities.

Terne Steel

Although aluminium is prevalent in equipment handled by humans, terne steel - essentially a steel sheet coated with a lead-tin alloy renowned for its exceptional corrosion resistance - is widely employed in Southeast Asia for constructing diesel vehicle fuel tanks (Yung *et al*., 2018). Yung *et al*. (2018) studied the compatibility of terne steel with palm biodiesel and its various blends with conventional diesel fuel. The research demonstrated that no corrosion or adverse reactions occur when terne steel is exposed to palm biodiesel blends, even after long periods at high temperatures. After being exposed to palm biodiesel and its mixtures at 80°C for 1,000 hr, the terne steel coating's mass remained stable at roughly 40 g/m^2. Detailed surface examination using scanning electron microscopy (SEM) revealed no corrosion or pitting. Furthermore, there was no detection of heavy metal leaching in the fuel samples. Therefore, the study concluded that terne steel was compatible with palm biodiesel mixtures as long as the biodiesel used was of high quality. Furthermore, Tsuchiya *et al*. (2006) explored how different concentrations of biodiesel mixtures affect metal corrosion, particularly using a range of mixtures from pure diesel (B0) to a blend with 5% biodiesel (B5), assessed through a specialised cup test method. They discovered that the B2 blend, which contains 2% biodiesel, was particularly corrosive to the metal test cups. This corrosion was linked to the presence of short-chain organic acids that formed in the biodiesel blends as they broke down. When they conducted tests that simulated the movement of fuel in a vehicle's fuel system, they found that blends with a high level of oxidation stability, determined by a 9.6 hr Rancimat induction period, did not corrode the metal. Specifically, terne sheet metal, a material used in diesel fuel tanks and tested at a plating exposure of 40, showed no significant corrosion. The research concluded that controlling three critical factors oxidation stability, the acid number (AN) and organic acid concentration was essential to prevent metal corrosion. To safeguard metal components, especially those in fuel tanks, the study suggested that the acid number should be kept below 0.13 mg KOH/g, and the total organic acid concentration should not exceed 30 ppm. Therefore, it can be confirmed that terne steel is compatible with palm biodiesel mixtures as long as the biodiesel used is of high quality which translates to the emphasis on the three critical factors; oxidation stability, the AN and organic acid concentration.

To conclude, biodiesel, composed of FAME can nourish microorganisms like bacteria, fungi and algae in fuel storage systems. These microorganisms form biofilms that produce corrosive byproducts

such as hydrogen sulphide and acetic acid, accelerating the corrosion of metals like carbon steel. Water in storage systems exacerbates this MIC. The corrosiveness of biodiesel varies with its composition, storage conditions, and exposure to air or high temperatures. Mitigating this involves using corrosion-resistant materials, proper storage practices and potentially adding corrosion-inhibiting additives to the fuel. In biodiesel processing, copper is valued for its thermal and electrical conductivity, strength, and corrosion resistance. It is used in equipment like heat exchangers, pipelines, and electrical components. The corrosion behaviour of copper in biodiesel varies with factors like fuel composition, temperature and biodiesel blend. Carbon steel, while cost-effective and durable, is more susceptible to biodiesel-induced corrosion, impacted by chemical properties and moisture. Factors influencing corrosion include biodiesel's chemical properties, water content and microorganisms. Different types of carbon steel show varying compatibility with biodiesel and moisture significantly increases corrosion rates. Preferred for its corrosion resistance, stainless steel (particularly types 316 and 304) is more suitable for biodiesel applications than regular carbon steel and copper. It withstands biodiesel's corrosive effects better, leading to lower maintenance and longer service life. Understanding the interaction between biodiesel properties and tank materials is crucial for long-term performance of biodiesel storage and handling equipment.

PASSIVE CORROSION MITIGATION USING FIBRE REINFORCED POLYMERIC COATING

Corrosion is a serious problem that affects many materials, including metals, alloys, and concrete. Corrosion can result in structural failure, reduced performance and increased maintenance costs. One effective way to mitigate corrosion is by using polymeric coatings. In this response, we will explain the use of polymeric coatings for corrosion mitigation, with a focus on non-reinforced coatings. Polymeric coatings are applied to surfaces to create a barrier that prevents the corrosive environment from coming into contact with the underlying material. The coating acts as a sacrificial layer, which corrodes preferentially to the underlying substrate. This sacrificial corrosion of the coating protects the substrate from further corrosion. Non-reinforced polymeric coatings do not contain any glass fibre reinforcement. These coatings are typically applied by spray or brush application and consist of a single layer. Non-reinforced coatings are generally less expensive than reinforced coatings and are used in less demanding environments.

Passive corrosion mitigation using FRP coatings involves several methods which mainly divided into two main components, resin and fibre reinforcement as outlined in *Table 6*.

Polymeric coatings provide several benefits for corrosion mitigation, including: (1) Chemical resistance – Polymeric coatings are highly resistant to chemical attack, which makes them an excellent choice for harsh environments (Li *et al*., 2019; Yi *et al*., 2018); (2) Water resistance – Polymeric coatings provide a barrier against water and moisture, which is essential for corrosion mitigation (Singh *et al*., 2020); (3) UV resistance – Polymeric coatings can be formulated to resist UV degradation, which is important for outdoor applications (Jiang *et al*., 2019; Touazi *et al*., 2020); (4) Easy to apply – Polymeric coatings can be easily applied using a variety of methods, including spray or brush application (Ouarga *et al*., 2022); and (5) Cost-effective – Polymeric coatings are generally less expensive than other corrosion mitigation methods, such as stainless steel or galvanised coatings (Thirumal *et al*., 2023).

Biodiesel exposure can also cause degradation of non-metal materials used in processing plants and storage facilities. Studies have found that biodiesel can have detrimental effects on materials such as rubber, plastic and composites. One study found that exposure to biodiesel can cause swelling and loss of mechanical properties in natural rubber seals and gaskets. It has been observed that biodiesel can cause cracking and loss of mechanical properties in polyurethane materials, leading to equipment leaks and failure. Moreover, studies have found that biodiesel can cause degradation of FRP composites, which are commonly used in the construction of tanks and piping in biodiesel processing plants and storage facilities. Exposure to biodiesel can degrade the polymer matrix, resulting in a loss of mechanical properties and failure of the composite. It is crucial to note that the effects of biodiesel on non-metal materials can vary based on the fuel's specific composition and the conditions of storage and usage. Factors such as high-water content or impurities in biodiesel, elevated temperatures, and exposure to air can intensify its detrimental effects. Consequently, the degradation of non-metal materials used in processing plants and storage facilities due to biodiesel corrosion can lead to equipment failure and leaks. Further research is necessary to fully comprehend the effects of biodiesel on non-metal materials and to develop effective methods for mitigation.

FRP is a composite material that consists of a polymer matrix reinforced with fibres, such as carbon or glass. FRP has been found to be an effective solution for corrosion mitigation in various

TABLE 6. THE TYPES OF FRP BASED ON RESIN AND FIBRE REINFORCEMENT SELECTION

Resin	Fibre reinforcement
Epoxy-based FRP: These coatings are widely used for their strong adhesion and good corrosion resistance. Epoxy-based FRP can effectively protect metal surfaces from corrosive environments.	**Glass FRP:** Glass fibres are commonly used in FRP composite to provide additional strength and durability. They help in distributing stress over a larger area, thus reducing the impact of localised corrosion.
Vinyl ester-based FRP: These FRPs are known for their excellent chemical resistance, particularly in acidic and caustic environments. They are often used in chemical processing industries.	**Carbon FRP:** Carbon fibres are used for high-performance applications. They offer superior strength, stiffness, and corrosion resistance, though at a higher cost compared to glass fibres.
Polyester-based FRP: These are used for their good balance of cost and performance. They offer decent corrosion resistance and are suitable for less aggressive environments.	**Aramid FRP:** Known for their excellent toughness and impact resistance, aramid fibres like Kevlar are sometimes used in FRP composite for extreme environments.

Note: FRP - Fibre-reinforced polymer.

industrial applications. The fibres in FRP provide mechanical reinforcement to the polymer matrix, while the polymer matrix provides a barrier to protect the fibres from the corrosive environment. In the context of biodiesel corrosion in processing plants and storage facilities, FRP has been found to be an effective solution for corrosion mitigation. Studies have shown that FRP can provide superior corrosion resistance compared to traditional materials, such as steel, in the presence of biodiesel. This is because the polymer matrix of FRP provides a barrier to protect the fibres from the corrosive environment, while the fibres provide mechanical reinforcement to the polymer matrix. One study found that FRP was more effective than steel in preventing corrosion in biodiesel storage tanks. The study found that FRP was able to resist corrosion for longer periods of time than steel when exposed to biodiesel. Another study found that FRP was an effective corrosion barrier for aluminium when used in biodiesel processing equipment. In addition to its corrosion resistance, FRP has other benefits when used in biodiesel processing plants and storage facilities. It is lightweight, easy to fabricate, and has a high strength-to-weight ratio. It also has excellent chemical resistance, making it suitable for use in harsh environments. In conclusion, FRP has been found to be an effective solution for corrosion mitigation in biodiesel processing plants and storage facilities. Its corrosion resistance, light weight, and ease of fabrication make it an attractive option for use in these applications. Additionally, its chemical resistance makes it suitable for use in harsh environments. Further research is needed to fully understand the potential of FRP as a solution for biodiesel corrosion.

Atikpo *et al*. (2022) proposed the use of a Codeposition method to create a novel mild steel coating using eggshell waste. The authors evaluated the microstructure, hardness values, viscosity and density of the samples in a *Jatropha curcas* biodiesel environment. The Zn-10% $CaCO_3$-ESP double layer exhibited a corrosion protection efficiency of 68.87%. Elias *et al*. (2020) investigated the corrosion of as-cast Al-7.5% Si alloy and Al-7.5wt% composite immersed in B100, B50 and BDE blends. The study revealed that the Al/Si composite exhibited lower corrosion susceptibility than the as-cast sample in all biofuels tested. Surprisingly, an increase in water content led to a decrease in the corrosion behaviour of the composite. These studies highlight the potential application of protective coatings and linings to enhance the corrosion resistance of metallic structures in biodiesel environments. By developing innovative coating materials and deposition techniques, it is possible to mitigate the corrosive effects of biodiesel and improve the durability and reliability of equipment. GFRP has excellent corrosion resistance properties and can withstand exposure to acids, water and other corrosive substances that are commonly found in biodiesel. GFRP also has high durability and can withstand cyclic loading and temperature fluctuations, which can contribute to stress corrosion cracking in traditional materials. Several laboratory experiments and field trials have been conducted to evaluate the effectiveness of GFRP in mitigating corrosion in biodiesel storage tanks. A study by Xue *et al*. (2021) investigated the corrosion behaviour of carbon steel and GFRP-reinforced epoxy coatings in biodiesel. The results showed that GFRP-reinforced epoxy coatings had significantly lower corrosion rates than carbon steel and uncoated epoxy coatings. Another study by Wei *et al*. (2021) evaluated the performance of GFRP-reinforced concrete for biodiesel storage tanks. The study found that GFRP-reinforced concrete had lower corrosion rates and higher durability than traditional reinforced concrete. The study also showed that GFRP-reinforced concrete had better resistance to cracking and spalling caused by cyclic loading and temperature fluctuations. Field trials have also shown promising results for the use of GFRP in biodiesel storage tanks. A case study

by Ram *et al*. (2020) evaluated the performance of GFRP-reinforced polyethylene terephthalate (PET) tanks for biodiesel storage. The study found that the GFRP-reinforced PET tanks had significantly lower corrosion rates than traditional steel tanks. The study also showed that the GFRP-reinforced PET tanks had lower maintenance costs and longer life service than traditional tanks.

The experiments included buckling strength, compression strength, low-velocity impact strength, and three-point bending tests to investigate the degrading behaviour of GFRP materials. The findings of these experiments demonstrated that when treated to diverse circumstances, GFRP materials could degrade. Eslami *et al*. (2015) conducted a study on the buckling strength of an E-glass/vinyl ester composite after exposure to seawater for 185 and 212 days. The results indicated that moisture absorption was more significant in tap water, while mechanical strength and bonding were adversely affected under high-temperature immersion conditions. Fitriah *et al*. (2017) investigated the compression strength of glass/epoxy pipes hydrothermally aged in hot water at 80°C for different durations. The study found that moisture absorption impaired the fibre-matrix bonding, leading to increased strength loss over time. Hawa *et al*. (2016) examined the low-velocity impact strength and burst strength of glass/epoxy FRP pipes with a winding angle of 55° immersed in hot water at 80°C for varying durations. The study revealed that the energy absorption of the aged pipes decreased after prolonged exposure, except for the 1,500 hr immersion, which exhibited slightly higher energy absorption due to material plasticisation. Ma *et al*. (2015) evaluated the low-velocity impact strength of glass/epoxy FRP pipes with different diameters after immersion in seawater for different durations. According to the study, a smaller diameter pipe had a more significant failure region, and the energy absorption of the pipes dropped as the pipe diameter grew. Kanerva *et al*. (2019) evaluated the three-point bending test ISO 178:2010 of E-glass/vinyl ester and vinyl ester GFRP reactors submerged in SAC solution for six months and one year, respectively. After one year of immersion, the flexural modulus of the epoxy-vinyl ester matrix reduced by 22%, but the ultimate strength improved by 109%. In their study, Kumarasamy *et al*. (2020) examined the degradation behaviour of E-glass/epoxy GFRP laminates with a fibre volume fraction ranging from 45%-55%. The laminates were manufactured using the vacuum-assisted resin-transfer moulding (VARTM) technique. The investigation focused on the effects of exposure to different fuels, namely Kerosene or Jet-A fuel, biodiesel fuel and an 80% kerosene with 20% biodiesel volume-based ratio blend fuel. The study discovered that deterioration happened predominantly due to the creation of voids and microcracks during immersion due to internal tension in the polymer network generated by the penetration of the fuel molecule.

Eslami *et al*. (2015) found that tap water conditions led to higher moisture absorption, while high-temperature immersion weakened the mechanical strength and bonding. Fitriah *et al*. (2017) found that tap water conditions led to higher moisture absorption, while high-temperature immersion weakened the mechanical strength and bonding. Hawa *et al*. (2016) reported slightly higher energy absorption in aged pipes (except for 1,500 hr) due to material plasticisation. Kanerva *et al*. (2019) discovered that the ultimate strength of an epoxy-vinyl ester matrix increased by 109% after one year of immersion. These studies provide valuable insights into the degradation behaviour of GFRP materials under different exposure conditions. However, it is essential to consider the specific type of GFRP material used and the specific exposure conditions when interpreting the results. Further research is needed to gain a comprehensive understanding of the effects of biodiesel on GFRP materials and develop effective strategies for corrosion mitigation and mechanical reinforcement. Then the study will examine the GFRP performance under various biodiesel storage conditions before evaluating the influence of GFRP geometrical parameters on the corrosion mitigation and mechanical reinforcement of carbon steel storage tank. Based on these, a deeper understanding of application of optimised GFRP parameters for various biodiesel storage conditions may be gained to improve the tank structural integrity and equipment integrity of oil and gas processing and storage facility. Overall, the use of GFRP in biodiesel storage tanks has shown promising results in reducing corrosion and improving tank integrity. GFRP has excellent corrosion resistance properties, high durability and can withstand cyclic loading and temperature fluctuations. Nevertheless, the efficacy of GFRP may be contingent upon various elements, such as the specific makeup of the biodiesel, the structural configuration of the storage tank, and the prevailing operational circumstances. Additional investigation is required to enhance the utilisation of GFRP in the context of storing biodiesel, as well as to assess its durability over an extended period. *Table 7* presents a comprehensive overview of multiple studies investigating the degradation characteristics of GFRP composites across diverse ageing conditions and materials employed. The research encompasses various categories of materials, diverse ageing methodologies, the maximum duration of the experiments, comprehensive details, the type of study conducted in accordance with ASTM

TABLE 7. THE VARIOUS AGEING CONDITIONS ON GFRP PIPE AND THEIR FAILURE CONDITIONS

Type of materials	Type of ageing	Max duration	Details	Type of study/ ASTM standards	Degradation behaviour	Observations	Ref.
E-glass/vinyl ester	Seawater Tap water	185 days 212 days	The temperature of both the seawater and the tap water was 25°C. Normal water was also conditioned at a lower temperature of 2°C.	Buckling strength (ASTM D5229)	59.70% 64.18%	More moisture absorption occurred with tap water. Immersion at a high temperature weakened both the mechanical strength and bonding.	Eslami *et al*. (2015)
Glass/epoxy	Hydrothermal	1,500 hr	Pipes were subjected to hydrothermal ageing in 80°C hot water for 500, 1,000 and 1,500 hr. The compressive test was conducted at 45°C to 65°C temperatures.	Compression strength (ASTM D695-10)	34.60%	The fibre-matrix bond deteriorated because of moisture absorption. There is a more significant loss of strength under the 1,500 hr condition.	Fitriah *et al*. (2017)
Glass/epoxy	Hydrothermal	1,500 hr	The GFRP pipe was manufactured with a winding angle of 55° and immersed in water heated to 80°C for 500, 1,000 and 1,500 hr.	Low velocity impact strength (ASTM D2444) Burst strength (ASTM D1599)	Increased 30.00%	The fibre-matrix bond deteriorated as a result of moisture absorption. There is a more significant loss of strength under the 1,500 hr condition. After ageing for 1,500 hr, GFRP pipes absorbed less energy. Due to material plasticisation, the energy absorption of aged pipes (except for those aged for 1,500 hr) was marginally more remarkable than that of new pipes.	Hawa *et al*. (2016)
Glass/epoxy	Seawater	12 months	The GFRP pipe was manufactured with 50, 75, 100, and 150 mm diameters. All the pipes were submerged for three, six, nine and twelve months in saltwater. On each aged pipe, impact loads of 15, 20 and 25 J were applied.	Low velocity impact strength	Increased	The failure area of a smaller diameter pipe was greater. As pipe diameter increased, the energy absorption of the pipes decreased.	Ma *et al*. (2015)

TABLE 7. THE VARIOUS AGEING CONDITIONS ON GFRP PIPE AND THEIR FAILURE CONDITIONS (continued)

Type of materials	Type of ageing	Max duration	Details	Type of study/ ASTM standards	Degradation behaviour	Observations	Ref.
Kevlar / HDPE	Hydrostatic pressure	10,000 hr	The pipe was immersed in 65°C hot water, subjected to 15 MPa of water pressure, and passed through a series of pipes for 10,000 hr. To predict pipe life, data were collected during the test pressure time at the failure stage.	Monotonic internal pressure (ASTM D2992)	40.45%	Compared to its initial state, the pipe's pressure resistance it decreased over time. The number of undamaged pipes was determined to be three for pipes older than 10,000 hr and ten for those older than 1,000 hr.	Chen *et al*. (2018)
E-glass / vinyl ester Vinyl ester		6 months 1 year	The laminates and matrix samples were immersed at elevated temperatures and pressures (90°C, 15 bar) in sulphuric acid (SAC) medium (50 g / L H2SO4 solution in water) in GFRP reactors. In addition, 0.5 g / L of $Fe_2(SO_4)_3$ was added to prevent corrosion in the metallic components of the conditioning system. In order to observe deterioration due to ageing, the laminates were aged for six months and the resin samples for one year.	Three-point bending test (ISO 178:2010)	5.6%-17.0% 22.0%	After one year of immersion, the flexural modulus of the matrix composed of epoxy-vinyl ester decreased by 22%, while the ultimate strength increased by 109%. After six months of conditioning, the GFRP cross-ply laminate's tensile Young's modulus decreased by 5.6%-2.1%, while its ultimate strength decreased by 13.4%-4.0%. Lower and on the layer length scale cause tensile property degradation. After six months of conditioning, the composite's flexural stiffness was 4%-69% less, and its flexural strength was 26%-34% less than before conditioning. On a microscopic scale, ageing primarily affects the fibres; however, the ageing of interfaces cannot be ruled out in terms of the linear elastic response within bending.	Kanerva *et al*. (2019)
E-glass / epoxy	Kerosene or Jet-A fuel, biodiesel fuel, and an 80% kerosene with 20% biodiesel volume-based ratio blend fuel	66 days	GFRP laminates are manufactured via vacuum-assisted resin transfer moulding (VARTM) with a fibre volume fraction between 45% and 55%.	ASTM D5229, ASTM D3039, ASTM D3410	Decrease	Due primarily to the formation of voids and microcracks during immersion. When the fuel molecule penetrates the polymer network, these deformations occur due to the internal stress within the polymer network.	Kumarasamy *et al*. (2020)

Standards, the behaviour of degradation exhibited by the materials, the observations made during the study and the references cited.

FUTURE RECOMMENDATION

As the biodiesel industry continues its rapid expansion and solidifies its position as a pivotal renewable energy source, it becomes increasingly imperative to confront and overcome the multifaceted challenges posed by corrosion within distribution and terminal operations. Building upon the comprehensive materials compatibility review undertaken in this study, a series of proactive recommendations emerge to elevate the corrosion resistance standards across biodiesel infrastructure. To begin, it is crucial to initiate long-term field trials that specifically assess material performance under the complex and dynamic conditions of biodiesel storage, including potential biodiesel contamination, temperature and humidity variations and its influence on distribution and terminal operations. In the realm of biodiesel storage, a critical need arises for a thorough and meticulous assessment of GFRP performance. This investigation must encompass various aspects, including the examination of internal lining applications enduring constant contact with biodiesel and its potential contaminants. Additionally, it should extend to the evaluation of external wrapping scenarios facing challenges such as prolonged exposure to UV radiation and the dynamic atmospheric conditions associated with biodiesel storage, which encompass humidity and the potential threat of seawater exposure. Furthermore, the development of a GFRP composite capable of effectively leveraging both the load-bearing properties of epoxy and the impressive chemical corrosion resistance demonstrated by vinylester becomes imperative. This dual-performance approach should be further enhanced through a careful selection of glass fibre types that can augment the composite's load-bearing capacity while concurrently enhancing its resistance to chemical corrosion. The integration of these elements, combined with a strategic incorporation of metallic components, represents a groundbreaking strategy aimed at extending and enhancing the durability and overall performance of metallic materials operating within the challenging biodiesel storage environment. Furthermore, the adoption of advanced corrosion monitoring systems, facilitated by the integration of cutting-edge technologies such as 3D scanning, finite element modeling (FEM) and IoT sensors, offers the potential to revolutionise our approach to managing biodiesel corrosion risks within storage facilities. These systems can not only provide early detection of corrosion issues but also enable predictive strategies to proactively address them.

CONCLUSION

The exploration and utilisation of biodiesel as a renewable energy source contribute to the goal of achieving energy sustainability and reducing carbon and toxic gas emissions. However, it is crucial to address the potential threats to food security and increased deforestation associated with biodiesel production.

In processing and storage facilities, which predominantly consist of metallic structures and equipment parts, the corrosion behaviour of biodiesel poses significant challenges to structural integrity and equipment reliability. To overcome these challenges, many researchers have suggested the potential application of GFRP as a lining material to act as a corrosion barrier and improve the mechanical strength of metallic structures involved in biodiesel processing and storage. It is important to conduct further research to fully understand the corrosion behaviour of biodiesel and develop effective mitigation methods that enhance its attractiveness as a sustainable energy transition option. The implementation of biodiesel as a sustainable energy source has the potential to significantly reduce carbon and toxic gas emissions and decrease dependency on conventional fossil fuels. On the other hand, oil palm wastes can be the potential alternative source of energy. In addition, the corrosive nature of biodiesel can threaten the structural integrity and equipment reliability of processing, storage facilities and equipment parts, which are predominantly made of metallic structures. This can lead to increased maintenance costs, equipment downtime, and safety hazards. To address this issue, the potential application of GFRP as a lining material for tanks and pipes has been proposed as a corrosion barrier and to improve the mechanical strength of the metallic structures. GFRP has been shown to provide excellent resistance to corrosion and chemical attack, and it can be customised to meet specific design requirements. However, more research is needed to fully understand the corrosion behaviour of biodiesel and to identify the most effective mitigation methods. This research can help to improve the attractiveness of biodiesel as a transitional energy source and promote the sustainability of the energy industry.

In conclusion, while biodiesel offers many benefits as a sustainable energy source, it also presents significant challenges related to corrosion and food security. Further research and development

are needed to overcome these challenges and ensure the successful implementation of biodiesel as a viable energy source.

ACKNOWLEDGEMENT

This study was supported financially under the Fundamental Research Grant Scheme awarded by the Ministry of Higher Education Malaysia with grant number: FRGS/1/2019/TK03/UM/02/12 (FP143-2019A). The authors also gratefully acknowledge the support from grants, RMF0400-2021, ST049-2022, AMMP Centre, Centre for Energy Sciences and Department of Mechanical Engineering, Universiti Malaya to conduct this research work.

REFERENCES

Aatola, H., Larmi, M., Sarjovaara, T., & Mikkonen, S. (2009). Hydrotreated vegetable oil (HVO) as a renewable diesel fuel: Trade-off between NO_x, particulate emission, and fuel consumption of a heavy duty engine. *SAE International Journal of Engines*, *1*(1), 1251–1262. https://doi.org/10.4271/2008-01-2500

Alves, S., Dutra-Pereira, F., & Bicudo, T. (2019). Influence of stainless steel corrosion on biodiesel oxidative stability during storage. *Fuel*, *249*, 73–79. https://doi.org/10.1016/j.fuel.2019.03.097

Anand, A., Meenakshi, H. N., Krishnamurthy, S. R., Mani, S. R., & Papavinasam, S. (2011, March). *Compatibility of metals in Jatropha oil*. The Corrosion 2011, Houston, USA.

Anand, A., Meenakshi, H. N., & Shyamala, R. (2011). Study on the impact of *Jatropha curcus* biodiesel on selected metals. *The Ecoscan*, *1*, 291–294.

Aquino, I., Hernandez, R., Chicoma, D., Pinto, H., & Aoki, I. (2012). Influence of light, temperature and metallic ions on biodiesel degradation and corrosiveness to copper and brass. *Fuel*, *102*, 795–807. https://doi.org/10.1016/j.fuel.2012.06.011

Atikpo, E., Aigbodion, V., & Von Kallon, D. (2021). $CaCO_3$-derived from eggshell waste for improving the corrosion resistance of zinc composite coating on mild steel for biodiesel storage tank. *Chemical Data Collections*, *37*, 100794. https://doi.org/10.1016/j.cdc.2021.100794

Batista, C., Fabris, J., Cavalcante, L., Ferraz, V., Andrade, B., Junior, Ardisson, J., Lemos, L., & Damasceno, S. (2019). Monitoramento da composição em ésteres do biodiesel do óleo de amêndoa da macaúba (*Acrocomia aculeata* (Jacq.) Lodd. ex Mart.) em contato direto com o aço carbono e o aço carbono galvanizado [Monitoring the composition in esters of the biodiesel from the macauba (*Acrocomia aculeata* (Jacq.) Lodd. ex Mart.) kernel oil put in direct contact with carbon steel and galvanized carbon steel]. *Quimica Nova*, *42*(4), 387–396. https://doi.org/10.21577/0100-4042.20170356

Borugadda, V. B., & Goud, V. V. (2012). Biodiesel production from renewable feedstocks: Status and opportunities. *Renewable and Sustainable Energy Reviews*, *16*(7), 4763–4784. https://doi.org/10.1016/j.rser.2012.04.010

Chandran, D. (2020). Compatibility of diesel engine materials with biodiesel fuel. *Renewable Energy*, *147*, 89–99. https://doi.org/10.1016/j.renene.2019.08.040

Chandran, D., Khalid, M., Raviadaran, R., Lau, H. L. N., Yung, C. L., Kanesan, D., & Salim, M. (2019). Sustainability of water in diesel emulsion fuel: An assessment of its corrosion behaviour towards copper. *Journal of Cleaner Production*, *220*, 1005–1013. https://doi.org/10.1016/j.jclepro.2019.02.210

Chandran, D., Ng, H. K., Lau, H. L. N., Gan, S., & Choo, Y. M. (2016). Investigation of the effects of palm biodiesel dissolved oxygen and conductivity on metal corrosion and elastomer degradation under novel immersion method. *Applied Thermal Engineering*, *104*, 294–308. https://doi.org/10.1016/j.applthermaleng.2016.05.044

Chandran, D., Raviadaran, R., Lau, H. L. N., Numan, A., Elumalai, P., & Samuel, O. D. (2023). Corrosion characteristic of stainless steel and galvanized steel in water emulsified diesel, diesel and palm biodiesel. *Engineering Failure Analysis*, *147*, 107129. https://doi.org/10.1016/j.engfailanal.2023.107129

Chen, W., Bai, Y., Yan, H., & Xiong, H. (2017). Analysis on the long-term hydrostatic strength of Kevlar fibre reinforced flexible pipe. *Ships and Offshore Structures*, *13*(2), 226–232. https://doi.org/10.1080/17445302.2017.1354660

Chevron Corporation (2007). *Diesel fuels technical review.* Retrieved October 9, 2023, from https://www.chevron.com/-/media/chevron/operations/documents/diesel-fuel-tech-review.pdf

Cursaru, D., Nassreddine, S., Riachi, B., Neagu, M., Mihai, S., Matei, D., & Brănoiu, G. (2018). Impact of moisture on the corrosion behavior of copper and mild carbon steel in corn biodiesel. *Corrosion Reviews*, *36*(6), 559–574. https://doi.org/10.1515/corrrev-2018-0015

Deshpande, S., Joshi, A., Vagge, S., & Anekar, N. (2019). Corrosion behavior of nodular cast iron in biodiesel blends. *Engineering Failure Analysis*, *105*, 1319–1327. https://doi.org/10.1016/j.engfailanal.2019.07.060

Elias, A. L. P., Koizumi, M. S., Ortiz, E. L., Rodrigues, J. F. Q., Bortolozo, A. D., Osório, W. R., & Da Silva Padilha, G. (2020). Corrosion behavior of an Al-Si casting and a sintered Al/Si composite immersed into biodiesel and blends. *Fuel Processing Technology*, *202*, 106360. https://doi.org/10.1016/j.fuproc.2020.106360

Eslami, S., Honarbakhsh-Raouf, A., & Eslami, S. (2015). Effects of moisture absorption on degradation of E-glass fiber reinforced vinyl ester composite pipes and modelling of transient moisture diffusion using finite element analysis. *Corrosion Science*, *90*, 168–175. https://doi.org/10.1016/j.corsci.2014.10.009

Fazal, M. A., Haseeb, A. S. M. A., & Masjuki, H. H. (2011). Effect of temperature on the corrosion behaviour of mild steel upon exposure to palm biodiesel. *Energy*, *36*(5), 3328–3334. https://doi.org/10.1016/j.energy.2011.03.02

Fazal, M. A., Haseeb, A. S. M. A., & Masjuki, H. H. (2012). Degradation of automotive materials in palm biodiesel. *Energy*, *40*(1), 76–83. https://doi.org/10.1016/j.energy.2012.02.026

Fazal, M. A., Haseeb, A. S. M. A., & Masjuki, H. H. (2013). Corrosion mechanism of copper in palm biodiesel. *Corrosion Science*, *67*, 50–59. https://doi.org/10.1016/j.corsci.2012.10.006

Fazal, M. A., Suhaila, N. R., Haseeb, A. S. M. A., Rubaiee, S., & Al-Zahrani, A. (2018). Influence of copper on the instability and corrosiveness of palm biodiesel and its blends: An assessment on biodiesel sustainability. *Journal of Cleaner Production*, *171*, 1407–1414. https://doi.org/10.1016/j.jclepro.2017.10.144

Fernandes, D. M., Squissato, A. L., Lima, A. F., Richter, E. M., & Munoz, R. A. (2019). Corrosive character of *Moringa oleifera* Lam biodiesel exposed to carbon steel under simulated storage conditions. *Renewable Energy*, *139*, 1263–1271. https://doi.org/10.1016/j.renene.2019.03.034

Fitriah, S., Majid, A., Ridzuan, M., Daud, R., Gibson, A., & Assaleh, T. (2017). Influence of hydrothermal ageing on the compressive behaviour of glass fibre/epoxy composite pipes. *Composite Structures*, *159*, 350–360. https://doi.org/10.1016/j.compstruct.2016.09.078

Grainawi, L. (2009). *Testing for compatibility of steel with biodiesel* [Paper presentation]. The Corrosion 2009, Atlanta, USA.

Gunstone, F. D. (2004). *The chemistry of oils and fats: Sources, composition, properties and uses*. Blackwell Publishing.

Haseeb, A. S. M. A., Masjuki, H. H., Ann, L. J., & Fazal, M. A. (2010). Corrosion characteristics of copper and leaded bronze in palm biodiesel. *Fuel Processing Technology*, *91*(3), 329–334. https://doi.org/10.1016/j.fuproc.2009.11.004

Hawa, A., Majid, M. S. A., Afendi, M., Marzuki, H. F. A., Amin, N. A. M., Mat, F., & Gibson, A. G. (2016). Burst strength and impact behaviour of hydrothermally aged glass fibre/epoxy composite pipes. *Materials & Design*, *89*, 455–464. https://doi.org/10.1016/j.matdes.2015.09.082

Jiang, F., Zhao, W., Wu, Y., Dong, J., Zhou, K., Lu, G., & Pu, J. (2019). Anti-corrosion behaviors of epoxy composite coatings enhanced via graphene oxide with different aspect ratios. *Progress in Organic Coatings*, *127*, 70–79. https://doi.org/10.1016/j.porgcoat.2018.11.008

Kanerva, M., Jokinen, J., Sarlin, E., Pärnänen, T., Lindgren, M., Järventausta, M., & Vuorinen, J. (2019). Lower stiffness of GFRP after sulfuric acid-solution aging is due to degradation of fibre-matrix interfaces? *Composite Structures*, *212*, 524–534. https://doi.org/10.1016/j.compstruct.2019.01.006

Kaul, S., Saxena, R. C., Kumar, A., Negi, M. S., Bhatnagar, A. K., Goyal, H. B., & Gupta, A. K. (2007). Corrosion behavior of biodiesel from seed oils of Indian origin on diesel engine parts. *Fuel Processing Technology*, *88*(3), 303–307. https://doi.org/10.1016/j.fuproc.2006.10.011

Komariah, L. N., Arita, S., Prianda, B. E., & Dewi, T. K. (2021). Technical assessment of biodiesel storage tank; A corrosion case study. *Journal of King Saud University - Engineering Sciences*, *35*(3), 232–237. https://doi.org/10.1016/j.jksues.2021.03.016

Kugelmeier, C. L., Monteiro, M. R., Da Silva, R., Kuri, S. E., Sordi, V. L., & Della Rovere, C. A. (2021). Corrosion behavior of carbon steel,

stainless steel, aluminium and copper upon exposure to biodiesel blended with petrodiesel. *Energy*, *226*, 120344. https://doi.org/10.1016/j.energy.2021.120344

Kumarasamy, S., Mazlan, N. M., Abidin, M. S. Z., & Anjang, A. (2019). Influence of fuel absorption on the mechanical properties of glass-fiber-reinforced epoxy laminates. *Journal of King Saud University - Engineering Sciences*, *32*(8), 548–554. https://doi.org/10.1016/j.jksues.2019.09.002

Li, S., Shao, M., Duan, C., Yan, Y., Wang, Q., Wang, T., & Zhang, X. (2019). Tribological behavior prediction of friction materials for ultrasonic motors using Monte Carlo-based artificial neural network. *Journal of Applied Polymer Science*, *136*(10), 47157. https://doi.org/10.1002/app.47157

Ma, Y., Sugahara, T., Yang, Y., & Hamada, H. (2015). A study on the energy absorption properties of carbon/aramid fiber filament winding composite tube. *Composite Structures*, *123*, 301–311. https://doi.org/10.1016/j.compstruct.2014.12.067

Martins, L. F., Cubides-Roman, D. C., Da Silveira, V. C., Aquije, G., Romão, W., Dos Santos, R. B., Neto, A. C., & Lacerda, V. (2020). Synthesis of new phenolic-schiff base and its application as antioxidant in soybean biodiesel and corrosion inhibitor in AISI 1020 Carbon Steel. *Journal of the Brazilian Chemical Society*. https://doi.org/10.21577/0103-5053.20190217

Milano, J., Umar, H., Shamsuddin, A. H., Silitonga, A. S., Irfan, O. M., Sebayang, A. H., Fattah, I. M. R., & Mofijur, M. (2021). Experimental study of the corrosiveness of ternary blends of biodiesel fuel. *Frontiers in Energy Research*, *9*, 778801. https://doi.org/10.3389/fenrg.2021.778801

Norouzi, S., Eslami, F., Wyszynski, M. L., & Tsolakis, A. (2012). Corrosion effects of RME in blends with ULSD on aluminium and copper. *Fuel Processing Technology*, *104*, 204–210. https://doi.org/10.1016/j.fuproc.2012.05.016

Ouarga, A., Lebaz, N., Tarhini, M., Noukrati, H., Barroug, A., Elaissari, A., & Youcef, H. B. (2022). Towards smart self-healing coatings: Advances in micro/nano-encapsulation processes as carriers for anti-corrosion coatings development. *Journal of Molecular Liquids*, *354*, 118862. https://doi.org/10.1016/j.molliq.2022.118862

Parameswaran, M. H. N., Anand, A., & Krishnamurthy, S. R. (2013). A comparison of corrosion behavior of copper and its alloy in *Pongamia pinnata* oil at different conditions. *Journal of Energy*, *2013*, 932976. https://doi.org/10.1155/2013/932976

Parveez, G. K. A., Tarmizi, A. H. A., Sundram, S., Loh, S. K., Ong-Abdullah, M., Palam, K. D. P., Salleh, K. M., Ishak, S. M., & Idris, Z. (2021). Oil palm economic performance in Malaysia and R&D progress in 2020. *Journal of Oil palm Research*, *33(2)*, 181–214. https://doi.org/10.21894/jopr.2021.0026

Pusparizkita, Y. M., Aslan, C., Schmahl, W. W., Devianto, H., Harimawan, A., Setiadi, T., Ng, Y. J., Bayuseno, A. P., & Show, P. L. (2023). Microbiologically influenced corrosion of the ST-37 carbon steel tank by *Bacillus licheniformis* present in biodiesel blends. *Biomass and Bioenergy*, *168*, 106653. https://doi.org/10.1016/j.biombioe.2022.106653

Pusparizkita, Y. M., Schmahl, W., Setiadi, T., Ilsemann, B., Reich, M., Devianto, H., & Harimawan, A. (2020). Evaluation of bio-corrosion on carbon steel by *Bacillus megaterium* in biodiesel and diesel oil mixture. *Journal of Engineering and Technological Sciences*, *52*(3), 370–384. https://doi.org/10.5614/j.eng.technol.sci.2020.52.3.5

Ram, D. S., Kumar, P. N. B., Kumar, R. S., & Ramnath, B. V. (2020). Evaluation of mechanical properties of sugarcane reinforced hybrid natural fibre composites by conventional fabrication and finite element method. *Key Engineering Materials*, *841*, 327–334. https://doi.org/10.4028/www.scientific.net/kem.841.327

Rocha, J. G., Dos Santos, M. D. R., Madeira, F. B., Rocha, S., Bauerfeldt, G. F., Da Silva, W. L. G., Salomao, A. A., & Tubino, M. (2019). Influence of fatty acid methyl ester composition, acid value, and water content on metallic copper corrosion caused by biodiesel. *Journal of the Brazilian Chemical Society*, *30(8)*, 1751–1761. https://doi.org/10.21577/0103-5053.20190078

Samuel, O. D., & Gulum, M. (2019). Mechanical and corrosion properties of brass exposed to waste sunflower oil biodiesel-diesel fuel blends. *Chemical Engineering Communications*, *206*(5), 682–694. https://doi.org/10.1080/00986445.2018.1519508

Serqueira, D. S., Pereira, J. F., Squissato, A. L., Rodrigues, M. A., Lima, R. C., Faria, A. M., Richter, E. M., & Munoz, R. A. (2021).

Oxidative stability and corrosivity of biodiesel produced from residual cooking oil exposed to copper and carbon steel under simulated storage conditions: Dual effect of antioxidants. *Renewable Energy*, *164*, 1485–1495. https://doi.org/10.1016/j.renene.2020.10.097

Singh, S. K., Pandey, A., Islam, S. S., Ransingchung, G. R., & Ravindranath, S. S. (2020). Significance of frequency in quantifying the deterioration in the properties of SBS modified binders and rutting performance. *Construction and Building Materials*, *262*, 120872. https://doi.org/10.1016/j.conbuildmat.2020.120872

Thirumal, V., Mahato, N., Yoo, K., & Kim, J. (2023). High performance Li-ion battery-type hybrid supercapacitor devices using antimony based composite anode and Ketjen black carbon cathode. *Journal of Energy Storage*, *61*, 106756. https://doi.org/10.1016/j.est.2023.106756

Touazi, Y., Abdi, A., Leshaf, A., & Khimeche, K. (2020). Influence of heat treatment of iron oxide on its effectiveness as anticorrosion pigment in epoxy based coatings. *Progress in Organic Coatings*, *139*, 105458. https://doi.org/10.1016/j.porgcoat.2019.105458

Tsuchiya, T., Shiotani, H., Goto, S., Sugiyama, G., & Maeda, A. (2006). Japanese standards for diesel fuel containing 5% FAME: Investigation of acid generation in FAME blended diesel fuels and its impact on corrosion. *SAE Technical Paper Series, 2006-01-3303*. https://doi.org/10.4271/2006-01-3303

Wei, Z., Zandi, Y., Gholizadeh, M., Selmi, A., Roco-Videla, A., & Konbr, U. (2021). On the optimization of building energy, material, and economic management using soft computing. *Advances in Concrete Construction*, *11*(6), 455–468. https://doi.org/10.12989/acc.2021.11.6.455

Xue, J., Balamurugan, S., Li, T., Cai, J., Chen, T., Wang, X., Yang, W., & Li, H. (2021). Biotechnological approaches to enhance biofuel producing potential of microalgae. *Fuel*, *302*, 121169. https://doi.org/10.1016/j.fuel.2021.121169

Yi, C., Rostron, P., Vahdati, N., Gunister, E., & Alfantazi, A. (2018). Curing kinetics and mechanical properties of epoxy based coatings: The influence of added solvent. *Progress in Organic Coatings*, *124*, 165–174. https://doi.org/10.1016/j.porgcoat.2018.08.009

Yung, C. L., Jalil, N., Miyamoto, M., Sakamoto, S., Maruyama, K., Loh, S. K., & Lim, W. S. (2018). Compatibility of terne sheet with palm biodiesel blends. *Journal or Oil Palm Research, 30*(4), 655–665. https://doi.org/10.21894/jopr.2018.0036

Journal of Oil Palm Research Vol. 37 (3) September 2025 p. 421-429
DOI: https://doi.org/10.21894/jopr.2024.0020

EFFECT OF OIL PALM FROND UTILISATION AS GREEN ROUGHAGE FEED ON KATJANG GOAT'S BODY WEIGHT

MD ZAINAL RASYIDI MAT RODI[1]*; KAMIL AZMI TOHIRAN[1] and RAJA ZULKIFLI RAJA OMAR[1]

ABSTRACT

The impact of providing various types of fodders as the primary green feed for Katjang goats was assessed. Twelve male Katjang goats were divided into three groups and randomly assigned to three experimental diets: (1) oil palm frond (OPF) ad libitum*; (2) undergrowth (UG)* ad libitum*; and (3) Napier grass (NG)* ad libitum*. The results of this study indicated that the daily fresh intake of green roughage was significantly higher (*$p<0.05$*) in the UG treatment group than in the OPF and NG treatment groups. However, feeding green roughage from OPF is equivalent to increasing the body weight of goats compared to using UG and NG. OPF is the most considered because it is more cost-effective than NG, which must be planted and maintained. Furthermore, OPF is a by-product of oil palm cultivation, whereas UG is limited in oil palm areas. Therefore, OPF is recommended for use as green roughage feed for Katjang goat farming in oil palm agriculture.*

Keywords: Katjang, Napier grass, oil palm frond, roughage feed, undergrowth.

Received: 11 June 2023**; Accepted:** 29 December 2023**; Published online:** 13 March 2024.

INTRODUCTION

The Katjang goat is a meat-type goat breed that is native to Southeast Asia, including Malaysia, Indonesia, Thailand, Philippines, Taiwan and the Southwest Japan Islands (Devendra, 1983; Mohamad *et al*., 2018; Tsukahara *et al*., 2008). As an indigenous goat, this breed has the advantages of natural tolerance towards heat stress and diseases such as parasitic infestation (Ernie-Muneerah *et al*., 2010; Thukahara *et al*., 2008), which are believed to be inherited genetically (Pralomkarn & Boonsanit 2012). Devendra (1983) has highlighted the advantage of the Katjang goat, where it performs well under low levels of nutrition, which is highly anticipated in smallholder production systems. In many instances, incorporating native breeds is suggested to retain their unique adaptive qualities and ensure successful participation in goat production (Khandoker *et al*., 2016; Shrestha & Fahmy, 2005). The local indigenous Katjang goat is highly prolific but has a small body size and poor growth performance compared to exotic breeds such as the Boer goat. A study has been done by Predith *et al*. (2020) by cross-breeding Katjang and Boer, but it involves only minimal alternation with genetics and still requires access to sufficient feed and nutrients to ascertain their genetic potential. Even though breed improvement may be used to enhance livestock performance (Liu *et al*., 2022), it is time-consuming and expensive to apply, particularly for small farms.

Some researchers have highlighted the importance of management practices rather than breeds as the key success factor for goat production (Nor-Azlina *et al*., 2011). Improvements in livestock management methods may have a direct effect on the performance of animals. Feed management is one of the most crucial aspects of livestock management that ensures success (Liu *et al*., 2022). Therefore, more focus should be given to the management practices, specifically the feeding, that can be altered for improvement as required by goat farmers. Feeding management involves the provision of a roughage source as the main feed input for goats, which is normally

[1] Malaysian Palm Oil Board,
6, Persiaran Institusi, Bandar Baru Bangi,
43000 Kajang, Selangor, Malaysia.

* *Corresponding author e-mail: zainal.rasyidi@mpob.gov.my*

green forage such as natural grass, pasture, or improved pasture. Green roughage feed is the most important component since it is the primary source of energy for goats (Banakar *et al*., 2018). However, as a green roughage feed source, natural pasture paddocks are rare in this country, and their availability is extremely limited for goat grazing. Therefore, goat farmers in Malaysia need to grow improved pastures as a green roughage source for feeding large numbers of goats. Commonly planted improved pastures are Napier grass (NG) and some other grasses that have the potential to survive in the long term, such as *Stenotaphrum secundatum*, *Panicum laxum*, *Paspalum notatum*, *P. wettsteinii*, *Brachiaria humidicola* and *Panicum maximum* (Ng *et al*., 1997). NG and *B. humidicola* are the two improved pastures that are popularly grown by farmers as green roughage feed for feeding ruminant livestock through the cut-and-carry system. However, growing the improved pastures involves higher costs in terms of paddock establishment, maintenance and harvesting, which are less affordable, specifically for small farmers or smallholders. Growing improved pastures for feeding goats does not look viable from an economic and profitability point of view. Therefore, alternative green roughage feeds that are technically and economically viable should be established to support goat farming development in Malaysia.

As an alternative, goat farmers may shift to using agriculture by-products as roughage feed for goat farming. Oil palm fronds (OPF) are one of the agriculture by-products that are abundantly available for use as green roughage feed, especially for goat farming in the oil palm industry. It is estimated that this country's annual harvest of OPF totals at 50 million tonnes (Tafsin *et al*., 2019). After harvesting, almost all these OPF are arranged in the frond stacking rows for nutrient recycling (Abu Hassan & Ishida, 1992). The abundance of OPF in this country has resulted in a major interest in its potential use as ruminant livestock feed. Several studies found that OPF can be used successfully as a viable ruminant livestock forage source (Ghani *et al*., 2017). Previous studies have shown that OPF is suitable for use as feed for ruminants, especially cattle (Ghani *et al*., 2017). However, the optimum inclusion of OPF in the diet ratio for beef and dairy cattle should not exceed 30% (Wong & Wan Zahari, 2011) for optimal growth, body weight gain and milk production. Nevertheless, study findings regarding OPF utilisation as the main green roughage source and its effect as feed on small ruminants, especially goats, are extremely limited. Therefore, this study was carried out to determine the suitability of OPF as a source of green roughage feed for goat farming in the oil palm agriculture system.

MATERIALS AND METHODS

Study Site and Experimental Diets

This study was carried out at the MPOB Research Station in Keratong (2° 77′ N latitude and 102° 91′ E longitude), Pahang, Malaysia. The care of livestock was carried out according to the guidelines established by the Department of Veterinary Services (DVS), Malaysia (DVS, 1992). Fresh OPF from harvesting activities of fresh fruit bunches (FFB) were collected daily at the station in the oil palm plantation. Only half of the OPF in the upper part was taken as the green roughage feed for goats in this trial. NG was planted in between rows of the Double Avenue oil palm planting area. NG was harvested daily from different plots in the trial plot. It was harvested at 45-50 day intervals to obtain similar quality throughout the experimental period. The NG plots were fertilised using 200 kg of compound NPK 15:15:15 fertiliser and 75 kg of urea fertiliser/ha annually. Undergrowth (UG) was harvested from oil palm planting areas in the station daily. No herbicide spray was permitted in the oil palm planting areas allocated for UG collection. Green roughage feeds of OPF, NG and UG were managed following a cut-and-carry system for feeding goats in the goat house. The OPF, NG, and UG were chopped into 5-7 cm lengths using a chopper machine. The chopped materials were fed to the goats on a fresh basis according to the diet treatments. Commercial soyhull pellets as a supplemental feed for goats in this trial were supplied by an appointed supplier every month.

Management of Animals

Goats for this study were selected from an available stock at the MPOB Research Station in Keratong, Pahang, Malaysia. Twelve males of the Katjang goat breed, aged between 13 and 15 months, were used in this feeding trial. The initial body weight of goats falls within the range of 15-25 kg. Goats were individually weighed and divided into three groups with an approximately similar total weight. Goats were familiarised with the feeding management for 14 days before the start of the actual feeding trial and data collection. Each group was fed a specific green roughage feed diet treatment (*ad libitum*) and supplemented with commercial soyhull pellets at 200 g/day/ahead (Zainal Rasyidi *et al*., 2019). The feeding trial was carried out for 95 days after a 14-day adaptation period. Three green roughage feed diet treatments were tested on goats in this trial as follows: Treatment 1 - OPF, Treatment 2 - NG and Treatment 3 - UG. All goats were supplemented at 3.0% of body weight (BW) in dry matter (DM) intake,

based on the maximum body weight gain per day. These green roughage feeds were fed *ad libitum* to the respective groups, normally about 130.0% of the average fresh intake of the previous day, twice daily (morning and afternoon). A supplemental feed of soy hull pellets was fed to all goats once in the morning before their green roughage diet treatment. The nutritional composition of soy hulls includes 26.2% crude protein, 8.8% crude fat, 22.8% crude fibre, 64.2% total digestible nutrients and metabolic energy content is 9.68 MJ/kg. For internal parasite control, all goats were dewormed prior to the feeding trial using Ivermectin according to the prescription by the product's manufacturer (Merial Limited, Duluth, GA 30096, USA). The goats were penned separately according to the specific diet treatment group. Clean water and mineral blocks were made available at all times in the pens.

Feed Intake and Body Weight Change

The intake of green roughage feed by goats was measured by weighing the amount of feed offered and the amount of feed balance refused by individual goats. Remnants of green roughages (refusal feed) were collected and weighed every morning before feeding the supplemental feed. The difference between the amount of green roughage offered and the amount of remaining green roughage is the quantity of green roughage fed to the goats. The dry matter intake of roughage feed was calculated by multiplying the intake of green roughage feed by the percentage of dry matter in the respective green roughage feed. The body weight changes in goats in response to the different green roughage feed diet treatments were measured by taking each individual goat's initial body weight before the start of the feeding trial. Then, it was followed by weighing an individual goat on a monthly basis until the end of the feeding trial period (Upreti *et al*., 2008). The final weight of the goats was taken on day 95. The difference between the goat's final live weight and initial live weight divided by the number of days of the feeding trial served as the basis for calculating average daily weight gain (ADG).

Feed Sampling and Analysis

Green roughage feeds were sampled on a biweekly basis. Samples were dried in an oven at 70°C for two days or until a constant weight was reached. The dry matter content of the green roughages was calculated by dividing the sample's oven-dry weight by the sample's fresh weight. The value was then converted to a percentage. The dried samples were prepared for analysis by grinding with a mill and sieving through a 1 mm sieve. Ground composite samples were analysed following the method of the Association of Official Analytical Chemists (AOAC, 1990) for dry matter, ash, and nitrogen (N). Crude protein was calculated by multiplying N by 6.25 (N x 6.25). Fibre fractionation analysis was conducted using the Goering and Van Soest's method (1970). Metals analysis was done with an atomic absorption spectrophotometer, and phosphorus was analysed using the Molybdate-metavanadate complex method. Crude fat was measured after being treated by boiling with diluted sulphuric acid. The total digestible nutrient was determined according to McDowell *et al*. (1974). Metabolisable energy was analysed using Menke's "Gas Test" methods (1979).

Statistical Analysis

Data on feed intake and body weight changes were analysed using SAS (version 9.2, SAS Institute Inc., Cary, NC, USA). An analysis of variance was performed, and mean values were tested for differences between treatments with the least significant difference using Duncan's Multiple Range Test (DMRT).

RESULTS AND DISCUSSION

Nutritional Composition Oil Palm Fronds (OPF), Napier Grass (NG) and Undergrowth (UG)

Other than concentrates, vitamins, and minerals, forage is the most important feed component for ruminants to meet their daily nutritional needs. In this study, the nutrient content of OPF, natural UG, and NG, three commonly used forage sources by oil palm growers in livestock farming, was evaluated. *Table 1* presents a summary of these nutritional analysis findings. The dry matter of OPF was 43%. It was higher than NG and UG. However, NG and UG had a similar dry matter percentage (13%). For nutritional content, OPF had lower crude protein (7%) compared to NG and UG, which contained an approximately similar percentage of crude protein (11%). The fibre content of OPF (37%) was also higher than that of NG (34%) and UG (31%). Total digestible nutrients of OPF (52%) were lower than those of NG (61%) and UG (60%). Meanwhile, metabolisable energy was also slightly lower in OPF compared to those of NG and UG. Overall, OPF had slightly lower nutritional attributes as goat feed compared to NG and UG. However, UG and NG had about the same nutritional level.

The most important nutrient discussed and concerned about is the protein content of a feedstuff. Protein is required for all forms of life, including animals and plants. Ruminant animals can utilise urea or plants with poor protein and carbohydrate quality for growth, wool production,

TABLE 1. NUTRITIONAL COMPOSITION (%, DRY MATTER)

Parameter	OPF	NG	UG
Dry matter (DM), %	43.00	13.00	13.00
Crude protein (N x 6.25), %	7.20	11.10	11.50
Crude fat, %	1.33	0.90	0.97
Crude fibre, %	37.07	33.73	31.57
Ash content, %	5.27	9.93	9.27
Calcium (Ca), %	0.27	0.23	0.17
Phosphorous (P), %	0.10	0.10	0.08
Total digestible nutrient (TDN), %	52.30	60.50	60.33
Metabolisable energy, MJ/kg DM	7.74	9.24	9.04

Note: OPF - oil palm frond; NG - Napier grass; UG - undergrowth.

and milk production. This process is performed by rumen microbes that may use urea nitrogen, inorganic nitrogen, or nitrogen from low-quality plant proteins for their own needs. Among the three green roughage feed sources examined in this study, OPF contained the least amount of crude protein (average: 7.2%). The findings of this study also indicated that the UG vegetation (average: 11.5%) and NG (average: 11.1%) had better crude protein content compared to OPF (*Table 1*). Dahlan *et al*. (1992) reported a leaflet crude protein content of 11.0%, while Zainal *et al*. (2016) observed an even higher crude protein content in leaflets, reaching 12.3%. These values fall within the range of crude protein typically quantified for UG vegetation, which spans from 11.5%-16.3%. The National Research Council (NRC) suggests that a modest range of 11.0%-14.0% crude protein is recommended for ruminant production (NRC, 2007). In line with this, Devendra and McLeroy (1982) noted that 11.0% crude protein is considered ideal for achieving normal weight gain in goats, as reported by Bamigboye *et al*. (2013). To overcome the issue of low crude protein in OPF, one strategy is to utilise the upper one-third portion of the OPF, which contains more leaflets. This can contribute to an increased protein content in the overall feed.

In this study, TDN values in the OPF diet treatment (average: 52.30%) were lower than those in the NG (average: 60.50%) and UG (average: 60.33%) diet treatments, respectively (*Table 1*). The difference in TDN value was about 8.00% lower in OPF compared to NG and UG. Otherwise, NG and UG had about the same amount of TDN. The TDN value indicates the energy that can be extracted from feedstuffs and is a crucial factor in determining the amount of energy provided to animals. According to Jayanegara *et al*. (2019), there is a negative association between TDN values and neutral detergent fibre and lignin concentration. OPF contain a higher level of neutral detergent fibre (NDF), indicating a greater presence of structural carbohydrates compared to NG and UG. This contributes to a lower TDN in OPF. Akmar *et al*. (1996) reported that OPF are more in lignin and silica, contributing to a reduction in their nutritive value when utilised as feed for ruminants. Lignin, known for its resistance to degradation, poses a challenge as it is not readily digestible by most animals. Therefore, providing feed with highly neutral detergent fibre and lignin content is ineffective as an energy source for animals. The quantity of fibre and lignin in plants is contingent on the plant type and age. Research by Imsya *et al.* (2013) indicates that, in comparison to NG, OPF generally exhibit higher lignin content. Additionally, as plants age, there is a tendency for fibre content to increase.

Nutritionally, fibre contributes to the physical and chemical functions of the ruminant digestive system, involving chewing activity and enzymatic degradation through the fermentation process (Banakar *et al*., 2018). The process of chewing determines the amount of saliva produced for digestion, and it is influenced by the type of forage, the forage-to-concentrate ratio, forage intake, and the physiological status of livestock (Banakar *et al*., 2018). OPF have a slightly higher crude fibre content (average: 37.07%), followed by NG (average: 33.73%) and UG (average: 31.57%). According to the findings of Haji Baba *et al*. (1998), crude fibre content was adequate for the growth of goats. Lu *et al.* (2005) recommend a diet with a crude fibre content exceeding 23.00% for the optimal growth of goats. In general, the results of this study indicated that OPF had lower nutritional attributes compared to NG and UG - Improving the performance of OPF can be achieved through physical processing, employing mechanical methods such as chopping, grinding, or shredding to reduce particle size. This enhances digestibility, making OPF more palatable for livestock. Additionally, chemical treatments, such as exploring alkaline or ammonia treatments, can be employed to break down lignin and enhance the nutritional quality of OPF.

Factors Affecting Feed Intake

In contrast, the daily dry matter intake of roughage feed was significantly higher for the OPF diet treatment compared to those of the NG and UG diet treatments (*Table 2*). Dry matter intake was 2-3 times higher for the OPF treatment compared to the NG and UG diet treatments. However, the NG and UG intakes were not significantly different. Supplemental feed was readily consumed by all goats without any balance. Therefore, the feed's total dry matter intake was significantly higher for the OPF treatment. It was two times higher than those of the NG and UG diet treatments.

The level of feed palatability reflects the level of feed intake by livestock. The higher the palatability of the feed, the higher the feed intake. In this study, fresh feed intake of green roughage by the goats for the UG diet treatment (average: 3.24 kg/day) was significantly higher (p<0.05) compared to NG (average: 2.63 kg/day) and OPF (2.68 kg/day) diet treatments, whereas the intake of fresh NG was similar to that of the OPF. A significantly higher intake of UG vegetation could be due to the higher palatability of the UG, which improved intake compared to other treatment diets. The higher palatability of UG could be due to the varieties of underbrush vegetation species that comprise the diet treatment. UG in this study consists of a combination of grasses and foliage such as *Asystasia gigantica*, *Paspalum conjugatum*, *Fimbristylis miliacea*, *Ageratum haustonianum*, and *Cleome pentaphyll*. The variety of grass and foliage types offers freedom of choice and increases the rate of feed intake (Fedele *et al*., 2002). *Asystasia gigantica* is the most preferred foliage by goats that graze in oil palm planting areas (Nobilly *et al*., 2021). Norlindawati *et al*. (2019) revealed that the crude protein content of *A. gigantica* ranged from 19.0%-21.9%.

In contrast, the other two treatments have only one type of green roughage that is similar in palatability. The similar palatability of NG or OPF might limit the goats' daily fresh intake of that feed. According to Kalio *et al*. (2006), plant species, presentation style, stage of maturity, processing techniques, and the chemical components of the fodder, all affect the intake of forage. The level of anti-nutritional factors such as tannins may also affect the palatability of forages and hence the animals' preferences. The smell of the foliage also influences the intake of green roughage. Tannins are one of the chemical compounds in foliage that influence the smell and are known to reduce palatability and intake by ruminants (Mueller-Harvey, 2006). The OPF contains a high level of tannins (Jaffri *et al*., 2011) and is also high in NG (Johnson & Chime, 2018). Tannins act as a defence mechanism in plants against pathogens, herbivores and hostile environmental conditions. Tannin in the feed usually reduces feed intake in ruminant animals. Tannins may reduce intake by decreasing palatability.

Palatability, which depends on both plant and animal factors, influences the choice of feed. Among the plant characteristics that affect palatability are species, intraspecific variation, chemical composition, morphology or physical characteristics, succulence or maturation, and forage shape. Chemical composition such as phenolics, alkaloids, and tannins, irrespective of the nutritional value of the feed (Marten, 1978). Animal elements include the senses, breeds, species, individual variance, previous exposures, and physiological state (Marten, 1978). According to Personius *et al*. (1987), herbivores are able to identify some harmful substances by scent before eating or just after the first bite. Flavour (taste and odour) is thought to be the most significant food sign. The inclusion of taste, smell, or texture in the assessment implies that these sensory factors may play a significant role in determining the palatability of each feed, as noted by Ngwa *et al*. (2003).

Effect of Oil Palm Fronds (OPF)on Body Weight Gain

Feed intake has a direct effect on body weight gain in livestock under a feeding trial. Different diet treatments may have different effects on body weight gain in goats. Showed that, although it is

TABLE 2. DAILY DRY MATTER INTAKE OF FEED BASED ON DIFFERENT DIETS

Treatment	Roughage (g/day/head)	Supplemental feed (g/day/head)	Total feed intake (g/day/head)
Oil palm fronds (OPF)	1,152.30[a]	180.00[a]	1,332.30[a]
Napier grass (NG)	368.35[b]	180.00[a]	548.35[b]
Undergrowth (UG)	420.92[b]	180.00[a]	600.92[b]
$LSD_{(0.05)}$	59.71	0	59.71
$CV_{(\%)}$	31.25	0	24.45

Note: Mean values in the same column with a similar superscript are not significantly different at p<0.05 (Duncan's Multiple Range Test (DMRT).

not significantly different, numerically the UG-fed goats had the highest body weight gain (average: 5.33 kg), followed by goats in NG (average: 4.50 kg) and OPF (average: 4.33 kg) diet treatments (*Table 3*). The difference in body weight gain was 1.0 kg higher for the UG diet treatment compared to that of the OPF diet treatment. The goats in the NG diet treatment had a 0.83 kg higher body weight gain compared to those in the OPF diet treatment (*Table 3*). However, the difference in body weight gain of the goats in this study did not differ significantly between diet treatment groups. Similarly, goats in the UG diet treatment showed a daily weight gain of 56.00 g/day compared to those in the NG (47.33 g/day) and the OPF diet treatments (45.67 g/day), respectively. These average daily weight gains were also not significantly different between goats in diet treatment groups at $p< 0.05$ (*Table 4*).

Farming ruminant livestock in oil palm planting areas is a good approach for increasing domestic livestock production by maximising the usage of oil palm land and its natural resources. UG or understory vegetation in oil palm planting areas is a vital natural source of green roughage feed for ruminant livestock rearing in oil palm planting areas. Cattle, goats and sheep can graze on the UG vegetation available in oil palm planting areas for their daily feed requirements. Grassing of ruminants in oil palm planting areas is normally carried out following a continuous grazing system or a rotational grazing system. A free grazing practice is also carried out, especially by oil palm smallholders. Grazing livestock in oil palm planting areas can reduce production costs for feed, especially roughage feed. This, will in turn improve the overall economic return from the livestock production system.

Success in livestock integration with oil palm also largely depends on the availability of good UG as a green roughage feed source. Sometimes, the availability of UG vegetation for livestock grazing is affected by several factors, such as herbicide spraying activity, oil palm age, drought, flooding, and replanting programmes. Contaminated UG caused by herbicide spraying is fatal to livestock when grazed. Old oil palm areas and the drought season can also reduce the growth rate and dry matter yield of UG vegetation for livestock. Meanwhile, flooding and replanting programmes may require the livestock to be relocated to other suitable areas. Therefore, alternatives should be sought to overcome these limitations that affect the rearing of livestock in an oil palm ecosystem.

Goats grazing in the oil palm ecosystem usually face the problem of insufficient green forage where UG limitations are caused by problems such as floods, droughts, and the effects of oil palm management programmes such as weeding, replanting, *etc*. Therefore, a wider grazing area is needed since the goats are vulnerable to predators, the threat of grazing poisonous weeds, and eating rodenticide, all of which can directly cause death to the goats. The UG's cut-and-carry system is less effective due to the difficulty of harvesting the diverse and uneven UG, leading to a longer harvest time. Meanwhile, green roughage from NG requires a suitable area to be planted and needs to be maintained from time to time in open areas, which costs more. Therefore, with the existence of available green roughage feed sources in the oil palm planting areas, such as OPF, which can also be considered agricultural product waste, there are alternatives for farmers seeking a cost-effective source of green roughage. Although OPF has a low nutritional value compared to UG and NG, OPF feed provides an almost similar body weight gain effect as using UG and NG did not make a significant difference.

CONCLUSION

OPF is abundant and available year-round as agricultural waste in oil palm planting areas and is the alternative for farmers seeking a cost-effective source of green roughage feed. A comparison has been made in this study by using UG and NG as a control, and it was found that the effect of daily weight gain is not significant, whereas the effect of weight gain is almost equivalent for Katjang goats for all three green roughages used in this study. Therefore, goat farmers, especially

TABLE 3. BODY WEIGHT CHANGE OF GOATS FED DIFFERENT GREEN ROUGHAGE DIETS

Treatment diet group	Initial weight (kg)	1st month weight (kg)	2nd month weight (kg)	Final weight (kg)	Difference in BW (kg)	ADG (g/day)
Oil palm fronds (OPF)	19.33[a]	21.67[a]	22.67[a]	23.67[a]	4.33[a]	45.67[a]
Napier grass (NG)	17.00[a]	19.17[a]	21.50[a]	21.50[a]	4.50[a]	47.33[a]
Undergrowth (UG)	18.67[a]	20.83[a]	22.83[a]	24.00[a]	5.33[a]	56.00[a]
$LSD_{(0.05)}$	7.45	10.27	11.01	11.77	4.95	52.06
$CV_{(\%)}$	20.33	25.00	24.68	25.55	52.47	52.46

Note: Mean values in the same column with a similar superscript are not significantly different at $p<0.05$ (Duncan's Multiple Range Test (DMRT). BW - body weight; ADG - average daily weight.

TABLE 4. BODY WEIGHT CHANGE OF GOATS FED WITH OIL PALM FROND (OPF), NAPIER GRASS (NG) AND UNDERGROWTH (UG)

Parameter	Diets		
	OPF	NG	UG
Initial body weight (kg)	19.33 [a]	17.00 [a]	18.67 [a]
Final body weight (kg)	23.67 [a]	21.50 [a]	24.00 [a]
Body weight gain (g/day)	45.67 [a]	47.33 [a]	56.00 [a]
Gain to feed ratio	0.034 [b]	0.086 [a]	0.093 [a]

Note: Mean values in the same row having a similar superscript are not significantly different at $p<0.05$.

oil palm growers, should embrace OPF as an untapped green roughage resource that produces a similar effect on livestock performance as other commonly planted roughage such as NG. Indeed, the current era presents an opportunity to champion sustainable agriculture practices. Advocacy for the heightened utilisation of OPF is crucial in this context. This entails maximising OPF usage while concurrently minimising its environmental impact.

ACKNOWLEDGEMENT

The authors would like to thank the Director-General of MPOB for permission to publish this article. We would also like to acknowledge all staff members of the Crop and Livestock Integration Unit for their assistance in carrying out this project. Last but not least, thank you to all the contributors.

REFERENCES

Abu Hassan, O., & Ishida, M (1992). Status of utilization of selected fibrous crop residues and animal performance with emphasis on processing of oil palm frond (OPF) for ruminant feed in Malaysia. *Tropical Agriculture Research Series: Proceeding of a Symposium on Tropical Agriculture Researches, 25*, 134-143.

Asada, T., Konno, T., & Saito, T. (1991). Study on the conversion of oil palm leaves and petioles into feeds for ruminants. In *Proceeding of the Third International Symposium on the Nutrition of Herbivores* (p. 104).

Association of Official Analytical Chemists (AOAC) (1990). *Official methods of analysis. 15th edition.* AOAC.

Astuti, T., Santoso, U., & Amir, Y. (2017). Nutritional value of fermented palm oil fronds as a basis for complete feed for ruminants. *Pakistan Journal of Nutrition*, *16*(2), 96–100. https://doi.org/10.3923/pjn.2017.96.100

Banakar, P. S., Kumar, N. A., Shashank, C. G., & Lakhani, N. (2018). Physically effective fibre in ruminant nutrition: A review. *Journal of Pharmacognosy and Phytochemistry, 7*(4), 303–308.

Bamigboye, F., Babayemi, O., & Adekoya, A. (2013). Feed resources and seasonal nutrient composition of predominant forages for small ruminant production in Iwo local government area of Osun State, Nigeria. *Journal of Biology, Agriculture and Healthcare*, *3*(17), 15–24.

Dahlan, I. (1992). The nutritive values and utilization of oil palm leaves as a fibrous feed for goat and sheep. In C. Reodecha & P. Bunvaveichewin (Eds.), *Proceedings of the Sixth Asian-Australasian Association of Animal Production: Animal Science Congress on Recent Advances in Animal Production, 3*, 271.

Department of Veterinary Services of Malaysia (DVS). (1992). *Panduan penternakan kambing, bingkisan penternakan* [Goat farming guide, farming gift pack].

Devendra, C. (1983). The energy and protein requirements during pregnancy of Katjang goats in Malaysia. *Mardi Research Bulletin*, *11*(2), 193–205.

Devendra, C., & McLeroy, G. B. (1982). *Goats and sheep production in the tropics*. Longman.

Ernie-Muneerah, M. A., Salleh, S. I., Raymond, A. K., Zawawi, I., Hafiz, A. R., Kamarulrizal, M. I., Hafizal, A. M., Kamaruddin, M. I., & Abu Hassan, M. A. (2010). *Development of Katjang goat conservation centre.* https://research.dvs.gov.my/ral/wp-content/uploads/2022/02/201020AgBioDConf2010-Katjang2.pdf

Fedele, V., Claps, S., Rubino, R., Calandrelli, M., & Pilla, A. M. (2002). Effect of free-choice and traditional feeding systems on goat feeding behaviour and intake. *Livestock Production Science*, *74*(1), 19–31. https://doi.org/10.1016/s0301-6226(01)00285-8

Ghani, A. A. A., Rusli, N. D., Shahudin, M. S., Goh, Y. M., Zamri-Saad, M., Hafandi, A. & Hassim, H. A. (2017). Utilisation of oil palm fronds as ruminant feed and its effect on fatty acid metabolism. *Pertanika Journal: Tropical Agricultural Science, 40(2)*, 215–224.

Goering, K. H., & Van Soest, P. J. (1970). *Forage fibre analysis (apparatus, reagents, procedures, and some application)*. United States Department of Agriculture.

Haji Baba, A. S., Azillah, A., Mukherjee, T. K., & Abdullah, R. B. (1998). Growth and reproductive performance of small ruminants under intergrated livestock-oil palm production system. *Asian-Australasian Journal of Animal Sciences*, *11*(5), 573–579. https://doi.org/10.5713/ajas.1998.573

Imsya, A., Laconi, E. B., Wiryawan, K. G., & Widyastuti, Y. (2013). *In vitro* digestibility of ration containing different level of palm oil frond fermented with *Phanerochaetae chrysosporium*. *Media Peternakan*, *36*(2), 131–136. https://doi.org/10.5398/medpet.2013.36.2.131

Jaffri, J. M., Mohamed, S., Ahmad, I. N., Mustapha, N. M., Manap, Y. A., & Rohimi, N. (2011). Effects of catechin-rich oil palm leaf extract on normal and hypertensive rats' kidney and liver. *Food Chemistry*, *128*(2), 433–441. https://doi.org/10.1016/j.foodchem.2011.03.050

Jayanegara, A., Ridla, M., Nahrowi, N., & Laconi, E. B. (2019). Estimation and validation of total digestible nutrient values of forage and concentrate feedstuffs. *IOP Conference Series Materials Science and Engineering*, *546*(4), 042016. https://doi.org/10.1088/1757-899x/546/4/042016

Johnson-Ajinwo, O. R., & Chime, J. (2018). Mineral content and chemical composition of Napier (*Pennisetum purpureum*) grass. *Saudi Journal of Medical and Pharmaceutical Sciences*, *4*(4), 382–386.

Kalio, G. A., Oji, U. I., & Larbi, A. (2006). Preference and palatability of indigenous and exotic acid soil-tolerant multipurpose trees and shrubs by West African dwarf sheep. *Agroforestry Systems*, *67*(2), 123–128. https://doi.org/10.1007/s10457-005-4278-z

Khandoker, M. A. M. Y., Syafiee, M., & Rahman, M. S. R. (2016). Morphometric characterization of Katjang goat of Malaysia. *Bangladesh Journal of Animal Science*, *45*(3), 17–24.

Liu, Y., Li, R., Ying, Y., Zhang, Y., Huang, Y., Wu, H., & Lin, K. (2022). Non-genetic factors affecting the meat quality and flavor of Inner Mongolian lambs: A review. *Frontiers in Veterinary Science*, *9*, 1067880. https://doi.org/10.3389/fvets.2022.1067880

Lu, C., Kawas, J., & Mahgoub, O. (2005). Fibre digestion and utilization in goats. *Small Ruminant Research*, *60*(1–2), 45–52. https://doi.org/10.1016/j.smallrumres.2005.06.035

Marten, G. C. (1978). The animal-plant complex in forage palatability phenomena. *Journal of Animal Science*, *46*(5), 1470–1477. https://doi.org/10.2527/jas1978.4651470x

McDowell, L. R., Conrad, J. E., Thomas, J. E., & Harris, L. E. (1974). *Latin American tables of feed composition*. University of Florida.

Menke, K. H., Raab, L., Salewski, A., Steingass, H., Fritz, D., & Schneider, W. (1979). The estimation of the digestibility and metabolizable energy content of ruminant feedingstuffs from the gas production when they are incubated with rumen liquor *in vitro*. *The Journal of Agricultural Science*, *93*(1), 217–222. https://doi.org/10.1017/s0021859600086305

Mohamad, H. R., Nor Amma, A. M., Izuan, B. A. J., Arnie Marini, A. B., & Mohd Hafiz, A. W. (2018). *Manipulating of Katjang goat genetic material for sustainable goat industry in Malaysia.* FFTC Agricultural Policy Platform (FFTC-AP). Retrieved August 14, 2019 from https://ap.fftc.org.tw/article/1364

Mueller-Harvey, I. (2006). Unravelling the conundrum of tannins in animal nutrition and health. *Journal of the Science of Food and Agriculture*, *86*(13), 2010–2037. https://doi.org/10.1002/jsfa.2577

National Research Council (NRC). (2007). *Nutrient requirements of small ruminants: Sheep, goats, cervids, and new world camelids.* National Academies Science Engineering Medicine.

Ng, K. F., Stür, W. W., & Shelton, H. M. (1997). New forage species for integration of sheep in rubber plantations. *The Journal of Agricultural Science*, *128*(3), 347–356. https://doi.org/10.1017/s0021859696004248

Ngwa, A. T., Nsahlai, I. V., & Bonsi, M. L. K. (2003). Feed intake and dietary preferences of sheep and goats offered hay and legume-tree pods in South Africa. *Agroforestry Systems*, *57*, 29–37.

Nobilly, F., Atikah, S. N., Yahya, M. S., Jusoh, S., Cun, G. S., Norhisham, A. R., Tohiran, K. A., Zulkifli, R., & Azhar, B. (2022). Rotational cattle grazing improves understory vegetation biodiversity and structural complexity in oil palm plantations. *Weed Biology and Management*, *22*(1), 13–26. https://doi.org/10.1111/wbm.12246

Norlindawati, A. P., Haryani, H., Sabariah, B., Noor, M. I., Samijah, A., Supie, M. J. & Edham, A. Z. W. (2019). Chemical composition of weeds as potential forage in integrated farming. *Malaysia Journal of Veterinary Research, 10*(2), 19–24.

Nor-Azlina, A. A., Sani, R. A. & Ariff, O. M. (2011). Management practices affecting helminthiasis in goats. *Pertanika Journal of Tropical Agricultural Science, 34*(2), 295–301.

Personius, T. L., Wambolt, C. L., Stephens, J. R., & Kelsey, R. G. (1987). Crude terpenoid influence on mule deer preference for sagebrush. *Journal of Range Management*, *40*(1), 84–88. https://doi.org/10.2307/3899368

Pralomkarn, W., & Boonsanit, D. (2012). Knowledge in goats in Thailand. *Walailak Journal of Science and Technology, 9*(2), 93–105.

Predith, M., Shanmugavelu, S., Hifzan, R. M., & Mohd Hafiz, A. W. (2020). Pre-weaning growth performance of F1 and F2 Katjang-Boer crossbreds fed formulated creep feed. *Malaysian Journal of Animal Science, 23*(2), 62–71.

Shrestha, J., & Fahmy, M. (2003). Breeding goats for meat production: A review. *Small Ruminant Research*, *58*(2), 93–106. https://doi.org/10.1016/s0921-4488(03)00183-4

Tafsin, M., Hanafi, N. D., Yunilas, N., & Mulianda, R. (2019). Nutrient quality of oil palm frond fermented by local microorganism (MOL) with different dosage and incubation time. *IOP Conference Series Earth and Environmental Science*, *260*(1), 012050. https://doi.org/10.1088/1755-1315/260/1/012050

Tsukahara, Y., Chomei, Y., Oishi, K., Kahi, A., Panandam, J., Mukherjee, T., & Hirooka, H. (2008). Analysis of growth patterns in purebred Kambing Katjang goat and its crosses with the German Fawn. *Small Ruminant Research*, *80*(1–3), 8–15. https://doi.org/10.1016/j.smallrumres.2008.07.030

Upreti, C. R., & Orden, E. A. (1970). Effect of rice bran and *Leucaena* supplementation on the growth performance of goats fed with urea treated rice straw. *Nepal Journal of Science and Technology*, *9*, 29–36. https://doi.org/10.3126/njst.v9i0.3161

Wong, H. K., & Wan Zahari, M. (2011). Utilisation of oil palm by-products as ruminant feed in Malaysia. *Journal of Oil Palm Research, 23*(2), 1029–1035.

Zainal Rasyidi, M. R., Kamil, A. T., & Raja Zulkifli, R. O. (2016). Intensive integration of Katjang goat in oil palm area. *MPOB Information Series No. 719*.

Zainal Rasyidi, M. R., Kamil, A. T., & Raja Zulkifli, R. O. (2019). *Intensive integration of Katjang goat in oil palm plantation* [Viva No. 990/2019(72)]. Malaysian Palm Oil Board.

Journal of Oil Palm Research Vol. 37 (3) September 2025 p. 430-440
DOI: https://doi.org/10.21894/jopr.2024.0026

STUDY ON THE EFFECT OF VARIOUS TYPES OF FERTILISER ON THE PRODUCTION OF OIL PALM ROOT CUTTING

CECEP IJANG WAHYUDIN[1]; HARIYADI[1]*; SUDRAJAT[1]; SUDIRMAN YAHYA[1] and SYAIFUL ANWAR[2]

ABSTRACT

In the context of Indonesia, the cultivation of oil palm (Elaeis guineensis) *is extremely significant and the application of diverse fertiliser variants can affect crop yield through the implementation of root-cutting methods. The modification of root morphology is also a strategy to address the issue of suboptimal nutrient uptake and soil physical properties exert a significant influence on the development. Therefore, this study used a nested plot design as the main plot, comprising plants aged 7, 12 and 16 years. The subplots were demarcated by fertiliser types, including control (no fertilisation), single fertiliser potassium (K) (2.25 kg KCl/tree), palm frond litter (65 kg/tree) and empty fruit bunches (65 kg/tree). Furthermore, the treatment was replicated four times, resulting in a total of 48 experimental units. The results showed that plants aged 7 years exhibited the most robust growth compared to 12 and 16 years, across all fertiliser types, as indicated by stem circumference, stem diameter, and NDVI values. Regarding the primary, secondary, and tertiary optimal root distribution, 7 year old plants responded to K fertiliser. However, tertiary distribution did not significantly differ from 12 year-old plants when K fertiliser was applied. The nutrient levels in 7 and 12 years old plants varied in terms of pH, organic carbon (C-organic), and K.*

Keywords: fertility soil, oil palm, root cutting.

Received: 20 July 2023; **Accepted:** 29 December 2023; **Published online:** 4 April 2024.

INTRODUCTION

Oil palm (*Elaeis guineensis* Jacq.) is a significant plantation crop in the agricultural sector. Among different oil-producing plants, it holds economic value as a foreign exchange source and Indonesia, Malaysia, and Thailand are the world's largest producers. Several activities are conducted to enhance palm oil production, including expansion, rehabilitation of existing plantations, and intensification (Nurcahyo & Arian, 2017). Fertilisation can be applied to oil palm plants subjected to root pruning to improve their production and quality.

[1] Department of Agronomy and Horticulture, IPB University, Bogor, 16680 Indonesia.

[2] Department of Soil Science and Land Resources, Faculty of Agriculture, IPB University, Bogor, 16680 Indonesia.

* *Corresponding author e-mail: hariyadibdp@apps.ipb.ac.id*

Root pruning can result in drought stress for plants due to disrupted nutrient and water absorption. It can also inhibit stem and shoot diameter growth (Fini *et al.*, 2015; Watson, 1998). However, root pruning enhances plant nutrient uptake through morphological and physiological mechanisms. Morphological mechanisms include root hair distribution and formation, where cutting roots stimulate the growth of new ones at the cut ends (Miller & Neely, 1993). Root pruning increases the percentage of dry-weight growth and root dry weight in oil palms (Raharjo *et al.*, 2017). Physiological mechanisms for improving nutrient uptake through root include root kinetics and nutrient mobilisation through root exudation (Rao *et al.*, 1999). Root pruning is performed on different plants with varying distances from the stem, pruning depth, and intensity. In the case of oil palm, it possesses a fibrous root system, with tertiary and quaternary roots playing a crucial role in nutrient and water absorption (Yahya *et al.*, 2010). This condition

leads to changes in organic acids expressed by roots as plants adapt to enhance nutrient uptake and optimise the absorption of essential nutrients when provided with the right types of fertiliser.

The application of fertiliser can enhance the production and quality of root-pruned plants. Proper application provides the necessary nutrients for optimal growth and development of plants. Previous studies have shown that providing fertiliser with the appropriate concentration, composition, and dosage can increase plant productivity. One nutrient that aids in plant recovery after drought stress is potassium, enhancing plant resilience to drought stress. This is influenced by physiological and biochemical processes related to the synthesis of compounds such as proline, antioxidant activity and phenols. Under drought stress conditions, the osmotic pressure in the environment is higher than inside plant cells, making it difficult for plants to absorb water. Plants increase the concentration of intracellular solutes such as proline and reduce the intracellular osmotic potential to maintain potential water balance (Cha-um *et al.*, 2010). These compounds actively contribute to the physiological mechanisms that enable plants to withstand drought stress (Egilla *et al.*, 2001). Additionally, using organic and potassium (K) fertiliser offers more environmentally friendly options providing additional benefits to root-pruned plants. Organic fertiliser derived from well-packaged oil palm plant waste can serve as a nutrient source.

The waste generated by oil palm plantations can manifest as solid waste, including empty fruit bunches (EFB), palm fronds and palm leaves. Sarwono (2008) states the advantages of EFB compost, such as the high K content, absence of starter and chemicals, enrichment of existing soil nutrients, and improvement of physical, chemical, and biological properties. This can be used as organic mulch or incorporated into soil to enhance soil fertility. The physical properties of soil are one of the factors that influence root growth, and inadequate physical properties can impede root development (Andiyarto & Purnomo, 2012). La Habi (2015) explains that the increase in soil pore space occurs due to the stimulation of soil aggregates by organic matter, resulting in a decrease in soil bulk density. Additionally, Widodo and Kusuma (2018) state that the increase in organic matter content acts as a binder in soil aggregate formation, leading to the creation of more inter-aggregate (macropores) and intra-aggregate spaces (micropores), enhancing air and water availability in soil.

Applying organic matter increases the total pore space, reduces soil volume (Wolf & Synder, 2003), and improves soil porosity by 13.00% (Endriani *et al.*, 2003). Oil palm plantations possess abundant organic matter in the form of leaf litter and EFB. Oil palm EFB is an abundant waste product derived from palm oil mills. This is known to improve the physical, chemical, and biological properties of soil, in addition to having a high nutrient content. Sarwono (2008) reports that EFB compost contains essential plant nutrients, including 1.50% nitrogen (N), 0.50% phosphorus (P), 7.30% K and 0.90% magnesium (Mg). Furthermore, Hayat and Andayani (2014) indicate that EFB compost's nutrient content includes total N (1.91%), K (1.51%), calcium (Ca) (0.83%), P (0.54%), Mg (0.09%), organic carbon (C-organic) (51.23%), C/N ratio (26.82%) and a pH of 7.

EFB compost serves a dual function by adding nutrients to soil and increasing its organic matter content crucial for improving the physical properties of soil. The increased organic matter enhances the stability of soil structure and improves its water retention capacity. These improvements in soil's physical properties positively impact root growth and nutrient uptake by plants (Rozy *et al.*, 2013). Apart from EFB, there is a significant accumulation of palm frond litter around oil palm trees. Therefore, palm frond litter has the potential to serve as a source of organic matter to improve the physical and chemical properties of soil in oil palm plantations. Using palm frond litter as fertiliser for oil palm trees is viable since it contains an average nutrient content of 1.67% N, 0.17% P, 0.23% K, 0.83% Ca and 0.26% Mg (Yuniati & Widyastuti, 2014).

The application of palm frond litter and EFB aims to increase the organic matter content, improving the physical properties of soil. The use of EFB is a common practice in oil palm plantations. However, the comprehensive exploration of palm frond litter, particularly in the context of its impact on root pruning, remains an area that has not received extensive attention. EFB compost, derived from palm oil mills, is a readily available waste product known to enhance soil's physical, chemical and biological properties. The compost is abundant throughout the year, accounting for approximately 20%-27% of processed fresh fruit bunches (FFB) (Bariyanto *et al.*, 2015). Increasing the dosage has been found to correlate with an increase in root volume (Amri *et al.*, 2018). The advantages of compost derived from palm frond litter include its high K content, the use of bio decomposers obtained from microbial isolates found beneath palm frond stacks in the field, the enrichment of soil nutrients, and the ability to improve the physical, chemical and biological properties of soil (Yuniati & Widyastuti, 2014).

Using palm waste as fertiliser holds great potential for enhancing the productivity of root-pruned crops. Therefore, this study aims to enhance the understanding of how root-pruned crops respond to various fertilisers. It provides valuable information for farmers and agricultural

practitioners to improve production efficiency and promote agricultural sustainability in the context of root-pruned crops. By understanding the nutrient requirements of these crops and applying suitable fertiliser, farmers can enhance the quality and quantity of their root-pruned crop yields.

MATERIALS AND METHODS

The study was conducted from October 2022 to May 2023 in Teluk Merbau Village, Dayun District, Siak Sriindrapura Regency, Riau, Indonesia. Soil nutrient analysis was performed at the Department of Soil Science and Land Resources, Faculty of Agriculture, IPB University. The study used K fertiliser, palm frond litter and EFB as materials. Furthermore, the tools employed included a measuring tape, hoe, soil auger, digital scale, SPAD-502, Haga Altimeter and GPS. The study followed a nested design, with plant age as the main plot and fertiliser types as the subplot. The plant age factor consisted of three levels, namely 7, 12 and 16 years, while the fertiliser types factor had four levels, including Control (without fertilisation), single K fertiliser (2.25 kg KCl/tree), palm frond litter (65 kg/tree) and EFB (65 kg/tree). Each treatment was replicated four times, resulting in 48 experimental units of four plants, totalling 192 (Darmosarkoro *et al.*, 2008).

The data were analysed using analysis of variance (ANOVA) with SAS software at a 95% confidence level (α = 5%). Duncan's Multiple Range Test (DMRT) was conducted at a 95% confidence level (α = 5%) when ANOVA indicated a significant treatment effect. The observed variables included plant height, measured from the ground surface to the rudimentary spine on the front using a Haga Altimeter. Stem circumference and diameter were measured with a tape by calculating the average circumference at the base of the stem. Root distribution was assessed after pruning, and samples were taken from one plant in each experimental unit, resulting in 28 sampling points. The number and weight of fruit bunches were observed at 1, 2, 3, 4, 5, and 6 months after the treatment. Furthermore, soil nutrient observations and natrium (Na) with Kjedhal method, P with Bray I, and K with washing method using ammonium acetate (NH_4OAc) at pH 7 in root were conducted.

RESULTS AND DISCUSSION

Agronomic and Production Characteristics

The ANOVA showed a significant variation in the height of oil palm plants due to the application of different fertilisers at the beginning and end of the observation period for each plant age, as shown in *Table 1*.

Table 1 shows that the tallest plant height was observed in 16 year old plants compared to those aged 12 and 7. Among the different types of fertiliser used, including the control, K fertiliser, midrib litter and EFB, there were no significant differences at each plant age. Generally, the height of oil palm plants increased from the initial to the final for each combination of plant age and fertiliser types. A higher plant height indicates better growth; as plants age, their height tends to increase compared to younger plants.

The application of different fertilisers did not significantly impact plant height, resulting in no differences observed among the treatments. Several factors influence the availability of nutrients in the soil for plant absorption and use. Fangeria *et al.* (2009) state that climate, soil conditions, plant-related factors and interactions influence nutrient

TABLE 1. OIL PALM PLANT HEIGHT FOR DIFFERENT PLANTING AGES AND THE APPLICATION OF VARIOUS FERTILISER

Plant age (yr)	Types of fertiliser	Initial plant height	Final plant height
7	Control	343.06 c	373.06 c
	K fertiliser	352.56 c	382.56 c
	Leaf litter	350.69 c	380.69 c
	EFB	338.06 c	368.06 c
12	Control	610.31 b	642.31 b
	K fertiliser	645.50 b	677.50 b
	Leaf litter	629.50 b	661.50 b
	EFB	643.25 b	675.25 b
16	Control	712.31 a	752.31 a
	K fertiliser	747.50 a	787.50 a
	Leaf litter	731.50 a	771.50 a
	EFB	745.25 a	785.25 a

Note: EFB - empty fruit bunches; K - potassium.

availability. Additionally, Syakir and Gusmaini (2012) emphasise the importance of considering factors that ensure plant nutrient availability for growth and development. Nutrients play a vital role in the formation of plant tissue, and any imbalances in soil nutrient levels can disrupt this process.

Even though fertiliser treatments did not yield significant differences, applying K fertiliser resulted in taller plants compared to other types across different ages of oil palm plants. K fertiliser contains the essential macronutrient, which is crucial for various physiological processes in plants, including protein synthesis, photosynthesis, cell osmotic pressure regulation and water and sugar balance control. Applying K fertiliser to oil palm can increase growth, such as plant height, productivity and fruit quality.

Based on the ANOVA, there were significant differences in oil palm trunk circumference among different plant ages. The largest trunk circumference, both at the beginning and end of the measurement, was observed in plants aged seven years, as shown in *Table 2*.

The trunk circumference of oil palm aged seven years showed a greater circumference than aged 12 and 16 years at the beginning and end of the observations. The use of different types of fertiliser at each age did not show significant differences for control, K fertiliser, midrib leaf litter and EFB.

The diameter of the oil palm stem from the ANOVA reported a significant difference in the diameter of the stem at each age. The largest diameter was shown in aged seven compared to 12 and 16 years old. The application of different types of fertiliser at each age showed no significant difference, as reported in *Table 3*.

The diameter of the stem is an indicator that can be used to determine plant growth and development. Oil palms aged seven years have a larger trunk diameter than others. Plants aged seven years experience faster growth in the vegetative phase using various types of fertiliser, which can spur growth in stem diameter. The application of various types of fertiliser is more optimally used in oil palms aged seven compared to plants aged 12 and 16 years, hence the diameter is more significant.

TABLE 2. OIL PALM TRUNK CIRCUMFERENCE FOR VARIOUS PLANTING AGES AND APPLICATION OF DIFFERENT FERTILISER

Plant age (yr)	Types of fertiliser	Initial trunk circle	Final trunk circle
7	Control	350.43 a	353.43 a
	K fertiliser	362.50 a	365.50 a
	Leaf litter	360.18 a	363.18 a
	EFB	354.43 a	357.43 a
12	Control	294.43 b	298.43 b
	K fertiliser	306.50 b	310.50 b
	Leaf litter	304.18 b	306.31 b
	EFB	298.43 b	302.43 b
16	Control	259.43 c	263.43 c
	K fertiliser	271.50 c	275.50 c
	Leaf litter	267.31 c	271.31 c
	EFB	263.43 c	267.43 c

Note: EFB - empty fruit bunches; K - potassium.

TABLE 3. OIL PALM TRUNK DIAMETER FOR VARIOUS TYPES OF PLANTING AGES AND THE APPLICATION OF VARIOUS TYPES OF FERTILISER

Plant age (yr)	Types of fertiliser	Initial bar diameter	Final bar diameter
7	Control	111.62 a	112.56 a
	K fertiliser	115.50 a	116.50 a
	Leaf litter	113.62 a	114.81 a
	EFB	112.87 a	113.56 a
12	Control	93.81 b	95.00 b
	K fertiliser	97.62 b	98.81 b
	Leaf litter	96.81 b	97.65 b
	EFB	95.06 b	96.37 b
16	Control	82.65 c	83.87 c
	K fertiliser	86.50 c	87.62 c
	Leaf litter	85.06 c	86.56 c
	EFB	83.87 c	85.18 c

Note: EFB - empty fruit bunches; K - potassium.

Oil palm fruit weight from the ANOVA showed a significant difference to the observations at the 1st, 2nd , 3rd , 4th , 6th , 7th and 8th months. During the 5th month of observation, there was no significant difference in using different fertilisers at various plant ages, as shown in *Table 4*.

The highest total fruit weight of oil palms was found in oil palm aged seven years with the application of K fertiliser and midrib leaf litter and in plants aged 12 years with the application of EFB. These three types of fertiliser contributed essential nutrients, resulting in an augmentation of the weight of oil palm fruit. Kasem *et al.* (2010) stated that using nitrogen fertiliser combined with P and K and organic fertiliser increased oil palm yields and fruit colour, weight, weight and length.

Based on the ANOVA, the number of oil palm bunches showed no significant difference in the age of the plants and the application of various types of fertiliser, as shown in *Table 5*.

The bunches are the number of fruits produced by oil palms. The number shows no significant difference with applying various types of fertiliser at different ages of oil palms. Appropriate fertiliser application can affect the growth and productivity of oil palms and the number of bunches produced. Fertilisers rich in N, P and K can be absorbed by plants, influencing the growth and formation of bunches (Syahfitri, 2008).

The formation of oil palm bunches is not solely contingent on fertiliser application, a multitude of factors exert influence, including genetic factors and environmental conditions. Genetic factors, including plant varieties, play an important role in determining the number of bunches produced, with certain varieties exhibiting superior bunch production owing to inherent genetic traits related to bunch formation. Furthermore, environmental conditions, such as the availability of water, sunlight exposure and nutrient levels, exert a profound influence on the proliferation of oil palm bunches. Plants thriving under optimal conditions, characterised by water resources, sufficient sunlight exposure and a well-balanced nutrient supply, tend to manifest an enhanced propensity for bunch production.

The ANOVA showed significant differences in the distribution of oil palm root based on the age and various types of fertiliser applications on the distribution of primary, secondary, and tertiary roots. There were no significant differences in the plant's age and the application of various types of fertiliser, as shown in *Table 6*.

The distribution of roots reported significant differences among primary, secondary, and tertiary roots. *Table 6* shows that the overall distribution of roots is influenced by the age of the plant and the types of fertiliser used. The use of K fertiliser significantly affected the distribution of roots at various ages of the plants. Fertiliser had the highest primary, secondary and tertiary root distribution values for oil palms aged seven years, even for plants aged 12 and 16 years. It also affected the distribution of roots of oil palms aged 12 and 16 years but towards secondary and tertiary roots (Syafitri, 2008).

The use of K fertiliser increased the distribution of primary, secondary and tertiary roots in oil palms. K fertiliser application also affected root distribution by increasing root growth. K fertiliser stimulated primary root growth, cell division and extension of primary root, which supported plant growth and development. Another function was to influence plant growth hormones such as auxin, which affected root formation and increased the distribution of roots.

The ANOVA showed a significant difference in the Normalised Difference Vegetation Index (NDVI) for plants of different ages, with the highest value found in plants aged seven years. However, there was no significant difference for plants aged 12 and 16 years, as shown in *Table 7*.

The NDVI index is a form of vegetation index used to evaluate, and monitor plant conditions and calculate the ratio of the spectral values of the red and near-infrared bands reflected from plants (Cahyono *et al.*, 2019; Yuniasih, 2022). A 7-year-old oil palm with a high NDVI value compared to the age of other plants at 0.736-0.756 indicates that the plant is in healthy condition and actively carrying out photosynthesis. Furthermore, the plant has a sufficient amount of chlorophyll and can absorb red light optimally for the process. Healthy plants also have dense, healthy cells, affecting near-infrared light's reflection. Oil palm aged seven years shows that the plants have sufficient chlorophyll content and dense cells, reflecting good photosynthetic activity and optimal growth conditions. According to (Lilles *et al.*, 2015; Sum & Shukor, 2019;), healthy plants provide low and high reflectance values in red and near-infrared waves, and the NDVI is expressed in the range -1 to 1. Negative and positive values indicate non-vegetative and vegetative objects, where an NDVI value close to 1 indicates dense and healthy vegetation.

Nutrient Analysis Results

Soil analysis showed significant difference in the parameters of pH H_2O, C-Organic, P and K. There was no difference in soil nitrogen content on land planted with oil palm aged 7, 12 and 16 years. The application of various fertilisers did not affect soil N content as shown in *Table 8*.

TABLE 4. OIL PALM FRUIT WEIGHT FOR VARIOUS TYPES OF PLANTING AGES AND APPLICATION OF VARIOUS TYPES OF FERTILISER

Plant age (yr)	Types of fertiliser	Fruit weight								
		1st month	2nd month	3rd month	4th month	5th month	6th month	7th month	8th month	Total
7	Control	19.35 b	17.88 bc	26.37 abc	20.56 ab	18.81 a	21.25 abc	21.33 bcd	27.01 ab	145.58 ab
	K fertiliser	23.18 ab	16.28 bc	29.45 ab	24.26 ab	20.81 a	25.40 ab	25.50 abc	25.07 ab	164.95 a
	Leaf litter	22.30 ab	24.50 ab	31.25 a	24.87 ab	20.31 a	30.68 a	15.38 cd	16.27 b	169.51 a
	EFB	27.93 ab	15.48 c	18.31 c	27.37 a	14.06 a	23.12 abc	31.52 ab	24.02 ab	157.83 ab
12	Control	21.22 b	27.01 a	18.68 c	27.27 a	23.30 a	19.18 bcd	22.26 bcd	18.38 b	158.96 ab
	K fertiliser	25.55 ab	25.07 ab	22.75 abc	21.95 ab	22.77 a	11.18 d	25.32 abc	19.41 b	153.91 ab
	Leaf litter	15.38 bc	16.25 bc	27.03 abc	18.30 ab	16.08 a	18.00 bcd	33.45 a	19.37 b	144.54 ab
	EFB	31.52 a	24.05 ab	18.00 c	20.93 ab	24.23 a	15.12 bcd	23.07 bcd	16.45 b	164.54 a
16	Control	15.38 c	23.87 ab	19.96 bc	20.56 ab	15.76 a	20.05 abc	18.81 cd	21.25 ab	131.54 b
	K fertiliser	19.52 b	25.25 ab	24.77 abc	25.81 ab	22.52 a	21.12 abc	20.81 cd	25.41 ab	159.82 ab
	Leaf litter	23.75 ab	25.18 ab	25.63 abc	17.65 b	22.37 a	14.30 cd	20.31 cd	30.68 a	141.56 ab
	EFB	17.97 bc	26.31 ab	22.90 abc	22.81 ab	20.97 a	18.42 bcd	14.06 d	23.12 ab	143.47 ab

Note: EFB - empty fruit bunches; K - potassium.

TABLE 5. THE NUMBER OF OIL PALM BUNCHES FOR VARIOUS TYPES OF PLANTING AGES AND THE APPLICATION OF VARIOUS TYPES OF FERTILISER

Plant age (yr)	Types of fertiliser	Number of bunches (month)								
		1st month	2nd month	3rd month	4th month	5th month	6th month	7th month	8th month	Total
7	Control	2 a	1 a	2 a	1 a	2 a	1 a	2 a	2 a	13 a
	K fertiliser	2 a	2 a	2 a	2 a	2 a	2 a	2 a	1 a	15 a
	Leaf litter	2 a	2 a	2 a	2 a	2 a	2 a	2 a	1 a	15 a
	EFB	2 a	1 a	2 a	2 a	2 a	2 a	2 a	2 a	15 a
12	Control	2 a	1 a	2 a	1 a	2 a	2 a	2 a	2 a	14 a
	K fertiliser	2 a	1 a	2 a	1 a	2 a	1 a	2 a	2 a	13 a
	Leaf litter	2 a	1 a	2 a	1 a	2 a	1 a	2 a	2 a	13 a
	EFB	2 a	2 a	2 a	1 a	2 a	2 a	2 a	2 a	15 a
16	Control	1 a	1 a	1 a	2 a	2 a	2 a	2 a	2 a	13 a
	K fertiliser	2 a	1 a	1 a	2 a	1 a	2 a	2 a	2 a	13 a
	Leaf litter	2 a	1 a	1 a	1 a	2 a	2 a	2 a	2 a	13 a
	EFB	1 a	1 a	1 a	2 a	2 a	2 a	2 a	2 a	13 a

Note: EFB - empty fruit bunches; K - potassium.

TABLE 6. DISTRIBUTION OF OIL PALM ROOT TO VARIOUS TYPES OF PLANTING AGES AND APPLICATIONS OF VARIOUS TYPES OF FERTILISER

Plant age (yr)	Types of fertiliser	Distribution of root		
		Primary	Secondary	Tertiary
7	Control	0.41 ab	0.27 ab	0.16 ab
	K fertiliser	0.66 a	0.42 a	0.25 a
	Leaf litter	0.49 ab	0.34 ab	0.20 ab
	EFB	0.51 ab	0.34 ab	0.20 ab
12	Control	0.31 b	0.22 ab	0.13 ab
	K fertiliser	0.49 ab	0.35 a	0.21 a
	Leaf litter	0.36 ab	0.28 ab	0.17 ab
	EFB	0.38 ab	0.28 ab	0.17 ab
16	Control	0.13 c	0.10 c	0.05 c
	K fertiliser	0.19 c	0.14 bc	0.08 bc
	Leaf litter	0.16 c	0.11 c	0.07 c
	EFB	0.16 c	0.11 c	0.06 c

Note: EFB - empty fruit bunches; K - potassium.

TABLE 7. OIL PALM NDVI FOR VARIOUS TYPES OF PLANTING AGES AND APPLICATIONS OF VARIOUS TYPES OF FERTILISER

Plant age (yr)	Types of fertiliser	NDVI
7	Control	0.736 A
	K fertiliser	0.754 A
	Leaf litter	0.737 A
	EFB	0.756 A
12	Control	0.682 B
	K fertiliser	0.681 B
	Leaf litter	0.694 B
	EFB	0.682 b
16	Control	0.682 b
	K fertiliser	0.681 b
	Leaf litter	0.694 b
	EFB	0.682 b

Note: EFB - empty fruit bunches; K - potassium.

Soil pH from *Table 8* showed significant difference for plants of different ages with the application of various types of fertiliser. Plants aged 7 years with the application of leaf litter and EFB had the highest pH values, namely 5.65 and 6.00 (slightly acidic) and the lowest were found in plants aged 12 years with control treatments and application of K fertiliser (4.38 and 4.30 with very acidic criteria). The use of midrib and EFB, both rich sources of organic matter, significantly influenced soil pH levels when subjected to decomposition. The breakdown of these organic materials generated compounds that altered the pH of the soil. Furthermore, the humification process stemming from coarse organic matter decomposting produces humic and fulvic acids, both of which increased soil pH. Butterley *et al.* (2013) affirmed that the use of dry matter in the form of residue, at a rate of 10 g/kg, was capable of augmenting soil pH values, leading to a temporary shift towards alkalinity. The condition was a consequence of the decomposition processes, driven by abiotic association reactions between H+ ions and the introduced organic matter. Additionally, the processes of ammonification and decarboxylation, occurring during decomposition, contributed to the generation of alkaline conditions in soil.

The application of leaf litter fertiliser and EFB on plants aged 12 years increased the C-organic content of the soil to around 9.72-10.3 (very high). The use of midrib litter and EFB as a source of organic matter increased the availability of soil C-organic when decomposed. The application of these two materials was also a form of using oil palm waste which was returned to the soil as a source of nutrients. Some results showed that the use of waste palm fronds and leaf residues restored soil nutrients and increased soil C-organic (Ariyanti *et al.*, 2019; Singh *et al.*, 2013).

Table 8 shows that the soil P content of 16-year-old oil palms was much higher than 7 and 12-year-old plants for various types of fertiliser applications. However, the application of different types of fertiliser did not have a significant effect on the phosphorus content in oil palms aged 16 years for both controls, K fertiliser, midrib leaf litter, and EFB with P values ranging from 144.19-152.45 (very high). This was due to the accumulation of P during fertilisation which was carried out until the age of 16 years. For soil K content there were also significant differences in the use of various types of fertiliser at various plant ages. The highest K value was found in the treatment of plant leaf litter aged 7 years after planting with the application of leaf litter to provide the needs in soil.

N content in soil at various ages of oil palm with the use of various types of fertiliser did not show

significantly different results with N values ranging from 0.17-3.05 (low-very high). The nitrogen content that did not differ in soil was influenced by the availability of sufficient amounts in soil. This nutrient was the most important limiting factor for plant productivity, and its availability was very important (Niu *et al.*, 2016). Excessive use of fertiliser in agricultural management causes loss of N through leaching and denitrification processes (Liu *et al.*, 2010).

Root NPK levels based on ANOVA reported significant differences in observed parameters both in N, P and K content. *Table 9* showed that plant age and the application of various types of fertiliser had a significant effect on root NPK.

Table 9 shows the NPK levels in the roots of various ages of oil palms due to the application of fertiliser. Root N content in oil palms aged 12 and 16 years with the use of frond litter fertiliser showed the highest N content compared to others. The use of midrib litter was able to provide nitrogen in the roots of oil palms and was used for plant growth. Yama (2018) stated that midrib litter contained a C/N ratio of 16, C-organic 34.18, N 2.09%, P 826 ppm and K 1790 ppm. This litter was obtained from fallen fruit, fronds, and stems stored in the armpits of fronds and experienced weathering. Meanwhile, weathered organic matter enriched the planting medium and the planting medium became fertile, loose, and grew freely. The results of other studies indicated that litter on oil palm stems was used to replace topsoil as a nursery medium for *Pueraria javanica* plants.

For the P content in the root, oil palms at the age of 12 years reported the highest content compared to the ages of 7 and 16 years using K fertiliser, leaf litter and EFB. *Table 9* shows that the numerical content of leaf litter has a high value compared to K fertiliser and EFB. This was because the leaf litter

TABLE 8. OIL PALM NORMALISED DIFFERENCE VEGETATION INDEX (NDVI) FOR VARIOUS TYPES OF PLANTING AGES AND APPLICATIONS OF VARIOUS TYPES OF FERTILISER

Plant age (yr)	Types of fertiliser	Soil analysis				
		pH H_2O	C-organic	N	P	K
7	Control	4.86 ab	2.12 b	0.30 a	24.75 b	0.65 b
	K fertiliser	4.68 ab	4.29 ab	0.31 a	46.25 ab	1.09 b
	Leaf litter	6.00 a	5.75 ab	0.31 a	55.81 ab	2.18 a
	EFB	5.65 a	1.93 b	0.17 a	22.77 b	1.51 ab
12	Control	4.38 b	5.96 ab	0.30 a	97.36 ab	0.26 b
	K fertiliser	4.30 b	9.25 ab	0.41 a	103.59 ab	0.40 b
	Leaf litter	5.46 ab	10.3 a	0.34 a	120.71 ab	0.93 b
	EFB	4.88 ab	9.72 a	0.30 a	101.83 ab	0.82 b
16	Control	4.95 ab	6.45 ab	2.76 a	145.49 a	0.37 b
	K fertiliser	4.80 ab	9.31 ab	0.50 a	152.45 a	0.34 b
	Leaf litter	5.15 ab	6.89 ab	3.05 a	147.06 a	0.40 b
	EFB	4.70 ab	5.98 ab	0.63 a	144.19 a	0.45 b

Note: EFB - empty fruit bunches; K - potassium; N - nitrogen; P - phosphorus; H_2O - water.

TABLE 9. NPK CONTENT OF OIL PALM PLANT ROOT FOR VARIOUS TYPES OF PLANTING AGES AND THE APPLICATION OF VARIOUS TYPES OF FERTILISER

Plant age (yr)	Types of fertiliser	Root NPK levels		
		N	P	K
7	Control	0.15 c	0.22 b	0.68 a
	K fertiliser	0.17 c	0.22 b	0.54 ab
	Leaf litter	0.19 bc	0.18 b	0.78 a
	EFB	0.12 c	0.15 b	0.56 ab
12	Control	0.30 ab	0.22 b	0.31 b
	K fertiliser	0.21 ab	0.58 a	0.51 ab
	Leaf litter	0.38 a	0.68 a	0.70 a
	EFB	0.20 ab	0.51 a	0.50 ab
16	Control	0.19 bc	0.27 b	0.58 ab
	K fertiliser	0.16 c	0.36 b	0.63 ab
	Leaf litter	0.35 a	0.31 b	0.66 ab
	EFB	0.19 bc	0.23 b	0.24 b

Note: EFB - empty fruit bunches; K - potassium; N - nitrogen; P - phosphorus.

had a high P content and when applied as fertiliser more nutrient was provided to be absorbed. The application of EFB of fertiliser to 12-year-old palms also provided high P. According to Hayat and Andayani (2014), the nutrient content of EFB compost contained a total of N (1.91%), K (1.51%) and Ca (0.83%), P (0.54%), Mg (0.09%), C-organic (51.23%), C/N ratio 26.82% and pH 7.

The application of K fertiliser indirectly increased the P content in the root of oil palms. The use provides potassium to plants and indirectly affects the absorption of P in the root. Potassium fertiliser given correctly can increase the efficiency of P use by plants, and assist in the process of transporting the element in plants to increase the efficiency of absorption. The element improves the quality of plant roots and explores more areas of soil, including areas rich in P.

CONCLUSION

In conclusion, the growth of plants aged 7 years was the best response compared to plants aged 12 and 16 years in terms of stem circumference, stem diameter, and NDVI values for all types of fertiliser applied. The primary root distribution for plants aged 7 years with the use of K fertiliser showed the best results for the distribution of secondary and tertiary roots and was not significantly different from those aged 12 years. Soil analysis showed that there were differences in the use of various types of fertiliser on soil nutrient content, specifically on pH, C-organic, P, and K values. The use of midrib and EFB affected plants aged 7 years, while those aged 12 years had C content. The high organic matter with the use of leaf litter and EFB for oil palms aged 16 years had the best effect on P values compared to those aged 7 and 12 years.

ACKNOWLEDGEMENT

The authors are grateful to the Indonesian Endowment Fund for Education (LPDP) 2019 (0007721/TRP/D/BUDI-2019), Ministry of Finance, Indonesia for their financial support.

REFERENCES

Amri, A. I., Armaini, A., & Purba, M. R. A. (2018). Aplikasi kompos tandan kosong kelapa sawit dan dolomit pada medium sub soil inceptisol terhadap bibit kelapa sawit (*Elaeis guineensis* Jacq.) di pembibitan utama. [Application of empty palm fruit bunch compost and dolomite on inceptisol subsoil medium to oil palm (*Elaeis guineensis* Jacq.) seedlings in main nurseries]. *Jurnal Agroteknologi, 8*(2), 1. https://doi.org/10.24014/ja.v8i2.3349

Ariyanti, M., Maxiselly, Y., Rosniawaty, S., & Indrawan, R. A. (2019). Pertumbuhan kelapa sawit belum menghasilkan dengan pemberian pupuk haract asal pelepah kelapa sawit dan asam humat [The growth of immature oil palm with the application of oil palm midrib organic fertilizer and humic acid]. *Jurnal Penelitian Kelapa Sawit*, *27*(2), 71–82.

Bariyanto, Nelvia, & Wardati. (2015). Pengaruh pemberian kompos tandan kosong kelapa sawit (TKSS) pada pertumbuhan bibit kelapa sawit (*Elaeis guineensis* Jacq.) di main-nursery pada medium subsoil ultisol [The effect of compost empty palm oil bunches (EFB) on the growth of seed oil palm (*Elaeis guineensis* Jacq.) main-nursery in the medium subsoil ultisol. *Jurnal Online Mahasiswa Fakultas Pertanian Universitas Riau, 2*(1), 1-8.

Budiarto, R., Poerwanto, R., Santosa, E., & Efendi, D. (2019). A review of root pruning to regulate citrus growth. *Journal of Tropical Crop Science*, *6*(01), 1–7. https://doi.org/10.29244/jtcs.6.01.1-7

Butterly, C. R., Baldock, J. A., & Tang, C. (2013). The contribution of crop residues to changes in soil pH under field conditions. *Plant and Soil*, *366*(1–2), 185–198. https://doi.org/10.1007/s11104-012-1422-1

Cahyono, B. E., Febriawan, E. B., & Nugroho, A. T. (2019). Analisis tutupan lahan menggunakan metode klasifikasi tidak terbimbing citra Landsat di Sawahlunto, Sumatera Barat [Land cover analysis using unsupervised classification method of Landsat imagery in Sawahlunto, West Sumatera]. *Jurnal Teknotan*, *13*(1), 8. https://doi.org/10.24198/jt.vol13n1.2

Cha-um, S., Samphumphuang, T., & Kirdmanee, C. (2013). Glycinebetaine alleviates water deficit stress in *indica* rice using proline accumulation, photosynthetic efficiencies, growth performances and yield attributes. *Australian Journal of Crop Science, 7(2)*, 213–218.

Endriani, Zurhalena, & Refliaty. (2003). Perbaikan sifat fisika tanah ultisol dan hasil tanaman melalui pemberian pupuk bokashi [Improvement of ultisol soil physical properties and crop yields through the application of bokashi fertilizer]. In *Prosiding Buku I. Kongres Nasional VIII Himpunan Ilmu Tanah*

Indonesia [*Proceedings Book I. 8th National Congress of the Indonesian Soil Science Society*]. Himpunan Ilmu Tanah Indonesia. Padang, Indonesia.

Fageria, N. K., Filho, M. P. B., & Da Costa, J. H. C. (2009). Potassium in the use of nutrients in crop plants. In N. K. Fageria (Ed.), *The use of nutrients in crop plants* (pp. 131–163). CRC Press, Taylor & Francis Group.

Fini, A., Frangi, P., Faoro, M., Piatti, R., Amoroso, G., & Ferrini, F. (2015). Effects of different pruning methods on an urban tree species: A four-year-experiment scaling down from the whole tree to the chloroplasts. *Urban Forestry & Urban Greening*, *14*(3), 664–674. https://doi.org/10.1016/j.ufug.2015.06.011

Hayat, E. S. & Andayani, S. (2014). Pengelolaan limbah tandan kosong kelapa sawit dan aplikasi biomassa *Chromolaena odorata* terhadap pertumbuhan dan hasil tanaman padi serta sifat tanah sulfaquent [Oil palm empty bunches waste management and aplication of biomass *Chromolaena odorata* on growthand yield of rice plant and sulfaquent soil properties]. *Jurnal Teknologi Pengelolaan Limbah, 17(22)*, 44–51.

Kassem, H. A., & Marzouk, H. A. (2010). Improving yield and fruit quality of date palm by organic fertilizer sources. *Journal of Applied Horticulture*, *12*(2), 145–150.

La Habi, M. (2015). Pengaruh aplikasi kompos granul ela sagu diperkaya pupuk ponska terhadap sifat fisik tanah dan hasil jagung manis di inceptisol [The effect of enriched sago palm frond granular compost application on soil physical properties and sweet corn yield in inceptisol]. *Biopendix Jurnal Biologi Pendidikan Dan Terapan*, *1*(2), 126–139. https://doi.org/10.30598/biopendixvol1issue2page126-139

Lillesand, T. M., Kiefer, R. W. & Chipman, J. (2015). *Remote sensing and image interpretation, 7th edition*. Wiley.

Liu, J., You, L., Amini, M., Obersteiner, M., Herrero, M., Zehnder, A. J. B., & Yang, H. (2010). A high-resolution assessment on global nitrogen flows in cropland. *Proceedings of the National Academy of Sciences*, *107*(17), 8035–8040. https://doi.org/10.1073/pnas.0913658107

Miller, F. D., & Neely, D. (1993). The effect of trenching on growth and plant health of selected species of shade trees. *Arboriculture & Urban Forestry*, *19*(4), 226–229. https://doi.org/10.48044/jauf.1993.036

Niu, S., Classen, A. T., Dukes, J. S., Kardol, P., Liu, L., Luo, Y., Rustad, L., Sun, J., Tang, J., Templer, P. H., Thomas, R. Q., Tian, D., Vicca, S., Wang, Y., Xia, J., & Zaehle, S. (2016). Global patterns and substrate-based mechanisms of the terrestrial nitrogen cycle. *Ecology Letters*, *19*(6), 697–709. https://doi.org/10.1111/ele.12591

Nurcahyo, N. E. & Arian, E. (2017). Pengaruh pupuk Gandasil-D dan berbagai limbah perkebunan kelapa sawit terhadap pertumbuhan bibit kelapa sawit (*Elaeis guineensis* Jacq.) di pembibitan utama [The effect of Gandasil fertilizer and a variety of waste oil palm plantation on the growth of seedlings of oil palm (*Elaeis guineensis* Jacq.) seedlings in the main nursery]. *Jurnal Online Mahasiswa Fakultas Pertanian Universitas Riau, 4(1)*, 1-13.

Rao, I. M., Borrero, V., Ricaurte, J., & García, R. (1999). Adaptive attributes of tropical forage species to acid soils. V. Differences in phosphorus acquisition from less available inorganic and organic sources of phosphate. *Journal of Plant Nutrition*, *22*(7), 1175–1196. https://doi.org/10.1080/01904169909365703

Raharjo, K. T. P., Nubatonis, J., & Neonbeni, E. Y. (2017). Pengaruh pemangkasan akar dan waktu aklimatisasi terhadap pertumbuhan bibit tanaman kemiri (*Aleurites moluccana* Willd) asal stum [Effect of root pruning and acclimation time on the growth of seedlings of candlenut (*Aleurites moluccana* Willd) from stump]. *Savana Cendana*, *2*(02), 19–22. https://doi.org/10.32938/sc.v2i02.87

Rozy, F., Rosmawaty, T., & Fatrrahman. (2013). Pemberian pupuk N P K Mutiara 16:16:16 dan kompos tandan kosong kelapa sawit pada tanaman terung (*Solanum melongena* L) [Application of NPK Mutiara 16:16:16 fertilizer and oil palm empty fruit bunch compost on eggplant (*Solanum melongena* L.)]. *Jurnal Relevensi, Akurasi dan Tepat Waktu, 1*(2), 228–239.

Sarwono, E. (2008). Pemanfaatan janjang kosong sebagai substitusi pupuk tanaman kelapa sawit [Utilization of empty fruit bunches as fertilizer substitute for oil palm plants]. *Aplika: Jurnal Ilmu Pengetahuan dan Teknologi*, *8*(1), 19–23.

Singh, P., Sulaiman, O., Hashim, R., Peng, L. C., & Singh, R. P. (2013). Evaluating biopulping as an alternative application on oil palm trunk using the white-rot fungus *Trametes*

versicolor. *International Biodeterioration & Biodegradation*, *82*, 96–103. https://doi.org/10.1016/j.ibiod.2012.12.016

Sum, A. F. W., & Shukor, S. (2019). Oil palm plantation monitoring from satellite image. *IOP Conference Series Materials Science and Engineering*, *705*(1), 012043. https://doi.org/10.1088/1757-899x/705/1/012043

Syakir, M., & Gusmaini. (2012). Pengaruh penggunaan sumber pupuk kalium terhadap produksi dan mutu minyak tanaman nilam [Effect of potassium sources on application yield and quality of patchouli]. *Jurnal Littri*, *18*(2), 60–65.

Watson, G. W. (1998). Tree growth after trenching and compensatory crown pruning. *Arboriculture & Urban Forestry*, *24*(1), 47–53. https://doi.org/10.48044/jauf.1998.007

Widodo, K. H., & Kusuma, Z. (2018). Pengaruh kompos terhadap sifat fisik tanah dan pertumbuhan tanaman jagung di inceptisol [Effects of compost on soul physical properties and growth of maize on an inceptisol]. *Jurnal Tanah dan Sumberdaya Lahan*, *5*(2), 959–967.

Wolf, B., & Snyder, G. H. (2003). *Sustainable soils: The place of organic matter in sustaining soils and their productivity*. Haworth Press.

Yahya, Z., Husin, A., Talib, J., Othman, J., Ahmed, O. H. & Jalloh, M. B. (2010). Oil palm (*Elaeis guineensis*) roots response to mechanization in Bernam series soil. *American Journal of Applied Sciences*, *7*(3), 343–348. https://doi.org/10.3844/ajassp.2010.343.348

Yama, D. I. (2018). Analisis pertumbuhan pembibitan *Pueraria javanica* pada komposisi media seresah dalam ketiak pelepah pada batang kelapa sawit [Analysis of *Pueraria javanica* seedling growth on litter media composition in oil palm frond axils]. *Jurnal Citra Widya Edukasi*, *10*(3), 199–206.

Yuniati, S. & Widyastuti, R. (2014). *Composting palm oil midrib-leaf with different biodecomposters and used as ameliorant*. Master thesis. Institut Pertanian Bogor.

Yuniasih, B., Adji, A. R. P., & Budi, B. (2022). Evaluation of pre-replanting oil palm plant health using the NDVI Index from Landsat 8 satellite imagery. *Jurnal Teknik Pertanian Lampung*, *11*(2), 304. https://doi.org/10.23960/jtep-l.v11i2.304-313

Journal of Oil Palm Research Vol. 37 (3) September 2025 p. 441-450
DOI: https://doi.org/10.21894/jopr.2024.0034

ALUMINIUM TOXICITY TOLERANCE OF DIFFERENT VARIETIES OF OIL PALM (*Elaeis guineensis* L. Jacq.) SEEDLINGS

HUSEIN ABDUL GANI[1]; NURAZMIUDDIN BACHO[1] and NUR QURSYNA BOLL KASSIM[2]*

ABSTRACT

Aluminium (Al) toxicity is one of the problems experienced by crops cultivated on acid soil, inhibiting root growth and nutrient absorption capability. This study evaluated the effects of different concentrations of Al-toxicity (0 μM-control; 100, 200 and 300 μM) on the physiological growth, chlorophyll content and selected nutrient uptake in roots and shoots of different varieties of oil palm seedlings, specifically the Elite Deli Dura *x BM119 AVROS* Pisifera*, Elite Deli* Dura *x Elite AVROS* Pisifera*, Ulu Remis Deli* Dura *x Dumpy AVROS and Ulu Remis Deli* Dura *x Ulu Remis* Tenera *varieties. Results showed that Al-toxicity has no significant effect on the height of shoots for all oil palm seedling varieties. The Ulu Remis Deli* Dura *x Ulu Remis* Tenera *seedlings appeared to be more tolerant, showing no significant effect on bole diameter, chlorophyll content and biomass of both shoot and roots upon Al-toxicity treatment. For selected nutrient uptake, all tested oil palm seedling varieties showed significant effects upon Al-toxicity treatment primarily from the 100 μM Al-toxicity application. The findings from this study suggested that the Elite Deli* Dura *x BM119 AVROS* Pisifera *oil palm variety exhibited the lowest tolerance towards Al-toxicity compared to the other oil palm varieties tested.*

Keywords: aluminium, oil palm, seedling, tolerance, toxicity.

Received: 13 September 2023**; Accepted:** 7 April 2024**; Published online:** 10 June 2024.

INTRODUCTION

Approximately 72% of the land area in Malaysia is from the soil order of Ultisols and Oxisols, which contain kaolinite, gibbsite, goethite, and hematite in the clay fractions (Shamshuddin & Noordin, 2011). These soils are often deep red, friable and high in iron (Fe) and aluminium oxide content. Aluminium (Al) toxicity is a major constraint that could limit plant development, eventually affecting crop yield. Study showed that there is a close relationship between exchangeable Al and root density of mature oil palms (Cristancho *et al*., 2007). The most observed symptom of Al-toxicity in plants is the inhibition of root growth. The study by Cristancho *et al*. (2011) showed that there is a significant interaction between the Al concentration and oil palm progeny on the number of leaves, root volume, lateral root growth length, magnesium (Mg) and potassium (K) content in root and shoot tissues, and calcium (Ca) and natrium (Na) content in shoot tissues. Different Al concentrations also significantly affect the morphology and physiology of oil palm varieties (Supene *et al*., 2014).

The physicochemical properties of soils in an oil palm agro-ecosystem will change with time. These changes are often related to the soil pH, which tends to decrease over time (Ng *et al*., 2011). A high rate of fertilisers applied around the palm base planted on Musang series soil for seven

[1] Malaysian Palm Oil Board,
6, Persiaran Institusi, Bandar Baru Bangi,
43000 Kajang, Selangor, Malaysia.

[2] Faculty of Plantation and Agrotechnology,
Universiti Teknologi MARA Cawangan Melaka Kampus Jasin,
77300 Merlimau, Melaka, Malaysia.

* *Corresponding author e-mail: qursyna@uitm.edu.my*

years led to a marked decline in soil pH to 3.8, a reduction of almost 10% (Kee *et al*., 1995; Nelson *et al.,* 2018). Continuous decline of soil pH will increase the availability of Al in the soil and may affect the morphology and physiology of oil palm seedlings. Kochian *et al.* (2004) found that when soil pH is below 5.0, Al^{3+}, which is the most rhizotoxic Al species, is solubilised in the soil. High concentrations of Al in the soil result in a toxic Al level which affects growth performance of crops. Kochian (1995) and Yang and Horst (2015) found that Al-toxicity inhibits root growth while Krstic *et al*. (2012) showed that there is inhibition of root elongation, resulting in extensive root injury which leads to difficulties in nutrient and water uptake by the crop. Root growth in mature oil palms is reduced by 0.1 cm cm^{-3} soil due to 1 cmol of exchangeable Al kg^{-1} soil (Cristancho *et al*., 2007). Al also significantly affects the primary root growth of oil palm seedlings from different varieties (Supena *et al*., 2014).

Many of the existing studies lack comprehensive data regarding the Al-toxicity tolerance of specific oil palm varieties. The genetic diversity present within oil palm seedlings may lead to variations in their ability to tolerate Al-toxicity. It is important to understand how distinct varieties respond to Al-toxicity to formulate targeted and effective planting management strategies. Consequently, the identification and characterisation of genotypic differences in tolerance levels can contribute significantly to the development of more resilient and productive oil palm varieties. As such, this study intended to evaluate the effects of different concentrations of Al-toxicity on the growth and chlorophyll content in oil palm seedlings and to examine the effects of nutrient uptake in roots and shoots of different varieties of oil palm seedlings due to Al-toxicity.

MATERIALS AND METHODS

Study Area

This study was conducted under greenhouse-controlled conditions located at the Faculty of Plantation and Agrotechnology, UiTM Kampus Jasin, Melaka, Malaysia. The mean daily temperature was 20°C-32°C with average rainfall 2,200-2,400 mm yr^{-1} (Malaysian Meteorology Department, 2017).

Oil Palm Seeds Preparation

Four different oil palm varieties were used, *i.e.*, Elite Deli *Dura* x BM119 AVROS *Pisifera*, Elite Deli *Dura* x Elite AVROS *Pisifera*, Ulu Remis Deli *Dura* x Dumpy AVROS and Ulu Remis Deli *Dura* x Ulu Remis *Tenera*. Their germinated seeds were collected from a local company and sown in a hydroponic system. These varieties were selected based on the major planting materials being used by plantations in Malaysia.

Preparation of Nutrient Solution

The Hoagland nutrient solution (*Table 1*) was prepared according to Supena *et al.* (2014).

TABLE 1. NUTRIENT COMPOSITION IN ONE L OF SOLUTION

No.	Mineral salts	Molarity	Quantity
1	$Ca(NO_3)_2.4H_2O$	1	5.00 mL
2	KNO_3	1	5.00 mL
3	KH_2PO_4	1	1.00 mL
4	$MgSO_4.7H_2O$	1	2.00 mL
5	H_3BO_3	-	2.86 g
6	$MnCl_2.4H_2O$	-	1.81 g
7	$ZnSO_4.7H_2O$	-	0.22 g
8	$CuSO_4.5H_2O$	-	0.08 g
9	$H_2MoO_4.H_2O$	-	0.02 g
10	Fe EDTA	-	1.00 mL

Al Treatment

Four different Al concentrations were applied to four different varieties of oil palm seeds after transplanting to the hydroponic system. The Al concentrations applied were: Treatment 0 (control), Treatment 1 (100 µM), Treatment 2 (200 µM), and Treatment 3 (300 µM). The range of treatments was based on the findings from Christancho *et al.* (2011). Al chloride ($AlCl_3.6H_2O$) was used as the Al source. Al chloride was mixed evenly into the nutrient solution at different concentrations according to the treatments. For control treatment, the pH was set at pH 5.5 (Supena *et al.,* 2014) which mimics the average soil pH in Malaysia, while the other Al treatments were adjusted to approximately pH 4.0 to ensure the availability of the Al. The pH adjustment was conducted by the addition of sulfuric acid (H_2SO_4) into the nutrient solution. The Al solution was monitored and replenished once a week to ensure that the concentration of Al was stable and constant.

Field Preparation

The oil palm seedlings were transplanted into a hydroponic system. Each tray containing 20 L of aerated Hoagland nutrient solution was replenished once a week. Dimensions of the hydroponic basin were 410 x 240 x 140 mm and each tray contained four different varieties of oil palm seedlings. There were 16 trays used in this study, with a total of 64 seedlings (*Figure 1*).

The treatments in this study were arranged based on a split plot design with two treatment factors. The Al stress was the first factor, and the second factor was the different oil palm varieties. There were four replications for each treatment and the arrangement is shown in *Figure 2*.

Parameters Measured

A week after the treatments were applied, the seedlings' height, root length, chlorophyll value and plant bole diameter were recorded once a week to observe the effects of Al application on the morphology and physiology of the plants. As for plant nutrient content and plant biomass, the samples were collected on the third month after the seedlings were sown. The height of the seedling was measured from the base of the seedling to the tip of the shoot weekly for a total of 90 days (Cristancho *et al.*, 2011). The root length was also measured weekly for 90 days. Only the longest root was measured for each seedling. Root length parameter is a better indicator of Al-toxicity compared to roots and leaf dry weight (Boudot *et al.*, 1994). Additionally, the bole diameter was measured once a week with a vernier calliper.

The plant nutrient content was analysed using a wet digestion method, with a 1:2 ratio of nitric acid (HNO_3)-hydrochloric acid (HCl) (Zhao *et al.*, 2023). The samples were analysed for their concentrations of selected plant nutrients, specifically P, K, Ca, and Mg, using the Inductively Coupled Plasma-Optical Emission Spectrometry (ICP-OES Model DV7300). Leaf chlorophyll content was measured using

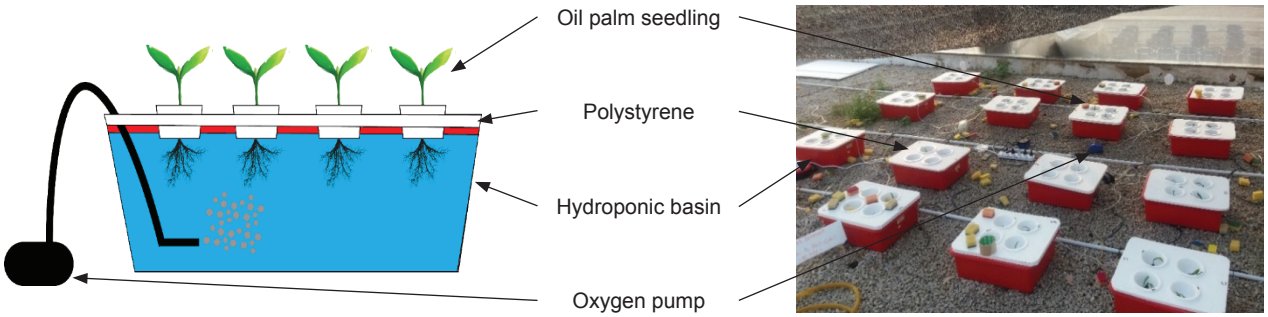

Figure 1. Preparation of the hydroponic system.

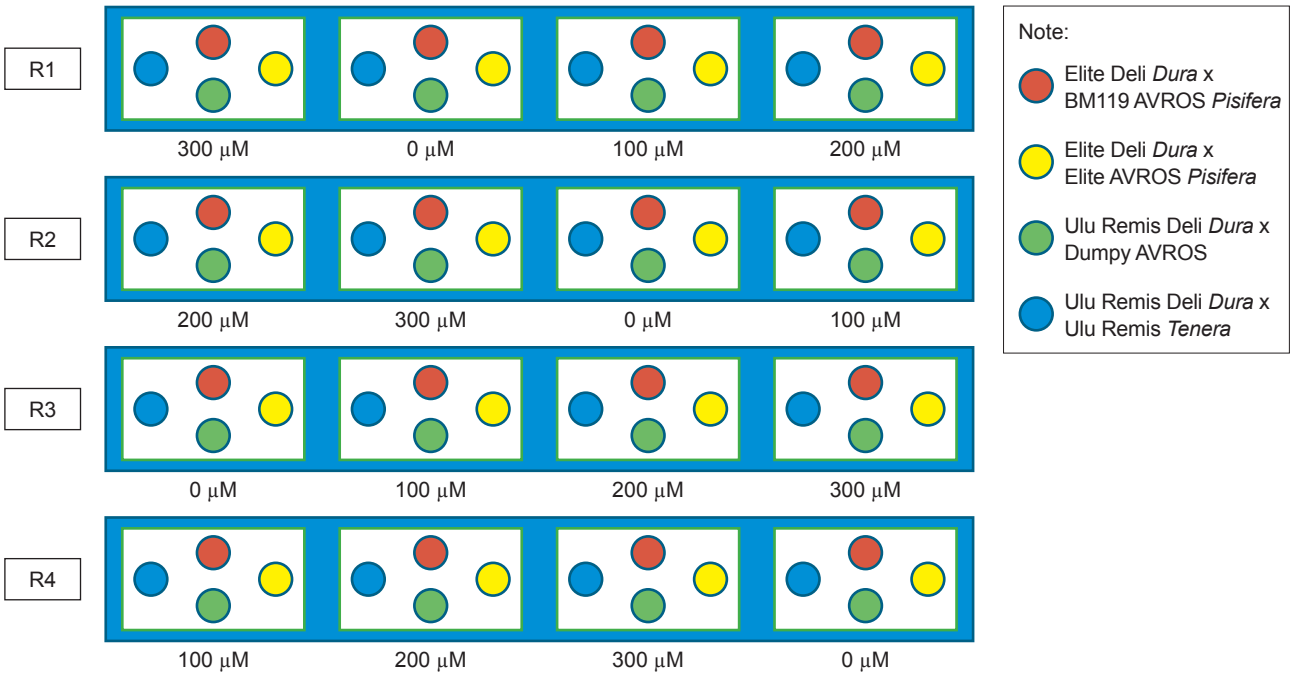

Note: R1 to R4 indicate the replication rows. The Al concentrations (0, 100, 200 and 300 µM) applied are shown at the bottom of each row. The arrangements of four oil palm varieties are indicated in the legend on the right.

Figure 2. Split plot experimental design.

Soil Plant Analysis Development meter (SPAD) on the 90th day after initiating treatment. Finally, the biomass of the seedlings was measured after 90 days. The root and shoots were separated and weighed. The plant was then air-dried in a forced-air oven at 65°C for 48 hr. After which the dry weight of plant roots and shoots were measured and recorded.

Statistical Analysis

The data obtained were analysed using SPSS version 26. Two-way ANOVA was used to analyse the variance of the treatments. The significant factors were then analysed using multiple comparison tests to compare the effects of Al-toxicity on the different oil palm seedling varieties.

RESULTS AND DISCUSSION

Effects of Different Concentrations of Al-toxicity on Growth and Chlorophyll Content of Oil Palm Seedlings

Table 2 shows the effects of different concentrations of Al-toxicity on the growth and chlorophyll content of oil palm seedlings variety Elite Deli *Dura* x BM119 AVROS *Pisifera*, Elite Deli *Dura* x Elite AVROS *Pisifera*, Ulu Remis Deli *Dura* x Dumpy AVROS and Ulu Remis Deli *Dura* x Ulu Remis *Tenera*, respectively.

The roots and chlorophyll content of oil palm seedling varieties Elite Deli *Dura* x BM119 AVROS *Pisifera* and Elite Deli *Dura* x Elite AVROS *Pisifera* were affected by all Al-toxicity treatments, leading

TABLE 2. EFFECTS OF DIFFERENT AL-TOXICITY ON DIFFERENT OIL PALM SEEDLING VARIETY

Parameters	Treatment 0 (Control): 0 µM	Treatment 1: 100 µM	Treatment 2: 200 µM	Treatment 3: 300 µM
Elite Deli *Dura* x BM119 AVROS *Pisifera*				
Mean length of roots (cm)	19.019^{a}	13.217^{b}	14.236^{c}	15.383^{bc}
Mean height of shoots (cm)	12.406^{a}	10.452^{a}	8.297^{a}	8.505^{a}
Mean of bole diameter (mm)	1.104^{a}	0.894^{a}	0.757^{a}	0.772^{a}
Mean of SPAD value (SPAD unit)	53.500^{a}	22.500^{b}	20.500^{b}	15.400^{b}
Root biomass (g)	0.900^{a}	0.610^{b}	0.330^{c}	0.300^{c}
Shoot biomass (g)	2.130^{a}	1.840^{b}	1.670^{b}	1.620^{b}
Elite Deli *Dura* x Elite AVROS *Pisifera*				
Mean length of roots (cm)	7.136^{a}	4.586^{b}	3.553^{b}	4.574^{b}
Mean height of shoots (cm)	2.044^{a}	1.956^{a}	1.631^{a}	1.656^{a}
Mean of bole diameter (mm)	0.811^{a}	0.861^{a}	0.808^{a}	0.634^{a}
Mean of SPAD value (SPAD unit)	32.300^{a}	18.100^{b}	16.500^{b}	18.900^{b}
Root biomass (g)	0.550^{a}	0.490^{b}	0.230^{c}	0.230^{c}
Shoot biomass (g)	2.070^{a}	2.050^{b}	1.800^{c}	1.030^{c}
Ulu Remis Deli *Dura* x Dumpy AVROS *Pisifera*				
Mean length of roots (cm)	19.238^{a}	21.241^{a}	21.898^{a}	17.113^{a}
Mean height of shoots (cm)	10.157^{a}	9.651^{a}	9.047^{a}	7.802^{a}
Mean of bole diameter (mm)	1.020^{a}	0.890^{a}	0.830^{a}	0.640^{b}
Mean of SPAD value (SPAD unit)	25.800^{a}	15.900^{b}	14.300^{bc}	9.600^{c}
Root biomass (g)	0.640^{a}	0.290^{b}	0.290^{b}	0.270^{b}
Shoot biomass (g)	2.470^{a}	1.310^{b}	1.070^{b}	1.060^{b}
Ulu Remis Deli *Dura* x Ulu Remis *Tenera*				
Mean length of roots (cm)	21.856^{ab}	19.017^{ab}	16.615^{a}	14.208^{b}
Mean height of shoots (cm)	12.566^{a}	11.026^{a}	8.359^{a}	6.808^{a}
Mean of bole diameter (mm)	1.432^{a}	1.444^{a}	1.273^{a}	1.122^{a}
Mean of SPAD value (SPAD unit)	22.200^{a}	14.400^{a}	21.000^{a}	18.400^{a}
Biomass of roots (g)	0.520^{a}	0.500^{a}	0.460^{a}	0.500^{a}
Biomass of shoots (g)	2.220^{a}	1.770^{b}	1.230^{c}	1.180^{c}

Note: Different superscript letters in the same row indicate significant difference at $p \leq 0.05$.

to significant effects on the biomass of roots and shoots (*Table 2*). On the other hand, the height of shoots for all varieties was not significantly affected by the application of Al-toxicity as high as 300 µM but the shoot biomass was affected. The bole diameter showed a similar pattern with the shoots, with exception of the Ulu Remis Deli *Dura* x Dumpy AVROS variety, where the highest concentration of Al-toxicity affected the bole diameter.

Effects of Nutrient Uptake in Root and Shoot of Different Varieties of Oil Palm Seedlings to Al-toxicity

A similar pattern in nutrient uptake, specifically P, K, Ca and Mg was observed in both roots and shoots of the oil palm seedlings (*Table 3*). For all oil palm varieties, the uptake of selected nutrients by both roots and shoots was significantly different among treatments. The uptake of P in shoots and roots was affected by a minimum of 100 µM Al-toxicity application for all oil palm seedling varieties. Upon increment of Al-toxicity level to 200 and 300 µM, the uptake of P in both roots and shoots fluctuated in all seedling varieties. The application of 100 µM Al-toxicity had a significant effect on the uptake of K, Ca and Mg in the seedling's roots and shoots, for all oil palm varieties.

These findings revealed that the uptake of nutrients specifically P, K, Ca and Mg was affected by Al-toxicity at as low as 100 µM level.

Discussion

The overall results indicated reduction in root growth at 100, 200 and 300 µM Al-toxicity for Elite Deli *Dura* x BM119 AVROS *Pisifera* seedlings (*Table 2* and *3*). A reduction was also observed for Elite Deli *Dura* x Elite AVROS *Pisifera* and Ulu Remis Deli *Dura* x Ulu Remis *Tenera* seedlings. The decrease in root length may be due to a reduction in cell division and elongation activity. Cristancho *et al.* (2010) also reported a reduction in total root length in Nigerian *Dura* x Nigerian *Dura* and Deli *Dura* x AVROS *Pisifera* oil palm progenies. In addition, Supena *et al.* (2014) similarly observed a reduction in primary root length in oil palm varieties toward Al stress conditions. Li *et al*. (2008) found that exposure of the root tips of several wheat varieties to Al led to a reduction in mitotic activities in the root. In plants, the presence of Al ions in the soil solution is much more destructive than H ions, even at the same concentration (Krstic *et al*., 2012).

The relationship between the pectin group and Al in root cells could be the reason for the reduction in root growth (Klimashevskii & Dedov, 1975; Yang & Horst, 2015). A reduction in cell division was attributed to the decrease in the root length of oil palm seedlings treated with high Al concentrations (Supena *et al*., 2014). Inhibition of root growth was also due to the binding of Al ions to the pectin and other cell wall parts, which caused changes in cell characteristics such as extensibility, enzyme activities and cell porosity. On the other hand, despite high Al concentrations, Ulu Remis Deli *Dura* x Dumpy AVROS seedlings exposed to 100 µM of Al exhibited increased root length. Cristancho *et al*. (2011) also observed a positive effect of Al exposure to the root volume of Nigerian *Dura* x Nigerian *Dura* oil palm progeny at 100 µM of Al. In other plants such as *Melastoma malabathrichum* L., addition of Al into its water culture solution increased the root growth (Osaki *et al*., 1997; Watanabe *et al.,* 2005). This plant is known as an Al-accumulation shrub. However, results in the present study indicate that the application of 100 µM of Al does not affect the mean height of the shoot and mean length of roots of three oil palm seedlings (Elite Deli *Dura* x BM119 AVROS *Pisifera*, Elite Deli *Dura* x Elite AVROS *Pisifera* and Ulu Remis Deli *Dura* x Ulu Remis *Tenera*). Apart from the Ulu Remis Deli *Dura* x Dumpy AVROS variety, the oil palm seedling varieties tested in this study showed retardation in shoot growth at 200 and 300 µM Al concentrations.

In response to Al alleviation, retarded shoot growth and chlorosis on the leaves have been observed in oil palm seedlings, which may be due to the reduction of some essential nutrient elements such as P (Cristancho *et al*., 2009). Al effects on foliar resembled effects from P deficiency, such as overall stunting, smaller size, dark green colour and delayed maturity (Rout *et al*., 2001). Apart from that, a reduction of 31.8% in height was observed in oil palm seedlings exposed to 200 µM Al (Cristancho *et al*., 2011). In this study, we observed a negative effect on the bole diameter size of Ulu Remis Deli *Dura* x Dumpy AVROS oil palm seedlings treated with 300 µM Al. Most of the oil palm varieties tested showed a reduction in bole diameter size. Cristancho *et al*. (2011) reported that oil palm seedlings exhibited a 28.9% reduction in bole diameter size when subjected to 200 µM Al. Currently, there are not many studies examining the effects of high Al concentrations on bole diameter size.

All varieties showed negative effects on chlorophyll content upon exposure to Al-toxicity. The chlorophyll content reduction was observed even at 100 µM Al concentration. The decrease in chlorophyll content from 200 µM Al exposure might be due to a significant reduction in root and shoot nitrogen (N) and Mg (Cristancho *et al*., 2011). In maize plants, chlorophyll content was severely affected upon exposure to 200 µM Al (Mihailovic *et al*., 2008). The reduction in chlorophyll content may reduce net photosynthesis due to its vital function in the photosynthesis process.

TABLE 3. EFFECTS OF DIFFERENT AL CONCENTRATIONS ON NUTRIENT UPTAKE IN ROOTS AND SHOOTS OF DIFFERENT OIL PALM SEEDLING VARIETIES

Parameters	Treatment 0 (Control): 0 µM	Treatment 1: 100 µM	Treatment 2: 200 µM	Treatment 3: 300 µM
Elite Deli *Dura* x BM119 AVROS *Pisifera*				
P in root (mg/kg)	18,916.670^{a}	19,813.330^{b}	13,850.000^{c}	21,390.000^{d}
K in root (mg/kg)	45,556.670^{a}	46 546.670^{a}	28,536.670^{b}	32,400.330^{c}
Ca in root (mg/kg)	5,352.330^{a}	6,510.000^{b}	5,080.330^{c}	5,213.330^{d}
Mg in root (mg/kg)	23,275.220^{a}	24,290.000^{b}	15,822.330^{c}	19,667.890^{a}
P in shoot (mg/kg)	16,556.670^{a}	26,273.330^{b}	7,462.333^{c}	13,426.670^{d}
K in shoot (mg/kg)	20,650.000^{a}	16,846.670^{b}	15,136.670^{c}	20,840.000^{a}
Ca in shoot (mg/kg)	5,352.330^{a}	6,510.000^{b}	5,080.330^{c}	5,213.330^{d}
Mg in shoot (mg/kg)	2,548.000^{a}	2,482.330^{ac}	2,326.670^{b}	2,459.000^{c}
Elite Deli *Dura* x Elite AVROS *Pisifera*				
P in root (mg/kg)	14,020.000^{a}	7,725.670^{b}	8,903.330^{c}	12,823.330^{d}
K in root (mg/kg)	159,086.700^{a}	18,030.000^{b}	20,373.330^{c}	25,743.330^{d}
Ca in root (mg/kg)	8,889.000^{a}	5,341.667^{b}	5,277.330^{b}	8,596.330^{c}
Mg in root (mg/kg)	4,721.670^{a}	2,486.000^{b}	2,497.330^{b}	3,741.670^{c}
P in shoot (mg/kg)	15,856.670^{a}	28,563.330^{b}	16,980.000^{c}	20,610.000^{d}
K in shoot (mg/kg)	25,213.330^{a}	39,663.330^{b}	40,700.000^{b}	40,686.670^{b}
Ca in shoot (mg/kg)	8,112.000^{a}	7,372.670^{b}	6,980.330^{c}	11,470.000^{d}
Mg in shoot (mg/kg)	3,035.670^{a}	6,664.000^{b}	5,963.330^{c}	5,789.000^{c}
Ulu Remis Deli *Dura* x Dumpy AVROS *Pisifera*				
P in root (mg/kg)	8,733.670^{c}	7,317.670^{d}	13,620.000^{a}	9 563.000^{b}
K in root (mg/kg)	16,723.330^{a}	15,596.670^{d}	16,040.000^{c}	16,593.330^{b}
Ca in root (mg/kg)	4,820.667^{ab}	4,994.667^{b}	4,791.000^{b}	5,452.333^{a}
Mg in root (mg/kg)	2,555.000^{a}	2,123.000^{b}	2,374.667^{b}	2,125.000^{c}
P in shoot (mg/kg)	19,136.670^{c}	25,903.330^{a}	15,883.330^{d}	25,446.670^{b}
K in shoot (mg/kg)	36,960.000^{a}	28,850.000^{b}	3,7530.000^{b}	53,506.670^{b}
Ca in shoot (mg/kg)	9,750.000^{a}	7,683.667^{b}	8,883.000^{c}	10,483.330^{d}
Mg in shoot (mg/kg)	4,976.000^{a}	5,804.667^{b}	5,000.667^{c}	7,025.6670^{c}
Ulu Remis Deli *Dura* x Ulu Remis *Tenera*				
P in root (mg/kg)	20,733.330^{a}	23,200.000^{b}	27,003.330^{c}	14,686.670^{d}
K in root (mg/kg)	37,066.670^{a}	19,486.670^{b}	31,056.670^{c}	20,453.330^{b}
Ca in root (mg/kg)	6,529.670^{a}	4,448.000^{b}	10,326.670^{c}	4,771.670^{d}
Mg in root (mg/kg)	4,049.330^{a}	2,872.330^{b}	4,935.330^{c}	2,732.330^{d}
P in shoot (mg/kg)	22,183.330^{a}	21,376.670^{b}	30,386.670^{c}	18,990.000^{d}
K in shoot (mg/kg)	47,910.000^{a}	38,466.670^{b}	46,243.330^{a}	43,853.330^{c}
Ca in shoot (mg/kg)	11,886.670^{a}	16,943.330^{b}	13,056.670^{c}	8,411.000^{d}
Mg in shoot (mg/kg)	7,213.000^{a}	6,002.670^{b}	6,815.670^{c}	5,783.670^{a}

Note: Different superscript letters in the same row indicate significant difference at $p \leq 0.05$.

Of the four different oil palm varieties tested, the root biomass of three varieties (Elite Deli *Dura* x BM119 AVROS *Pisifera*, Elite Deli *Dura* x Elite AVROS *Pisifera*, Ulu Remis Deli *Dura* x Dumpy AVROS) were affected due to Al-toxicity treatments. Root biomass was observed in Ulu Remis Deli *Dura* x Ulu Remis *Tenera* seedlings, treated with up to 200 µM Al. This positive effect can be correlated with the availability of P in the root. Increasing P availability in the root cell protects the cell membrane against Al toxic actions (Batista *et al*., 2009). Decreasing root and shoot biomass was correlated with the reduction of root and shoot growth. A reduction in root biomass was also reported in red spruce trees exposed to Al-toxicity (Graefe *et al*., 2008; Raynal *et al*., 1990). It is well

known that the most significant effect of Al-toxicity in plants is on the root growth and development which will eventually affect the root biomass. On the other hand, shoot biomass of the Ulu Remis Deli *Dura* x Dumpy AVROS variety was found to be the most affected. Similarly, 57.5% reduction in the shoot dry weight was observed in a Nigerian *Dura* x Nigerian *Dura* oil palm progeny (Christancho *et al*., 2011). Reduction in the shoot's dry mass of corn plants was also observed when the plants were treated with 100 mg kg^{-1} Al (Batista *et al*., 2009). In the present study, K content in the roots of Elite Deli *Dura* x BM119 AVROS *Pisifera* seedlings decreased upon exposure to Al concentrations of 200 and 300 µM.

Similarly, reduction trends in root K content had been observed previously in Angola *Dura,* Nigerian *Dura* and Deli *Dura* x AVROS *Pisifera* oil palm seedlings at 200 µM Al exposure (Cristancho *et al*., 2011) and in various oil palm seedlings treated with 225 ppm Al (Supena *et al*., 2014). K deficiency symptoms such as necrosis of old oil palm fronds were observed after treatment with high concentrations of Al for about five to six months. In contrast, increased K content in the roots of Elite Deli *Dura* x Elite AVROS *Pisifera* and Ulu Remis Deli *Dura* x Ulu Remis *Tenera* seedlings were observed. Increased K content was also observed in the shoots of Elite Deli *Dura* x Elite AVROS *Pisifera* oil palm seedlings. Increased K content was also observed in Al-treated Deli *Dura* x Dumpy AVROS *Pisifera* (Cristancho *et al*., 2011) and five oil palm progenies (Supena *et al*., 2014). Al-tolerant maize genotypes are able to accumulate high concentrations of K when exposed to high Al concentrations (Giannakoula *et al*., 2008). Al can block the inward K channels in the root hair (Cristancho *et al*., 2011). This was in line with a study by Liu and Luan (2001) on Al inhibition of K uptake and root elongation.

Phosphorus (P) uptake in both roots and shoots of Ulu Remis Deli *Dura* x Ulu Remis *Tenera* seedlings appeared to increase at 200 µM Al level. For other varieties however, a negative effect in P absorption was observed at as low as 100 µM Al. Shoot P content in Elite Deli *Dura* x BM119 AVROS *Pisifera,* Elite Deli *Dura* x Elite AVROS *Pisifera* and Ulu Remis Deli *Dura* x Dumpy AVROS varieties showed decreasing pattern at 200 µM Al. The root P content for Elite Deli *Dura* x Elite AVROS *Pisifera* and Elite Deli *Dura* x BM119 AVROS *Pisifera* decreased from exposure to 100 µM and 200 µM, respectively. On the other hand, root P content increased in Ulu Remis Deli *Dura* x Dumpy AVROS seedlings subjected to 200 µM Al. These observations are in line with a report by Cumming *et al*. (1986) on red spruce, where the P concentrations increased in roots but decreased in shoots. Al-toxicity may lead to the fixation of P into a less available form in the soil and in plant root (Fleming *et al*., 1974). Depending on the concentration, Al may function as an inducer or inhibitor of Ca inflow (Cristancho *et al*., 2011). In this study, the patterns in shoot and root Ca contents upon exposure to the different Al concentrations were inconsistent.

Decreased Ca content in roots of oil palm seedlings is most probably due to the destruction of the roots. Cristancho *et al*. (2011) also reported a 31.8% reduction in root Ca content in Nigerian *Dura* x Nigerian *Dura* oil palm seedlings on Al exposure. The presence of Al also inhibited the uptake of Ca in Al sensitive wheat varieties (Huang *et al*., 1992). High Al concentrations in soil also inhibits Ca uptake in garlic crops (Liu *et al*., 1993). In this study, Mg content in the roots of oil palm seedling also decreased from exposure to the lowest Al concentration used here 100 µM, but the shoot Mg content increased in all oil palm varieties. Cristancho *et al*. (2011) also reported a reduction in root Mg content in oil palm seedlings treated with Al with decreased shoot Mg content observed in the Nigerian *Dura* oil palm progeny. Several studies have reported that the reduction in uptake of most nutrient elements was due to a major destruction of the roots of oil palm seedlings and other plants in high Al concentrations. The reduction of nutrient uptake could be the declining effects in plant roots traits, especially the length of lateral roots, total root volume and root tips (Cristancho *et al*., 2009 2010, 2011; Li *et al*., 2008). Pteridophyta families also exhibited imbalanced nutrient uptake especially in Ca, Mg, P and K, due to the accumulation of Al (Olivares *et al*., 2009).

Apart from that, inconsistencies in nutrient absorption may also be due to effects of high Al concentrations on water uptake and movement in plants. Water plays an essential role in transporting nutrients throughout the plant. For example, the stomata of *Arabidopsis* plants closed after 9 hr of exposure to 100 µM Al (Sivaguru *et al*., 2003). The transpiration rate in wheat also decreased after exposure to 148 µM Al for 28 days (Ohki, 1986).

CONCLUSION

Different oil palm varieties show different responses towards high Al concentrations, suggesting differences in the levels of Al tolerated. The most affected part of oil palm seedlings exposed to high concentration of Al was the roots. The Elite Deli *Dura* x BM119 AVROS *Pisifera* seedlings appeared to have a low tolerance to high Al concentrations as compared to the other three varieties. In terms of shoot growth, Elite Deli *Dura* x Elite AVROS *Pisifera* and Ulu Remis Deli *Dura* x Dumpy AVROS varieties showed a high tolerant level towards Al esposure. Besides that, Elite Deli

Dura x Elite AVROS *Pisifera* demonstrated a steady bole diameter growth as compared to the other three varieties. On the other hand, the Ulu Remis Deli *Dura* x Ulu Remis *Tenera* variety exhibited the highest chlorophyll content. The Ulu Remis Deli *Dura* x Ulu Remis *Tenera* and Elite Deli *Dura* x Elite AVROS *Pisifera* varieties produced the highest root and shoot biomass growth respectively. In terms of root and shoot nutrient contents, Ulu Remis Deli *Dura* x Dumpy AVROS roots and Elite Deli *Dura* x Elite AVROS *Pisifera* shoots contained high amounts of K while Ulu Remis Deli *Dura* x Ulu Remis *Tenera* shoots and roots contained high amounts of P. High Ca contents were observed in the Elite Deli *Dura* x BM119 AVROS *Pisifera* roots and shoots, Ulu Remis Deli *Dura* x Dumpy AVROS roots and Ulu Remis Deli *Dura* x Ulu Remis *Tenera* shoots. Finally, Mg content was relatively higher in the roots and shoots of Elite Deli *Dura* x BM119 AVROS *Pisifera* and Ulu Remis Deli *Dura* x Dumpy AVROS seedlings as well as in Elite Deli *Dura* x Elite AVROS *Pisifera* shoots. From this study, the Elite Deli *Dura* x BM119 AVROS *Pisifera* oil palm seedlings exhibited the lowest tolerance towards high Al concentrations as compared to the other three oil palm varieties tested.

ACKNOWLEDGEMENT

The authors would like to thank the Faculty of Plantation and Agrotechnology, UiTM for providing the experimental plot and lab facilities for this research.

REFERENCES

Batista, M. A., Pintro, J. C., Da Costa, A. C. S., Tormena, C. A., Bonato, C. M., & Batista, M. F. (2009). Mineral composition and dry mass production of the corn plants in response to phosphorus sources and aluminum concentration. *Brazilian Archives of Biology and Technology*, *52*(3), 541–548. https://doi.org/10.1590/s1516-89132009000300004

Boudot, J., Becquer, T., Merlet, D., & Rouiller, J. (1994). Aluminium toxicity in declining forests: A general overview with a seasonal assessment in a silver fir forest in the Vosges mountains (France). *Annales Des Sciences Forestières*, *51*(1), 27–51. https://doi.org/10.1051/forest:19940103

Cristancho, R. J. A., Hanafi, M. M., Syed Omar, S. R. & Rafii, Y. M. (2009). Chemical characteristic of representative high aluminium saturation soil as affected by addiction of soil amendment in a closed incubation system. *Malaysian Journal of Soil Science, 13*, 13–28.

Cristancho, R. J. A., Hanafi, M. M., Syed Omar, S. R., & Rafii, Y. M. (2010). Variations in oil palm (*Elaeis guineensis* Jacq.) progeny response to high aluminium concentrations in solution culture. *Plant Biology*, *13*(2), 333–342. https://doi.org/10.1111/j.1438-8677.2010.00378.x

Cristancho, R. J. A., Hanafi, M. M., Syed Omar, S. R., Rafii, Y. M., Martinez, F. M. & Carlos, E. C. C. (2011). Alleviation of aluminium in acidic soils and its effect on growth of hybrid and clonal oil palm seedlings. *Journal of Plant Nutrition, 34*(3), 387–401. https://doi.org/10.1080/01904167.2011.536880

Cristancho, R. J. A., Munevar, M. F., Acosta, G. A., Santacruz, A. L. & Torres, V. M. (2007). Relationship between soil characteristics and distribution of mature oil palm (*Elaeis guineensis* Jacq.) root system. *Palmas, 28,* 24–30.

Cumming, J. R., Eckert, R. T., & Evans, L. S. (1986). Effect of aluminum on 32P uptake and translocation by red spruce seedlings. *Canadian Journal of Forest Research*, *16*(4), 864–867. https://doi.org/10.1139/x86-152

Fleming, A. L., Schwartz, J. W. & Foy, C. D. (1974). Soil: Aluminium toxicity in plants. *Argonomy Journal, 66*, 715-719.

Giannakoula, A., Moustakas, M., Mylona, P., Papadakis, I., & Yupsanis, T. (2008). Aluminum tolerance in maize is correlated with increased levels of mineral nutrients, carbohydrates and proline, and decreased levels of lipid peroxidation and Al accumulation. *Journal of Plant Physiology*, *165*(4), 385–396. https://doi.org/10.1016/j.jplph.2007.01.014

Graefe, S., Hertel, D., & Leuschner, C. (2008). Estimating fine root turnover in tropical forests along an elevational transect using minirhizotrons. *Biotropica*, *40*(5), 536–542. https://doi.org/10.1111/j.1744-7429.2008.00419.x

Huang, J., Grunes, D., & Kochian, L. (1992). Aluminum effects on the kinetics of calcium uptake into cells of the wheat root apex. *Planta*, *188*(3), 414–421. https://doi.org/10.1007/bf00192809

Kee, K. K., Goh, K. J., & Chew, P. S. (1995). Effects of NK fertiliser on soil pH and exchangeable K status on acid soils in an oil palm plantation

in Malaysia. In R. A. Date, N. J. Grundon, G. E. Rayment, & M. E. Probert (Eds.), *Plant-soil interactions at low pH: Principles and management* (Vol. 64, pp. 785–791). Springer. https://doi.org/10.1007/978-94-011-0221-6_130

Klimashevskii, E. L., & Dedov, V. M. (1975). Localization of growth inhibiting action of aluminiumions in elongating cell walls. *Fiziologiia Rastenii*, *22*(6), 1183–1190.

Kochian, L. V. (1995). Cellular mechanisms of aluminum toxicity and resistance in plants. *Annual Review of Plant Physiology and Plant Molecular Biology*, *46*(1), 237–260. https://doi.org/10.1146/annurev.pp.46.060195.001321

Kochian, L. V., Hoekenga, O. A., & Piñeros, M. A. (2004). How do crop plants tolerate acid soils? Mechanisms of aluminum tolerance and phosphorous efficiency. *Annual Review of Plant Biology*, *55*(1), 459–493. https://doi.org/10.1146/annurev.arplant.55.031903.141655

Krstic, K., Djalovic, I., Nikezic, D., & Bjelic, D. (2012). Aluminium in acid soils: Chemistry, toxicity and impact on maize plants. In A. Aladjadjiyan (Ed.), *Food production – Approaches, challenges and tasks* (pp. 231–243). InTechOpen. https://doi.org/10.5772/33077

Li, Y., Yang, G., Luo, L., Ke, T., Zhang, J., Li, K., & He, G. (2008). Aluminium sensitivity and tolerance in model and elite wheat varieties. *Cereal Research Communications*, *36*(2), 257–267. https://doi.org/10.1556/crc.36.2008.2.6

Liu, D., Jiang, W., & Li, D. (1993). Effects of aluminium ion on root growth, cell division, and nucleoli of garlic (*Allium sativum* L.). *Environmental Pollution*, *82*(3), 295–299. https://doi.org/10.1016/0269-7491(93)90132-8

Liu, K., & Luan, S. (2001). Internal aluminum block of plant inward K+ channels. *The Plant Cell*, *13*(6), 1453–1466. https://doi.org/10.1105/tpc.13.6.1453

Malaysian Meteorology Department. (2017). *Annual Report 2016*.

Mihailovic, N., Drazic, G., & Vucinic, Z. (2008). Effects of aluminium on photosynthetic performance in Al-sensitive and Al-tolerant maize inbred lines. *Photosynthetica*, *46*(3), 476–480. https://doi.org/10.1007/s11099-008-0082-0

Nelson, P. N., Sheaves, M., Bessou, C., Pardon, L., Lim, H. S., & Kookana, R. S. (2018). Modelling environmental impacts of agriculture, focusing on oil palm. In A. Rival (Ed.), *Achieving sustainable cultivation of oil palm. Volume 2: Diseases, pests, quality and sustainability* (pp. 285–334). Burleigh Dodds Science Publishing.

Ng, P. H. C., Gan, H. H., & Goh, K. J. (2011). Soil nutrient changes in Ultisols under oil palm in Johor, Malaysia. *Journal of Oil Palm & the Environment*, *2*, 93–104.

Ohki, K. (1986). Photosynthesis, chlorophyll, and transpiration responses in aluminum stressed wheat and sorghum. *Crop Science*, *26*(3), 572–575. https://doi.org/10.2135/cropsci1986.0011183x002600030030x

Olivares, E., Pena, E., Marcano, E., Mostacero, J., Aguiar, G., Benitez, M., & Rengifo, E. (2009). Aluminum accumulation and its relationship with mineral plant nutrients in 12 pteridophytes from Venezuela. *Environmental and Experimental Botany*, *65*(1), 132–141. https://doi.org/10.1016/j.envexpbot.2008.04.002

Osaki, M., Watanabe, T., & Tadano, T. (1997). Beneficial effect of aluminum on growth of plants adapted to low pH soils. *Soil Science & Plant Nutrition*, *43*(3), 551–563. https://doi.org/10.1080/00380768.1997.10414782

Raynal, D. J., Joslin, J. D., Thornton, F. C., Schaedle, M., & Henderson, G. S. (1990). Sensitivity of tree seedlings to aluminum: III. Red spruce and loblolly pine. *Journal of Environmental Quality*, *19*(2), 180–187. https://doi.org/10.2134/jeq1990.00472425001900020003x

Rout, G. R., Samantaray, S., & Das, P. (2001). Aluminium toxicity in plants: A review. *Agronomie*, *21*(1), 3–21. https://doi.org/10.1051/agro:2001105

Shamshuddin, J., & Noordin, W. D. (2011). Classification and management of highly weathered soils in character for production of plantation crops. In B. Ö. Güngör (Ed.), *Principles, application and assessment in soil science* (pp. 75–86). InTechOpen. https://doi.org/10.5772/29490

Sivaguru, M., Ezaki, B., He, Z., Tong, H., Osawa, H., BalušKa, F., Volkmann, D., & Matsumoto, H. (2003). Aluminum-Induced gene expression and protein localization of a cell Wall-Associated receptor kinase in *arabidopsis*. *Plant Physiology*, *132*(4), 2256–2266. https://doi.org/10.1104/pp.103.022129

Supena, N., Soegianto, A. & Soetopo, L. (2014). Response of oil palm varieties to aluminium stress. *Journal of Tropical Life Science*, *4*(1), 51–60. https://doi.org/10.11594/jtls.04.01.09

Watanabe, T., Jansen, S., & Osaki, M. (2005). The beneficial effect of aluminium and the role of citrate in Al accumulation in *Melastoma malabathricum*. *New Phytologist*, *165*(3), 773–780. https://doi.org/10.1111/j.1469-8137.2004.01261.x

Yang, Z. B., & Horst, W. J. (2015). Aluminium-induced inhibition of root growth: Roles of cell wall assembly, structure, and function. In F. Baluška & S. K. Panda (Eds.), *Aluminium stress adaptation in plants* (pp. 253–274). Springer.

Zhao, X., Jiao, C., Yang, F., Zhang, Z., & Ma, Y. (2023). Analytical techniques for detection of nanomaterials in soil-plant system. In P. Zhang, I. Lynch, J. C. White, & R. D. Handy (Eds.), *Analytical techniques for detection of nanomaterials in soil-plant system* (pp. 391–417). Elsevier. https://doi.org/10.1016/b978-0-323-91233-4.00016-8

Journal of Oil Palm Research Vol. 37 (3) September 2025 p. 451-460
DOI: https://doi.org/10.21894/jopr.2024.0035

MOLECULAR CHARACTERISATION OF OIL PALM (*Elaeis guineensis* Jacq.) HYBRIDS

ROJA RAMANI, G[1]*; KALPANA, M[1]; VENKATSWAMI, D[1] and KALYANABABU, B[2]

ABSTRACT

For genetic mapping research in a crop like oil palm, polymorphic simple sequence repeat (SSR) markers are crucial. Thirty four SSR loci were used for screening in the current work to test a total of 10 hybrids at molecular level. There were between two and four alleles in these, with 22 of them being polymorphic and 12 being monomorphic. The primer SMG00026 *had the greatest Polymorphism Information Content (PIC) value (0.60), while mEgCIR0408 had the lowest (0.14), with a mean PIC value of 0.22. Genetic variation scores varied between 0.15 (mEgCIR0408) and 0.66 (SMG00026), with an average of 0.286. Seven highly polymorphic markers, SMG00026, mEgCIR0074, mEgCIR0353, mEgCIR3350, mEgCIR0555, mEgCIR3886, and mEgCIR0905, were identified based on PIC and other genetic criteria. The oil palm crop development programme can effectively utilise the found polymorphic SSR loci in genetic diversity investigations and mapping. The 10 hybrids were divided into two primary clusters by a total of 22 polymorphic SSRs, and the observed clustering was based on geographic origin. These polymorphic primers can be used effectively because they make it easier to choose promising varieties at nursery stage, which helps both researchers and farmers to modernise the plant breeding programme for oil palm.*

Keywords: allele, polymorphism, primer.

Received: 31 August 2023; **Accepted:** 7 April 2024; **Published online:** 11 June 2024.

INTRODUCTION

The oil palm produces universal and distinctive oil that is most widely manufactured and commercialised of all vegetable oil crops. *Elaeis guineensis* Jacq. an oil palm species is a member of the Arecaceae family (tribe: Cocoineae) and is a monocot that is allogamous and arborescent native to West Africa (Hartley, 1988). Its genetic code, which has 16 homologous chromosome pairs and is diploid (2n = 32), is thought to be 1.800 gigabases (Gb) in size. The reference genome assembly for *E. guineensis* (AVROS, *pisifera* fruit form), which has a total size of 1.535 Gb, was made available to the general public in 2013 (Singh *et al*., 2013). Flow cytometry determined its physical size as 3.79 pg/2C (Rival *et al*., 1997). It can meet market demand in conjunction with a lower planting area than other oil crops due to its better productivity and extremely low production costs, which is especially beneficial for the food industry (Cadena *et al*., 2013; Mozzon *et al*., 2013). This golden palm is one of the greatest possibilities for meeting the nation's needs for edible oil because of its great oil production (4-6 t/ha) capability, which is five times greater than that of other annual oil-yielding crops (Basiron, 2000).

Malaysia and Indonesia are the two countries that produce the most palm oil (Yarra *et al*., 2019), although India is still in the early stages of its expansion in this area. Genetic research is aimed at increasing the effectiveness of oil palm farming because oil palm is naturally highly heterozygous. Genetic diversity assessment and the characterisation of germplasm of oil palm play a significant part in terms of genetic development

[1] Dr. Y.S.R. Horticultural University, Venkatramannagudem, Andhra Pradesh, 534101, India.

[2] ICAR-Indian Institute of Oil Palm Research, Pedavegi, Andhra Pradesh, 534450, India.

* *Corresponding author e-mail: rojaramanigorle60@gmail.com*

of the oil palm (Zhou *et al*., 2015). To quantify the genetic variability of germplasm (Zhao *et al*., 2019) morphological, biochemical and molecular approaches can be used (Mohammadi & Prasanna, 2003).

Oil palm molecular research has advanced somewhat as a result of the development of molecular marker innovation (Zhou *et al*., 2020). Mayes *et al.* (1997) pioneered the use of genetic markers in the oil palm industry by performing Restriction Fragment Length Polymorphism (RFLP)-based genetic mapping. Genetic diversity studies (Bakoume *et al*., 2014), linkage mapping studies (Singh *et al*., 2009), association mapping studies (Pootakham *et al*., 2015), and linkage map construction studies in oil palm all used DNA markers like Rapid Amplified Polymorphic DNA (RAPD) (Sathish & Mohankumar, 2007), Amplified Fragment Length Polymorphism (AFLP) (Rance *et al*., 2001), and simple sequence repeats (SSR) (Billotte *et al*., 2005).

Genomic DNA typification-based molecular assays have been acknowledged as effective techniques for assessing genetic diversity and creating molecular marker-based genetic mapping investigations (Liu *et al*., 2018). Amplification of the SSR is a common molecular method because of its benefits including hypervariability, broad genomic distribution, co-dominant inheritance, polymorphism, and chromosome-specific locations (Osorio-Guarín *et al*., 2020). In addition to being more practical to use in comparison to other DNA typification assays, PCR-based SSRs are regarded as being the most promising markers to comprehend population genetics (Asadi *et al*., 2019) and identifying probable parental genotypes in the oil palm. Using molecular markers, only some attempts have been done in India to increase the genetic diversity of local germplasm (Satish & Mohankumar, 2007).

Additionally, the data present enough proof to distinguish each variation between the three fruit forms namely, *dura, pisifera* and *tenera* individually (Babu *et al*., 2017), besides the parent *dura* and *pisifera* jointly. DNA-based polymorphism assays were conducted; this is the initial instance to assess the degree of variation in oil palm types (Satish & Mohankumar, 2007). There have not been any findings, though, on how genetically diverse the indigenous oil palm germplasm is. In order to use SSR markers in marker-assisted selection, genetic diversity, and mapping, it is essential to discover more polymorphic SSRs (Xiao *et al*., 2014).

Because of this, we used high yield related 34 SSR markers in the current work to identify polymorphic SSRs for genetic diversity investigations in certain genotypes. As a result, the use of SSR markers in oil palm breeding could be beneficial in differentiating high yielding hybrids at early stage, so that best performing hybrids could be multiplied and supplied to farmers in our country by reducing their time and expenses before going for commercial planting at field level and may increase their income.

The objectives of the current study were to identify polymorphic SSR markers of oil palm germplasm and use those markers to analyse the genetic diversity of the chosen germplasm.

MATERIALS AND METHODS

DNA Extraction from Plant Materials

Indian Institute of Oil Palm Research, Palode, Kerala made 10 cross combinations which were collected and planted at Horticultural Research Station, Vijayrai, Eluru with three replications (six palms per plot) in total were employed and *Table 1* contains information about each hybrid. Genomic DNA was extracted from an unopened oil palm spear leaflet stored in a field gene bank (Gawel & Jarret, 1991) using liquid nitrogen by following standard protocol of CTAB method with few modifications (Babu *et al*., 2019).

TABLE 1. LIST OF 10 HYBRIDS APPLIED IN THE STUDY AND THEIR CROSS COMBINATION

No.	Hybrids	Cross combination
1	NRCOP-1	78 x 435
2	NRCOP-2	90 x 577
3	NRCOP 3	158 x 116
4	NRCOP-4	131 x 435
5	NRCOP-5	5 x 577
6	NRCOP-6	173 x 435
7	NRCOP-7	183 x 577
8	NRCOP-8	70 x 577
9	NRCOP-9	28 x 435
10	NRCOP-10	345 x 577

SSR Amplification using PCR

A total of 34 SSR markers were used to amplify DNA of 10 oil palm hybrids (*Table 2*). The primers forward and reverse sequences came from Billotte *et al*. (2005). A reaction mixture (20 µL) of 10 X buffer (Hi media), 2 µL of 15 mm $MgCl_2$, 0.2 mM forward and reverse primers, 2 µL of 2 mM dNTPs, 0.2 µL of 1 U Taq DNA polymerase (Invitrogen, USA), and 25-50 ng template DNA was prepared to conduct the thermal reaction. Thermocycler (Biorad, USA) with a programmed initial denaturation of 3 min at 95°C, 35 cycles of 30 s at 95°C, 30 s at 50°C

temperature of annealing, extension of 1 min at 72°C, final extension of 10 min at 72°C, followed by a hold at 4°C was used to carry out the PCR amplifications. On an agarose gel with a 3% super fine resolution (SFR), the PCR results were fractionated. The electrophoresis was conducted at ambient temperature for 3 hr at 100 volts. Agarose gel was manually scored depending on the size of the 100 bp ladder after being viewed using the Bioimaging System (Bio Rad) and stained with ethidium bromide. Power Marker 3.0 was used for the UPGMA analysis and statistical analysis of polymorphism for the generation of dendrograms. The Power Marker V3.0 software was utilised to compute PIC, heterozygosity, gene diversity, allele frequency, and inbreeding co-efficient (Liu & Muse, 2005).

RESULTS AND DISCUSSION

In order to investigate variability in our set of evaluated samples, highly polymorphic SSRs reported by Billotte *et al.* (2005) were sufficient. Using 34 SSR markers, the oil palm's hybrids genetic DNA (*Table 3*) was amplified and produced bands that could be scored. The 34 SSRs were uniformly distributed across the oil palm chromosomes. Out of the 34 primers, 22 loci (64.7% of the total) were discovered to be polymorphic, detecting 58 alleles on average with for each locus, while 12 SSR loci (35.2%) were monomorphic.

With polymorphic primers, the oil palm hybrids produced between 2 and 4 alleles. This figure is less than, the 13.1 alleles per locus discovered by Bakoume *et al*. (2015). Evidently, the quantity of polymorphic alleles per locus depends on the number of investigated samples and sample origin. The modest amount of materials employed in this study *i.e.*, a few number of parents in a breeding programme and a small number of descendants for their intercrosses likely contributed to the low number of alleles. Allele variability tends to decline and the population is impacted by this hybridisation and selection. The SSR loci *mEgCIR0408*, *mEgCIR3808*, *mEgCIR3382*, *mEgCIR3705*, *mEgCIR2347*, and *SMG00227* with 2 alleles were determined to have the most alleles. The SSR locus *SMG00026* registered 4 alleles. *Figure 1* and *2* showed the band pattern suggesting SSR loci polymorphism of *mEgCIR0350* and *mEgCIR0074*, respectively.

The results observed are good, as the markers employed have a 95% efficiency in differentialy unique palms. The capacity of the polymorphic primers to distinguish between different hybrids was demonstrated by the PIC values, which varied between 0.14-0.60 for all 10 oil palm hybrids, with an average value of 0.22. It is comparable to PIC values from previous oil palm studies that used markers from comparable sources and were tested on six unique crossings (Budiman *et al*., 2019), also on plants with similar ancestors (Arias *et al*., 2014). The marker's level of informativeness increases with its PIC.

Out of 34 primers, primer SMG00026 had the highest PIC value in our samples, which was 0.60, is considered to be moderately informative, best in screening oil palm genotypes loci, capable of discriminating between genotypes which can be used for genetic fingerprinting in breeding programmes and the mEgCIR3808 primer exhibited the lowest PIC value (0.14) (Zaki *et al*., 2012).

Expected heterozygosity (H_e), often known as gene diversity, the values ranged from 0.15 (*mEgCIR0408*) to 0.66 (*SMG00026*), with a mean of 0.286. The observed heterozygosity (H_o), also

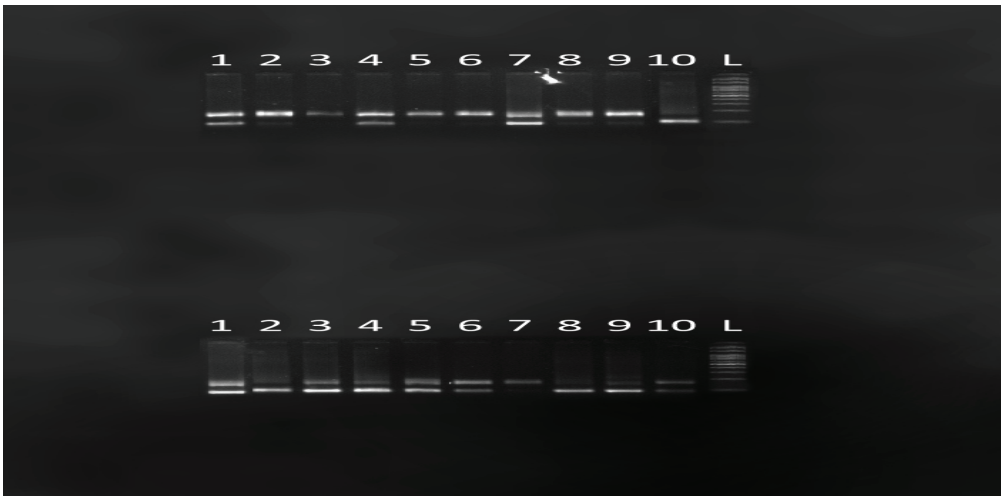

Figure 1. The mEgCIR3350 *loci's SSR banding profile among the 10 oil palm hybrids, where L = 100 bp DNA ladder lane (1-10) oil palm hybrids (please refer to* Table 1 *for label).*

TABLE 2. SSR MARKERS USED TO DETERMINE GENETIC DIVERSITY IN TEN OIL PALM HYBRIDS

No.	Locus	Repeat motif	Primer sequence (5′-3′)		Annealing temperature (°C)	Link age group location[b]
			Forward	Reverse		
1	*SMG00217*	NA	GGTGGAATTAGTTGCTCAGAAG	CGCAGATGTTTCATAATCGAG	52	NA
2	*SPSC00185*	NA	AAGGAGAACTACCACGCGAA	AATTATGTGCGGTTGTTGAGC	52	NA
3	*SMG00227*	NA	TCTATTTCATCCAAATCTGCAC	TTTTCAGTTAGCGCATAGCAT	52	NA
4	*SEG00125*	NA	TACCCTTTTCCCTCCCTCCATA	CATCATCTCCGTTGCCAGTATT	58	NA
5	*SMG00026*	NA	CCCCTACCTTTCTTTCTTACC	ATGAGCAGGAGTTGGAATAG	52	NA
6	*mEgCIR0059*	(GA)15	TGCAGGGGATGCTTTTATT	CCCTTAATTCCTGCCTTATT	52	4
7	*mEgCIR0074*	(GT)7ga	AAGAGAGTTTCACGGTCATA	GACCTCTGCTTGTGTTTCTA	52	4
8	*mEgCIR0195*	(GA)21	CCCACCACCCCTAGCTTCTC	ACCCCGGTCCAAATAAAATC	58	6
9	*mEgCIR0246*	(GA)19	GGTAAGAGATGAGATGGGTTGTC	AGGAATTAAGGGTTGTAGGTGAA	52	8
10	*mEgCIR0353*	(GT)11 (GA)15	AGAGAGAGAGAGTGCGTATG	GTCCCTGTGGCTGCTGTTTC	52	16
11	*mEgCIR0874*	(CA)11 (GA)18	TCCAGTTGTCGAGTTGTAGT	ATTATGGGGTTATGCTTTCA	52	1
12	*mEgCIR0894*	(GA)18	TGCTTCTTGTCCTTGATACA	CCACGTCTACGAAATGATAA	52	7
13	*mEgCIR0555*	(GA)18	TACCATCACTGACCAATAAC	GTCTTTCTTGCTAACTACAC	52	8
14	*mEgCIR0878*	(GA)22	CAAAGCAACAAAGCTAGTTAGTA	CAAGCAACCTCCATTTAGAT	52	11
15	*mEgCIR0773*	NA	GCAAAATTCAAAGAAAACTTA	CTGACAGTGCAGAAAATGTTATAGT	52	NA
16	*mEgCIR2347*	(GA)15	ATTTTGCATGTGTTGAGAGC	CAACCAATTGCACCCTAAAG	52	8
17	*mEgCIR2291*	(GA)11	ATGCCCGGATCTTTGTGTAG	TTGTTCGTGTTAATCAAGTGTATG	52	7
18	*mEgCIR3300*	(GA)19	CATGCACGTAAAGAAAGTGT	CCAAATGCACCCTAAGA	52	7
19	*mEgCIR3382*	(GA)24	TGTAGGTGGTGGTTAGG	TGTCAGACCCACCATTA	52	11
20	*mEgCIR3350*	(GA)16	GGAATAAAGCTTCCAACAAC	CCTGGTCGTTTGGTAGAGA	52	14
21	*mEgCIR3683*	(GA)15	GTAGCTTGAACCTGAAA	AGAACCACCGGAGTTAC	52	2
22	*mEgCIR3555*	(GA)18	CATCAGAGCCTTCAAACTAC	AGCCTGAATTGCCTCTC	52	13
23	*mEgCIR3546*	(GA)15	GCCTATCCCCTGAACTATCT	TGCACATACCAGCAACAGAG	52	14
24	*mEgCIR3569*	(GA)25	AAGGCTTGGAGTTGAGGTAT	CACCATTGCATCATTATTCC	52	14
25	*mEgCIR3705*	(GA)16	CCACCATGCAGAATAGTAAG	GTGTGCCCTCAAAAAGTATG	52	4
26	*mEgCIR3775*	(GA)18	TCTTGATATTAAAAGGTCAGGAGAA	CGTTCCCTTTTTCCATAGAT	52	4
27	*mEgCIR3711*	(GA)17	GTCTCATGTGGCTACCTCTC	AGGCTCCCTGCTTTTAAGT	52	8
28	*mEgCIR3732*	(GA)19	ATTTTATTTGGCTTGGTATA	ACTTTTCTATCTAATTCTTGAAGAT	52	8
29	*mEgCIR3808*	(GA)22	CCGCTAACTTGGTATAC	ATTTCCAGCAGCTAATC	52	8
30	*mEgCIR3557*	NA	CATTGCCATTCCCTTCAAGT	TCCCCTCTGTTCACTCAAGC	52	NA
31	*mEgCIR3260*	NA	GGGCAAGTCATGTTTCCTACA	TAAGGGCGAGGTATTTCTGC	52	NA
32	*mEgCIR0408*	NA	AGCGCAGTTGCTCGGTATAA	CCCTGCAGTGTCCCTCTTTA	52	NA
33	*mEgCIR3886*	NA	TTCTAGGGTCTATCAAAGTCATAAG	AGCCACCACCACCATCTACT	52	NA
34	*mEgCIR0905*	NA	CACCACATGAAGCAAGCAGT	CCTACCACAACCCCAGTCTC	52	NA

known as the heterozygosity range (*mEgCIR0074*, *mEgCIR0353*, *mEgCIR0555*, *mEgCIR3886*, *mEgCIR0905*), was seen with an average of 0.10 (*SEG00125*) to 1.00 (*mEgCIR0074*, *mEgCIR3886*, *mEgCIR0905*). But the H_o determined in our investigation, was higher than the projected H_e, demonstrating greater diversity and no heterozygosity deficiency and could be justified by the advanced breeding population (Sarimana *et al*., 2021) and the stated H_o value is comparable to prior publication (Arias *et al*., 2015).

The major allele at the locus with the highest frequency was *mEgCIR0408* (140 bp allele), which was followed by *mEgCIR3808* (190 bp allele), which was at 88%, *SMG00227* (240 bp allele), which was at 83%, and *mEgCIR3382* (140 bp allele), which was at 83%. This study aids in the identification of small population based on the amount of acquired alleles (Romeo *et al.*, 2003). Different populations had different allele frequencies at each locus, and some alleles were exclusive to one or a few populations. The most frequent factors influencing allele frequencies are genetic drift and reproductive isolation which is common in out crossing plants like oil palm, where random mating is expected (Bakoume *et al*., 2009).

Given that genetic diversity functions in various strategies to determine population relationships, the relatively low average gene diversity of all the hybrids (28%), which indicates that the genotypes had low degrees of polymorphism and the lack of correlation between variations assessed by molecular markers should not be regarded as a constraint.

UPGMA analysis generated dendrogram divided the 10 oil palm hybrids into two major categories. NRCOP-5 established a unique cluster that was relatively characteristic of their heterotic group and two further sub clusters were created from cluster II which includes NRCOP-2, NRCOP-1, NRCOP-4, NRCOP-3 and NRCOP-6 in one sub cluster whereas NRCOP-7, NRCOP-8, NRCOP-9 and NRCOP-10 in another sub cluster (*Figure 3*). Both clusters include parents chosen for their high combining ability and production potential.

Figure 2. The SSR banding profile of the 10 oil palm hybrids of mEgCIR0074 *loci, where L = 100 bp DNA ladder lane (1-10) oil palm hybrids (please refer to* Table 1 *for label).*

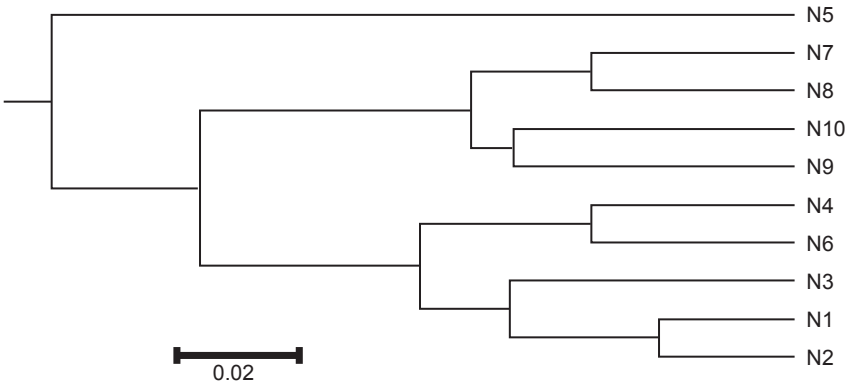

Note: N1 - NRCOP-1; N2 - NRCOP-2; N3 - NRCOP-3; N4 - NRCOP-4; N5 - NRCOP-5; N6 - NRCOP-6; N7 - NRCOP-7; N8 - NRCOP-8; N9 - NRCOP-9; and N10 - NRCOP-10

Figure 3. The rectangular dendrogram of 10 oil palm hybrids as determined by UPGMA analysis using the software POWER MARKER.

TABLE 3. PARAMETERS FOR 34 SSR LOCI GENETIC ANALYSIS OVER THE 10 OIL PALM HYBRIDS

No.	Locus	Major allele frequency	Allele no.	Gene diversity	Heterozygosity	PIC
1	*SMG00217*	0.5714	2.0000	0.4898	0.8571	0.3698
2	*SMG00026*	0.4286	4.0000	0.6633	0.8571	0.6003
3	*mEgCIR0074*	0.5000	2.0000	0.5000	1.0000	0.3750
4	*mEgCIR0195*	0.5556	2.0000	0.4938	0.6667	0.3719
5	*mEgCIR0246*	0.5556	2.0000	0.4938	0.8889	0.3719
6	*SPSC00185*	1.0000	1.0000	0.0000	0.0000	0.0000
7	*SMG00227*	0.8333	2.0000	0.2778	0.3333	0.2392
8	*SEG00125*	0.6500	2.0000	0.4550	0.1000	0.3515
9	*mEgCIR0059*	1.0000	1.0000	0.0000	0.0000	0.0000
10	*mEgCIR0353*	0.5000	2.0000	0.5000	1.0000	0.3750
11	*mEgCIR0874*	1.0000	1.0000	0.0000	0.0000	0.0000
12	*mEgCIR0894*	0.5833	2.0000	0.4861	0.1667	0.3680
13	*mEgCIR0555*	0.5000	2.0000	0.5000	1.0000	0.3750
14	*mEgCIR0878*	0.5556	2.0000	0.4938	0.8889	0.3719
15	*mEgCIR0773*	0.5556	2.0000	0.4938	0.4444	0.3719
16	*mEgCIR2347*	0.7500	2.0000	0.3750	0.0000	0.3047
17	*mEgCIR2291*	1.0000	1.0000	0.0000	0.0000	0.0000
18	*mEgCIR3300*	1.0000	1.0000	0.0000	0.0000	0.0000
19	*mEgCIR3382*	0.8333	2.0000	0.2778	0.3333	0.2392
20	*mEgCIR3350*	0.5000	2.0000	0.5000	0.1111	0.3750
21	*mEgCIR3683*	1.0000	1.0000	0.0000	0.0000	0.0000
22	*mEgCIR3555*	1.0000	1.0000	0.0000	0.0000	0.0000
23	*mEgCIR3546*	0.6000	2.0000	0.4800	0.8000	0.3648
24	*mEgCIR3569*	1.0000	1.0000	0.0000	0.0000	0.0000
25	*mEgCIR3705*	0.7000	2.0000	0.4200	0.2000	0.3318
26	*mEgCIR3775*	1.0000	1.0000	0.0000	0.0000	0.0000
27	*mEgCIR3711*	1.0000	1.0000	0.0000	0.0000	0.0000
28	*mEgCIR3732*	1.0000	1.0000	0.0000	0.0000	0.0000
29	*mEgCIR3808*	0.8889	2.0000	0.1975	0.0000	0.1780
30	*mEgCIR3557*	1.0000	1.0000	0.0000	0.0000	0.0000
31	*mEgCIR3260*	0.6000	2.0000	0.4800	0.8000	0.3648
32	*mEgCIR0408*	0.9167	2.0000	0.1528	0.1667	0.1411
33	*mEgCIR3886*	0.5000	2.0000	0.5000	1.0000	0.3750
34	*mEgCIR0905*	0.5000	2.0000	0.5000	1.0000	0.3750
Mean	**-**	**0.7523**	**1.7059**	**0.2862**	**0.3710**	**0.2233**

According to UPGMA results, genetic similarity is typically not correlated with geographic distance but rather is consistent with geographic dispersal. Combining morphological and agronomic data with similarity groups can be used to select and cross superior plants, maximising the expression of "interpopulation heterosis" and enabling more effective utilisation of the genetic diversity already present.

Jaccard's similarity co-efficient between genotypes ranged from 3.850%-32.000% (*Table 4*) with an average of 18.000%, suggesting a moderate genetic relationship within oil palm hybrids. The highest similarity coefficient value of 32.000% was observed between hybrids of NRCOP-5 and NRCOP-9 and the least similarity of 3.850% was noticed between hybrids of NRCOP-1 and NRCOP-2. In nine D-P cross combinations, Arias *et al.* (2013) showed similarity coefficients ranging from 0.015%-0.039% (Zulkifli *et al*., 2012), with a mean genetic distance of 0.251 among oil palm germplasm originating from eleven different African states. Our findings, however, indicated that high similarity values were also seen among oil palm hybrids, indicating that there was either no inter-crossing between them or there was significant inbreeding.

The anticipated heterozygosity of 0.280 was comparable to 0.200, which Arias *et al*. (2013) reported as a high value, and 0.390, which Okoye *et al*. (2016a) recorded for African oil palm. The findings of the genetic diversity analysis conducted to study H_e and H_o published among the utilising genotypes of oil palm using microsatellites are very similar. H_e and H_o measurements collected from Nigeria and Malaysia ranged from 0.167-0.778 and 0.153-0.643, respectively. With NIFOR oil palm germplasm, H_e of 0.700 and H_o of 0.690 were reported by Okoye *et al*. (2016b). Twelve of the 34 SSRs were monomorphic, and 22 were polymorphic. The gel image depicts the polymorphic SSRs banding patterns, which are seen in *Figure 1* and *2*.

There were 18 microsatellites according to the PIC value that were more numerous, higher than usual due to their comparatively high levels of polymorphism: SSR loci *SMG00026*, *mEgCIR0074*, *mEgCIR0353*, *mEgCIR3350*, *mEgCIR0555*, *mEgCIR3886*, and *mEgCIR0905* stood out among the others. Eighteen SSR loci in all fell into the 0.3-0.6 PIC range, with an average rate of 0.3, whereas four loci fell into the 0.14-0.23 PIC range, with 0.18 as the mean. A marker is considered more informative if its PIC is higher.

Out of 22 primers, SMG00026 has the highest PIC value of 0.6, followed by mEgCIR0074, mEgCIR0195, mEgCIR0246, mEgCIR0353, mEgCIR0555, mEgCIR0878, mEgCIR0773, mEgCIR3350, mEgCIR3886 and mEgCIR0905. The highest PIC value in commercial oil palm material was stated by Arias *et al*. (2010) at 0.822 and Okoye *et al*. (2016a) attained an incredibly elevated mean proportion of polymorphism (85.09%).

The oil palm breeding programme may have involved crossing 10 hybrids into two major groups, and the dendrogram suggests that these geographical regions may have sprung from a single genetic background or from genetic origins that are comparable. Similar findings were made in a study by Bakoume *et al*. (2009) using SSR markers on a natural population of oil palms. Since the female lines, namely *dura*, originated from four palms and that oil palm is very heterozygous, it is possible that the same genes contributed to the clustering pattern.

Nevertheless, we offer our SSR results that can be combined with additional markers or used independently for further validation by other authors in search of the most effective identification formula. SSRs are more effective as a quality check to establish the accuracy of the pedigree and authenticity. However, screening more SSRs could make this method better, and more accessions should be developed to create new strains for confirming the findings.

TABLE 4. JACCARD'S SIMILARITY COEFFICIENT VALUES BASED ON 34 SSR PRIMERS SEQUENCE DATA OF OIL PALM HYBRIDS

Hybrids	NRCOP-1	NRCOP-10	NRCOP-2	NRCOP-3	NRCOP-4	NRCOP-5	NRCOP-6	NRCOP-7	NRCOP-8	NRCOP-9
NRCOP-1	0.0000	0.1522	0.0385	0.0652	0.1250	0.2391	0.1250	0.2000	0.1731	0.1923
NRCOP-10		0.0000	0.1200	0.1591	0.1458	0.2083	0.1800	0.0625	0.1042	0.0800
NRCOP-2			0.0000	0.0962	0.0556	0.1731	0.0769	0.1800	0.1731	0.1852
NRCOP-3				0.0000	0.1087	0.1739	0.1458	0.1522	0.1667	0.2000
NRCOP-4					0.0000	0.1923	0.0577	0.1667	0.1538	0.1731
NRCOP-5						0.0000	0.1875	0.1667	0.2400	0.3200
NRCOP-6							0.0000	0.1600	0.1400	0.2115
NRCOP-7								0.0000	0.0577	0.0926
NRCOP-8									0.0000	0.1071
NRCOP-9										0.0000

CONCLUSION

Vegetable oil from the golden palm is valuable, and polymorphic markers must be found to identify significant QTLs in the germplasm for use in a breeding program to increase oil yield. Seven highly polymorphic SSR markers (SMG00026, mEgCIR0074, mEgCIR0353, mEgCIR3350, mEgCIR0555, mEgCIR3886, and mEgCIR0905) were discovered in this study determined by the following criteria: Polymorphic alleles of ≥2, gene diversity of ≥48, and PIC value of ≥37.

In conclusion, the novel information presented here shows that the developed hybrids are a valuable resource to support additional research to create countrywide breeding plans and conservation initiatives for this vital crop in India. These polymorphic primers and QTL mapping studies can be used effectively because they make it easier to choose promising varieties at an early stage, which helps to shorten the oil palm's lengthy breeding cycle. Additionally, because they showed extremely high polymorphism over other loci, they may also help to modernise the plant breeding programme for oil palm.

ACKNOWLEDGEMENT

The first author is grateful to Dr. Y.S.R. Horticultural University in Venkatramannagudem and the Directors of the ICAR-IIOPR in Pedavegi, Andhra Pradesh for providing the tools needed for me to conduct my study as part of my M.Sc. thesis.

REFERENCES

Arias, D., González, M., Prada, F., Ayala-Diaz, I., Montoya, C., Daza, E., & Romero, H. M. (2015). Genetic and phenotypic diversity of natural American oil palm (*Elaeis oleifera* (H.B.K.) Cortés) accessions. *Tree Genetics & Genomes*, *11*(6). https://doi.org/10.1007/s11295-015-0946-y

Arias, D., González, M., Prada, F., Restrepo, E., & Romero, H. (2013). Morpho-agronomic and molecular characterisation of oil palm *Elaeis guineensis* Jacq. material from Angola. *Tree Genetics & Genomes*, *9*(5), 1283–1294. https://doi.org/10.1007/s11295-013-0637-5

Arias, D., Montoya, C., & Romero, H. M. (2010). Preliminary results on the molecular characterization of oil palm using microsatellites markers. *Palmas*, *31*(3), 35–45.

Arias, D., Ochoa, I., Castro, F., & Romero, H. (2014). Molecular characterization of oil palm *Elaeis guineensis* Jacq. of different origins for their utilization in breeding programmes. *Plant Genetic Resources*, *12*(3), 341–348. https://doi.org/10.1017/s1479262114000148

Asadi, A., Ebrahimi, A., Rashidi-Monfared, S., Basiri, M., & Akbari-Afjani, J. (2020). Comprehensive functional analysis and mapping of SSR markers in the chickpea genome (*Cicer arietinum* L.). *Computational Biology and Chemistry*, *84*, 107169. https://doi.org/10.1016/j.compbiolchem.2019.107169

Babu, B. K., Mathur, R. K., Kumar, P. N., Ramajayam, D., Ravichandran, G., Venu, M. V. B., & Babu, S. S. (2017). Development, identification and validation of *CAPS* marker for *SHELL* trait which governs *dura, pisifera* and *tenera* fruit forms in oil palm (*Elaeis guineensis* Jacq.). *PLoS ONE*, *12*(2), e0171933. https://doi.org/10.1371/journal.pone.0171933

Babu, B. K., Rani, K. L. M., Sahu, S., Mathur, R. K., Kumar, P. N., Ravichandran, G., Anitha, P., & Bhagya, H. P. (2019). Development and validation of whole genome-wide and genic microsatellite markers in oil palm (*Elaeis guineensis* Jacq.): First microsatellite database (OpSatdb). *Scientific Reports*, *9*(1), 1899. https://doi.org/10.1038/s41598-018-37737-7

Bakoume, C., Wickneswari, R., Rajanaidu, N., Kushairi, A., & Billotte, N. (2009). Screening natural oil palm (*Elaeis guineensis* Jacq.) populations using SSR markers. In *International Society for Oil Palm Breeders Seminar* (pp. 1–10).

Bakoumé, C., Wickneswari, R., Siju, S., Rajanaidu, N., Kushairi, A., & Billotte, N. (2015). Genetic diversity of the world's largest oil palm (*Elaeis guineensis* Jacq.) field genebank accessions using microsatellite markers. *Genetic Resources and Crop Evolution*, *62*(3), 349–360. https://doi.org/10.1007/s10722-014-0156-8

Basiron, Y. (2000). Techno-economic aspects of research and development in the Malaysian oil palm industry. In Y. Basiron, B. S. Jalani, & K. W. Chan (Eds.), *Advances in oil palm research* (pp. 1-18). Malaysian Palm Oil Board.

Billotte, N., Marseillac, N., Risterucci, A., Adon, B., Brottier, P., Baurens, F., Singh, R., Herrán, A., Asmady, H., Billot, C., Amblard, P., Durand-Gasselin, T., Courtois, B., Asmono, D., Cheah, S. C., Rohde, W., Ritter, E., & Charrier, A. (2005). Microsatellite-based high density

linkage map in oil palm (*Elaeis guineensis* Jacq.). *Theoretical and Applied Genetics*, *110*(4), 754–765. https://doi.org/10.1007/s00122-004-1901-8

Budiman, L. F., Apriyanto, A., Pancoro, A., & Sudarsono, S. (2019). Genetic diversity analysis of *Tenera* × *Tenera* and *Tenera* × *Pisifera* Crosses and D-self of oil palm (*Elaeis guineensis*) parental populations originating from Cameroon. *Biodiversitas Journal of Biological Diversity*, *20*(4), 937–949. https://doi.org/10.13057/biodiv/d200402

Cadena, T., Prada, F., Perea, A., & Romero, H. M. (2013). Lipase activity, mesocarp oil content, and iodine value in oil palm fruits of *Elaeis guineensis*, *Elaeis oleifer*a, and the interspecific hybrid O×G (*E. oleifera* × *E. guineensis*). *Journal of the Science of Food and Agriculture*, *93*(3), 674–680. https://doi.org/10.1002/jsfa.5940

Gawel, N. J., & Jarret, R. L. (1991). A modified CTAB DNA extraction procedure for *Musa* and *Ipomoea*. *Plant Molecular Biology Reporter*, *9*(3), 262–266. https://doi.org/10.1007/bf02672076

Hartley, C. W. S. (1988). *The oil palm. 2nd edition*. Longman.

Liu, K., & Muse, S. V. (2005). PowerMarker: An integrated analysis environment for genetic marker analysis. *Bioinformatics*, *21*(9), 2128–2129. https://doi.org/10.1093/bioinformatics/bti282

Liu, Z., Shao, W., Shen, Y., Ji, M., Chen, W., Ye, Y., & Shen, Y. (2018). Characterization of new microsatellite markers based on the transcriptome sequencing of *Clematis finetiana*. *Hereditas*, *155*(1), 23. https://doi.org/10.1186/s41065-018-0060-x

Mayes, S., Jack, P. L., Corley, R. H. V., & Marshall, D. F. (1997). Construction of a RFLP genetic linkage map for oil palm (*Elaeis guineensis* Jacq.). *Genome*, *40*(1), 116–122. https://doi.org/10.1139/g97-016

Mohammadi, S. A., & Prasanna, B. M. (2003). Analysis of genetic diversity in crop plants – Salient statistical tools and considerations. *Crop Science*, *43*(4), 1235–1248. https://doi.org/10.2135/cropsci2003.1235

Mozzon, M., Pacetti, D., Lucci, P., Balzano, M., & Frega, N. G. (2013). Crude palm oil from interspecific hybrid *Elaeis oleifera* × *Elaeis guineensis*: Fatty acid regiodistribution and molecular species of glycerides. *Food Chemistry*, *141*(1), 245–252. https://doi.org/10.1016/j.foodchem.2013.03.016

Okoye, M. N., Bakoumé, C., Uguru, M. I., Singh, R., & Okwuagwu, C. O. (2016a). Genetic relationships between elite oil palms from Nigeria and selected breeding and germplasm materials from Malaysia via simple sequence repeat (SSR) Markers. *Journal of Agricultural Science*, *8*(2), 159. https://doi.org/10.5539/jas.v8n2p159

Okoye, M. N., Uguru, M. I., Bakoumé, C., Singh, R., & Okwuagwu, C. O. (2016b). Assessment of genetic diversity of NIFOR oil palm main breeding parent genotypes using microsatellite markers. *American Journal of Plant Sciences*, *07*(01), 218–237. https://doi.org/10.4236/ajps.2016.71022

Osorio-Guarín, J. A., Berdugo-Cely, J. A., Coronado-Silva, R. A., Baez, E., Jaimes, Y., & Yockteng, R. (2020). Genome-wide association study reveals novel candidate genes associated with productivity and disease resistance to *Moniliophthora* spp. in cacao (*Theobroma cacao* L.). *G3 Genes Genomes Genetics*, *10*(5), 1713–1725. https://doi.org/10.1534/g3.120.401153

Pootakham, W., Jomchai, N., Ruang-Areerate, P., Shearman, J. R., Sonthirod, C., Sangsrakru, D., Tragoonrung, S., & Tangphatsornruang, S. (2015). Genome-wide SNP discovery and identification of QTL associated with agronomic traits in oil palm using genotyping-by-sequencing (GBS). *Genomics*, *105*(5–6), 288–295. https://doi.org/10.1016/j.ygeno.2015.02.002

Rance, K. A., Mayes, S., Price, Z., Jack, P. L., & Corley, R. H. V. (2001). Quantitative trait loci for yield components in oil palm (*Elaeis guineensis* Jacq.). *Theoretical and Applied Genetics*, *103*(8), 1302–1310. https://doi.org/10.1007/s122-001-8204-z

Rival, A., Beule, T., Barre, P., Hamon, S., Duval, Y., & Noirot, M. (1997). Comparative flow cytometric estimation of nuclear DNA content in oil palm (*Elaeis guineensis* Jacq.) tissue cultures and seed-derived plants. *Plant Cell Reports*, *16*(12), 884–887. https://doi.org/10.1007/s002990050339

Romero, C., Pedryc, A., Muñoz, V., Llácer, G., & Badenes, M. L. (2003). Genetic diversity of different apricot geographical groups determined by SSR markers. *Genome*, *46*(2), 244–252. https://doi.org/10.1139/g02-128

Sarimana, U., Herrero, J., Erika, P., Indarto, N., Wendra, F., Santika, B., Ritter, E., Sembiring, Z., & Asmono, D. (2021). Analysis of genetic diversity and discrimination of oil palm DxP populations based on the origins of *pisifera*

elite parents. *Breeding Science*, *71*(2), 134–143. https://doi.org/10.1270/jsbbs.20043

Sathish, D. K. & Mohankumar, C. (2007). RAPD markers for identifying oil palm (*Elaeis guineensis* Jacq.) parental varieties (*dura* and *pisifera*) and the hybrid *tenera*. *Indian Journal of Biotechnology, 6*, 354-358.

Singh, R., Ong-Abdullah, M., Low, E. L., Manaf, M. a. A., Rosli, R., Nookiah, R., Ooi, L. C., Ooi, S., Chan, K., Halim, M. A., Azizi, N., Nagappan, J., Bacher, B., Lakey, N., Smith, S. W., He, D., Hogan, M., Budiman, M. A., Lee, E. K., . . . Sambanthamurthi, R. (2013). Oil palm genome sequence reveals divergence of interfertile species in Old and New worlds. *Nature*, *500*(7462), 335–339. https://doi.org/10.1038/nature12309

Singh, R., Tan, S. G., Panandam, J. M., Rahman, R., Ooi, L. C., Low, E. L., Sharma, M., Jansen, J., & Cheah, S. (2009). Mapping quantitative trait loci (QTLs) for fatty acid composition in an interspecific cross of oil palm. *BMC Plant Biology*, *9*(1), 114. https://doi.org/10.1186/1471-2229-9-114

Xiao, Y., Zhou, L., Xia, W., Mason, A. S., Yang, Y., Ma, Z., & Peng, M. (2014). Exploiting transcriptome data for the development and characterization of gene-based SSR markers related to cold tolerance in oil palm (*Elaeis guineensis*). *BMC Plant Biology*, *14*(1), 384. https://doi.org/10.1186/s12870-014-0384-2

Yarra, R., Jin, L., Zhao, Z., & Cao, H. (2019). Progress in tissue culture and genetic transformation of oil palm: An overview. *International Journal of Molecular Sciences*, *20*(21), 5353. https://doi.org/10.3390/ijms20215353

Zaki, N. M., Singh, R., Rosli, R., & Ismail, I. (2012). *Elaeis oleifera* genomic-SSR Markers: Exploitation in oil palm germplasm diversity and cross-amplification in Arecaceae. *International Journal of Molecular Sciences*, *13*(4), 4069–4088. https://doi.org/10.3390/ijms13044069

Zhao, Y., Zhang, J., Zhang, Z., & Xie, W. (2019). *Elymus nutans* genes for seed shattering and candidate gene-derived EST-SSR markers for germplasm evaluation. *BMC Plant Biology*, *19*(1), 102. https://doi.org/10.1186/s12870-019-1691-4

Zhou, L., Xiao, Y., Xia, W., & Yang, Y. (2015). Analysis of genetic diversity and population structure of oil palm (*Elaeis guineensis*) from China and Malaysia based on species-specific simple sequence repeat markers. *Genetics and Molecular Research*, *14*(4), 16247–16254. https://doi.org/10.4238/2015.december.8.15

Zhou, L., Yarra, R., Zhao, Z., Jin, L., & Cao, H. (2020). Development of SSR markers based on transcriptome data and association mapping analysis for fruit shell thickness associated traits in oil palm (*Elaeis guineensis* Jacq.). *3 Biotech*, *10*(6), 280. https://doi.org/10.1007/s13205-020-02269-3

Zulkifli, Y; Maizura, I and Rajinder, S (2012). Evaluation of oil palm germplasm (*Elaeis guineensi*s Jacq.) populations using EST-SSR. *J. Oil Palm Res., 24*: 1368-1377.

Journal of Oil Palm Research Vol. 37 (3) September 2025 p. 461-475
DOI: https://doi.org/10.21894/jopr.2024.0036

DISTINCT GENE CLUSTERS ARE EXPRESSED IN OIL PALM LEAF AND ROOT TISSUES IN RESPONSE TO DROUGHT STRESS

TISHA MELIA[1]*; FATAYAT[1]; SUKAMTO[1] and RIKI ARIO NUGROHO[1]

ABSTRACT

Elaeis guineensis *is a significant source of vegetable oil, yet it does not thrive in dry conditions. Thus, it is essential to understand the molecular response to drought in multiple oil palm tissues. This study analysed publicly available transcriptomic data from the leaves and roots of oil palms following drought. The data identified ~5,000 genes with significant gene expression changes, further clustered based on their expression patterns into 12 groups. The gene clusters showed distinct expression patterns in the two tissues examined, highlighting the different biological mechanisms. The involvement of the phytohormone abscisic acid in drought is implicated in both tissues by the differential expression of the activating transcription factor (TF) families homodomain-leucine zipper (HD-ZIP), ethylene response element binding factors (ERF) and no apical meristem (NAM),* Arabidopsis thaliana *activating factor (ATAF) and cup-shaped cotyledon (CUC) NAC. Gene clusters uniquely upregulated in leaves are enriched for TF family DNA binding one zinc finger (DOF) and lateral organ boundaries domain (LBD), which regulate hormone homeostasis and stomatal closure. Photosynthetic-related genes are downregulated in leaves, hypothesised to reduce photosynthesis activity, whereas heat shock proteins are enriched in upregulated genes found in roots. Finally, this study assembled ribonucleic acid (RNA) sequencing reads to discover ~6,200 novel genes whose expression are sensitive to drought. Our results expand the knowledge of molecular response following drought and demonstrate how identifying gene clusters can help to form hypotheses of molecular mechanisms.*

Keywords: bioinformatics, clustering, drought, sequencing, transcriptome.

Received: 31 August 2023**; Accepted:** 7 April 2024**; Published online:** 21 June 2024.

INTRODUCTION

The African oil palm (*Elaeis guineensis*) is an essential source of edible oil, providing an average yield of 3.5 t ha^{-1}. It is one of the most efficient species to produce oil while occupying a small land footprint (Barcelos *et al.*, 2015). Global oil palm producers are Indonesia and Malaysia, which boast a climate that enables oil palm to meet its water requirement of 2,000 mm yr^{-1} (Corley *et al.*, 2017). Palms subjected to water-deficit stress for more than 90 days exhibited a decrease in oil yield ranging from 25%-35% (Afandi *et al*., 2022; Woittiez *et al*., 2017). Drought caused physical changes in *E. guineensis*, including lower female/male flower ratio, higher floral abortion, and lower photosynthetic rate (Afandi *et al*., 2022; Suharyanti *et al*., 2020), all of which directly reduce oil yield. Therefore, it is crucial to understand how oil palm tolerate water deficits, particularly in the face of climate change. *El Niño* brings anomalous weather conditions in Southeast Asia, resulting in elevated temperatures, reduced precipitation and increased aridity (Khor *et al*., 2021).

Understanding molecular responses to drought stress is an active area of research in plants, particularly in *Arabidopsis thaliana* and *Zea mays* L. (maize). When exposed to drought stress, maize activates numerous phytohormones, alters ion fluxes, and accumulates reactive oxygen species (ROS) as stress signals (Gupta *et al*., 2020; Leng & Zhao, 2020). These stress signals activate transcription factors (TF) that regulate a complex system of stress-responsive genes. Known TFs that have been shown to regulate plants' response to drought stress are basic region / leucine zipper (ZIP),

[1] Computer Science Department,
Faculty of Mathematics and Natural Sciences,
Universitas Riau, Pekanbaru, 28293 Riau, Indonesia.

* *Corresponding author e-mail: tisha.melia@lecturer.unri.ac.id*

AP2/ERF, No apical meristem (NAM), *A. thaliana* activating factor (ATAF) and Cup-shaped cotyledon (CUC) NAC, WRKY and nuclear transcription factor Y (NF-Y) (Leng & Zhao, 2020). One of the main phytohormones used in drought stress is abscisic acid (ABA), which was shown to regulate multiple TFs (Jiao *et al*., 2022b; Wu *et al*., 2022; Yang *et al*., 2022; Zhao *et al*., 2014). TFs that were triggered by ABA (ABA-dependent) and other mechanisms (ABA-independent) regulate the transcription of downstream stress-related genes. Many of these genes coordinate molecular mechanisms to reduce water loss by closing the stomatal aperture, decreasing the photosynthesis rate, and altering root systems (Hong *et al*., 2020; Jiao *et al*., 2022a; Leng & Zhao, 2020). Furthermore, plants that undergo water-deficit stress must control the accumulation of ROS since its highly reactive hydroxyl radical may damage photosynthesis-related proteins and thylakoidal membranes (De Carvalho, 2008).

Transcriptomic changes following drought treatment have been reported in oil palm roots (Wang *et al*., 2020) and leaves (Salgado *et al*., 2022), with the latter focusing only on microRNA changes. Root transcriptome analyses confirmed the involvement of hormone regulation and ABC transporters. In terms of cellular functions, Wang *et al*. (2020) found an enrichment of cell wall biogenesis, phenylpropanoid biosynthesis, cellular ketone metabolism, ion transport and homeostasis as well as small molecule biosynthesis. Many of these functional categories have previously been identified in other plants as playing a role in phytohormone signalling mechanisms, altered growth rates and maintaining ROS homeostasis. The same study reported water deficit regulates several ABA-dependent TFs. In a separate study, Salgado *et al.* (2022) discovered miRNA affected by drought in oil palm leaves, which were predicted to target TFs, including myeloblastosis (MYB), homeobox (HOX) and NF-Y. These findings emphasise the importance of noncoding RNA in understanding the molecular response to drought. A recent study by Leão *et al.* (2022) showed that drought stress has a significant impact on protein phosphorylation and carbohydrate metabolism in leaves. This highlights the importance of phosphorylation in protein modification and the role of carbohydrates in signal transduction and energy production, which can enhance drought tolerance in plants.

Despite previous research, it is unclear how protein-coding genes in oil palm leaves respond to drought and how their gene expression patterns differ from the root transcriptome. This information is essential for identifying ways to improve oil palm genetics and increase drought tolerance. The present study addresses this knowledge gap by collecting publicly available RNA-sequencing datasets from the roots and leaves of oil palms following drought treatment. Water deficit stress regulates approximately 5,000 genes, which we cluster into 12 groups. Various gene clusters exhibited distinct patterns of gene expression profiles and were enriched with unique functional categories. Common transcription factors, namely homeodomain-leucine zipper (HD-ZIP), ERF and NAC, were identified as significantly activated in both tissues, alongside TFs that were uniquely enriched and upregulated in leaves, DNA binding one zinc finger (DOF) and LBD. Many of these TFs regulate stress-related genes to improve drought tolerance. Furthermore, we identified approximately 6,000 novel transcripts displaying characteristics commonly found in protein-coding genes. The majority of these transcripts exhibited significant expression alterations in response to drought. Thus, the present study enhances our understanding of how oil palm responds to drought stress, with significant implications for crop improvement and molecular-based drought tolerance phenotyping.

MATERIALS AND METHODS

RNA Sequencing Datasets

We obtained RNA sequencing data from 15 young *tenera E. guineensis* samples subjected to drought treatment from published studies (SRA accession PRJNA573093 and PRJDB9517, *Table 1*) (Ferreira *et al*., 2022; Salgado *et al*., 2022; Wang *et al*., 2020). Apical leaves were collected from the first nine palms after either no drought treatment (controls) or withholding water for seven and 14 days; the following six samples were taken from the roots of control palms and palms that were not given water for 14 days. Leaf samples were taken from clones, while root samples were from seedlings. All raw reads showed good sequencing quality as assessed by FastQC (Andrews, 2010). We mapped raw reads to the oil palm genome version EG 5.1 (Sanusi *et al*., 2018) using spliced transcripts aligment to a reference (STAR) (Dobin & Gingeras, 2015). To visualise the mapped reads, we created normalised bigwig tracks using DeepTools (Ramírez *et al*., 2016), excluding any reads that were mapped into multiple places in the genome. We used normalisation factors extracted from the trimmed mean of the M-values (TMM) method in edgeR (McCarthy *et al*., 2012) to normalise bigwig files.

Novel Gene Discovery and Characterisation

Mapped sequencing reads from each sample were used to assemble transcripts using StringTie (Shumate *et al*., 2022) based on the EG5.1 annotation as the starting point. We merged assembled

TABLE 1. RNA-SEQUENCING SAMPLES USED IN THIS STUDY

Sample	Tissue	Treatment	Accession #	Uniquely mapped reads	Citation
1	Leaf	Control replicate 1	SRR10219438	20,576,526	Ferreira *et al*. (2022); Salgado *et al*. (2022)
2	Leaf	Control replicate 2	SRR10219439	27,106,414	
3	Leaf	Control replicate 3	SRR10219424	22,015,317	
4	Leaf	Drought (7 days) replicate 1	SRR10219435	33,554,595	
5	Leaf	Drought (7 days) replicate 2	SRR10219436	21,634,316	
6	Leaf	Drought (7 days) replicate 3	SRR10219437	20,702,478	
7	Leaf	Drought (14 days) replicate 1	SRR10219432	30,894,589	
8	Leaf	Drought (14 days) replicate 2	SRR10219433	26,408,182	
9	Leaf	Drought (14 days) replicate 3	SRR10219434	25,008,000	
10	Root	Control replicate 1	DRR286073	29,891,464	Wang *et al.* (2020)
11	Root	Control replicate 2	DRR286072	45,118,907	
12	Root	Control replicate 3	DRR286077	35,989,393	
13	Root	Drought (14 days) replicate 1	DRR286076	16,035,703	
14	Root	Drought (14 days) replicate 2	DRR286075	11,582,438	
15	Root	Drought (14 days) replicate 3	DRR286074	25,066,789	

transcripts from all samples into one final assembly. Assembled transcripts were filtered to exclude genes that are <200 nucleotides in length and overlapping with known gene annotations. Novel gene structures are provided as a Gene Transfer Format (GTF) file available to be downloaded from https://my.unri.ac.id/8cjruY.

We produced mature transcripts for each gene by concatenating exon sequences defined by our gene structures. We used the mature mRNA sequences to find all open reading frames (ORFs) in the six reading frames (three reading frames in the sense direction and another three in the antisense direction). For each reading frame, we search for the occurrence of a Pfam domain using the Perl web service provided by the European Bioinformatics Institute. We only consider a match for an E-value less than 0.05. Mature mRNA transcripts were also used to identify TF sequences using the search feature in PlantTFDB (Jin *et al*., 2017).

Gene Expression Quantification

Gene expression levels for annotated and novel genes were quantified using featureCounts (Liao *et al*., 2014), counting only uniquely mapped reads at exons. A gene is considered expressed when the total reads across conditions is at least 15, with at least one sample having a minimum of 10 reads. The edgeR package (McCarthy *et al*., 2012) was used to normalise and perform differential expression analyses. To quantify gene expression level changes between two conditions, we directly compared the normalised gene expression counts between the two conditions (fold-changes). The statistical significance of fold-changes is assessed by edgeR with false discovery rate (FDR) correction applied. A gene is said to be differentially expressed if the $|\log2(\text{fold-changes})| > 2$ at FDR <0.05. Negative log2(fold-changes) indicates downregulation of gene expression patterns, while upregulation of gene expression will have positive log2(fold-changes).

Gene Clustering

We used consensus clustering (Monti *et al*., 2003) to identify a robust grouping of genes based on fold-changes of the four differential expression analyses described above. Briefly, we used the k-means method to cluster genes into 2-15 clusters, where the clustering is repeated fifty times in each choice of cluster number. We randomly subsampled (80%) of the data in each repeat of the k-means clustering. Cluster robustness is assessed in the form of a consensus matrix, whose value at row i and column j is the frequency of genes i and j clustered together across all repetitions. To aid in choosing the appropriate number of clusters, a cumulative distribution function (CDF) graph of the values in the consensus matrix is created. The changes in the area under the CDF curves (delta K) were also provided to delineate small differences between cluster number choices.

Functional Enrichment

To understand the significance of the identified gene clusters, we performed functional enrichment analyses to determine if there is a greater prevalence of genes with known functions in a cluster, as compared to by chance. The four types of functional enrichment we performed are detailed below. For each functional enrichment type,

p-values of the enrichment strength were adjusted with the Benjamini-Hochberg method, setting the significance level at <0.05.

Kyoto* Encyclopedia *of Genes and Genomes Orthology (KO) and Gene Ontology (GO) enrichment. We downloaded EG5.1 coding sequences (CDS) from PalmXplore (Sanusi *et al*., 2018), which were then used to identify Kyoto Encyclopedia of Genes and Genomes (KEGG) pathways and GO categories for each gene using EggNOG (Huerta-Cepas *et al*., 2019). The enrichment was done by comparing the number of genes found in a specific KEGG pathway/GO category to all genes that are differentially expressed at any point during drought treatments (5,168 genes). The enrichment analyses were done using the enricher function in clusterProfiler (Yu *et al*., 2012).

Transcription factor (TF) enrichment. We downloaded 2910 TF sequences found in oil palm from PlantTFDB (Jin *et al*., 2017) comprising 58 TF families. We used these annotated TFs to identify TFs in the *E. guineensis* CDS by BLAST. The enrichment score of having TF family *f* in cluster *c* was calculated as Equation (1):

$$\frac{g_{f,c}}{g_{f',c}} \Big/ \frac{g_{f,c'}}{g_{f',c'}} \quad (1)$$

where, $g_{f,c}$ is the number of genes that are TF family *f* in cluster *c*; $g_{f',c}$ is the number of genes that are NOT TF family *f* in cluster *c*; $g_{f,c'}$ is the number of genes that are TF family *f* in the cluster other than *c* and $g_{f',c'}$ is the number of genes that are NOT TF family *f* in the cluster other than *c*. Enrichment significance was determined using Fisher's exact test.

Fatty acid biosynthesis genes enrichment. A total of 42 fatty acid biosynthesis genes were collected from PalmXplore (Sanusi *et al*., 2018), which were then used to perform enrichment in the same way we performed TF enrichment.

RESULTS AND DISCUSSION

Massive Transcriptomic Changes Occurred in Response to Drought

We collated RNA-sequencing data that had been generated from 15 young *E. guineensis* palms that had been subjected to drought treatments or served as controls (*Table 1*). Drought treatments consisted of withholding water for seven or 14 days. Leaves were collected from nine palms (three palms each for controls, seven day drought and 14 day drought) (Wang *et al*., 2020) and roots were collected from the remaining palms (three palms each for controls and 14 day drought) (Ferreira *et al*., 2022; Salgado *et al*., 2022). The average number of uniquely mapped reads to the EG5.1 genome per sample is 25.3 and 27.2 million for leaf and root samples, respectively.

The transcriptomic data from these samples showed the expected grouping, as shown in the PCA plot in *Figure 1a*. The first principal component, accounting for 48% of the total variance, clearly separates the samples by the tissue of origin. The second principal component (16% of total variance) correlates well with drought severity from controls (bottom) to 14 day drought (top). All but one of the control samples do not overlap with the seven day drought samples, suggesting that the drought response is well underway by day seven. All 14 day drought samples are clustered together at the top of the PCA plot, indicating massive transcriptomic changes occurred in response to drought.

To quantify the extent of the gene expression response to aridity, we conducted differential expression analyses on the 23,539 genes expressed in these samples. As leaf samples cover three time points, we compared Day 7 drought with control samples (D7/Control), Day 14 with Day 7 samples (D14/D7), and Day 14 with control samples (D14/Control); however, only the D14/Control comparison was possible for root samples. For all comparisons, a greater number of genes exhibited downregulation of expression than upregulation (on average of 62% *vs.* 38%, *Table 2*) at a minimum of four fold-change. This pattern suggests that young palms responded to drought stress by significantly reducing their transcription activity. The prevalence of downregulated expression was also reported for miRNAs after exposure to drought and genes affected by high salinity stress (Ferreira *et al*., 2022; Salgado *et al*., 2022). A total of 5168 genes were identified as differentially expressed in at least one of the four comparative analyses (*Figure 1b* and *1c*, *Table S1*), which corresponds to slightly less than a quarter (~22%) of all expressed genes.

We examined the 10 most differentially expressed genes at each time point (Day 7 and 14 in leaf samples, as well as Day 14 in root samples) to better understand the transcriptomic changes brought about by drought (*Table 3*). Three out of 10 genes whose expression significantly changed on Day 7 following drought in leaves are TFs, which may be involved in regulating the early response to drought stress. Two of these, namely p5.00_sc00016_p0198 and p5.00_sc00135_p0003, showed strong upregulation. The former is a HD-ZIP TF family member. Members of this TF family are involved in the initiation of drought response in maize (Jiao *et al*., 2022a), while p5.00_sc00135_p0003 is an auxin-responsive IAA protein, which has been associated with enhanced drought tolerance in *A. thaliana* (Shani *et al*., 2017). At Day 14 post

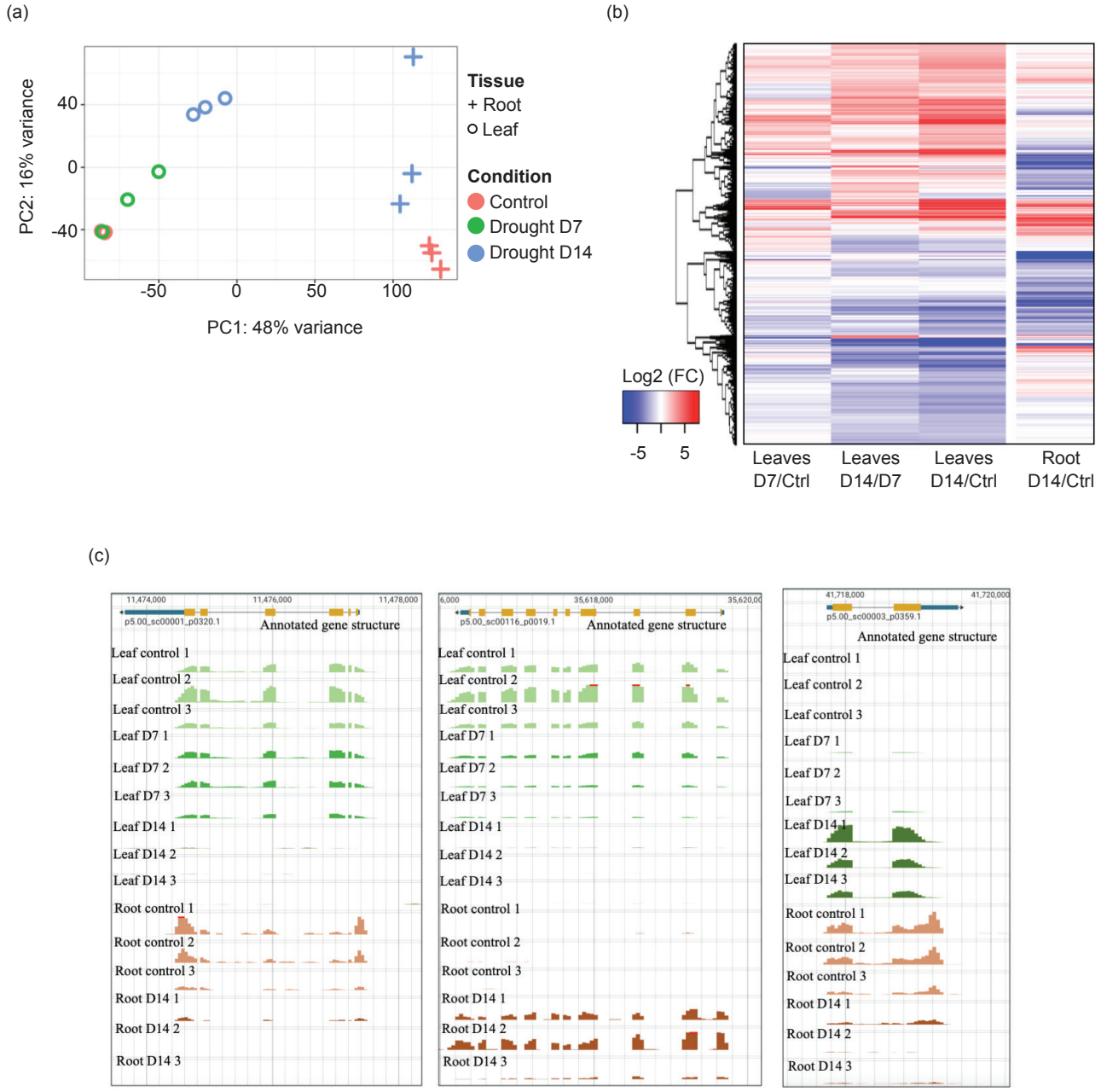

Figure 1. Transcriptomic response to drought treatment. (a). PCA of the 15 RNA-seq samples. (b) Heatmap depicting gene expression level changes for 5,168 regulated genes in response to drought treatment. The rows correspond to genes and columns correspond to the four treatment comparisons discussed in the text. The colours indicate the log2(fold-changes) of gene expression patterns. (c) Genome browser screenshots for three genes that are differentially expressed following drought treatment. The top track presents gene structures, followed by gene expression tracks showing read pileups in every sample.

drought treatment, eight of the 10 most regulated genes in leaves showed robust downregulation. Genes that were downregulated include two known transcriptional regulators, whereby the maize orthologue of p5.00_sc00127_p0068 is involved in kernel storage (Zhan *et al*., 2018), while orthologues of p5.00_sc00034_p0162 are involved in plant response to stress (Qian *et al*., 2021). The p5.00_sc00034_p0162 gene exhibited a significant 3-fold increase in expression on Day 7 of the drought treatment, followed by downregulation by Day 14, suggesting that its expression may only be essential during the early stages of the stress response. In roots of oil palm seedlings subjected to 14 days of drought treatment, the top 10 differentially expressed genes were downregulated except for a heat shock protein gene, p5.00_sc00001_p0173. The heat shock protein family are molecular chaperones in distressed plants. Members of this family were found to be significantly upregulated in the roots of *Canavalia rosea* following drought treatment (Zhao *et al*., 2018).

TABLE 2. NUMBER OF GENES THAT ARE DIFFERENTIALLY EXPRESSED IN RESPONSE TO DROUGHT

	D7/control	D14/D7	D14/control	
	Leaves	Leaves	Leaves	Root
Fold change <-4	261	1,319	1,936	1,114
Fold change >4	218	1,079	1,619	344
Total	**479**	**2,398**	**3,555**	**1,458**

TABLE 3. TOP DIFFERENTIALLY EXPRESSED GENES IN EACH TIME POINT

Comparison	Gene name	Top 10 differentially expressed genes	
		Direction of regulation	Annotation
D7/control leaves	*p5.00_sc00001_p0582*	Down	-
	p5.00_sc00016_p0198	Up	TF from HD-ZIP family; a homeobox-leucine zipper protein
	p5.00_sc00018_p0081	Up	-
	p5.00_sc00087_p0033	Up	-
	p5.00_sc00089_p0007	Down	-
	p5.00_sc00107_p0001	Down	Isoprene synthase
	p5.00_sc00127_p0028	Up	Remorin (C-terminal region) protein
	p5.00_sc00135_p0003	Up	Aux IAA protein, known as a TF
	p5.00_sc00360_p0022 (CCA1)	Down	TF belonging to MyB Family; a protein LHY-like isoform X1
	p5.00_sc15516_p0001	Down	-
D14/d7 leaves	*p5.00_sc00001_p0732*	Down	-
	p5.00_sc00006_p0051	Down	Protoporphyrinogen oxidase
	p5.00_sc00044_p0061	Up	Alpha beta hydrolase domain-containing protein
	p5.00_sc00104_p0041	Down	UAA transporter family
	p5.00_sc00107_p0001	Down	Isoprene synthase
	p5.00_sc00127_p0068	Down	TF from bZIP family; regulatory protein opaque-2
	p5.00_sc00135_p0039	Down	-
	p5.00_sc00389_p0013 (PARP3)	Up	Poly (ADP-ribose) polymerase
	p5.00_sc00034_p0162	Down	TF from the bHLH family
	p5.00_sc00059_p0119	Down	-
D14/control root	*p5.00_sc00001_p0173*	Up	Heat shock protein
	p5.00_sc00006_p0166	Down	Glycosyl hydrolase family 9
	p5.00_sc00018_p0026	Down	Glycosyltransferase 2 family
	p5.00_sc00019_p0112	Down	-
	p5.00_sc00038_p0180	Down	Plastocyanin-like domain
	p5.00_sc00058_p0071	Down	-
	p5.00_sc00078_p0012	Down	Microtubule associated protein (MAP65/ASE1 family)
	p5.00_sc00123_p0044	Down	-
	p5.00_sc00271_p0007	Down	-
	p5.00_sc00063_p0036	Down	Soluble NSF attachment protein, SP

Note: The symbol "-" indicates that no annotation was found for the gene.

Distinct Clusters of Differential Expression Profiles were Observed in Response to Drought

To discern the biological mechanisms of drought response, we clustered all differentially expressed genes (5,168) based on fold-change profiles obtained from the four differential expression analyses discussed earlier (*Figure 1b*). A consensus clustering method was employed to identify robust clusters. This method repeats the clustering algorithm multiple times and identifies consistent groupings across iterations. We determined the optimal number of clusters by evaluating the consensus matrix (*Figure 2a*), which displays how frequently pairs

of genes are clustered together across repetitions. Consistent clustering in the consensus matrix (*Figure 2a*) established twelve distinct groups.

Increasing the number of clusters did not enhance the stability of the identified groups, as observed by the negligible change in the consensus matrix. Distinct gene expression patterns were evident for the 12 identified clusters in the four differential expression analyses (*Figure 2b* and *2c*). Of these, five clusters (cluster 4, 9, 11, 8 and 2) exhibited common regulation patterns across both examined tissues (1438 genes, 27.8% of regulated genes, *Figure 2b* and *2c*). Five additional clusters (clusters 1, 3, 5, 7, and 12) showed expression regulation occurring exclusively in either roots or leaves, indicating the likely tissue-specificity of these genes' function. The bulk of the regulated genes (3,283, 63.5%) belong to these five clusters. Cluster 6 and 10, comprising 8.6% of the genes (447), exhibited contrasting expression patterns.

Functional Enrichment of Gene Clusters

To identify the biological mechanisms associated with each cluster, we assess whether any enrichment exists for specific functional gene groups. A significant enrichment for a particular functional group may indicate the biological mechanisms involved. Initially, we assessed the significant enrichment of genes from KEGG Orthology (KO) (Kanehisa *et al.*, 2023) in any of the 12 clusters. KO is a manually curated database of molecular functions derived from pathways, modules and BRITE hierarchies. We found that seven clusters

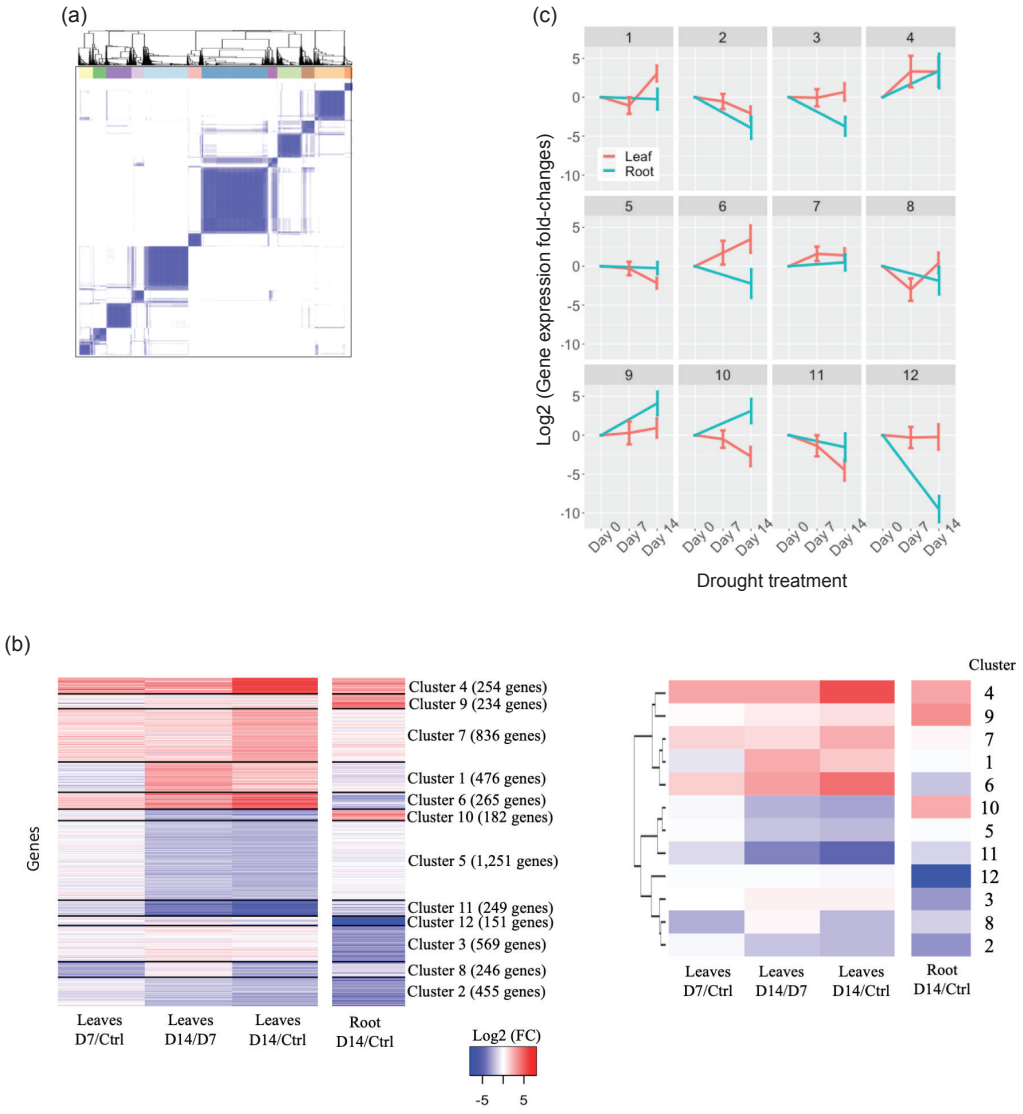

Figure 2. (a) A heatmap of the consensus matrix showing the frequency genes being clustered together in a specific row and column. The darker the blue colour, the more frequently the genes cluster together. (b) Left: expression heatmap of the four differential expression analyses (columns). Colour corresponds to the magnitude of changes in expression (log2(fold-changes)) in each comparison. Genes are arranged into the 12 identified clusters. Right: a similar heatmap on the left, but it depicts the average log2(fold-change) per cluster instead of the fold changes of individual genes. (c) The same information as in (b, right) is plotted as line graphs. Error bars are standard deviations.

exhibited significant enrichment for nine distinct KOs at an adjusted *p*-value <0.05 (*Figure 3a*). Next, we analysed GO terms, which are a collection of controlled vocabularies explaining gene products' functions and locations (Carbon *et al*., 2009), where we found five distinct clusters enriched for 22 GO terms (*Figure 3b*). We identified five unique clusters with 23 enriched GO terms (*Figure 3b*). Subsequently, we examined whether any of the 56 TF families defined in PlantTFDB (Jin *et al*., 2017) were significantly present in any of the clusters, which led to the discovery of four such clusters (*Figure 3c*). Finally, we assessed significant enrichment for the biosynthesis of fatty acids, whereby we identified that only cluster 3 was enriched.

Drought-induced Gene Expression Responses that are Common in Leaves and Roots

Genes in cluster 4 and 9 are upregulated in both tissues, with genes in cluster 4 exhibiting a stronger upregulation pattern as early as Day 7 of drought (*Figure 2b*). Cluster 4 is enriched for HD-ZIP, auxin-responsive IAA proteins (*Figure 3a*), Ethylene Response Element Binding Factors (ERF) TF family (*Figure 3c*) and cellulase activity (*Figure 3b*). The first three enriched functional categories, *i.e*., HD-ZIP, auxin-responsive IAA proteins and ERF, are known transcriptional regulators. HD-ZIP are TFs that regulate responses to abiotic stress and plant growth (Elhiti & Stasolla, 2009; Li *et al*., 2022), including initiating drought response by activating downstream stress-related genes in maize, rice and *A. thaliana* through ROS signaling and/or ABA-dependent pathways (Jiao *et al*., 2022a; Leng & Zhao, 2020; Li *et al*., 2022; Zhao *et al*., 2014). Similarly, the ERF TF family has been implicated in regulating plant tolerance in response to stress mediated by both ABA-dependent and ABA-independent pathways (Leng & Zhao, 2020; Qin *et al*., 2007; Wu *et al*., 2022; Xie *et al*., 2019). ERF was also shown to activate a subset of auxin-responsive proteins (Shani *et al*., 2017), which are known as transcriptional repressors hypothesised to regulate organogenesis, growth and environmental responses through auxin-signaling pathways (Shani *et al*., 2017; Wang *et al*., 2010). Auxin-responsive proteins are regulated following drought in oil palms (Ferreira *et al*., 2022; Wang *et al*., 2020), potentially coordinating growth rate and direction during such stressors.

Cluster 9 is enriched with the TF family NAC (NAM, ATAF1/2, CUC2; *Figure 3c*), which is known to respond to stress through ABA-dependent signaling pathways in maize (Leng and Zhao, 2020). Our results confirm previous observations in young oil palms, where the three ABA-dependent TFs (HD-ZIP, ERF and NAC) and pathways (hormone regulation and cell wall biogenesis) are regulated following drought (Wang *et al*., 2020). Taken together, common drought stress responses in both leaves and roots of oil palms are similar to the responses observed on model plants (Leng & Zhao, 2020; Shani *et al*., 2017; Xie *et al*., 2019). In summary, water scarcity triggers the production of diverse phytohormones including ABA and others, evidenced through the activation of ABA-dependent TFs (HD-ZIP, ERF and NAC) (Leng & Zhao, 2020; Li *et al*., 2022) along with ABA-independent pathways (Xie *et al*., 2019).

Upregulated Gene Expression Patterns in Responses to Drought Uniquely Found in Leaves

Clusters with marked differences in the direction of gene regulation between leaf and root samples are particularly interesting, characterised by unique stress responses in the two tissues. Cluster 1, 6 and 7 showed robust upregulation of gene expression patterns in leaves, with contrasting downregulation (cluster 6) or no regulation (cluster 1 and 7) of gene expression levels in roots (*Figure 2b* and *2c*). Cluster 6 is uniquely enriched for β-glucosidases (*Figure 3a* and *3b*), which have been shown to regulate the activation of phytohormones, cell wall lignification and stress response (Kongdin *et al*., 2021; Opassiri *et al*., 2006). β-glucosidases are classified into multiple glycoside hydrolase families (Cairns & Esen, 2010), which were reported to be essential in the activation of the phytohormone ABA by hydrolysing inactive ABA in *A. thaliana* (Jiao *et al*., 2022a). ABA, in turn, triggers different signaling pathways to increase stress tolerance (Leng & Zhao, 2020; Xie *et al*., 2019) (*Figure 3d*).

Cluster 1 is enriched for the DOF TF family (*Figure 3a)* (Bhaskara *et al*., 2012; Liu *et al*., 2021), which is a plant-specific transcriptional regulator involved in seed development, hormone regulation and abiotic stress response (Leng & Zhao, 2020; Zou & Sun, 2023). The DOF TF family was shown to be sensitive to ABA under water-deficit conditions and was implicated in increased drought tolerance in *A. thaliana* (Corrales *et al*., 2017), apple (Chen *et al*., 2020) and tomato (Corrales *et al*., 2014) by enhancing ROS scavenging ability (Zang *et al*., 2017; Zou & Sun, 2023). In *A. thaliana*, the DOF gene named CDF3 regulates genes involved in protecting stressed plants from osmotic and oxidative stress (Corrales *et al*., 2017). Through conducting metabolite profiling, the same study revealed that protective metabolites were present in a higher concentration in plants with overexpressed CDF3.

Cluster 7 showed significant enrichment for the LBD TF family, which has been demonstrated to enhance drought tolerance in maize (Jiao *et al*., 2022b; Wu *et al*., 2023) and *A. thaliana* (Guo *et al*., 2020b). It was suggested that *Zm*LBD, an LBD in maize, interacts with the IAA5 protein to regulate

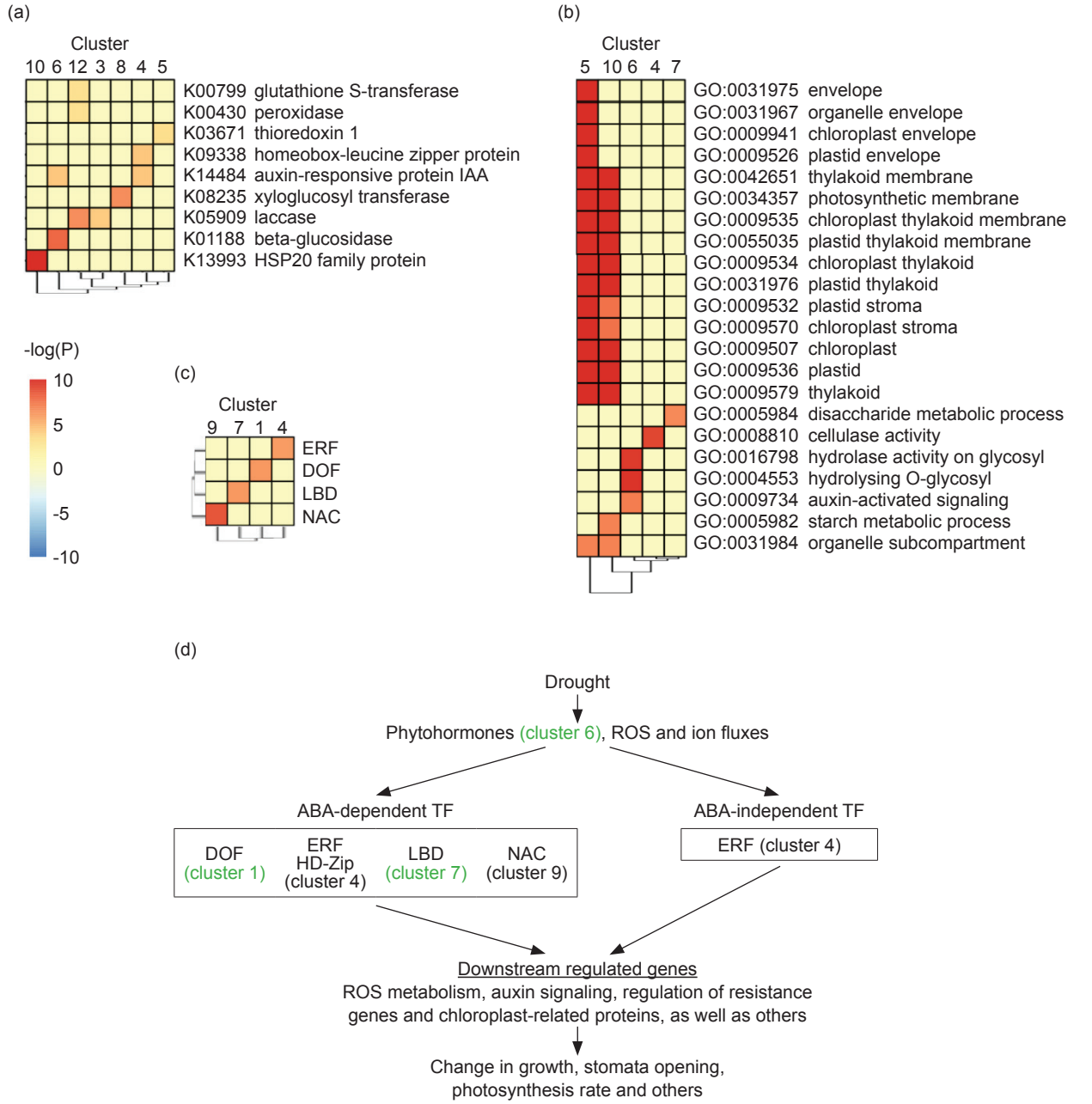

Figure 3. (a) Functional enrichments of the identified gene clusters for KEGG Orthology, (b) GO terms and (c) TF Family. Colours represent the –log(P value) for each enrichment analysis. (d) Hypothesised molecular mechanisms following drought. Cluster names were added next to/under each molecular mechanism involved. Clusters that were specific to leaves were written in green.

auxin biosynthesis genes, modulating H_2O_2 levels and increasing resistance to drought (Jiao *et al*., 2022a). Additionally, LBD15 in *A. thaliana* was shown to bind directly to the promoter of ABI4, a gene in the ABA signaling pathway, resulting in the closure of stomata. In conclusion, clusters with strong upregulation patterns, exclusively in leaves, are enriched for ABA-responsive transcription factors DOF and LBD. These factors were shown to regulate genes to enhance drought tolerance by facilitating the biosynthesis of protective metabolites and limiting water loss through stomatal closure (*Figure 3d*).

Downregulated Gene Expression Patterns Found in Leaves During Water Deficit

Cluster 5 and 10 exhibit significant reduction in gene expression patterns in leaves, with cluster 10 presenting upregulation and cluster 5 showing no regulation in roots (*Figure 2b* and *2c*). Both clusters show enrichment in chloroplast-related proteins (*Figure 3b*). These proteins were markedly suppressed in drought-stressed *A. thaliana*, cassava and potato plants (Chang *et al*., 2019; Hong *et al*., 2020; Tamburino *et al*., 2017). Moreover, chloroplast-related proteins were shown intimately linked with

photosynthetic activity and stomatal closure to retain water during stress (Hong *et al*., 2020). Cluster 10 exhibits a unique enrichment for heat-shock protein HSP20 (*Figure 3a*). The HSP20 protein family acts as molecular chaperones, contributing to a tolerance of biotic and abiotic stresses by stabilising cell structure and function and folding and transporting auxiliary proteins (Chini *et al*., 2004; Guo *et al*., 2020a).

Root-specific Gene Expression Changes in Response to Drought

Genes in cluster 3 and 12 exhibited a marked decrease in gene expression levels in roots resulting from drought treatment (*Figure 2b* and *2c*). Both clusters are enriched for laccase genes (*Figure 3a*), and cluster 3 exhibits additional enrichment in genes related to fatty acid biosynthesis. Laccase genes are known to play a role in lignin biosynthesis (Liu *et al*., 2017; Zhu *et al*., 2023), while fatty acid biosynthesis is implicated in forming callus and lateral root development. Tea plants subjected to water-deficit stress exhibited significant downregulation of genes associated with lignin and long-chain fatty acid biosynthesis. This led to reduced accumulation of necessary enzymes in the respective biosynthesis pathways during drought. As a result, the plants could better adapt to challenging conditions (Gu *et al*., 2020).

Many Drought-responsive Genes are Novel

Many genes are only transcribed following a stimulus, which reduces their likelihood of being discovered and included in published annotations. We assembled genome-wide transcriptomic data to catalogue all drought-responsive genes, a subset of which may be novel. This effort uncovered 9,329 transcribed regions that do not overlap with annotated genes in the EG5.1 genome; 2,475 of these transcripts contain multiple exons (multi-exonic, *Figure 4a*). We further analysed these uncharacterised transcript regions by examining features commonly present in known genes, including an open reading frame (ORF) of 150 amino acids or more, splicing evidence, a protein family (PFAM) domain, sequence similarity to known TFs, and significant changes in gene expression levels following exposure to drought stress. We identified 6,209 transcripts exhibiting at least one of the five properties we evaluated (*Table 3*). We designated these 6,209 transcripts as novel genes (*Table 4*, *Figure 4a* and *4b*). The data highlights that a considerable proportion of the novel genes (73.8% or 4,583) possess a PFAM domain, with a subset of 247 (equivalent to 3.9% of the novel genes) being identified as TFs. Furthermore, 2,121 new genes are significantly differentially expressed following water deficit stress (*Table 5*), which account for 41% of all differentially expressed genes. Given the sizable number of novel drought-responsive genes, our discovery of new genes offers a valuable resource for understanding oil palm's response to drought stress. Overall, we have demonstrated that our 6,209 new genes are likely to function as protein-coding genes.

TABLE 4. PROPERTIES OF THE NOVEL TRANSCRIBED REGIONS

Item	Novel transcripts	Novel genes
Number of transcripts/genes	9,329	6,209
Average #exons/gene	2.4	3.0
Average width (bp)	1,979.4	2,624.0
Average longest ORF (aa)	160.6	207.4
% Genes with PFAM domains	49.1%	73.8%
% Genes that are putative TF	2.6%	3.9%

TABLE 5. NUMBER OF NOVEL GENES THAT ARE DIFFERENTIALLY EXPRESSED IN RESPONSE TO DROUGHT

Item	D7/control	D14/D7	D14/control	
	Leaves		Leaves	Root
Fold change <-4	118	631	900	334
Fold change >4	89	426	635	129
Total	**207**	**1,057**	**1,535**	**463**

CONCLUSION

Elaeis guineensis is a crucial source of vegetable oils. However, arid conditions markedly lower the oil output, emphasising the necessity of breeding drought-resistant oil palms. Accordingly, understanding how oil palms respond to drought stress is essential. Here, we present the first report to compare transcriptomic changes in two oil palm tissues, including roots and leaves, under drought conditions. This study comprehensively compares the transcriptomic profiles and aims to pinpoint any tissue-specific changes caused by drought stress. A total of 6,209 genes were identified as differentially expressed following water-deficit stress. These genes were then organised into 12 robust gene clusters, with several clusters showing significant enrichments for specific functional categories. Gene clusters upregulated in both tissues are enriched for three ABA-dependent TFs: HD-ZIP, ERF and NAC, known regulators of stress-related genes. The leaf transcriptome exhibited a unique enrichment for upregulated LBD and DOF TFs, previously implicated in facilitating protective metabolite production and stomatal

closure. Furthermore, chloroplast-related proteins were strongly downregulated in leaves, indicating a potential reduction in photosynthesis rate. Genes involved in lignin and fatty acid biosynthesis were enriched in clusters downregulated solely in roots, suggesting the cessation of non-essential activities under stressful conditions. Finally, we discovered and characterised 6,209 novel transcripts with features commonly found in genes, such as protein domains, long ORF, sequence similarity to known TFs and splicing evidence. A notable 41% of differentially expressed genes responding to drought treatment were novel, emphasising their significant contribution to drought tolerance. Our findings provide essential resources in comprehending oil palm's response to drought, revealing distinct biological mechanisms induced in various tissues.

ACKNOWLEDGEMENT

Computational resources to complete this work were provided by MAHAMERU BRIN HPC, National Research and Innovation Agency of Indonesia (BRIN).

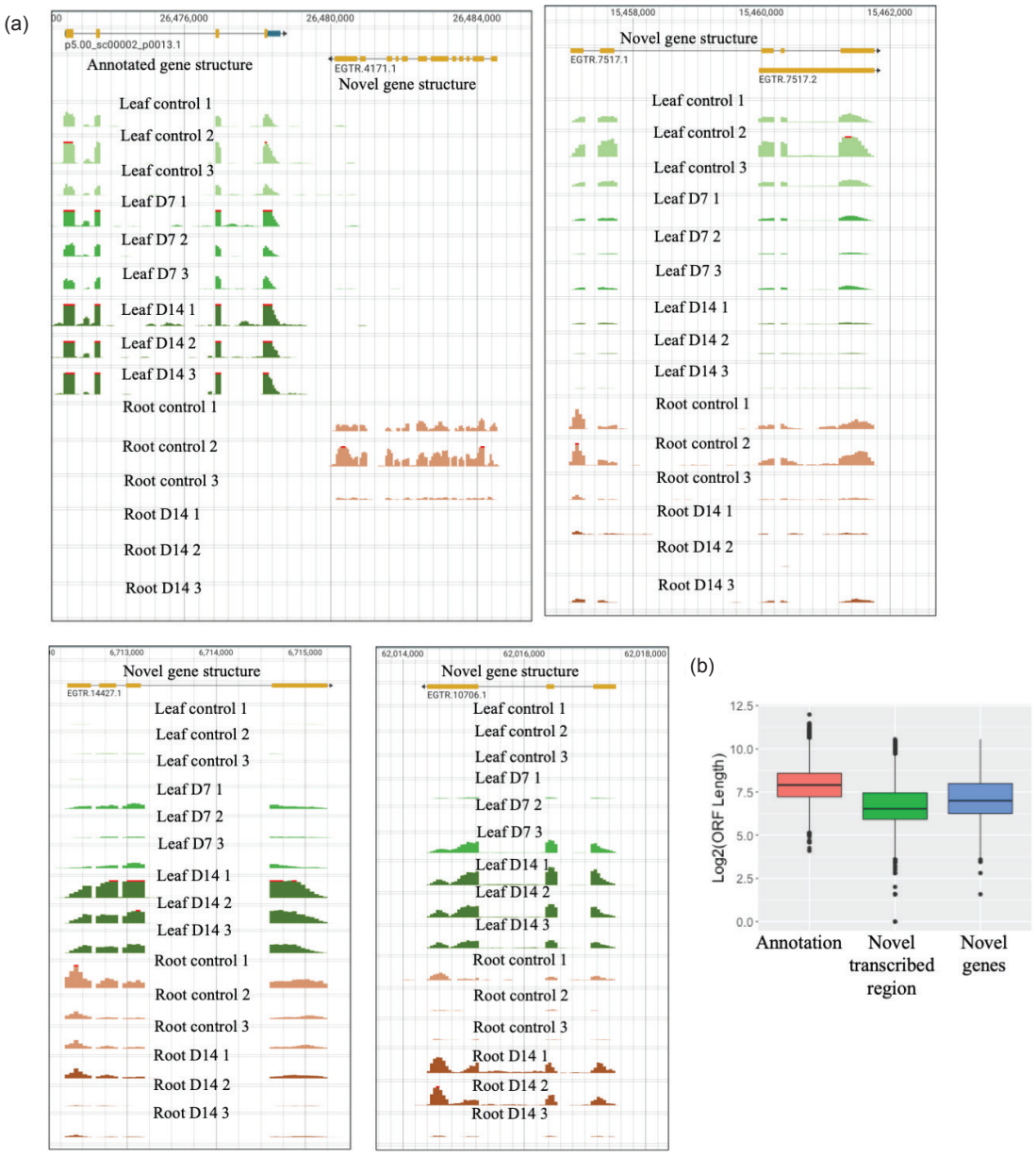

Figure 4. (a) Genome browser screenshots for four novel genes that are differentially expressed following drought treatment. The top track illustrates gene structures, followed by gene expression tracks depicting read pileups in each samples. These novel genes demonstrate significant downregulation in either roots (top-left) or both tissues; upregulation in leaves, but downregulation in roots (bottom-left); and upregulation in both tissues (bottom-right). (b) The distribution of ORFs (as log2) for these three categories is shown. In this study, we discovered annotated genes to have the longest open reading frame (ORF), followed by novel genes and then transcribed regions.

REFERENCES

Afandi, A. M., Zulkifli, H., Nur Zuhaili, H. A. Z. A., Norliyana, Z. Z., Hisham, H., Saharul, A. M., Dzulhelmi, M. N., & Vu Thanh, T. A. (2022). Oil palm water requirement and the need for irrigation in dry Malaysian areas. *Journal of Oil Palm Research*, *35*(2), 391–405. https://doi.org/10.21894/jopr.2022.0052

Andrews, S. (2010). *FastQC: A quality control tool for high throughput sequence data*. http://www.bioinformatics.babraham.ac.uk/projects/fastqc/

Barcelos, E., Rios, S. D. A., Cunha, R. N. V., Lopes, R., Motoike, S. Y., Babiychuk, E., Skirycz, A., & Kushnir, S. (2015). Oil palm natural diversity and the potential for yield improvement. *Frontiers in Plant Science*, *6*, 190. https://doi.org/10.3389/fpls.2015.00190

Bhaskara, G. B., Nguyen, T. T., & Verslues, P. E. (2012). Unique drought resistance functions of the highly ABA-induced clade A protein phosphatase 2Cs. *Plant Physiology*, *160*(1), 379–395. https://doi.org/10.1104/pp.112.202408

Cairns, J. R., K., & Esen, A. (2010). β-Glucosidases. *Cellular and Molecular Life Sciences*, *67*(20), 3389–3405. https://doi.org/10.1007/s00018-010-0399-2

Carbon, S., Ireland, A., Mungall, C. J., Shu, S., Marshall, B., & Lewis, S. (2009). The AmiGO hub and the web presence working group: AmiGO: Online access to ontology and annotation data. *Bioinformatics*, *25*(2), 288–289. https://doi.org/10.1093/bioinformatics/btn615

Chang, L., Wang, L., Peng, C., Tong, Z., Wang, D., Ding, G., Xiao, J., Guo, A., & Wang, X. (2019). The chloroplast proteome response to drought stress in cassava leaves. *Plant Physiology and Biochemistry*, *142*, 351–362. https://doi.org/10.1016/j.plaphy.2019.07.025

Chen, P., Yan, M., Li, L., He, J., Zhou, S., Li, Z., Niu, C., Bao, C., Zhi, F., Ma, F., & Guan, Q. (2020). The apple DNA-binding one zinc-finger protein *MdDof54* promotes drought resistance. *Horticulture Research*, *7*(1), 195. https://doi.org/10.1038/s41438-020-00419-5

Chini, A., Grant, J. J., Seki, M., Shinozaki, K., & Loake, G. J. (2004). Drought tolerance established by enhanced expression of the CC-NBS-LRR gene, *ADR1*, requires salicylic acid, *EDS1* and *ABI1*. *The Plant Journal*, *38*(5), 810–822. https://doi.org/10.1111/j.1365-313X.2004.02086.x

Corley, R. H. V., Rao, V., Palat, T., & Praiwan, T. (2017). Breeding for drought tolerance in oil palm. *Journal of Oil Palm Research*, *30*, 26–35. https://doi.org/10.21894/jopr.2017.0011

Corrales, A., Carrillo, L., Lasierra, P., Nebauer, S. G., Dominguez-Figueroa, J., Renau-Morata, B., Pollmann, S., Granell, A., Molina, R., Vicente-Carbajosa, J., & Medina, J. (2017). Multifaceted role of cycling DOF factor 3 (*CDF3*) in the regulation of flowering time and abiotic stress responses in *Arabidopsis*. *Plant Cell & Environment*, *40*(5), 748–764. https://doi.org/10.1111/pce.12894

Corrales, A., Nebauer, S. G., Carrillo, L., Fernández-Nohales, P., Marqués, J., Renau-Morata, B., Granell, A., Pollmann, S., Vicente-Carbajosa, J., Molina, R. V., & Medina, J. (2014). Characterization of tomato cycling Dof factors reveals conserved and new functions in the control of flowering time and abiotic stress responses. *Journal of Experimental Botany*, *65*(4), 995–1012. https://doi.org/10.1093/jxb/ert451

De Carvalho, M. H. C. (2008). Drought stress and reactive oxygen species: Production, scavenging and signaling. *Plant Signaling & Behavior*, *3*(3), 156–165. https://doi.org/10.4161/psb.3.3.5536

Dobin, A., & Gingeras, T. R. (2015). Mapping RNA-seq reads with STAR. *Current Protocols in Bioinformatics*, *51*(1), 1–19. https://doi.org/10.1002/0471250953.bi1114s51

Elhiti, M., & Stasolla, C. (2009). Structure and function of homodomain-leucine zipper (HD-Zip) proteins. *Plant Signaling & Behavior*, *4*(2), 86–88. https://doi.org/10.4161/psb.4.2.7692

Ferreira, T. M. M., Filho, J. A. F., Leão, A. P., De Sousa, C. A. F., & Souza, M. T. (2022). Structural and functional analysis of stress-inducible genes and their promoters selected from young oil palm (*Elaeis guineensis*) under salt stress. *BMC Genomics*, *23*(1), 735. https://doi.org/10.1186/s12864-022-08926-6

Gu, H., Wang, Y., Xie, H., Qiu, C., Zhang, S., Xiao, J., Li, H., Chen, L., Li, X., & Ding, Z. (2020). Drought stress triggers proteomic changes involving lignin, flavonoids and fatty acids in tea plants. *Scientific Reports*, *10*(1), 15504. https://doi.org/10.1038/s41598-020-72596-1

Guo, L. M., Li, J., He, J., Liu, H., & Zhang, H. M. (2020a). A class I cytosolic HSP20 of rice enhances

heat and salt tolerance in different organisms. *Scientific Reports*, *10*(1), 1383. https://doi.org/10.1038/s41598-020-58395-8

Guo, Z., Xu, H., Lei, Q., Du, J., Li, C., Wang, C., Yang, Y., Yang, Y., & Sun, X. (2020b). The *Arabidopsis* transcription factor *LBD15* mediates ABA signaling and tolerance of water-deficit stress by regulating *ABI4* expression. *The Plant Journal*, *104*(2), 510–521. https://doi.org/10.1111/tpj.14942

Gupta, A., Rico-Medina, A., & Caño-Delgado, A. I. (2020). The physiology of plant responses to drought. *Science*, *368*(6488), 266–269. https://doi.org/10.1126/science.aaz7614

Hong, Y., Wang, Z., Liu, X., Yao, J., Kong, X., Shi, H., & Zhu, J. K. (2020). Two chloroplast proteins negatively regulate plant drought resistance through separate pathways. *Plant Physiology*, *182*(2), 1007–1021. https://doi.org/10.1104/pp.19.01106

Huerta-Cepas, J., Szklarczyk, D., Heller, D., Hernández-Plaza, A., Forslund, S. K., Cook, H., Mende, D. R., Letunic, I., Rattei, T., Jensen, L. J., von Mering, C., & Bork, P. (2019). eggNOG 5.0: A hierarchical, functionally and phylogenetically annotated orthology resource based on 5090 organisms and 2502 viruses. *Nucleic Acids Research*, *47*(D1), D309–D314. https://doi.org/10.1093/nar/gky1085

Jiao, P., Jiang, Z., Wei, X., Liu, S., Qu, J., Guan, S., & Ma, Y. (2022a). Overexpression of the homeobox-leucine zipper protein *ATHB-6* improves the drought tolerance of maize (*Zea mays* L.). *Plant Science*, *316*, 111159. https://doi.org/10.1016/j.plantsci.2021.111159

Jiao, P., Wei, X., Jiang, Z., Liu, S., Guan, S., & Ma, Y. (2022b). *ZmLBD2* a maize (*Zea mays* L.) lateral organ boundaries domain (*LBD*) transcription factor enhances drought tolerance in transgenic *Arabidopsis thaliana*. *Frontiers in Plant Science*, *13*, 1000149. https://doi.org/10.3389/fpls.2022.1000149

Jin, J., Tian, F., Yang, D-C., Meng, Y-Q., Kong, L., Luo, J., & Gao, G. (2017). Plant TFDB 4.0: Toward a central hub for transcription factors and regulatory interactions in plants. *Nucleic Acids Research*, *45*(D1), D1040–D1045. https://doi.org/10.1093/nar/gkw982

Kanehisa, M., Furumichi, M., Sato, Y., Kawashima, M., & Ishiguro-Watanabe, M. (2023). KEGG for taxonomy-based analysis of pathways and genomes. *Nucleic Acids Research*, *51*(D1), D587–D592. https://doi.org/10.1093/nar/gkac963

Khor, J. F., Ling, L., Yusop, Z., Tan, W. L., Ling, J. L., & Soo, E. Z. X. (2021). Impact of *El Niño* on oil palm yield in Malaysia. *Agronomy*, *11*(11), 2189. https://doi.org/10.3390/agronomy11112189

Kongdin, M., Mahong, B., Lee, S-K., Shim, S-H., Jeon, J-S., & Ketudat Cairns, J. R. (2021). Action of multiple rice β-glucosidases on abscisic acid glucose ester. *International Journal of Molecular Sciences*, *22*(14), 7593. https://doi.org/10.3390/ijms22147593

Leão, A. P., Bittencourt, C. B., Da Silva, T. L. C., Neto, J. C. R., De Oliveira Braga, Í., Vieira, L. R., De Aquino Ribeiro, J. A., Abdelnur, P. V., De Sousa, C. A. F., & Júnior, M. T. S. (2022). Insights from a multi-omics integration (MOI) study in oil palm (*Elaeis guineensis* Jacq.) response to abiotic stresses: Part Two – Drought. *Plants*, *11*(20), 2786. https://doi.org/10.3390/plants11202786

Leng, P., & Zhao, J. (2020). Transcription factors as molecular switches to regulate drought adaptation in maize. *Theoretical and Applied Genetics*, *133*(5), 1455–1465. https://doi.org/10.1007/s00122-019-03494-y

Li, Y., Yang, Z., Zhang, Y., Guo, J., Liu, L., Wang, C., Wang, B., & Han, G. (2022). The roles of HD-ZIP proteins in plant abiotic stress tolerance. *Frontiers in Plant Science*, *13*, 1027071. https://doi.org/10.3389/fpls.2022.1027071

Liao, Y., Smyth, G. K., & Shi, W. (2014). featureCounts: An efficient general purpose program for assigning sequence reads to genomic features. *Bioinformatics*, *30*(7), 923–930. https://doi.org/10.1093/bioinformatics/btt656

Liu, Q., Dong, G., Ma, Y., Zhao, S., Liu, X., Li, X., Li, Y., & Hou, B. (2021). Rice glycosyltransferase gene *UGT85E1* is involved in drought stress tolerance through enhancing abscisic acid response. *Frontiers in Plant Science*, *12*, 790195. https://doi.org/10.3389/fpls.2021.790195

Liu, Q., Luo, L., Wang, X., Shen, Z., & Zheng, L. (2017). Comprehensive analysis of rice laccase gene (*OsLAC*) family and ectopic expression of *OsLAC10* enhances tolerance to copper stress in *Arabidopsis*. *International Journal of Molecular Sciences*, *18*(2), 209. https://doi.org/10.3390/ijms18020209

McCarthy, D. J., Chen, Y., & Smyth, G. K. (2012). Differential expression analysis of multifactor

RNA-Seq experiments with respect to biological variation. *Nucleic Acids Research*, *40*(10), 4288–4297. https://doi.org/10.1093/nar/gks042

Monti, S., Tamayo, P., Mesirov, J., & Golub, T. (2003). Consensus clustering: A resampling-based method for class discovery and visualization of gene expression microarray data. *Machine Learning*, *52*(1/2), 91–118. https://doi.org/10.1023/A:1023949509487

Opassiri, R., Pomthong, B., Onkoksoong, T., Akiyama, T., Esen, A., & Cairns, J. R. K. (2006). Analysis of rice glycosyl hydrolase family 1 and expression of *Os4bglu12* β-glucosidase. *BMC Plant Biology*, *6*(1), 33. https://doi.org/10.1186/1471-2229-6-33

Qian, Y., Zhang, T., Yu, Y., Gou, L., Yang, J., Xu, J., & Pi, E. (2021). Regulatory mechanisms of bHLH transcription factors in plant adaptive responses to various abiotic stresses. *Frontiers in Plant Science*, *12*, 677611. https://doi.org/10.3389/fpls.2021.677611

Qin, F., Kakimoto, M., Sakuma, Y., Maruyama, K., Osakabe, Y., Tran, L-S. P., Shinozaki, K., & Yamaguchi-Shinozaki, K. (2007). Regulation and functional analysis of *ZmDREB2A* in response to drought and heat stresses in *Zea mays* L.: *ZmDREB2A* in drought and heat stress response. *The Plant Journal*, *50*(1), 54–69. https://doi.org/10.1111/j.1365-313X.2007.03034.x

Ramírez, F., Ryan, D. P., Grüning, B., Bhardwaj, V., Kilpert, F., Richter, A. S., Heyne, S., Dündar, F., & Manke, T. (2016). deepTools2: A next generation web server for deep-sequencing data analysis. *Nucleic Acids Research*, *44*(W1), W160–W165. https://doi.org/10.1093/nar/gkw257

Salgado, F. F., Da Silva, T. L. C., Vieira, L. R., Silva, V. N. B., Leão, A. P., Costa, M. M. D. C., Togawa, R. C., De Sousa, C. A. F., Grynberg, P., & Souza, M. T. (2022). The early response of oil palm (*Elaeis guineensis* Jacq.) plants to water deprivation: Expression analysis of miRNAs and their putative target genes, and similarities with the response to salinity stress. *Frontiers in Plant Science*, *13*, 970113. https://doi.org/10.3389/fpls.2022.970113

Sanusi, N. S. N. M., Rosli, R., Halim, M. A. A., Chan, K. L., Nagappan, J., Azizi, N., Amiruddin, N., Tatarinova, T. V., & Low, E-T. L. (2018). PalmXplore: Oil palm gene database. *Database*, *2018*, bay095. https://doi.org/10.1093/database/bay095

Shani, E., Salehin, M., Zhang, Y., Sanchez, S. E., Doherty, C., Wang, R., Mangado, C. C., Song, L., Tal, I., Pisanty, O., Ecker, J. R., Kay, S. A., Pruneda-Paz, J., & Estelle, M. (2017). Plant stress tolerance requires auxin-sensitive Aux/IAA transcriptional repressors. *Current Biology*, *27*(3), 437–444. https://doi.org/10.1016/j.cub.2016.12.016

Shumate, A., Wong, B., Pertea, G., & Pertea, M. (2022). Improved transcriptome assembly using a hybrid of long and short reads with StringTie. *PLOS Computational Biology*, *18*(6), e1009730. https://doi.org/10.1371/journal.pcbi.1009730

Suharyanti, N. A., Mizuno, K., & Sodri, A. (2020). The effect of water deficit on inflorescence period at palm oil productivity on peatland. *E3S Web of Conferences*, *211*, 05005. https://doi.org/10.1051/e3sconf/202021105005

Tamburino, R., Vitale, M., Ruggiero, A., Sassi, M., Sannino, L., Arena, S., Costa, A., Batelli, G., Zambrano, N., Scaloni, A., Grillo, S., & Scotti, N. (2017). Chloroplast proteome response to drought stress and recovery in tomato (*Solanum lycopersicum* L.). *BMC Plant Biology*, *17*(1), 40. https://doi.org/10.1186/s12870-017-0971-0

Wang, L., Lee, M., Ye, B., & Yue, G. H. (2020). Genes, pathways and networks responding to drought stress in oil palm roots. *Scientific Reports*, *10*(1), 21303. https://doi.org/10.1038/s41598-020-78297-z

Wang, S., Bai, Y., Shen, C., Wu, Y., Zhang, S., Jiang, D., Guilfoyle, T. J., Chen, M., & Qi, Y. (2010). Auxin-related gene families in abiotic stress response in *Sorghum bicolor*. *Functional & Integrative Genomics*, *10*(4), 533–546. https://doi.org/10.1007/s10142-010-0174-3

Woittiez, L. S., Van Wijk, M. T., Slingerland, M., Van Noordwijk, M., & Giller, K. E. (2017). Yield gaps in oil palm: A quantitative review of contributing factors. *European Journal of Agronomy*, *83*, 57–77. https://doi.org/10.1016/j.eja.2016.11.002

Wu, M., He, W., Wang, L., Zhang, X., Wang, K., & Xiang, Y. (2023). *PheLBD29*, an *LBD* transcription factor from Moso bamboo, causes leaf curvature and enhances tolerance to drought stress in transgenic *Arabidopsis*. *Journal of Plant Physiology*, *280*, 153865. https://doi.org/10.1016/j.jplph.2022.153865

Wu, Y., Li, X., Zhang, J., Zhao, H., Tan, S., Xu, W., Pan, J., Yang, F., & Pi, E. (2022). ERF subfamily transcription factors and their function in plant responses to abiotic stresses. *Frontiers in Plant*

Science, *13*, 1042084. https://doi.org/10.3389/fpls.2022.1042084

Xie, Z., Nolan, T. M., Jiang, H., & Yin, Y. (2019). AP2/ERF Transcription factor regulatory networks in hormone and abiotic stress responses in *Arabidopsis*. *Frontiers in Plant Science*, *10*, 228. https://doi.org/10.3389/fpls.2019.00228

Yang, C., Huang, Y., Lv, P., Antwi-Boasiako, A., Begum, N., Zhao, T., & Zhao, J. (2022). NAC transcription factor *GmNAC12* improved drought stress tolerance in soybean. *International Journal of Molecular Sciences*, *23*(19), 12029. https://doi.org/10.3390/ijms231912029

Yu, G., Wang, L-G., Han, Y., & He, Q-Y. (2012). clusterProfiler: An R package for comparing biological themes among gene clusters. *OMICS: A Journal of Integrative Biology*, *16*(5), 284–287. https://doi.org/10.1089/omi.2011.0118

Zang, D., Wang, L., Zhang, Y., Zhao, H., & Wang, Y. (2017). *ThDof1.4* and *ThZFP1* constitute a transcriptional regulatory cascade involved in salt or osmotic stress in *Tamarix hispida*. *Plant Molecular Biology*, *94*(4-5), 495–507. https://doi.org/10.1007/s11103-017-0620-x

Zhan, J., Li, G., Ryu, C-H., Ma, C., Zhang, S., Lloyd, A., Hunter, B. G., Larkins, B. A., Drews, G. N., Wang, X., & Yadegari, R. (2018). Opaque-2 regulates a complex gene network associated with cell differentiation and storage functions of maize endosperm. *Plant Cell*, *30*(10), 2425–2446. https://doi.org/10.1105/tpc.18.00392

Zhao, P., Wang, D., Wang, R., Kong, N., Zhang, C., Yang, C., Wu, W., Ma, H., & Chen, Q. (2018). Genome-wide analysis of the potato Hsp20 gene family: Identification, genomic organization and expression profiles in response to heat stress. *BMC Genomics*, *19*(1), 61. https://doi.org/10.1186/s12864-018-4443-1

Zhao, Y., Ma, Q., Jin, X., Peng, X., Liu, J., Deng, L., Yan, H., Sheng, L., Jiang, H., & Cheng, B. (2014). A novel maize homeodomain-leucine zipper (HD-Zip)I gene, *Zmhdz10*, positively regulates drought and salt tolerance in both rice and *Arabidopsis*. *Plant and Cell Physiology*, *55*(6), 1142–1156. https://doi.org/10.1093/pcp/pcu054

Zhu, J., Zhang, H., Huang, K., Guo, R., Zhao, J., Xie, H., Zhu, J., Gu, H., Chen, H., Li, G., Wei, C., & Liu, S. (2023). Comprehensive analysis of the laccase gene family in tea plant highlights its roles in development and stress responses. *BMC Plant Biology*, *23*(1), 129. https://doi.org/10.1186/s12870-023-04134-w

Zou, X., & Sun, H. (2023). DOF transcription factors: Specific regulators of plant biological processes. *Frontiers in Plant Science*, *14*, 1044918. https://doi.org/10.3389/fpls.2023.1044918

Journal of Oil Palm Research Vol. 37 (3) September 2025 p. 476-491
DOI: https://doi.org/10.21894/jopr.2024.0043

A COMPREHENSIVE ASSESSMENT OF COMPOSITION AND NUTRIENT CONTENT IN VARIOUS COMMERCIAL FERTILISERS USED IN INDONESIAN OIL PALM PLANTATIONS

SUKARMAN[1,2]; LILIK SUTIARSO[1]*; ANDRI PRIMA NUGROHO[1]; ARDAN WIRATMOKO[1]; TAKASHI OKAYASU[3]; SUWARDI[1,4]; SEPTA PRIMANANDA[4]; AHMAD HASANUDDIN[4] and HERRY WIRIANATA[5]

ABSTRACT

The objective of this study was to evaluate the composition and nutrient content of various types of commercial fertilisers used in oil palm plantations in Indonesia. The utilisation of non-conforming fertilisers harms soil fertility and health, leading to decreased plant productivity and affecting product quality. Combating non-conforming fertilisers is therefore crucial in supporting the sustainability of oil palm plantations. This study is classified as evaluative, with primary data comprising fertiliser analysis results, interviews, and field observations. Fertiliser samples were obtained from oil palm plantations in eight provinces in Indonesia, namely Central Kalimantan, South Kalimantan, West Kalimantan, East Kalimantan, South Sumatra, West Sumatra, Riau and North Sumatra. The results demonstrate that the quality of the tested fertilisers can be categorised into three criteria: Original fertilisers, adulterated fertilisers and counterfeit fertilisers. NPK fertiliser tends to be a target for counterfeiting due to its relatively high price, widespread usage across various agricultural commodities and ease of imitation with available technology. In conclusion, this comprehensive assessment sheds light on the varying compositions and nutrient content of fertilisers used in oil palm plantations. The findings can assist plantation managers in making informed decisions to enhance overall productivity and sustainability in oil palm cultivation.

Keywords: adulterated, counterfeit fertilisers, non-conforming fertilisers, nutrient content, soil health.

Received: 13 December 2023**; Accepted:** 16 June 2024**; Published online:** 5 September 2024.

[1] Smart Agriculture Research,
Department of Agricultural and Biosystems Engineering,
Faculty of Agricultural Technology,
Universitas Gadjah Mada,
Jln. Flora No. 1 Bulaksumur,
Yogyakarta 55281, Indonesia.

[2] Department of Agribusiness,
Faculty of Agriculture, Darwan Ali University,
Jl. Batu Berlian No. 10, Mentawa Baru Hulu,
Kotawaringin Timur, Central Kalimantan 74322, Indonesia.

[3] Department of Agro-Environmental Sciences,
Faculty of Agricultural Technology,
Kyushu University, 744 Motooka, Nishi-ku,
Fukuoka 810-0395, Japan.

[4] Wilmar International Plantation,
Region of Central Kalimantan, Indonesia.

[5] Department of Agrotechnology,
Faculty of Agriculture, STIPER Agricultural Institute,
Yogyakarta 55281, Indonesia.

* *Corresponding author e-mail: lilik-soetiarso@ugm.ac.id*

INTRODUCTION

Oil palm plantations are a crucial agricultural sector for Indonesia's economy (Abdul-Hamid *et al.*, 2022; Dermawan *et al.*, 2022; Krishna *et al.*, 2017; Waudby & Zein, 2021). The cultivation of oil palm significantly contributes to palm oil production, one of Indonesia's primary export commodities (Afriyanti *et al.*, 2016; Lam *et al.*, 2019; Xin *et al.*, 2022). To support the sustainable and optimal productivity of oil palm plantations, proper fertilisation plays a crucial role (Essono *et al.*, 2023; Lim *et al.*, 2023; Zainuddin *et al.*, 2022). Fertilisers are essential sources of nutrients for plants, fulfilling their nutritional requirements for growth, development and optimal yields (Albuquerque *et al.*, 2022; Georgieva *et al.*, 2022; Wilson & Shakya, 2023). Selecting and using the right type of fertiliser directly influences the quality and

productivity of oil palm (Liu *et al.*, 2023; Morra *et al.*, 2021; Shahwar *et al.*, 2023). As a result, fertilisation becomes a key factor in enhancing productivity, with fertiliser costs accounting for approximately 37% of total production expenses, or around 60% of the total maintenance costs for oil palm cultivation (Aji *et al.*, 2021; Arifin *et al.*, 2022; Firmansyah *et al.*, 2021; Saprida & Saruksuk, 2021).

However, farmers and plantation managers often face numerous choices of fertiliser options, each with different nutrient compositions (Chen *et al.*, 2023; Hu *et al.*, 2024; Li *et al.*, 2018; Martin *et al.*, 2023). Given the variety of fertilisers available in the market, it is essential to evaluate the composition and nutrient content of each fertiliser (Dhankhar & Kumar, 2023; Nektarios *et al.*, 2022). This becomes more complex with the prevalence of counterfeit fertilisers, posing a serious threat in the agricultural sector (Khor & Zeller, 2014; Michelson *et al.*, 2021; Pujawati & Kurniati, 2021). This phenomenon arises due to the increased demand for fertilisers by farmers and plantation managers, leading to illegal practices in fertiliser production and distribution (Bold *et al.*, 2017). Many cases have been reported where counterfeit fertilisers are sold in the market with deceptive labels and packaging, raising concerns among farmers about the quality and safety of the fertilisers that they use (Jamilah *et al.*, 2022; Pujawati & Kurniati, 2021). These cases are not limited only to Indonesia but have also been reported in Malaysia (San, 2022), Nigeria (Dania, 2023), India (TNN, 2022), California (Fromartz, 2011), Tanzania (Michelson *et al.*, 2021; Norton *et al.*, 2020), Vietnam (Nam, 2008), Ghana (Beidou Company, 2019) and several other countries.

Such unethical practices can lead to potential financial losses and reduced production for farmers. The use of inappropriate fertilisers can negatively impact soil fertility and health, decrease crop yields, affect product quality and hamper overall agricultural productivity (Huang *et al.*, 2023; Li *et al.*, 2018; Liu *et al.*, 2022; Quemada *et al.*, 2019). From a cost perspective, it can result in significant financial burdens due to increased fertilisation expenses without proportional gains in production. The use of counterfeit fertilisers also renders the subsequent application of the 5R approach (right source, right method, right timing, right application site), ineffective. Cases of counterfeit fertiliser application typically occur among oil palm industry stakeholders who seldom or never conduct nutrient content identification and testing of the received fertilisers (Fitrya *et al.*, 2022; Wongmaneeroj *et al.*, 2019). Various reasons cited by farmers and plantation managers include lack of knowledge, expensive analysis costs, prolonged analysis results and inconsistent employee performance in fertiliser sampling (Rui *et al.*, 2012; Vuthy, 2020). Therefore, it is crucial to combat non-conforming fertilisers.

The use of counterfeit fertilisers can be considered to have the same effect as not fertilising at all, as only the fertiliser material is provided, without supplying the necessary nutrients for oil palm plants. This becomes even more severe when it occurs in the plantations of Indonesian farmers because almost 90% exhibit potassium (K) deficiency, 50% lack nitrogen (N) and 67% lack phosphorus (P) (Lim *et al.*, 2023). Rhebergen *et al.* (2016) explain that with poor nutrient management, the yield gap in oil palm production can reach 5 t ha^{-1} yr^{-1}. Continuous N fertilisation in oil palms can maintain yields above 30 t ha^{-1} yr^{-1}, but cessation can lead to a drastic decrease (Anuar *et al.*, 2008). However, excessive use of fertilisers in oil palm plantations can increase leaching processes and alter nutrient reserves in the soil without a significant increase in production compared to sufficient doses (Dubos *et al.*, 2016).

Earlier studies have focused on oil palm fertilisation, providing insights into fertiliser usage in general. However, specific data regarding the composition and nutrient content of commonly used fertilisers in oil palm plantations remain limited. The objective of this study was to evaluate the composition and nutrient content of various types of fertilisers commonly used in oil palm plantations. Analysing the nutrient content of different fertilisers is expected to provide in-depth information on the benefits and efficiency of each fertiliser for oil palm growth.

MATERIALS AND METHODS

Research Location

The research was conducted from March to June 2023 at PT. Mustika Sembuluh (PT. MS), located on Jl. Jenderal Sudirman Km 62 Sampit – P. Bun, Kab. Kotawaringin Timur, Central Kalimantan, Indonesia. This study was carried out in several oil palm plantations situated in different regions. The selection of these locations ensured a broader representation of fertiliser usage across various oil palm plantations. Samples were collected from eight provinces in Indonesia, namely Central Kalimantan, South Kalimantan, West Kalimantan, East Kalimantan, South Sumatra, West Sumatra, Riau, and North Sumatra (*Figure 1*).

Research Method

This study belongs to the category of evaluative research, involving the assessment of the composition and nutrient content of various fertilisers in different oil palm plantations. The types of fertilisers used in the study include nitrogen phosphorus potassium (NPK), nitrogen

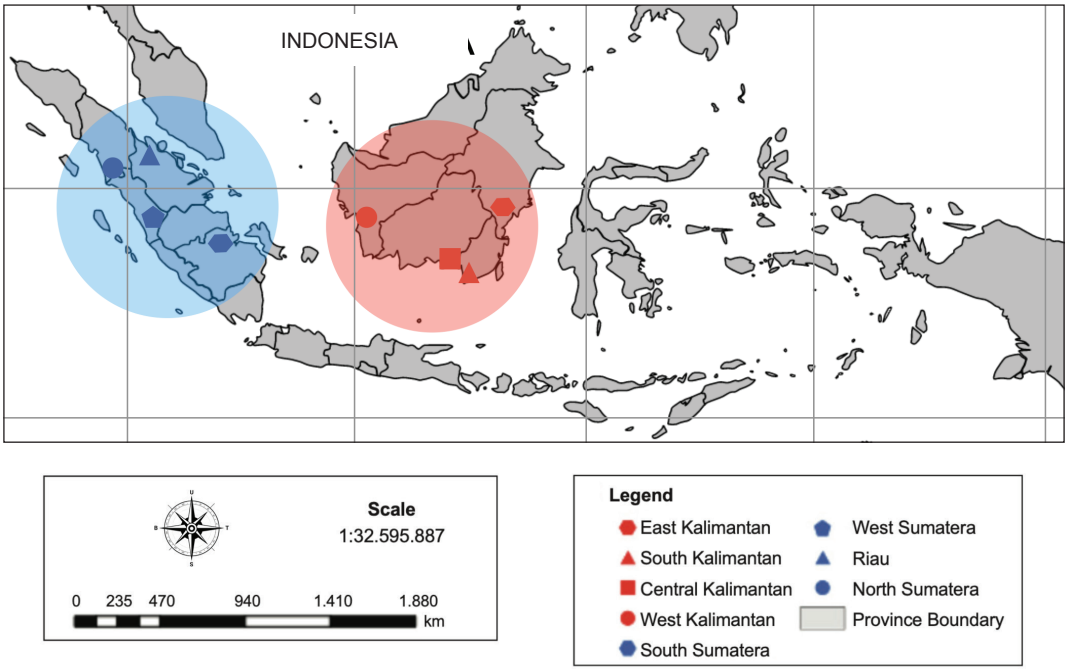

Figure 1. Locations where fertiliser samples were taken.

potassium (NK), rock phosphate Peru (RP Peru), dolomite, muriate of potash (MOP), kieserite, magnesium sulfate heptahydrate (MgSB), sulphuric acid (SOA), borate and urea. Primary data collection includes fertiliser analysis results, interviews, and field observations. Interviews were conducted with farmers, farmer groups and plantation staff or managers. Fertiliser samples were analysed in the laboratory to determine their composition and nutrient content. Direct observations were made in the oil palm plantations to understand the specifications of various fertiliser types, fertiliser sampling methods and how non-conforming fertilisers were handled. The secondary data consists of previous studies and reports, fertiliser product knowledge and relevant regulations and policies.

Research Procedure

Samples of various types and brands of fertilisers were collected from different oil palm plantations. The sampling of solid fertiliser in sack packaging followed the Indonesian National Standard (SNI) 19-0428-1998. Upon receiving the fertilisers, standard checks were performed on the packing and labels, including the condition of the sack thread, the condition of the inner plastic, the number of torn sacks, packaging labels, and the type and origin of the fertiliser. Each sampled sack was given a number using a marker to facilitate identification of the sack's source truck and other relevant details. Each sample sack was weighed to assess the consistency of sack weights per arrival.

Sampling of fertiliser from the sacks was conducted using a probe. Each sack sample was sampled diagonally from the bottom left and right sides. The sack sample was laid horizontally and probed from the bottom to the top, or from two opposite corners, using a stainless-steel probe. The fertiliser obtained from the probe was mixed in a bucket to create a composite sample. When sampling from the fertiliser sack, the hole in the stainless-steel pipe should face downward. Once the pipe is fully inserted, it is rotated 180° until the hole faces upwards and is filled before removing the pipe. Each sample sack is referred to as a primary sample, and several sacks will be sampled as per SNI 19-0428-1998. All primary samples will be combined to create composite samples, totalling more than 750 g (*Figure 2*).

Interviews were conducted in a structured manner with farmers, members of farming groups, and staff/managers of oil palm plantations, who were selected through specific inclusion criteria to ensure sufficient knowledge about oil palm fertilisation. The interview questions, based on literature and research objectives, will explore respondents' experiences with different types of fertilisers and their effectiveness, quality, and selection challenges. Interviews were conducted in an atmosphere that supported honesty, informed consent agreement, and accurate recording to ensure data reliability. Data analysis will use qualitative content methods with coding to identify the main themes and data triangulation to enhance the reliability and validity of the findings. This systematic and ethical approach aimed to

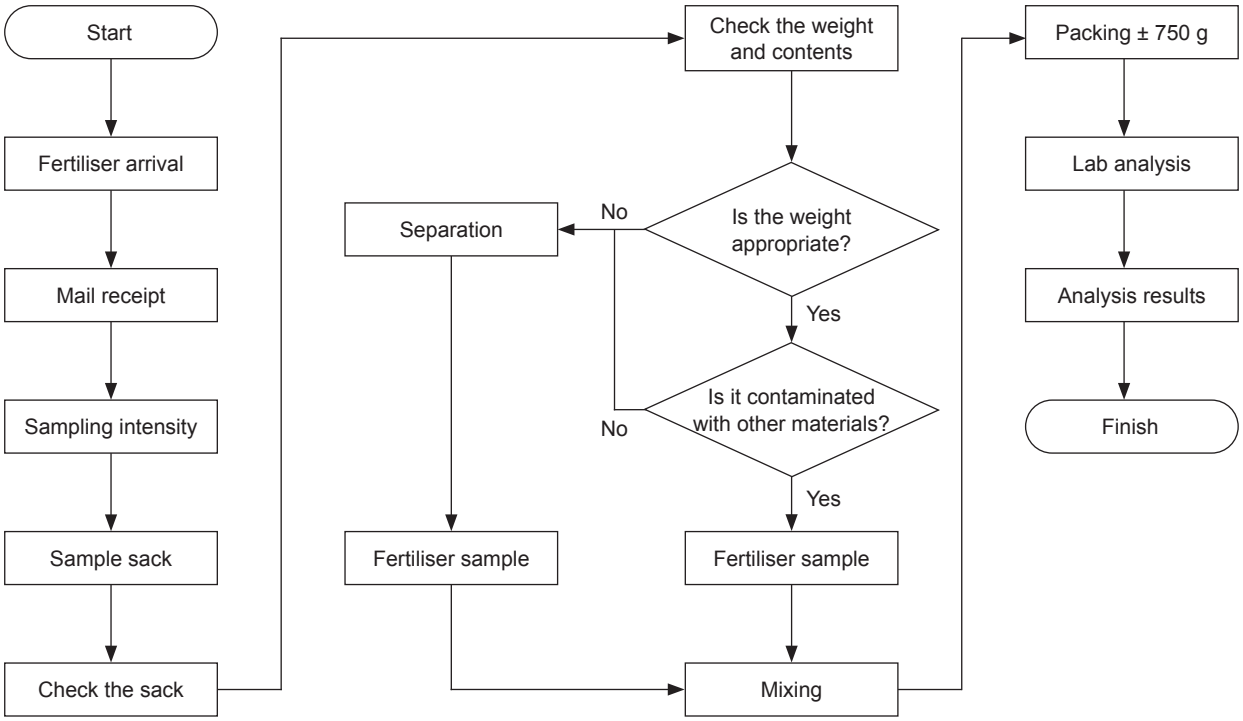

Figure 2. Flow diagram of fertiliser sampling.

produce valuable insights into the evaluation of fertiliser composition and nutrient levels in palm oil plantations, with reliable and credible findings.

Data Analysis

Descriptive and comparative analysis methods were used to analyse the data. Descriptive analysis provides detailed insights into the composition and nutrient content of each evaluated fertiliser type. Descriptive and comparative analyses were used for data analysis. A descriptive analysis was used to provide a detailed overview of the composition and nutrient content of each type of fertiliser. The comparative analysis in this study utilised advanced statistical methods to objectively compare the composition and nutrient content of various types of fertilisers, identifying statistically significant differences through Analysis of Variance (ANOVA). *Post-hoc* Least Significant Difference (LSD) and independent t-test <5% analyses were used to determine specific differences between fertiliser groups. This approach was strengthened by correlation and regression analyses to uncover the relationship between fertiliser composition and its effects on oil palm growth. This study ensured reliability and validity by using a representative sample and accurate data processing using SPSS Statistics 29 software. The results are credible and offer evidence-based recommendations regarding the selection of the most effective fertilisers for oil palm plantations.

RESULTS AND DISCUSSION

Fertiliser Quality Criteria Analysis

The laboratory analysis of composition and nutrient content showed that the presence of non-conforming fertilisers reached 2.8%. Among the tested samples throughout the year, NPK fertiliser had the highest percentage of non-conforming at 2.4%, followed by kieserite at 0.3% and MgSB at 0.1% from a total of 723 samples. No non-conforming fertilisers were found in the samples of NPK, NK, RP Peru, dolomite, MOP, SOA, borate, and urea during the year 2022. There are two types of NPK, namely NPK 10/6/24/5+0.96 B, which for convenience are referred to as NPK 10, and NPK 12/12/17/2, are referred to as NPK 12. Although MOP fertiliser was found to contain some other mixed materials, resulting in a non-conforming condition, its nutrient content still fell within the permissible tolerance range. The SNI has set the standard for the content of NPK and NK fertilisers (SNI 2803-2012), RP (SNI 02-3776-2005), dolomite (SNI 02-2804-2005), MOP (SNI 02-2805-2005), kieserite (SNI 02-2807-1992), SOA (SNI 02-1760-2005), borate (SNI 02-4959-1999), and urea (SNI 2801-2010). These standards regulate the quality criteria of the fertilisers concerning their composition and nutrient content that must be met.

Figure 3 and *4* compare the chemical compositions of various fertiliser samples, grouped according to the percentage of components that meet the specifications (content on-spec),

following the SNI, and those that did not meet the specifications (non-conforming). Each bar is labelled with lowercase letters below it (a, b, d, e, g, m, n), representing the notation from the LSD test at the 5% significance level; numbers with the same lowercase letter notation indicate no significant statistical difference.

Based on the mentioned standard, a tolerance of 8% SNI 2803-2012 is allowed for the nutrient content stated on the fertiliser NPK label. For example, NPK 10 fertiliser has a tolerance of N min 9.2%, phosphate (P_2O_5) min 5.5%, potassium oxide (K_2O) min 22.1%, magnesium oxide (MgO) min 4.6%, boron oxide (B_2O_3) min 0.9% and maximum moisture of 3.0%. Other fertilisers such as NK, RP Peru, dolomite, MOP, kieserite, MgSB and SOA also have tolerance standards based on SNI, as shown in *Figure 3*. For the tested NPK 10 fertiliser, its nutrient content was found to be significantly below the standard specified on the label and SNI 2803-2012. The nutrient content of this NPK fertiliser was only about 50% of the established standard. Specifically, the N content was 4.0% (min 9.92%), P_2O_5 was 2.4% (min 5.5%), and K_2O was 10.7% (min 22.1%). Furthermore, the B_2O_3 content was low, at 0.8% (min 0.9%), while the MgO content was excessively high at 9.1% (min 4.6%). These significant discrepancies between the found nutrient contents and the standard indicate that the fertilisers can be categorised as non-conforming fertiliser. Such inconsistency points to potential errors or fraudulence in the production or distribution process, resulting in the received fertiliser not meeting the specified standards. Similar deviations were also observed for Kieserite (MgO 18.6% and S 1.3% below the standard) and MgSB (MgO 1.5% and S 1.9% below the standard), with B_2O_3 exceeding the standard significantly. In the context of NK and NPK 12 fertilisers, no significant difference was found between these fertilisers and the SNI, thus, no non-conforming fertilisers were detected.

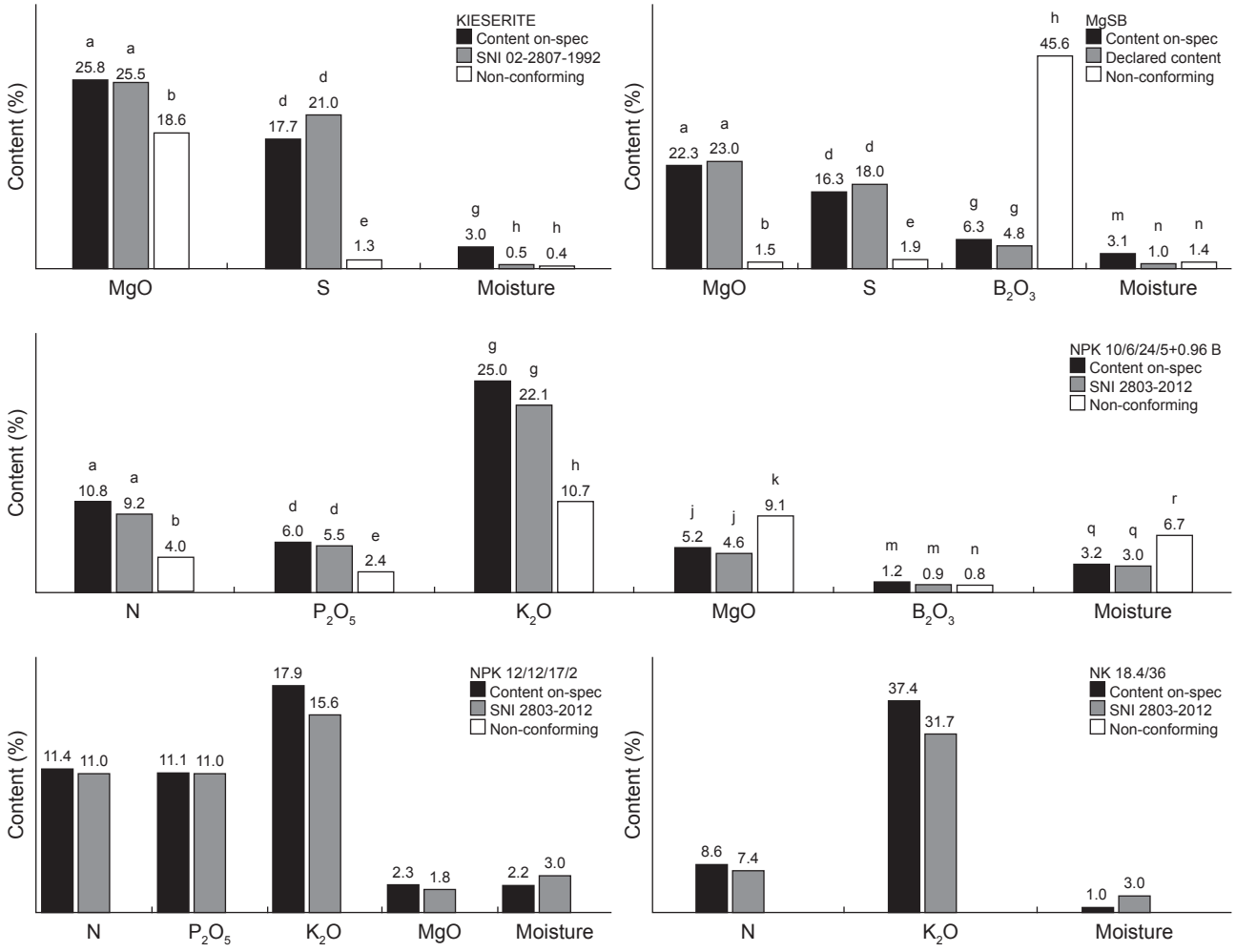

Note: Each bar labelled with the same lowercase letter notation indicates no statistically significant difference from the LSD test at the 5% significance level.

Figure 3. The average nutrient content of various types of fertilisers analysed in the laboratory (kieserite, MgSB, NPK and NK).

The results in *Figure 4* indicate that the nutrient content in RP Peru, Dolomite, MOP, SOA, Borate and Urea fertilisers generally comply with the applicable SNI. For RP Peru, the total P_2O_5 (30.1% and min 28.0%) and moisture content (4.0% and max 5.0%) were very close to the SNI 02-3776-2005 standard. Meanwhile, Dolomite exhibited compliance with the SNI 02-2804-2005 for MgO (18.6% and min 18.0%), CaO (32.1% and min 29.0%), and moisture content (1.4% and max 3.0%). Similarly, MOP met the SNI 02-2805-2005 requirements for total K_2O (60.4% and min 60.0%) and moisture (0.4% and max 1.0%). For SOA, the N (20.9% and min 20.8%) and S content (23.3% and min 23.8%), as well as moisture (0.1% and max 1.0%), appeared to be in line with SNI 02-1760-2005. For Borate, the B_2O_3 content (49.4% and min 45.0%) and moisture 2.3% complied with SNI 02-4959-1999. And finally, Urea adhered to the SNI 2801-2010 standard for N content (46.4% and min 46.0%) and moisture (0.3% and max 0.5%). Overall, there are no statistically significant differences in terms of nutrient content and moisture between the analysed samples and the SNI standards, with no fertilisers identified as non-conforming.

Based on field observations and the nutrient content results as shown in *Figure 3* and *4*, the fertiliser quality can be categorised into three criteria: On-spec fertilisers (original), adulterated fertilisers and counterfeit fertilisers. On-spec fertilisers maintain the nutrient content as specified on the label and comply with the SNI standards. It can be relied upon to provide the necessary nutrients for plant growth. Non-conforming adulterated fertilisers contain a nutrient content of only about 50% of the label and SNI. Its use may reduce productivity and harvest quality due to inadequate nutrient supply. Counterfeit fertilisers, on the other hand, contain nutrient content far below the label and SNI specifications for that fertiliser type, even less than 1%. This classification aids in identifying the different qualities of fertilisers available in the market and facilitates standardisation for fertiliser users, such as farmers and plantation managers.

Figure 5 shows a series of scatter plots of the distribution of nutrient levels in the NPK 10 fertiliser samples. Each plot represents one type of nutrient, with red dots indicating samples with nutrient levels below the tolerance standard of

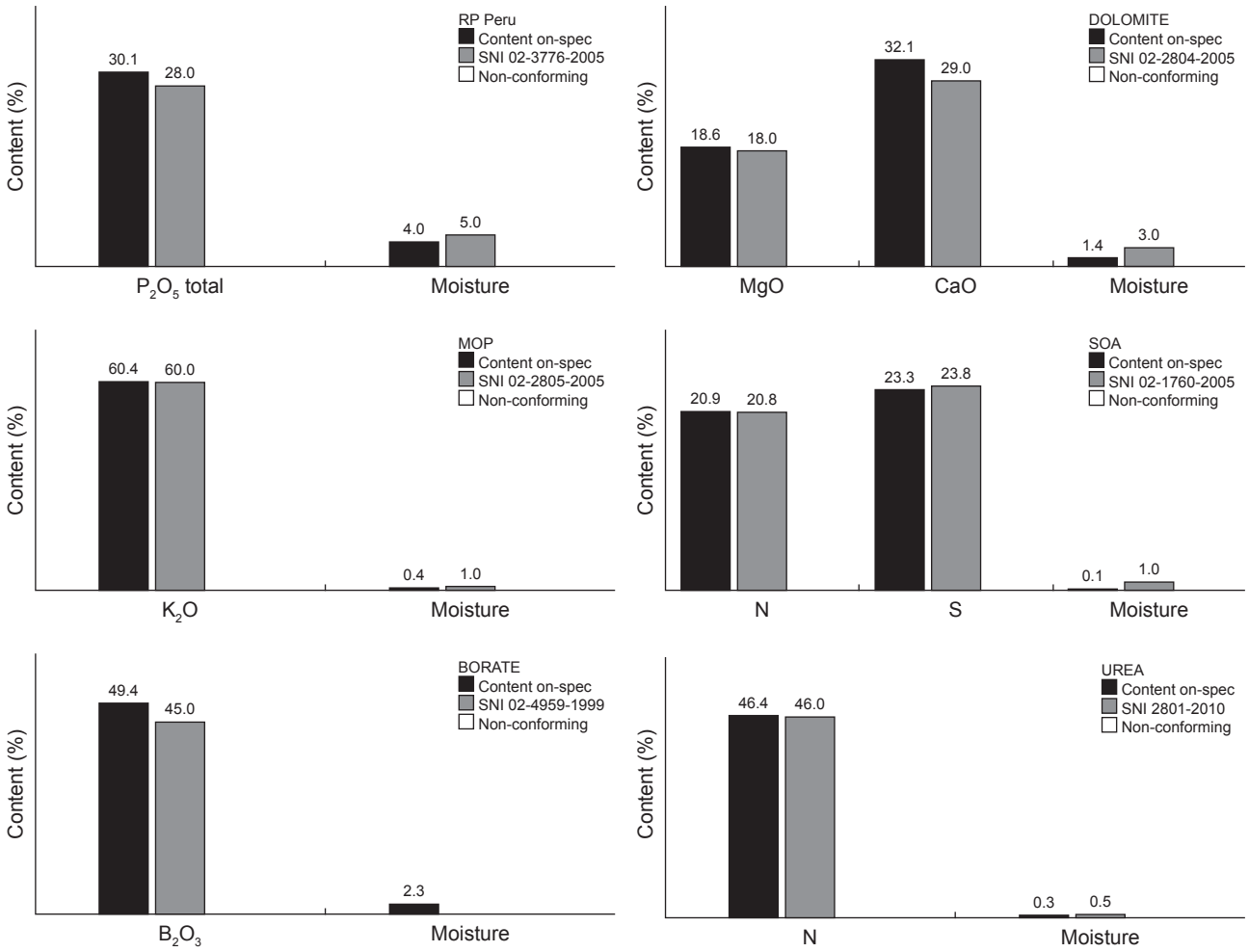

Figure 4. The average nutrient content of various types of fertilisers analysed in the laboratory (RP Peru, dolomite, MOP, SOA, borate, urea).

SNI 2803-2012 (non-conforming) and blue dots indicating samples with nutrient levels above the standard (original). The red and blue colours were also used to illustrate the significant difference between the original and non-conforming fertilisers, based on the results of the independent t-test <5%. The results of the independent t-test at <5% level indicate that the contents of N, P_2O_5, K_2O, MgO and moisture showed significantly different results between the original NPK 10 and the non-conforming, with only B_2O_3 not showing a significant difference. This figure assists in identifying fertiliser samples that meet or do not meet the specified requirements based on SNI standards and provides a visual representation of the variation in nutrient content among samples.

In *Figure 5*, N shows that most samples are above the 9.20% standard (blue), with a small portion below the standard (red). P_2O_5 levels were displayed similarly, with a minimum standard of 5.52%, also showing a majority above the standard. K_2O samples exceeded the 22.08% threshold in large numbers. The MgO and B_2O_3 plots followed the same pattern, with standards set at 4.60% and 0.96%, respectively. Moisture content is marked in red for levels above 3.00% and in blue for below. These plots clearly illustrate that most samples are above the nutrient standards; however, caution is advised, as there are samples below the standard for all NPK 10 nutrient contents tested.

In some cases, slight deviations below the minimum tolerance level set by SNI 2803-2012 may be found for one nutrient content in the on-spec fertiliser in *Figure 5*. However, the differences are not significant, and other nutrient contents remain at high levels. This indicates that although there is a slight discrepancy in one nutrient content, the fertiliser still maintains relatively good quality. Through this visualisation and comparison, the distribution of nutrient levels in NPK 10 fertiliser and its compliance with the established standard can be seen clearly.

Figure 6 presents a visual comparison between original and adulterated NPK Mix 10 fertilisers. The original NPK Mix 10 is marked by the presence of dominant white and yellowish granules (such as urea, kieserite and borate) and the absence of dark brown granules. Furthermore, the original NPK 10 fertiliser exhibits richer colour variations, with around five different colours in the mixture. Conversely, the confirmed adulterated NPK fertiliser displays dark and dominant brown granules, even causing the white granules to fade. Additionally, only four colour variations are visible in the mixture, indicating an imbalance in fertiliser composition. This is further evidenced by the absence of urea granules (yellowish-white and round) and the difficulty in differentiating kieserite and borate granules due to their colour fading caused by the adulterated granules. Other visual differences may also be observed in the quality of the fertilisers. The original fertilisers tend to have a uniform texture and do not contain foreign or additional materials that should not be present. On the other hand, counterfeit fertilisers often appear non-homogeneous, unevenly granulated, or even contain hazardous materials. These visual differences are crucial for farmers and fertiliser users as they can be an initial indication of the authenticity and quality of the purchased fertiliser.

The presence of non-conforming fertiliser with unsuitable nutrient content can also be due to the addition of other materials. There are some common examples of non-conforming fertilisers, such as adulterated fertilisers and counterfeit fertilisers. Firstly, adulterated fertiliser occurs when the original fertiliser is mixed with additional materials that should not be present in its composition. For instance, *Figure 7* shows MOP fertiliser mixed with materials like sand, brick, or laterite soil. This is done to increase the volume of the fertiliser, reduce production costs, or is deliberately carried out by irresponsible parties by reducing the amount of original fertiliser in the sack and refilling it with unsuitable materials. Secondly, non-conforming fertiliser refers to a situation where the original fertiliser is replaced with other materials that may appear to have similar characteristics but differ in their actual composition and nutrient content. For example, kieserite fertiliser is substituted with dolomite, which is, in fact, a different material (*Figure 7*). This can result in differences in nutrient content and composition that should be present in the original fertiliser.

Prevalence of Counterfeit NPK Fertilisers in the Market

The field observations and *Figure 7* above provide valuable insights into the prevalence of counterfeit NPK fertilisers in the market. NPK fertilisers are more susceptible to counterfeiting, compared to other types of fertilisers, and several relevant factors explain this phenomenon. Firstly, it is crucial to note that the use of NPK fertilisers has become widespread and significantly increased across various agricultural commodities. NPK fertilisers are popular and extensively utilised in agriculture due to their combination of three essential nutrients: N, P and K. These elements play a crucial role in supporting plant growth and development. Given the high demand from farmers, NPK fertilisers have become an attractive target for counterfeiters.

This trend is also observed in the oil palm plantation industry, where the use of NPK 10 fertiliser has the highest average compared to other types of fertilisers (*Figure 8*). The high demand

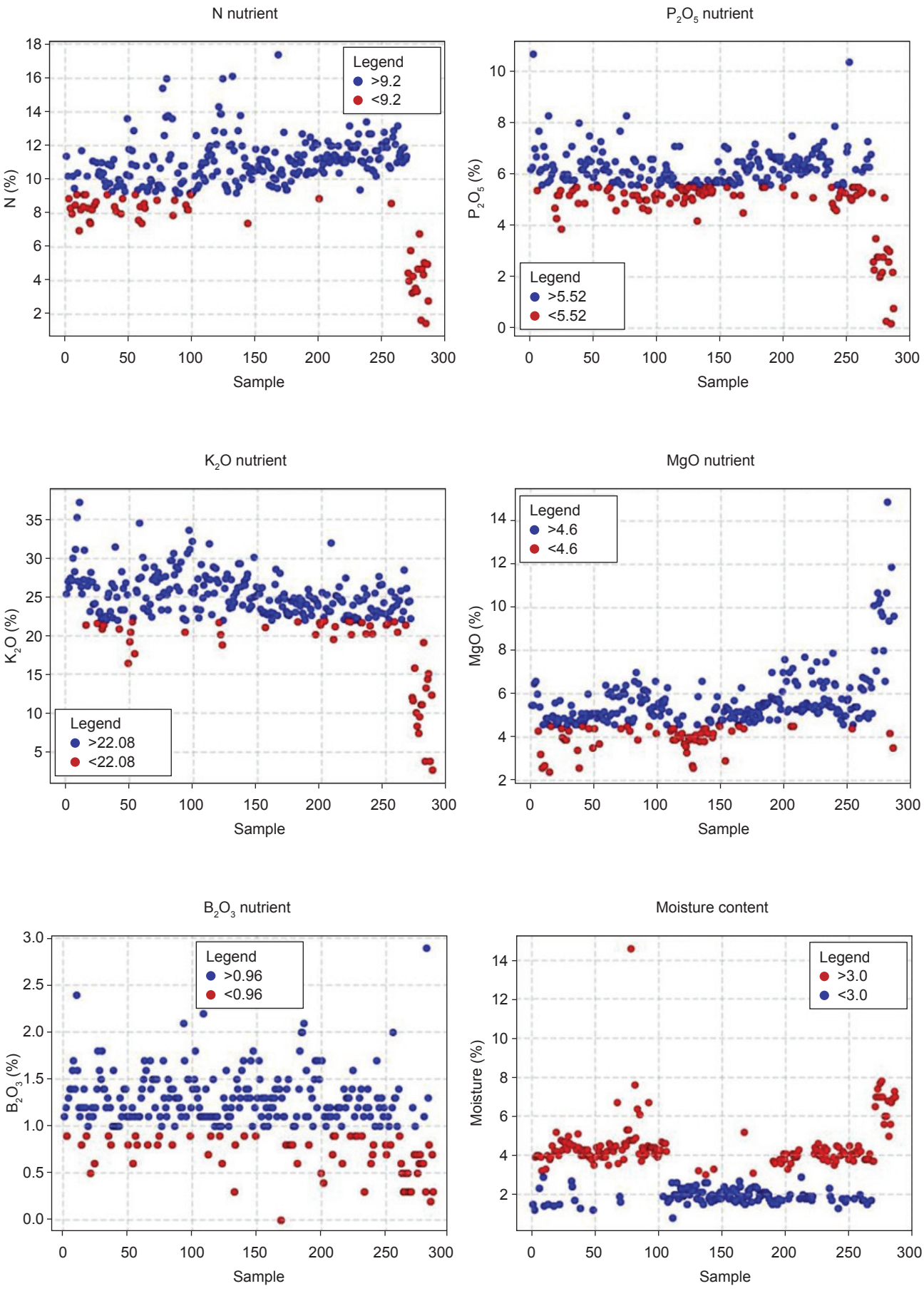

Figure 5. Distribution of nutrient content of NPK 10 from laboratory analysis compared to SNI 2803-2010 standard (tolerance 8%).

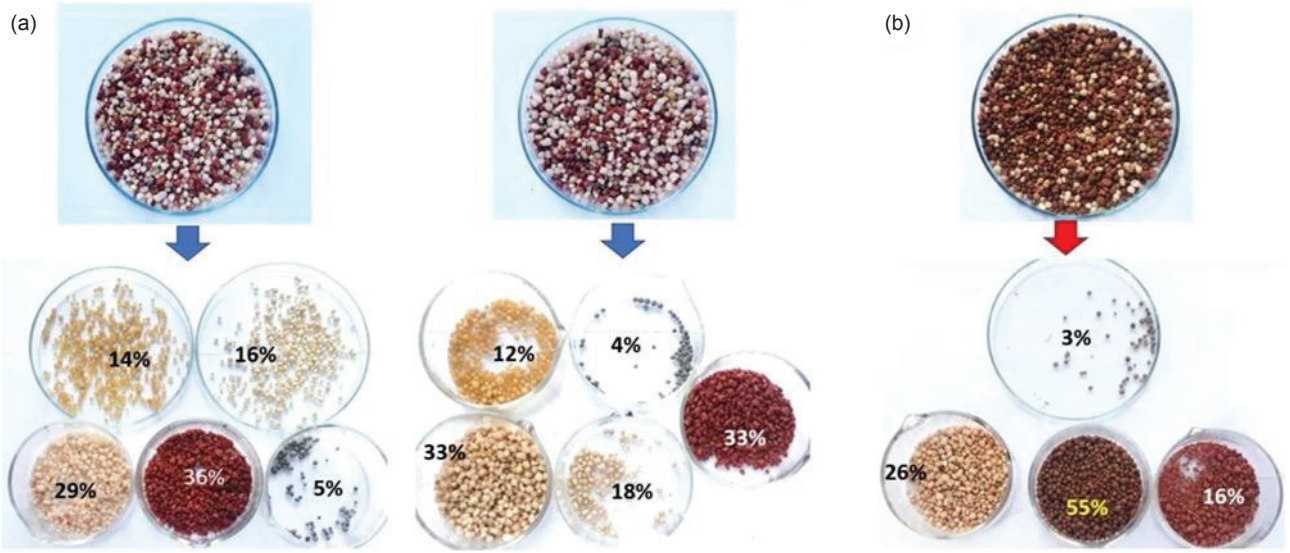

Figure 6. Visual comparison of NPK Mix 10; (a) original and (b) adulterated.

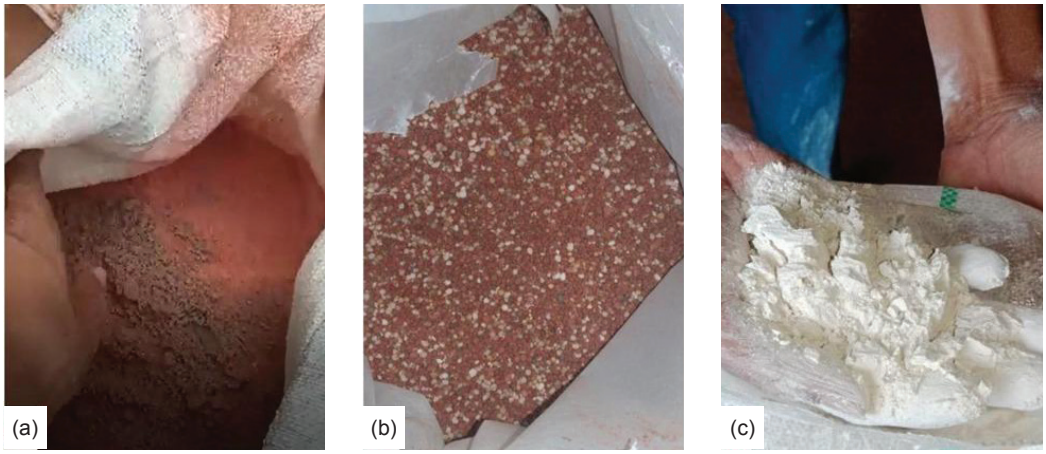

Figure 7. Mixed fertiliser; (a) MOP mixed with other materials such as sand, bricks, lattice soil, (b) NPK Mix mixed with granular clay and dolomite and non-conforming fertiliser (c) Kieserit replaced by Dolomite.

for NPK fertilisers creates a potential market for counterfeit manufacturers, as unscrupulous actors see an opportunity to exploit this demand. The large market size and high demand make the supervision of NPK fertilisers increasingly important. In such situations, the risk of counterfeit NPK fertilisers increases due to economic incentives to produce and market substandard fertilisers. Irresponsible actors may try to imitate popular NPK fertiliser brands and compositions, aiming to gain financial profit without considering the negative impact on plant growth and the environment.

Figure 8 shows that NPK fertiliser dominated the usage at 34%, followed by NK at 18%, dolomite at 10%, MOP, kieserite and urea at 7%, and RP and kieserbor at 5%. The borate had the lowest proportion (1%). The use of NPK fertiliser, reaching the largest proportion of 34%, signifies its importance in oil palm plantations. If NK fertiliser is not used, the proportion of NPK usage could increase to over 50%. The chart presented is not a representation of the quantity of fertiliser given in one year but is the general dose of fertiliser per palm. In practice, the given fertiliser dose is adjusted based on various factors, such as soil classification, plant age, production targets, nutrient loss due to leaching, and other relevant agronomic factors. Because of these factors, the applied fertiliser dose can vary from location to location.

The second factor is the relatively high price of NPK fertilisers (*Table 1*). The high cost provides an incentive for unscrupulous actors to counterfeit NPK fertilisers and sell them at lower prices. Counterfeit fertilisers are often offered at a lower cost than original fertilisers, tempting farmers to choose the more financially accessible option. In situations

where farmers have limited finances, or the expected harvest profits are insufficient, they may be inclined to opt for cheaper counterfeit fertilisers as a more economical alternative. This is especially true if farmers lack adequate access to information or knowledge about the risks and consequences of using counterfeit fertilisers.

Based on the non-subsidised fertiliser price table, NPK 12 fertiliser has a maximum price of USD1.00 kg^{-1}. Compared to other fertilisers, NPK 10 is sold at a lower maximum price of USD0.53, making NPK 10 47% cheaper than NPK 12. NK fertiliser (maximum USD0.80) was 20% cheaper than NPK 12. RP Peru and kieserite have the same maximum price of USD0.40, or 60% cheaper than NPK 12. Dolomite, with the lowest maximum price in *Table 1* at USD0.10, is 90% cheaper than NPK 12, presenting a much more economical choice for buyers if they need MgO and CaO.

The MOP has a price almost identical to NPK 12 at USD0.93; thus, it is only 7% cheaper. However, MgSB with a maximum price of USD1.33, was 33% more expensive than NPK 12, indicating a significant additional cost for certain nutrients. SOA is sold at a maximum price of USD0.37 or 63% cheaper than NPK 12. Urea, with a maximum price of USD0.50, shows to be 50% cheaper than NPK 12, offering a more affordable alternative for buyers in need of high N nutrients. Overall, these prices illustrate the cost spectrum that farmers may face when selecting fertilisers, with some options being much cheaper than NPK 12, while others, such as MgSB offer different nutrients at a higher cost.

Thirdly, it is essential to be vigilant about the relatively easy process of imitating NPK fertilisers using available technology. This provides opportunities for unscrupulous actors to produce and distribute counterfeit fertilisers in the market. *Figure 9* shows two samples of NPK fertiliser taken from the field. Sample A is a fertiliser that meets the standards (original), whereas sample B is a fertiliser that is non-conforming. Although these two samples have differences in quality and composition based on laboratory tests, they appear to be visually very similar. This similarity poses a challenge for farmers and fertiliser users to distinguish between them, through visual inspection alone. This situation underscores the challenges present in the fertiliser industry, where the physical appearance of a fertiliser does not always reflect its nutrient content, and without more in-depth analysis, non-conforming products can easily be mistaken for those that meet the standards (original).

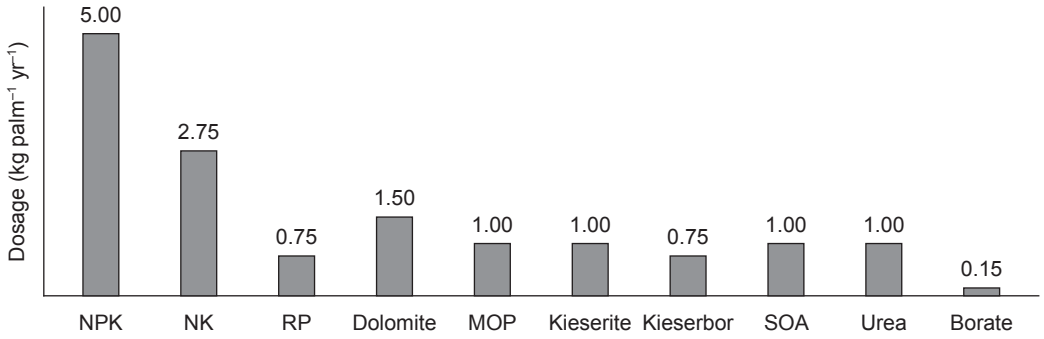

Figure 8. Average fertiliser usage during the TM phase in oil palm plantations.

TABLE 1. RANGE OF NON-SUBSIDISED FERTILISER PRICES AT AGRICULTURAL STORES (JUNE 2023)

No.	Fertiliser type	Composition	Price kg^{-1} (USD)
1	NPK 12	N 12.00%, P_2O_5 12.00%, K_2O 17.00%, MgO 2.00%	0.80 to 1.00
2	NPK 10	N 10.00%, P_2O_5 6.00%, K_2O 24.00%, MgO 5.00%, B_2O_3 0.96%	0.43 to 0.53
3	NK 8.4/36	N 8.40%, K_2O 36.00%	0.70 to 0.80
4	RP Peru	P_2O_5 28.00%	0.33 to 0.40
5	Dolomite	MgO 18.00%, CaO 29.00%	0.07 to 0.10
6	MOP	K_2O 60.00%	0.83 to 0.93
7	Kieserite	MgO 25.50%, S 21.00%	0.33 to 0.40
8	MgSB	MgO 23.00%, S 18.00%, B_2O_3 4.80%	1.16 to 1.33
9	SOA	N 20.80%, S 23.80%	0.31 to 0.37
10	Urea	N 46.00%	0.43 to 0.50

Note: USD1.00 = IDR15,026.00 per 30 June 2023.

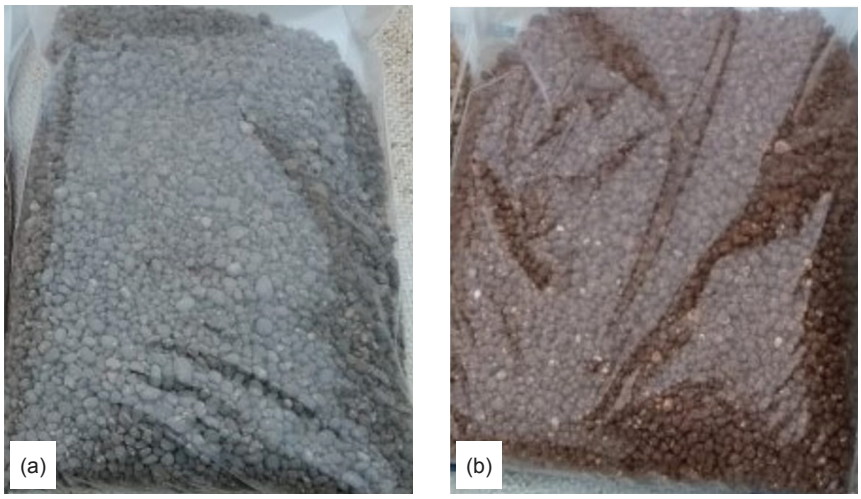

Figure 9. NPK 13/6/27 compound fertiliser (a) on-spec, and (b) non-conforming criteria found in the field are challenging to differentiate.

The above data reveals serious concerns regarding the presence of non-conforming fertilisers, especially counterfeit NPK fertilisers circulating in the field. The existence of non-conforming fertilisers has severe consequences for agriculture and farmers, including reduced productivity, nutrient imbalances, low harvest yields, poor product quality and environmental risks. Farmers also experience financial losses as non-conforming fertilisers do not yield the expected results. Therefore, it is essential to implement an effective fertiliser quality verification system and control the usage of non-conforming fertilisers in oil palm plantations to minimise the negative impacts and promote productive and sustainable agriculture. Identifying the most vulnerable types of fertilisers to becoming non-conforming provides valuable insights and enables targeted improvement actions focused on NPK fertilisers. This information forms a critical basis for formulating appropriate strategies and corrective actions to reduce the use of non-conforming fertilisers and enhance the efficiency and productivity of oil palm plantations.

Negative Impact of Non-conforming Fertilisers on Oil Palm

The use of counterfeit fertilisers over the years had significant negative consequences for agriculture and the environment. The first impact of using counterfeit fertilisers is reduced soil fertility. Counterfeit fertilisers often have low and unbalanced nutrient content, leading to inadequate nutrient supply for plants (Pujawati & Kurniati, 2021). As a result, the soil becomes deficient in essential nutrients such as N, P, K and other micronutrients (Chen *et al.*, 2023). Soil fertility decline can hinder the growth of oil palm plants, reduce fruit production and ultimately decrease the income of farmers and plantation managers (Loh *et al.*, 2019; Maity *et al.*, 2022; Zainuddin *et al.*, 2022).

Moreover, the use of counterfeit fertilisers can damage the overall health of the soil. Additional substances present in counterfeit fertilisers can disrupt soil structure and reduce its ability to retain nutrients. Unhealthy soil will struggle to provide optimal conditions for oil palm roots to absorb nutrients and water, negatively impacting overall plant growth and development (Pérez-Sato *et al.*, 2023; Romanyuk *et al.*, 2023; Salomon & Cavagnaro, 2022).

Furthermore, the use of counterfeit fertilisers can lead to reduced crop production. With inadequate nutrient content, oil palm plants will not thrive and produce optimally, resulting in a significant decline in oil palm fruit production, leading to economic losses for farmers and plantation managers (Chukwu *et al.*, 2023; Ganesapillai *et al.*, 2016). Additionally, reduced crop production affects the availability of palm oil, an essential commodity for food and industrial needs (Monzon *et al.*, 2023; Sugianto *et al.*, 2023; Zhao *et al.*, 2023).

Lastly, the use of counterfeit fertilisers also negatively impacts the quality of food and the final products of palm oil. Oil palm plants exposed to counterfeit fertilisers may have low nutrient content and contain harmful residue from these counterfeit fertilisers. Consequently, the resulting palm oil may have poor quality and lack essential nutrients, affecting the quality of food and the competitiveness of palm oil products in the international market (Dubey *et al.*, 2021; Milošević *et al.*, 2022; Nakayama & Matsuda, 2022).

To address the issue of counterfeit fertiliser use, it is crucial for farmers and plantation managers to always choose fertilisers that have been tested

for quality and comply with official standards (Pujawati & Kurniati, 2021). Strict government supervision and enforcement are also necessary to reduce the prevalence of counterfeit fertilisers in the market (Fitrya *et al.*, 2022; Nasrin *et al.*, 2019; Yang & Lin, 2020). Additionally, education and awareness regarding the importance of selecting and using appropriate fertilisers need to be enhanced to raise awareness of the negative impacts of counterfeit fertilisers and promote the use of quality and licensed fertilisers (Kautsar *et al.*, 2020; Kholis & Setiaji, 2020). With appropriate preventive and corrective measures, it is hoped that the agricultural and oil palm plantation sectors can operate more sustainably and produce high-quality products for the benefit of society and the environment.

CONCLUSION

To facilitate plantation managers in determining fertiliser application policies in the field, fertiliser quality can be categorised into three criteria: Original fertiliser (composition and content in line with the label), diluted fertiliser (nutrient content around 50% of the label and standard) and counterfeit fertiliser (nutrient content significantly deviating from the label and standard, even less than 1%). Visual inspections can identify fertilisers with improper compositions (non-conforming), such as MOP mixed with other materials (sand, bricks, laterite soil), NPK granules mixed with clay and dolomite granules, and the substitution of kieserite with dolomite. Original NPK Mix fertiliser is characterised by dominant white and yellowish granules and a rich variety of colours with around five variations in the mixture, whereas counterfeit NPK Mix has dominant dark brown granules, only four variations in colours, and lacks the characteristic white to yellowish granules.

NPK fertilisers have the highest percentage of non-conforming at 2.4%, followed by kieserite at 0.3%, and MgSB at 0.1% out of 723 samples tested over a year. NPK fertilisers are more prone to counterfeiting due to their relatively high price, widespread use, increasing demand in various agricultural commodities, and their relatively easy production process to replicate with available technology. The use of non-conforming fertilisers negatively impacts the growth and development of oil palm plants.

In conclusion, it is essential to address the prevalence of counterfeit and non-conforming fertilisers in the market to ensure the productivity and sustainability of oil palm plantations. Plantation managers should prioritise the use of original and quality fertilisers, that comply with official standards, to maximise the yield and quality of oil palm produce. Additionally, rigorous government supervision and strict law enforcement are crucial to reducing the circulation of counterfeit fertilisers. Raising awareness among farmers about the detrimental effects of counterfeit and non-conforming fertilisers can also contribute to making informed decisions regarding their fertiliser choices. By taking appropriate actions and implementing preventive measures, the oil palm plantation sector can achieve better outcomes, benefiting both the industry and the environment.

ACKNOWLEDGEMENT

The author would like to express gratitude to the Research Directorate at Universitas Gadjah Mada and the UGM Reputation Improvement Team Towards World-Class University for their support under the research scheme of the Post-Doctoral Program (3662/UN1.P.II/Dit-Lit/PT.01.03/2023). Additionally, the research received support from the Smart Agriculture Research Group, the Department of Agricultural and Biosystems Engineering, Universitas Gadjah Mada, and Wilmar International Plantation-Central Kalimantan Region.

REFERENCES

Abdul-Hamid, A., Ali, M. H., Osman, L. H., Tseng, M., & Lim, M. K. (2022). Industry 4.0 quasi-effect between circular economy and sustainability: Palm oil industry. *International Journal of Production Economics*, *253*, 108616. https://doi.org/10.1016/j.ijpe.2022.108616

Afriyanti, D., Kroeze, C., & Saad, A. (2016). Indonesia palm oil production without deforestation and peat conversion by 2050. *The Science of the Total Environment*, *557–558*, 562–570. https://doi.org/10.1016/j.scitotenv.2016.03.032

Aji, W. A., Utami, A. D., Nugroho, B., Toyyibah, T., & Nurcahya, M. A. (2021). Fertilization effectiveness on the productivity of fresh fruit bunches and maintenance costs of oil palm. *Buletin Penelitian Sosial Ekonomi Pertanian Fakultas Pertanian Universitas Haluoleo*, *22*(2), 66–71. https://doi.org/10.37149/bpsosek.v22i2.13874

Albuquerque, A. R., Merino, A., Angélica, R. S., Omil, B., & Paz, S. P. (2022). Performance of ash from Amazonian biomasses as an alternative source of essential plant nutrients:

An integrated and eco-friendly strategy for industrial waste management in the lack of raw fertilizer materials. *Journal of Cleaner Production*, *360*, 132222. https://doi.org/10.1016/j.jclepro.2022.132222

Anuar, A. R., Goh, K. J., Heoh, T. B., & Ahmed, O. H. (2008). Spatial-temporal yield trend of oil palm as influenced by nitrogen fertilizer management. *American Journal of Applied Sciences*, *5*(10), 1376–1383. https://doi.org/10.3844/ajassp.2008.1376.1383

Arifin, I., Hanafi, M. M., Roslan, I., Ubaydah, M. U., Karim, Y. A., Tui, L. C., & Hamzah, S. (2022). Responses of irrigated oil palm to nitrogen, phosphorus and potassium fertilizers on clayey soil. *Agricultural Water Management*, *274*, 107922. https://doi.org/10.1016/j.agwat.2022.107922

Beidou Company. (2019). *5 big lies and 8 big sweet-talk of fertiliser industry!* LinkedIn. Retrieved July 23, 2023 from https://www.linkedin.com/pulse/5-big-lies-8-sweet-talk-fertiliser-industry-beidou-company

Bold, T., Kaizzi, K. C., Svensson, J., & Yanagizawa-Drott, D. (2017). Lemon technologies and adoption: Measurement, theory and evidence from agricultural markets in Uganda. *The Quarterly Journal of Economics*, *132*(3), 1055–1100. https://doi.org/10.1093/qje/qjx009

Chen, H., Yang, G., Xiao, Y., Zhang, G., Yang, G., Wang, X., & Hu, Y. (2023). Effects of nitrogen and phosphorus fertilizer on the eating quality of indica rice with different amylose content. *Journal of Food Composition and Analysis*, *118*, 105167. https://doi.org/10.1016/j.jfca.2023.105167

Chukwu, E., Udoh, B., Afangide, A., & Osisi, A. (2023). Evaluation of soil quality under oil palm cultivation in a coastal plain sands area of Akwa Ibom State Nigeria. *Soil Security*, *10*, 100087. https://doi.org/10.1016/j.soisec.2023.100087

Dania, O. (2023, April 20). *Fake fertilizer supplier arraigned for N20m fraud*. Punch Newspapers. https://punchng.com/fake-fertilizer-supplier-arraigned-for-n20m-fraud/

Dermawan, A., Hospes, O., & Termeer, C. (2022). Between zero-deforestation and zero-tolerance from the state: Navigating strategies of palm oil companies of Indonesia. *Forest Policy and Economics*, *136*, 102690. https://doi.org/10.1016/j.forpol.2022.102690

Dhankhar, N., & Kumar, J. (2023). Impact of increasing pesticides and fertilizers on human health: A review. *Materials Today Proceedings*. https://doi.org/10.1016/j.matpr.2023.03.766

Dubey, A. K., Sharma, R. M., Deepak, N., & Kumar, A. (2021). Long term performance of mango varieties on five polyembryonic rootstocks under subtropical conditions: Effect on vigour, yield, fruit quality and nutrient acquisition. *Scientia Horticulturae*, *280*, 109944. https://doi.org/10.1016/j.scienta.2021.109944

Dubos, B., Snoeck, D., & Flori, A. (2016). Excessive use of fertilizer can increase leaching processes and modify soil reserves in two Ecuadorian oil palm plantations. *Experimental Agriculture*, *53*(2), 255–268. https://doi.org/10.1017/s0014479716000363

Essono, D. M., Nkoué, B. B., Voundi, E., Kono, L., Verrecchia, E., Ghazoul, J., Mala, A. W., Buttler, A., & Guillaume, T. (2023). Nutrient availability challenges the sustainability of low-input oil palm farming systems. *Farming System*, *1*(1), 100006. https://doi.org/10.1016/j.farsys.2023.100006

Firmansyah, E., Dewi, S. I., & Umami, A. (2021). Pembangunan sistem rekomendasi pemupukan berbasis web bagi perkebunan kelapa sawit rakyat [Development of web-based fertilization recommendation system for smallholder palm oil plantation]. *Jurnal Pertanian Agros 23 (1), 109-120.*

Fitrya, N., Wirman, S. P., & Rumzi, M. (2022). Rancang bangun sistem optik metode *Laser Speckle Imaging (LSI) model backscattering* untuk identifikasi pupuk oplosan [Optical system method of Laser Speckle Imaging (LSI) backscattering model for identification of oplosan fertilizers]. *Photon Jurnal Sain Dan Kesehatan, 12(2).* https://doi.org/10.37859/jp.v12i2.2362

Fromartz, S. (2021, April 7). *California schemin': How a fake organic fertilizer bamboozled farmers and watchdogs alike*. Grist. https://grist.org/organic-food/2011-05-18-california-how-a-fake-organic-fertilizer-bamboozled-farmers/

Ganesapillai, M., Simha, P., Beknalkar, S. S., & Sekhar, D. (2016). Low-grade rock phosphate enriched human urine as novel fertilizer for sustaining and improving agricultural productivity of *Cicer arietinum*. *Sustainable Production and Consumption*, *6*, 62–66. https://doi.org/10.1016/j.spc.2016.01.005

Georgieva, R., Delibaltova, V., & Chavdarov, P. (2022). Change in agronomic characteristics and essential oil composition of coriander after application of foliar fertilizers and biostimulators. *Industrial Crops and Products*, *181*, 114819. https://doi.org/10.1016/j.indcrop.2022.114819

Hu, M., Wade, A. J., Shen, W., Zhong, Z., Qiu, C., & Lin, X. (2024). Effects of organic fertilizers produced using different techniques on rice grain yield and ammonia volatilization in double-cropping rice fields. *Pedosphere*, *34*(1), 110–120. https://doi.org/10.1016/j.pedsph.2023.03.004

Huang, R., Mao, P., Xiong, L., Qin, G., Zhou, J., Zhang, J., Li, Z., & Wu, J. (2023). Negatively charged nano-hydroxyapatite can be used as a phosphorus fertilizer to increase the efficacy of wollastonite for soil cadmium immobilization. *Journal of Hazardous Materials*, *443*, 130291. https://doi.org/10.1016/j.jhazmat.2022.130291

Jamilah, J., Syahrial, S., Z, Y. R., Ernita, M., Zahanis, Z., & Mutia, Y. D. (2022). Dissemination of fertilizer packaging literature and soil conservation on farming group in Sungai Aur District Pasaman Barat. *Jurnal Pengabdian Kepada Masyarakat DEWANTARA*, *5*(2), 1. https://doi.org/10.31317/jpmd.v5i2.819

Kautsar, M. R., Sofyan, & Makmur, T. (2020). Analisis kelangkaan pupuk bersubsidi dan pengaruhnya terhadap produktivitas padi (*Oryza sativa*) di Kecamatan Montasik Kabupaten Aceh Besar [The scarcity analysis of subsidized fertilizer and its effect on rice productivity in Montasik Subdistrict, Aceh Besar Regency]. *Jurnal Ilmiah Mahasiswa Pertanian, 5(1)*, 97–107.

Kholis, I., & Setiaji, K. (2020). Analisis efektivitas kebijakan subsidi pupuk pada petani padi. [Analysis of the effectiveness of fertilizer subsidy policy for rice farmers]. *Economic Education Analysis Journal*, 9(2), 503–515.

Khor, L. Y., & Zeller, M. (2014). Inaccurate fertilizer content and its effect on the estimation of production functions. *China Economic Review*, *30*, 123–132. https://doi.org/10.1016/j.chieco.2014.06.003

Krishna, V., Euler, M., Siregar, H., & Qaim, M. (2017). Differential livelihood impacts of oil palm expansion in Indonesia. *Agricultural Economics*, *48*(5), 639–653. https://doi.org/10.1111/agec.12363

Lam, W. Y., Kulak, M., Sim, S., King, H., Huijbregts, M. A., & Chaplin-Kramer, R. (2019). Greenhouse gas footprints of palm oil production in Indonesia over space and time. *The Science of the Total Environment*, *688*, 827–837. https://doi.org/10.1016/j.scitotenv.2019.06.377

Li, W., Guo, S., Liu, H., Zhai, L., Wang, H., & Lei, Q. (2018). Comprehensive environmental impacts of fertilizer application vary among different crops: Implications for the adjustment of agricultural structure aimed to reduce fertilizer use. *Agricultural Water Management*, *210*, 1–10. https://doi.org/10.1016/j.agwat.2018.07.044

Lim, Y. L., Tenorio, F. A., Monzon, J. P., Sugianto, H., Donough, C. R., Rahutomo, S., Agus, F., Slingerland, M. A., Darlan, N. H., Dwiyahreni, A. A., Farrasati, R., Mahmudah, N., Muhamad, T., Nurdwiansyah, D., Palupi, S., Pradiko, I., Saleh, S., Syarovy, M., Wiratmoko, D., & Grassini, P. (2023). Too little, too imbalanced: Nutrient supply in smallholder oil palm fields in Indonesia. *Agricultural Systems*, *210*, 103729. https://doi.org/10.1016/j.agsy.2023.103729

Liu, D., Shi, Z., Ma, Q., Zhang, Y., Cai, T., Zhang, P., & Jia, Z. (2023). Strategy for matching fertilizer application with soil water before sowing can stabilize maize productivity under rainwater harvesting and mulching planting in dry areas: A six-year field experiment. *Agricultural Water Management*, *287*, 108452. https://doi.org/10.1016/j.agwat.2023.108452

Liu, H., Zhang, X., Zhang, G., Kou, X., & Liang, W. (2022). Partial organic substitution weakens the negative effect of chemical fertilizer on soil micro-food webs. *Journal of Integrative Agriculture*, *21*(10), 3037–3050. https://doi.org/10.1016/j.jia.2022.07.043

Loh, S. K., Lai, M. E., & Ngatiman, M. (2019). Vegetative growth enhancement of organic fertilizer from anaerobically-treated palm oil mill effluent (POME) supplemented with chicken manure in food-energy-water nexus challenge. *Food and Bioproducts Processing*, *117*, 95–104. https://doi.org/10.1016/j.fbp.2019.06.016

Maity, A., Marathe, R. A., Sarkar, A., & Basak, B. (2022). Phosphorus and potassium supplementing bio-mineral fertilizer augments soil fertility and improves fruit yield and quality of pomegranate. *Scientia Horticulturae*, *303*, 111234. https://doi.org/10.1016/j.scienta.2022.111234

Martin, T. M., Aubin, J., Gilles, E., Auberger, J., Esculier, F., Levavasseur, F., McConville, J., & Houot, S. (2023). Comparative study of environmental impacts related to wheat production with human-urine based fertilizers versus mineral fertilizers. *Journal of Cleaner Production*, *382*, 135123. https://doi.org/10.1016/j.jclepro.2022.135123

Michelson, H., Fairbairn, A., Ellison, B., Maertens, A., & Manyong, V. (2021). Misperceived quality: Fertilizer in Tanzania. *Journal of Development Economics*, *148*, 102579. https://doi.org/10.1016/j.jdeveco.2020.102579

Milošević, T., Milošević, N., & Mladenović, J. (2022). The influence of organic, organo-mineral and mineral fertilizers on tree growth, yielding, fruit quality and leaf nutrient composition of apple cv. 'Golden Delicious Reinders.' *Scientia Horticulturae*, *297*, 110978. https://doi.org/10.1016/j.scienta.2022.110978

Monzon, J. P., Lim, Y. L., Tenorio, F. A., Farrasati, R., Pradiko, I., Sugianto, H., Donough, C. R., Edreira, J. I. R., Rahutomo, S., Agus, F., Slingerland, M. A., Zijlstra, M., Saleh, S., Nashr, F., Nurdwiansyah, D., Ulfaria, N., Winarni, N. L., Zulhakim, N., & Grassini, P. (2023). Agronomy explains large yield gaps in smallholder oil palm fields. *Agricultural Systems*, *210*, 103689. https://doi.org/10.1016/j.agsy.2023.103689

Morra, L., Bilotto, M., Baldantoni, D., Alfani, A., & Baiano, S. (2021). A seven-year experiment in a vegetable crops sequence: Effects of replacing mineral fertilizers with Biowaste compost on crop productivity, soil organic carbon and nitrates concentrations. *Scientia Horticulturae*, *290*, 110534. https://doi.org/10.1016/j.scienta.2021.110534

Nakayama, M., & Matsuda, H. (2022). Soilless cultivation of 'Ruby Star' passion fruit: Effects of NO_3-N application, pH, and temperature on fruit quality. *Scientia Horticulturae*, *306*, 111462. https://doi.org/10.1016/j.scienta.2022.111462

Nam, T. (2008, October 16). *Ha noi companies making fake fertilizers busted.* SGGP English Edition. https://en.sggp.org.vn/ha-noi-companies-making-fake-fertilizers-busted-post55916.html

Nasrin, M., Bauer, S., & Arman, M. (2019). Dataset on measuring perception about fertilizer subsidy policy and factors behind differential farm level fertilizer usage in Bangladesh. *Data in Brief*, *22*, 851–858. https://doi.org/10.1016/j.dib.2019.01.005

Nektarios, P. A., Ischyropoulos, D., Kalozoumis, P., Savvas, D., Yfantopoulos, D., Ntoulas, N., Tsaniklidis, G., & Goumenaki, E. (2022). Impact of substrate depth and fertilizer type on growth, production, quality characteristics and heavy metal contamination of tomato and lettuce grown on urban green roofs. *Scientia Horticulturae*, *305*, 111318. https://doi.org/10.1016/j.scienta.2022.111318

Norton, B., Hoel, J., & Michelson, H. (2020, July 26–28). *The demand for (fake?) fertiliser: Using an experimental auction to examine the role of beliefs on agricultural input demand in Tanzania* [Paper presentation]. Agricultural and Applied Economics Association 2020 Annual Meeting, Kansas City, United States. https://doi.org/10.22004/ag.econ.304444

Pérez-Sato, M., Gómez-Gutiérrez, Á., López-Valdez, F., Ayala-Niño, F., Soni-Guillermo, E., González-Graillet, M., & Pérez-Hernández, H. (2023). Soil physicochemical properties change by age of the oil palm crop. *Heliyon*, *9*(6), e16302. https://doi.org/10.1016/j.heliyon.2023.e16302

Pujawati, U., & Kurniati, G. (2021). Tinjauan yuridis penyelesaian sengketa konsumen akibat penjualan pupuk bersubsidi palsu [Juridical review of consumer dispute resolution due to the sale of fake subsidized fertilizer]. *Wajah Hukum*, *5*(2), 473-480. https://doi.org/10.33087/wjh.v5i2.529

Quemada, M., Alonso-Ayuso, M., Castellano-Hinojosa, A., Bedmar, E. J., Gabriel, J. L., González, I. G., Valentín, F., & Calvo, M. (2019). Residual effect of synthetic nitrogen fertilizers and impact on Soil Nitrifiers. *European Journal of Agronomy*, *109*, 125917. https://doi.org/10.1016/j.eja.2019.125917

Rhebergen, T., Fairhurst, T.; Zingore, S., Fisher, M., Oberthür, T., & Whitbread, A. (2016). Adapting oil palm best management practices to Ghana: Opportunities for production intensification. *Better Crops, 100*(4), 12–15.

Romanyuk, N., Ednach, V., Nukeshev, S., Troyanovskaya, I., Voinash, S., Kalimullin, M., & Sokolova, V. (2023). Improvement of the design of the plow-subsoiler-fertilizer to increase soil fertility. *Journal of Terramechanics*, *106*, 89–93. https://doi.org/10.1016/j.jterra.2023.01.001

Rui, Y., Hao, J., & Rui, F. (2012). Determination of seven plant nutritional elements in potassium dihydrogen phosphate fertilizer from northeastern China. *Journal of Saudi Chemical*

Society, *16*(1), 89–90. https://doi.org/10.1016/j.jscs.2010.11.003

Salomon, M. J., & Cavagnaro, T. R. (2022). Healthy soils: The backbone of productive, safe and sustainable urban agriculture. *Journal of Cleaner Production*, *341*, 130808. https://doi.org/10.1016/j.jclepro.2022.130808

San, K. G. (2022, May 20). *Farmers hit by fake fertiliser scams*. The Malaysian Insight. https://www.themalaysianinsight.com/s/382255

Saprida, & Saruksuk, W. (2021). Analisis pengaruh biaya pemupukan tanaman dan biaya panen terhadap pendapatan petani [Analysis of the influence of plant fertilization costs and harvest costs on farmer income]. *Agriprimatech*, *4*(2), 46–56. https://doi.org/10.34012/agriprimatech.v4i2.1702

Shahwar, D., Mushtaq, Z., Mushtaq, H., Alqarawi, A. A., Park, Y., Alshahrani, T. S., & Faizan, S. (2023). Role of microbial inoculants as bio fertilizers for improving crop productivity: A review. *Heliyon*, *9*(6), e16134. https://doi.org/10.1016/j.heliyon.2023.e16134

Sugianto, H., Monzon, J. P., Pradiko, I., Tenorio, F. A., Lim, Y. L., Donough, C. R., Sunawan, N., Rahutomo, S., Agus, F., Cock, J., Amsar, J., Farrasati, R., Iskandar, R., Edreira, J. I. R., Saleh, S., Santoso, H., Tito, A. P., Ulfaria, N., Slingerland, M. A., & Grassini, P. (2023). First things first: Widespread nutrient deficiencies limit yields in smallholder oil palm fields. *Agricultural Systems*, *210*, 103709. https://doi.org/10.1016/j.agsy.2023.103709

TNN. (2022, February 6). *Fake fertilizer racket stumps farmers*. The Times of India. https://timesofindia.indiatimes.com/city/mysuru/fake-fertilizer-racket-stumps-farmers/articleshow/89375217.cms

Vuthy, T. (2020). The supply of fertiliser for rice farming in Takeo. In R. Cramb (Ed.) *White gold: The commercialisation of rice farming in the lower Mekong Basin* (pp. 291–308). Springer. https://doi.org/10.1007/978-981-15-0998-8_14

Waudby, H., & Zein, S. H. (2021). A circular economy approach for industrial scale biodiesel production from palm oil mill effluent using microwave heating: Design, simulation, techno-economic analysis and location comparison. *Process Safety and Environmental Protection*, *148*, 1006–1018. https://doi.org/10.1016/j.psep.2021.02.011

Wilson, W. W., & Shakya, S. (2023). Quantifying impacts of competition and demand on the risk for fertilizer plant locations. *Journal of Commodity Markets*, *30*, 100326. https://doi.org/10.1016/j.jcomm.2023.100326

Wongmaneeroj, A., Pitakdantham, R., Thawornpruek, S., Verapattananirund, P., Yost, R. S., & Attanandana, T. (2019). Soil clinics: Farmers teaching smart-farming to farmers. *Agricultural Sciences*, *10*(09), 1194–1205. https://doi.org/10.4236/as.2019.109089

Xin, Y., Sun, L., & Hansen, M. C. (2022). Oil palm reconciliation in Indonesia: Balancing rising demand and environmental conservation towards 2050. *Journal of Cleaner Production*, *380*, 135087. https://doi.org/10.1016/j.jclepro.2022.135087

Yang, J., & Lin, Y. (2020). Driving factors of total-factor substitution efficiency of chemical fertilizer input and related environmental regulation policy: A case study of Zhejiang Province. *Environmental Pollution*, *263*, 114541. https://doi.org/10.1016/j.envpol.2020.114541

Zainuddin, N., Keni, M. F., Ibrahim, S. A. S., & Masri, M. M. M. (2021). Effect of integrated biofertilizers with chemical fertilizers on the oil palm growth and soil microbial diversity. *Biocatalysis and Agricultural Biotechnology*, *39*, 102237. https://doi.org/10.1016/j.bcab.2021.102237

Zhao, J., Elmore, A. J., Lee, J. S. H., Numata, I., Zhang, X., & Cochrane, M. A. (2023). Replanting and yield increase strategies for alleviating the potential decline in palm oil production in Indonesia. *Agricultural Systems*, *210*, 103714. https://doi.org/10.1016/j.agsy.2023.103714

Journal of Oil Palm Research Vol. 37 (3) September 2025 p. 492-505
DOI: https://doi.org/10.21894/jopr.2024.0016

DELIGNIFICATION METHODS FOR EMPTY FRUIT BUNCH CO-SUBSTRATE IN POME ANAEROBIC DIGESTION: AN EXPERIMENTAL COMPARATIVE ANALYSIS

MUHAMMAD ALPLEX FIRSTONDA KATON[2,4]; FRENDY RIAN SAPUTRO[1]; BAMBANG MUHARTO[1]; ZULAICHA DWI HASTUTI[1]; ADE SYAFRINALDY[1]; ALDRIN SANOVA[2]; MUHAMMAD ILHAM AKBAR[2]; AGUS KISMANTO[1]; RINALDI MEDALI RACHMAN[2]; NURUL AIYSHAH MAZLAN[3]; AHMAD MUHSIN ITHNIN[3] and DHANI AVIANTO SUGENG[1]*

ABSTRACT

Empty fruit bunches (EFB) enhances biogas production in the anaerobic digestion of palm oil mill effluent (POME) by acting as a co-substrate. Yet, lignin in EFB inhibits the performance boost. Therefore, EFB was delignified before using it as a co-substrate as much as 4%. This study compared three delignification techniques using the pairwise comparison method: Bacterial, chemical and hydrothermal. Three parameter variations were selected for each method, namely bacterial concentration, molar concentration and temperatures. Chemical delignification (CDP) at a NaOH concentration of 2 M yielded the largest production of biogas and methane (302.0 and 153.8 mL, respectively), followed by hydrothermal at 180°C (260.0 and 83.8 mL, respectively). Although bacterial delignification (BDP) required a long time (2 weeks), it was the simplest to implement and yielded the largest lignin reduction. However, the bacterial method yielded lower biogas (103-204 mL) than hydrothermal and chemical, probably because of lower hemi- and cellulose contents. Based on biogas and methane yield, production hazards, preparation time, and required infrastructure, CDP was selected as the best method because of its gas production, followed closely by hydrothermal due to its efficiency and safety.

Keywords: anaerobic co-digestion, biogas, delignification, EFB, POME.

Received: 28 July 2023; **Accepted:** 28 December 2023; **Published online:** 14 February 2024.

INTRODUCTION

Indonesia and Malaysia are the world's biggest palm oil producers, with 54.0% and 32.0% of the total world's crude palm oil (CPO) production (Aziz *et al.*, 2020). In the last five years, the Indonesian Ministry for Agriculture reported an annual increase in CPO production of around 11.1% (Direktorat Jenderal Perkebunan Kementerian Pertanian Republik Indonesia, 2021), while the Malaysian Palm Oil Board (MPOB) reported a 5.6% annual growth in the same period (MPOB, 2020).

Processing 1 t of oil palm fresh fruit bunches (FFB) emits 583 kg palm oil mill effluent (POME), 210-230 kg empty fruit bunches (EFB), 65 kg shells and 40 kg wet mud (Hambali & Rivai, 2017). POME is an environmental pollutant because of the high value of chemical oxygen demand (COD) between 15,000 and 100,000 mg O_2/L, acidity (pH 3.4-5.2), and discharge temperatures between 80°C and 90°C (Chow *et al.*, 2020). Anaerobic-digesting lagoons are

[1] Center for Energy Conversion and Conservation, KST BJ Habibie, National Research and Innovation Agency, Tangerang Selatan 15314, Indonesia.

[2] Department of Chemical Engineering, Universitas Pertamina, Jakarta 12220, Indonesia.

[3] Advanced Vehicle System, Malaysia Japan International Institute of Technology, Universiti Teknologi Malaysia, 54100 Kuala Lumpur, Malaysia.

[4] Department of Chemical Engineering, Bandung Institute of Technology, Bandung, 40132, Indonesia.

* *Corresponding author e-mail: dhan001@brin.go.id*

widely applied in palm oil mills before POME is discharged into the environment to lower their COD (Chow *et al.*, 2020).

Anaerobic digestion is an anaerobic fermentation process that involves the degradation of organic materials to produce biogas and digestate through the activities of microorganisms (Nwokolo *et al.*, 2020). One t of POME produces approximately 28 m^3 of biogas, consisting of methane (CH_4), carbon dioxide (CO_2) and traces of hydrogen sulfide (H_2S) (Suksong *et al.*, 2020). CH_4 is a greenhouse gas that contributes 20 times more to global warming than CO_2 (Chow *et al.*, 2020). However, its energy content can substitute fossil fuels in households and various industries.

When the process involves only one substrate, the fermentation process is called mono-digestion, while if there is more than one substrate, the process is called co-digestion. While POME is highly biodegradable due to the rich cellulolytic material and oil (Dominic & Baidurah, 2022), EFB has poor biodegradability (Liew *et al.*, 2021). However, the co-digestion of POME and EFB has proven beneficial, with EFB providing extra nutrients that increase biogas production (Chow *et al.*, 2020; Octiva *et al.*, 2018).

EFB is lignocellulosic with a large cellulose content of 24%-65%. Other components are typically hemicellulose (21%-34%), lignin (14%-31%) and ash (1%) (Yiin *et al.*, 2019). The main concern with EFB utilisation in anaerobic co-digestion is the proper breakdown of the lignocellulosic substrate due to its recalcitrant and complex nature. Although hemicellulose, cellulose and lignin are sources of nutrients for anaerobic bacteria, their decomposition rates vary wildly. Lignin, which accounts for 17%-32% w/w in oil palm lignocellulose, is the slowest to decompose, limiting the co-digestion's performance boost (Nwokolo *et al.*, 2020).

Exposed cellulose and hemicellulose in EFB are important for efficient enzyme access (Patinvoh *et al.*, 2017). Delignification, which involves removing the lignin seal, improves the accessibility of cellulose and hemicellulose. In the case of mono-digestion, delignification enhanced methane production in waste-paper anaerobic digestion by up to 141% compared to untreated situations (Yuan *et al.*, 2012). Delignification can be performed biologically, chemically or hydrothermally (Sołowski *et al.*, 2020).

Bacterial delignification (BDP) is a biological process via fungi or bacteria by their ligninolytic enzymes. Research in BDP shows significant lignin degradation in lignocellulosic biomasses (Van Fan *et al.*, 2018). The bacteria or fungi used in delignification are usually commercial microbial inoculants containing yeasts, lactic acid bacteria, and photosynthetic bacteria, such as *Lactobacillus* sp., *Streptomyces* sp., and *Actinomycetes* sp. (Dewi *et al.*, 2018). The biological degradation of solid organic materials consumes low energy and is environment and budget-friendly (Dewi *et al.*, 2018; Van Fan *et al.*, 2018).

Chemical delignification (CDP) destroys lignin using chemicals such as NaOH. NaOH effectively degrades lignin, as was observed in previous works on EFB, wheat straw, and pine wood (Javanmard *et al.*, 2024; McIntosh & Vancov, 2011; O-Thong *et al.*, 2012; Salehian *et al.*, 2013).

Lastly, hydrothermal pretreatment involves hot-compressed water in a sealed pressure reactor, where water is the sole solvent (Niu *et al.*, 2022). This method has the advantage of increasing enzymes' access to lignocellulosic biomass by reducing its particle size and increasing its pore volume (Abo *et al.*, 2019). Interestingly, pre-soaking the biomass in NaOH before hydrothermal treatment resulted in even higher lignin degradation (O-Thong *et al.*, 2012; Rahmani *et al.*, 2023; Sun *et al.*, 2021).

The novelty of this work remains that the comparison of EFB delignification by bacterial, chemical and hydrothermal methods has never been explored in the context of providing a co-substrate for anaerobic digestion of POME. Therefore, this study compares the three methods of EFB delignification on biogas production in the anaerobic digestion of POME.

MATERIALS AND METHODS

The scope of the experiment covered EFB preparation and delignification, followed by combining POME, inoculum, and delignified EFB into different digesters. The delignification of the samples was analysed using the Chesson-Datta 1981 method (Ishola *et al.*, 2014). This method quantifies the hemicellulose, cellulose, and lignin levels within a lignocellulosic specimen. The remaining components are ash and extractive compounds.

POME's chemical oxygen demand (COD) was measured before and after digestion using the spectrophotometric closed reflux method by the Indonesian National Standard (SNI) 6989.2:2009 (Badan Standardisasi Nasional [BSN], 2009; Baird *et al.*, 2017).

The resulting gas samples were sent to a Shimadzu 8A gas chromatograph-thermal conductivity detector (GC-TCD) for methane content analysis. *Table 1* shows the operational conditions for the methane content analysis.

Materials

POME was collected from a palm oil mill in Serang, Indonesia, whereas EFB was obtained from Padang, Indonesia. A methane capture plant at the same mill in Padang was the source of inoculum/

starter. Inoculum is a dark, POME-based liquid which readily contains methanogenic microorganisms. It is commonly used to speed up the gas-producing bacteria's incubation in other anaerobic digestion plants.

This study employed bacterial, chemical, and hydrothermal delignification (HTP) methods. An agricultural-grade bacteria labeled Effective Microorganism 4 (EM4) from PT. Songgolangit Persada was used for the bacterial process, which contains 1.09 x 10^7 CFU/mL *Lactobacillus* sp. and 4.30 x 10^7 *Saccharomyces* sp. Analytical grade NaOH (99.9%) from PT Bumi Agung Kimia was used for the CDP. As for the hydrothermal method, the process used by O-Thong *et al.*, (2012) which pre-soaked the EFB in low-concentration NaOH, was selected. All materials except EM4 were stored in a cooler at 4°C.

TABLE 1. OPERATIONAL CONDITIONS FOR THE METHANE CONTENT ANALYSIS

Parameter	Notes
Apparatus	Shimadzu 8A
Detector temperature	100°C
Injector temperature	100°C
Column type	Shincarbon ST 50-80 MESH 2.0 m x 3.0 mm I.D
Column temperature	50°C hold for 7 min (rate 20°C /min) to 100°C hold for 10 min
Gas carrier	Argon
Carrier gas flow	25 mL/min

Empty Fruit Bunch (EFB) Preparation

Small EFB particles were prepared to provide a large contact surface for the microbes to process the lignocellulose. Therefore, the EFB was shredded to between 2 and 5 cm before oven-drying to a maximum water content of 10% (dry basis) (Dewi *et al.*, 2018).

Bacterial Delignification (BDP)

BDP was performed aerobically to supply oxygen to the bacteria and remove the resulting toxic gases. Three perforated plastic bins were prepared as containers for the process. Dried EFB samples of 300 g each were placed in perforated plastic bins measuring 17.5 cm in diameter and a depth of 10.0 cm. The plastic bins were then sealed with hollow fabric to allow breathing while retaining the heat and moisture (Dewi *et al.*, 2018).

Three EM4 solutions of 200 mL at concentrations of 1.96%, 3.85% and 5.66% v/v were prepared by diluting EM4 with distilled water designated as B-196, B-385 and B-566. The solutions were allowed to stand for around 12 hr. Following the study of Arbaain, each solution was sprayed evenly into the specimens and then kept for 14 days (Arbaain *et al.*, 2019). The specimens were then rinsed with distilled water through a filter cloth until the rinsing water was clear (Dewi *et al.*, 2018).

Chemical Delignification (CDP)

CDP was first performed by soaking 20 g of dried EFB in NaOH solutions with variable molar concentrations of 0.50, 1.25 and 2.00 M (C-050, C-125 and C-200). The specimens were then left to stand for 10 min at ambient temperature. Next, the mixture was incubated in an oven at 100°C for 60 min, with periodic shaking every 10 min. After the incubation, the specimens were centrifuged, washed with distilled water and vacuum-filtered (Tepsour *et al.*, 2019).

Hydrothermal Delignification (HTP)

HTP was performed by pre-soaking the shredded EFB in a low concentration of NaOH (0.1% eq. 0.0025 M) at ambient temperature for one day. The specimens were centrifuged, washed with distilled water and vacuum-filtered (Tepsour *et al.*, 2019). A total of 30 g samples were then treated hydrothermally using a 0.5 L autoclave, stirring at 100 rpm for 30 min in steam at 150°C, 180°C and 200°C (H-150, H-180 and H-200) (O-Thong *et al.*, 2012).

Drying and Pulverising

All EFB samples were oven-dried again to obtain a maximum water content of 10% (dry basis) before being milled using a high-speed pulverising machine to pass a 40-mesh screen (0.420 mm). The EFB samples were stored in airtight plastic bags at 4°C before use (Tepsour *et al.*, 2019).

Anaerobic Co-digestion

After delignification, the digesters were operated simultaneously for all methods. Erlenmeyer flasks of 500 mL were used as batch mesophilic digesters at an ambient temperature of around 27°C (*Figure 1*). The working digestion volume was set at 300 mL, and no substrates were added during the experiment. Referring to the study by Octiva, the digesters contained a mixture of POME/EFB at a ratio of 35:1 volume/mass.

Two control digesters were prepared: O-01 mono-digested POME and O-02 co-digested POME with untreated EFB. Nine other digesters were filled with POME and delignified EFB, designated as C-050, C-125, C-200, H-150, H-180, H-200, B-196,

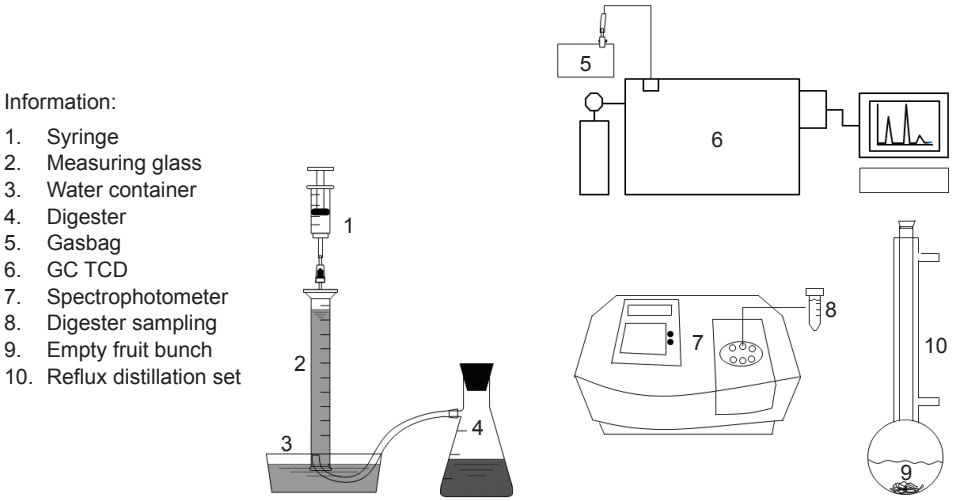

Figure 1. Experimental setup of anaerobic co-digestion.

B-385 and B-566. Inoculum comprised 15% v/v of the working volume (Octiva *et al.*, 2018). The biogas produced in the digester would fill the top of the measuring glass and consequently push down the water level in the measuring glass. The water displacement was recorded daily as the volume of the produced biogas. Every alternating day until day 21, the accumulated gas was suctioned from the measuring glass by a syringe and transferred to a sampling bag. The gas bags were then sent for analysis after 21 days.

The methane content was calculated using the Equation (1) and (2):

$$V_{CH4,i} = \%CH_{4,i}.V_{biogas,i} \quad (1)$$

$$sCH_{4,i} = \frac{V_{CH4,i}}{COD_{red,i}} \quad (2)$$

where, $V_{CH4,i}$ is the methane production of method i in mL, $\%CH_{4,i}$ the methane content of method i in %, $V_{biogas,i}$ is the biogas production of method i in mL, $sCH_{4,i}$ is the specific methane of method i in mL/g COD reduction, and finally $COD_{red,i}$ is the reduction of COD of method i in g COD reduction.

Pairwise Comparison

The delignification methods were evaluated using the pairwise comparison method (Fürnkranz & Hüllermeier, 2011). Comparison of the delignification methods was subjected to several objectives: Biogas production, methane content, preparation time, preparation requirements, and preparation hazards. Each objective was appraised and given a mark on the scale of 1-5. The details of the five-point scale are shown in *Table 2*.

TABLE 2. FIVE-POINT SCALE

Scale	Description
1	Very poor
2	Poor
3	Satisfactory
4	Good
5	Very good

RESULTS AND DISCUSSION

Lignocellulosic Analysis

All delignification methods showed similar visuals. EFB was initially light brown, rough, smelled of oil, and was irregularly sized. It transformed from rough to smooth after the final oven drying, resembling a sample of 90% ripeness from the study of Indriati *et al.*, 2020. The fine texture shall enable the anaerobic microbe to decompose the lignocellulose more easily (Indriati *et al.*, 2020). EFB's colour changed from light to dark brown, caused by intermediate products from lignin degradation (Poh *et al.*, 2010; Rodriguez-Yupanqui *et al.*, 2023). The processes also changed EFB's smell from oil to earthy, which might be caused by accelerated decomposition, conforming to Van Fan *et al.* (2018). Similar to the study of delignification also made the EFB easier to pulverise and sieve to 40 mesh (Dewi *et al.*, 2018).

Table 3 shows that delignification reduced the lignin in all samples between 5.23% (C-050) and 50.51% (B-566). Biological delignification showed noticeably higher lignin reduction than both other methods. The hemicellulose was also reduced across all samples between 5.57% (H-150) and 78.30% (C-200). CDP performance was far superior

in reducing hemi than other methods, followed by biological and hydrothermal. Cellulose increase is observable, where CDP is again the largest among all samples.

Bacterial delignification (BDP). BDP degraded the lignin between 27.00% and 51.00%, with maximum degradation in B-566 of 50.51%. The rising degradation trend was probably caused by higher EM4 concentrations having larger populations of *Actinomycetes* sp., thus producing more peroxidase extracellular enzymes. Peroxidase enzymes accelerate the bacteria in depolymerising and solubilising the lignin content (Dewi *et al*., 2018).

The results also show that hemicellulose degraded between 11.00% and 29.00%, with B-385 as the maximum at 29.18%. Hemicellulose's amorphous and branched structure makes it susceptible to EM4 microorganisms biological hydrolysis (Dewi *et al*., 2018; Van Fan *et al*., 2018). Decreases in lignin break hemicellulose bonds with cellulose, yielding an increment in hemicellulose.

It should be noted that B-385, not B-566, was the highest in hemicellulose reduction and cellulose increase. This trend was probably because the biological pretreatment used microorganisms (mainly fungi) to degrade lignin and hemicellulose, but the microorganisms left the cellulose intact (Xu *et al*., 2021). The whole composition of the lignocellulose was altered, keeping the cellulose from increasing at higher bacterial concentrations.

The cellulose increased between 45.00% and 65.00%, with B-385 as the maximum at 64.68%. The increase might be caused by trapped cellulose between lignin and hemicellulose before delignification. The losses in lignin and hemicellulose released and exposed the cellulose from the lignocellulosic barriers (Silva *et al*., 2021).

Chemical delignification (CDP). CDP reduced lignin between 5.00% and 27.00%, with the highest reduction in C-200 at 26.45%. The delignification was caused by NaOH breaking the bonds between lignin and carbohydrates. The Na^+ ions in lignin formed water-soluble phosphate salt compounds (Fengel & Wegener, 2011). The decrease in lignin relates to the concentration of NaOH, where higher NaOH concentration resulted in higher lignin degradation, conforming to the study by Wadchasit *et al*. (2020).

Hemicellulose also decreased between 41.00% and 79.00%, with C-200 again as the maximum at 78.30%. The decrease in hemicellulose conforms with the study of Fengel and Wegener (2011), which observed that higher NaOH concentrations also resulted in a higher reduction in hemicellulose. The higher reduction might be caused by hemicellulose's susceptibility to acids and base chemicals, high temperatures and solubility (Saha *et al*., 2018). Alkali pretreatment, such as NaOH, is generally known to partially break down lignin and hemicellulose (Kulshreshtha, 2022). Some studies have shown that hemicellulose can be solubilised as NaOH concentrations increase (Modenbach & Nokes, 2014). The degradation process involves the action of hemicellulases, a group of enzymes that specifically degrade hemicellulose. These enzymes, including exoglycosidases and endo-hemicellulases, target the hemicellulose structure, releasing monomeric units and oligosaccharides (Kerr & Goring, 2011).

Cellulose increased between 72.00% and 100.00%, with C-200 again the highest at 99.84%. The extensive increase in cellulose was caused by changes in composition after the loss of lignin and hemicellulose.

Hydrothermal Delignification (HTP). HTP combined with NaOH pre-soaking yielded moderate lignin reductions between 19.00% and 34.00%. However, it could be observed that the lignin reduction peaked at 180°C (H-180) at 33.96%. Syaftika and Matsumura study obtained a similar trend at temperatures of 180°C and beyond (Syaftika & Matsumura, 2018). Their study showed that at 180°C, a large part of lignin was destroyed, exposing the cellulose. Lignin remains unaltered or stable when the temperature increases to 200°C

TABLE 3. CHANGES IN THE LIGNOCELLULOSIC CONTENT BY DELIGNIFICATION

Lignocellulosic content	Initial composition (% w/w)	Final composition (% w/w)								
	Untreated	B-196	B-385	B-566	C-050	C-125	C-200	H-150	H-180	H-200
Lignin	17.58	12.67 (-27.93)	10.78 (-38.68)	8.70 (-50.51)	16.66 (-5.23)	14.36 (-18.32)	12.93 (-26.45)	14.11 (-19.74)	11.61 (-33.96)	13.33 (-24.18)
Hemicellulose	24.06	18.29 (-23.98)	17.04 (-29.18)	21.20 (-11.89)	14.07 (-41.52)	8.55 (-64.46)	5.22 (-78.30)	22.72 (-5.57)	21.75 (-9.60)	12.59 (-47.67)
Cellulose	36.50	53.20 (+45.75)	60.11 (+64.68)	59.16 (+62.08)	62.81 (+72.08)	71.52 (+95.95)	72.94 (+99.84)	56.27 (+54.16)	59.82 (+63.89)	65.19 (+78.60)

Note: ± indicates an increase or decrease in %

and 230°C, while cellulose degrades (Syaftika & Matsumura, 2018). Also, the stable lignin percentage at temperatures higher than 180°C is likely due to the re-polymerisation or condensation of lignin droplets, known to occur at higher temperatures (Donohoe *et al.*, 2008).

With hydrothermal processes, hemicellulose degrades more as temperatures increase, jumping to 47.67% at 200°C. The jump might be caused by hydronium ions formed in the presence of water at high temperatures, resulting in an acidic medium due to the autohydrolysis of EFB bonds. Also, acetic acid is generated from the thermal separation of acetyl groups from hemicellulose. The auto-ionisation of acetic acid due to the elevated temperature and pressure pushed these chemicals into catalysts, which encouraged further hemicellulose degradation (Syaftika & Matsumura, 2018).

The cellulose content rose steadily from 54.00%-79.00% across the experiment temperature despite the re-polymerisation of lignin. The cellulose increase of H-200 is still high at 78.60% because the high-temperature cellulose degradation only starts at 200°C (Syaftika & Matsumura, 2018).

Cumulative Biogas Production

Figure 2 shows the cumulative biogas production, measured every other day. EFB pretreatment was proven to be effective. Delignified co-digesting reactors started producing earlier than O-02, where untreated EFB was used.

O-01 started to produce biogas very early, compared to other digesters, which shows the ease of the bacteria to mono-digest than co-digest (Wellinger *et al.*, 2013). The substrate in O-01 readily provided the specific active site for methanogenic enzymes, requiring almost no time to adapt (Sołowski *et al.*, 2020). However, O-01 production slowed down after day 7 before entering the death phase on day 14. The organic nutrients of POME were depleted, resulting in the death of the anaerobic bacteria (Barragán *et al.*, 2016).

All co-digesting reactors showed that biogas production steadily grew after the bacteria acclimatised with EFB. Even after O-01 died, the co-digesting reactors showed no sign of slowing down, indicating that abundant nutrients could be converted (Chow *et al.*, 2020).

At the end of the experiment, C-200 produced the largest cumulative volume of biogas, although the initial production was slower than B-566 and O-01. C-200's initial production slope is also the highest, probably caused by the lowest lignin and highest cellulose. In the anaerobic process, cellulose and hemicellulose work together as substrates to accelerate methane production. Meanwhile, lignin is more difficult to digest and inhibits the rate of methane production.

On days 2-4 of production, B-566's production slope is the steepest, probably due to the lowest lignin composition (Patinvoh *et al.*, 2017). The high hemicellulose content of B-566 could cause the rapid initial production of biogas. Hemicellulose decomposes faster than cellulose due to its lower degree of polymerisation molecular weight (Brodeur *et al.*, 2011; Nwokolo *et al.*, 2020). However, C-200 ultimately produced higher yield and biogas production due to the high cellulose content (72.94 w/w% of cellulose) in C-200 compared to B-566 (59.16 w/w% of cellulose).

From the production slope on day 21, it is obvious that all co-digesting reactors were still active. Adding EFB as a co-substrate causes a balance of C/N and increases the acceptable organic content to produce more biogas (Chow *et al.*, 2020).

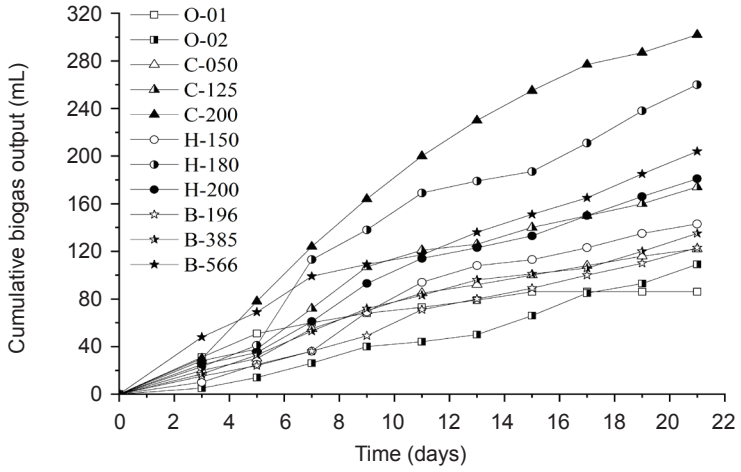

Figure 2. Cumulative biogas production (measured on alternating days).

Bacterial delignification (BDP). BDP increased the cumulative biogas production by 43.00%-137.00% compared to O-01. B-566 showed the most rapid initial output among the bacterial group reactors, most probably caused by its lowest lignin and highest hemicellulose. Hemicellulose decomposes faster than cellulose due to its low degree of polymerisation and low molecular weight (Brodeur *et al.*, 2011; Nwokolo *et al.*, 2020).

Chemical delignification (CDP). CDP produced 42.00% to 251.00% more biogas compared to O-01. The large spread in lignin and hemicellulose reduction probably caused the large spread of biogas production (42.00%-251.00%). C-200 had the least lignin among the chemical group digesters. Hence, it yielded the highest accumulated biogas and initial production slope.

Hydrothermal delignification (HTP). HTP combined with NaOH pre-soaking cumulatively produced 66.00%-202.00% more biogas than O-01. H-180 was observed to have the lowest lignin among hydrothermal group reactors. Hence, H-180 yielded the highest cumulative production and initial production slope, followed by H-200 and H-150.

Chemical Oxygen Demand (COD)

The COD value is used as a metric of the amount of oxygen needed in the chemical decomposition of organic matter. In anaerobic digestion, the COD value indicates the abundance of nutrients for the bacteria to produce biogas (Chow *et al.*, 2020). However, a high COD value is unwanted in the environment because it could kill aquatic life forms (Sumardiono *et al.*, 2013; Yusof *et al.*, 2023).

Figure 3 shows that the addition of EFB elevated the organic content, reflected in the higher initial COD values. O-01 had the lowest starting COD of 28,444 mg O_2/L, while the addition of untreated EFB in O-02 increased the initial COD to 40,927 mg O_2/L. With the addition of pretreated EFB, the chemical group averaged 41,000 mg O_2/L, the hydrothermal group averaged 38,000 mg O_2/L, and the bacterial group averaged 47,000 mg O_2/L. The average initial COD of the hydrothermal group is noticeably lower than O-02. This lower value was probably caused by the lower additional organic content in hemicellulose and cellulose (*Table 3*).

Adding EFB causes a jump in COD because EFB comprises various organic compounds. Delignification further increases the COD because the lignocellulosic material is broken down into simpler sugars and organic acids (Fitrah *et al.*, 2019; Muryanto *et al.*, 2022; Octiva *et al.*, 2018)

After 21 days, the COD of O-01 was the lowest. All samples showed reductions in COD, but the co-digesters' COD was still higher than the mono-digesting O-01, indicating high contents of nutrients remained for further biogas production (Chow *et al.*, 2020). Since O-01 died on day 14, its final COD value of 24,590 mg O_2/L could measure where other digesters would stop producing biogas. O-02's COD after 21 days of 33,183 mg O_2/L is the lowest among the co-digesters.

Methane Production

Methane contents of the produced biogas are an index of the biogas quality. *Figure 4* shows the methane percentages of each reactor, where the impact of EFB addition is obvious. C-200 produced biogas with the highest quality, with 47.61% biogas with a total methane volume of 143.77 mL and COD removal of 9.37%. Interestingly, O-02 produced

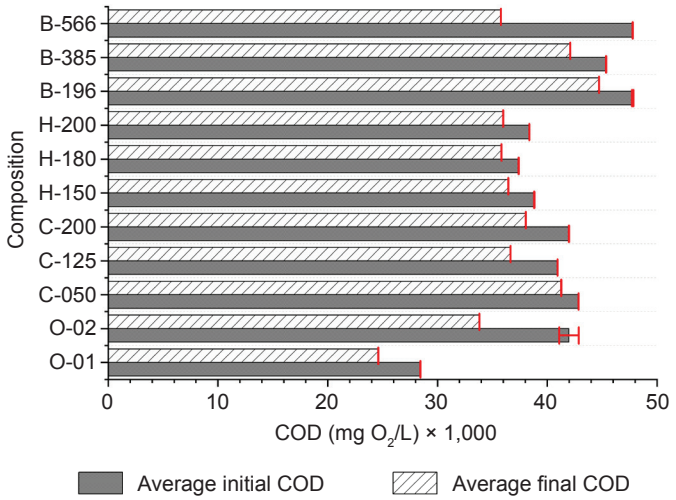

Figure 3. Chemical oxygen demand (COD) of samples before and after 21 days of anaerobic digestion.

the second-best quality of biogas. However, its production was the slowest among the co-digesting reactors due to the time required for the bacteria to process untreated EFB.

Mono-digesting O-01 produced the lowest methane compared to the co-digesting samples. C-200 produced biogas with the highest methane after 21 days, followed by H-180 (*Figure 5*). The lignocellulosic contents of both C-200 and H-180 most likely caused the spike in methane production.

H-180 yielded the highest specific methane production (SMP), defined as the ratio of produced methane over absolute COD reduction (*Figure 6*). Thus, H-180 potentially produce the most methane when the organic contents are fully consumed. The results in the methane production of hydrothermal group reactors closely resemble the study of O-Thong *et al.*, where they found the optimal hydrothermal temperature of 175°C. The spike of SMP in H-180 was most probably caused by the conversion of lignin into acetic acid under alkaline conditions, which is beneficial for methanogenic microorganisms (Kaparaju & Felby, 2010; O-Thong *et al.*, 2012).

Production Scale-up Scenario

A typical covered lagoon for anaerobic digestion can measure 150 m by 50 m, with a depth of 7 m. If the delignified EFB ratio is kept the same as in the experiment, around 1.91 t of delignified EFB will need to be prepared. This quantity of delignified EFB would require a well-planned infrastructure.

After EFB is cut into size, BDP can be performed in a covered warehouse, which would take 14 days to complete before it is washed and ground to size. On the other hand, delignification methods by chemical and hydrothermal methods can be completed within a much shorter time of 60 and 30 min, respectively.

CDP would need containers to perform the NaOH soaking and washing. A large container of around 5 m^3 can perform the soaking, and the delignification can be performed in batches until the required volume is reached. It should be noted that the spent NaOH cannot be freely disposed of after use since it is an environmental hazard; thus, it requires a recycling process.

HTP will require a small processing plant where the NaOH pre-soaking could occur and a boiler as a heat source for the hydrothermal reactor. All three methods require a grinding facility to get the delignified EFB to size.

Pairwise Comparison

A pairwise comparison arranged the level of importance of each selection objective (*Table 4*). A pairwise comparison chart was constructed by comparing each of the objectives with one another. The scoring marks for the comparison process were 0.0, 0.5 and 1.0 points, indicating the less, equal, and most favoured, respectively.

The obvious preferred objectives are biogas quality (MC) and volume (BP), with weighted scores of 0.37 and 0.32, respectively. Safety (PH) is also considered high and scored 0.21, followed by preparation time (PT) and infrastructure (PI). *Table 5* lists the objectives arranged in their respective order of importance (score) and their respective description.

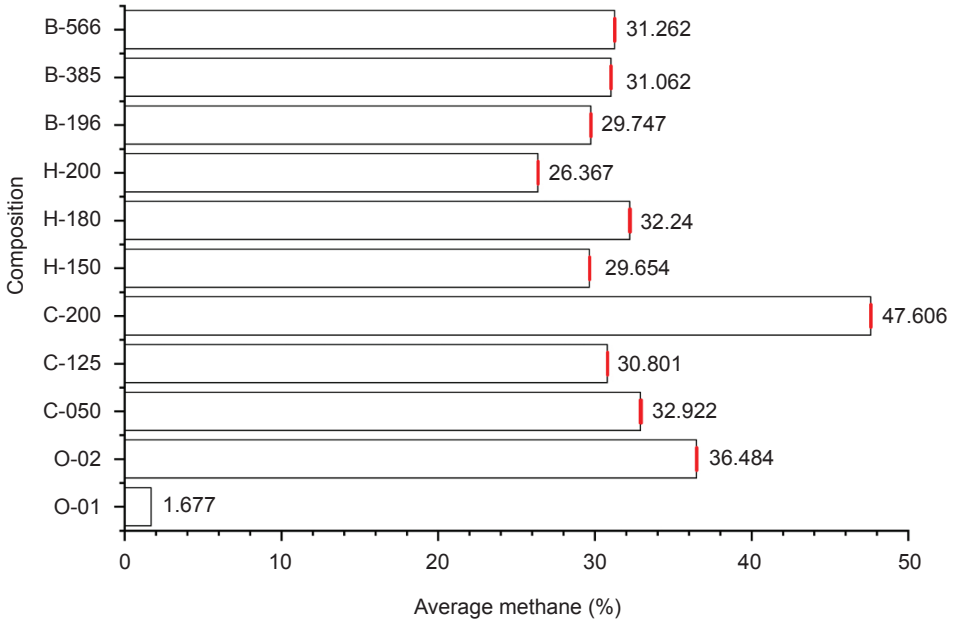

Figure 4. Methane content.

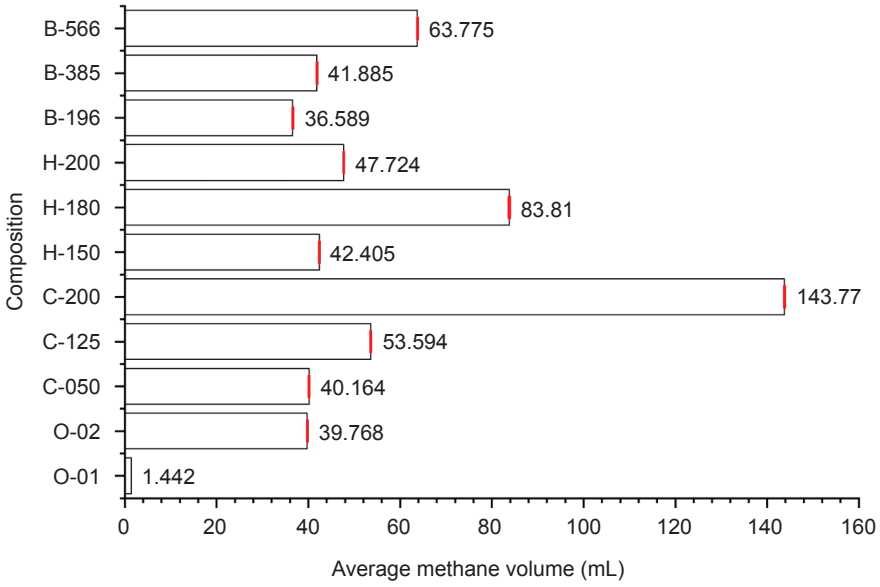

Figure 5. Methane production.

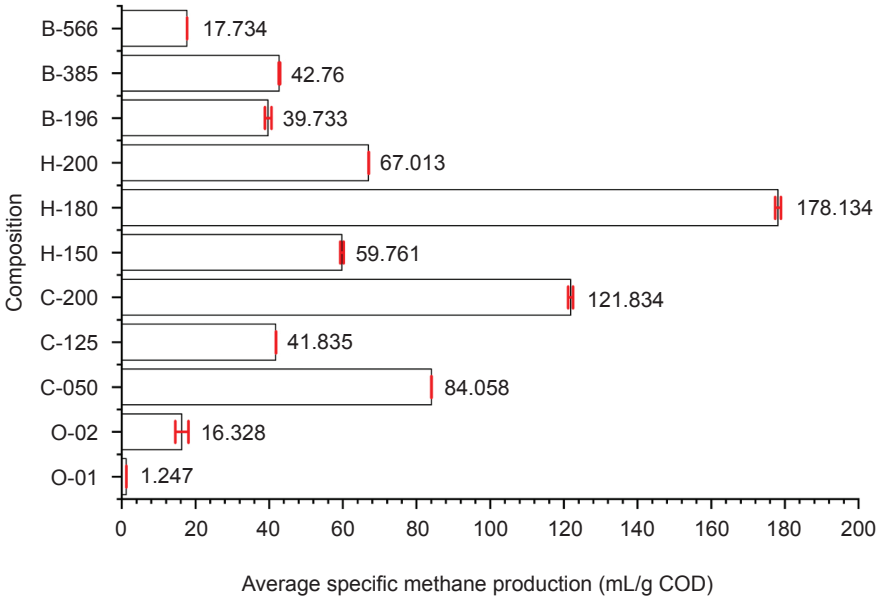

Figure 6. Specific methane production.

The delignification methods were ranked with the weight objective method. The calculation of weighting and rating is shown in *Table 6*. Each option was appraised and marked on a scale of 1-5. The score was weighted through the pairwise comparison chart from *Table 4* and used to rank each method. The high methane contents of the produced biogas ranked the chemical group as the highest, with 5 points for methane content (MC). Due to the high volume of chemicals required for the chemical process, it ranked the lowest in the hazard objective (PH). On the other hand, BDP was considered the safest to operate since it is mainly a biological process. However, due to its long preparation time of 14 days (PT), biological delignification ranked the lowest, with HTP the highest. If the pre-soaking is performed in batches, it only takes 30 min to prepare. Due to the complex required investment and maintenance, HTP is ranked lowest in the infrastructure objective (PI).

The pairwise comparison shows that CDP ranked the highest (3.64) due to the biogas produced and its quality. Also, it requires simple infrastructure. However, its productional hazards rendered it almost equally preferred to hydrothermal (3.63).

TABLE 4. PAIRWISE COMPARISON CHART OF VARIOUS OBJECTIVES

Objective	BP	MC	PT	PI	PH	Score	Weight
Biogas production (BP)	-	0.50	1.00	0.50	1.00	3.00	0.32
Methane content (MC)	0.50	-	1.00	1.00	1.00	3.50	0.37
Preparation time (PT)	0.00	0.00	-	0.50	0.00	0.50	0.05
Preparation infrastructure (PI)	0.00	0.00	0.50	-	0.00	0.50	0.05
Preparation hazards (PH)	0.00	0.00	1.00	1.00	-	2.00	0.21

TABLE 5. OBJECTIVES ARRANGED BY THE ORDER OF IMPORTANCE

Rank	Objective	Description
1	MC	High methane content is desired for the quality of biogas as fuel.
2	BP	High biogas production volume is much desired because it is a potential fuel source for households and small industries.
3	PH	The hazardous processes carry an inherent health and safety risk to the processing personnel and the environment.
4	PT	The preparation time of the co-substrate is important in the continuous production of biogas. However, the co-substrate can be prepared inbatch for multiple production.
4	PI	The required infrastructure to process the co-substrate is key to the efficiency of the selected delignification method.

Note: MC - methane content; BP - biogas production; PH - preparation hazards; PT - preparation time; PI - preparation infrastructure.

TABLE 6. PAIRWISE SCORING OF THE DELIGNIFICATION METHOD SELECTION

Objectives	Weight	Bacterial (BDP)		Chemical (CDP)		Hydrothermal (HTP)	
		Score	Weighted score	Score	Weighted score	Score	Weighted score
MC	0.37	2.00	0.74	5.00	1.85	4.00	1.48
BP	0.32	2.00	0.64	4.00	1.28	3.00	0.96
PH	0.21	5.00	1.05	1.00	0.21	4.00	0.84
PT	0.05	1.00	0.05	3.00	0.15	5.00	0.25
PI	0.05	5.00	0.25	3.00	0.15	2.00	0.10
Score		**2.73**		**3.64**		**3.63**	
Rank		**3**		**1**		**2**	

Note: MC - methane content; BP - biogas production; PH - preparation hazards; PT - preparation time; PI - preparation infrastructure.

CONCLUSION

There is a close correlation between the EFB's lignocellulosic composition and biogas/methane production. The maximum delignification of 50.51% was reached with bacterial B-566. However, chemical C-200 showed the highest cellulose increase of 99.84% and a hemicellulose reduction of 78.30%. Consequently, after 21 days, C-200 produced the largest volume of biogas and methane (302.0 and 153.8 mL, respectively). A pairwise comparison of the three delignification methods has concluded that CDP was the most preferred method, followed very closely by hydrothermal. CDP scored the highest due to its biogas production and quality. HTP was second highest because of its efficiency, safety, and modest biogas production and quality.

ACKNOWLEDGEMENT

The highest appreciation goes to the New Energy and Industrial Technology Development Organization (NEDO), Japan, for their financial support through the cooperative agreement between NEDO and Badan Riset dan Inovasi Nasional Republik Indonesia (BRIN), number 30/III.3/HK/2023.

REFERENCES

Abo, B. O., Gao, M., Wang, Y., Wu, C., Ma, H., & Wang, Q. (2019). Lignocellulosic biomass for bioethanol: An overview on pretreatment, hydrolysis and fermentation processes. *Reviews on Environmental Health*, *34*(1), 57–68. https://doi.org/10.1515/reveh-2018-0054

Arbaain, E. N. N., Bahrin, E. K., Ibrahim, M. F., Ando, Y., & Abd-Aziz, S. (2019). Biological pretreatment of oil palm empty fruit bunch by *Schizophyllum commune* ENN1 without washing and nutrient addition. *Processes*, *7*(7), 402. https://doi.org/10.3390/pr7070402

Aziz, M. M. A., Kassim, K. A., ElSergany, M., Anuar, S., Jorat, M. E., Yaacob, H., Ahsan, A., Imteaz, M. A., & Arifuzzaman, N. (2020). Recent advances on palm oil mill effluent (POME) pretreatment and anaerobic reactor for sustainable biogas production. *Renewable and Sustainable Energy Reviews*, *119*, 109603. https://doi.org/10.1016/j.rser.2019.109603

Badan Standardisasi Nasional (BSN). (2009). *Air dan air limbah – Bagian 2: Cara uji Kebutuhan Oksigen Kimiawi (Chemical Oxygen Demand/COD) dengan refluks tertutup secara spektrofotometri* (SNI 06-6989.2-2009) [Water and wastewater – Part 2: Test method for Chemical Oxygen Demand (COD) with closed reflux spectrophotometry (SNI 06-6989.2-2009)].

Baird, R. B., Eaton, A. D., & Rice, E. W. (Eds.). (2017). *Standard methods for the examination of water and wastewater* (23rd ed.). American Public Health Association.

Barragán, L. A. P., Figueroa, J. J. B., Durán, L. V. R., González, C. N. A., & Hennigs, C. (2016). Fermentative production methods. In P. Poltronieri & O. F. D'Urso (Eds.), *Biotransformation of agricultural waste by-products for food, feed, fibre, fuel and economic development* (pp. 189–217). Springer. https://doi.org/10.1016/b978-0-12-803622-8.00007-0

Brodeur, G., Yau, E., Badal, K., Collier, J., Ramachandran, K. B., & Ramakrishnan, S. (2011). Chemical and physicochemical pretreatment of lignocellulosic biomass: A review. *Enzyme Research*, *2011*, 1–17. https://doi.org/10.4061/2011/787532

Chow, W., Chong, S., Lim, J., Chan, Y., Chong, M., Tiong, T., Chin, J., & Pan, G. (2020). Anaerobic co-digestion of wastewater sludge: A review of potential co-substrates and operating factors for improved methane yield. *Processes*, *8*(1), 39. https://doi.org/10.3390/pr8010039

Dewi, I. A., Ihwah, A., & Wijana, S. (2018). Optimization on pulp delignification from Nypa palm (*Nypa fruticans*) petioles fibre of chemical and microbiological methods. *IOP Conference Series Earth and Environmental Science*, *187*, 012019. https://doi.org/10.1088/1755-1315/187/1/012019

Direktorat Jenderal Perkebun Kementerian Pertanian Republik Indonesia. (2021). *Statistik Perkebunan Unggulan Nasional 2019-2021* [Statistical of national leading estate crops commodity 2019-2021].

Dominic, D., & Baidurah, S. (2022). Recent developments in biological processing technology for palm oil mill effluent treatment – A review. *Biology*, *11*(4), 525. https://doi.org/10.3390/biology11040525

Donohoe, B. S., Decker, S. R., Tucker, M. P., Himmel, M. E., & Vinzant, T. B. (2008). Visualizing lignin coalescence and migration through maize cell walls following thermochemical pretreatment. *Biotechnology and Bioengineering*, *101*(5), 913–925. https://doi.org/10.1002/bit.21959

Fengel, D., & Wegener, G. (2011). *Wood: Chemistry, ultrastructure, reactions*. Walter de Gruyter. (Original work published 1984).

Fitrah, R., Ahmad, A., & Amri, I. (2019). Enhanced biogas production by mesophilic and thermophilic anaerobic co-digestion of palm oil mill effluent with empty fruit bunches in expanded granular sludge bed reactor. *IOP Conference Series Materials Science and Engineering*, *550*(1), 012029. https://doi.org/10.1088/1757-899x/550/1/012029

Fürnkranz, J., & Hüllermeier, E. (2003). Pairwise Preference Learning and Ranking. In N. Lavrač, D. Gamberger, H. Blockeel, & L. Todorovski (Eds.), *Machine learning: ECML 2003* [Lecture Notes in Computer Science, 2837, (pp. 145-156)]. Springer. https://doi.org/10.1007/978-3-540-39857-8_15

Hambali, E., & Rivai, M. (2017). The potential of palm oil waste biomass in Indonesia in 2020 and 2030. *IOP Conference Series Earth and Environmental Science*, *65*, 012050. https://doi.org/10.1088/1755-1315/65/1/012050

Indriati, L., Elyani, N., & Dina, S. F. (2020). Empty fruit bunches, potential fiber source

for Indonesian pulp and paper industry. *IOP Conference Series Materials Science and Engineering*, *980*(1), 012045. https://doi.org/10.1088/1757-899x/980/1/012045

Ishola, M. M., Isroi, N., & Taherzadeh, M. J. (2014). Effect of fungal and phosphoric acid pretreatment on ethanol production from oil palm empty fruit bunches (OPEFB). *Bioresource Technology*, *165*, 9–12. https://doi.org/10.1016/j.biortech.2014.02.053

Javanmard, A., Daud, W. M. a. W., Patah, M. F. A., Zuki, F. M., Ai, S. P., Azman, D. Q., & Chen, W. (2024). Breaking barriers for a green future: A comprehensive study on pre-treatment techniques for empty fruit bunches in the bio-based economy. *Process Safety and Environmental Protection*, *182*, 535–558. https://doi.org/10.1016/j.psep.2023.11.053

Kaparaju, P., & Felby, C. (2010). Characterization of lignin during oxidative and hydrothermal pre-treatment processes of wheat straw and corn stover. *Bioresource Technology*, *101*(9), 3175–3181. https://doi.org/10.1016/j.biortech.2009.12.008

Kerr, A. J., & Goring, D. A. I. (1975). The role of hemicellulose in the delignification of wood. *Canadian Journal of Chemistry*, *53*(6), 952–959. https://doi.org/10.1139/v75-134

Kulshreshtha, A. (2022). Sustainable energy generation from municipal solid waste. In C. M. Hussain, S. Singh, & L. Goswomi (Eds.), *Waste-to-energy approaches towards zero waste–Interdisciplinary methods of controlling waste* (pp. 315–342). Elsevier.

Li, W., Khalid, H., Zhu, Z., Zhang, R., Liu, G., Chen, C., & Thorin, E. (2018). Methane production through anaerobic digestion: Participation and digestion characteristics of cellulose, hemicellulose and lignin. *Applied Energy*, *226*, 1219–1228. https://doi.org/10.1016/j.apenergy.2018.05.055

Liew, Z. K., Chan, Y. J., Ho, Z. T., Yip, Y. H., Teng, M. C., Bin, A. I. T. a. A., Chong, S., Show, P. L., & Chew, C. L. (2021). Biogas production enhancement by co-digestion of empty fruit bunch (EFB) with palm oil mill effluent (POME): Performance and kinetic evaluation. *Renewable Energy*, *179*, 766–777. https://doi.org/10.1016/j.renene.2021.07.073

Malaysian Palm Oil Board (MPOB). (2020). *Overview of the Malaysian oil palm industry*. https://bepi.mpob.gov.my/images/overview/Overview_of_Industry_2020.pdf

McIntosh, S., & Vancov, T. (2011). Optimisation of dilute alkaline pretreatment for enzymatic saccharification of wheat straw. *Biomass and Bioenergy*, *35*(7), 3094–3103. https://doi.org/10.1016/j.biombioe.2011.04.018

Modenbach, A. A., & Nokes, S. E. (2014). Effects of sodium hydroxide pretreatment on structural components of biomass. *Biosystems and Agricultural Engineering Faculty Publications*. 84. https://uknowledge.uky.edu/bae_facpub/84

Muryanto, M., Amelia, F., Izzah, M. N., Maryana, R., Triwahyuni, E., Bardant, T. B., Filailla, E., Sudiyani, Y., & Gozan, M. (2022). Delignification of empty fruit bunch using deep eutectic solvent for biobased-chemical production. *IOP Conference Series Earth and Environmental Science*, *1108*(1), 012013. https://doi.org/10.1088/1755-1315/1108/1/012013

Niu, M., Sun, R., Ding, K., Gu, H., Cui, X., Wang, L., & Hu, J. (2022). Synergistic effect on thermal behavior and product characteristics during co-pyrolysis of biomass and waste tire: Influence of biomass species and waste blending ratios. *Energy*, *240*, 122808. https://doi.org/10.1016/j.energy.2021.122808

Nwokolo, N., Mukumba, P., Obileke, K., & Enebe, M. (2020). Waste to energy: A focus on the impact of substrate type in biogas production. *Processes*, *8*(10), 1224. https://doi.org/10.3390/pr8101224

Octiva, C. S., Irvan, N., Sarah, M., Trisakti, B., & Daimon, H. (2018). Production of biogas from co-digestion of empty fruit bunches (EFB) with palm oil mill effluent (POME): Effect of mixing ratio. *RASAYAN Journal of Chemistry*, *11*(2), 791–797. https://doi.org/10.31788/rjc.2018.1123022

O-Thong, S., Boe, K., & Angelidaki, I. (2012). Thermophilic anaerobic co-digestion of oil palm empty fruit bunches with palm oil mill effluent for efficient biogas production. *Applied Energy*, *93*, 648–654. https://doi.org/10.1016/j.apenergy.2011.12.092

Patinvoh, R. J., Osadolor, O. A., Chandolias, K., Horváth, I. S., & Taherzadeh, M. J. (2017). Innovative pretreatment strategies for biogas production. *Bioresource Technology*, *224*, 13–24. https://doi.org/10.1016/j.biortech.2016.11.083

Poh, P. E., Yong, W., & Chong, M. F. (2010). Palm oil mill effluent (POME) characteristic in high crop season and the applicability of high-rate

anaerobic bioreactors for the treatment of POME. *Industrial & Engineering Chemistry Research*, *49*(22), 11732–11740. https://doi.org/10.1021/ie101486w

Rahmani, A. M., Tyagi, V. K., Gunjyal, N., Kazmi, A., Ojha, C. S. P., & Moustakas, K. (2023). Hydrothermal and thermal-alkali pretreatments of wheat straw: Co-digestion, substrate solubilization, biogas yield and kinetic study. *Environmental Research*, *216*, 114436. https://doi.org/10.1016/j.envres.2022.114436

Rodriguez-Yupanqui, M., De La Cruz-Noriega, M., Quiñones, C., Otiniano, N. M., Quezada-Alvarez, M. A., Rojas-Villacorta, W., Vergara-Medina, G. A., León-Vargas, F. R., Solís-Muñoz, H., & Rojas-Flores, S. (2023). Lignin-degrading bacteria in paper mill sludge. *Microorganisms*, *11*(5), 1168. https://doi.org/10.3390/microorganisms11051168

Saha, K., Dwibedi, P., Ghosh, A., Sikder, J., Chakraborty, S., & Curcio, S. (2018). Extraction of lignin, structural characterization and bioconversion of sugarcane bagasse after ionic liquid assisted pretreatment. *3 Biotech*, *8*(8), 374. https://doi.org/10.1007/s13205-018-1399-4

Salehian, P., Karimi, K., Zilouei, H., & Jeihanipour, A. (2013). Improvement of biogas production from pine wood by alkali pretreatment. *Fuel*, *106*, 484–489. https://doi.org/10.1016/j.fuel.2012.12.092

Silva, J. P., Ticona, A. R. P., Hamann, P. R. V., Quirino, B. F., & Noronha, E. F. (2021). Deconstruction of lignin: From enzymes to microorganisms. *Molecules*, *26*(8), 2299. https://doi.org/10.3390/molecules26082299

Sołowski, G., Konkol, I., & Cenian, A. (2020). Production of hydrogen and methane from lignocellulose waste by fermentation. A review of chemical pretreatment for enhancing the efficiency of the digestion process. *Journal of Cleaner Production*, *267*, 121721. https://doi.org/10.1016/j.jclepro.2020.121721

Suksong, W., Tukanghan, W., Promnuan, K., Kongjan, P., Reungsang, A., Insam, H., & O-Thong, S. (2019). Biogas production from palm oil mill effluent and empty fruit bunches by coupled liquid and solid-state anaerobic digestion. *Bioresource Technology*, *296*, 122304. https://doi.org/10.1016/j.biortech.2019.122304

Sumardiono, S., Syaichurrozi, I., Budiyono, & Sasongko, S. B. (2013). The effect of COD/N ratios and pH control to biogas production from vinasse. *International Journal of Biochemistry Research & Review*, *3*(4), 401–413. https://doi.org/10.9734/ijbcrr/2013/3797

Sun, S., Sun, D., Li, H., Cao, X., Sun, S., & Wen, J. (2021). Revealing the topochemical and structural changes of poplar lignin during a two-step hydrothermal pretreatment combined with alkali extraction. *Industrial Crops and Products*, *168*, 113588. https://doi.org/10.1016/j.indcrop.2021.113588

Syaftika, N., & Matsumura, Y. (2018). Comparative study of hydrothermal pretreatment for rice straw and its corresponding mixture of cellulose, xylan, and lignin. *Bioresource Technology*, *255*, 1–6. https://doi.org/10.1016/j.biortech.2018.01.085

Tepsour, M., Usmanbaha, N., Rattanaya, T., Jariyaboon, R., O-Thong, S., Prasertsan, P., & Kongjan, P. (2019). Biogas production from oil palm empty fruit bunches and palm oil decanter cake using solid-state anaerobic co-digestion. *Energies*, *12*(22), 4368. https://doi.org/10.3390/en12224368

Van Fan, Y., Lee, C. T., Klemeš, J. J., Chua, L. S., Sarmidi, M. R., & Leow, C. W. (2017). Evaluation of Effective Microorganisms on home scale organic waste composting. *Journal of Environmental Management*, *216*, 41–48. https://doi.org/10.1016/j.jenvman.2017.04.019

Wadchasit, P., Siripattana, C., & Nuithitikul, K. (2020). The effect of pretreatment methods for improved biogas production from oil-palm empty fruit bunches (EFB): Experimental and model. *IOP Conference Series Earth and Environmental Science*, *463*(1), 012126. https://doi.org/10.1088/1755-1315/463/1/012126

Wellinger, A., Murphy, J., & Baxter, D. (2013). *The biogas handbook: Science, production and applications*. Elsevier Inc.

Xu, C., Su, X., Wang, J., Zhang, F., Shen, G., Yuan, Y., Yan, L., Tang, H., Song, F., & Wang, W. (2021). Characteristics and functional bacteria in a microbial consortium for rice straw lignin-degrading. *Bioresource Technology*, *331*, 125066. https://doi.org/10.1016/j.biortech.2021.125066

Yiin, C. L., Ho, S., Yusup, S., Quitain, A. T., Chan, Y. H., Loy, A. C. M., & Gwee, Y. L. (2019). Recovery of cellulose fibers from oil palm empty fruit bunch for pulp and paper using green delignification approach. *Bioresource Technology*, *290*, 121797. https://doi.org/10.1016/j.biortech.2019.121797

Yuan, X., Cao, Y., Li, J., Wen, B., Zhu, W., Wang, X., & Cui, Z. (2012). Effect of pretreatment by a microbial consortium on methane production of waste paper and cardboard. *Bioresource Technology*, *118*, 281–288. https://doi.org/10.1016/j.biortech.2012.05.058

Yusof, M. A. B. M., Chan, Y. J., Chong, C. H., & Chew, C. L. (2023). Effects of operational processes and equipment in palm oil mills on characteristics of raw palm oil mill effluent (POME): A comparative study of four mills. *Cleaner Waste Systems*, *5*, 100101. https://doi.org/10.1016/j.clwas.2023.100101

Journal of Oil Palm Research Vol. 37 (3) September 2025 p. 506-518
DOI: https://doi.org/10.21894/jopr.2024.0030

EVALUATING THE EFFECT OF LOW AND HIGH TEMPERATURE MODE OF SUBCRITICAL WATER PRE-TREATED EMPTY FRUIT BUNCHES ON CO-DIGESTION PERFORMANCE AND KINETIC STUDY FOR METHANE PRODUCTION

ADILA FAZLIYANA AILI HAMZAH[1]; MUHAMMAD HAZWAN HAMZAH[1,2]*; KHAIRUDIN NURULHUDA[1,2]; HASFALINA CHE MAN[1,2]; MUHAMMAD HEIKAL ISMAIL[3] and PAU LOKE SHOW[4,5,6,7]

ABSTRACT

Anaerobic digestion of oil palm empty fruit bunches (EFB) is considered an effective method for non-renewable energy substitution through biogas production. However, lignocellulosic recalcitrance structure of EFB is one of the main difficulties in achieving high biogas production for anaerobic co-digestion with palm oil mill effluents (POME). In this study, EFB was pre-treated with subcritical water (SCW) at low (120°C) and high (180°C) temperatures for 10-30 min to enhance biogas production. The characteristics of EFB after SCW pre-treatment were evaluated to identify changes in physicochemical characteristics. The combination pre-treatment of 180°C for 10 min with 546.18 mL g^{-1} volatile solid (VS) biogas yield and 421.41 mL CH_4 g^{-1} VS methane yield revealed the highest biogas production. Meanwhile, co-digestion of SCW pre-treated EFB with POME led to a removal of more than 66% VS. The sugars released were analysed in liquid fraction of SCW pre-treated EFB where glucose, xylose, cellobiose, mannose and galactose were detected. Notably, kinetic study of biogas production of pre-treated EFB using modified Gompertz model revealed that pre-treatment improved the lag phase, and the highest biogas production rate was observed at 19.80 mL g^{-1} VS. day. In conclusion, co-digestion of EFB with POME for methane production can be improved with the use of SCW pre-treatment.

Keywords: biogas, co-digestion, methane, pre-treatment, subcritical water.

Received: 7 October 2023**; Accepted:** 19 February 2024**; Published online:** 8 May 2024.

INTRODUCTION

The world's oil palm production is predicted to reach 240 million tonnes by 2050 as the market for palm oil products expands (Sulaiman *et al*., 2022). Malaysia's palm oil sector can currently generate 115.86 million tonnes of fresh fruit bunches (FFB), making it the second-largest producer of palm

[1] Department of Biological and Agricultural Engineering, Faculty of Engineering, Universiti Putra Malaysia, 43400 UPM Serdang, Selangor, Malaysia.

[2] Smart Farming Technology Research Centre, Faculty of Engineering, Universiti Putra Malaysia, 43400 UPM Serdang, Selangor, Malaysia.

[3] Department of Environment, Faculty of Forestry and Environment, Universiti Putra Malaysia, 43400 UPM Serdang, Selangor, Malaysia.

[4] Department of Chemical and Petroleum Engineering, Khalifa University, P.O. Box 127788, Abu Dhabi, United Arab Emirates.

[5] Zhejiang Provincial Key Laboratory for Subtropical Water Environment and Marine Biological Resources Protection, Wenzhou University, Wenzhou 325035, China.

[6] Department of Chemical and Environmental Engineering, Faculty of Science and Engineering, University of Nottingham Malaysia, Jalan Broga, 43500 Semenyih, Selangor, Malaysia.

[7] Department of Sustainable Engineering, Saveetha School of Engineering, SIMATS, Chennai 602105, India.

* *Corresponding author e-mail: hazwanhamzah@upm.edu.my*

oil in the world (Awoh *et al*., 2023). However, the process also produces a significant amount of waste. Following the process of extracting crude palm oil (CPO) from FFB, palm oil empty fruit bunches (EFB) are subsequently produced. For every tonne of palm oil produced, typically between 23% and 25% or 1.07 t of EFB, are created (Dolah *et al*., 2021). EFB can be used as a raw material for biogas production. Meanwhile, POME, which is also produced from the same stream as EFB, contains numerous organic matter, solids that are suspended in the water, different nitrogenous compounds, and a mixture of smaller organic and mineral parts that can contribute to water pollution (Tan & Lim, 2019). Due to the rapid expansion of the palm oil industry, a large volume of oil palm waste is produced, thereby raising environmental concerns. These events highlight the need for effective management to ensure environmental sustainability and agricultural productivity (Liew *et al*., 2021). To sustain the oil palm industry, waste treatment is one of the top priorities of palm oil companies. An interesting approach is to use biotechnological methods to transform this waste into an energy resource, which may bring additional financial benefits to the industry (Mahmod *et al*., 2021).

Palm oil wastes such as EFB, decanter cake, and trunk have a high potential for biomethane production. However, due to the high C/N ratio, the use of oil palm wastes as a single substrate in mono digestion often results in poor digester performance (Park *et al*., 2021). The high carbon content in these wastes led to poor buffering capacity and excessive volatile fatty acid production in the biogas digester. Nevertheless, co-digestion with nitrogenous feedstock would eliminate the problem (Hamzah *et al*., 2024). Co-digestion of EFB with another waste stream from palm oil production is considered a viable waste management option in palm oil mills. Liew *et al*. (2021) found that co-digestion of EFB and POME produced relatively high methane-rich biogas, with a performance that was 2.36 times better than using each of them as a single feedstock. Despite anaerobic co-digestion, biogas yield is not satisfying due to the intricate nature of the composition. The application of pre-treatment before biogas production breaks down the lignocellulosic bond, subsequently making it accessible for hydrolysis (Aili Hamzah *et al*., 2023).

Due to the resistant structure of the EFB, the rate of anaerobic digestion of the EFB is constrained at the hydrolysis stage. Consequently, biogas production can be severely impacted by the inability of lignocellulosic components like lignin and cellulose to degrade into simple sugars (Saritpongteeraka *et al*., 2022). The disruption in the morphological structure of lignocellulosic substrates through pre-treatment has gained remarkable attention as a viable strategy for biogas enhancement (Ahmad *et al*., 2018). Several studies have demonstrated the effectiveness of biological, chemical, and hydrothermal pre-treatment of palm oil solid wastes in enhancing the yield of methane-rich biogas (Mamimin *et al*., 2021; Saritpongteeraka *et al*., 2022; Sitthikitpanya *et al*., 2018). SCW pre-treatment is widely recognised as a sustainable and greener technology that facilitates structure-breaking and the accessibility of substrates. Moreover, the pre-treatment does not need recycling of acid and is environmentally friendly (Chen *et al*., 2021). Water in the SCW region penetrates the lignocellulosic structure and subsequently hydrates cellulose, dissolving hemicellulose and eliminating lignin partially (Sarker *et al*., 2021). Thus, SCW pre-treatment can facilitate enzymatic hydrolysis and digestion of lignocellulosic biomass, leading to fast and significant biogas production.

To date, limited studies are available detailing the physiochemical properties of EFB after SCW pre-treatment. Most previous studies focused on the impacts of the SCW pre-treatment on biogas production. Tian *et al*. (2020) conducted a pre-treatment for wheat straw and sludge at a temperature of 175°C. Resultantly, the co-digestion process of the pre-treatment improved biogas production, thus promoting 52.0% of biogas production as compared to untreated samples. At temperatures of 120°C and 180°C, Xiang *et al*. (2021) observed an increased production of biogas from the pre-treated rice straw by 38.0% and 14.0%, respectively. Lignin in the solid fraction was also reported to increase as time increased due to recombination between lignin and hemicellulose (Ahmad *et al*., 2018). Pre-treatment at 120°C resulted in a 4.9% reduction of total solids (TS), which was further reduced to 6.4% upon increasing the pre-treatment time (Dasgupta & Chandel, 2019). Furthermore, Aili Hamzah *et al*. (2023) suggested that energy can be saved by less reaction time than by longer reaction time.

However, the effectiveness of the pre-treatment regarding the unique characteristic of SCW pre-treatment is based on the process parameters itself as a function of reaction temperature and time. The sugar production increased with temperature (170°C-210°C), and temperatures below 120°C were not high enough to cause differential breakdown of hemicellulose and cellulose into simple sugar (Saritpongteeraka *et al*., 2022). On the other hand, methanogenesis inhibitors known as furan derivatives were formed at pre-treatment temperatures higher than 200°C (Lee & Park, 2020). It was observed that a 6.9% reduction in methane yield after pre-treatment at 175°C (Tian *et al*., 2020). At 180°C, Wang *et al*. (2018) reported that biogas produced from pre-treated rice straw improved 3.0% compared to untreated rice straw.

While temperature 210°C presented a 30.0% reduction with a more extended lag period. The optimum biogas yield was obtained at low severity of 2.65. The SCW on cocoa pod waste observed that temperature influences the lignin solubilisation compared to reaction time (Antwi *et al.*, 2019). Pre-treatment temperature up to 120°C resulted in enhanced methane content as pre-treatment time was increased. While, higher SCW temperature has resulted in more significant degradation and soluble sugars produced from hemicellulose solubilisation (Dasgupta & Chandel, 2019). SCW is aimed to improve biogas production but at the same time balance the fermentable sugar yield with lower operational cost. The SCW pre-treatment parameters, temperature and reaction time are the three main factors that influence pre-treatment efficiency and subsequently, anaerobic digestion.

This study aims (1) to investigate the effect of SCW pre-treatment at low (120°C) and high-temperature (180°C) modes on the physicochemical properties of EFB, (2) to determine the sugar production after SCW water pre-treatment, (3) to evaluate the biogas profiles and yield from the co-digestion of SCW pre-treated EFB with POME, and (4) to identify the changes in initial and final effluent of anaerobic digestion process parameters and their kinetic analysis.

MATERIALS AND METHOD

Sample Collection

The EFB and POME used in this study were obtained from the Palm Oil Mill, Selangor in Malaysia. The inoculum was collected from the anaerobic digester treating POME. The inoculum was pre-incubated for three days at 37°C ± 1°C before being used to remove any background methane from the inoculum and adjust the microorganisms to mesophilic environments (Chan *et al.*, 2021). The EFB was dried at 60°C and then went through a grinding process to 500 µm size using a universal cutting mill pulverisette 19 (Fritsch, Germany). The POME and inoculum were stored at 4°C in the refrigerator before further use.

Subcritical Water Pre-treatment

The SCW pre-treatment was carried out in a high-temperature reaction bath with reactors fitted on a rocking bed. In a 40 mL steel reactor, EFBs were poured into the reactor along with water at a ratio of 1:10 (EFB:Water). Thereafter, the reactor head was assembled and tightened after nitrogen gas was purged for 1 min at 2 mL min^{-1}. The SCW pre-treatment was conducted at 120°C and 180°C at 10 and 30 min, respectively. Then the oil was heated to achieve the desired temperature before each pre-treatment. The reactor was attached to the rocking bed in the oil bath, and once the pre-determined amount of time had passed, they were taken out and quickly being immersed in the ice bath. To lower the pressure inside, the mixtures were left prior to usage. The SCW pre-treated EFBs were then co-digested with POME to produce biogas. To quantify the SCW pre-treatment combined effect of time and temperature, the pre-treatment severities (S) were measured for each set of pre-treatments. The S was calculated using Equation (1), where t is the time (min) and T is the SCW temperature (°C) (Vakalis *et al.*, 2022).

$$Log\ S = Log\left[t.EXP\left(\frac{T\text{-}100}{14.75}\right)\right] \quad (1)$$

Biogas Production

The batch co-digestion using SCW pre-treated EFB and POME was performed in 125 mL serum bottles at mesophilic temperature. The working volume of each digester was 100 mL with an organic

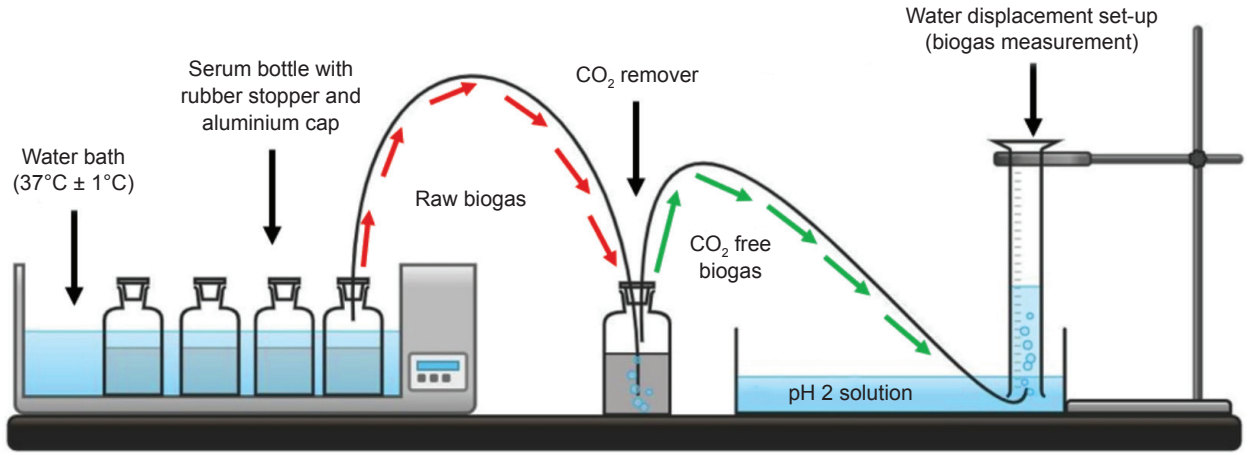

Figure 1. Anaerobic co-digestion set-up.

loading of 11 g VS L^{-1} as described by Liew *et al*. (2021). The bottles were submerged in a water bath during the digestion period at 37°C ± 1°C (Memmert, Germany). Meanwhile, the substrate's pH was adjusted to 7 using 3M sodium hydroxide and hydrochloric acid. Batch testing was conducted until the biogas generation rate was constant (60 days). This procedure was conducted until the plateau of the generated gas was achieved. Each sample was prepared in triplicate to increase the reliability of the measures. Gas production was collected daily using the water displacement method (*Figure 1*).

Analytical Methods

The total solid (TS), VS and total ammonia nitrogen (TAN) were determined using the standard method (APHA, 1998). The TAN measurements were performed according to standard procedure #4500-D. The CHN628 Series (LECO, United States) was used to analyse the carbon (C) and nitrogen (N) contents, whereas a pH meter was employed to measure the pH value. The percentage of lignin in EFB waste was determined based on the Technical Association of the Pulp and Paper Industry (TAPPI) standard procedure (TAPPI, 1950), while the measurement of sugars was performed using a high-performance liquid chromatograph (HPLC) with a refractive index detector (RID). Gas chromatography (GC) with a thermal conductivity detector (TCD) analyser (Agilent 6890N, United States) was used to identify the methane composition of the biogas.

Kinetic Study

A modified Gompertz model equation kinetically analysed the cumulative biogas production data. The gas production curve corresponds to a slow, flat curve when complex solid organic materials are used as substrates (Xiang *et al.*, 2021). The kinetic study provides several essential parameters, such as the lag phase and the maximum biogas production rate for the digestion process. The lag phase (λ) is also an important factor used to reflect the efficiency of the digestion process. The modified Gompertz [Equation (2)] was applied to obtain a better understanding of the behaviour of the process (Tian *et al.*, 2020). The assumption using this model is that the biogas produced in the batch test corresponds to the specific growth rate of the methanogenic bacteria in the digester.

$$B = B_0 \, exp\left\{- exp\left[\frac{\mu.e}{B_0}(\lambda\text{-}t) + 1\right]\right\} \quad (2)$$

where B is biogas production yield (mL g^{-1} VS), B_0 is the maximum biogas yield (mL g^{-1} VS), μ is the maximum biogas production rate (mL g^{-1} VS.day), λ is the lag phase period, t is time and e is an Euler's function = 2.71828. B and t were determined from the experimental data, while B_0, μ and λ were determined from the model. R^2 is a coefficient of determination of the relationship between experimental and predicted values of biogas (Lim *et al.*, 2021). The high R^2 closer to 1 showed that the data adequately fit the model. The accuracy of the studied model is compared by computing the root mean square error (RMSE). The RMSE is calculated as the standard deviation between the predicted and experimental values, as shown in Equation (3) (Manogaran *et al.*, 2023). A smaller RMSE is considered more desirable.

$$RMSE = \sqrt{\sum_{i=1}^{n} \frac{(Y_{i,}\, experimental - Y_{i,}\, predicted)^2}{n}} \quad (3)$$

Statistical Analysis

The data were presented as mean ± standard deviation, and statistical analyses were performed using SAS software (Version 9.4). The data were analysed using analysis of variance, followed by Tukey's multiple comparison test. The *p*-value less than 0.05 was considered statistically significant.

RESULTS AND DISCUSSION

Properties of EFB

Table 1 depicts the main characteristics of EFB, POME, and inoculum used in evaluating the potential of biogas production from SCW pre-treated EFB. As shown in the characterisation results, TS and VS of the EFB were 95.77% and 94.38%, respectively. These findings are consistent with the results by Tepsour *et al*. (2019), in which the values of TS and VS were 96.38% and 90.22%, respectively. The C/N ratio is crucial in anaerobic digestion, as it indicates the nutritional supply for the microorganisms in the reactor. It is appropriate to add POME in this instance due to the EFB's high C content (43.24%) as a carbon source to improve biogas yield. Typically, the reported C/N ratio of EFB is 60-80 (Liew *et al.*, 2021; Mamimin *et al.*, 2021). In the present study, the C and N of the POME were 35.65% and 2.04%, thereby resulting in a C/N ratio of 17.47. In terms of pH, the acidity obtained is similar to that reported in a previous study (Tan & Lim, 2019). The TS, VS and pH of the inoculum were 1.75%, 35.56% and 7.55, respectively.

The solid yields of EFB decreased with an increase in the SCW pre-treatment temperature (*Table 2*). Moreover, the solid yield decreased with an increasing pre-treatment time, from 10 to 30 min. The lower solid yields at the longest pre-

treatment time were due to the extension of the pre-treatment time, which increased delignification and carbohydrate dissolution (Jomnonkhaow *et al*., 2022). Similarly, the VS of the EFB was also reduced with SCW temperature. An increase in the SCW pre-treatment time from 10 to 30 min further reduced the VS of SCW pre-treated EFB. Higher pre-treatment temperature and time resulted in solubilisation, structural changes and modification of the lignocellulosic fraction in the biomass, thereby reducing the solid fraction (Chen *et al*., 2021). Higher pre-treatment severity also led to a relatively higher solid recovery in the pre-treated biomass (Ahmad *et al*., 2018). Pre-treatment severity reflects the intensity of the pre-treatment, whereby the severity increases in line with an increment in the pre-treatment temperature and time. Low pre-treatment severity might be insufficient to overcome the recalcitrance structure of biomass, thus leading to poor microbial performance (He *et al*., 2022).

The severity of SCW pre-treatment in this study ranged from 1.59-3.83. Meanwhile, the pH of SCW pre-treated EFB decreased towards a higher pre-treatment severity. According to Simanungkalit *et al*. (2017), a decrease in pH resulted from the formation of soluble sugar and organic acids in the liquid fraction along with pre-treatment severity. Notably, the lignin content of SCW pre-treated EFB in the present study increased in comparison to the untreated EFB at a higher temperature and longer reaction time. As found in previous studies, increasing pre-treatment time and temperature, along with pre-treatment severity, were reported to increase the biomass's lignin content (Ahmad *et al*., 2018; Jomnonkhaow *et al*., 2022). The increase in lignin may be attributed to the formation of pseudo-lignin under severe pretreatment conditions (He *et al*., 2022). From *Table 2*, it can be seen that hemicellulose content reduced from 22.40%-16.90% as the temperature and time increased. This result supports the hemicellulose trend from previous observations in which the hemicellulose fraction of wheat straw reduced from 24.52%-17.84% as the temperature increased from 125°C-175°C (Tian *et al*., 2020). As mentioned before, hemicellulose can be degraded at a temperature above 150°C (He *et al*., 2022). Hemicellulose degradation altered lignocellulosic structural complexity and improved microbial accessibility to cellulose, improving anaerobic digestibility (Wang *et al*., 2018). While for the cellulose fraction, a slight increase in cellulose can be observed from the study. This result further supports the observation from the previous study that the cellulose fraction did not change significantly when the pre-treatment temperature was promoted to 130°C, and the percentage increased more noticeably at higher temperatures (Xiang *et al*., 2021). This is likely related to the complexity of the cellulose, which is only partially soluble in water or organic solvents at temperatures below 200°C (Phuttaro *et al*., 2019).

TABLE 1. CHARACTERISTICS OF EFB, POME AND INOCULUM USED IN THIS STUDY

Characteristics	EFB	POME	Inoculum
TS (%)	95.77 ± 0.34	6.36 ± 0.03	1.75 ± 0.05
VS (%)	94.38 ± 0.21	79.62 ± 0.15	35.56 ± 0.55
C (%)	43.24 ± 0.05	35.65 ± 0.16	NA
N (%)	0.53 ± 0.01	2.04 ± 0.00	NA
C/N	82.21 ± 0.04	17.47 ± 0.28	NA
pH	NA	4.55 ± 0.02	7.55 ± 0.06

Note: Data in the table are exhibited in the form of mean ± standard deviation, NA - not available; TS - total solid; VS - volatile solid; C - carbon; N - nitrogen; C/N - carbon/nitrogen.

TABLE 2. PHYSICOCHEMICAL PROPERTIES OF SCW PRE-TREATED EFB AFTER PRE-TREATMENT

Pre-treatment	Severity	pH	Solid yield (%)	VS reduction (%)	Lignin (%)	Cellulose (%)	Hemicellulose (%)
120°C, 10 min	1.59	$5.38 \pm 0.05^{a,b}$	57.66 ± 0.11^{b}	$4.51 \pm 0.02^{a,b}$	$15.38 \pm 1.29^{a,b}$	50.36 ± 1.13^{a}	22.44 ± 1.29^{a}
120°C, 30 min	2.07	$5.21 \pm 0.01^{a,b}$	47.56 ± 0.14^{d}	5.61 ± 1.33^{b}	2.79 ± 0.64^{a}	$52.01 \pm 1.18^{a,b}$	$20.36 \pm 0.64^{a,b}$
180°C, 10 min	3.36	$4.78 \pm 0.04^{a,b}$	54.56 ± 0.10^{c}	2.89 ± 0.86^{c}	16.86 ± 0.74^{b}	$54.85 \pm 1.27^{a,b}$	$18.55 \pm 1.27^{a,b}$
180°C, 30 min	3.83	4.00 ± 0.05^{c}	36.07 ± 0.04^{e}	$3.66 \pm 0.39^{a,c}$	17.32 ± 2.06^{b}	57.79 ± 2.06^{b}	16.90 ± 1.59^{a}
Untreated	0.00	5.79 ± 0.05^{b}	100 ± 0.00^{a}	0 ± 0.00^{d}	16.19 ± 0.10^{b}	49.53 ± 4.96^{a}	24.43 ± 4.96^{b}

Note: Data in the table are exhibited in the form of mean ± standard deviation. Different lowercase letters indicate significant differences at $p<0.05$ using Tukey test.

Sugars Production

The SCW pre-treatment enhances biomass hydrolysis and organic matter breakdown during anaerobic digestion. Lignin, cellulose and hemicellulose are the main components in lignocellulosic biomass, whereas other extractive components may include ash, fats, protein and inorganics. Carbohydrate hydrolysis produces fermentable sugar, which can be used to produce biogas (Sarker *et al.*, 2021). Cellulose and hemicellulose are transformed into monosaccharides (glucose and xylose), which can later facilitate microbial hydrolysis in anaerobic digestion (Saritpongteeraka *et al.*, 2022).

In the present study, the concentration of glucose in the liquid fraction after SCW pre-treatment increased with increasing pre-treatment temperature (*Table 3*). A similar increasing trend was observed for cellobiose, arabinose, galactose, and mannose after SCW pre-treatment. Likewise, Akita *et al*. (2021) reported an increase in the concentration of glucose, cellobiose and mannose in the liquid fraction of pre-treated EFB along with the increasing temperature. Meanwhile, xylose composition was not detected at a lower temperature. A previous study revealed a similar result, as 346.5 mg L^{-1} of xylose was detected at 180°C for 45 min of pre-treatment time (Zerback *et al.*, 2022).

Results also revealed an increase in the cellobiose concentration in the liquid fraction from 206.94-333.79 mg L^{-1}. Through SCW pre-treatment, the EFB is hydrolysed and subsequently, hemicellulose and cellulose are broken down into cellobiose (Kurnin *et al.*, 2016). Since xylose cannot be detected in less severe conditions, furfural may be formed from the decomposition of arabinose (Zerback *et al.*, 2022). As for arabinose, the highest concentration (1,023.37 mg L^{-1}) was detected at the highest temperature (180°C). These findings align with the results by Zerback *et al*. (2022), who reported an increasing trend of arabinose content in a liquid fraction when pre-treating wheat straw within a temperature range of 160°C-180°C. A previous study also indicated that xylose and glucose can be degraded to furans by dehydration cyclisation (He *et al.*, 2022). Furans inhibit the biogas production process and are generated during the breakdown of hemicellulose into monosaccharides, oligosaccharides, and monomers (Dasgupta & Chandel, 2019). Furans may result in reduced biogas production in the anaerobic digestion process, depending on their availability and concentration levels throughout the process (Phuttaro *et al.*, 2019).

Biogas Production

The impact of the SCW pre-treatment condition on co-digestion of EFB and POME is presented in *Figure 2*. The biogas production of the low-temperature groups (120°C) reached a significant peak on the 4th day after digestion started. The rapid digestion of the easily soluble components in EFB may be responsible for the rapid biogas generation, which shifted the peak from the 6th day of the untreated EFB to the 4th day. Compared to untreated EFB, at 180°C for 10 min of pre-treatment, the biogas continued to produce peak after the 26th day. The continuous peak observed might have resulted from the changes in the lignocellulosic structure of EFB due to the SCW pre-treatment, which appears to promote biogas production by changing the physical and chemical structure of pre-treated EFB (Kim *et al.*, 2015). The second biogas peak at SCW pre-treatment of 180°C and 30 min was detected after the 16th day of the digestion period. Similarly, Xiang *et al*. (2021) experienced a delay in the biogas production of rice straw at high temperatures. The researchers reported that biogas production from rice straw pre-treated at a temperature of more than 180°C produced a second peak after the 14th to 15th day post-digestion.

Figure 3 depicts the improvements in SCW pre-treated EFB; there was no significant difference in the biogas output compared to those that were not SCW pre-treated at lower temperatures and for shorter periods (120°C, 10 min). This explains why the shorter reaction time and low temperature did not affect the biogas production from SCW pre-treated EFB. Previously, Park *et al*. (2021) observed that the reaction time of biogas produced at a temperature of 125°C was not significant and had no effects on biogas production. In addition to the water-to-solid ratio, Aili Hamzah *et al*. (2022) further highlighted that only the temperature of SCW pre-treatment reflected a significant impact on biogas yield.

TABLE 3. SUGAR YIELDS FROM THE RESIDUAL LIQUID FRACTION OF SCW PRE-TREATED EFB

Pre-treatment	Cellobiose (mg L^{-1})	Glucose (mg L^{-1})	Arabinose (mg L^{-1})	Galactose (mg L^{-1})	Mannose (mg L^{-1})	Xylose (mg L^{-1})
120°C, 10 min	206.94	335.05	520.10	416.38	ND	ND
120°C, 30 min	313.78	418.40	ND	449.72	656.30	ND
180°C, 10 min	315.09	637.68	1,028.37	505.08	ND	ND
180°C, 30 min	333.79	734.22	ND	513.77	2,405.24	400.08

Note: ND – not detected.

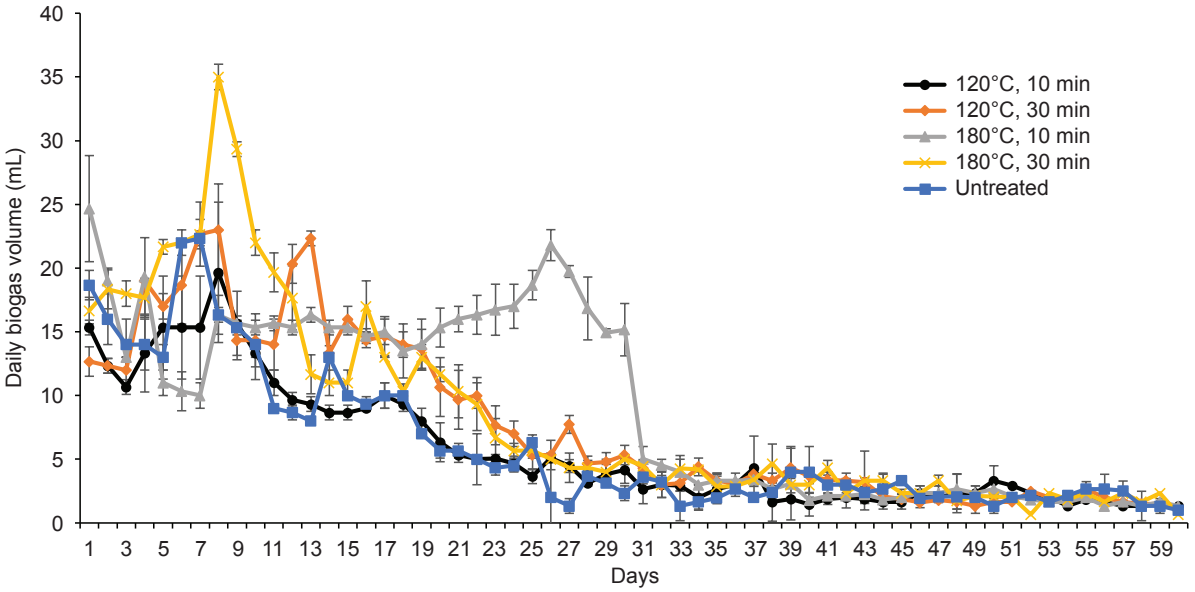

Figure 2. Daily biogas production of co-digestion of SCW pre-treated and untreated EFB with POME.

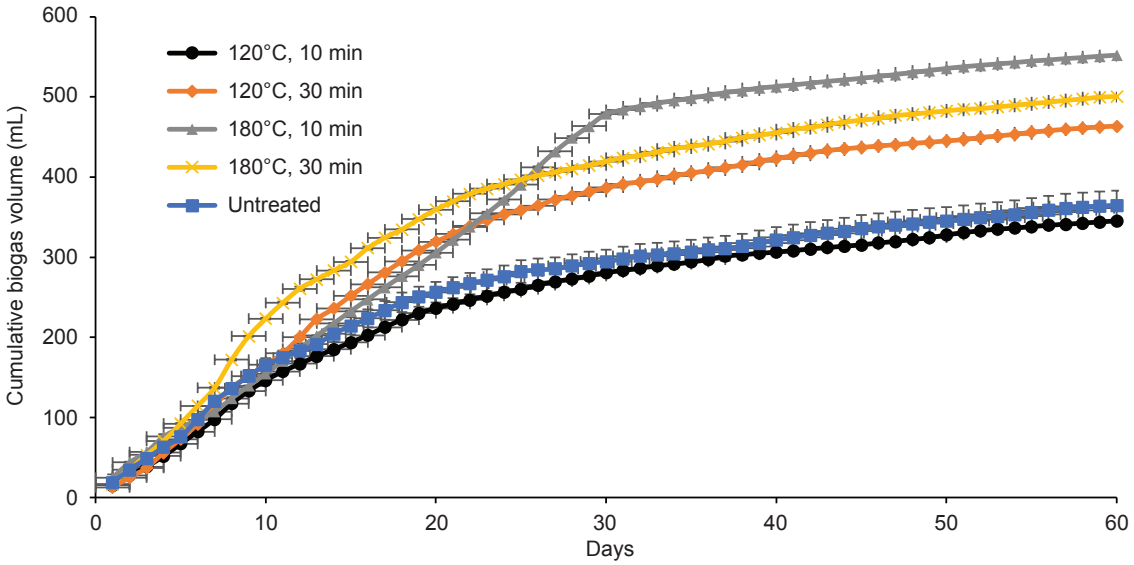

Figure 3. Cumulative biogas production of co-digestion of SCW pre-treated and untreated EFB with POME.

It can be seen from the data in *Table 4* that pre-treated EFB produced the highest biogas volume (547.27 mL), biogas yield (546.18 mL g^{-1} VS) and methane yield at 421.41 mL CH_4 g^{-1} VS, respectively. The results indicate that the aforementioned data for the pre-treated EFB were 32.0% higher than those for the untreated EFB. In addition, the methane content range of the pre-treated EFB was higher than that of the untreated EFB. Overall, the methane yield of SCW pre-treated EFB increased by 32.0% at 180°C compared to the untreated samples. In accordance with the present results, previous research has demonstrated that biogas production was only improved by 14.0% when rice straw was pre-treated to 180°C, while pre-treatment to 120°C led to a significant increment of biogas by 38.0% (Xiang *et al.*, 2021). In another study of hydrothermal SCW pre-treated acai processing waste and wheat straw, an increase in methane yield of 30.0% (Maciel-Silva *et al.*, 2019) and 32.0% (He *et al.*, 2022) was reported, respectively. These results further support an increase in the percentage of methane from 60.0%-85.0% in untreated to 92.0% in pre-treated. In another related study, methane production improved only by 63.4% upon pre-treatment of sludge at 180°C (Kim *et al.*, 2015). The percentage of methane after SCW pre-treatment observed in this study was higher (63.0%-92.0%) as compared to SCW pre-treated pineapple waste (75.0%-88.0%) reported by Aili Hamzah *et al.* (2022). Furthermore, SCW pre-treatment at a high

temperature promotes biomass degradation during anaerobic digestion of EFB. This demonstrated that hydrothermal SCW pre-treatment increased the ability to fully utilise the EFB potential and increased biogas and methane yield.

Effluents Characteristics

A few parameters, including the initial and final effluent of the anaerobic digestion of SCW pre-treated EFB, were assessed to assure the stability of the anaerobic digestion process. *Table 5* summarises the pH, VS removal, and TAN at different pre-treatment conditions. The pH decreased slightly from its initial value of 7.0 to acidic. A decrease in pH in an anaerobic process can inhibit methanogens through rapid acidogenesis, thus contributing to low biogas production (Tepsour *et al.*, 2019; Wenjing *et al.*, 2019). None of the effluent pH values of the co-digestion of pre-treated EFB and POME differed significantly from the starting pH of 7.0. The final effluents can decrease to 6.78. Similarly, Tian *et al*. (2020) stated that the co-digestion of hydrothermal pre-treated waste recovered faster at 175°C when treated and achieved a suitable pH for methanogens, ranging from 6.8-7.2. The final TAN levels in the process ranged from 173.13 to 211.98 mg L^{-1}. In contrast, no TAN inhibition occurred in the present study since the maximum TAN did not exceed the inhibition level. Low biogas production often results from an increase in the TAN level above the threshold value, which inhibits the methanogenic activity. In a previous study involving hydrothermal SCW pre-treated sewage sludge, operating the pre-treatment under 175°C produced a lower TAN concentration and reduced TAN inhibition risk (Park *et al*., 2021). The maximum VS removal from the co-digestion of SCW pre-treated EFB with POME was observed at 69.47%. This demonstrated that SCW pre-treatment aids in the degradation of organic matter into biogas by more than 50.00%. However, a prior study reported that fungal pre-treatment on EFB could achieve 60.00%-75.00% biodegradability (Suksong *et al*., 2020). The lowest VS removal was reported in the untreated sample, for only 62.71% of VS removal. According to the higher VS removal reported by Gaballah *et al*. (2020), rape straw pre-treated with a steam explosion at 180°C combined with grinding resulted in 71.20% VS removal, followed by dilute acid and a steam explosion at 190°C with 70.60% VS removal.

TABLE 4. SUMMARY OF ANAEROBIC CO-DIGESTION PERFORMANCE OF SCW PRE-TREATED AND UNTREATED EFB WITH POME

Pre-treatment	Cumulative biogas volume	Cumulative biogas yield	Methane composition	Methane yield	Improvement
	(mL)	(mL g^{-1} VS)	(%)	(mL CH_4 g^{-1} VS)	(%)
120°C, 10 min	345.37 ± 35.69^{d}	299.96 ± 25.28^{c}	74-90	229.15 ± 17.22^{a}	-28
120°C, 30 min	463.70 ± 29.63^{c}	444.27 ± 36.14^{a}	72-90	$347.02 \pm 16.19^{a,c}$	8
180°C, 10 min	547.27 ± 20.73^{a}	546.18 ± 44.80^{b}	68-89	421.41 ± 15.85^{a}	32
180°C, 30 min	500.53 ± 9.49^{b}	$489.19 \pm 11.58^{a,b}$	63-92	$380.79 \pm 16.88^{a,b}$	19
Untreated	364.83 ± 5.62^{d}	323.7 ± 6.85^{c}	60-85	320.44 ± 11.32^{c}	0

Note: Data in the table are exhibited in the form of mean ± standard deviation. Different lowercase letters indicate significant differences at $p<0.05$ using Tukey test.

TABLE 5. SUMMARY OF INITIAL AND FINAL EFFLUENTS CHARACTERISTIC OF SCW PRE-TREATED AND UNTREATED EFB WITH POME

Pre-treatment	pH		TAN		VS		VS removal
			mg L^{-1}	mg L^{-1}	g VS L^{-1}	g VS L^{-1}	
	Initial	Final	Initial	Final	Initial	Final	
120°C, 10 min	7	6.96 ± 0.12^{a}	122.13 ± 9.28^{e}	194.13 ± 7.81^{b}	17	5.78 ± 0.22^{ab}	66.00 ± 1.29^{ab}
120°C, 30 min	7	7.00 ± 0.50^{a}	161.93 ± 5.15^{d}	173.13 ± 6.11^{d}	17	5.50 ± 0.58^{ab}	67.65 ± 3.35^{ab}
180°C, 10 min	7	6.98 ± 0.36^{a}	204.40 ± 6.86^{a}	192.73 ± 6.61^{c}	17	5.19 ± 0.61^{a}	69.47 ± 3.59^{ab}
180°C, 30 min	7	6.78 ± 0.12^{a}	197.80 ± 8.92^{b}	173.60 ± 8.51^{d}	17	5.71 ± 0.23^{ab}	66.41 ± 2.35^{ab}
Untreated	7	7.18 ± 0.39^{a}	190.43 ± 5.09^{c}	211.98 ± 5.11^{a}	17	6.34 ± 0.99^{b}	62.71 ± 5.82^{ab}

Note: Data in the table are exhibited in the form of mean ± standard deviation. Different lowercase letters indicate significant differences at $p<0.05$ using Tukey test.

Kinetic Study

It is assumed, using the modified Gompertz model (MGM) equation, that the rate at which biogas is produced in the digester equals a specific rate at which methanogenic bacteria grow. It can be seen in *Figure 4* that SCW pre-treated EFB at 180°C for 30 min produced faster biogas production compared to other pre-treatment conditions, while the slowest production can be seen at 120°C for 10 min and untreated. This finding suggests that the microbial growth rate is lower at low temperatures and shorter pre-treatment times. This is because lower temperatures result in the production of less fermentable sugar. High-temperature production of fermentable sugar enhances microbial growth and increases the availability of sucrose for conversion into methane. *Table 6* summarises the predicted parameters of MGM's equation. Despite having the maximum biogas production, there is an increase in SCW pre-treatment at 180°C for 30 min. Xiang *et al*. (2021) found that increasing the pre-treatment temperature from 120°C-180°C released more fermentable sugars that facilitate the anaerobic digestion process. Thus, an increase in the amount of fermentable sugar in the pre-treated sample increases the λ. These results reflect those of Hamzah *et al*. (2024), who also observed a similar trend. Also, the λ of the solid fraction hydrothermal SCW pre-treated rice straw increased from 3.49-5.25 days (Xiang *et al*., 2021), a slight increase in λ from 3.23-3.45 and 3.79 was observed by fungal pre-treatment of rice straw (Kainthola *et al*., 2019) and λ increased from 1 day to a maximum of 9.9 using acid and alkali pre-treatment for tobacco stalk (Zhang *et al*., 2020).

The maximum biogas production rate (μ) demonstrated an increasing trend as the SCW temperature and reaction time increased. The highest μ was observed at 180°C for 30 min with mL g^{-1} VS. day and the lowest μ at 120°C for 10 min with only 12.73 mL g^{-1} VS. day. An increase in the μ, from 12.33-14.75 mL g^{-1} VS. day, was observed when pre-treated rice straw was subjected to a temperature increase from 120°C-180°C (Xiang *et al*., 2021). The kinetic study is crucial in predicting, modelling, and monitoring the performance of a process under various conditions (Cao *et al*., 2020). The model assists in predicting kinetic parameters and elucidating the digestion process. The RMSE is a primary metric used to evaluate the effectiveness of a regression model and offers an assessment of the model's ability to accurately forecast the target value (accuracy) (Manogaran *et al*., 2023). It is widely acknowledged that a lower RMSE indicates superior model performance (Pečar *et al*., 2020). A lower RMSE signifies a more outstanding outcome of the model prediction. The RMSE values in the present study varied between 0.2416 and 0.8746. The coefficient of determination (R^2) values of the ratios for the pre-treated EFB were also higher in comparison with untreated materials. The R^2 of pre-treated EFB suggested good agreement between the experimental data and model simulation for all pre-treatments. The fact that the R^2 values were near to one further demonstrated that the kinetics of the MGM fit with the actual biogas generation. Previously, a good fit was observed using MGM for anaerobic co-digestion of chemically pre-treated agricultural waste and animal manure, reported at a range of 0.979-0.994 (Almomani & Bhosale, 2020), while hydrothermal SCW pre-treated rice

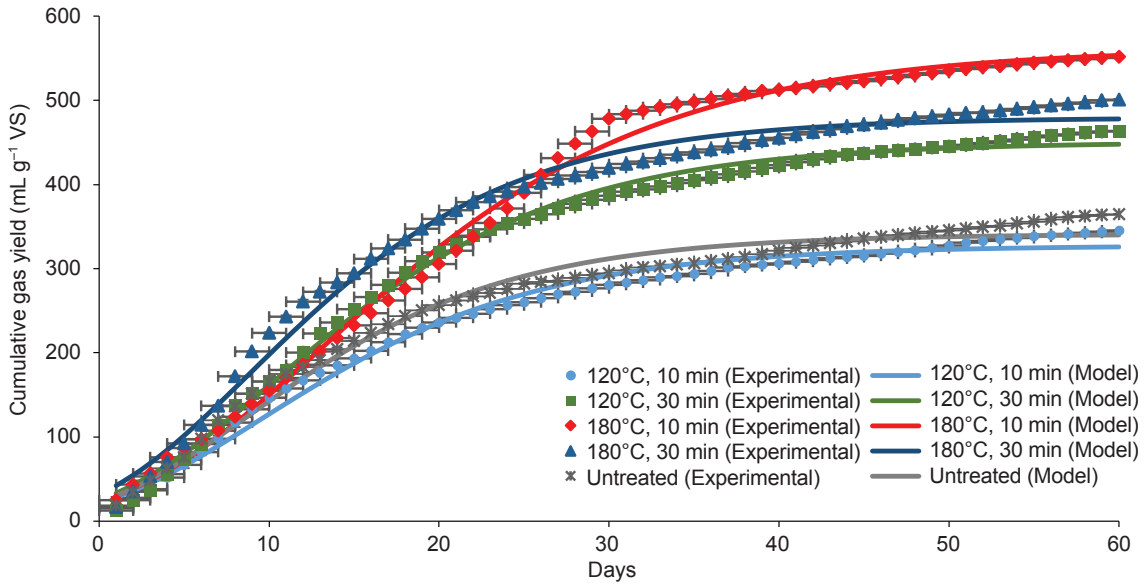

Figure 4. Cumulative biogas yield of co-digestion of SCW pre-treated EFB with POME.

TABLE 6. KINETIC PARAMETERS OF BIOGAS PRODUCTION DURING ANAEROBIC CO-DIGESTION - THE MODIFIED GOMPERTZ MODEL

Pre-treatment	120°C, 10 min	120°C, 30 min	180°C, 10 min	180°C, 30 min	Untreated
B_0 (mL g^{-1} VS)	327.37 ± 30.38^{c}	450.37 ± 28.97^{b}	562.28 ± 17.93^{a}	479.39 ± 7.40^{b}	341.04 ± 6.61^{c}
μ (mL g^{-1} VS day)	12.73 ± 1.79^{c}	$17.17 \pm 1.61^{a,b}$	18.25 ± 0.47^{b}	19.80 ± 0.25^{b}	$14.27 \pm 0.59^{a,c}$
λ (day)	0.00 ± 0.00^{b}	0.59 ± 0.40^{b}	1.82 ± 0.25^{a}	0.00 ± 0.11^{b}	0.00 ± 0.00^{b}
R^2	0.9874	0.9957	0.9953	0.9897	0.9805
RMSE	0.8567	0.7041	0.8724	0.2416	0.8746

Notes: B_0 - maximum biogas yield; μ - the maximum biogas production rate; λ - lag phase period; R^2 - coefficient of determination; RMSE - root mean square error. Data in the table are exhibited in the form of mean ± standard deviation. Different lowercase letters indicate significant differences at $p<0.05$ using Tukey test.

straw reported an increase in R^2 from 0.9944-0.9989 after being pre-treated at a SCW temperature of 150°C by using the same kinetic model (Wang *et al.*, 2018). The increase of R^2 values towards 1 and the gradual decrease of RMSE towards 0 imply a strong relationship between these models and the experimental results, suggesting a good fit (Hakimi *et al.*, 2023). Both the RMSE and the R^2 measure the degree to which a linear regression model accurately fits the experimental value. Thus, from this analysis, the MGM equation is suitable for the biogas prediction model because it has a low RMSE value and a good R^2 fit.

CONCLUSION

The impact of SCW pre-treatment process parameters on the methane production from co-digestion of EFB and POME was investigated in this study. The changes in the properties of EFB after pre-treatment depended on the SCW pre-treatment severity. Fermentable sugars such as glucose, xylose, mannose, cellobiose, and galactose were detected in the liquid fraction of SCW pre-treated EFB. High-temperature (180°C) SCW pre-treatment depicted better methane production than low-temperature pre-treatment. SCW pre-treatment at 180°C for 10 min achieved the maximum biogas volume of 547.27 mL, corresponding to 546.18 mL g^{-1} VS biogas yield and 421.41 mL CH_4 g^{-1} VS methane yields, respectively. Lignin reduction was observed in all pre-treated samples. Meanwhile, the SCW pre-treatment improved the VS removal and reduced the final TAN and pH of the anaerobic co-digestion process. Cumulative biogas production analysed by a modified Gompertz kinetic equation revealed that the longer λ observed at SCW pre-treatment produced the highest yield. This finding is likely to be related to the increase in the amount of fermentable sugar after the pre-treatments. This study demonstrated that SCW pre-treatment successfully increased methane production from the co-digestion of EFB and POME.

The SCW pre-treatment for a shorter time does not promote methane production. Though high-temperature (180°C) SCW pre-treatment depicted better methane production than low-temperature pre-treatment, a reduction in biogas production can be observed as the reaction time is prolonged to 30 min. The degradation of cellulose, hemicellulose, and lignin at SCW temperature, as well as the duration of the reaction, have an impact on the efficiency of biogas production, sugar yield, and the generation of inhibitory compounds. At elevated temperatures, there is an increased release of fermentable sugars, along with the potential presence of inhibitory compounds. The compounds exhibit toxicity toward the methanogens. Therefore, identification of the concentration of these compounds at high temperatures and longer reaction times is crucial. The integration of SCW pre-treatment can effectively remove lignin from lignocellulosic wastes, hence improving microbial hydrolysis. Selecting the SCW temperature and reaction time carefully is essential to maximising methane conversion and reducing inhibitor formation. Hence, there is still a need to investigate this pre-treatment method to achieve optimal methane production and the recovery of sugars while minimising the production of inhibitors.

ACKNOWLEDGEMENT

The authors are grateful for the research project under the Fundamental Research Grant Scheme (Ref. No: FRGS/1/2021/TK0/UPM/02/28) awarded by the Ministry of Higher Education Malaysia. The authors wish to acknowledge the support and technical facilities from the Faculty of Engineering, Universiti Putra Malaysia. The authors wish to thank Green Lagoon Technology Sdn. Bhd. for their kind assistance in raw material supply used in this study. The authors declare that they are free of any known conflicts of interest or direct personal connections that might have looked to have impacted the research presented in this study.

REFERENCES

Ahmad, F., Silva, E. L., & Varesche, M. B. A. (2018). Hydrothermal processing of biomass for anaerobic digestion – A review. *Renewable and Sustainable Energy Reviews*, *98*, 108–124. https://doi.org/10.1016/j.rser.2018.09.008

Aili Hamzah, A. F., Hamzah, M. H., Mazlan, N. I., Che Man, H., Jamali, N. S., Siajam, S. I., & Show, P. L. (2022). Optimization of subcritical water pre-treatment for biogas enhancement on co-digestion of pineapple waste and cow dung using the response surface methodology. *Waste Management*, *150*, 98–109. https://doi.org/10.1016/j.wasman.2022.06.042

Aili Hamzah, A. F., Hamzah, M. H., Che Man, H., Jamali, N. S., Siajam, S. I., & Show, P. L. (2023). Subcritical water pretreatment for anaerobic digestion enhancement: A review. *Pertanika Journal of Science & Technology*, *31*(2), 1011–1034. https://doi.org/10.47836/pjst.31.2.19

Akita, H., Yusoff, M. Z. M., & Fujimoto, S. (2021). Preparation of oil palm empty fruit bunch hydrolysate. *Fermentation*, *7*(2), 81. https://doi.org/10.3390/fermentation7020081

Almomani, F., & Bhosale, R. R. (2020). Enhancing the production of biogas through anaerobic co-digestion of agricultural waste and chemical pre-treatments. *Chemosphere*, *255*, 126805. https://doi.org/10.1016/j.chemosphere.2020.126805

Antwi, E., Engler, N., Nelles, M., & Schüch, A. (2019). Anaerobic digestion and the effect of hydrothermal pretreatment on the biogas yield of cocoa pods residues. *Waste Management*, *88*, 131–140. https://doi.org/10.1016/j.wasman.2019.03.034

American Public Health Association (APHA). (1998). *Standard methods for the examination of water and wastewater* (20th ed.)

Awoh, E. T., Kiplagat, J., Kimutai, S. K., & Mecha, A. C. (2023). Current trends in palm oil waste management: A comparative review of Cameroon and Malaysia. *Heliyon*, *9*(11), e21410. https://doi.org/10.1016/j.heliyon.2023.e21410

Cao, Z., Hülsemann, B., Wüst, D., Illi, L., Oechsner, H., & Kruse, A. (2020). Valorization of maize silage digestate from two-stage anaerobic digestion by hydrothermal carbonization. *Energy Conversion and Management*, *222*, 113218. https://doi.org/10.1016/j.enconman.2020.113218

Chan, Y. J., Lee, H. W., & Selvarajoo, A. (2021). Comparative study of the synergistic effect of decanter cake (DC) and empty fruit bunch (EFB) as the co-substrates in the anaerobic co-digestion (ACD) of palm oil mill effluent (POME). *Environmental Challenges*, *5*, 100257. https://doi.org/10.1016/j.envc.2021.100257

Chen, J., Wang, X., Zhang, B., Yang, Y., Song, Y., Zhang, F., Liu, B., Zhou, Y., Yi, Y., Shan, Y., & Lü, X. (2021). Integrating enzymatic hydrolysis into subcritical water pretreatment optimization for bioethanol production from wheat straw. *The Science of the Total Environment*, *770*, 145321. https://doi.org/10.1016/j.scitotenv.2021.145321

Dasgupta, A., & Chandel, M. K. (2019). Enhancement of biogas production from organic fraction of municipal solid waste using hydrothermal pretreatment. *Bioresource Technology Reports*, *7*, 100281. https://doi.org/10.1016/j.biteb.2019.100281

Dolah, R., Karnik, R., & Hamdan, H. (2021). A comprehensive review on biofuels from oil palm empty fruit bunch (EFB): Current status, potential, barriers and way forward. *Sustainability*, *13*(18), 10210. https://doi.org/10.3390/su131810210

Gaballah, E. S., Abomohra, A. E.-F., Xu, C., Elsayed, M., Abdelkader, T. K., Lin, J., & Yuan, Q. (2020). Enhancement of biogas production from rape straw using different co-pretreatment techniques and anaerobic co-digestion with cattle manure. *Bioresource Technology*, *309*, 123311. https://doi.org/10.1016/j.biortech.2020.12331

Hakimi, M., Manogaran, M. D., Shamsuddin, R., Johari, S. A. M., Hassan, M. A. M., & Soehartanto, T. (2023). Co-anaerobic digestion of sawdust and chicken manure with plant herbs: Biogas generation and kinetic study. *Heliyon*, *9*(6), e17096. https://doi.org/10.1016/j.heliyon.2023.e17096

Hamzah, A. F. A., Hamzah, M. H., Man, H. C., Jamali, N. S., Siajam, S. I., & Show, P. L. (2024). Biogas production through mono- and co-digestion of pineapple waste and cow dung at different substrate ratios. *BioEnergy Research*, *17*(2), 1179–1190. https://doi.org/10.1007/s12155-022-10478-2

He, C., Hu, J., Shen, F., Huang, M., Zhao, L., Zou, J., Tian, D., Jiang, Q., & Zeng, Y. (2022). Tuning hydrothermal pretreatment severity of wheat

straw to match energy application scenarios. *Industrial Crops and Products*, *176*, 114326. https://doi.org/10.1016/j.indcrop.2021.114326

Jomnonkhaow, U., Sittijunda, S., & Reungsang, A. (2022). Assessment of organosolv, hydrothermal, and combined organosolv and hydrothermal with enzymatic pretreatment to increase the production of biogas from Napier grass and Napier silage. *Renewable Energy*, *181*, 1237–1249. https://doi.org/10.1016/j.renene.2021.09.099

Kainthola, J., Kalamdhad, A. S., Goud, V. V., & Goel, R. (2019). Fungal pretreatment and associated kinetics of rice straw hydrolysis to accelerate methane yield from anaerobic digestion. *Bioresource Technology*, *286*, 121368. https://doi.org/10.1016/j.biortech.2019.121368

Kim, D., Lee, K., & Park, K. Y. (2015). Enhancement of biogas production from anaerobic digestion of waste activated sludge by hydrothermal pre-treatment. *International Biodeterioration & Biodegradation*, *101*, 42–46. https://doi.org/10.1016/j.ibiod.2015.03.025

Kurnin, N. A. A., Ismail, M. H. S., Yoshida, H., & Izhar, S. (2016). Recovery of palm oil and valuable material from oil palm empty fruit bunch by sub-critical water. *Journal of Oleo Science*, *65*(4), 283–289. https://doi.org/10.5650/jos.ess15209

Lee, J., & Park, K. Y. (2020). Impact of hydrothermal pretreatment on anaerobic digestion efficiency for lignocellulosic biomass: Influence of pretreatment temperature on the formation of biomass-degrading byproducts. *Chemosphere*, *256*, 127116. https://doi.org/10.1016/j.chemosphere.2020.127116

Liew, Z. K., Chan, Y. J., Ho, Z. T., Yip, Y. H., Teng, M. C., Ameer Abbas, B. A. I. T., Chong, S., Show, P. L., & Chew, C. L. (2021). Biogas production enhancement by co-digestion of empty fruit bunch (EFB) with palm oil mill effluent (POME): Performance and kinetic evaluation. *Renewable Energy*, *179*, 766–777. https://doi.org/10.1016/j.renene.2021.07.073

Lim, Y. F., Chan, Y. J., Hue, F. S., Ng, S. C., & Hashma, H. (2021). Anaerobic co-digestion of palm oil mill effluent (POME) with decanter cake (DC): Effect of mixing ratio and kinetic study. *Bioresource Technology Reports*, *15*, 100736. https://doi.org/10.1016/j.biteb.2021.100736

Maciel-Silva, F. W., Mussatto, S. I., & Forster-Carneiro, T. (2019). Integration of subcritical water pretreatment and anaerobic digestion technologies for valorization of açai processing industries residues. *Journal of Cleaner Production*, *228*, 1131–1142. https://doi.org/10.1016/j.jclepro.2019.04.362

Mahmod, S. S., Jahim, J. M., Abdul, P. M., Luthfi, A. A. I., & Takriff, M. S. (2021). Techno-economic analysis of two-stage anaerobic system for biohydrogen and biomethane production from palm oil mill effluent. *Journal of Environmental Chemical Engineering*, *9*(4), 105679. https://doi.org/10.1016/j.jece.2021.105679

Mamimin, C., Chanthong, S., Leamdum, C., O-Thong, S., & Prasertsan, P. (2021). Improvement of empty palm fruit bunches biodegradability and biogas production by integrating the straw mushroom cultivation as a pretreatment in the solid-state anaerobic digestion. *Bioresource Technology*, *319*, 124227. https://doi.org/10.1016/j.biortech.2020.124227

Manogaran, M. D., Hakimi, M., Ahmad, M. H. N. B., Shamsuddin, R., Lim, J. W., Hassan, M. A. M., & Sahrin, N. T. (2023). Effect of temperature on co-anaerobic digestion of chicken manure and empty fruit bunch: A kinetic parametric study. *Sustainability*, *15*(7), 5813. https://doi.org/10.3390/su15075813

Park, M., Kim, N., Jung, S., Jeong, T., & Park, D. (2021). Optimization and comparison of methane production and residual characteristics in mesophilic anaerobic digestion of sewage sludge by hydrothermal treatment. *Chemosphere*, *264*, 128516. https://doi.org/10.1016/j.chemosphere.2020.128516

Pečar, D., Pohleven, F., & Goršek, A. (2020). Kinetics of methane production during anaerobic fermentation of chicken manure with sawdust and fungi pre-treated wheat straw. *Waste Management*, *102*, 170–178. https://doi.org/10.1016/j.wasman.2019.10.046

Phuttaro, C., Sawatdeenarunat, C., Surendra, K., Boonsawang, P., Chaiprapat, S., & Khanal, S. K. (2019). Anaerobic digestion of hydrothermally-pretreated lignocellulosic biomass: Influence of pretreatment temperatures, inhibitors and soluble organics on methane yield. *Bioresource Technology*, *284*, 128–138. https://doi.org/10.1016/j.biortech.2019.03.114

Saritpongteeraka, K., Natisupacheevin, K., Tan, C., Rehman, S., Charnnok, B., Vaurs, L. P., Leu, S., & Chaiprapat, S. (2021). Comparative assessment between hydrothermal treatment and anaerobic digestion as fuel pretreatment for industrial

conversion of oil palm empty fruit bunch to methane and electricity - A preparation study to full scale. *Fuel*, *310*, 122479. https://doi.org/10.1016/j.fuel.2021.122479

Sarker, T. R., Pattnaik, F., Nanda, S., Dalai, A. K., Meda, V., & Naik, S. (2021). Hydrothermal pretreatment technologies for lignocellulosic biomass: A review of steam explosion and subcritical water hydrolysis. *Chemosphere*, *284*, 131372. https://doi.org/10.1016/j.chemosphere.2021.131372

Simanungkalit, S. P., Mansur, D., Nurhakim, B., Agustin, A., Rinaldi, N., Muryanto, N., & Fitriady, M. A. (2017). Hydrothermal pretreatment of palm oil empty fruit bunch. *AIP Conference Proceedings*, *1803*, 020011. https://doi.org/10.1063/1.4973138

Sitthikitpanya, S., Reungsang, A., & Prasertsan, P. (2018). Two-stage thermophilic bio-hydrogen and methane production from lime-pretreated oil palm trunk by simultaneous saccharification and fermentation. *International Journal of Hydrogen Energy*, *43*(9), 4284–4293. https://doi.org/10.1016/j.ijhydene.2018.01.063

Suksong, W., Wongfaed, N., Sangsri, B., Kongjan, P., Prasertsan, P., Podmirseg, S. M., Insam, H., & O-Thong, S. (2020). Enhanced solid-state biomethanisation of oil palm empty fruit bunches following fungal pretreatment. *Industrial Crops and Products*, *145*, 112099. https://doi.org/10.1016/j.indcrop.2020.112099

Sulaiman, N. S., Sintang, M. D., Mantihal, S., Zaini, H. M., Munsu, E., Mamat, H., Kanagaratnam, S., Jahurul, M. H. A., & Pindi, W. (2022). Balancing functional and health benefits of food products formulated with palm oil as oil sources. *Heliyon*, *8*(10), e11041. https://doi.org/10.1016/j.heliyon.2022.e11041

Tan, Y. D., & Lim, J. S. (2019). Feasibility of palm oil mill effluent elimination towards sustainable Malaysian palm oil industry. *Renewable and Sustainable Energy Reviews*, *111*, 507–522. https://doi.org/10.1016/j.rser.2019.05.043

Technical Association of the Pulp and Paper Industry. (TAPPI). (1950). *T.A.P.P.I. standards: Testing methods, recommended practices, specifications of the Technical Association of the Pulp and Paper Industry*.

Tepsour, M., Usmanbaha, N., Rattanaya, T., Jariyaboon, R., O-Thong, S., Prasertsan, P., & Kongjan, P. (2019). Biogas production from oil palm empty fruit bunches and palm oil decanter cake using solid-state anaerobic co-digestion. *Energies*, *12*(22), 4368. https://doi.org/10.3390/en12224368

Tian, W., Chen, Y., Shen, Y., Zhong, C., Gao, M., Shi, D., He, Q., & Gu, L. (2020). Effects of hydrothermal pretreatment on the mono- and co-digestion of waste activated sludge and wheat straw. *The Science of the Total Environment*, *732*, 139312. https://doi.org/10.1016/j.scitotenv.2020.139312

Vakalis, S., Georgiou, A., Moustakas, K., & Fountoulakis, M. (2022). Assessing the effect of hydrothermal treatment on the volatile solids content and the biomethane potential of common reed (*phragmites australis*). *Bioresource Technology Reports*, *17*, 100923. https://doi.org/10.1016/j.biteb.2021.100923

Wang, D., Shen, F., Yang, G., Zhang, Y., Deng, S., Zhang, J., Zeng, Y., Luo, T., & Mei, Z. (2018). Can hydrothermal pretreatment improve anaerobic digestion for biogas from lignocellulosic biomass? *Bioresource Technology*, *249*, 117–124. https://doi.org/10.1016/j.biortech.2017.09.197

Wenjing, L., Chao, P., Lama, A., Xindi, F., Rong, Y., & Dhar, B. R. (2019). Effect of pre-treatments on biological methane potential of dewatered sewage sludge under dry anaerobic digestion. *Ultrasonics Sonochemistry*, *52*, 224–231. https://doi.org/10.1016/j.ultsonch.2018.11.022

Xiang, C., Tian, D., Hu, J., Huang, M., Shen, F., Zhang, Y., Yang, G., Zeng, Y., & Deng, S. (2021). Why can hydrothermally pretreating lignocellulose in low severities improve anaerobic digestion performances? *The Science of the Total Environment*, *752*, 141929. https://doi.org/10.1016/j.scitotenv.2020.141929

Zerback, T., Schumacher, B., Weinrich, S., Hülsemann, B., & Nelles, M. (2022). Hydrothermal pretreatment of wheat straw – Evaluating the effect of substrate disintegration on the digestibility in anaerobic digestion. *Processes*, *10*(6), 1048. https://doi.org/10.3390/pr10061048

Zhang, H., Wang, L., Dai, Z., Zhang, R., Chen, C., & Liu, G. (2019). Effect of organic loading, feed-to-inoculum ratio, and pretreatment on the anaerobic digestion of tobacco stalks. *Bioresource Technology*, *298*, 122474. https://doi.org/10.1016/j.biortech.2019.122474

Journal of Oil Palm Research Vol. 37 (3) September 2025 p. 519-532
DOI: https://doi.org/10.21894/jopr.2024.0042

SULPHONIC ACIDS SUPPORTED ON Fe_3O_4/PVA MAGNETIC COMPOSITE AS CATALYSTS FOR ESTERIFICATION OF FREE FATTY ACIDS

ANDREW T H YEOW[1,2]; ADEEB HAYYAN[1,2]*; MOHD USMAN MOHD JUNAIDI[1,2]; MUNEER M BA-ABBAD[3] and MOHD ALI HASHIM[1]

ABSTRACT

Low-quality palm oil (LPO) with high free fatty acid (FFA) content (9.66%) can be pretreated for biodiesel production through acid-catalysed esterification. However, homogeneous acid catalysts exhibit challenges in recyclability and separation despite their high catalytic efficiency. Magnetic composites (Fe_3O_4/PVA) as support materials for acid catalysts are a viable protocol for improving recyclability and separation performances. In this study, sulphonic acids and their deep eutectic solvent (DES) counterparts (formed with paracetamol at a 3:1 molar ratio) were supported on Fe_3O_4/PVA to yield heterogeneous solid acid catalysts for FFA esterification in LPO. From the screening results, Fe_3O_4/PVA/PTSA was determined as the best performing catalyst. The optimised reaction conditions were determined: 10 wt.% catalyst loading, 20:1 methanol-to-oil molar ratio, 5 hr of contact time and at 60°C, resulting in an FFA conversion of 79.81%. Fe_3O_4/PVA/PTSA exhibited fair recyclability performances and stability with >65% FFA conversion after five successive runs. FFA esterification reaction using Fe_3O_4/PVA/PTSA was determined to require an activation energy of 43.72 kJ/mol following a simplified pseudo first order rate of reaction. Pristine sulphonic acids exhibited higher compatibility to be supported on Fe_3O_4/PVA magnetic composite than their DES counterpart, with Fe_3O_4/PVA/PTSA being a viable catalyst for the pretreatment of low-quality oils through FFA esterification.

Keywords: deep eutectic solvents, esterification, free fatty acid, magnetic composite, sulphonic acid.

Received: 11 January 2024; **Accepted:** 13 June 2024; **Published online:** 4 September 2024.

INTRODUCTION

Fossil fuel depletion and increased carbon emissions have spurred the need for renewable and sustainable alternative energy resources. Among such alternatives, biofuels such as biodiesels have garnered significant development as the most promising replacement for non-renewable, petroleum-derived diesel (Ghorbani-Choghamarani *et al.*, 2022). In the conventional production of biodiesel, edible vegetable oils from high yielding oil crops such as palm and sunflower oil undergo a highly scalable alkali-catalysed transesterification reaction process to yield fatty acid methyl esters (FAME), a form of biodiesel and glycerol. The use of edible, refined vegetable oils in biodiesel production poses concerns over food supply competition and high production costs (Tropecêlo *et al.*, 2016). Recently, biodiesel production through the valorisation of low value, non-edible feedstocks such as sludge oils, waste vegetable oils or animal fats and used cooking oil has garnered significant attention (Maleki *et al.*, 2022; Yu *et al.*, 2021). Here, the feedstocks can undergo acid-catalysed esterification as a

[1] Department of Chemical Engineering, Faculty of Engineering, Universiti Malaya, 50603 Kuala Lumpur, Malaysia.

[2] Sustainable Process Engineering Centre (SPEC), Faculty of Engineering, Universiti Malaya, 50603 Kuala Lumpur, Malaysia.

[3] Gas Processing Center, College of Engineering, Qatar University, P.O. Box 2713 Doha, Qatar.

* *Corresponding author e-mail: adeeb.hayyan@yahoo.com*

pre-treatment step prior to the transesterification reaction to reduce the high free fatty acid (FFA) content. The utilisation of low value, non-edible feedstocks through catalytic esterification eliminates the aforementioned competition with food supply and improves the economic feasibility of biodiesel production (Bahadoran *et al.*, 2022; Chen *et al.*, 2023). Therefore, the development of acidic catalysts that are commercially significant is vital to enable effective valorisation of low value feedstocks to improve the economic feasibility of biodiesel production (Lou *et al.*, 2023).

Acidic catalysts in the esterification process for biodiesel production can be broadly classified into homogeneous- and heterogeneous-type catalysts. Mineral acids such as sulphuric acid are commonly employed as homogeneous catalysts, however, have significant drawbacks such as being highly corrosive, requiring complex downstream separation and exhibiting challenges in recyclability (Khan *et al.*, 2021). Recent advancements in homogeneous acidic catalysts such as ionic liquids and deep eutectic solvents (DESs) have been sought out due to their unique properties in overcoming the limitations of conventional mineral acids (Hayyan *et al.*, 2023; He *et al.*, 2023; Wang *et al.*, 2022). On the other hand, solid acid catalysts (SACs) have garnered significant development as a heterogeneous catalyst material for the biodiesel esterification process owing to its advantages over homogeneous catalysts, such as being recyclable, having lower corrosiveness and enabling sustainable catalyst design, particularly when derived from biomass (Zhou *et al.*, 2023). A relevant catalyst design protocol is through supporting homogeneous acids onto various types of support materials such as mesoporous silicas, layered double hydroxides, metal organic frameworks (MOFs), carbon-based materials and polymers (Borton *et al.*, 2019; Chen *et al.*, 2022; Mandari & Devarai, 2022; Zhong *et al.*, 2019). Furthermore, the catalyst recovery and recyclability of the SACs can be enhanced with the integration of a magnetic component such as ferromagnetic magnetite nanoparticles (Fe_3O_4), yielding magnetic responsive SACs that can be easily separated from the reaction mixture via magnetic forces introduced externally (Krishnan *et al.*, 2021). Hence, various magnetic composite/nanocomposite catalyst materials have been investigated for catalytic applications in biodiesel production (Xie & Li, 2023). For example, Ali *et al.* (2020) reported on the synthesis of cuprospinel ($CuFe_2O_4$)-based magnetic nanocatalyst for waste frying oil transesterification that exhibited exceptional biodiesel yield (90.24%) and ease of separation and recovery magnetically. 1-butyl-3-methylimidazolium hydrogen sulphate acidic ionic liquid was synthesised and supported on a Fe_3O_4/SiO_2 composite for the methyl esterification reaction of waste seed oils (Yu *et al.*, 2021). The authors reported high catalytic efficiency and stability (87.6% conversion after four reaction cycles) while exhibiting ease of separation due to its magnetic properties.

In a previous study, sulphonic acids in the form of DESs were reported for the esterification of mixed oils with high FFA content (Hayyan *et al.*, 2023). Herein, p-toluenesulphonic acid was combined with paracetamol to form a DES (3:1 molar ratio) acting as a recyclable, homogeneous catalysts for FFA esterification. Despite the appreciable catalytic activity, the DES and its pristine acid counterparts exhibited weak recyclability. Therefore, the potential of the acids as heterogeneous catalysts in esterification reactions remains unexplored. This study investigates the feasibility of supporting sulphonic acids (BZSA, PTSA and SSA) and their DESs onto a Fe_3O_4/polyvinyl alcohol (PVA) magnetic composite material to improve its recyclability performance of the SACs for the esterification of FFA in LPO. PVA is a synthetic biopolymer that is widely used in fields of research materials such as PVA-based hydrogels for biomedical applications, functional materials and composites and as catalyst support materials due to its high thermal stability and good chemical resistance (Zhang *et al.*, 2016). PVA has been demonstrated as a viable composite/nanocomposite material with Fe_3O_4 magnetic nanoparticles (Maleki *et al.*, 2019; Rahimi *et al.*, 2020b). Additionally, the use of a crosslinker for the linking of PVA strands may enable better incorporation of the sulphonic acid functional group in the SAC (Perez & Dumont, 2021).

EXPERIMENTAL METHODS

Materials and Chemicals

Low-quality palm oil (LPO) containing high FFA content of 9.66% was supplied by a palm oil mill in Selangor, Malaysia. Anhydrous iron (III) chloride ($FeCl_3$, ≥98.00%) was obtained from HmbG Chemicals Malaysia, and iron (II) sulphate heptahydrate ($FeSO_4 \cdot 7H_2O$,≥99.50%) was obtained from R&M Chemicals Malaysia. Polyvinyl alcohol (PVA, molecular weight ~60,000, ≥98.00% degree of hydrolysis) and maleic acid (≥99.00%, Analytical reagent) were purchased from Merck Malaysia. The sulphonic acids involved in this study were: benzenesulphonic acid (BZSA, 90.00% technical grade, Sigma Aldrich), p-toluenesulphonic acid (PTSA, ≥98.00%, Sigma Aldrich), and 5-sulphosalicylic acid dihydrate (SSA, >99.00%, Merck). The sulphonic acids were used as supplied without further purification. Paracetamol (PCM, ≥99.00%, BioXtra grade) was obtained from Sigma Aldrich. Ammonium hydroxide solution ($NH_3.H_2O$, 25.00% w/v solution) was purchased

from R&M Chemicals Malaysia. Methanol (≥99.85%) and propan-2-ol (ACS reagent) were purchased from Kollin Chemicals and Merck Malaysia respectively.

Synthesis of Fe_3O_4/PVA Magnetic Composite

Fe_3O_4/PVA magnetic composites were synthesised based on the *in-situ* co-precipitation method (Fazelinia *et al.*, 2023; Kamalzare *et al.*, 2021). A 5 w/v % PVA solution was produced by dissolving PVA in distilled water under vigorous stirring for 4 hr at 80°C. Subsequently, 12 mL of $NH_3.H_2O$ was added to the PVA solution to adjust the pH to 11. At the same time, 0.02 mol of $FeCl_3$ and 0.01 mol of $FeSO_4.7H_2O$ were dissolved in 10 mL of distilled water to form a 2:1 Fe^{3+}:Fe^{2+} ratio mixture, serving as the Fe^{3+} and Fe^{2+} precursors for the synthesis of Fe_3O_4 magnetic nanoparticles by co-precipitation. This mixture was added dropwise into the $NH_3.H_2O$–PVA solution under stirring at 350 rpm. The solution gradually turned black and was continuously stirred for 2 hr at 60°C under N_2 atmosphere. The black particles precipitate (denoted as Fe_3O_4/PVA) was recovered using an external magnet and washed several times with distilled water and dried at 60°C overnight.

Synthesis of Sulphonic Acid-based DESs

To synthesise the sulphonic acid-based DESs, the sulphonic acids (BZSA, PTSA or SSA) were combined with PCM at a molar ratio of 3:1 (Hayyan *et al.*, 2023). The DESs are thus labelled as [3BZSA:PCM], [3PTSA:PCM] and [3SSA:PCM], corresponding to the sulphonic acid component and PCM. The DESs were formed under magnetic stirring (350 rpm) at 80°C for 1-3 hr until a homogeneous solution was obtained. The DESs were then collected and stored in a desiccator. After 24 hr of storage, the DESs remained in liquid phases at elevated temperature (60°C) and no precipitation was observed.

Synthesis of Acids and DESs Supported on Fe_3O_4/PVA

The synthesis protocol was adapted from the proposed method described by Kamalzare *et al.* (2021) with slight modifications. To synthesise the acid-supported Fe_3O_4/PVA, a 1:1 by mass ratio of Fe_3O_4/PVA and acid/DES was taken (Swami *et al.*, 2023). A total of 1 g of Fe_3O_4/PVA was dispersed in 15 mL of distilled water, and simultaneously 1 g of acid (BZSA, PTSA or SSA) or DES compound [3BZSA:PCM], [3PTSA:PCM], [3SSA:PCM] was dissolved in 10 mL of distilled water. The acid solution was added to the Fe_3O_4/PVA solution and continuously stirred for 15 min at ambient temperature. Subsequently, 30 wt.% of maleic acid was added as the crosslinker for the composite according to a previous optimisation study (Mok *et al.*, 2020) and 1 mL of 37% HCl was added to catalyse the crosslinking process. Finally, the mixture of synthesised composite (denoted as Fe_3O_4/PVA/Acid) was stirred for 30 min at room temperature, and subsequently collected using an external magnet. To remove any residuals remaining with composite, the Fe_3O_4/PVA/Acid was washed several times using distilled water and dried at 60°C overnight.

Esterification Reaction Experimental Setup

LPO was preheated to 70°C to yield a red, liquid phase oil that is homogeneous compared to its semisolid physical state at room temperature. The Fe_3O_4/PVA/Acid catalyst was added to the reactants of 20 g of LPO and methanol in a sealed, jacketed reactor equipped with an overhead condenser, where the mixture was stirred at 350 rpm constantly throughout the experiment. A screening stage was conducted to preliminarily evaluate the catalytic performance of the FFA esterification reaction and determine the most suitable catalyst including either the sulphonic acids or DES compounds supported on the Fe_3O_4/PVA magnetic composite. Subsequently, the preferred catalyst material was determined from the screening procedure for further characterisation and optimisation (by single factor optimisation). The optimisation parameters include catalyst loading within the range of 5-20 wt.%, methanol requirement within 10:1-25:1 methanol-to-oil molar ratio, contact time within 1-6 hr, and reaction temperatures 30°C-70°C. The esterification experiments were triplicated and the average FFA content is presented along with the standard deviation.

The FFA content was determined according to the American Oil Chemists Society (AOCS) Official Method Ca 5a-40 using titrimetric method (AOCS, 2017). The FFA limit was set for below 2%, and percentage conversion of FFA into FAME was determined according to Equation (1):

$$Conversion = \frac{FFA_I - FFA_F}{FFA_I} \times 100\% \quad (1)$$

where FFA_I and FFA_F are the initial and final FFA values before and after esterification respectively. The recyclability performance of the heterogeneous magnetic catalyst was also conducted. At the end of reaction, the catalyst was easily recovered using an external magnet and regenerated by washing repeatedly up to three times with distilled water and subjected to oven drying at 60°C overnight. The recovered catalyst was added to fresh LPO and the extent of the esterification reaction was evaluated.

Characterisation of Fe_3O_4/PVA/Acid Magnetic Composite

The synthesised Fe_3O_4/PVA/Acid was characterised for its morphology and elemental composition using field emission scanning electron microscopy (FESEM) imaging and energy dispersive X-ray spectroscopy (EDX) analysis (FEI Quanta FEG 650 S scanning electron microscope). The structural phase of the synthesised Fe_3O_4/PVA and Fe_3O_4/PVA/Acid were revealed using X-ray diffraction (XRD) analysis, which was conducted on the Malvern PANalytical EMPYREAN diffractometer system using CuKα radiation (λ = 1.5406 Å) at two theta (2θ) angle range of 10-80 (0.01 step size), and operated at 45 kV volts and 40 mA current. The thermogravimetric analyses (TGA) were conducted using a PerkinElmer Pyris 6 TGA analyser and the thermal behaviour was observed from 30°C-800°C at a 10°C/min heating rate under nitrogen gas flow. The energy binding and oxidation states of the Fe_3O_4/PVA/Acid composite were determined through X-ray photoelectron spectroscopy (XPS) conducted on the Axis Ultra DLD (KRATOS model) X-ray photoelectron spectrometer using a monochromated Al Kα radiation (1486.6 eV) as the excitation source (15 kV).

RESULTS AND DISCUSSION

Screening of Catalyst Performance in FFA Esterification

The screening of the catalyst performance was conducted at excess operating conditions (10 wt.% catalyst loading, 20:1 methanol-to-oil molar ratio, 6 hr contact time and reaction temperature at 60°C) to enable the reaction to achieve equilibrium. From the screening results presented in *Figure 1*, PTSA supported on Fe_3O_4/PVA (denoted as Fe_3O_4/PVA/PTSA) exhibited the highest catalytic performance, reducing the FFA value down to 1.98% below the predetermined limit, equivalent to 79.53% conversion; followed by Fe_3O_4/PVA/SSA at 66.51% FFA conversion. Among the list of catalysts supported on Fe_3O_4/PVA, the pristine acid components exhibited greater FFA conversion than their counterpart composed within the DES system. A plausible explanation for this may be that the DES system exhibited stronger molecular bonding with the water solvent while it was solvated, leading to the formation of an aqueous DES system (Picciolini *et al.*, 2023; Wang *et al.*, 2021). Hence, the DESs may be inferred to be incompatible with the Fe_3O_4/PVA composite based on the low FFA conversion results as the support was unable to exhibit a catalytic effect. BZSA and [3SSA:PCM] DES exhibited the weakest FFA esterification performance at 31.29% and 29.70% FFA conversion when supported on Fe_3O_4/PVA, which may be attributed to the weak attachment of the molecules and functional groups to the Fe_3O_4/PVA support material. Hence, Fe_3O_4/PVA/PTSA was determined as the best performing catalyst from the screening stage and further optimisation studies were conducted.

Characterisation of Fe_3O_4/PVA/PTSA

FESEM imaging and EDX analysis were used to provide topographical and elemental information of the synthesised Fe_3O_4/PVA/PTSA composite as presented in *Figure 2*, accompanied with the photographic images of the magnetic response of the Fe_3O_4/PVA/PTSA composite in water. The spherical shape of the Fe_3O_4/PVA/PTSA composite (*Figure 2a-2c*) observed from the FESEM image agrees with previously reported studies on modified Fe_3O_4/PVA (Maleki *et al.*, 2019). Furthermore, the elemental distribution of C (23.21%), Fe (46.11%), O (27.83%) and S (2.85%)

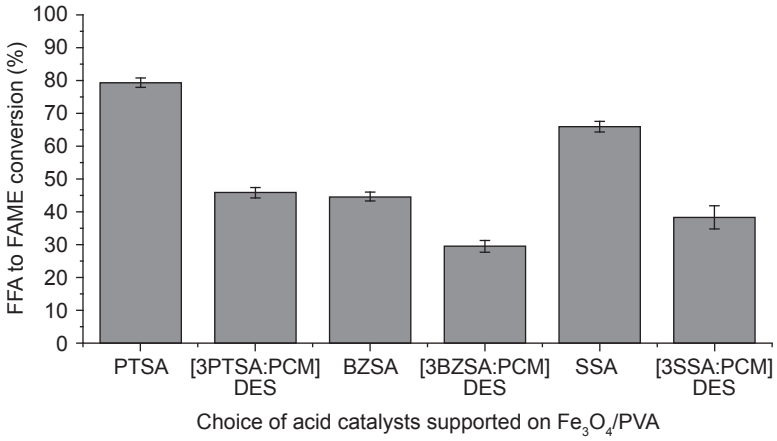

Figure 1. Screening of FFA esterification catalytic performance using sulphonic acids and DESs supported on Fe_3O_4/PVA magnetic composite.

was determined from the EDX analysis, suggesting that the PTSA is synthesised onto the Fe_3O_4/PVA matrix. The presence of the S element is contributed by the sulphonic acid functional group (-SO_3H) of the PTSA molecule, whereas the Fe and O element peaks in the EDX spectra plot affirm the presence of Fe_3O_4 (Ba-Abbad *et al.*, 2022). Additionally, the high carbon (C) element is attributed to the maleic acid-crosslinked PVA polymer chains and the benzene ring of the PTSA molecules. In summary, the EDX spectra plot elucidates the presence of Fe_3O_4, PVA and PTSA, thus supporting the screening results on the presence of catalytic activity for FFA esterification.

The TGA and derivative thermogravimetry (DTG) curves of the Fe_3O_4/PVA and Fe_3O_4/PVA/PTSA composite are presented in *Figure 3a* and *3b*. According to the DTG curves derived from the TGA data, two peaks were observed at 246.2°C-246.8°C and 441.4°C-460.2°C, which correspond to the breaking down of the polymer network of PVA and the dehydration of -OH groups among the PVA chains respectively (Kurchania *et al.*, 2014). Furthermore, the calculated peak at 86.17°C observed for the Fe_3O_4/PVA/PTSA curve may be attributed to the release of physically adsorbed water molecules arising from the acid modification step conducted extensively in the distilled water medium. The trends of the TGA curves were in good agreement with previously reported results in literature pertaining to the synthesis of Fe_3O_4/PVA (Maleki *et al.*, 2019).

The XRD pattern of the synthesised Fe_3O_4/PVA and Fe_3O_4/PVA/PTSA is presented in *Figure 3c*. The peaks appearing at 2θ = 30.15°, 35.54°, 43.33°, 53.58°, 57.32° and 62.78° are in good correlation with the standard JCPDS Card No. 88-0315 for Fe_3O_4 and affirms the synthesis. Furthermore, the broad peak centred at around 22° is assigned to the diffraction pattern of amorphous PVA (Maleki *et al.*, 2019). The XRD pattern for Fe_3O_4/PVA/PTSA revealed a fringe peak at 2θ = 32.69°, which may be attributed to the coating interaction between the PVA chains and the Fe_3O_4 particle (Rahimi *et al.*, 2020a, 2020b).

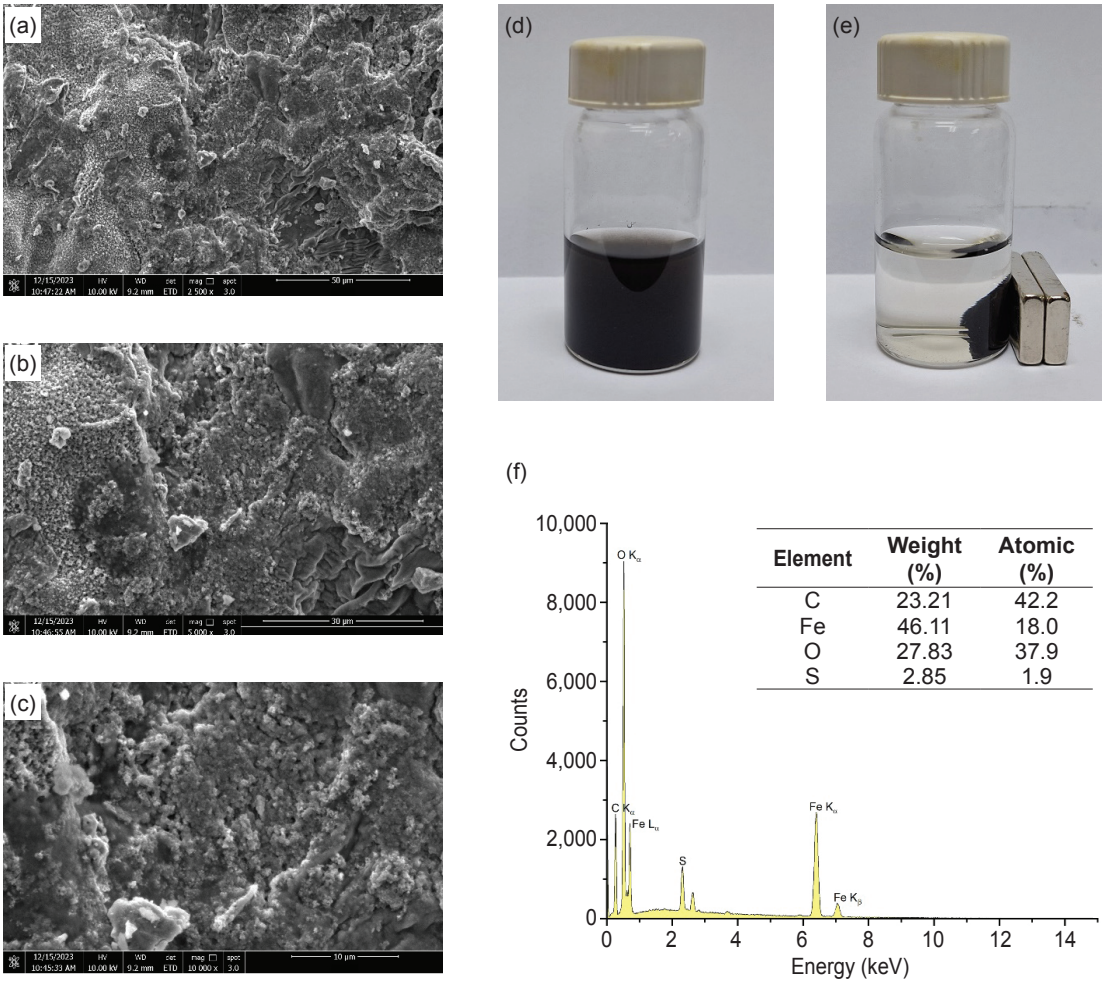

Figure 2. FESEM imaging of the Fe_3O_4/PVA/PTSA composite at (a) 2,500X, (b) 5,000X, and (c) 10,000X magnification; photographic image of (d) dispersion of Fe_3O_4/PVA/PTSA composite in water and (e) magnetic response of the Fe_3O_4/PVA/PTSA composite; and (f) EDX spectra plot of the Fe_3O_4/PVA/PTSA composite.

XPS spectra analysis was conducted to observe the near surface region of the Fe_3O_4/PVA/PTSA composite and determine the chemical states. *Figure 3d* presents the survey spectra of the Fe_3O_4/PVA/PTSA composite, indicating the detection of S 2p, O 1s, Fe 2p and C1s. The high resolution spectra of S 2p (*Figure 3e*) can be deconvoluted into two peaks at 168.3 and 169.6 eV that is assigned to the $-SO_3H$ groups of the PTSA molecule synthesised onto the surface of Fe_3O_4/PVA (Wang *et al.*, 2015; Zheng *et al.*, 2024). The three peaks determined in the deconvoluted O 1s spectra (*Figure 3f*) at 529.9, 531.2 and 532.4 eV may be assigned to oxygen in the form of Fe–O, H–O, and C–O respectively (Luo *et al.*, 2019). In the Fe 2p spectrum (*Figure 3g* and *3h*), the detection of asymmetric peaks at 710.5 and 724.1 eV (corresponding to the Fe $2p_{3/2}$ and Fe $2p_{1/2}$ phase) and the absence of a satellite peak at 719.0 eV verified the synthesis of Fe_3O_4-based composites (Ali *et al.*, 2018). The C 1s spectra were deconvoluted into three peaks at binding energies of 284.8, 286.3 and 288.6 eV that could be assigned to the functional groups of C–C, C–O and C=O respectively (Luo *et al.*, 2019). The XPS spectra did not reveal other peaks contributed by magnetic compounds such as FeO, FeOOH or Fe_2O_3. In summary, the XPS analysis confirms the successful synthesis of Fe_3O_4/PVA/PTSA composite, supported by the analytical results of XRD and TGA analysis.

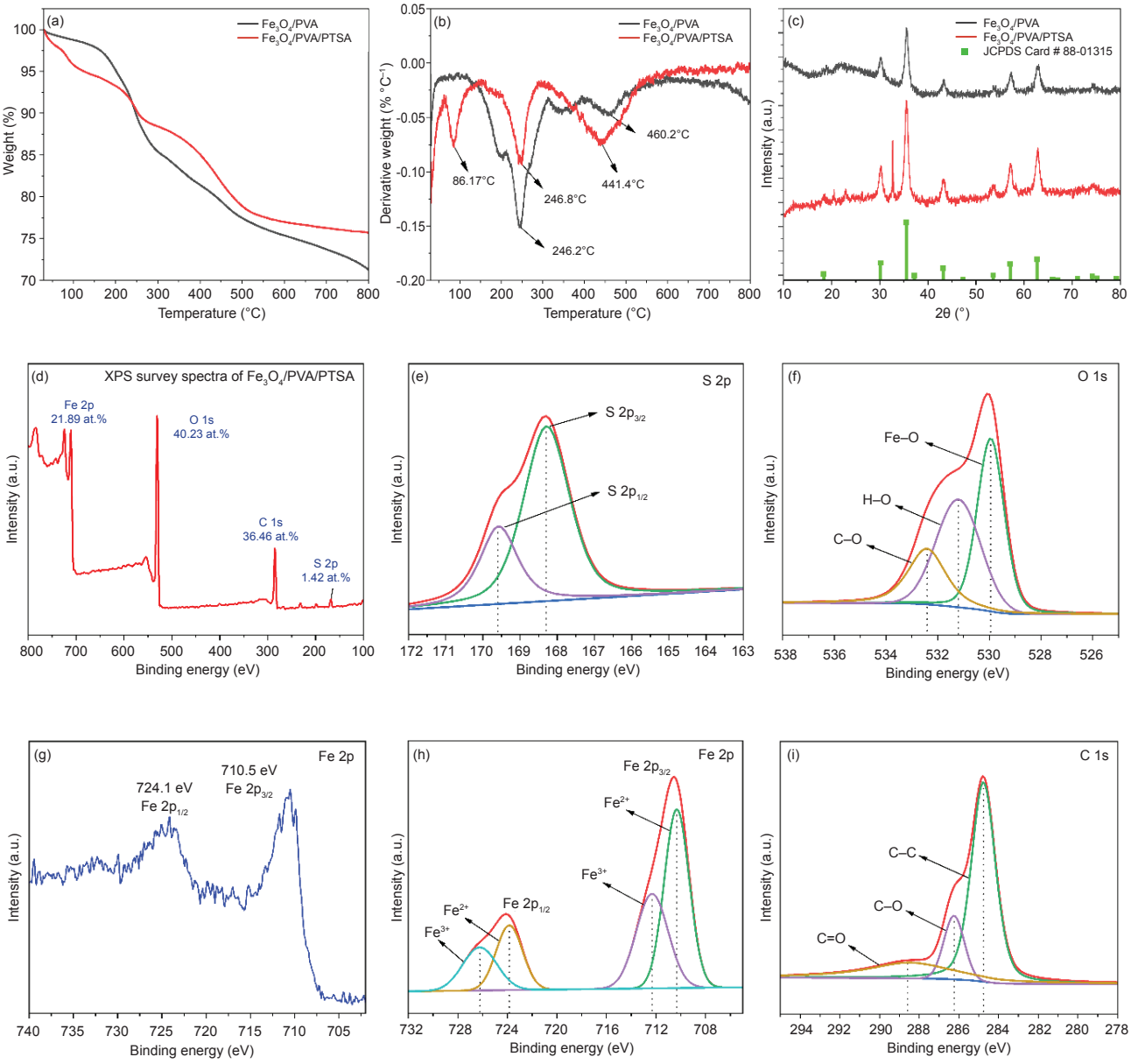

Figure 3. (a) TGA and (b) DTG curves of the Fe_3O_4/PVA and Fe_3O_4/PVA/PTSA composite; (c) XRD patterns for Fe_3O_4/PVA and Fe_3O_4/PVA/PTSA composite; (d) XPS survey spectrum and high-resolution XPS scan spectra over (e) S 2p, (f) O 1s, (g–h) Fe 2p and (i) C 1s for the Fe_3O_4/PVA/PTSA composite.

Effect of Catalyst Loading

The optimisation of Fe_3O_4/PVA/PTSA catalyst loading up to 20 wt.% on FFA esterification is presented in *Figure 4*. At 10 wt.% catalyst loading, the FFA value below 2.00% limit was achieved, equating to an FFA to FAME conversion percentage of 79.33%. At double catalyst loading as 20 wt.%, the FFA conversion rate of 84.38% was achieved. By increasing of catalyst loading, the FFA conversion rate was increased due to the increase of contact and density of the active sites to accelerate the reaction. Additionally, Wang *et al.* (2019) reported that novel synthesis of a magnetic sulphonated SAC based on zirconium and iron chelated using sodium alginate or sodium carboxymethylcellulose. The loading of the magnetic catalyst was studied from 3-11 wt.%, where 9 wt.% of catalyst loading achieved the highest biodiesel yield of 94.30% from the esterification of oleic acid. In another study, PTSA and methanesulphonic acid supported on UiO-66 MOFs were studied for the esterification of palmitic acids with methanol, n-butanol and n-decanol at 25 g/mol (10 wt.% of palmitic acid) of catalyst content (Liu *et al.*, 2020). Hence, the catalyst loading of 10 wt.% was reported in this study as optimum loading for the highest FFA conversion.

Effect of Methanol Requirement

Methanol is supplied as a reactant in excess by molar ratio to enable the forward shift of the FFA esterification reaction to yield FAME. The effects of the methanol ratio requirement on the FFA conversion rate are presented in *Figure 5*. At excess methanol: LPO molar ratio of 20:1, the final FFA content of 1.97% was attained, corresponding to a 79.61% FFA to FAME conversion. Increasing the methanol content to a 25:1 molar ratio resulted in a slight increase in the FFA conversion rate up to 81.07%. Considering the economic significance of excessive methanol with respect to the minute FFA conversion percentage, the optimum methanol: LPO molar ratio was selected as 20:1. In comparison, the methanol molar ratio requirement in the use of PTSA as a homogeneous catalyst is halved at 10:1 (Hayyan *et al.*, 2010). However, the excess methanol requirement is in good agreement with previous studies that used heterogeneous catalysts. Ibrahim *et al.* (2020) utilised oil palm empty fruit bunches to synthesise novel magnetic carbonaceous SAC for the esterification of palm fatty acid distillate. The magnetic catalyst enabled 96.00% conversion of the palm fatty acid distillate feedstock at the optimised methanol requirement of 16:1 molar ratio. Rokhum *et al.* (2022) reported on the influence and optimisation of a novel sugar-derived sulphonated aromatic carbon catalysts on oleic acid esterification, achieving 97.5% conversion at the optimised conditions of 20:1 methanol molar ratio and 5 wt.% catalyst loading.

Effect of Contact Time

Compared to homogeneous mineral acid catalysts applied in biodiesel esterification reactions, heterogeneous catalysts typically require extended contact time (Racar *et al.*, 2023). Hence, the catalyst contact time should be optimised to reach reaction equilibrium due to the increased mass transfer resistance and reduced surface area. The optimisation of catalyst contact time is presented in *Figure 6*. The FFA content was reduced down to 2.00% at the 5th hr of the reaction, and a slight reduction improvement in FFA content was recorded at 1.84% at the 6th hr. Durations of optimal catalyst contact time from 3-8 hr were reported in literature utilising various forms of heterogeneous catalysts. Sulphonated carbon catalysts derived from *Sargassum horneri* biomass were optimised for a high oleic acid conversion of 96.4% at a reaction time of 3 hr (Cao *et al.*, 2021). As reported, Xie and Wang (2020) synthesised polymeric 1-vinyl-3-(3-sulphopropyl)imidazolium hydrogen sulphate as acidic ionic liquids supported on Fe_3O_4/SiO_2 magnetic composites which yielded high oil conversion at 93.30% under optimal reaction time of 6 hr. Sulphonated ZnO-β-zeolite catalysts were reported to exhibit high catalytic performance (96.90% WCO conversion) in the simultaneous esterification and transesterification of waste cooking oil under optimal reaction time of 8 hr (Yusuf *et al.*, 2023).

Effect of Reaction Temperature

Higher reaction temperatures are required for FFA esterification reactions catalysed by heterogeneous catalysts (Maleki *et al.*, 2022). The influence of reaction temperature on the reduction of FFA content is presented in *Figure 7* and shows that the FFA conversion increased with increasing temperature from 40°C-70°C. At 60°C, the FFA was reduced to 1.96%, with no significant reduction observed for 70°C reaction temperature, indicating that the reaction equilibrium has been reached. Comparatively, phosphomolybdic acid was impregnated onto bismuth-based MOFs to yield SACs for the esterification of oleic acid (Zhang *et al.*, 2023). The esterification reaction was conducted in a sealed high-pressure autoclave that allowed reaction temperatures to be optimised between 120°C-170°C. As the reaction was conducted at atmospheric pressure in this study, the reaction temperature was optimised around the boiling point of methanol. Similarly,

the optimal reaction temperature was reported as 75°C in the transesterification of waste cooking oil in a glass batch reactor using a novel sulphonated Fe-Al-TiO_2 magnetic nanocomposite (Gardy *et al.*, 2018).

Validation of Reaction Conditions and Catalyst Recyclability

The reaction conditions determined in the optimum experiment conditions were: 10 wt.% acid catalyst loading, 20:1 methanol: LPO molar ratio of methanol loading, and 5 hr contact time at 60°C. The reaction conditions were revalidated and yielded a treated LPO sample with an FFA content value of 1.95% (79.81% FFA conversion). Subsequently, the catalyst recyclability study was conducted to evaluate the reusability of the Fe_3O_4/PVA/PTSA SAC. Upon completion of the first reaction run, the catalyst was easily recovered using an external magnet, washed continually several times using distilled water, and dried in a vacuum oven for 24 hr. Subsequently, the Fe_3O_4/PVA/PTSA catalyst was transferred to a fresh batch of LPO for the second used and succeeding reaction runs. The catalyst recyclability performance for five continuous reaction cycles is presented in *Figure 8*. The Fe_3O_4/PVA/PTSA catalyst maintained a relatively high FFA conversion rate in the first three runs, demonstrating a slight gradual decrease in FFA conversion from 79.81% to 78.89%. In the succeeding fourth and fifth reaction runs, the FFA conversion drops to 75.15% and 65.65% respectively. The decrease in

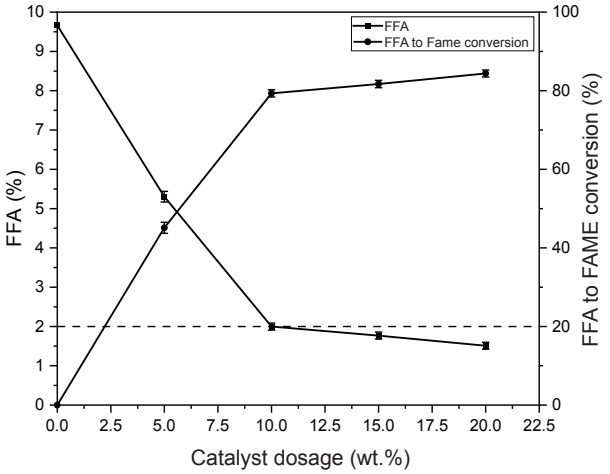

Figure 4. Effect of Fe_3O_4/PVA/PTSA catalyst loading on FFA content reduction and conversion. Experimental parameters were fixed at 20:1 methanol-to-oil molar ratio, 6 hr contact time and 60°C reaction temperature.

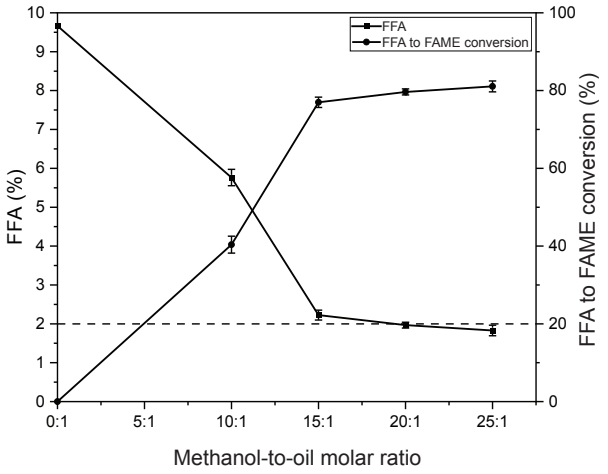

Figure 5. Effect of methanol requirement on FFA content reduction and conversion. Experimental parameters were fixed at 10 wt.% catalyst loading, 6 hr contact time and 60°C reaction temperature.

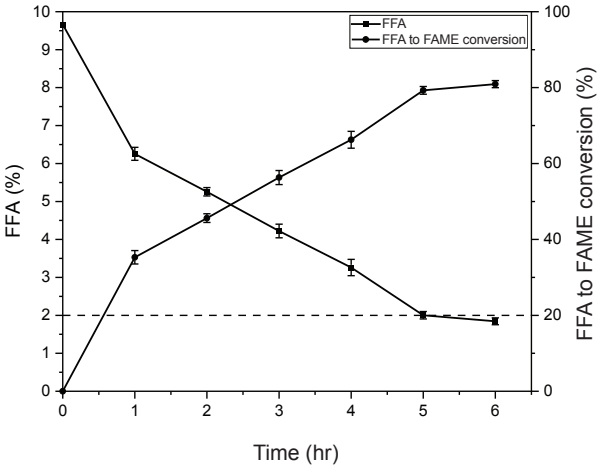

Figure 6. Effect of Fe_3O_4/PVA/PTSA catalyst contact time on FFA content reduction and conversion. Experimental parameters were fixed at 10 wt.% catalyst loading, 20:1 methanol-to-oil molar ratio and 60°C reaction temperature.

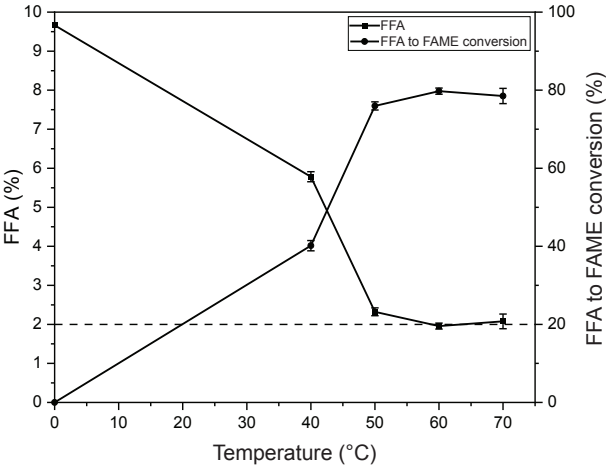

Figure 7. Effect of reaction temperature on FFA content reduction and conversion. Experimental parameters were fixed at 10 wt.% catalyst loading, 20:1 methanol-to-oil molar ratio and 5 hr contact time.

FFA conversion rate may be attributed to catalytic deactivation by water, by-product formation from the esterification reaction. To overcome this issue, the catalyst may be regenerated by re-sulphonation using PTSA (Cao *et al.*, 2021).

Evaluation of Reaction Kinetics and Thermodynamic Studies

The reaction kinetics and thermodynamic studies were presented for the FFA esterification reaction using Fe_3O_4/PVA/PTSA at the optimum reaction conditions at reaction temperatures of 40°C, 50°C and 60°C. Given that significant excess of methanol (20:1 molar ratio to oil) was used, and assuming the methanol concentration remained constant, the empirical data was fitted according to the pseudo first order kinetics based on a simple rate expression of the kinetic model (Hayyan *et al.*, 2023; Wang *et al.*, 2023). By plotting the rate constant (k) values against temperature, the activation energy (E_a) and frequency factor (A) were determined through the linearised form of the Arrhenius equation [Equation (2)].

$$k = Ae^{\frac{-E_a}{RT}} \tag{2}$$

Figure 9a depicts the Arrhenius plot with satisfactory coefficients of determination values ($R^2 > 0.9$) obtained. Here, the reaction kinetic factors of E_a and A values were calculated as 43.72 kJ/mol and 3.586/min respectively. The E_a values were in agreement with literature values on the esterification of low value oils using heterogeneous SACs between the range of 18.11-64.60 kJ/mol (Olagbende *et al.*, 2021; Zhang *et al.*, 2021).

Subsequently, the thermodynamic factors of the esterification reaction were studied through the Eyring-Polanyi model [Equation (3)]. The linearised plot of the Eyring-Polanyi model is expressed as Equation (4).

$$k = K\frac{k_B T}{h}e^{\left(\frac{\Delta G^\circ}{RT}\right)} \tag{3}$$

$$ln\left(\frac{k}{T}\right) = -\frac{\Delta H^\circ}{RT} + ln\left(\frac{k_B}{h}\right) + \frac{\Delta S^\circ}{R} + lnK \tag{4}$$

where, ΔH° is the standard enthalpy of the reaction system, ΔS° is the entropy of activation of the reaction system, k is the rate constant at temperature T, k_B is the Boltzmann constant, h is the Planck constant, K is the transmission coefficient ($K=1$), and R is the universal gas constant taken as 8.314 J/mol/K. The Gibbs free energy (ΔG°) was determined by Equation (5).

$$\Delta G^\circ = \Delta H^\circ - T\Delta S^\circ \tag{5}$$

The Eyring-Polanyi plot is illustrated in *Figure 9b*, showing satisfactory fitting based on the coefficients of determination values (R^2>0.9), and the thermodynamic parameters are presented in *Table 1*. Based on the results, the FFA esterification reaction using Fe_3O_4/PVA/PTSA was calculated as positive ΔH°, negative ΔS° and positive ΔG° values, which corresponds to the thermodynamics of the reaction process being dictated as endothermic, non-spontaneous and endergonic across the analysed temperature, respectively. The positive enthalpy values (ΔH°>0) dictate the requirement of external heat input for main product generation (FAME yield), attributed to the optimal reaction temperatures in FFA esterification. The results of this study were within range and in agreement with the thermodynamic parameters of SACs previously reported on the acid-catalysed esterification of FFA (Lieu *et al.*, 2016; Roslan *et al.*, 2022; Tang *et al.*, 2020).

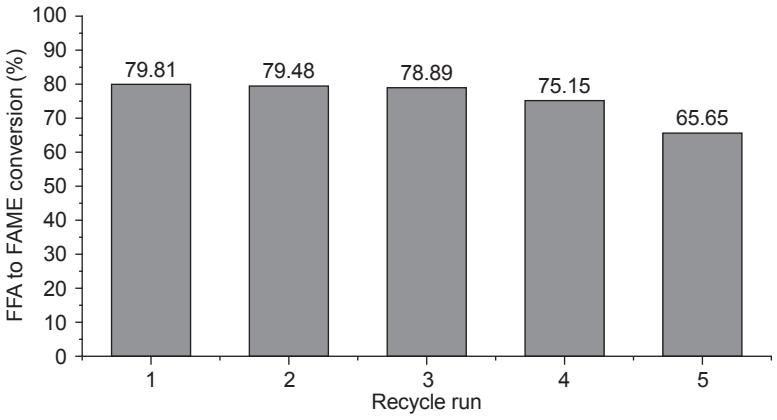

Figure 8. Evaluation of recyclability performance of Fe_3O_4/PVA/PTSA in FFA conversion.

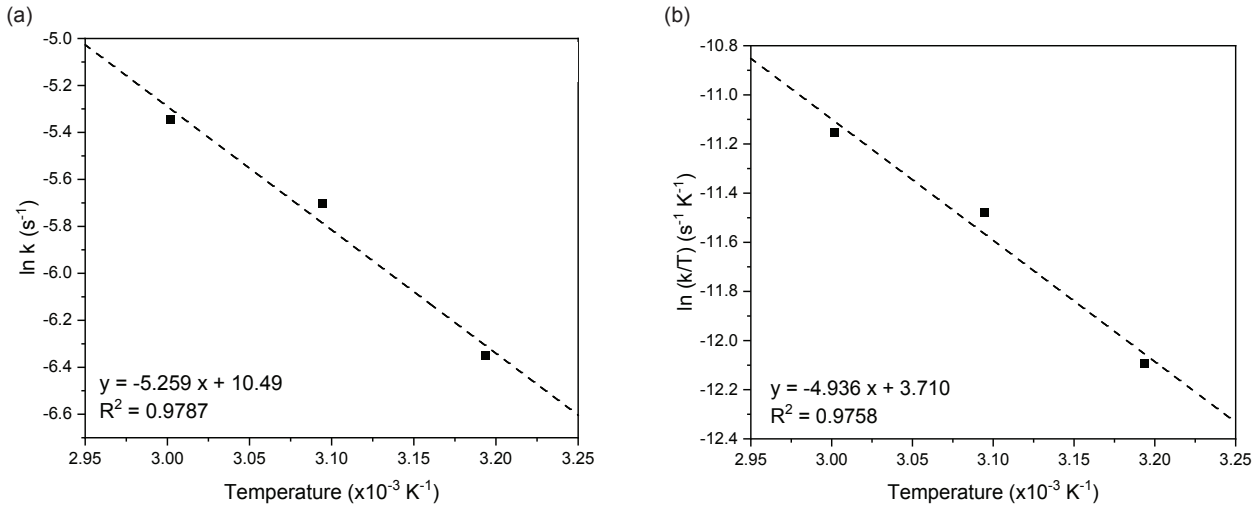

Figure 9. (a) Arrhenius plot; and (b) Eyring–Polanyi plot of temperature dependency in FFA esterification using Fe_3O_4/PVA/PTSA catalyst.

TABLE 1. VALUES OF THERMODYNAMIC FACTORS FOR THE FFA ESTERIFICATION REACTIONS CATALYSED BY Fe_3O_4/PVA/PTSA CATALYST

Standard enthalpy, ΔH° (kJ/mol)	Entropy of activation, ΔS° (kJ/mol)	Gibbs free energy, ΔG° (kJ/mol)			Coefficient of determination, R^2
		313.15 K	323.15 K	333.15 K	
41.04	-0.167	93.24	94.91	96.57	0.9758

CONCLUSION

In this study, sulphonic acids (BZSA, PTSA and SSA) and their DES counterparts (formed with PCM at a 3:1 molar ratio) were attempted to be supported on Fe_3O_4/PVA magnetic composites to yield heterogeneous SACs for the esterification of FFA in LPO. The screening results reveal that PTSA was compatible with the Fe_3O_4/PVA support material based on the catalytic activity in FFA esterification and that the pristine sulphonic acid components exhibited greater FFA conversion compared to the DES system. Subsequently, Fe_3O_4/PVA/PTSA was selected as the best performing catalyst for further optimisation in reaction conditions. At reaction conditions of 10 wt.% catalyst loading, 20:1 methanol-to-oil molar ratio, 5 hr of contact time and at 60°C, the LPO was pretreated to the FFA content value of 1.95%, corresponding to an FFA conversion of 79.81%. Additionally, the catalyst was recycled for five successive runs with fair stability and acceptable FFA conversion (>65%). The reaction kinetics revealed that the FFA esterification reaction using Fe_3O_4/PVA/PTSA follows the pseudo first order rate of reaction, requiring an activation energy of 43.72 kJ/mol. This study demonstrated the feasibility of certain sulphonic acids and DESs to be supported on the Fe_3O_4/PVA magnetic composite, with Fe_3O_4/PVA/PTSA being the viable catalyst choice for the pretreatment of low-quality oils through FFA esterification.

ACKNOWLEDGEMENT

The authors would like to acknowledge the grant provided by Universiti Malaya, RU Geran–Fakulti program – GPF015A-2023. The author Y. A. T. H. would like to extend their sincerest gratitude to Dr. Chan Mieow Kee and the Department of Chemical Engineering, SEGi University for providing assistance with laboratory facilities and equipment.

REFERENCES

Ali, R. M., Elkatory, M. R., & Hamad, H. A. (2020). Highly active and stable magnetically recyclable $CuFe_2O_4$ as a heterogenous catalyst for efficient conversion of waste frying oil to biodiesel. *Fuel*, *268*, 117297. https://doi.org/10.1016/j.fuel.2020.117297

Ali, S., Khan, S. A., Eastoe, J., Hussaini, S. R., Morsy, M. A., & Yamani, Z. H. (2018). Synthesis, characterization, and relaxometry studies of hydrophilic and hydrophobic superparamagnetic Fe_3O_4 nanoparticles for oil reservoir applications. *Colloids and Surfaces A: Physicochemical and Engineering Aspects*, *543*, 133–143. https://doi.org/10.1016/j.colsurfa.2018.02.002

American Oil Chemists Society (AOCS). (2017). *Official methods and recommended practices of the AOCS*.

Ba-Abbad, M. M., Benamour, A., Ewis, D., Mohammad, A. W., & Mahmoudi, E. (2022). Synthesis of Fe_3O_4 nanoparticles with different shapes through a co-precipitation method and their application. *JOM*, *74*(9), 3531–3539. https://doi.org/10.1007/s11837-022-05380-3

Bahadoran, A., Ramakrishna, S., Oryani, B., Al-Keridis, L. A., Nodeh, H. R., & Rezania, S. (2022). Biodiesel production from waste cooking oil using heterogeneous nanocatalyst-based magnetic polyaniline decorated with cobalt oxide. *Fuel*, *319*, 123858. https://doi.org/10.1016/j.fuel.2022.123858

Borton, J., Lopez, F. D. N., Doan, L., Holmes, W. E., & Benson, T. J. (2019). Conversion of high free fatty acid lipid feedstocks to biofuel using triazabicyclodecene catalyst (Homogeneous and heterogeneous). *Energy & Fuels*, *33*(4), 3322–3330. https://doi.org/10.1021/acs.energyfuels.9b00359

Cao, M., Peng, L., Xie, Q., Xing, K., Lu, M., & Ji, J. (2021). Sulfonated *Sargassum horneri* carbon as solid acid catalyst to produce biodiesel via esterification. *Bioresource Technology*, *324*, 124614. https://doi.org/10.1016/j.biortech.2020.124614

Chen, C., Wang, F., Li, Q., Wang, Y., & Ma, J. (2022). Embedding of SO_3H-functionalized ionic liquids in mesoporous MIL-101(Cr) through polyoxometalate bridging: A robust heterogeneous catalyst for biodiesel production. *Colloids and Surfaces A: Physicochemical and Engineering Aspects*, *648*, 129432. https://doi.org/10.1016/j.colsurfa.2022.129432

Chen, L., He, L., Zheng, B., Wei, G., Li, H., Zhang, H., & Yang, S. (2023). Bifunctional acid-activated montmorillonite catalyzed biodiesel production from non-food oil: Characterization, optimization, kinetic and thermodynamic studies. *Fuel Processing Technology*, *250*, 107903. https://doi.org/10.1016/j.fuproc.2023.107903

Fazelinia, F., Bayat, M., Nasri, S., Kamalzare, M., & Maleki, A. (2023). Chitosan@Tannic acid-supported Fe_3O_4 magnetic bionanocomposite as green and recyclable catalyst for the synthesis of Benzo[g]thiazolo[3,2-a] quinolones based on nitroketene N,S-Acetal. *Catalysis Surveys From Asia*, *27*(4), 391–405. https://doi.org/10.1007/s10563-023-09406-x

Gardy, J., Osatiashtiani, A., Céspedes, O., Hassanpour, A., Lai, X., Lee, A. F., Wilson, K., & Rehan, M. (2018). A magnetically separable SO_4/Fe-Al-TiO_2 solid acid catalyst for biodiesel production from waste cooking oil. *Applied Catalysis B: Environment and Energy*, *234*, 268–278. https://doi.org/10.1016/j.apcatb.2018.04.046

Ghorbani-Choghamarani, A., Taherinia, Z., & Tyula, Y. A. (2022). Efficient biodiesel production from oleic and palmitic acid using a novel molybdenum metal-organic framework as efficient and reusable catalyst. *Scientific Reports*, *12*(1), 10338. https://doi.org/10.1038/s41598-022-14341-4

Hayyan, A., Alam, M. Z., Mirghani, M. E., Kabbashi, N. A., Hakimi, N. I. N. M., Siran, Y. M., & Tahiruddin, S. (2010). Sludge palm oil as a renewable raw material for biodiesel production by two-step processes. *Bioresource Technology*, *101*(20), 7804–7811. https://doi.org/10.1016/j.biortech.2010.05.045

Hayyan, A., Qing, F. L. W., Salleh, M. Z. M., Basirun, W. J., Hamid, M. D., Saleh, J., Aljohani, A. S., Alhumaydhi, F. A., Zulkifli, M., Abdulmonem, W. A., Yeow, A. T., Nor, M. R. M., Hashim, M. A., & Al-Sabahi, J. N. (2023). Encapsulated paracetamol-based eutectic solvents for the treatment of low-grade palm oil mixed with microalgae oil. *Industrial Crops and Products*, *195*, 116322. https://doi.org/10.1016/j.indcrop.2023.116322

He, L., Chen, L., Zheng, B., Zhou, H., Wang, H., Li, H., Zhang, H., Xu, C. C., & Yang, S. (2023). Deep eutectic solvents for catalytic biodiesel production from liquid biomass and upgrading of solid biomass into 5-hydroxymethylfurfural. *Green Chemistry*, *25*(19), 7410–7440. https://doi.org/10.1039/d3gc02816j

Ibrahim, N. A., Rashid, U., Choong, T. S. Y., & Nehdi, I. A. (2020). Synthesis of nanomagnetic sulphonated impregnated Ni/Mn/Na_2SiO_3 as catalyst for esterification of palm fatty acid distillate. *RSC Advances*, *10*(10), 6098–6108. https://doi.org/10.1039/c9ra08115a

Kamalzare, M., Ahghari, M. R., Bayat, M., & Maleki, A. (2021). Fe_3O_4@chitosan-tannic acid bionanocomposite as a novel nanocatalyst for the synthesis of pyranopyrazoles. *Scientific Reports*, *11*(1), 20021. https://doi.org/10.1038/s41598-021-99121-2

Khan, Z., Javed, F., Shamair, Z., Hafeez, A., Fazal, T., Aslam, A., Zimmerman, W. B., & Rehman, F. (2021). Current developments in esterification

reaction: A review on process and parameters. *Journal of Industrial and Engineering Chemistry*, *103*, 80–101. https://doi.org/10.1016/j.jiec.2021.07.018

Krishnan, S. G., Pua, F., & Zhang, F. (2021). A review of magnetic solid catalyst development for sustainable biodiesel production. *Biomass and Bioenergy*, *149*, 106099. https://doi.org/10.1016/j.biombioe.2021.106099

Kurchania, R., Sawant, S. S., & Ball, R. J. (2014). Synthesis and characterization of magnetite/polyvinyl alcohol core-shell composite nanoparticles. *Journal of the American Ceramic Society*, *97*(10), 3208–3215. https://doi.org/10.1111/jace.13108

Lieu, T., Yusup, S., & Moniruzzaman, M. (2016). Kinetic study on microwave-assisted esterification of free fatty acids derived from *Ceiba pentandra* seed oil. *Bioresource Technology*, *211*, 248–256. https://doi.org/10.1016/j.biortech.2016.03.105

Liu, W., Wang, F., Meng, P., & Zang, S. (2020). Sulfonic acids supported on UIO-66 as heterogeneous catalysts for the esterification of fatty acids for biodiesel production. *Catalysts*, *10*(11), 1271. https://doi.org/10.3390/catal10111271

Lou, J., Babadi, M. R., Otadi, M., Tarahomi, M., Van Le, Q., Khonakdar, H. A., & Li, C. (2023). Agricultural waste valorization towards (nano) catalysts for the production of chemicals and materials. *Fuel*, *351*, 128935. https://doi.org/10.1016/j.fuel.2023.128935

Luo, N., Yang, Z., Tang, F., Wang, D., Feng, M., Liao, X., & Yang, X. (2019). Fe_3O_4/Carbon NanoDot hybrid nanoparticles for the indirect colorimetric detection of glutathione. *ACS Applied Nano Materials*, *2*(6), 3951–3959. https://doi.org/10.1021/acsanm.9b00854

Maleki, A., Niksefat, M., Rahimi, J., & Hajizadeh, Z. (2019). Design and preparation of Fe_3O_4@PVA polymeric magnetic nanocomposite film and surface coating by sulfonic acid via *in situ* methods and evaluation of its catalytic performance in the synthesis of dihydropyrimidines. *BMC Chemistry*, *13*(1), 19. https://doi.org/10.1186/s13065-019-0538-2

Maleki, B., Talesh, S. A., & Mansouri, M. (2022). Comparison of catalysts types performance in the generation of sustainable biodiesel via transesterification of various oil sources: A review study. *Materials Today Sustainability*, *18*, 100157. https://doi.org/10.1016/j.mtsust.2022.100157

Mandari, V., & Devarai, S. K. (2022). Biodiesel production using homogeneous, heterogeneous, and enzyme catalysts via transesterification and esterification reactions: A critical review. *BioEnergy Research*, *15*(2), 935–961. https://doi.org/10.1007/s12155-021-10333-w

Mok, C. F., Ching, Y. C., Osman, N. A. A., Muhamad, F., Junaidi, M. U. M., & Choo, J. H. (2020). Preparation and characterization study on maleic acid cross-linked poly(vinyl alcohol)/chitin/nanocellulose composites. *Journal of Applied Polymer Science*, *137*(35), 49044. https://doi.org/10.1002/app.49044

Olagbende, O. H., Falowo, O. A., Latinwo, L. M., & Betiku, E. (2021). Esterification of Khaya senegalensis seed oil with a solid heterogeneous acid catalyst: Modeling, optimization, kinetic and thermodynamic studies. *Cleaner Engineering and Technology*, *4*, 100200. https://doi.org/10.1016/j.clet.2021.100200

Perez, G. A. P., & Dumont, M. (2021). Polyvinyl sulfonated catalyst and the effect of sulfonic sites on the dehydration of carbohydrates. *Chemical Engineering Journal*, *419*, 129573. https://doi.org/10.1016/j.cej.2021.129573

Picciolini, E., Pastore, G., Del Giacco, T., Ciancaleoni, G., Tiecco, M., & Germani, R. (2023). Aquo-DESs: Water-based binary natural deep eutectic solvents. *Journal of Molecular Liquids*, *383*, 122057. https://doi.org/10.1016/j.molliq.2023.122057

Racar, M., Jerbić, I. Š., Glasovac, Z., & Jukić, A. (2023). Guanidine catalysts for biodiesel production: Activity, process modelling and optimization. *Renewable Energy*, *202*, 1046–1053. https://doi.org/10.1016/j.renene.2022.11.044

Rahimi, J., Niksefat, M., & Maleki, A. (2020a). Fabrication of Fe_3O_4@PVA-CU nanocomposite and its application for facile and selective oxidation of alcohols. *Frontiers in Chemistry*, *8*. https://doi.org/10.3389/fchem.2020.00615

Rahimi, J., Taheri-Ledari, R., Niksefat, M., & Maleki, A. (2020b). Enhanced reduction of nitrobenzene derivatives: Effective strategy executed by Fe_3O_4/PVA-10%Ag as a versatile hybrid nanocatalyst. *Catalysis Communications*, *134*, 105850. https://doi.org/10.1016/j.catcom.2019.105850

Rokhum, S. L., Changmai, B., Kress, T., & Wheatley, A. E. (2022). A one-pot route to tunable sugar-derived sulfonated carbon catalysts for

sustainable production of biodiesel by fatty acid esterification. *Renewable Energy*, *184*, 908–919. https://doi.org/10.1016/j.renene.2021.12.001

Roslan, N. A., Abidin, S. Z., Abdullah, N., Osazuwa, O. U., Rasid, R. A., & Yunus, N. M. (2022). Esterification reaction of free fatty acid in used cooking oil using sulfonated hypercrosslinked exchange resin as catalyst. *Process Safety and Environmental Protection*, *180*, 414–424. https://doi.org/10.1016/j.cherd.2021.10.020

Swami, P., Rathod, S., Choudhari, P., Patil, D., Patravale, A., Nalwar, Y., Sankpal, S., & Hangirgekar, S. (2023). Fe_3O_4@SiO_2@TDI@DES: A novel magnetically separable catalyst for the synthesis of oxindoles. *Journal of Molecular Structure*, *1292*, 136079. https://doi.org/10.1016/j.molstruc.2023.136079

Tang, Z., Lim, S., Pang, Y., Shuit, S., & Ong, H. (2020). Utilisation of biomass wastes based activated carbon supported heterogeneous acid catalyst for biodiesel production. *Renewable Energy*, *158*, 91–102. https://doi.org/10.1016/j.renene.2020.05.119

Tropecêlo, A. I., Caetano, C. S., Caiado, M., & Castanheiro, J. E. (2016). Biodiesel production from waste cooking oil over sulfonated catalysts. *Energy Sources Part A: Recovery Utilization and Environmental Effects*, *38*(2), 174–182. https://doi.org/10.1080/15567036.2012.747035

Wang, H., Zhou, H., Yan, Q., Wu, X., & Zhang, H. (2023). Superparamagnetic nanospheres with efficient bifunctional acidic sites enable sustainable production of biodiesel from budget non-edible oils. *Energy Conversion and Management*, *297*, 117758. https://doi.org/10.1016/j.enconman.2023.117758

Wang, R., Qin, H., Song, Z., Cheng, H., Chen, L., & Qi, Z. (2022). Toward reactive extraction processes for synthesizing long-chain esters: A general approach by tuning bifunctional deep eutectic solvent. *Chemical Engineering Journal*, *445*, 136664. https://doi.org/10.1016/j.cej.2022.136664

Wang, Y., Meng, X., Tian, Y., Kim, K. H., Jia, L., Pu, Y., Leem, G., Kumar, D., Eudes, A., Ragauskas, A. J., & Yoo, C. G. (2021). Engineered sorghum bagasse enables a sustainable biorefinery with p-hydroxybenzoic acid-based deep eutectic solvent. *ChemSusChem*, *14*(23), 5235–5244. https://doi.org/10.1002/cssc.202101492

Wang, Y., Wang, D., Tan, M., Jiang, B., Zheng, J., Tsubaki, N., & Wu, M. (2015). Monodispersed hollow SO_3H-functionalized carbon/silica as efficient solid acid catalyst for esterification of oleic acid. *ACS Applied Materials & Interfaces*, *7*(48), 26767–26775. https://doi.org/10.1021/acsami.5b08797

Wang, Y., Yang, X., Xu, J., Wang, H., Wang, Z., Zhang, L., Wang, S., & Liang, J. (2019). Biodiesel production from esterification of oleic acid by a sulfonated magnetic solid acid catalyst. *Renewable Energy*, *139*, 688–695. https://doi.org/10.1016/j.renene.2019.02.111

Xie, W., & Li, J. (2023). Magnetic solid catalysts for sustainable and cleaner biodiesel production: A comprehensive review. *Renewable and Sustainable Energy Reviews*, *171*, 113017. https://doi.org/10.1016/j.rser.2022.113017

Xie, W., & Wang, H. (2020). Immobilized polymeric sulfonated ionic liquid on core-shell structured Fe_3O_4/SiO_2 composites: A magnetically recyclable catalyst for simultaneous transesterification and esterifications of low-cost oils to biodiesel. *Renewable Energy*, *145*, 1709–1719. https://doi.org/10.1016/j.renene.2019.07.092

Yu, J., Wang, Y., Sun, L., Xu, Z., Du, Y., Sun, H., Li, W., Luo, S., Ma, C., & Liu, S. (2021). Catalysis preparation of biodiesel from waste schisandra chinensis seed oil with the ionic liquid immobilized in a magnetic catalyst: Fe_3O_4@SiO_2@[C4mim]HSO_4. *ACS Omega*, *6*(11), 7896–7909. https://doi.org/10.1021/acsomega.1c00504

Yusuf, B. O., Oladepo, S. A., & Ganiyu, S. A. (2023). Biodiesel production from waste cooking oil via β-zeolite-supported sulfated metal oxide catalyst systems. *ACS Omega*, *8*(26), 23720–23732. https://doi.org/10.1021/acsomega.3c01892

Zhang, H., Gao, J., Zhao, Z., Chen, G. Z., Wu, T., & He, F. (2016). Esterification of fatty acids from waste cooking oil to biodiesel over a sulfonated resin/PVA composite. *Catalysis Science & Technology*, *6*(14), 5590–5598. https://doi.org/10.1039/c5cy02133b

Zhang, Q., Lei, Y., Li, L., Lei, J., Hu, M., Deng, T., Zhang, Y., & Ma, P. (2023). Construction of the novel PMA@Bi-MOF catalyst for effective fatty acid esterification. *Sustainable Chemistry and Pharmacy*, *33*, 101038. https://doi.org/10.1016/j.scp.2023.101038

Zhang, Q., Luo, Q., Wu, Y., Yu, R., Cheng, J., & Zhang, Y. (2021). Construction of a Keggin heteropolyacid/Ni-MOF catalyst for esterification of fatty acids. *RSC Advances*, *11*(53), 33416–33424. https://doi.org/10.1039/d1ra06023f

Zheng, B., Chen, L., He, L., Wang, H., Li, H., Zhang, H., & Yang, S. (2024). Facile synthesis of chitosan-derived sulfonated solid acid catalysts for realizing highly effective production of biodiesel. *Industrial Crops and Products*, *210*, 118058. https://doi.org/10.1016/j.indcrop.2024.118058

Zhong, Y., Zhang, P., Zhu, X., Li, H., Deng, Q., Wang, J., Zeng, Z., Zou, J., & Deng, S. (2019). Highly efficient alkylation using hydrophobic sulfonic acid-functionalized biochar as a catalyst for synthesis of high-density biofuels. *ACS Sustainable Chemistry & Engineering*, *7*(17), 14973–14981. https://doi.org/10.1021/acssuschemeng.9b03190

Zhou, R., Ye, B., & Hou, Z. (2023). Synthesis of acetylglycerols over hierarchical porous sulfonated polymeric solid acid. *Fuel*, *354*, 129325. https://doi.org/10.1016/j.fuel.2023.129325

Journal of Oil Palm Research Vol. 37 (3) September 2025 p. 533-548
DOI: https://doi.org/10.21894/jopr.2025.0008

BIODIESEL PRODUCTION FROM PALM STEARIN PROCESS OPTIMISATION USING RESPONSE SURFACE METHODOLOGY (RSM)

P GOWTHAM[1]*; K PITCHANDI[2] and V MANIENIYAN[1]

ABSTRACT

The purpose of this study is to optimise biodiesel production from palm stearin using the Box-Behnken design in response surface methodology (RSM) for three key process parameters: Methanol volume, catalyst concentration and reaction time. The methanol (A) was fixed at three levels: -1, 0, and +1, corresponding to 200, 225 and 250 mL, respectively; the catalyst (B) concentration was varied between 8, 10, and 12 g; and the reaction time (C) ranged from 45-90 min. The experiments were conducted and analysed using Design Expert software (version 13) to maximise biodiesel yield. The highest yield of palm stearin methyl ester (910 mL, 89.25% yield) was achieved with 225 mL methanol, 10 g catalyst and a reaction time of 60 min. The optimised model predicted a yield of 913.4 mL, demonstrating strong agreement with experimental results. This study is significant in promoting more sustainable biodiesel production by improving efficiency and reducing both operational costs and environmental impact. By optimising process parameters, this work addresses the need for cost-effective renewable fuel alternatives, contributing to the long-term commercial viability of biodiesel in the energy market.

Keywords: biodiesel, Box-Behnken Design, catalyst, RSM, transesterification.

Received: 3 January 2024; **Accepted:** 22 November 2024; **Published online:** 20 February 2025.

INTRODUCTION

To address energy security concerns and reduce the environmental impact of fossil fuels, the search for sustainable and renewable energy sources has become crucial. Biodiesel, derived from animal fats and vegetable oils, presents a viable alternative to conventional fossil fuels by lowering greenhouse gas emissions and reducing reliance on non-renewable resources. Palm stearin, a product of palm oil fractionation with high saturated fat content, has been identified as a potential feedstock for biodiesel production. Sustainable palm oil practices are also being promoted to encourage the use of this renewable resource.

[1] Department of Mechanical Engineering, Government College of Engineering Srirangam, Tamil Nadu, India.

[2] Department of Mechanical Engineering, Sri Venkateswara College of Engineering, Tamil Nadu, India.

* *Corresponding author e-mail: gowthamvortex@gmail.com*

Vegetable oils and fats often contain impurities like gums, free fatty acids (FFA), and metal components that must be removed to improve oil quality (Adepoju *et al.,* 2022). Acid oil, a by-product of oil refining, is a low-cost alternative to refined oils and is suitable for biodiesel production when impurities are reduced (Muthuswamy & Veerasigamani, 2020).

Biodiesel produced from waste oil can match the quality of petroleum diesel, and palm stearin is a favourable feedstock for its synthesis. Extracted from the oil palm tree (*Elaeis guineensis*), particularly in Southeast Asia, palm stearin offers high yields at a lower cost than other feedstocks. Its composition, rich in saturated fatty acids, enhances the transesterification process, making it suitable for biodiesel production.

Edible palm stearin, with its high saturated fat content and solidification properties, was chosen over alternatives like palm kernel oil (PKO), palm oil mill effluent (POME) and palm fatty acid distillate (PFAD). Palm stearin's saturated fats, especially palmitic acid, provide higher cetane numbers,

improving combustion and ignition. Its solid fraction enhances cold flow properties, lowering the cloud point and improving performance in colder climates (Hazrat *et al.,* 2020). In contrast, PKO's lower saturated fat content may require additional processing to meet biodiesel standards. POME and PFAD, while potential feedstocks, contain impurities and FFA that complicate biodiesel production, raising costs (Zahan & Kano, 2018).

Biodiesel made from palm stearin, a by-product of the palm oil industry, offers significant environmental advantages, such as reducing greenhouse gas emissions and contributing to waste management by converting a low-value material into a renewable energy source. Additionally, palm stearin is a cost-effective feedstock compared to virgin oils, lowering the overall production costs and improving the market competitiveness of biodiesel. These factors not only make biodiesel from palm stearin environmentally sustainable but also economically viable, aligning with global efforts to reduce carbon emissions and promote renewable energy.

Jatropha oil may yield higher oil content, but palm stearin, as a by-product of palm oil processing, offers a more cost-effective and sustainable alternative. Waste oils, although potentially cheaper, often require more complex processing due to contamination and impurities.

Transesterification is a chemical process used in biodiesel production to convert vegetable oils, used frying oil and animal fats into biodiesel and glycerol. This reaction involves the use of an alcohol, typically ethanol or methanol, in the presence of a catalyst such as potassium hydroxide (KOH) or sodium hydroxide (NaOH), to produce biodiesel (Rajali *et al.,* 2022). Upon completion of the transesterification process, the biodiesel can either be used alone or blended with petroleum diesel in various proportions. Single-stage processes commonly use alkali-based catalysts, while two-stage methods may incorporate both alkali and acid catalysts.

Biodiesel exhibits physical properties similar to petroleum diesel, making it suitable for compression ignition (CI) engines without significant modifications (Sonachalam *et al.,* 2020). It can be used as a standalone fuel or blended with diesel in mixes such as B5 or B20, providing benefits like a higher cetane number, better combustion and reduced emissions of particulate matter and carbon monoxide (Ranjan *et al.,* 2022). However, biodiesel has slightly less energy content than petroleum diesel, potentially leading to lower fuel efficiency (Deivajothi *et al.,* 2018) and tends to produce higher nitrogen oxide (NOx) emissions, which can contribute to smog formation (Razak *et al.,* 2021). These challenges can be mitigated with technologies like selective catalytic reduction (SCR) systems.

Using palm stearin for biodiesel production offers environmental advantages by reducing waste and promoting a circular economy, as palm stearin is a by-product of palm oil processing (Bustamam *et al.,* 2022). Biodiesel derived from palm stearin also exhibits favourable combustion properties, including lower greenhouse gas emissions compared to traditional diesel fuels. These properties make palm stearin a promising feedstock for biodiesel synthesis, contributing to sustainable energy solutions.

KOH is widely used as a catalyst in biodiesel production due to its high reactivity, cost-effectiveness, and established industrial use. KOH efficiently catalyses the transesterification of triglycerides, accelerating reaction kinetics and reducing by-products, which simplifies downstream purification (Zhang *et al.,* 2019). Additionally, KOH is versatile across various feedstocks, including animal fats and vegetable oils. It is also more effective than NaOH, as potassium soaps formed during transesterification are softer, leading to less clogging during separation.

The next section will focus on the Box-Behnken design, a response surface methodology (RSM)-based experimental design, used to optimise key parameters in biodiesel production. Experiments are conducted by varying methanol volume, catalyst concentration and reaction time. RSM aims to optimise these process parameters, solving regression model equations using Design Expert (version 13) software and analysing three-dimensional surface plots to maximise biodiesel yield. Analysis of variance (ANOVA) helps identify the dominant factors influencing biodiesel production efficiency.

Design of Experiments (DOE)

Simsek *et al.* (2022) used the DOE as a systematic approach to test and analyse the effects of various factors on the outcome of a product or process. DOE assists in identifying significant factors and their optimal levels by systematically adjusting factor levels. This method enables the examination of specific results under various experimental conditions, facilitating the improvement of the process (Gupta *et al.,* 2022). ANOVA is commonly employed in experimental designs to visually evaluate the effects of different factors and their interactions on the response variables (Parak *et al.,* 2022).

Response Surface Methodology (RSM)

RSM is a statistical technique used to model and optimise the relationship between independent variables and a response. In biodiesel synthesis from palm stearin, RSM helps optimise key parameters

such as reaction time, catalyst concentration and methanol concentration to maximise yield. Experimental designs like the Box-Behnken Design (BBD) vary these variables systematically. A polynomial model is then used to represent the relationship, with regression analysis identifying the optimal conditions. The goal is to reduce the number of experiments while effectively exploring factor ranges.

Once optimal conditions are determined, confirmatory experiments validate the results to ensure reliability for real-world applications (Buasri *et al.,* 2024; Loryuenyong *et al.,* 2024; Yusoff *et al.,* 2022). Overall, RSM provides a systematic method for enhancing biodiesel production by building predictive models and improving yield and quality (Karimi & Saidi, 2022; Ngige *et al.,* 2023).

Box-Behnken Design (BBD)

BBD is a widely applied response surface design (RSD) in statistics, commonly used in the DOE to represent the relationships between multiple input factors and one or more output variables. The BBD offers advantages over full factorial designs because it requires fewer experiments while still providing reliable estimates of variable interactions (Manimaran *et al.,* 2022). This design proves particularly useful for determining the optimal conditions in product development and process optimisation.

BBD functions by selecting a set of independent variables, or factors, and assigning three levels to each-usually at the midpoint of the desired range (Kober *et al.,* 2022). These levels are then combined to create a subset of possible experiments, each exploring different combinations of factors. The value of this approach lies in its ability to optimise a response variable by analysing the interactions between input factors and output responses (Joorasty *et al.,* 2022).

The authors chose BBD over Central Composite Design (CCD) for several reasons: BBD requires fewer experimental runs, making it more efficient, especially when resources are limited. Additionally, BBD lacks axial points, which simplifies the interpretation of interactions among variables. It is well-suited for fitting second-order (quadratic) models, effectively capturing the relationships among methanol volume, catalyst quantity and reaction time without risking overfitting. BBD also provides a balanced design, ensuring equal examination of factors and allowing for flexibility in factor levels, enhancing the ability to identify optimal conditions for biodiesel production. Overall, BBD offers a robust and straightforward framework for this study's objectives.

In summary, applying BBD to optimise biodiesel synthesis from palm stearin is a pragmatic and effective strategy, especially considering the complexity of the process and resource constraints. Study by Buasri *et al.* (2023) demonstrates the efficacy of BBD in similar scenarios, highlighting its utility in achieving optimal experimental designs.

The novelty of this study lies in the comprehensive optimisation of palm stearin transesterification processes using RSM and BBD. While extensive research exists on biodiesel synthesis from palm oil and other raw materials, the potential of palm stearin-a by-product of palm oil fractionation-remains underexplored. This study identifies the most favourable conditions for biodiesel production while also enhancing the sustainable use of palm stearin, thereby increasing the value of a typically low-value by-product.

In addition, the application of RSM and BBD in this study provides a systematic and efficient approach for evaluating the combined effects of key process variables-namely methanol concentration, catalyst (KOH) loading and reaction time-on biodiesel production. This methodology allows for the identification of optimal conditions that maximise biodiesel yield while minimising the consumption of reactants and energy.

This study aimed to improve the transesterification process for biodiesel production from palm stearin through a systematic experimental methodology. A BBD was employed within the framework of RSM to model the interactions among critical process variables (methanol volume, catalyst quantity and reaction time) and their effects on biodiesel yield. We developed a quadratic model to predict optimal conditions for maximum biodiesel output. The research also involved an analysis of the physicochemical properties of the produced biodiesel to evaluate its suitability for practical applications. Overall, this study sought to enhance the understanding of biodiesel optimisation and to establish a more efficient production process using palm stearin as a feedstock.

MATERIALS AND METHODS

Materials

Fractionation is a process that yields palm stearin, a solid fraction of palm oil. Fractionation involves heating and cooling palm oil to separate its various components according to their melting points. Palm stearin has a higher melting point than other fractions of palm oil, such as palm olein and is therefore solid at room temperature.

The palm stearin used in this study was procured from Murugan Oil Mill, Namakkal, India. The chemicals used in the process were methanol

with a purity of 99.85% and grade AA, and KOH pellets with a purity of 85.00%. The chemicals, methanol and KOH, were obtained from Blulux Laboratories in Faridabad, India and Chemind Laboratory Chemicals in Thrissur, India respectively.

Palm stearin was stored in airtight containers at a temperature below its melting point of 52°C to maintain its solid state. The containers of palm stearin were placed in a dry environment to prevent moisture absorption and air exposure. Moisture can lead to hydrolysis, forming FFA that negatively affect the transesterification process (Bustamam *et al.*, 2022). To avoid contamination, handling and transferring of palm stearin was done using a clean, stainless-steel ladle.

Palm stearin was stored in airtight containers at a temperature below its melting point of 52°C to maintain its solid state. The containers of palm stearin were placed in a dry environment to prevent moisture absorption and air exposure. Moisture can lead to hydrolysis, forming FFA that negatively affect the transesterification process (Bustamam *et al.*, 2022). To avoid contamination, transferring and handling palm stearin was done by using a clean, stainless-steel ladle.

Biodiesel Production by Transesterification Method

The equipment used for the transesterification reaction consisted of a 1,000 mL Erlenmeyer flask, a thermometer and a magnetic stirrer. The palm stearin was originally in a solid state. Every sample preparation began with melting palm stearin at 50°C and pouring 1,000 mL of the melted palm stearin into an Erlenmeyer flask. We blended the melted palm stearin with the homogenous potassium methoxide solution, which was prepared by reacting the catalyst KOH and methanol, and the reaction mixture in the flask was subsequently stirred using a magnetic stirrer. The temperature of the reaction mixture was maintained below 60°C (the boiling point of methanol).

After the specified reaction time (45, 60, or 90 min), the reaction products (methyl ester and glycerol) were transferred to a separating funnel and allowed to settle for 24 hr. Then, high-density glycerol settled at the bottom of the funnel and was removed using a valve in the separator funnel. The methyl ester phase was washed with water to eliminate any unwanted impurities. Then the methyl ester was heated to 105°C to remove any moisture and to obtain pure biodiesel. The schematic diagram of the transesterification process is shown in *Figure 1*. The physicochemical properties of the produced biodiesel were determined using the standard methods mentioned in *Table 1*.

The characterisation of biodiesel was conducted using gas chromatography-mass spectrometry (GC-MS) to identify the fatty acid methyl esters (FAME) content. The Agilent 8890 GC System (Agilent Technologies, Santa Clara, CA, USA), equipped with a quadrupole mass selective (Agilent 5977B MSD) detector, was employed for capillary GC/MS analysis. A DB-5MS capillary column (30.00 m, 0.25 mm ID, 0.25 µm film thickness) was used for the separation. The injector was operated in split mode with a split ratio of 7500:1 and the injection volume was set at 1 µL.

The column temperature sequence involves holding the initial temperature at 60°C for 2 min, then increasing it by 10°C/min to 200°C and holding it for 5 min. Lastly, the temperature is increased by 5°C/min to 280°C and held for 10 min. Helium, with a constant flow rate of 1 mL/min, served as the carrier gas. In mass spectroscopy, the electron impact mode operates at 70 eV. The quadrupole temperature at 150°C, the ion source temperature at 230°C, and the transfer line temperature at 280°C are maintained. Mass range in full scan mode from m/z 50-550 to prevent solvent interference, with a solvent delay of 3 min is done.

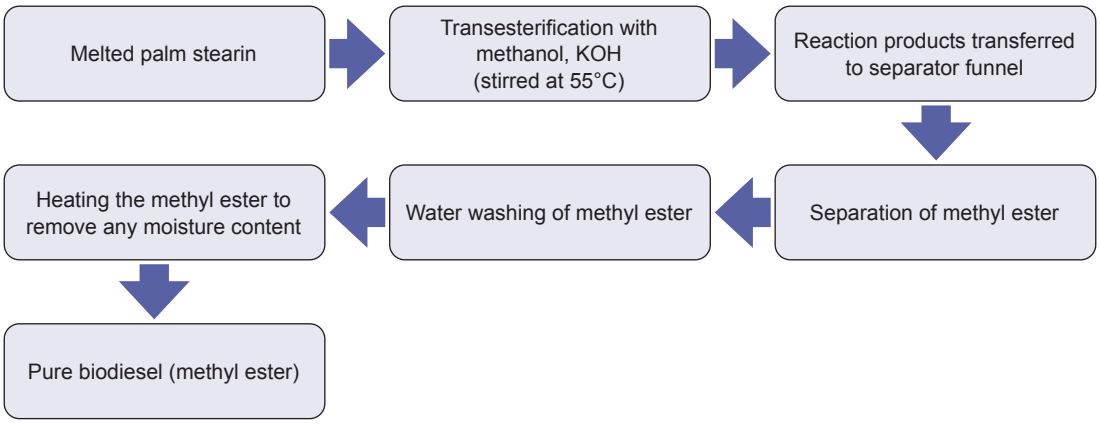

Figure 1. Schematic diagram of the transesterification process.

A calibration curve is generated by preparing a set of fatty acid methyl ester (FAME) standards in hexane at five different concentrations. The concentrations are 0.1, 0.2, 0.5, 1.0 and 2.0 mg/mL. To make the standard solutions, a concentrated FAME solution is diluted with hexane and then put through a 0.45 µm PTFE syringe filter before it is analysed. 1 µL of each standard solution was injected into the GC/MS system, and the peak areas corresponding to each concentration were recorded. Agilent MassHunter software conducts the data acquisition and processing. The compounds are identified by comparing retention times and mass spectra with standards and the NIST library.

Experimental Conditions by BBD for Biodiesel Yield

The three-level, two-factor BBD was identified as appropriate for designing the experimental settings in this research. Methanol (A) volume was varied at three levels: 200 (-1), 225 (0) and 250 mL (+1). The catalyst (B) was set at 8 (-1), 10 (0) and 12 g (+1). Similarly, reaction time (C) was tested at three durations: 45 (-1), 60 (0) and 90 min (+1). The experimental conditions proposed by RSM for biodiesel yield, in coded values, are presented in *Table 2*.

Statistical Summary of Model

In the present study, a quadratic model was selected to fit the experimental data based on statistical indicators, such as R^2 and adjusted R^2 (Adj-R^2). Although a cubic model demonstrated higher R^2 and Adj-R^2 values, aliasing problems hindered the distinction between the individual effects of the variables, thereby making the cubic model unsuitable. The linear relationship yielded R^2 and Adj-R^2 values of 0.2126 and 0.0960, respectively, clearly indicating its inadequacy for modelling the experimental data. Therefore, the quadratic model was determined to be the most appropriate, providing a better fit with an R^2 of 0.9967 and an Adj-R^2 of 0.9812 at a 99% confidence level. *Table 3* shows that the quadratic model fits the data significantly better than the linear or cubic models, which supports its choice for further analysis.

TABLE 1. DESCRIPTION OF STANDARD METHODS OF TESTING PARAMETERS

No.	Test parameters	Methods	Description
1.	Ash content	ASTM D482-13	The ash content was determined by weighing the residue remaining after the combustion of the biodiesel sample at 775°C.
2.	Density @ 15°C	IS:1448 Part 32: 2019	The density of the biodiesel was measured using a hydrometer at 15°C.
3.	Moisture content	IS:1448 Part 40: 2015	The moisture content was determined using the Karl Fischer titration method.
4.	Kinematic viscosity @ 40°C	ASTM D 445: 2015	The kinematic viscosity of the biodiesel was measured at 40°C using a capillary viscometer.
5.	Cetane index	ASTM D976-06	The cetane index was calculated based on the density and distillation range of the biodiesel.
6.	Acidity	IS:1448 Part 2: 2007	The acidity of the biodiesel was measured by titration with KOH.
7.	Sulphur content	IS:1448 Part 33: 1991	The sulphur content was determined using an X-ray fluorescence spectrometer.
8.	Flash point	IS 1448 Part 20: 1998	The flash point of the biodiesel was determined using a Pensky-Martens closed cup tester.
9.	Fire point	IS 1448 Part 20: 1998	The fire point was measured as the temperature at which the biodiesel produced a flame when ignited.
10.	Sulphated ash	ASTM D874-13	The sulphated ash content was measured by combustion of the sample and subsequent treatment with sulfuric acid.
11.	Relative density @ 15°C	IS:1448 Part 32: 2019	The relative density of the biodiesel was determined using a hydrometer at 15°C.
12.	Net calorific value	IS:1448 Part 6: 1984	The net calorific value was measured using a bomb calorimeter.

TABLE 2. BBD PROPOSED EXPERIMENTAL SETTINGS FOR BIODIESEL YIELD

Variable	Real values			
	Code	-1	0	1
Methanol (mL)	A	200	225	250
Catalyst (g)	B	8	10	12
Reaction time (min)	C	45	60	90

RESULTS AND DISCUSSION

Fit Statistics

Table 4 presents the fit statistics derived from Design Expert version 13. The close agreement between the Adj-R^2 (0.9967) and predicted R^2 (0.9812) confirms the robustness of the quadratic model. The adequate precision value of 57.8018, well above the threshold of 4, demonstrates a strong signal-to-noise ratio, which is crucial for model accuracy in navigating the design space. *Table 5* presents the experimental conditions proposed by the BBD for optimising biodiesel yield. It includes both coded and actual values for methanol, catalyst and reaction time, as well as the actual and predicted yields. The strong correlation between the actual and predicted biodiesel yields further validates the model's reliability.

Based on the model evaluation, the quadratic model [Equation (1)], expressed in coded terms, is presented below:

$$\text{Biodiesel yield} = 910.00 + 99.56(A) + 75.63(B) + 82.66(C) + 75.60(A*B) + 65.00(A*C) + 51.75\,(B*C) - 20.01(A)^2 - 13.97(B)^2 - 24.39(C)^2 \quad (1)$$

Equation (1) illustrates the relationship between biodiesel yield and the three key process factors: Methanol (A), catalyst (B) and reaction time (C). The positive coefficients of the linear and interaction terms indicate that increasing the factors, within the tested range, contributes positively to biodiesel yield.

TABLE 3. STATISTICAL SUMMARY

Source	Sequential *p*-value	Adj-R^2	Predicted R^2	
Linear	0.1384	0.2126	0.0960	
Quadratic	**< 0.0001**	**0.9967**	**0.9812**	**Suggested**
Cubic		1.0000		Aliased

TABLE 4. FIT STATISTICS WERE OUTPUT BY DESIGN EXPERT VERSION 13

Standard deviation	4.87	**R^2**	0.9988
Mean	790.67	**Adj-R^2**	0.9967
Coefficient of variation (%)	0.6164	**Predicted R^2**	0.9812
		Adequate precision	57.8018

TABLE 5. EXPERIMENTAL CONDITIONS PROPOSED BY BBD

Run	Coded values of variables			Actual level of variable			Actual	Predicted
	Methanol (mL)	Catalysts (g)	Reaction time (min)	Methanol (mL)	Catalysts (g)	Reaction time (min)		
1	-1	0	1	200	10	90	690	691.25
2	0	-1	1	225	8	90	745	748.13
3	-1	1	0	200	12	60	705	708.13
4	1	1	0	250	12	60	890	894.38
5	-1	0	-1	200	10	45	680	680.00
6	1	0	1	250	10	90	850	850.00
7	0	0	0	225	10	60	910	913.40
8	1	0	-1	250	10	45	760	758.75
9	0	0	0	225	10	60	910	913.40
10	1	-1	0	250	8	60	780	776.88
11	0	-1	-1	225	8	45	720	724.38
12	-1	-1	0	200	8	60	730	725.63
13	0	0	0	225	10	60	910	913.40
14	0	1	-1	225	12	45	750	746.88
15	0	1	1	225	12	90	830	825.63

The equation, expressed in the terminology of coded factors, can be applied to predict responses at different levels of each factor. By default, a high level of the factors is coded as +1, while a low level is coded as -1. By correlating the factor coefficients, the coded equation can be used to calculate the relative significance of the factors. In terms of actual factors, this same equation is capable of estimating responses at different levels of each factor. The levels for each factor must be indicated in their original units. Therefore, the coefficients are adjusted to fit the units of each factor, and the correlation coefficient is assessed at the design centre point. Thus, an equation should be used to calculate the comparative impact of each variable.

Model Accuracy Check

Table 6 displays the ANOVA results for the obtained model. ANOVA is an analytical technique that uses a t-test and an F-test to conclude the significance of a model and its variables. Using a *p*-value threshold, the Student's t-test was applied to evaluate the significance of the correlation coefficients. Larger F-values and smaller *p*-values generally demonstrate significant coefficient conditions. The F-value, standing at 471.23 with a *p*-value below 0.0001, indicates that only a minuscule fraction of the variability could justify such a significant F-value. Significant model terms have *p*-values below 0.0500. In this case, significant model terms include A, B, C, AB, AC, BC, A^2, B^2 and C^2. Model terms are not significant if the *p*-value is greater than 0.1000. Model reduction may be helpful if the model has many superfluous terms (excluding those required to maintain hierarchy).

The RSM design predicts a biodiesel yield value of 913.40 mL, which corresponds to a yield percentage of 89.59%, under conditions of 225 mL of methanol, a catalyst concentration of 10 g and a reaction time of 60 min. According to *Figure 2*, the desirability value is 1 under these conditions, with a biodiesel yield of 910 mL, equating to a yield percentage of 89.25%. In contrast, Hussanai and Kittisak (2023) predicted the highest yield of 96.73% and achieved a yield percentage of 92.74% in their experiment on the transesterification of palm oil with KOH catalyst supported on palm kernel shell ash. The RSM predicted value of biodiesel yield is found to be 99% accurate compared to the experimental result.

To establish an adequate model, an accuracy check is necessary. The comparison of anticipated and experimental biodiesel yields serves as evidence for the model's accuracy. The linear relationship between experimental and predicted biodiesel yield is shown in *Figure 3a.* A normal residual plot was also obtained between internally studentised residuals and normal probability (%). The internal residuals can be used to calculate the standard deviations between the predicted and experimental values. The residuals are then analysed to determine if the model aligns with the ANOVA interpretation. The relationship between the internally studentised residuals and normal probability (%) is depicted in *Figure 3b.* The straight line indicates that no reaction conversion is needed and that normality is not affected.

Response Analysis

Figure 4 depicts the interactions between biodiesel yield and these three factors. Each graph represents the impact of two parameters over their respective investigated intervals, with the third parameter set to zero. The response surface illustrates each factor's tendency to affect biodiesel yield. The contour plot's shape reveals the type and extent of factor interactions. An elliptical contour plot suggests a significant interaction, while a circular contour plot signifies a minor effect (Khan *et al.*, 2022).

TABLE 6. ANOVA CONSEQUENCES FOR THE OBTAINED MODEL

Source	Sum of squares	Degree of freedom	Mean square	F-value	*p*-value	Characteristic
Model	1.007E+05	9	11,191.62	471.23	< 0.0001	Significant
A-A	28,203.12	1	28,203.12	1,187.50	< 0.0001	
B-B	5,000.00	1	5,000.00	210.53	< 0.0001	
C-C	5,253.13	1	5,253.13	221.18	< 0.0001	
AB	4,556.25	1	4,556.25	191.84	< 0.0001	
AC	1,600.00	1	1,600.00	67.37	0.0004	
BC	756.25	1	756.25	31.84	0.0024	
A^2	20,769.23	1	2,0769.23	874.49	< 0.0001	
B^2	12,744.23	1	12,744.23	536.60	< 0.0001	
C^2	29,907.69	1	29,907.69	1,259.27	< 0.0001	
Residual	118.75	5	23.75			
Lack of fit	300.00	3	100.00	1.43	0.30	Not significant

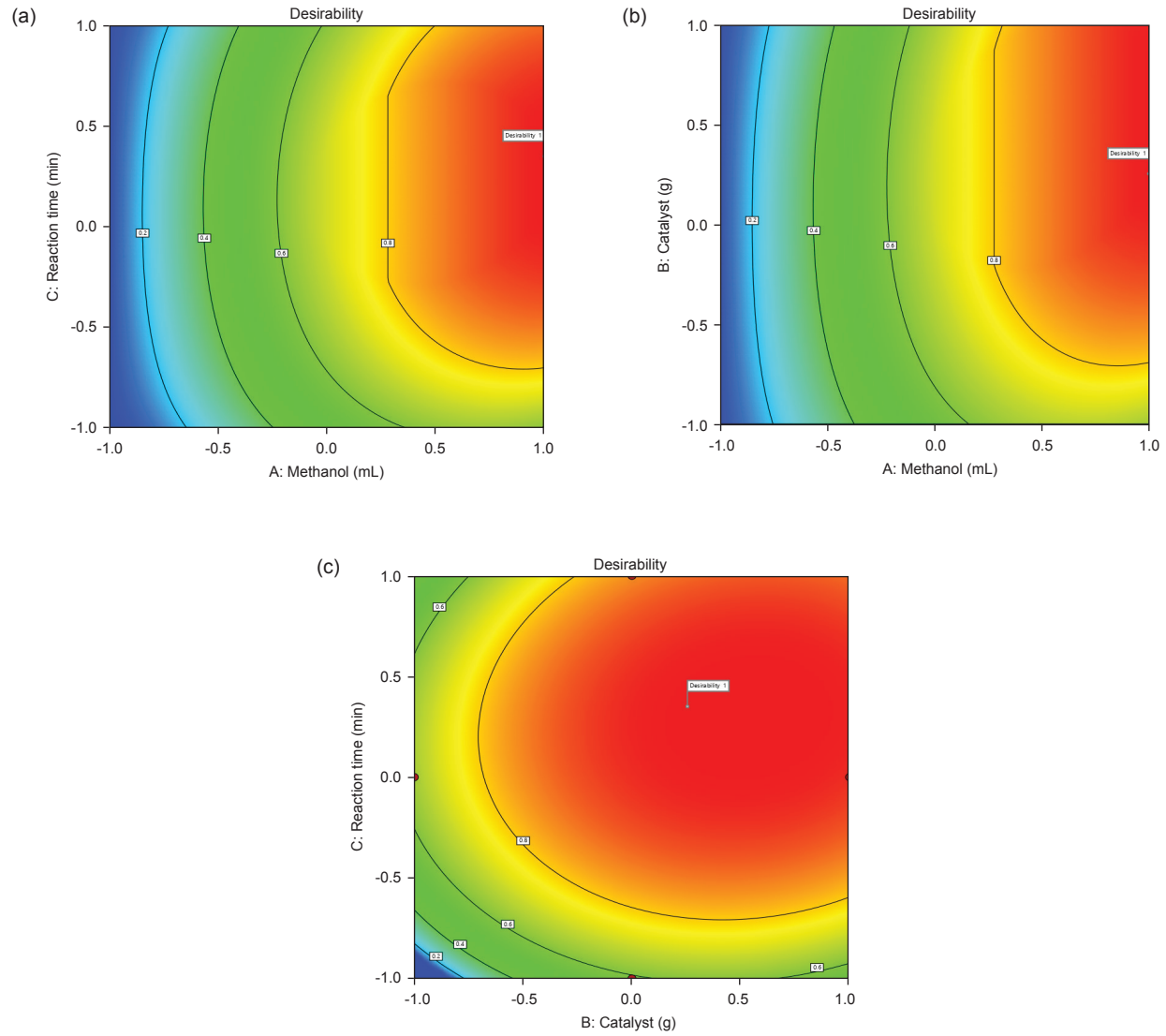

Figure 2. (a) Optimisation plot for methanol and reaction time, (b) methanol and catalyst and (c) reaction time and catalyst for the yield of biodiesel.

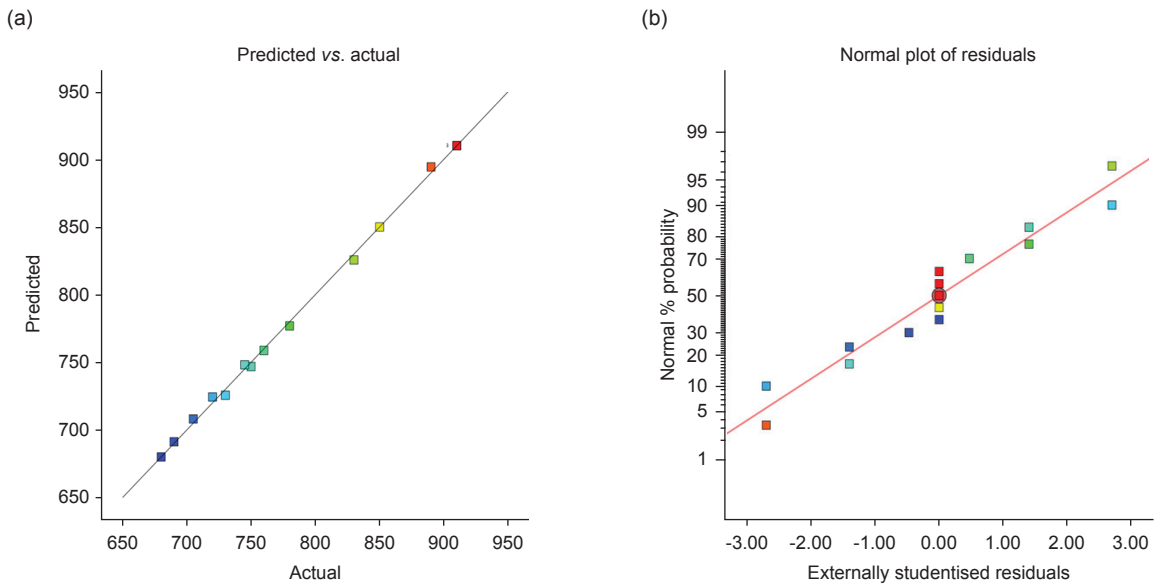

Figure 3. (a) Biodiesel yield predictions versus experimental results and (b) relationship between normal probability (%) and externally studentised residuals is depicted by a normal plot of residuals.

The plots show that biodiesel yield increases as methanol concentration increases. An increase in methanol above the 225 mL level, on the other hand, does not result in an additional increment in biodiesel yield but instead leads to a slight reduction. Therefore, there is an optimal methanol concentration of 225 mL and a catalyst concentration of 10 g. Concerning the effect of catalyst concentration, the biodiesel yield rises with increasing catalyst concentration from 8-12 g. Conversely, beyond this concentration, the biodiesel yield begins to decrease. Thus, there is an optimal catalyst concentration of 10 g and a reaction time of 60 min. Regarding the effect of reaction time, raising the reaction time from 45-60 min tends to increase the biodiesel yield. Moreover, once this concentration is reached, the biodiesel yield begins to decline (Bai *et al.*, 2022).

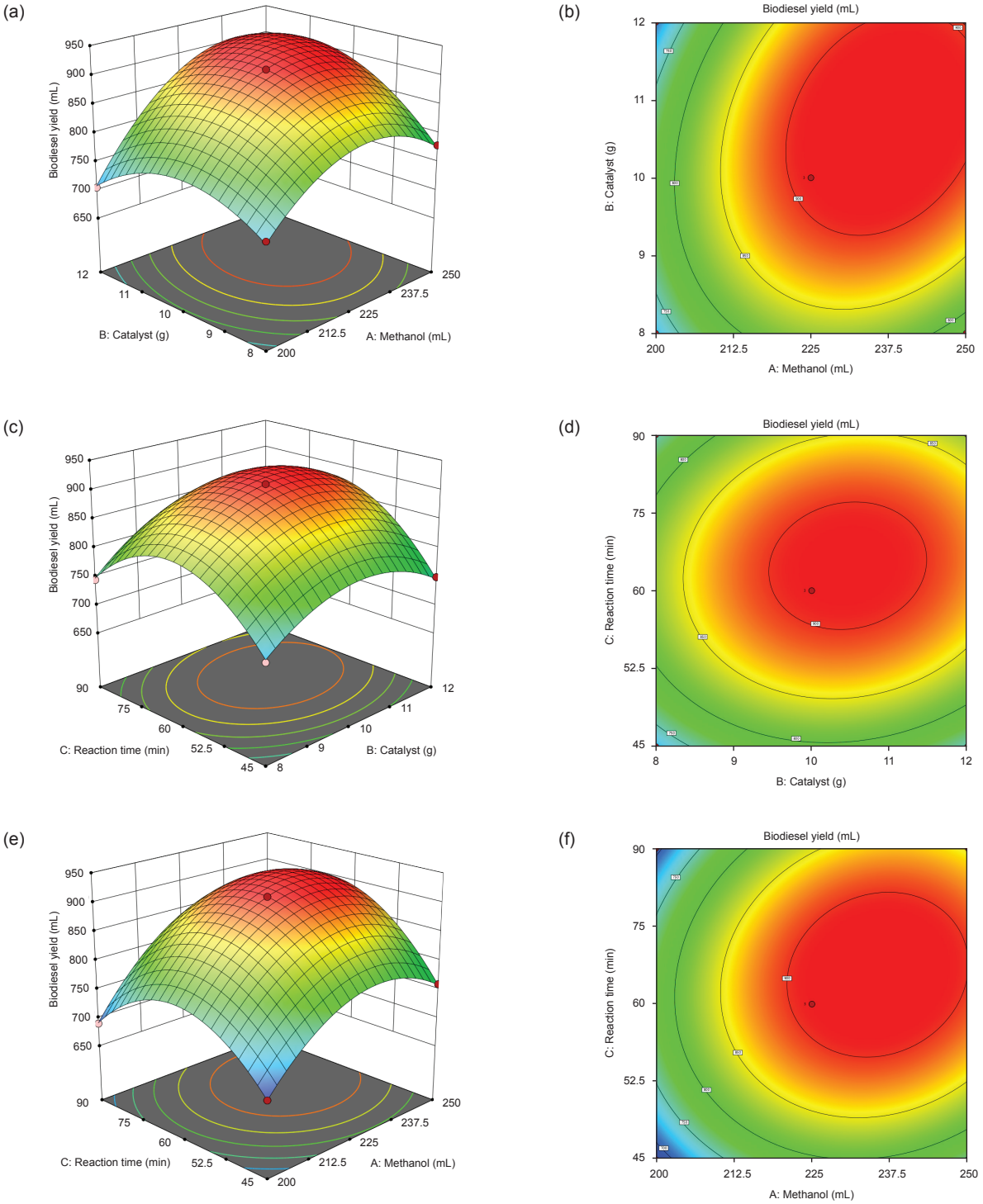

Figure 4. (a) Methanol and catalyst combined for biodiesel yield response surface, (b) methanol and catalyst contour plot of the expected biodiesel yield, (c) catalyst and reaction time combined for biodiesel yield response surface, (d) catalyst and reaction time contour plot of the expected biodiesel yield, (e) methanol and reaction time combined for biodiesel yield response surface and (f) reaction time combined contour plot of the expected biodiesel yield.

Therefore, there is an optimal reaction time of 60 min and a methanol concentration of 225 mL. At 225 mL methanol, with a 10 g catalyst and a reaction time of 60 min, the maximum biodiesel yield of 910 mL is achieved.

BBD necessitates fewer experimental runs and can effectively simulate quadratic relationships; nevertheless, it may underperform in situations with high values or pronounced non-linearities, where CCD may better capture intricate features. Future research could investigate hybrid methodologies that integrate the advantages of both CCD and BBD or utilise sophisticated techniques such as machine learning models for optimisation to uncover additional improvements in biodiesel production efficiency.

Biodiesel Yield

Effect of catalyst concentration. A stirrer blends the catalyst and methanol in a small reactor. The oil should first be charged into the reactor, after which the KOH/methanol mixture is added to the oil. Triglycerides may take longer to completely convert to biodiesel and glycerol if there is insufficient catalyst concentration, which can cause slower reaction rates. This prolonged reaction time may raise processing expenses and decrease manufacturing efficiency. Lower catalyst concentrations may cause the conversion of triglycerides to biodiesel to be incomplete, thereby reducing biodiesel production. The unreacted triglycerides that are still present in the reaction mixture necessitate more processing stages or reagents to achieve the required degree of conversion, which might escalate the cost and complexity even further. A higher catalyst concentration may cause the usage of more reactants than necessary, hence might lower the output of biodiesel. This occurs because of the excess catalyst, which can potentially trigger unintended reactions like saponification, reducing the output of biodiesel by forming soap. Since catalysts frequently account for a sizeable percentage of the total costs associated with producing biodiesel, using more catalysts than necessary raises production costs. Oil, alcohol and water combinations that are stable can create emulsions when there is an overabundance of catalysts present. Emulsions may obstruct the biodiesel's ability to separate from the reaction mixture, complicating subsequent steps and adding time and energy to the purifying process. Theam *et al.* (2015) achieved the highest yield at 1.00% (w/w) catalyst loading for the transesterification of palm stearin with a metal-doped methoxide solid catalyst. Verma and Sharma (2016) achieved the highest yield at 1.22% (w/w) catalyst loading for the transesterification of karanja oil with methanol and KOH as catalysts. The optimum concentration of the catalyst, KOH, for the highest biodiesel yield in this study is 10 g, corresponding to a catalyst loading of 1.12% (w/w), which falls within the range specified by Verma and Sharma (2016).

Effects of methanol. The amounts of methanol (200, 225 and 250 mL) were utilised in this experiment. The molar ratio is the most significant variable that affects conversion efficiency and biodiesel production costs. The conversion efficiency is defined as the process yield expressed as a percentage. An optimum molar ratio minimises excess methanol, which can cause side reactions and lower the yield while ensuring that there is enough methanol to react with all the fatty acid esters found in the palm stearin. The side reactions, including the production of soap and fatty acid methyl esters with shorter carbon chains, might result from using too much methanol. These side reactions have the potential to impair the biodiesel product's quality and make the separation procedure more difficult (Verma & Sharma, 2016). For the highest yield of 910 mL, the transesterification process uses a molar ratio of 5.58:1 between methanol and palm stearin. Theam *et al.* (2015) achieved the highest yield at a molar ratio of 6:1 between methanol and palm stearin for the transesterification of palm stearin with a metal-doped methoxide solid catalyst. Vyas *et al.* (2011) optimised the molar ratio to 6:1 for the transesterification of jatropha oil with methanol. The presence of both water and FFA tends to promote saponification (Danane *et al.*, 2022). Therefore, the oils and alcohols must mostly be anhydrous.

Effect reaction time. We investigated the impact of reaction time on palm stearin transesterification efficiency in biodiesel production. When transforming palm stearin, working with a reaction time that is below ideal can lead to a variety of problems, including inadequate phase separation, increased contaminants, inconsistent product quality and incomplete conversion. Shorter reaction periods may lead to the formation of soap, mono- and diglycerides and FFA. These contaminants may have a negative impact on the quality and characteristics of the biodiesel product, resulting in reduced fuel efficiency and potential engine issues. When transforming palm stearin, running at a reaction time longer than ideal can lead to resource waste, lower reaction selectivity, higher energy consumption, product deterioration and ineffective separation. Prolonging the reaction beyond the required duration results in excessive utilisation of catalysts, energy and raw materials, leading to decreased productivity and increased expenses in

the production process. Prolonged reaction times can lead to the formation of unwanted by-products, such as soap and glycerides, due to side reactions. This lowers the transesterification process's selectivity, resulting in lower biodiesel purity and yield. Therefore, to maximise the efficiency of biodiesel production while minimising expenses, it is imperative to carefully manage and optimise the reaction time. The optimum reaction time for the highest biodiesel yield is 60 min. Theam *et al.* (2015) achieved the highest yield at 180 min for the transesterification of palm stearin with a metal-doped methoxide solid catalyst. Vyas *et al.* (2011) achieved the highest yield at 30 min for the transesterification of jatropha oil with methanol, and Verma and Sharma (2016) achieved it at 90 min for the transesterification of karanja oil with methanol.

The molar ratio of methanol to palm stearin, as well as the weight-to-weight (w/w) catalyst loading, demonstrate consistency with Theam *et al.* (2015), Verma and Sharma (2016) and Vyas *et al.* (2011), affirming adherence to established practices in the transesterification process. The validation analysis of the quadratic response was carried out by performing an experimental study to verify the predicted optimised parameters obtained from Equation (2):

$$\begin{aligned}\text{Biodiesel yield} = {} & 910.00 + 99.56(225) + \\ & 75.63(10) + 82.66(60) \\ & + 75.60(225*10) + \\ & 65.00(225*60) + 51.75(10*60) \\ & - 20.01(225)^2 - 13.97(10)^2 - \\ & 2\ 4.39(60)^2 = 913.40\ \text{mL}\end{aligned} \quad (2)$$

Attaining an 89.25% biodiesel yield from palm stearin offers significant benefits in the industrial synthesis of biodiesel. From an economic perspective, elevated yield rates mean that a greater proportion of the raw feedstock is transformed into usable fuel, resulting in substantial cost savings on raw materials. This directly reduces the need for acquiring supplementary feedstock and lowers the overall per-unit manufacturing cost of biodiesel. In an industrial setting, efficient feedstock utilisation increases throughput, reducing the necessity for prolonged processing times or multiple reaction phases. This leads to decreased energy consumption and less wear on equipment, therefore lowering maintenance expenses and improving the long-term sustainability of industrial operations. Moreover, reduced energy usage correlates with a diminished carbon footprint, thereby enhancing the environmental benefits of biodiesel as a cleaner fuel alternative.

In addition to cost reductions, such a high yield ensures efficiency improvements across various industrial applications. An optimised transesterification process requires fewer resources to produce the same volume of biodiesel, potentially motivating more industries to adopt biodiesel as a viable alternative to conventional fossil fuels. Furthermore, a more efficient production process makes the scaling up of biodiesel production more feasible, enabling increased industrial output without a corresponding rise in operational costs or environmental impact. This is particularly crucial for industries aiming to achieve sustainability goals while maintaining profitability. Consequently, achieving high biodiesel yields not only improves economic feasibility but also strengthens biodiesel's position as a competitive, green energy source in both local and global energy markets.

Biodiesel Characteristics and Properties

Biodiesel properties. We conducted laboratory tests to determine the physical properties of the biodiesel. *Table 7* provides the standards used for the various properties of diesel and palm stearin biodiesel, along with ASTM D6751 (for the United States) and EN14214 (for the European Union) standards (DieselNet, 2009).

Palm stearin biodiesel meets the criteria for ash content, density @ 15°C, moisture content, kinetic viscosity @ 40°C, acidity, flash point, fire point, sulphated ash and relative density @ 15°C. The cetane number of palm stearin biodiesel is slightly below both ASTM D6751 and EN14214 standard values. The sulphur content of palm stearin biodiesel exceeds both ASTM D6751 and EN14214 standard values. The net calorific value of palm stearin biodiesel is slightly below the EN14214 standard value.

Blending diesel with palm stearin biodiesel at a ratio of 80% diesel to 20% biodiesel can meet ASTM D6751 and EN14214 minimum criteria. Diesel usually has a low sulphur level or complies with Ultra-Low Sulfur Diesel (ULSD) regulations. The total sulphur level of the mix drops by blending with diesel, which has a lower sulphur concentration, assisting in meeting the allowable limitations. In general, diesel fuel has a greater cetane number than biodiesel. Adding diesel to the mix may raise its cetane index and improve the blend's ignition and combustion properties. Diesel's high cetane number will still have a major effect on the blend, even though biodiesel alone helps to improve cetane (Sakkampang *et al.*, 2023).

In comparison to biodiesel, diesel fuel has greater flash and fire points. Combining the blend with diesel will increase its fire and flash points, thereby enhancing handling and storage

safety. By modifying the blend ratios to satisfy the required criteria, blending with diesel can also assist in producing the right density, viscosity and other qualities. Blending biodiesel with diesel can counteract its increased viscosity and bring it within the permissible limit (Sakthivel *et al.*, 2018).

Biodiesel characteristics. The GC-MS test can provide information about the FAMEs present in the biodiesel sample and also identify any impurities like glycerol or water (Manojkumar *et al.*, 2022). If the biodiesel passes the quality criteria established by regulatory agencies like the American Society for Testing and Materials (ASTM), the findings of the GC-MS test can be used to make that determination. The GC-MS analysis that was performed is shown in *Figure 5*. *Table 8* includes the sixteen chemicals found during the analysis. Five of the sixteen components are major, while the other twelve are minor.

Using the MS database library as a base, these peaks can be identified. Several derivatives of hexadecanoic acid, including methyl ester ($C_{17}H_{34}O_2$), were found in the highest concentration (24.79%). The MS database allows for the identification of these peaks, which include 9-Octadecenoic acid (Z)-, methyl ester ($C_{19}H_{36}O_2$) (21.90%), 9,12-Octadecadienoic acid (Z, Z)-, methyl ester ($C_{19}H_{34}O_2$) (13.64%), methyl stearate ($C_{19}H_{38}O_2$) (13.20%) and methyl tetradecanoate ($C_{15}H_{30}O_2$) (11.16%).

The FAME content in palm stearin biodiesel is shown in *Table 9*. In the biodiesel made from palm stearin, the saturated FAME percentage is 59.19%, the unsaturated FAME level is 38.47% and the overall FAME content is 97.66%. The remaining 2.34% of the palm stearin biodiesel comprises other substances or contaminants, such as methanol, water, glycerides, glycerol and small amounts of other components. These substances may be by-products, contaminants, or unreacted starting components.

Higher levels of saturated FAME in biodiesel are commonly associated with higher viscosities, improved oxidative stability, higher pour points and higher cloud points. Saturated FAME typically has higher melting temperatures and viscosities than unsaturated FAME. This can result in poorer low-temperature properties and increased viscosity, which can affect engine performance and flow characteristics, particularly in cold weather. Over time, biodiesel with saturated FAME exhibits superior oxidative stability because it is generally more resistant to oxidation than unsaturated FAME. A higher saturated FAME level in biodiesel raises its cloud point and pour point, which may impact its cold flow characteristics and suitability for use in colder regions.

Higher levels of unsaturated FAME in biodiesel are commonly associated with lower viscosities, poorer oxidative stability, lower pour and cloud points, and higher cetane numbers. When compared to saturated FAME, unsaturated FAME often has greater cetane values, which enhance biodiesel's ignition quality and combustion properties, leading to smoother engine operation and lower emissions.

In general, an elevated overall FAME concentration results in biodiesel having a higher energy content per unit volume, which provides more energy for combustion and may boost fuel efficiency. FAME components contribute to the lubricity of biodiesel, reducing engine wear and tear and prolonging engine life. Higher FAME content in biodiesel tends to make it more biodegradable, which lessens the impact of spills or leaks on

TABLE 7. BIODIESEL PROPERTIES

No.	Test parameters	Unit	Petroleum diesel	ASTM D6751	EN14214	Palm stearin biodiesel	Test method
1	Ash	% by mass	0.01	≤0.02%	≤0.02%	0.02	ASTM D 482:2013
2	Density @ 15°C	g/cm^3	0.85	0.82-0.90	0.86-0.90	0.8670	IS:1448 part 32:2019
3	Moisture	% by mass	0.01	≤0.05%	≤0.02%	BLQ	IS:1448 part 40:2015
4	Kinematic viscosity @ 40°C	mm^2/s (cSt)	4.5	1.9-6.0	3.5-5.0	4.7	ASTM D 445:2015
5	Cetane index	-	55	≥47	≥51	42.2	ASTM D976-06
6	Acidity	mg of KOH/g	0.02	≤0.50	≤0.50	0.2	IS:1448 part 2:2007
7	Sulphur	% by mass	0.001	≤0.0015	≤0.001	0.08	IS:1448 part 33:1991
8	Flash point	°C	96	≥93	≥95	170	IS 1448 Part 20:1998
9	Fire point	°C	96	N/A	≥140	179	IS 1448 Part 20:1998
10	Sulphated ash	% by mass	0.01	≤0.02	≤0.02	0.02	ASTM D 482:2013
11	Relative density @ 15°C	-	0.85	N/A	0.860-0.900	0.8678	IS:1448 part 32:2019
12	Net calorific value	cal/g	10038.241	N/A	≥ 8556.40	8503	IS:1448 part 6:1984

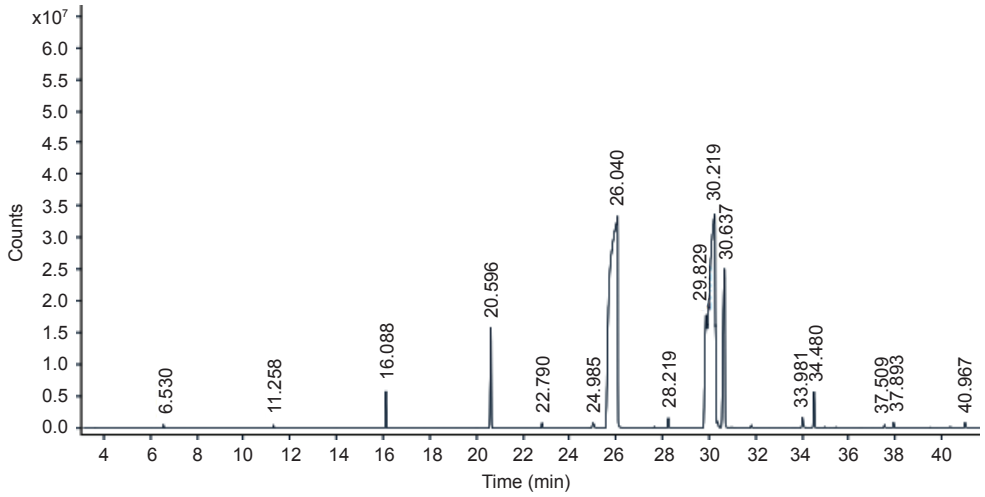

Figure 5. GC-MS test outcomes for biodiesel.

TABLE 8. ELEMENTS ACQUIRED IN GCMS RESULT

No.	Compound name	Peak	Area in %	Chemical formula
1	Octanoic acid, methyl ester	6.530	0.29	$C_9H_{18}O_2$
2	Decanoic acid, methyl ester	11.258	0.29	$C_{11}H_{22}O_2$
3	Dodecanoic acid, methyl ester	16.088	3.60	$C_{13}H_{26}O_2$
4	Methyl tetradecanoate	20.596	11.16	$C_{15}H_{30}O_2$
5	Pentadecanoic acid, methyl ester	22.790	0.63	$C_{16}H_{32}O_2$
6	Methyl hexadec-9-enoate	24.985	1.19	$C_{17}H_{32}O_2$
7	Hexadecanoic acid, methyl ester	26.040	24.79	$C_{17}H_{34}O_2$
8	Heptadecanoic acid, methyl ester	28.219	1.34	$C_{18}H_{36}O_2$
9	9,12-Octadecadienoic acid (Z, Z)-, methyl ester	29.829	13.64	$C_{19}H_{34}O_2$
10	9-Octadecenoic acid (Z)-, methyl ester	30.219	21.90	$C_{19}H_{36}O_2$
11	Methyl stearate	30.637	13.20	$C_{19}H_{38}O_2$
12	cis-Methyl 11-eicosenoate	33.981	1.74	$C_{20}H_{38}O_2$
13	Eicosanoic acid, methyl ester	34.480	4.39	$C_9H_{10}O_2$
14	Glycerol 1-palmitate	37.509	0.50	$C_{19}H_{38}O_4$
15	Docosanoic acid, methyl ester	37.893	0.74	$C_{23}H_{46}O_2$
16	Tetracosanoic acid, methyl ester	40.967	0.59	$C_{25}H_{50}O_2$

TABLE 9. FAME CONTENT IN PALM STEARIN BIODIESEL

FAME type	Compound name	Chemical formula	Content (%)
Saturated FAME	Octanoic acid, methyl ester	$C_9H_{18}O_2$	0.29
	Decanoic acid, methyl ester	$C_{11}H_{22}O_2$	0.29
	Dodecanoic acid, methyl ester	$C_{13}H_{26}O_2$	3.60
	Methyl tetradecanoate	$C_{15}H_{30}O_2$	11.16
	Hexadecanoic acid, methyl ester	$C_{17}H_{34}O_2$	24.79
	Heptadecanoic acid, methyl ester	$C_{18}H_{36}O_2$	1.34
	Methyl stearate	$C_{19}H_{38}O_2$	13.20
	Eicosanoic acid, methyl ester	$C_{20}H_{40}O_2$	4.39
	Docosanoic acid, methyl ester	$C_{23}H_{46}O_2$	0.74
	Tetracosanoic acid, methyl ester	$C_{25}H_{50}O_2$	0.59
Total saturated FAME			**59.19**
Unsaturated FAME	Methyl hexadec-9-enoate	$C_{17}H_{32}O_2$	1.19
	9,12-Octadecadienoic acid (Z, Z)-, methyl ester	$C_{19}H_{34}O_2$	13.64
	9-Octadecenoic acid (Z)-, methyl ester	$C_{19}H_{36}O_2$	21.90
	cis-Methyl 11-eicosenoate	$C_{20}H_{38}O_2$	1.74
Total unsaturated FAME			**38.47**
Total FAME			**97.66**

the environment. Biodiesel's physicochemical properties, such as viscosity, oxidative stability, cold flow properties, cetane number, energy content, lubricity and biodegradability, significantly depend on the proportion of FAME it contains. To maximise these qualities and ensure that biodiesel is suitable for various applications, such as power production, heating and transportation, it is imperative to balance the concentrations of saturated and unsaturated FAME (Brahma *et al.*, 2022).

CONCLUSION

This study effectively optimised the transesterification process for the production of biodiesel from palm stearin using a Box-Behnken design and RSM. We created a quadratic model to clarify the interactions between methanol volume, catalyst quantity, and reaction time. With a coefficient of determination (R^2) of 0.9849 and an Adj-R^2 of 0.9974, the model shows a great match to the experimental data, demonstrating its excellent predictive accuracy. Further evidence of the model's importance in maximising biodiesel output comes from the low *p*-value (<0.0001). The ideal parameters of 225 mL of methanol, 10 g of catalyst and a 60-min reaction period resulted in a maximum biodiesel output of 910 mL, with a percentage yield of 89.25%. We validated the model's effectiveness by finding that the expected biodiesel production nearly matches the experimental result. Physicochemical studies revealed that the produced biodiesel exhibited good viscosity, density and cold flow characteristics. These characteristics are essential for guaranteeing both environmental sustainability and optimal engine performance. While this study offers valuable insights, future research should explore scaling up the process for industrial applications to assess the practical feasibility of these optimised conditions at a larger scale. The study's limitations include the laboratory-scale nature of the experiments. Further studies could address potential variations in yield or biodiesel quality under different operational scales and raw materials, which would provide a more comprehensive understanding of the process's broader applicability.

ACKNOWLEDGEMENT

The authors would like to thank the IITM SAIF (Sophisticated Analytical Instrument Facility) for their vital role in delivering the GC-MS data required for the biodiesel sample analysis and characterisation.

REFERENCES

Adepoju, T., Victor, E., Ekop, E., Emberru, R., Balogun, T., & Adeniyi, A. (2022). Residual wood ash powder: A predecessor for the synthesis of $CaO\text{-}K_2O\text{-}SiO_2$ base catalyst employed for the production of biodiesel from *Asimina triloba* oil seed. *Case Studies in Chemical and Environmental Engineering, 6*, 100252. https://doi.org/10.1016/j.cscee.2022.100252

Bai, H., Tian, J., Talifu, D., Okitsu, K., & Abulizi, A. (2022). Process optimisation of esterification for deacidification in waste cooking oil: RSM approach and for biodiesel production assisted with ultrasonic and solvent. *Fuel, 318*, 123697. https://doi.org/10.1016/j.fuel.2022.123697

Brahma, S., Nath, B., Basumatary, B., Das, B., Saikia, P., Patir, K., & Basumatary, S. (2022). Biodiesel production from mixed oils: A sustainable approach towards industrial biofuel production. *Chemical Engineering Journal Advances, 10*, 100284. https://doi.org/10.1016/j.ceja.2022.100284

Buasri, A., Lertnimit, S., Nisapruksachart, A., Khunkha, I., & Loryuenyong, V. (2023). Box-Behnken design for optimization on esterification of free fatty acids in waste cooking oil using modified smectite clay catalyst. *ASEAN Journal of Chemical Engineering, 23*(1), 40–51. https://doi.org/10.22146/ajche.77009

Buasri, A., Kamsuwan, J., Dokput, J., Buakaeo, P., Horthong, P., & Loryuenyong, V. (2024). Green synthesis of metal oxides ($CaO\text{-}K_2O$) catalyst using golden apple snail shell and cultivated banana peel for production of biofuel from non-edible *Jatropha curcas* oil (JCO) via a central composite design (CCD). *Journal of Saudi Chemical Society*, 101836. https://doi.org/10.1016/j.jscs.2024.101836

Bustamam, F. K. A., Yeoh, C. B., Sulaiman, N., & Saw, M. H. (2022). Evaluation on the quality of Malaysian refined palm stearin. *OCL, 29*, 37. https://doi.org/10.1051/ocl/2022030

Danane, F., Bessah, R., Alloune, R., Tebouche, L., Madjene, F., Kheirani, A. Y., & Bouabibsa, R. (2022). Experimental optimisation of waste cooking oil ethanolysis for biodiesel production using response surface methodology (RSM). *Science and Technology for Energy Transition, 77*, 14. https://doi.org/10.2516/stet/2022014

Deivajothi, P., Manieniyan, V., & Sivaprakasam, S. (2018). An impact of ethyl esters of groundnut

acid oil (vegetable oil refinery waste) used as emerging fuel in DI diesel engine. *Alexandria Engineering Journal, 57*(4), 2215–2223. https://doi.org/10.1016/j.aej.2017.09.003

DieselNet. (2024). *Biodiesel standards & properties*. Retrieved January 30, 2024, from https://dieselnet.com/tech/fuel_biodiesel_std.php

Gupta, S., Patel, P., & Mondal, P. (2022). Biofuels production from pine needles via pyrolysis: Process parameters modeling and optimisation through combined RSM and ANN-based approach. *Fuel, 310*, 122230. https://doi.org/10.1016/j.fuel.2021.122230

Hazrat, M. A., Rasul, M. G., Mofijur, M., Khan, M. M. K., Djavanroodi, F., Azad, A. K., Bhuiya, M. M. K., & Silitonga, A. S. (2020). A mini review on the cold flow properties of biodiesel and its blends. *Frontiers in Energy Research, 8*. https://doi.org/10.3389/fenrg.2020.598651

Hussanai, S., & Kittisak, W. (2023). Optimisation of FAME production from waste cooking palm oil with KOH catalyst supported on palm kernel shells ash (PKSA) using response surface methodology (RSM). *Journal of Oil Palm Research, 35*(4), 668–681. https://doi.org/10.21894/jopr.2023.0005

Joorasty, M., Rahbar-Kelishami, A., & Hemmati, A. (2022). A performance comparison of cyclopentyl methyl ether (CPME) and hexane solvents in oil extraction from sewage sludge for biodiesel production; RSM optimisation. *Journal of Molecular Liquids, 368*, 120573. https://doi.org/10.1016/j.molliq.2022.120573

Karimi, S., & Saidi, M. (2022). Biodiesel production from *Azadirachta indica*-derived oil by electrolysis technique: Process optimisation using response surface methodology (RSM). *Fuel Processing Technology, 234*, 107337. https://doi.org/10.1016/j.fuproc.2022.107337

Khan, T. A., Khan, T. A., & Kumar Yadav, A. (2022). A hydrodynamic cavitation-assisted system for optimisation of biodiesel production from green microalgae oil using a genetic algorithm and response surface methodology approach. *Environmental Science and Pollution Research, 29*(32), 49465–49477. https://doi.org/10.1007/s11356-022-20474-w

Kober, R., Schwaab, M., Barbosa-Coutinho, E., & Pinto, J. C. (2022). Are empirical models based on the response surface methodology suitable for biodiesel production optimisation? *Industrial & Engineering Chemistry Research, 61*(34), 12458–12472. https://doi.org/10.1021/acs.iecr.2c01848

Loryuenyong, V., Rohing, S., Singhanam, P., Kamkang, H., & Buasri, A. (2024). Artificial neural network and response surface methodology for predicting and maximizing biodiesel production from waste oil with KI/CaO/Al_2O_3 catalyst in a fixed bed reactor. *ChemPlusChem, 89*. https://doi.org/10.1002/cplu.202400117

Manimaran, R., Venkatesan, M., & Kumar, K. T. (2022). Optimisation of okra (*Abelmoschus esculentus*) biodiesel production using RSM technique coupled with GA: Addressing its performance and emission characteristics. *Journal of Cleaner Production, 380*, 134870. https://doi.org/10.1016/j.jclepro.2022.134870

Manojkumar, N., Muthukumaran, C., & Sharmila, G. (2022). A comprehensive review on the application of response surface methodology for optimisation of biodiesel production using different oil sources. *Journal of King Saud University-Engineering Sciences, 34*(3), 198–208. https://doi.org/10.1016/j.jksues.2020.09.012

Muthuswamy, S., & Veerasigamani, M. (2020). Impact of secondary fuel injector in various distances on direct injection diesel engine using acetylene-biodiesel in reactivity controlled compression ignition mode. *Energy Sources, Part A: Recovery, Utilization, and Environmental Effects*, 1–15. https://doi.org/10.1080/15567036.2020.1810177

Ngige, G. A., Ovuoraye, P. E., Igwegbe, C. A., Fetahi, E., Okeke, J. A., Yakubu, A. D., & Onyechi, P. C. (2023). RSM optimisation and yield prediction for biodiesel produced from alkali-catalytic transesterification of pawpaw seed extract: Thermodynamics, kinetics, and multiple linear regression analysis. *Digital Chemical Engineering, 6*, 100066. https://doi.org/10.1016/j.dche.2022.100066

Parak, S., Nikseresht, A., Alikarami, M., & Ghasemi, S. (2022). RSM optimisation of biodiesel production by a novel composite of Fe (III)-based MOF and phosphomolybdic acid. *Research on Chemical Intermediates, 48*(9), 3773–3793. https://doi.org/10.1007/s11164-022-04783-w

Rajali, N. A., Radzi, S. M., Rehan, M. M., & Amin, N. A. M. (2022). Optimisation of the biodiesel production via transesterification reaction of palm oil using response surface methodology

(RSM): A review. *Malaysian Journal of Science, Health & Technology, 8*(2), 58–67. https://doi.org/10.33102/mjosht.v8i2.292

Ranjan, A., Dawn, S. S., Nirmala, N., Santhosh, A., & Arun, J. (2022). Application of deep eutectic solvent in biodiesel reaction: RSM optimisation, CI engine test, cost analysis and research dynamics. *Fuel, 307*, 121933. https://doi.org/10.1016/j.fuel.2021.121933

Razak, N. H., Hashim, H., Yunus, N. A., & Klemeš, J. J. (2021). Reducing diesel exhaust emissions by optimisation of alcohol oxygenates blend with diesel/biodiesel. *Journal of Cleaner Production, 316*, 128090. https://doi.org/10.1016/j.jclepro.2021.128090

Sakkampang, C., Sakkampang, K., Suwunnasopha, P., & Poojeera, S. (2023). Performance, exhaust emission, and wear behavior of a direct-injection engine using biodiesel from Yang-Na (*Dipterocarpus alatus*) oleoresins. *Case Studies in Chemical and Environmental Engineering, 7*, 100328. https://doi.org/10.1016/j.cscee.2023.100328

Sakthivel, R., Ramesh, K., Purnachandran, R., & Mohamed Shameer, P. (2018). A review on the properties, performance, and emission aspects of the third generation biodiesels. *Renewable and Sustainable Energy Reviews, 82*, 2970–2992. https://doi.org/10.1016/j.rser.2017.10.037

Simsek, S., Uslu, S., & Simsek, H. (2022). Proportional impact prediction model of animal waste fat-derived biodiesel by ANN and RSM technique for diesel engine. *Energy, 239*, 122389. https://doi.org/10.1016/j.energy.2021.122389

Sonachalam, M., PaulPandian, P., & Manieniyan, V. (2020). Emission reduction in diesel engine with acetylene gas and biodiesel using inlet manifold injection. *Clean Technologies and Environmental Policy, 22*, 2177–2191. https://doi.org/10.1007/s10098-020-01968-y

Theam, K. L., Islam, A., Choo, Y. M., & Taufiq-Yap, Y. H. (2015). Biodiesel from low cost palm stearin using metal doped methoxide solid catalyst. *Industrial Crops and Products, 76*, 281–289. https://doi.org/10.1016/j.indcrop.2015.06.058

Verma, P., & Sharma, M. P. (2016). Comparative analysis of effect of methanol and ethanol on Karanja biodiesel production and its optimisation. *Fuel, 180*, 164–174. https://doi.org/10.1016/j.fuel.2016.04.035

Vyas, A. P., Verma, J. L., & Subrahmanyam, N. (2011). Effects of molar ratio, alkali catalyst concentration, and temperature on transesterification of jatropha oil with methanol under ultrasonic irradiation. *Advances in Chemical Engineering and Science, 1*(2), 45–50. https://doi.org/10.4236/aces.2011.12008

Yusoff, M. N. A. M., Zulkifli, N. W. M., Sukiman, N. L., Kalam, M. A., Masjuki, H. H., Syahir, A. Z., Awang, M. S. N., Mujtaba, M. A., Milano, J., & Shamsuddin, A. H. (2022). Microwave irradiation-assisted transesterification of ternary oil mixture of waste cooking oil – *Jatropha curcas*-palm oil: Optimization and characterization. *Alexandria Engineering Journal, 61*(12), 9569–9582. https://doi.org/10.1016/j.aej.2022.03.040

Zahan, K. A., & Kano, M. (2018). Biodiesel production from palm oil, its by-products, and mill effluent: A review. *Energies (Basel), 11*(8), 2132. https://doi.org/10.3390/en11082132

Zhang, C., Chang, J., Wang, T., & Lu, C. (2019). Biodiesel production from waste cooking oil using a novel heterogeneous catalyst derived from hydrotalcite-supported KOH. *Fuel, 236*, 1016–1024. https://doi.org/10.3934/energy.2022049

Journal of Oil Palm Research Vol. 37 (3) September 2025 p. 549-559
DOI: https://doi.org/10.21894/jopr.2024.0019

TRIBOLOGICAL AND THERMAL CHARACTERISATION OF PALM GREASE WITH ORGANIC THICKENER

MUHAMMAD FAKHRUR RAZZI ZULKIFLI[1]; NURUL FARHANA MOHD YUSOF[1]*; NADIAH AQILAHWATI ABDULLAH[1] and ZAIDI MOHD RIPIN[1]

ABSTRACT

Grease is widely utilised in machinery to provide essential lubrication during component contact. However, the concern regarding the toxicity linked with mineral-based grease has attracted notable attention. With a thickener content of up to 30%, the properties of the thickener can likewise impact the characteristics of the grease. Organic or green thickeners have gained significant attention from researchers due to their biodegradability and environmentally friendly properties. In this study, a refined, bleached and deodorised (RBD) palm olein grease was formulated utilising a cellulose and chitosan organic thickener and subsequently, its tribological and thermal properties were assessed. The palm grease formulated with organic thickeners exhibited a lower coefficient of friction than lithium-based and food-grade grease. Mass loss analysis of the pin indicated comparable values among all grease samples. The grease containing organic thickener exhibited a shallower wear groove depth on the plate with white particles, resulting from elevated levels of carbon and oxygen attributed to the organic thickener material. Thermal analysis indicated good thermal stability of the organic thickener grease. The finding discovered the potential of organic thickener formulated with RBD palm olein as a sustainable grease.

Keywords: grease, organic thickener, palm oil.

Received: 28 August 2023**; Accepted:** 28 January 2024**; Published online:** 7 March 2024.

INTRODUCTION

Grease plays a vital role in ensuring the smooth functioning of machinery components by providing essential lubrication to the components in contact. Typically derived from mineral or synthetic oils, conventional grease has been a staple in various industries. However, it is worth noting that the constituents of conventional grease, while effective, can sometimes pose toxicity concerns. Recently, major concerns about grease toxicity in industrial applications, particularly in food processing, agriculture and manufacturing sectors, have led to an increase in the number of research and development efforts focused on green lubricants.

Green lubricants, also known as environmentally friendly or sustainable lubricants, are designed to address the environmental and health issues associated with traditional lubricants, including their potential toxicity and negative impact on users, labour and ecosystems. Previous study (Barboza *et al.*, 2023) found that the use of epoxidised gingelly methyl ester with 1.00% w/w alumina nanoparticle biolubricant leads to an 8.64% improvement in brake thermal efficiency compared to the baseline operation using B20 biodiesel fuel-mineral lubricant. In addition, significant decreases in emissions had been identified with reductions in the percentage of CO, NOx and HC concentrations, as well as smoke opacity, when compared to the baseline operation for the mentioned combination. Through a combination of biodegradability and reduced toxicity, green lubricants aim to lessen the harm caused by lubricant residues that might find their way into processed food in machinery and finally safe disposal into soil and water systems.

[1] School of Mechanical Engineering,
Universiti Sains Malaysia,
14300 Nibong Tebal, Pulau Pinang, Malaysia.

* *Corresponding author e-mail: mefarhana@usm.my*

One approach to produce a green lubricant involves substituting mineral oil-based substances or materials with environmentally friendly alternatives such as vegetable oils. Several research have evaluated vegetable-based oil performance including their rheological, tribological and thermal characteristics (Hamnas & Unnikrishnan, 2023). Grease generally is a semi-solid lubricant that contains 70%-90% base oil, 10%-30% thickener and 5%-10% additives (Japar *et al.*, 2019). Therefore, the portion of the thickener also played a crucial role in producing a safe and environmentally friendly lubricant. Organic or green thickeners have gained significant attention from researchers due to their biodegradability and environmentally friendly properties. Several works have been done to evaluate the performance of vegetable oil-based grease, such as castor oil (Ahme *et al.*, 2023; García-Zapateiro *et al.*, 2014; Japar *et al.*, 2019; Sanchez *et al.*, 2011; Vafaei *et al.*, 2022), sunflower oil (García-Zapateiro *et al.*, 2014), karanja oil (Panchal *et al.*, 2015), soybean oil (Sanchez *et al.*, 2011; Saxena *et al.*, 2021) and palm oil (Muhammad *et al.*, 2023; Yap *et al.*, 2022), however, there is very limited literature available on the topic of green thickeners. Sánchez *et al.* (2011) formulated grease using chitosan, chitin and acylated derivatives as organic thickener agents while castor oil and soybean oil as base oil and found that the greases formulated with the organic thickeners oleogel exhibited a comparable coefficient of friction value with standard lithium greases, however, these greases generally display quite poor mechanical stability. The study observed that, as the thickener concentration increases, the NLGI grade tends to rise, whereas the use of soybean oil instead of castor oil in the formulation leads to a decrease in the NLGI grade. It was observed that 23% of chitin, 25% and 27% of chitosan with castor oil exhibit NLGL greater than 1. Another work by Japar *et al.* (2019) used polypropylene, chitosan and chitin thickener with a percentage range of 25%-35% in the formulation and observed that the formulation produced greases with National Lubricating Grease Institute (NLGI) 000 to 1. It was found that these formulated greases could be used for low-temperature applications only as the greases start to lose their stability at high temperatures. Sanchez *et al.* (2014) observed that the formulated acylated chitosan-thickened grease poses better thermal resistance than lithium and calcium greases with good mechanical stability behaviour. However, the friction coefficient at low speeds was slightly higher than the others and had larger wear marks. In the study by Acar *et al.* (2018), biodegradable greases were developed using sunflower oil and castor oil with various thickeners including natural cellulose fibre and traditional lithium hydro stearate. It was observed that the biodegradable grease from cellulose fibre posed a lower friction coefficient and wear volume. Abdulbari and Zuhan (2011) used spent bleaching earth obtained from natural clay as a thickening agent in grease formulation and found that the addition of a fumed silica additive is required to increase the penetration number of the grease to NLGI 1.

With the limited literature available regarding the advantages of green thickeners, the unexplored potential of utilising such thickeners in the creation of biodegradable and environmentally sustainable green grease remains to be investigated. This study aims to pioneer sustainable alternatives that reduce environmental impact while maintaining or even enhancing performance levels. Through innovative research and development in this field, it is expected to improve lubrication practices, setting new standards for eco-friendly, high-performance lubricants that align with our global commitment to a greener environment. In this work, the palm olein grease is developed utilising organic thickeners, and the tribological and thermal performance of the resulting grease in comparison to both conventional grease and thickeners were accessed. Through this endeavour, it is anticipated that the produced grease will contribute to secure disposal practices of grease waste in the environment, while also ensuring the safe process of food machinery and workers while handling the machine.

MATERIALS AND METHODS

Grease Preparation

In this study, the grease is developed by using refined, bleached and deodorised (RBD) palm olein as the base oil and added with three different thickeners which were cellulose microcrystalline powder 20 µm $(C_6H_{10}O_5)n$, chitosan [Deacetylated chitin, Poly(D-glucosamine)] and lithium hydrostearate. Chitosan and cellulose were categorised as organic thickeners, whereas lithium is a widely used conventional inorganic thickener with improved superior performance (Zhou *et al.*, 2022). The RBD palm olein viscosity at 40°C and 100°C is 46.76 mm^2/s and 8.91 mm^2/s respectively. The performance of the developed greases was then compared with commercial food-grade grease available in the market as a benchmarking performance for the greases. The greases were prepared following the sets of compositions as shown in *Table 1*. The composition was selected based on previous work of producing greases with a green thickener (Japar *et al.*, 2019; Muhammad *et al.*, 2023) with the aim of producing NLGI grade 1 to grade 2 grease. These grades are widely used as multipurpose grease applied in machinery. For a set of 100 g final weights of grease using lithium thickener, 87 wt.% of palm

olein (87 g) and 13 wt.% of lithium thickener (13 g) were needed. Meanwhile, the organic grease requires higher thickener compositions as stated in *Table 1*.

Firstly, the beaker was placed on a hotplate and heated above the water's boiling temperature for about 10 min to clear all the moisture content in the base oil. Subsequently, the thickener was added to the base oil. The hotplate temperature was adjusted accordingly, either raised or lowered, based on the thickener's melting point. The solution was then stirred for 10 min to completely dissolve the thickener. Then, the remaining base oil was poured into the mixture to cool it down. The mixture temperature was slowly reduced and the stirring process was continued for 30 min for homogenisation.

A penetration test was performed according to ASTM D217 standard to evaluate the NLGI grade consistency of the developed grease. The HK-2020 cone and needle penetrometer were used. Before the test, the grease underwent 60 double strokes using an HK-269G mechanical grease worker machine. A stainless steel-tipped brass cone, weighing 102.5 grams, was used to penetrate the grease for 5 s. From the test, the lithium grease penetration value was in the range of 265-295 dmm which was under NLGI grade 2 consistency.

Tribological Testing

The tribological test for each grease was performed using a pin-on-plate tribometer machine (DUCOM TR-20). Before testing, the pin and plates were cleaned using acetone to remove all the unwanted material that was deposited on the samples. During the test, the pin was fixed to the machine holder while the plate was undergoing reciprocating motion continuously at a specific time as shown in *Figure 1*. The normal load during the test was set to 98.1 N by applying a 10 kg mass of weight. The test was run at room temperature conditions with the 100-rpm speed of the reciprocating plate for 60 min.

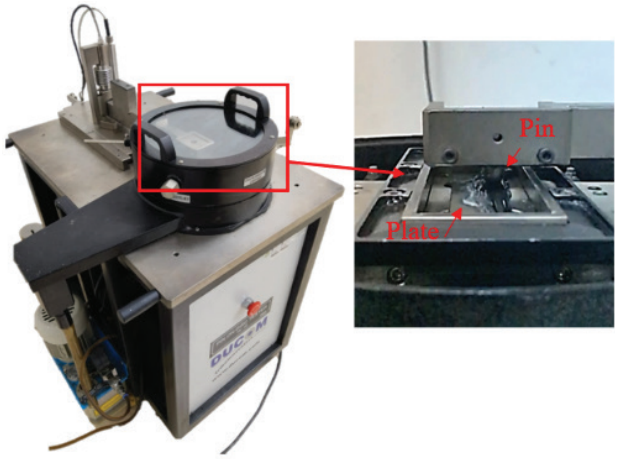

Figure 1. Pin-on-plate experiment set up.

Both pin and plate were fabricated using a mild steel material as shown in *Figure 2*. The pins have a hemispherical shape with a 12 mm diameter and a 25 mm cylindrical body length. The plates were machined in cuboid shape with the dimensions of 100 × 28 × 6 mm. All the pins and plates were fabricated according to the ASTM G99 for the standard pin-on-plate test.

TABLE 1. COMPOSITIONS OF THE GREASE FORMULATIONS

Thickener agent	Thickener concentration (%)	Base oil	Name	Type of thickener
Cellulose	30	Palm olein	POCl	Organic
Chitosan	30	Palm olein	POCt	Organic
Lithium	13	Palm olein	POLi	Inorganic
Food grade grease	unknown	unknown	FG	unknown

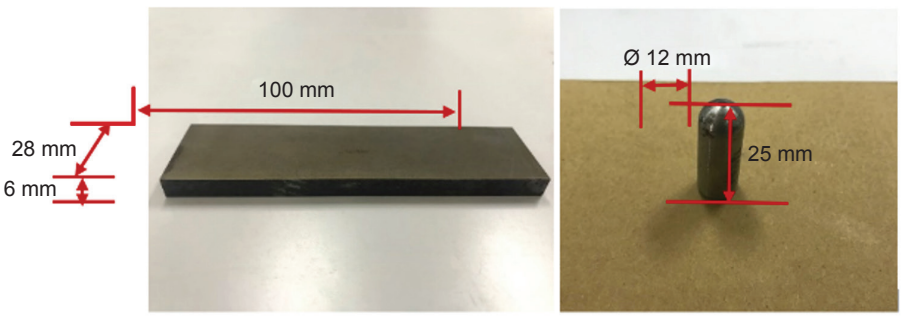

Figure 2. Plate and pin used in testing.

Surface Characterisation

Surface characterisation was performed by using Hitachi S3400N Scanning Electron Microscope and Zeiss LSCM 700 Laser Scanning Confocal Microscope. Using this technique, the surface micrograph, morphology and wear profile of the tested pin and plate were evaluated. Elemental analysis was carried out using Energy-dispersive X-ray (EDX) analysis to further evaluate the material elements in the surface micrograph.

Thermal Analysis

Thermal analysis was performed to evaluate the thermal resistance of the grease before undergoing degradation. The grease's thermal resistance was explored through thermogravimetric analysis, which provides insights into the thermal decomposition of the utilised materials. The interception between the temperature at which the grease starts to degrade and the tangent of the curve is denoted by T_{onset} while T_{max} is the temperature of the grease when there is a rapid change in mass (from the temperature derivative graph). T_{offset} is the interception between the temperature of grease at which the mass does not change as the process continues and the tangent of the curve. These values were taken from the weight against the temperature graph. The thermogravimetric analysis was performed with a thermogravimetric Analyzer Pyris 1 (Perkin Elmer) where each sample was weighed at around 10 mg (± 5 mg), and the temperature was scanned from 25°C-700°C at a heating rate of 10°C min^{-1}. TGA was performed by placing the substance in platinum crucibles under the nitrogen flow of 100 mL min^{-1}.

RESULTS AND DISCUSSION

Grease Characteristics

The physical appearance of palm grease with thickeners is shown in *Figure 3*. From *Figure 3a*, it can be seen that the grease formulated with cellulose thickener (POCl) has a brownish-cream colour. The POCl grease also has a soft like ketchup consistency, providing relatively low viscosity. The physical appearance of palm grease with chitosan thickener (POCt) is shown in *Figure 3b*. It is observed that the completed POCt grease has a brownish-cream colour with a soft texture. From *Figure 3c* the formulated lithium thickener (POLi) grease turns into a soft white cream with colour. The POLi grease also has a soft semi-solid consistency with relatively high viscosity. From visual inspection, the POLi grease also has high or uniform homogeneity compared to other greases. Previous work employing chiton, chitosan-based thickeners exhibited values of COF comparable to standard lithium greases, however, these greases generally display quite poor mechanical stability (Sanchez *et al.*, 2011).

Tribological Properties

Coefficient of friction. *Figure 4* shows the specific average of the coefficient of friction (COF) obtained from the pin-on-disc test lubricated with various greases. Grease with organic thickener (POCl and POCt) recorded the lowest COF value at 0.0840 followed by POLi and food grade (FG) greases with their corresponding value of 0.1015 and 0.1250 respectively. Theoretically, a higher COF value means that higher force is required to initiate and maintain the motion between the surfaces thus increasing the resistance while making it harder to move (Zeren *et al.*, 2007). The coefficient of friction obtained in this study shows that the newly developed greases using organic substances which are cellulose and chitosan thickeners give a promising result as compared to the others. This result indicates that organic thickeners used in this experiment pose excellent friction and better performance than the lithium and food-grade grease in terms of COF.

Pin wear mass loss analysis. The mass of the pin subjected to contact during the pin-on-disc test was measured before and after testing to evaluate the amount of material removed after the pin and

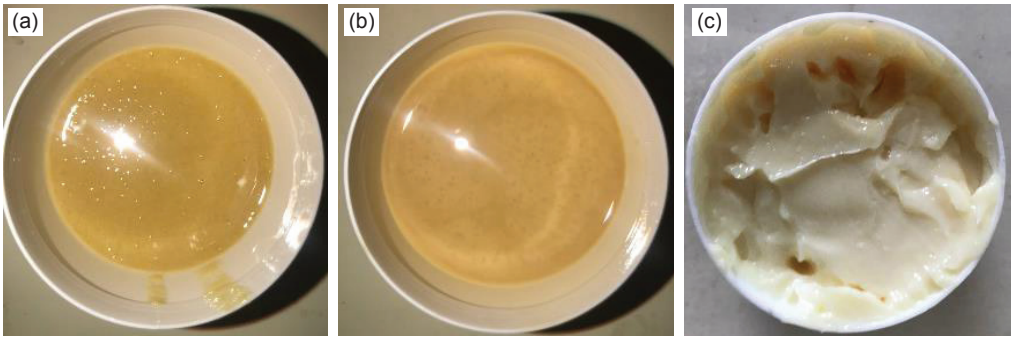

Figure 3. Palm grease developed with (a) cellulose (POCl), (b) chitosan (POCt) and (c) lithium thickener (POLi).

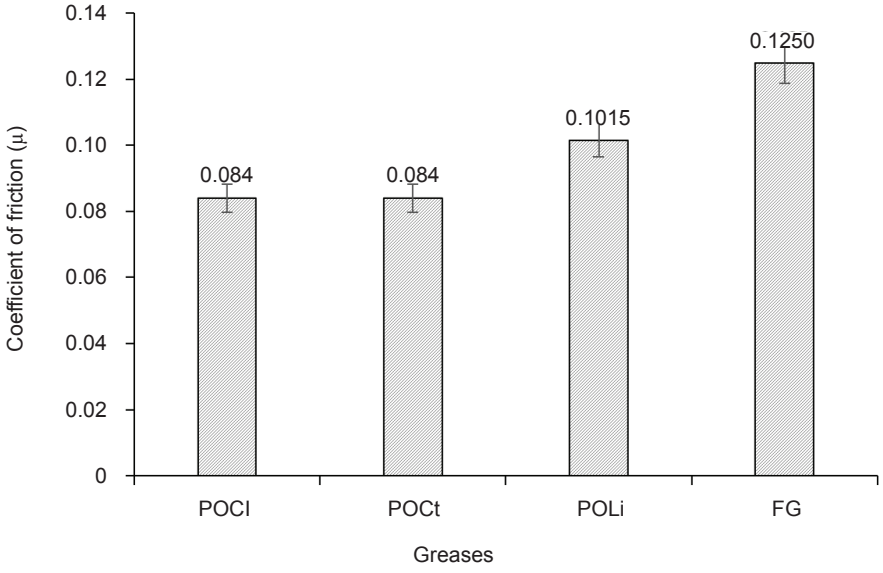

Figure 4. Coefficient of friction for all greases.

plate sliding contact. *Figure 5* shows the pin mass loss analysis for all greases. Overall, all pins show a minuscule and almost similar mass loss percentage in a range of 2 to 6 $x10^{-5}$%. The pin lubricated with POCl and POCt has a slightly higher mass loss percentage with a value of 6.1388 $x10^{-5}$% and 6.1388 $x10^{-5}$% respectively. FG grease shows the lowest mass loss with a value of 2.6486 $x10^{-5}$% followed by POLi with 4.6158 $x10^{-5}$% mass reduction. This finding shows that the formulated palm olein grease with organic thickener shows comparable properties compared to the conventional POLi and commercial food grade grease. POLi has been proven to have superior performance in mineral grease application (Sukirno *et al.*, 2009; Zhou *et al.*, 2022). Meanwhile, the FG has been commercially used and the properties have been enhanced with additives by the manufacturer.

Plate wear groove depth analysis. *Figure 6* shows the three-dimensional (3D) morphology of the plate groove formed during the pin-on-plate test and the related c value is shown in *Figure 7*. From the figure, the POCl and POCt grease show almost identical surface topography with the lowest wear depth of 13.7 μm. Most of the groove regions in POCl and POCt are in light blue colour which indicates that it has lower depth as compared to POLl and FG greases. The highest groove wear depth occurs on the FG grease plate with a value of 16.1 μm. The dark blue colour on the height map shows the highest depth region while the red one indicates the upper surface of the plate. The high depth indicates that more material was removed during the contact. POLi grease shows a slightly lower depth groove formed on the surface with a depth of 15.6 μm. The deep groove formed on the plate surface indicates the lubricant failure in protecting the surface from wear. This finding shows that the developed palm grease with organic thickener can protect the surface from wear by forming a shallower groove depth. In addition, the COF of the contact lubricated by these lubricants are shown to be low in *Figure 4*. This shows the good agreement between friction and wear analysis where low COF during contact causes less wear or material removal.

Surface characterisation. The SEM micrographs of the plates are shown in *Figure 8*. *Figure 8a* displays the initial plate surface condition before contact as a reference and *Figure 8b-8d* show the images of the samples after being subjected to sliding contact applied with different greases. The image on the left displays the surface micrograph at 100x and the right side displays the enlarged micrograph image at 500x magnification. The yellow arrow shows the movement of the sliding plate during the test. The wear groove produced on the plate is highlighted in the rectangular area. For the POCl plate in *Figure 8b*, the groove marks can be seen at the area of contact with the pin. A brighter colour is observed at the area where a groove formed on the plate for all the samples after the test. Apart from groove formation, we can see that the area which is in contact with the pin is smoother than the other part of the plate as expected due to surface smoothening by sliding of the surface asperities (Yusof & Ripin, 2014, 2016). This deformation can be attributed to the contact stress developed during the surface

Samples	Mass before (g)	Mass after (g)	Total mass loss (g)	Reduction ($x10^{-5}$%)
POLi	25.9978	25.9966	0.00113	4.6158
POCl	26.0637	26.0621	0.00160	6.1388
POCt	26.0433	26.0416	0.00170	6.5275
FG	26.0429	26.0422	0.00070	2.6486

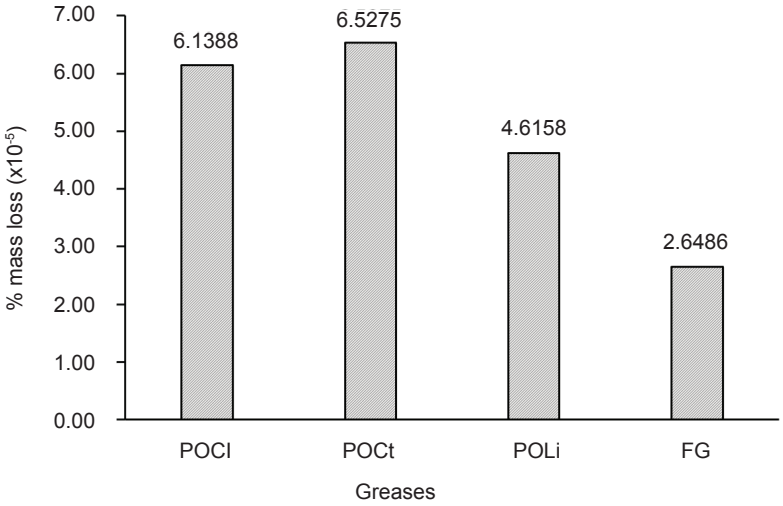

Note: POCl - cellulose; POCt - chitosan; POLi - lithium thickener; FG - food grade.

Figure 5. Percentage of mass loss of the pin for all greases.

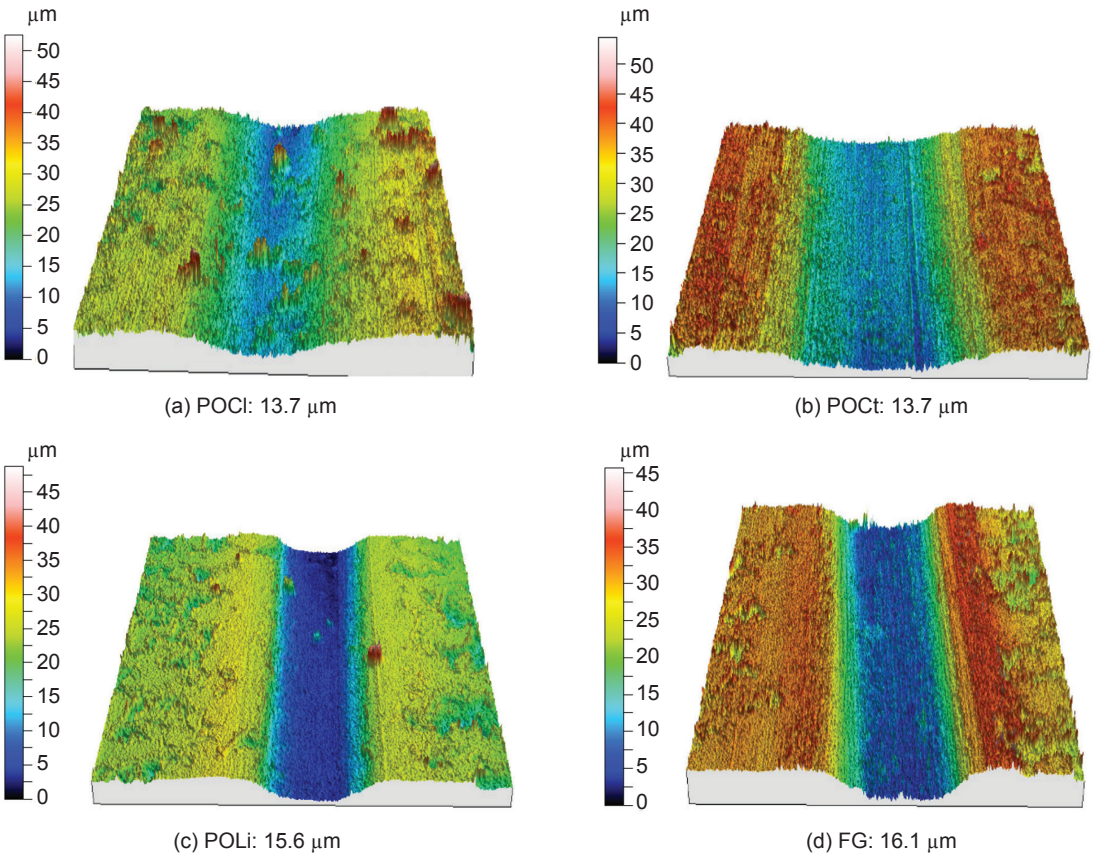

Figure 6. 3D surface topography of the plate groove for (a) cellulose (POCl), (b) chitosan (POCt), (c) lithium thickener (POLi) and (d) food grade (FG) greases.

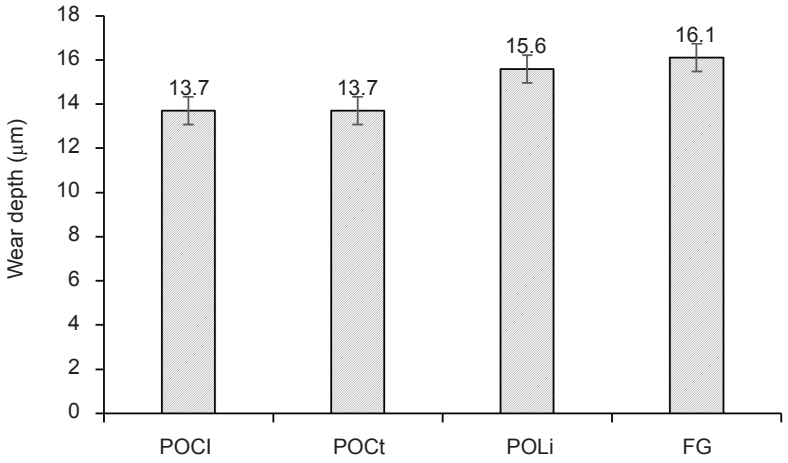

Figure 7. Groove wear depth.

contact (Adman & Yusof, 2020). The enlarged image in *Figure 8b* shows the presence of white particles deposited on the surface of the plate. It is expected that these particles are from cellulose thickener that protects the plate surface by acting as a pressure absorber hence reducing the groove wear depth produced on the plate. According to Gupta *et al.* (2019) cellulose is a complex polysaccharide composed of repeating units of glucose molecule with the material composition mainly consisting of carbon, hydrogen and oxygen atoms arranged in a specific molecular structure. This was also observed by Hussein *et al.* (2019) where some portion of the pressure was carried by fine particles and reduced adhesion wear. This could be a reason why there is no distinct groove formed on the plate with the lubrication using POCl grease. *Figure 8c* shows the image micrograph for the POCt sample. The enlarged image shows medium-sized white particles presumably originating from the chitosan thickener. Chitosan is a naturally occurring polysaccharide derived from chitin, which is found in the exoskeletons of crustaceans such as shrimp, crabs and lobsters with the material composition of carbon, hydrogen, oxygen and nitrogen atoms, with a specific arrangement (Ramawat & Mérillon, 2015). Elemental analysis of both white particle substances indicates the presence of a high quantity of carbon and oxygen elements, hence resulting in a high percentage of carbon and oxygen detected on the surface.

Figure 8d shows the groove formation on the surface of the plate using POLi grease lubrication. It is observed that the sliding movement of the pin has generated a significant wear depth on the plate and initiation of micro crack. Based on the previous surface topography analysis in *Figure 6*, this image is taken at the groove depth of 15.6 μm. It is expected that at this depth, continuous sliding contact has started to disrupt the materials by crack initiation and severe material loss. *Figure 8e* shows the groove formation on the surface of the plate using FG grease lubrication. The sliding marks are obvious and the enlarged image shows that the surface starts to form a lot of microcracks at the groove depth of 16.1 μm. In addition, it is observed that white colour tiny particles are present, expected from the additive that is used in the food grade grease. Further elemental analysis revealed the presence of silicon in the area of the white particles. Based on existing literature, the silicon derivative is incorporated into the material composition as an additive during the grease preparation process, fulfilling its role in enhancing the grease's properties such as increasing thermal resistance (Liang & Ji, 2022).

Thermal analysis. *Figure 9* shows thermogravimetric analysis curves in terms of weight against temperature for all greases and *Table 2* shows the related temperature. It is observed that the *Tonset* of the grease that is made of organic thickeners (POCl and POCt) is slightly lower than grease using POLi which is within the range of 370.00°C-390.00°C. FG sample shows the lowest T_{onset} around 338.31°C which means that the grease starts to degrade earlier than the others. The T_{onset} is often used as an indicator of the thermal stability of a material. A lower onset temperature suggests that the material cannot withstand higher temperatures and undergo significant decomposition or weight loss early. In the previous work, Sanchez *et al.* (2014) observed that the formulated acylated chitosan displayed better thermal resistance than the lithium and calcium thickened grease.

The decomposition temperature range for both POCl and POCt are 264.08°C-544.66°C and 253.77°C-543.22°C respectively. These ranges are close to the grease made from POLi. In addition,

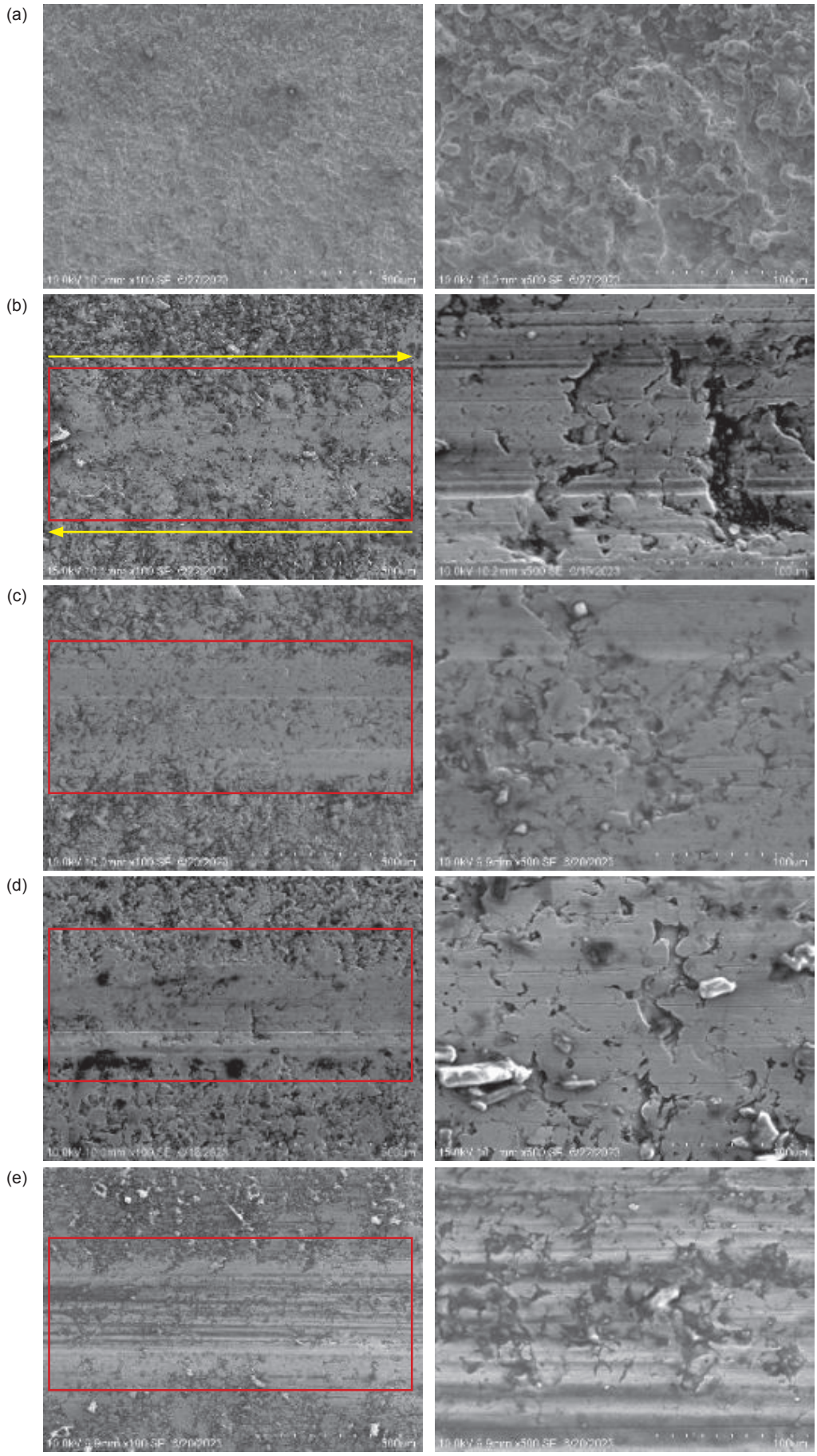

Figure 8. (a) New, (b) cellulose (POCl), (c) chitosan (POCt), (d) lithium (POLi) and (e) food grade grease (FG).

three of them also show the widest range of T_{onset} and T_{offset} as compared to FG grease. Thermal characteristics for both organic thickeners show a slightly similar behaviour in which their decomposition range is in between 250.00°C-545.00°C. Besides, the thermal decomposition of greases that contain cellulose and chitosan also exhibits a two-stage process, whereas the other two greases undergo thermal decomposition in a single stage. Based on the existing literature, in the case of organic thickeners, the derivative function of weight loss against temperature reveals the presence of two distinct peaks, which indicates the thermal decomposition process occurs in two stages. According to Sánchez *et al.* (2011), the first stage of decomposition–belonged to the degradation of the thickener itself while the second one is associated with the thermal degradation of the base oil (palm olein).

Implications and Limitations of Study

The study of green lubricants holds significant implications for both environmental sustainability and technological advancement in renewable energy. Based on the findings of this study, the grease performance in the aspect of tribological and thermal characteristics shows the potential of grease as an alternative to conventional mineral-based lubricants. This supports the need for a safe and sustainable lubricant, consequently leading to a decrease in pollution and ensuring a safe working environment. While the findings of this study focused on the performance of the developed grease, further work needs to be done to evaluate the level of biodegradability of the developed grease. This requires a commitment from multidiscipline studies with the aspiration to create lubricants of exceptional performance and unwavering reliability.

TABLE 2. THERMOGRAVIMETRIC ANALYSIS OF TEMPERATURES

Item	T_{onset} (°C)	T_{max} (°C)	T_{offset} (°C)	Decomposition range (°C)
POCl	387.38	429.68	448.04	264.08-544.66
POCt	378.83	435.80	454.09	253.77-543.22
POLi	395.78	429.64	454.88	274.50-540.27
FG	338.31	400.55	418.90	228.04-462.66

Note: POCl - cellulose; POCt - chitosan; POLi - lithium thickener; FG - food grade.

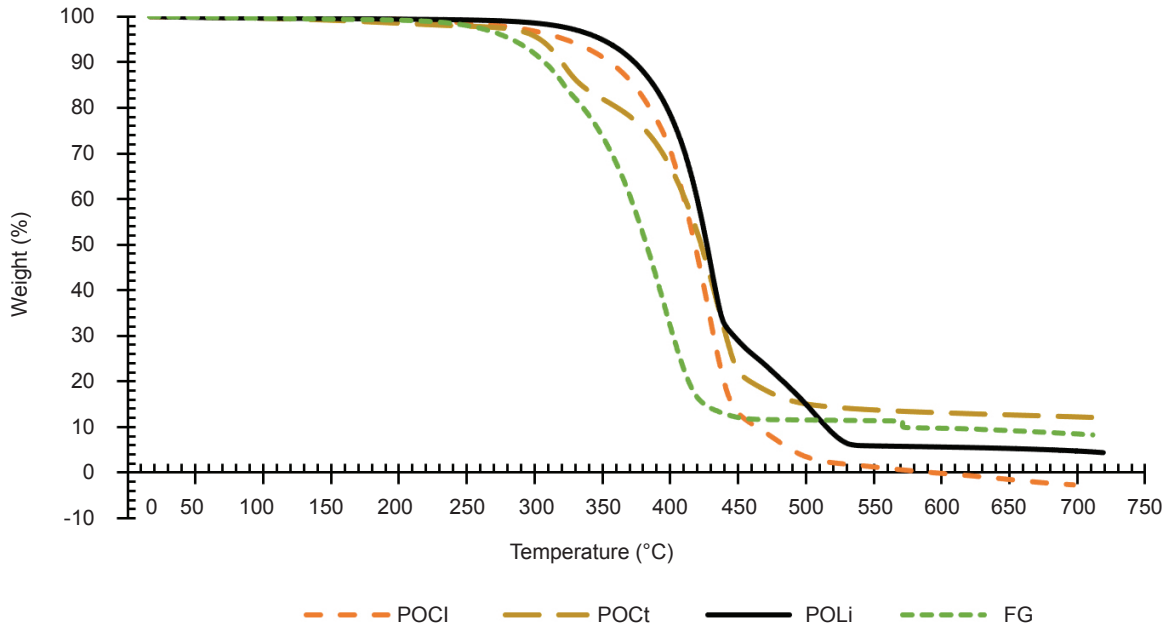

Figure 9. Weight percentage as a function of temperature.

CONCLUSION

This study revealed that the palm grease formulated with organic thickeners exhibits a lower coefficient of friction (0.0840) in comparison to both lithium-based (0.1015) and food-grade grease (0.1250). Mass loss analysis of the pin indicates comparable mass loss among all grease samples in a range of 2 to 6 $x10^{-5}$%. The grease containing organic thickener exhibits a shallower wear groove depth on the plate with the existence of white particles. Elemental analysis indicated that the particles result from elevated levels of carbon and oxygen which is attributed to the organic thickener material. The grease formulated with organic thickeners exhibits a slightly lower onset temperature (378.83°C) compared to the grease containing lithium thickeners (395.78°C), yet superior to the food grade grease (338.31°C), indicating good thermal stability. The finding indicated that RBD palm olein greases formulated with organic thickeners demonstrate positive performance attributes, in terms of coefficient of friction, groove wear depth, and thermal stability.

ACKNOWLEDGEMENT

The authors thank the Ministry of Higher Education Malaysia for providing a research fund (FRGS/1/2019/TK03/USM/03/4) and Universiti Sains Malaysia for providing a workspace to complete this study.

REFERENCES

Abdulbari, H. A., & Zuhan, N. (2018). Grease formulation from palm oil industry wastes. *Waste and Biomass Valorization*, *9*(12), 2447–2457. https://doi.org/10.1007/s12649-018-0237-6

Acar, N., Kuhn, E., & Franco, J. M. (2018). Tribological and rheological characterization of new completely biogenic lubricating greases: A comparative experimental investigation. *Lubricants*, *6*(2), 45. https://doi.org/10.3390/lubricants6020045

Adman, A. A., & Yusof, N. F. M. (2020). Analysis of contact stress and vibration of rolling element bearing. *IOP Conference Series Materials Science and Engineering*, *815*(1), 012001. https://doi.org/10.1088/1757-899x/815/1/012001

Ahme, L., Kuhn, E., & Canto, M. Á. D. (2023). On the optical assessment of the structural degradation of rheologically stressed lubricating greases. *Tribology International*, *187*, 108771. https://doi.org/10.1016/j.triboint.2023.108771

Barboza, A. B. V., Dinesha, P., & Rosen, M. A. (2023). Effect of green fuel and green lubricant with metallic nanoparticles on emissions of HC, CO, NOx, and smoke for a compression ignition engine. *Environmental Science and Pollution Research*, *30*(39), 91344–91354. https://doi.org/10.1007/s11356-023-28645-z

García-Zapateiro, L., Valencia, C., & Franco, J. (2014). Formulation of lubricating greases from renewable basestocks and thickener agents: A rheological approach. *Industrial Crops and Products*, *54*, 115–121. https://doi.org/10.1016/j.indcrop.2014.01.020

Gupta, P. K., Raghunath, S. S., Prasanna, D. V., Venkat, P., Shree, V., Chithananthan, C., Choudhary, S., Surender, K., & Geetha, K. (2019). An update on overview of cellulose, its structure and applications. In A. R. Pascual & M. E. Martin (Eds.), *Cellulose*. IntechOpen Ltd. https://doi.org/10.5772/intechopen.84727

Hussein, H. A., Mahdi, H. H., & Ghazi, A. K. (2019). Tribological behavior and lubrication mechanism of fine particles in the base oil SN500. *Journal of Engineering and Sustainable Development*, *23*(05), 108–116. https://doi.org/10.31272/jeasd.23.5.8

Hamnas, A., & Unnikrishnan, G. (2023). Bio-lubricants from vegetable oils: Characterization, modifications, applications and challenges – Review. *Renewable and Sustainable Energy Reviews*, *182*, 113413. https://doi.org/10.1016/j.rser.2023.113413

Japar, N. S. A., Aziz, M. A. A., Razali, M. N., Zakaria, N. A., & Rahman, N. W. A. (2019). Preparation of grease using organic thickener. *Materials Today Proceedings*, *19*, 1303–1308. https://doi.org/10.1016/j.matpr.2019.11.141

Liang, X., & Ji, H. (2022). Tribological properties of lubricating grease additives made of silica and silicon carbide nanomaterials. *Integrated Ferroelectrics*, *225*(1), 212–224. https://doi.org/10.1080/10584587.2021.1911243

Muhammad, A. I., Yusof, N. F. M., & Ripin, Z. M. (2023). The tribological performance analysis of palm olein-based grease lubricants containing copper nanoparticle additive. *Proceedings of the Institution of Mechanical Engineers Part J Journal of Engineering Tribology*, *237*(12), 2162–2177. https://doi.org/10.1177/13506501231190695

Panchal, T., Chauhan, D., Thomas, M., & Patel, J. (2015). Bio based grease: A value added product from renewable resources. *Industrial Crops and Products*, *63*, 48–52. https://doi.org/10.1016/j.indcrop.2014.09.030

Ramawat, K. G., & Mérillon, J. M. (2015). *Polysaccharides: Bioactivity and Biotechnology*. Springer.

Sánchez, R., Stringari, G., Franco, J., Valencia, C., & Gallegos, C. (2011). Use of chitin, chitosan and acylated derivatives as thickener agents of vegetable oils for bio-lubricant applications. *Carbohydrate Polymers*, *85*(3), 705–714. https://doi.org/10.1016/j.carbpol.2011.03.049

Sánchez, R., Valencia, C., & Franco, J. M. (2014). Rheological and tribological characterization of a new acylated chitosan-based biodegradable lubricating grease: A comparative study with traditional lithium and calcium greases. *Tribology Transactions*, *57*(3), 445–454. https://doi.org/10.1080/10402004.2014.880541

Saxena, A., Kumar, D., & Tandon, N. (2021). Development of eco-friendly nano-greases based on vegetable oil: An exploration of the character via structure. *Industrial Crops and Products*, *172*, 114033. https://doi.org/10.1016/j.indcrop.2021.114033

Sukirno, Fajar, R., Bismo, S., & Nasikin, M. (2009). Biogrease based on palm oil and lithium soap thickener: Evaluation of antiwear property. *World Applied Sciences Journal, 6*(3), 401-407.

Vafaei, S., Jopen, M., Jacobs, G., König, F., & Weberskirch, R. (2022). Synthesis and tribological behavior of bio-based lubrication greases with bio-based polyester thickener systems. *Journal of Cleaner Production*, *364*, 132659. https://doi.org/10.1016/j.jclepro.2022.132659

Yap, J. H., Lee, A. Y., & Yusof, N. F. M. (2022). A contact characteristic of roller bearing with palm oil-based grease lubrication. *Journal of Advanced Research in Fluid Mechanics and Thermal Sciences*, *89*(2), 139–149.

Yusof, N. F. M., & Ripin, Z. M. (2014). Analysis of surface parameters and vibration of roller bearing. *Tribology Transactions*, *57*(4), 715–729. https://doi.org/10.1080/10402004.2014.895887

Yusof, N. F. M., & Ripin, Z. M. (2016). A technique to measure surface asperities plastic deformation and wear in rolling contact. *Wear*, *368–369*, 496–504. https://doi.org/10.1016/j.wear.2016.09.017

Zeren, A., Feyzullahoglu, E., & Zeren, M. (2007). A study on tribological behaviour of tin-based bearing material in dry sliding. *Materials & Design*, *28*(1), 318–323. https://doi.org/10.1016/j.matdes.2005.05.016

Zhou, C., Ren, G., Fan, X., & Lv, Y. (2022). Probing the effect of thickener microstructure on rheological and tribological properties of grease. *Journal of Industrial and Engineering Chemistry*, *111*, 51–63. https://doi.org/10.1016/j.jiec.2022.03.010

Journal of Oil Palm Research Vol. 37 (3) September 2025 p. 560-572
DOI: https://doi.org/10.21894/jopr.2024.0049

ENVIRONMENTAL ASSESSMENT OF FATTY ACIDS PRODUCTION FROM PALM OIL USING LIFE CYCLE APPROACH

NOORAZAH ZOLKARNAIN[1]*; ZULINA ABD MAURAD[1]; VIJAYA SUBRAMANIAM[1] and RAZMAH GHAZALI[1]

ABSTRACT

To date, no comprehensive life cycle assessment (LCA) study has been conducted on palm-based fatty acids, the powerhouse of the oleochemical industry. Thus, a cradle-to-gate LCA for the production of palm-based fatty acids in Malaysia was performed to assess their potential environmental impacts. The life cycle impact assessment (LCIA) findings showed that the significant impacts for palm-based fatty acids were mainly attributed to the production of the feedstocks used, which are crude palm kernel oil (CPKO) and refined, bleached and deodorised palm stearin (RBDPS). The greenhouse gas (GHG) emission for the fatty acids studied is in the range of 1.39-9.43 kg CO_2 eq. per kg fatty acid and dropped to a range of 0.07-0.18 kg CO_2 eq. per kg fatty acids by excluding contributions from the production of feedstock. For CPKO-based fatty acid production, the energy substitution using oil palm biomass led to a reduction of up to 13% in global warming potential compared to grid electricity. The findings from this study can be used to establish baseline information on the environmental profile of fatty acids and draw up policies pertaining to the carbon credit scheme or green labelling for the sustainable production of palm-based fatty acids in the future.

Keywords: environmental impact, greenhouse gases, LCA, palm-based fatty acids, sustainability.

Received: 16 April 2024; **Accepted:** 4 September 2024; **Published online:** 8 November 2024.

INTRODUCTION

Fatty acids, which are one of the basic oleochemicals, play an important role in the development of the oleochemical industry as well as other non-food industries. Intermediate chemicals such as fatty acid methyl esters, fatty alcohols and fatty amines can also be produced from fatty acids feedstock (Kiatkittipong *et al.*, 2022). *Figure 1* shows the processing routes for basic oleochemicals and their derivatives. The expansion of the global market and the diversification of the use of fatty acids in various applications are among the major factors increasing the demand for these fatty acid products. The availability of supplies of raw materials such as palm oil and coconut oil, along with good infrastructure and facilities, has made Southeast Asia as the hub for fatty acid manufacturing. Accordingly, several new oleochemical plants producing fatty acids have been built in Southeast Asia. Meanwhile, fatty acid manufacturers in Malaysia and Indonesia are also taking proactive steps to increase their production capacity to meet the growing demand.

Currently, there are 19 oleochemical plants operating in Malaysia (Parveez *et al.*, 2022), which exported about 2.86 million tonnes of oleochemicals in 2023 (Malaysian Palm Oil Board [MPOB], 2024). In 2023 alone, fatty acids represent approximately 36% of the total oleochemical products exported from Malaysia. *Figure 2* shows the volume of fatty acid exports from 2010 to 2023. Generally, fatty acids are carboxylic acids with hydrocarbon chains comprising four to 36 carbon atoms. They can be classified into short chains with two to four carbon atoms, medium chains with six to 10 carbon atoms and long chains consisting of 12-26 carbon atoms (Siram *et al.*, 2019). There are three types of fatty acids, namely saturated, mono-unsaturated and

[1] Malaysian Palm Oil Board,
6, Persiaran Institusi, Bandar Baru Bangi,
43000 Kajang, Selangor, Malaysia.

* *Corresponding author e-mail: azah@mpob.gov.my*

polyunsaturated, where saturated fatty acids do not contain any double bonds or other functional groups along the carbon chain. Monounsaturated fatty acids have only one double bond in their alkyl chain. Meanwhile, polyunsaturated fatty acids contain more than one double bond in their alkyl chain. A common method for the production of fatty acids is the separation or splitting process of fats at high temperatures and pressures. In addition, fractionation and distillation are common processes involved in the production of fatty acids. Apart from these processes, there are also other processes involved, such as hydrogenation, bleaching, and cooling separation. The number of fractionations used for fatty acid production may differ from one plant to another, depending on the plant's design and capacity. Several fatty acid manufacturers introduced the bleaching process before the splitting process to purify the feedstock used. The hydrogenation process is also carried out to increase the number of saturated alkyl carbon chains in the feedstock used.

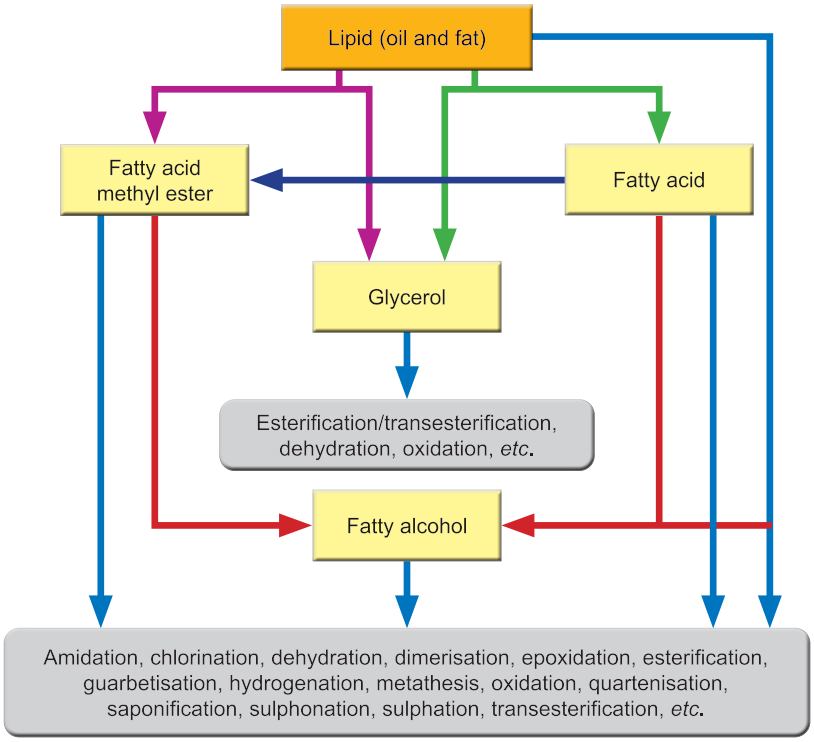

Source: Kiatkittipong *et al.* (2022).

Figure 1. Processing route of basic oleochemicals and its derivatives reaction.

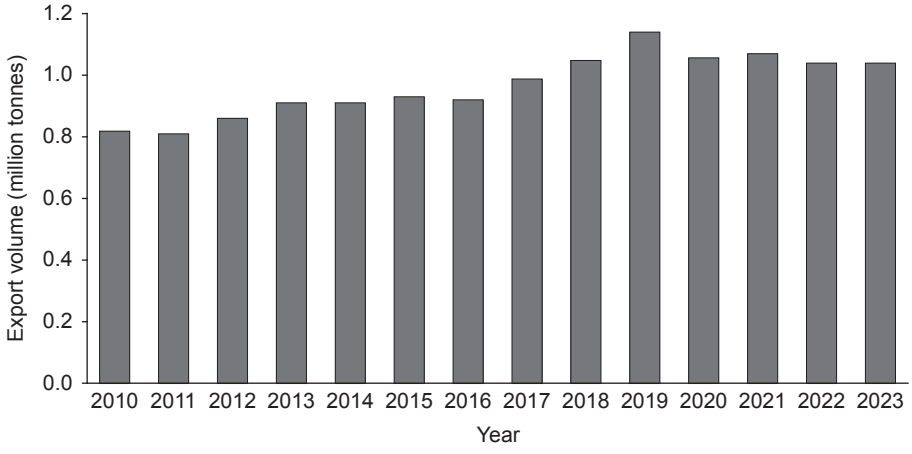

Source: MPOB (2011-2024).

Figure 2. Export of Malaysian fatty acids from 2010 to 2023.

Various fatty acids with different acid compositions (*Table 1*) have been produced in Malaysia using palm oil (PO) and palm kernel oil (PKO) products, including crude palm kernel oil (CPKO), crude palm oil (CPO), refined, bleached and deodorised palm oil (RBDPO), refined, bleached and deodorised palm kernel oil (RBDPKO) and refined, bleached and deodorised palm stearin (RBDPS). Caproic acid, caprylic acid, capric acid, lauric acid, myristic acid, palmitic acid, stearic acid and oleic acid are among the types of fatty acids that are often produced in Malaysia. With proper selection of carbon chain length with targeted properties, fatty acids can be used as starting materials to produce valuable oleochemical derivatives. These fatty acids can be used as feedstocks in the production of soaps, medium-chain triglycerides, polyol esters, detergents, emulsifiers, plastics, textiles, cosmetics, lubricants and many other products (Gervajio, 2005).

TABLE 1. FATTY ACID COMPOSITION IN PALM OIL AND PALM KERNEL OIL

Fatty acid	Composition (%)	
	Palm oil	Palm kernel oil
Caproic acid (6:0)	-	0.2
Caprylic acid (8:0)	-	3.3
Capric acid (10:0)	-	3.5
Lauric acid (12:0)	0.2	47.8
Myristic acid (14:0)	1.1	16.3
Palmitic acid (16:0)	44.0	8.5
Stearic acid (18:0)	4.5	2.4
Oleic acid (18:1)	39.2	15.4
Linoleic acid (18:2)	10.1	2.4
Linolenic acid (18:1)	0.4	-
Arachidic acid (18:2)	0.1	0.1

Source: Mancini *et al.* (2015).

The life cycle assessment (LCA) is highly recommended as a suitable tool for environmental evaluation of products or services that can be used to promote their sustainability (Salvador *et al.*, 2018). LCA provides a mechanism to evaluate the environmental impacts of products or processes by considering their entire life cycle. Currently, LCA on palm-based fatty acids produced by Malaysian fatty acid manufacturers is not available. However, the LCA approach is not new in the oil palm (OP) industry; in fact, several LCA studies on this industry have been conducted to address issues of sustainability and the environment. Hansen (2007) conducted the first LCA study on OP, which included a feasibility study of CPO performance in Malaysia. The most significant impact categories for CPO production were fossil fuels (FF) and respiratory inorganics, with minor impacts on global warming and acidification/eutrophication. On the other hand, continual environmental improvements were necessary for the OP industry in order to remain competitive in facing new challenges ahead. This fact was then proven by Subramaniam *et al.* (2010) through the LCA study on CPO production, where global warming was found to be the most significant impact caused by biogas from the anaerobic treatment of palm oil mill effluent (POME). Apart from that, an LCA study by Subramaniam *et al.* (2010) on the CPKO produced through a simple mechanical pressing method showed that the main impact contributors in the CPKO production were from OP upstream activities, *i.e.*, production and application of fertiliser and biogas emissions. It was suggested that integration between the palm kernel-crushing (PKC) plant and palm oil mill (POM) is the best approach in order to have the least environmental impacts for CPKO production.

There were also several LCA studies conducted on midstream PO products, *i.e.*, RBDPO, RBDPS, refined bleached and deodorised palm olein (RBDPOo) and biodiesel (Angarita *et al.*, 2009; Castanheira & Freira, 2017; Puah *et al.*, 2010; Silalertruksa & Gheewala, 2012; Siregar *et al.*, 2015; Tan *et al.*, 2010; Yee *et al.*, 2009; Yung *et al.*, 2020). In addition, a few LCA studies were also conducted on downstream (oleochemical) products, *i.e.*, polyol, methyl ester and methyl ester sulphonate (MES) as reported by Noorazah *et al.* (2015, 2016, 2017). All the LCA findings from these downstream studies showed that the major impact contributors in oleochemical production were from the production of feedstock used and/or utilities, which significantly contributed to climate change and FF depletion impact categories.

The overall greenhouse gas (GHG) emissions for each OP supply chain conducted in Malaysia were reported by Choo *et al.* (2011). The sustainability of the OP supply chain was proven through the complete cradle-to-gate LCA studies, where the best scenario practices and approaches were used. As concern for environmental issues increases, it is deemed necessary to evaluate the environmental performance of palm-based fatty acids, which are the major basic oleochemicals exported and commonly used in many consumer products. As of now, there have not been any LCA studies carried out for the production of palm-based fatty acids in Malaysia and this study is the first of its kind. Therefore, this article aims to evaluate the potential environmental impacts of fatty acid production in Malaysia using PO products as feedstock and different energy sources, which include electricity from the power grid and energy substitution using biomass from PO. As an outcome, the findings

of this study can be used as a benchmark for sustainable production of palm-based fatty acids in the future.

MATERIALS AND METHODS

Goal and Scope Definition

This LCA aims to develop baseline information for the production of fatty acids in Malaysia using CPKO and RBDPS as feedstocks, specifically to identify the impacts contributed by the production of fatty acids. The scope of this study covers the assessment of the production of the main fatty acids, *i.e.*, lauric acid, myristic acid, palmitic acid and stearic acid, at commercial fatty acid plants in Malaysia. The environmental impacts of fatty acid production were evaluated for a cradle-to-gate system boundary, covering OP nursery, OP plantation, POM and PO refinery up to the fatty acid plant with the exclusion of its use and distribution.

Functional Unit

The functional unit of this study is 1 kg of lauric acid, myristic acid, palmitic acid and stearic acid produced.

Inventory Data Source and Allocation

The original production data were obtained from fatty acid manufacturers based in Malaysia through actual on-site quantification of the raw materials, water, electricity, energy, chemicals, products and wastes. The inventory data were collected, verified and then back-calculated according to the functional units. The source of data used in this study is listed in *Table 2*. Other established background data were also used in order to support the site-specific foreground data, including from the Ecoinvent 3.4 and Agri-footprint databases. In this study, mass allocation was used as the main allocation for the baseline assessment, which was based on the yield of the product from fat splitting process, *i.e.*, 95.0% fatty acids (main product) and 12.0% glycerol (co-product). In this case, the mass allocation used for utilities and chemical among the fatty acid was the same based on the percentage yield of the fatty acids production in Malaysia, which made mass allocation as 88.7% (fatty acids) and 11.3% (glycerol). Besides, the economic values were volatile, fluctuated based on time, and required data to be updated frequently. However, the economic allocation was conducted through a sensitivity analysis, as described in the scenario of the study in *Table 2*.

TABLE 2. SOURCES AND SCENARIOS OF THE OIL PALM SUPPLY CHAIN USED IN THIS STUDY

Stage	Source
OP nursery	Muhamad *et al.* (2014) • Seedling cultivated for 10-12 months
OP plantation	Hashim *et al.* (2014) • Land use change from OP to OP • Cultivated on mineral soils • OP tree life cycle: 25 years
POM	Subramaniam *et al.* (2020) • Biogas capture scenario at 90% capture efficiency • Mass allocation: CPO (58%), palm kernel (24%), palm kernel shell (18%)
PKC plant	Subramaniam *et al.* (2020) • Plant operating in the proximity of ports
PO refinery plant	Yung *et al.* (2020)
Fatty acids plant	• Data obtained from fatty acids manufacturers in Malaysia • Scenarios for LCA study: 1) Scenario 1: Production of fatty acids using continued land use (OP to OP) with biogas capture, energy source from electricity grid - using cradle-to-gate system boundary 2) Scenario 2: Production of fatty acids using continued land use (OP to OP) with biogas capture, energy source from OP biogas capture - using cradle-to-gate system boundary 3) Sensitivity analysis: Production of fatty acids as in Scenario 1 based on economic allocation

Note: OP - oil palm; PO - palm oil; PKC - palm kernel-crushing; CPO - crude palm oil; LCA - life cycle assessment; POM - palm oil mill.

System Boundary

Figure 3 shows a system boundary for the life cycle impact assessment (LCIA) of fatty acid production. In the OP nursery, the growth and development of OP seedlings for the first 10-12 months are closely monitored before transporting the seedlings to the OP plantation (Haryati *et al.*, 2022; Muhammad *et al.*, 2010). The OP seedlings are field-planted on mineral soils at the OP plantation when they reach 12-15 months old. The OP is first harvested within two to three years after being planted in the plantation and this is a continuous process for the next 20-25 years, where one fresh fruit bunches (FFB) is produced every 10-21 days (Zulkifli *et al.*, 2010). Both the nursery and plantation activities involve the use of pesticides and fertiliser for OP growth. Then, the harvested FFB is immediately delivered to POMs to ensure the production of high-quality CPO (Foong *et al.*, 2019).

At this stage, the extracted CPO is clarified in order to remove any water, dirt and impurities, before being transferred into the storage tank. Later, the CPO is sent for refining or export purposes (Subramaniam *et al.*, 2010). Meanwhile, the palm kernel (PK) is transported to the kernel crushing plants for CPKO extraction, while the PK shell is used as a boiler fuel. Apart from CPO, PK and PK shell, other main by-products produced at the POMs are empty fruit bunches (EFB), pressed mesocarp fibre and POME or sludge. At the kernel crushing plant, the cleaned PK is processed using a continuous screw press (expeller) and PK cake is discharged from this process as a by-product (Subramaniam *et al.*, 2010). The CPO from POM is then sent to the refining plant for the production of refined PO products. At this refining stage, the CPO undergoes a purification process to remove any undesired minor components, *e.g.,* gums, free fatty acids (FFA), heavy metals, colour pigments and others before the products, *i.e.,* RBDPO and palm fatty acid distillate (PFAD), are obtained (Yung *et al.*, 2020). The RBDPO is then fractionated into RBDPS and RBDPOo products.

Generally, a common method employed for fatty acid production is fat splitting, which is carried out at high temperatures between 240°C and 260°C and at high pressure. The CPKO or RBDPS, which are used as feedstock, will hydrolyse at high temperatures and high pressures to become fatty acids and sweet water, also known as crude glycerol. The raw fatty acids are then fractionated or distilled based on different boiling points to produce the desired fatty acid chain length composition. The fatty acids obtained through this process are referred to as light-cut (consists mainly of caproic acid, caprylic acid, and capric acid), mid-cut (mixtures of lauric acid and myristic acid), and heavy-cut (from palmitic acid upwards). Sometimes, the hydrogenation process will also be introduced to harden the fatty acids by modifying their unsaturation level.

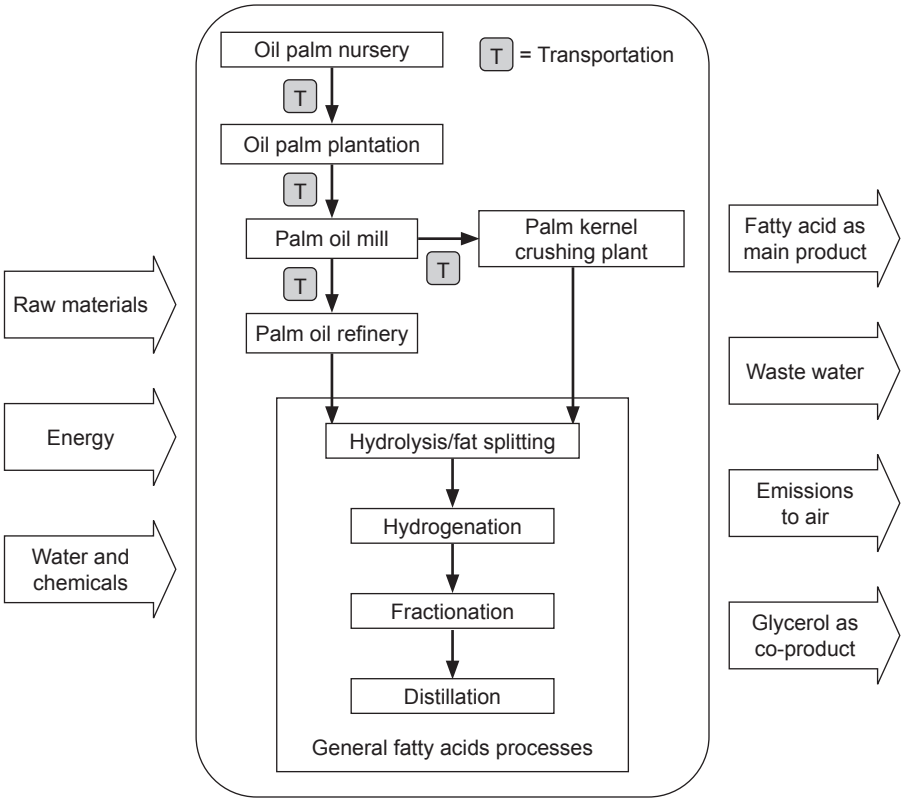

Figure 3. System boundary for fatty acid production using palm oil products as feedstock.

Life Cycle Impact Assessment

The LCA study was performed based on International Organization for Standardization (ISO) 14040:2006 and 14044:2006 standards (ISO, 2006a; 2006b), while SimaPro 9.1.1.1 software was chosen to assess the LCIA of this study. The LCIA aims to describe the environmental impacts of the process. The ReCiPe 2016 midpoint methodology was applied using the 'hierarchist' perspective to estimate the potential environmental impacts from fatty acid production. The environmental impacts of the study were analysed and discussed.

Sensitivity Analysis

The sensitivity analysis is performed in order to investigate the changes in the calculation of the final LCA results by setting different parameters or values for the most significant contributors in the study, with any assumptions unchanged throughout the study. In accordance with the ISO 14044:2006 standard (ISO, 2006b), sensitivity analysis is a procedure to check if changes in data affect the results of the LCIA. In this study, sensitivity analysis on economic allocation was conducted using the average prices of fatty acids and glycerol.

RESULTS AND DISCUSSION

Life Cycle Inventory (LCI)

Table 3 shows the consolidated average data for fatty acid production, encompassing OP nursery, plantation, POM, PO refinery and fatty acid plants. These data are the average data of six fatty acid manufacturers (for lauric acid, myristic acid and palmitic acid) and five fatty acid manufacturers (for stearic acid). In this study, weight allocation was carried out for the input and output flows of each product stage. The transportation in the consolidated data is for all product stages except for the fatty acid production boundary. Natural gas was used only at the PO refinery and fatty acid plants. The power supply for the whole supply chain was obtained from a non-renewable energy source where FF was consumed and wastes were generated along the process. The electricity data were taken from the Malaysian electricity profile generated at power stations as national grid source. For the electricity process flow, the input data was collected, including the mining process and extraction of FF (natural gas, coal, *etc.*), the production of electricity, and its distribution to the grid at the points of use. In this case, the power consumption from electricity using the national grid per kg of fatty acids produced varies, depending on the processes involved in each fatty acid production. Some of the fatty acid manufacturers used a combination of biomass (about 13% in total) and natural gas to produce heat for their boiler systems. Furthermore, the number of fractionation processes also varies for all fatty acids, from single fractionation up to triple fractionations, depending on the plant design and its capacity. The use of triple fractionations with hydrogenation processes elucidated why natural gas consumption somehow was higher in some fatty acid production.

Three types of water were used in the overall process, *i.e.*, deionised water (for high-pressure steam), softened water (for boiler feed water and low-pressure steam) and tap water (mainly for cleaning and cooling water). During the oil

TABLE 3. CONSOLIDATED AVERAGE DATA ON FATTY ACID PRODUCTION

Input (nursery-plantation-mill-refinery-fatty acids)	Average per t fatty acids			
	Lauric acid	Myristic acid	Palmitic acid	Stearic acid
Seedlings	5.02	14.87	17.93	27.77
FFB (t)	15.22	45.05	54.32	84.15
Palm kernel (t)	5.23	15.48	-	-
CPO (t)	-	-	10.65	16.50
RBDPO (t)	-	-	10.09	15.64
Pesticides (kg)	20.58	60.91	73.44	113.78
Fertilisers (kg)	737.42	2,182.69	2,631.82	4,077.10
Fuels, total (kg)	32.74	96.96	121.12	187.64
Water, total (m^3)	12.44	36.78	97.92	151.22
Electricity, total (kWh)	635.08	1,813.14	430.45	573.80
Natural gas (m^3)	66.40	162.00	96.92	182.97
Chemicals (kg)	25.3	9.60	148.06	207.16
Hydrogen (m^3)	-	-	51.2	90.3
Transportation, total (tkm)	586.68	586.68	654.08	654.08

Note: FFB - fresh fruit bunches; PK - palm kernel; CPO - crude palm oil; RBDPO - refined, bleached and deodorised palm oil.

splitting process in fatty acid production, crude glycerol or sweet water was also produced as a co-product. In most oleochemical plants, this crude glycerol will be purified up to 99.5% for high-end applications. Overall, there were many differences in fatty acid processes between the manufacturers, which include the number of steps in the process, utilities, and source of energy. The different ranges in energy consumption might be due to the plant design requirements, fractionator efficiency, boiler efficiency and the number of steps in the processes in each fatty acid production.

Life Cycle Impact Assessment (LCIA)

The characterised LCIA for all fatty acid production at midpoint level is shown in *Figure 3*. CPKO production was found to be the single major contributor in all impact categories evaluated for lauric acid and myristic acid productions (*Figure 4a* and *4b*), whereas RBDPS, which is produced from RBDPO, was the largest contributor in palmitic acid and stearic acid productions (*Figure 4c* and *4d*). Other than that, there were also contributions from the production and consumption of natural gas and electricity in almost all impact categories for all fatty acid production. The intensity of energy for the production of CPKO-fatty acids is higher compared to RBDPS-fatty acids due to the processes involved, mainly at the milling stage.

Scenario 1: Cradle-to-gate of fatty acid production using continued land use (OP to OP) and biogas capture, with energy sources from the electricity grid. The environmental impacts for 1 kg of each fatty acid studied were quantified for all impact categories, as shown in *Table 4*. Among these impact categories, only six contribute significantly to fatty acid production, with more than 0.5 units (cut-off criteria) of their respective impact categories is elaborated in detail, which are global warming, terrestrial ecotoxicity, freshwater ecotoxicity, marine ecotoxicity, human non-carcinogenic toxicity and fossil resource scarcity.

Global warming. Global warming is known as one of the most applied environmental impact indicators in any LCA study and is expressed in kg CO_2 eq. Consequently, this study measured how much GHG was emitted from fatty acid production and trapped in the atmosphere and was calculated using the global warming potential factors published in the Intergovernmental Panel on Climate Change (IPCC) report (IPCC, 2013; Yung *et al.*, 2020). The results indicated that the production of myristic acid had the highest impact on global warming compared to other fatty acids (*Table 4*) due to the contribution from the production of CPKO used as feedstock, *i.e.,* the amount of CPKO required to produce 1 kg of myristic acid is almost three times higher than lauric acid on average. This could be caused by the different fatty acid composition in PKO as described in *Table 1*, where a huge amount of CPKO is required to produce 1 kg of myristic acid compared to lauric acid. Meanwhile, palmitic acid, which is produced from RBDPS, had the lowest impact on global warming, 36% lower than the impact generated by stearic acid. The significant contributors to GHG emissions from CPKO production are POME, N-based fertiliser and the production of electricity. Both POME from the POM and fertiliser used in the plantations are burdens carried by the feedstock from upstream activities.

It was observed that the higher the amount of feedstock and energy used, the higher the GHG emitted. The GHG emissions for all fatty acid productions vary due to the different types and amounts of feedstock used for each production. The GHG emission for myristic acid was higher among all fatty acids in this study due to the higher amount of feedstock used, *i.e.,* PK to produce CPKO with 9.43 kg CO_2 eq. per kg myristic acid, followed by lauric acid with 3.22 kg CO_2 eq. per kg lauric acid. However, the GHG values for RBDPS-based fatty acids, *i.e.,* palmitic acid and stearic acid, were slightly lower than those for CPKO-based fatty acids (lauric acid and myristic acid), which are 1.39 and 2.39 kg CO_2 eq. per kg of fatty acid, respectively. This is because the RBDPS process had a lower impact than the CPKO process due to the allocation made along the RBDPS supply chain. Nevertheless, through this study, the GHG emissions for all fatty acid production were reduced up to >90% when gate-to-gate system boundary analysis was performed, where the GHG dropped to a range of 0.07-0.18 kg CO_2 eq. per kg of fatty acids. This finding is consistent with most LCA studies conducted for the downstream product, in which the possible impacts are primarily driven by the feedstock used, which bears the burdens of upstream processes.

Ecotoxicity and human toxicity. The toxicity was assessed using the maximum tolerable concentrations of substances that exist in the water and is expressed as kg 1,4-dichlorobenzene (1,4-DCB) equivalent. The ecotoxicity impact analysed in this study is a combination of impacts on terrestrial, freshwater, and marine ecotoxicity. In all fatty acid production, the ecotoxicity impact on the terrestrial ecosystem was found to be 93 times higher compared to the freshwater ecosystem. Meanwhile, the ecotoxicity impact on the marine ecosystem is less than 0.5 kg 1,4-DCB eq. for all fatty acids produced. The impact on ecotoxicity is mainly caused by the manufacturing of fertilisers and the consumption of pesticides

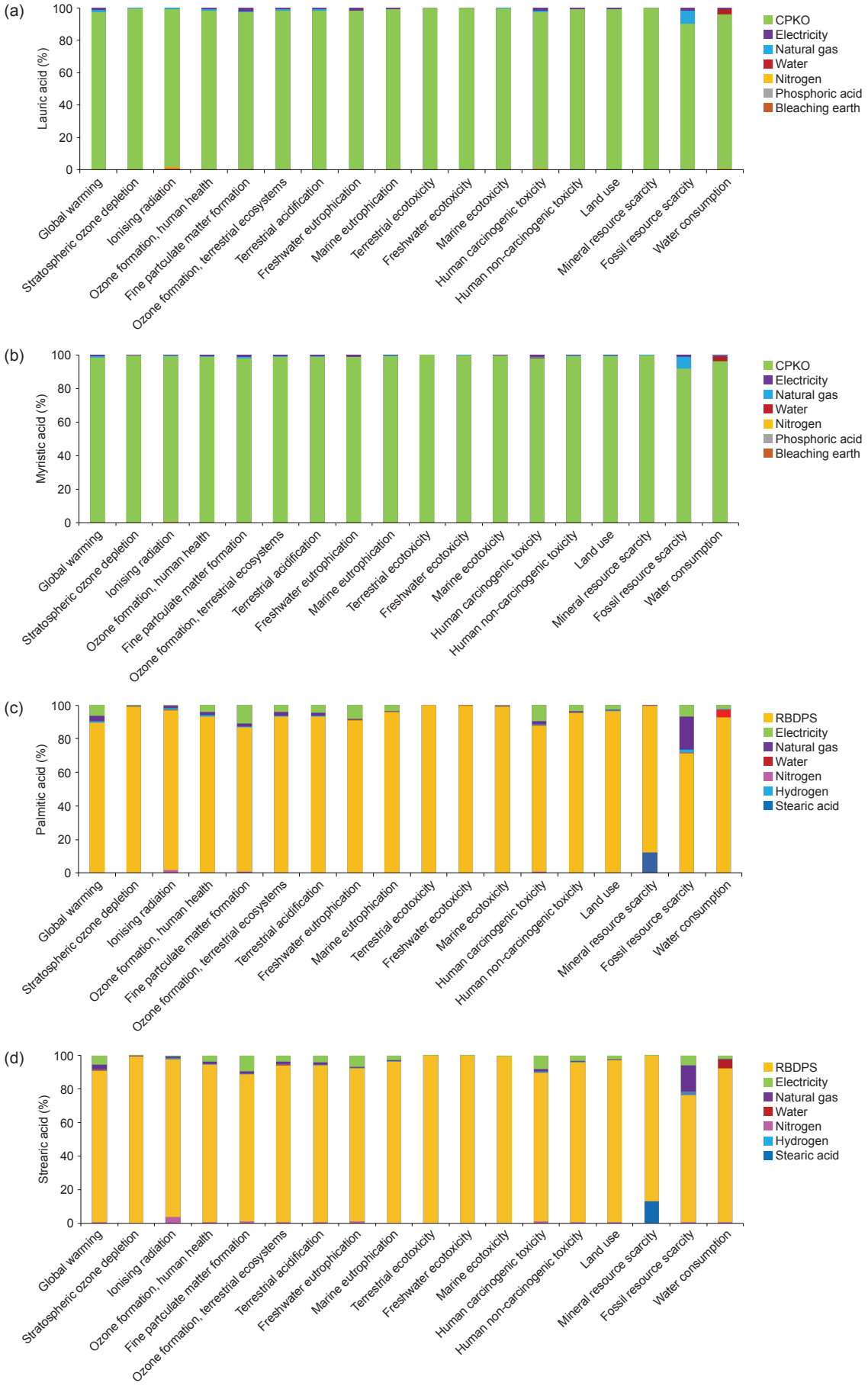

Figure 4. Characterised life cycle impact assessment (LCIA) to produce 1 kg of: (a) Lauric acid, (b) myristic acid, (c) palmitic acid and (d) stearic acid.

during agricultural activities, in this case at the OP plantation and nursery. Panichelli *et al.* (2009) reported that cypermethrin, used as a pesticide in the supply chain, is also responsible for the impact on ecotoxicity. Results show that the production of myristic acid had the highest impact on the terrestrial ecotoxicity impact category compared to other fatty acids (*Table 4*).

Human non-carcinogenic toxicity. For this impact category, the production of feedstock used, *i.e.*, CPKO and RBDPS, has a prominent impact with a contribution of 99% and 95% of the total contribution, respectively. Meanwhile, the main contributors were the background process for the production of electricity and also activities during FFB production itself, including pesticide usage.

Fossil resource scarcity. This impact category is related to the use of FF as a source of energy and feedstock for production; in this case, the production of electricity and also natural gas, which were measured in a kg of oil equivalent (addressed as the fossil resource scarcity category). *Figure 5* shows the major impact contributors to the fossil resource scarcity impact category, where the production of raw materials (CPKO and RBDPS) was identified as the major contributor to this impact category due to the accumulation of FF used along their supply chain.

The findings showed that the higher the amount of natural gas used to produce steam at the plant's boiler and electricity used during fatty acid production, the higher the depletion of FF. In these fatty acid productions, there were differences in energy source and consumption, which were mainly due to the number of fractionation processes involved and also the efficiency of the plant since there were newer and older fatty acid plants evaluated in this study. The higher the number of fractionations required, the higher the energy consumption. Generally, the production of RBDPS-based fatty acids (palmitic acid and stearic acid) only involved a single-step fractionation process, while the production of CPKO-based fatty acids could be single, or double, or may go up to a maximum of triple fractionations, depending on the plant design and also its capacity. Eventually, the impact it has depends heavily on the nature of the feedstock itself.

Overall, the LCIA results indicated that the impacts of fatty acid production from CPKO were greater than those from RBDPS, mainly because of the allocation and upstream burdens from each process, *i.e.*, plantation, milling and refinery, besides the energy usage during the fatty acid production itself, *i.e.*, number of fractionations involved. Clearly, the main contributor to environmental impacts in fatty acid production was dominated by the production of CPKO and RBDPS, with more

TABLE 4. ENVIRONMENTAL IMPACTS OF 1 KG OF LAURIC ACID, MYRISTIC ACID, PALMITIC ACID AND STEARIC ACID (SCENARIO 1)

Input category	Unit	Impact per kg fatty acid			
		Lauric acid	Myristic acid	Palmitic acid	Stearic acid
Global warming	kg CO_2 eq.	3.22	9.43	1.39	2.19
Stratospheric ozone depletion	kg CFC_{11} eq.	1.80E-05	5.33E-05	7.40E-06	1.15E-05
Ionising radiation	kBq Co-60 eq.	0.05	0.15	0.03	0.04
Ozone formation, human health	kg NO_x eq.	0.01	0.02	3.43E-03	0.01
Fine partculate matter formation	kg PM2.5 eq.	4.73E-03	0.01	2.03E-03	3.19E-03
Ozone formation, terrestrial ecosystems	kg NO_x eq.	0.01	0.02	3.50E-03	0.01
Terrestrial acidification	kg SO_2 eq.	0.01	0.04	0.01	0.01
Freshwater eutrophication	kg P eq.	1.15E-03	3.38E-03	4.63E-04	7.24E-04
Marine eutrophication	kg N eq.	1.87E-04	5.51E-04	7.63E-05	1.19E-04
Terrestrial ecotoxicity	kg 1,4-DCB	261.87	774.65	109.20	169.26
Freshwater ecotoxicity	kg 1,4-DCB	2.85	8.42	1.17	1.81
Marine ecotoxicity	kg 1,4-DCB	0.78	2.30	0.32	0.50
Human carcinogenic toxicity	kg 1,4-DCB	0.15	0.44	0.07	0.11
Human non-carcinogenic toxicity	kg 1,4-DCB	3.37	9.91	1.45	2.27
Land use	m^2a crop eq.	0.06	0.18	0.03	0.05
Mineral resource scarcity	kg Cu eq.	0.02	0.06	0.01	0.02
Fossil resource scarcity	kg oil eq.	0.69	1.98	0.34	0.56
Water consumption	m^3	0.04	0.12	0.03	0.05

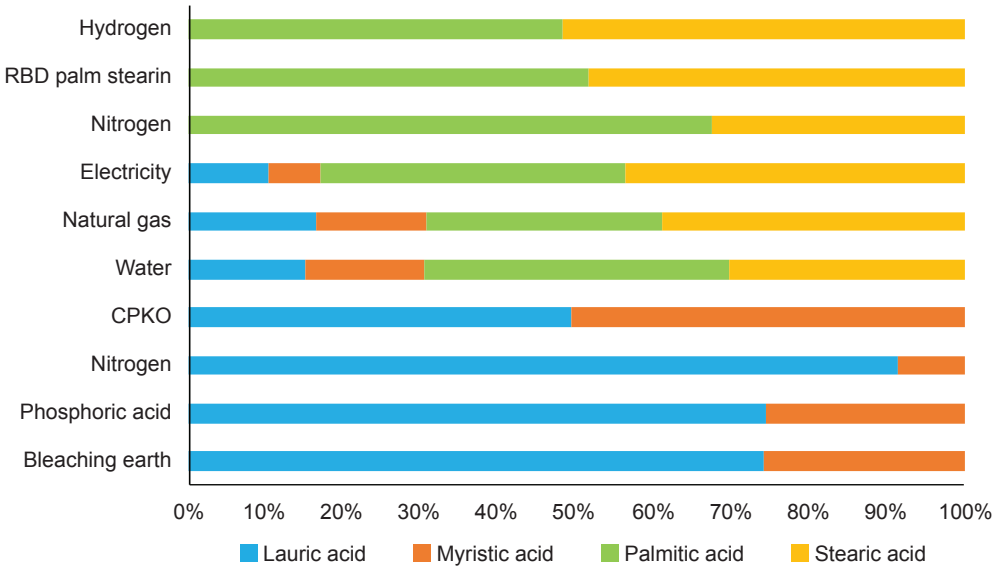

Note: RBD - refined, bleached and deodorised; CPKO - crude palm kernel oil.

Figure 5. Percentage of the major contributors to the fossil resource scarcity impact category for the production of 1 kg of lauric acid, myristic acid, palmitic acid and stearic acid.

than 90% contribution in all impact categories. Along with that, the consumption of natural gas and electricity, which were used as energy and heat sources in fatty acid production, also had significant impacts on the environment. All these contributors were similar for all fatty acid productions assessed.

Scenario 2: Cradle-to-gate of fatty acid production using continued land use (OP to OP) and biogas capture, with replacement of energy sources with OP biomass. In this study, the utilisation of OP biomass, *i.e.,* shell and mesocarp fibre, as an alternative to replace the current energy source from FF is proposed. The purpose of this scenario is to find out how much environmental impact or burden associated with fatty acid production can be reduced by replacing the energy source at all stages without any change to other parameters or processes. At the POM, the OP biomass is directly burned to be used as a fuel for boiler plants in order to produce heat to convert water into steam (Noorazah *et al.*, 2015). In this fatty acid production, the total non-renewable primary energy demand is in the range of 0.86-6.53 MJ per kg fatty acid. Overall, for the CPKO-based fatty acid production, the utilisation of OP biomass managed to reduce about 13% and 16% of impacts in the global warming and fossil resource scarcity impact categories, respectively, as compared to using energy from the electricity grid in Scenario 1 according to the ReCiPe methodology (*Figure 6*). Meanwhile, for RBDPS-based fatty acid production, only 1.4% of the impact can be reduced for both impact categories as compared to Scenario 1 studied.

This shows that the CPKO-based fatty acid production process is most energy-intensive as compared to RBDPS-based fatty acid production. The replacement of fossil-based energy from grid electricity with OP biomass-based renewable energy, even at a small amount, can definitely help to reduce the climate change impact and the industry's dependency on FF (Subramaniam *et al.*, 2021). Indirectly, these initiatives will help to lessen the related impacts generated from fatty acid production through better energy substitution and also improve the sustainability performance of the OP supply chain by maximising the use of by-products from their industry itself.

Sensitivity analysis (Production of fatty acids as described in Scenario 1 based on economic allocation). The initial allocation in this study was weight allocation. A sensitivity analysis was conducted via economic allocation based on price between fatty acid and glycerol as a co-product with a ratio of 61:39. The economic evaluation was difficult to conduct due to the daily price fluctuation, and in this case, the value of fatty acids was higher than glycerol (prices based on MPOB). In this study, the allocation went from 88.7% (mass allocation) to 61.0% (economic allocation). As a result, the impacts decreased by about 31.0% in selected impact categories when economic allocation was used, which is more favourable for fatty acid production compared to mass allocation (*Table 5*). This also shows that allocation choice can change the results significantly. Additionally, Yung *et al.* (2021) suggested that economic allocation seems more beneficial for palm biodiesel production than allocation by mass or energy content.

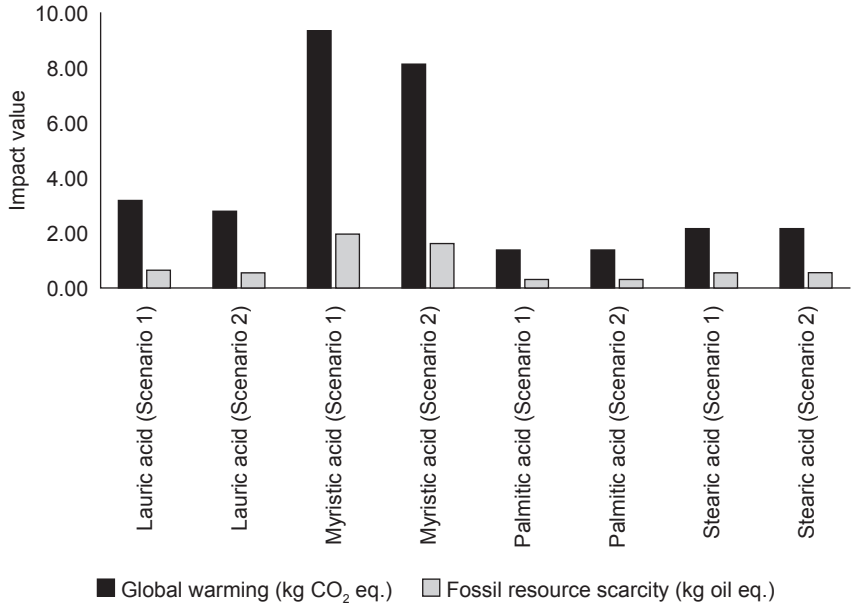

Figure 6. Comparison of impacts from all fatty acid productions for Scenario 1 and 2.

TABLE 5. SELECTED ENVIRONMENTAL IMPACTS OF 1 KG OF LAURIC ACID, MYRISTIC ACID, PALMITIC ACID AND STEARIC ACID (MASS ALLOCATION *vs.* ECONOMIC ALLOCATION)

Fatty acid	Impact category					
	Global warming (kg CO_2 eq.)		Terrestrial ecotoxicity (kg 1,4-DCB)		Fossil resource scarcity (kg oil eq.)	
	Mass allocation	Economic allocation	Mass allocation	Economic allocation	Mass allocation	Economic allocation
Lauric acid	3.22	2.25	261.87	183.04	0.69	0.48
Myristic acid	9.43	6.59	774.65	541.47	1.98	1.38
Palmitic acid	1.39	0.97	109.20	76.33	0.34	0.24
Stearic acid	2.19	1.53	169.26	118.31	0.56	0.39

CONCLUSION

This study specifically evaluates the environmental performance of palm-based fatty acid manufacturers in Malaysia, who are also part of the OP industry supply chain. The environmental hotspots identified in this LCA will help the manufacturers identify the environmental impacts of their production and the industry can take steps to mitigate this by improving their processes. Overall, the GHG emissions for this study demonstrated that the selected impacts generally for CPKO-based fatty acid production are reduced by about 16% by replacing the energy source from the electricity grid with OP biomass. The LCA results based on economic allocation also showed that the impact can be reduced by up to 31% in all impact categories, which gives more benefits to all fatty acid production as compared to weight allocation.

In general, the downstream process, as in the production of fatty acids, will carry the burdens and impacts of the upstream processes. As a recommendation, the manufacturers can consider looking into other potential sources for energy generation. It is suggested that the manufacturer explore other alternative energy sources and heat-producing techniques for their current and future plant operations, such as energy efficiency technology, biogas utilisation, solar system, cogeneration system and heat integration system in order to reduce their dependency on fossil fuels such as coal, natural gas, *etc.* By implementing these approaches, it could help reduce the total impact generated from the production of feedstock and the production of fatty acids. Better and greener technologies for energy efficiency are suggested to be implemented and introduced to the oleochemical industry, which is believed to reduce environmental impacts, especially the global warming potential and fossil resource scarcity impact categories.

On the other hand, it is also essential for the respective manufacturer to maintain and continuously use feedstock from certified sources, *i.e.,* with RSPO or MSPO certification,

the implementation of good agriculture practices (GAP) at the OP plantation, the application of biogas capture facility at POM, a good wastewater treatment system, *etc.* In the end, the findings from this study, which are GHG emissions, can also be used by manufacturers to determine the level of carbon footprint of their products and this information is also required in the product market.

ACKNOWLEDGEMENT

The authors wish to thank the Director-General of MPOB for permission to publish this article. Thanks are also extended to all fatty acids' producers in Malaysia for their contributions and supports for this study.

REFERENCES

Angarita, E. E. Y., Lora, E. E. S., Da Costa, R. E., & Torres, E. A. (2009). The energy balance in the palm oil-derived methyl ester (PME) life cycle for the cases in Brazil and Colombia. *Renewable Energy*, *34*(12), 2905–2913. https://doi.org/10.1016/j.renene.2009.05.007

Castanheira, É. G., & Freire, F. (2016). Environmental life cycle assessment of biodiesel produced with palm oil from Colombia. *The International Journal of Life Cycle Assessment*, *22*(4), 587–600. https://doi.org/10.1007/s11367-016-1097-6

Choo, Y. M., Muhamad, H., Hashim, Z., Subramaniam, V., Puah, C. W., & Tan, Y. (2011). Determination of GHG contributions by subsystems in the oil palm supply chain using the LCA approach. *The International Journal of Life Cycle Assessment*, *16*(7), 669–681. https://doi.org/10.1007/s11367-011-0303-9

Foong, S. Z., Goh, C. K., Supramaniam, C. V., & Ng, D. K. (2019). Input-output optimisation model for sustainable oil palm plantation development. *Sustainable Production and Consumption*, *17*, 31–46. https://doi.org/10.1016/j.spc.2018.08.010

Gervajio, G. C. (2005). Fatty acids and derivatives from coconut oil. In *Bailey's industrial oil and fat products* (pp. 15-18). John Wiley and Sons.

Hansen, S. (2007). Feasibility study of performing an life cycle assessment on crude palm oil production in Malaysia (9 pp). *The International Journal of Life Cycle Assessment*, *12*(1), 50–58. https://doi.org/10.1065/lca2005.08.226

Haryati, Z., Subramaniam, V., Noor, Z. Z., Hashim, Z., Loh, S. K., & Aziz, A. A. (2022). Social life cycle assessment of crude palm oil production in Malaysia. *Sustainable Production and Consumption*, *29*, 90–99. https://doi.org/10.1016/j.spc.2021.10.002

Hashim, Z., Muhamad, H., Subramaniam, V., & May, C. Y. (2014). Water footprint: Part 2 – FFB production for oil palm planted in Malaysia. *Journal of Oil Palm Research*, *26*(4), 282–291.

Intergovernmental Panel on Climate Change (IPCC) (2013). *Climate Change 2013: The physical science basis.* Retrieved June 8, 2023 from https://www.ipcc.ch/site/assets/uploads/2018/03/WG1AR5_SummaryVolume_FINAL.pdf

International Organization for Standardization (ISO) (2006a). *Environmental management - Life cycle assessment - Principles and framework (2nd ed.)* (ISO 14040:2006).

International Organization for Standardization (ISO) (2006b). *Environmental management - Life cycle assessment - Requirements and guidelines (1st ed.)* (ISO 14044:2006).

Kiatkittipong, W., Pongsiriyakul, K., Lim, J. W., Kiatkittipong, K., Wongsurakul, P., Yodpetch, V., Boonyasuwat, S., & Assabumrungrat, S. (2022). Bioresources and biofuels – From classical to perspectives and trends. In N. Thongchul, A. Kokossis, & S. Assabumrungrat (Eds.), *A-Z of biorefinery* (pp. 165–220). Elsevier.

Malaysian Palm Oil Board (MPOB). (2011-2024). *Malaysian oil palm statistics 2010, 2011, 2012, 2013, 2014, 2015, 2016, 2017, 2018, 2019, 2020, 2021, 2022, 2023.*

Mancini, A., Imperlini, E., Nigro, E., Montagnese, C., Daniele, A., Orrù, S., & Buono, P. (2015). Biological and nutritional properties of palm oil and palmitic acid: Effects on health. *Molecules*, *20*(9), 17339–17361. https://doi.org/10.3390/molecules200917339

Muhamad, H., Hashim, Z., Subramaniam, V., Khairuddin, N. S. K., & Choo, Y. M. (2014). Water footprint: Part 1 - Production of oil palm seedlings in Peninsular Malaysia. *Journal of Oil Palm Research*, *26*(4), 273–281.

Muhamad, H., Hashim, Z., Subramaniam, V., Tan, Y. A., Puah, C. W., & Choo, Y. M. (2010). Life cycle assessment of oil palm seedling production (Part 1). *Journal of Oil Palm Research*, *22*, 878–886

Noorazah, Z., Sumiani, Y., Subramaniam, V., Zulina, A. M., Zailan, A. B., Razmah, G., & Hazimah, A. H. (2015). Evaluation of environmental impacts and GHG of palm polyol production using life cycle assessment approach. *Journal of Oil Palm Research*, *27*(2), 144–155.

Noorazah, Z., Zulina, A. M., Razmah, G., & Hazimah, A. H. (2016). Environmental performance of palm-based methyl ester sulphonates production using life cycle approach. *Journal of Oil Palm Research*, *28*(1), 104–113.

Noorazah, Z., Zulina, A. M., Razmah, G., & Zainab, I. (2017). Environmental assessment on methylester production from palm feedstock: A case study. *Journal of Oil Palm Research*, *29*, 414–423.

Panichelli, L., Dauriat, A., & Gnansounou, E. (2009). Life cycle assessment of soybean-based biodiesel in Argentina for export. *The International Journal of Life Cycle Assessment*, *14*(2), 144–159. https://doi.org/10.1007/s11367-008-0050-8

Parveez, G. K. A., Nur Nadia, K., Norliyana, Z. Z., Meilina, O. A., Rahmawati, R., Soh, L. K., Selvaduray, K. R., Hoong, S. S., & Zainab, I. (2022). Oil palm economic performance in Malaysia and R&D progress in 2021. *Journal of Oil Palm Research*, *34*(2), 185–218. https://doi.org/10.21894/jopr.2022.0036

Puah, C. W., Choo, Y. M., & Ma, A. N. (2010). Life cycle assessment for the production and use of palm biodiesel (Part 5). *Journal of Oil Palm Research*, *22*, 927–933.

Salvador, R., Barros, M. V., De Paula Do Rosário, J. G., Piekarski, C. M., Da Luz, L. M., & De Francisco, A. C. (2018). Life cycle assessment of electricity from biogas: A systematic literature review. *Environmental Progress & Sustainable Energy*, *38*(4), 13133. https://doi.org/10.1002/ep.13133

Silalertruksa, T., & Gheewala, S. H. (2012). Environmental sustainability assessment of palm biodiesel production in Thailand. *Energy*, *43*(1), 306–314. https://doi.org/10.1016/j.energy.2012.04.025

Siram, K., Habibur Rahman, S. M., Balakumar, K., Duganath, N., Chandrasekar, R., & Hariprasad, R. (2019). Pharmaceutical nanotechnology: Brief perspective on lipid drug delivery and its current scenario. In *Biomedical applications of nanoparticles* (pp. 91–115). Elsevier.

Siregar, K., Tambunan, A. H., Irwanto, A. K., Wirawan, S. S., & Araki, T. (2015). A comparison of life cycle assessment on oil palm (*Elaeis guineensis* Jacq.) and physic nut (*Jatropha curcas* Linn.) as feedstock for biodiesel production in Indonesia. *Energy Procedia*, *65*, 170–179. https://doi.org/10.1016/j.egypro.2015.01.054

Subramaniam, V., Choo, Y. M., Muhamad, H., Hashim, Z., Tan, Y. A., & Puah, C. W. (2010). Life cycle assessment of the production of crude palm oil (Part 3a). *Journal of Oil Palm Research*, *22*, 904–912.

Subramaniam, V., Hashim, Z., Loh, S. K., & Astimar, A. A. (2020). Assessing water footprint for the oil palm supply chain – A cradle to gate study. *Agricultural Water Management*, *237*, 106184. https://doi.org/10.1016/j.agwat.2020.106184

Subramaniam, V., Loh, S. K., & Aziz, A. A. (2021). GHG analysis of the production of crude palm oil considering the conversion of agricultural wastes to by-products. *Sustainable Production and Consumption*, *28*, 1552–1564. https://doi.org/10.1016/j.spc.2021.09.004

Tan, Y. A., Muhamad, H., Hashim, Z., Subramaniam, V., Puah, C. W., Chong, C. L., Ma, A. N., & Choo, Y. M. (2010). Life cycle assessment of refined palm oil production and fractionation (Part 4). *Journal of Oil Palm Research*, *22*, 913–926.

Yee, K. F., Tan, K. T., Abdullah, A. Z., & Lee, K. T. (2009). Life cycle assessment of palm biodiesel: Revealing facts and benefits for sustainability. *Applied Energy*, *86*, S189–S196. https://doi.org/10.1016/j.apenergy.2009.04.014

Yung, C. L., Subramaniam, V., & Sumiani, Y. (2020). Life cycle assessment for palm oil refining and fractionation. *Journal of Oil Palm Research*, *32*, 341–354. https://doi.org/10.21894/jopr.2020.0029

Yung, C. L., Subramaniam, V., & Sumiani, Y. (2021). Life cycle assessment for the production of palm biodiesel. *Journal of Oil Palm Research*, *33*, 140–150. https://doi.org/10.21894/jopr.2020.0080

Zulkifli, H., Halimah, M., Chan, K. W., Choo, Y. M., & Mohd Basri, W. (2010). Life cycle assessment for oil palm fresh fruit bunch production from continued land use for oil palm planted on mineral soil (Part 2). *Journal of Oil Palm Research*, *22*, 887–894.

SHORT COMMUNICATION

Journal of Oil Palm Research Vol. 37 (3) September 2025 p. 573-580
DOI: https://doi.org/10.21894/jopr.2024.0053

BIRD FUNCTIONAL GROUPS CAN REDUCE INSECT PESTS IN OIL PALM SMALLHOLDINGS IN RUPAT ISLAND, RIAU PROVINCE, INDONESIA

DIMAS HARYO PRADANA[1]; MUFTI PETALA PATRIA[1]; YASMAN[1] and NURUL LAKSMI WINARNI[2]*

ABSTRACT

Insect pests are one of the causes of yield reduction in oil palm. Birds from adjacent forest remnants can provide pest control services to address this problem. Insect pest control service by birds is available if the ecosystem is functioning with the presence of certain functional groups of birds. Our study aimed to examine bird functional groups that affect the number of insect pests. We assessed the herbivory rate using bird exclosure treatment. We classified birds according to foraging strategy, foraging strata, diet and body mass traits. Our results showed that gleaning, sallying, omnivorous and large body-size birds have a significant negative relationship with herbivory rates. However, there were no significant differences between treatment and control of herbivory rates. Thus, the pest control service by these bird groups is equal to ecosystem disservices from adjacent forest remnants.

Keywords: bird, ecosystem services, functional group, oil palm, pest control.

Received: 24 September 2023; **Accepted:** 6 September 2024; **Published online:** 26 November 2024.

INTRODUCTION

Oil palm plantation expansion is often accused of causing the deforestation of tropical rainforests (Carlson *et al*., 2012; Stibig *et al*., 2014). Yield gaps are often used as an argument to expand oil palm plantations that cause deforestation (Soliman *et al*., 2016). Pests are one of the causes of crop yield reduction. Leaf-eating insect pests can cause a 15%-50% yield reduction in case of complete defoliation. Severe Rhinoceros beetle (*Oryctes rhinoceros*) attacks in young plantations can lead to 20%-50% yield loss. Severe infestation of rat populations that reach >300 individuals per ha can reduce oil production by about 5% in mature plantations (Woittiez *et al*., 2017).

[1] Department of Biology,
Faculty of Mathematics and Natural Sciences,
Universitas Indonesia,
16424, Depok, West Java, Indonesia.

[2] Research Center for Climate Change-Universitas Indonesia,
Faculty of Mathematics and Natural Sciences,
Universitas Indonesia,
16424, Depok, West Java, Indonesia.

* *Corresponding author e-mail: nwinarni@gmail.com*

Common pests in oil palm plantations include nettle caterpillar (*Setora nitens*) (Koh, 2008) and *Setothosea asigna* (Chenon & Agus, 2006), bagworm (Lepidoptera: Psychidae) (Basri *et al*., 1995; Kamarudin & Wahid, 2010) and rats (*Rattus rattus*) (Abidin *et al*., 2014). Caterpillars primarily feed on the leaflets (Koh, 2008; Murphy 2007; Sheil *et al*., 2009) while rats consume the male inflorescences (Puan *et al*., 2011; Silmi, 2013; Wood & Fee, 2003). In Malaysia, rats are also known to prey on the larva of oil palm pollinating weevil (*Elaeidobius kamerunicus*), which resides within the male inflorescences (Wood & Fee, 2003).

These pest problems, especially insect pests, can be solved by pest control services provided by birds from remnant forests adjacent to the oil palm plantation. Most of the previous studies in natural and agroecosystems have found that birds reduce the population densities of insects (Whelan *et al*., 2015). This service has been studied quantitatively by Denmead *et al*. (2017) and Koh (2008). They quantified insect pest control service by measuring the herbivory rate of the oil palm leaflets using bird exclosure treatment. Their studies revealed different results. Koh (2008), who conducted the study in an industrial oil palm plantation complex,

showed that the herbivory rates in bird exclosure treatment were higher than the control group, while Denmead *et al*. (2017), who carried out the study in smallholdings, showed no significant difference. Thus, more studies are needed.

Insect pest control service by forest birds to the oil palm plantations, and ecosystem services in general, is available if the ecosystem functions. The ecosystem will function if bird species with specific functional characteristics or traits are present (Van Bodegom & Price, 2015). On the other hand, certain traits in the ecosystem are affected by environmental conditions (Keddy, 1992; Van Bodegom & Price, 2015). The study on trait-based bird functional groups associated with insect pest control services was conducted by Phillpott *et al*. (2009) in coffee and cacao plantations. Their research showed that bird species that forage in the understory and canopy, gleaners, omnivores and tiny sizes were related to the reduction of insect pests. Another study by Luck *et al*. (2012) on apple plantations indicated that bird forage by hawking and sallying have a higher potential to reduce insect pests. Only a few studies on bird functional groups have been done in tropical agroecosystems (Sekercioglu, 2012). Denmead *et al*. (2017) and Koh (2008) studied the insect pest control services in the oil palm plantation but did not study the related bird traits. Understanding the bird traits related to insect pest control services in oil palm plantation is crucial to ensure that the oil palm plantations are managed properly. Therefore, this study investigated the bird functional groups that can potentially decrease the population of insect pests in smallholdings. With this understanding, we can formulate strategies to effectively manage the environmental conditions of smallholdings, ensuring the preservation and sustenance of the identified bird functional groups.

MATERIALS AND METHODS

Our study was conducted in six oil palm smallholdings owned by different independent smallholders in Rupat Island, Riau Province, Sumatra, Indonesia, from 14 September to 14 October 2022. The area of each smallholding spans approximately 2 ha, with distance among them between 1.0 and 17.0 km, except for two smallholdings which were separated by only 0.2 km, as depicted in *Figure 1*. Among the six smallholdings, only three retained adjacent forest remnants, specifically riparian and coastline mangrove forests. The width of these forest remnants averaged around 200 m.

Two bird exclosure treatments and two control groups were set at each smallholding, positioned at 200 m apart. The size of each exclosure was 100 x 100 x 120 cm (length x width x height) and featured a net cage with a mesh size of 2.5 x 2.5 cm. These cages were carefully placed over oil palm seedlings. The control group consisted of oil palm seedlings without protective net cages. The distance between the two treatment types was maintained at 10 m (*Figure 2*). All seedlings were obtained from the same nursery on Rupat Island and had similar height (approximately 1 m) and age (approximately 1 year old). Twenty undamaged leaflets were randomly chosen from each seedling, and their lamina bases were marked using a waterproof permanent marker. After 21-22 days, the marked leaflets were collected and photographed, adhering to the procedures outlined by Koh (2008).

Herbivory rates were measured based on the missing lamina areas using ImageJ (Rasband, 2018). The missing lamina area was quantified per leaflet per day the seedling remained at the sampling site. Since we wanted to look at the direct relationship between the missing lamina area and herbivory rate by insect pest species, we only recorded insect species that perched on the leaflet of the treatment or control seedlings. We did not record the overall insect pest species or count their abundance.

Bird observations were carried out from 06:00-08:00 and 15:00-17:00 hr using point count method (Bibby *et al*., 1998). Each point count was carried out for 15 min and covered a radius of 50 m, with the bird exclosure treatment as the central point of reference. The distance between points was 200 m. The bird observation for each smallholding was replicated twice on different days and different orders of point. The number of individual bird species observed were recorded. In addition, the foraging strategies and foraging strata observed during surveys were documented.

The recorded bird species were then classified into functional groups based on four distinct traits: Foraging strategies, foraging strata, diet and body size (*Table 1*). This classification of the bird functional group followed the traits used by Philpott *et al*. (2009). Based on observation, birds were classified into three foraging strategy groups: Gleaning, hawking and sallying, following Remsen & Robinson's terminology (Remsen and Robinson, 1990). Bird species observed foraging on the ground or in the understorey were classified as understorey foragers, while those foraging in the mid or upper canopy were classified as canopy foragers. Birds displaying foraging behaviour across all strata or in aerial environments were categorised as all-strata foragers. Bird diets were classified into three: Insectivores, omnivores and carnivores. Moreover, birds' body sizes were classified into four distinct body size groups: Tiny (<15 g), small (15 to <30 g), medium (30 to <60 g) and large (60 to <120 g). The diet and body size classifications were based on Cornell Lab of Ornithology (2022).

Note: Sampling sites which were separated by only 0.2 km.

Figure 1. The location of smallholdings on Rupat Island, Riau Province, Indonesia.

Figure 2. (a) The control, and (b) the bird exclosure treatment at one of the smallholdings.

The Wilcoxon-test was carried out to evaluate significant differences in herbivory rates between the bird exclosure treatment and the control group because the data did not follow normal distribution. Binomial Generalised Linear Mixed Model (GLMM) was used to determine the relationship between bird functional group and herbivory rates. We used binomial GLMM with the missing lamina area as the response variable. The fixed effect was the bird's individual number at each functional group, and the random effects were sampling sites and points. The response variable was the herbivory rates of the control treatment, aiming to assess whether bird access to seedlings led to a reduction in herbivory rates. The statistical analysis was done using R version 4.2.2. (R Core Team, 2022), using the GLMM package (Knudson, 2022).

TABLE 1. BIRD FUNCTIONAL CLASSIFICATION BASED ON FORAGING STRATEGY, FORAGING STRATA, DIET AND BODY SIZE TRAITS

Trait	Functional group
Foraging strategy	Gleaning
	Hawking
	Sallying
Foraging strata	Understorey
	Canopy
	All strata
Diet	Insectivore
	Omnivore
	Carnivore
Body size	Tiny (<15 g)
	Small (15 to <30 g)
	Medium (30 to <60 g)
	Large (60 to <120 g)

RESULTS AND DISCUSSION

We found a total of 10 bird species from all sampling sites with 71 individual birds. The most abundant bird functional group was insectivores. The most prevalent foraging strategy among these birds was hawking, and their preferred foraging stratum encompassed all strata. The dominant body size group among the recorded birds was tiny (*Table 2*). Similar to this study, Chenon and Agus (2006), in their study on oil palm plantation estates in North Sumatra, also reported the dominance of insectivores and tiny birds. However, their study revealed different dominant foraging strategies and strata, with gleaning and the understorey being prominent, respectively. Furthermore, they found that *Centropus bengalensis* and *Parus major* were consuming one of the essential defoliating pests *S. asigna*. Interestingly, we did not find these two birds at our sampling sites, but we observed them in the remnant forest adjacent to the smallholdings. The height of the seedlings we used in our treatment and the condition of the smallholdings (the oil palm height ranged from 2-3 m and the understorey was not in a well-developed stage) may explain the dominance of all strata birds in our study. Older smallholdings with taller oil palm and well-developed understorey may attract more canopy and understorey birds.

We found a significant negative relationship between the abundance of gleaning (z = -2.04, *p*-value = 0.04), sallying (z = -2.25, *p*-value = 0.02), omnivorous (z = -3.84, *p*-value = 0.00) and large birds (z = -3.92, *p*-value = 0.00) with missing lamina areas, suggesting the reduction of herbivory rates (*Table 3*, *Figure 3*). However, the sampling sites and points as random effects showed significance to the response variable indicating that these factors affect the relationship between bird's functional groups and missing lamina areas (*Table 3*). Our finding suggested that an increase in the number of these bird functional groups corresponded to a reduction in herbivory on oil palm leaflets. Thus, gleaning, sallying, omnivorous, and large birds provide insect pest control within the oil palm smallholdings. Gleaning birds such as *Acridotheres javanicus* and sallying birds such as *Halcyon smyrnensis* picked food items from a substrate, such as the leaflet of oil palm, although the latter can also pick aerial prey. Moreover, all omnivorous birds at our sampling sites, *Pycnonotus goiavier* and *A. javanicus*, were gleaners, and most of sallying, *H. smyrnensis* and *Todiramphus chloris*, were large birds (*Table 2*). This explains the negative relationship between the abundance of these bird groups and herbivory rate. On the other hand, most insectivorous birds (z = 6.79, *p*-value <0.01) that occupy all strata (z = 3.55, *p*-value <0.00) and use a hawking foraging strategy (z = 3.03, *p*-value <0.01), which attacks prey items in continuous flight such as *Collocalia esculenta* (*Table 2*), showed positive relationship with herbivory rates (*Table 3*, *Figure 3*), indicating that they could not reduce insect pests on oil palm leaflets. It is worth noting that previous studies on ecosystem services in oil palm plantations, such as those conducted by Denmead *et al*. (2017), Gray and Lewis (2014) and Koh (2008), did not include an analysis of the relationship between bird functional groups and herbivory rates. Gleaning, sallying, omnivorous, and large birds used understorey, canopy and all strata, therefore, heterogeneity of vegetation cover in remnant forests must be preserved (*Table 2*).

During the survey, one seedling in bird exclosure treatment was heavily damaged by animals and one seedling in control was missing. Consequently, subsequent analyses of herbivory rates can only be done on 22 seedlings, 11 seedlings from each

TABLE 2. FUNCTIONAL GROUP OF BIRD SPECIES FOUND AT THE SAMPLING SITES

Species	Individual number	Functional group			
		Foraging strategies	Foraging strata	Diet	Body size
Glossy Swiftlet (*Collocalia esculenta*)	42	Hawking	All strata	Insectivore	Tiny
White-throated Kingfisher (*Halcyon smyrnensis*)	3	Sallying	Understorey	Carnivore	Large
Collared Kingfisher (*Todiramphus chloris*)	1	Sallying	Understorey	Carnivore	Large
Blue-tailed Bee-eater (*Merops philippinus*)	2	Sallying	All strata	Insectivore	Medium
Pacific Swallow (*Hirundo tahitica*)	2	Hawking	All strata	Insectivore	Small
Yellow-vented Bulbul (*Pycnonotus goiavier*)	8	Gleaning	Canopy	Omnivore	Medium
Ashy Tailorbird (*Orthotomus ruficeps*)	4	Gleaning	All strata	Insectivore	Tiny
Yellow-bellied Prinia (*Prinia flaviventris*)	3	Gleaning	Understorey	Insectivore	Tiny
Malaysian Pied-Fantail (*Rhipidura javanica*)	3	Gleaning	Canopy	Insectivore	Small
Javan Myna (*Acridotheres javanicus*)	3	Gleaning	Understorey	Omnivore	Large
Total	**71**				

TABLE 3. RELATIONSHIP BETWEEN BIRD FUNCTIONAL GROUP AND HERBIVORY RATE OF CONTROL SEEDLINGS

Fixed effect			Random effect			Random effect		
	z	*p*-value		Z	*p*-value		z	*p*-value
Gleaning	**-2.04**	**0.04**	Site	1.60	0.06	Point	**2.16**	**0.02**
Hawking	**3.03**	**0.00**		**1.73**	**0.04**		**2.29**	**0.01**
Sallying	**-2.25**	**0.02**		**1.73**	**0.04**		**2.35**	**0.01**
Understorey	-1.44	0.15		**1.72**	**0.04**		**2.34**	**0.01**
Canopy	-0.97	0.33		**1.73**	**0.04**		**2.33**	**0.01**
All strata	**3.55**	**0.00**		**1.73**	**0.04**		**2.35**	**0.01**
Insectivore	**6.79**	**0.00**		**1.73**	**0.04**		**2.35**	**0.01**
Omnivore	**-3.84**	**0.00**		**1.73**	**0.04**		**2.35**	**0.01**
Carnivore	-1.55	0.12		**1.73**	**0.04**		**2.28**	**0.01**
Tiny	1.75	0.08		**1.73**	**0.04**		**2.31**	**0.01**
Small	-0.24	0.81		1.52	0.06		**2.35**	**0.01**
Medium	-1.21	0.23		**1.73**	**0.04**		**2.34**	**0.01**
Large	**-3.92**	**0.00**		**1.73**	**0.04**		**2.28**	**0.01**

Note: Significant z value (*p*-value <0.05) appears in boldface.

treatment. The difference between herbivory rates of bird exclosure treatment and control was not significant (W = 69, *p*-value = 0.60) (*Figure 4*). Our result was similar to the previous study carried out in oil palm smallholdings by Denmead *et al*. (2017), which also found no significant difference between herbivory rates in bird exclosure treatment and control groups, while Koh (2008) which conducted the study in industrial oil palm plantation found significant difference. Interestingly, the local farmers in our sampling sites reported that insect pests are not a significant problem in their plantations. These findings suggested that insect pest control service by gleaning, sallying, omnivorous and large birds is equal to ecosystem disservices stemming from

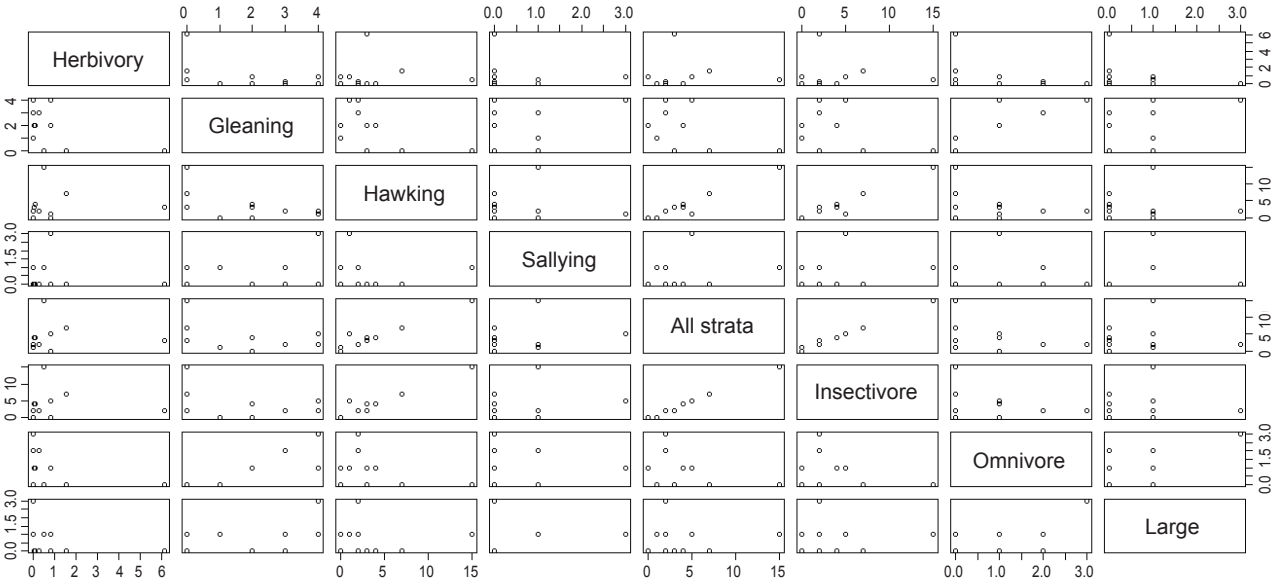

Figure 3. Relationship between herbivory rates and abundance of bird functional groups. Only significant relationships are shown.

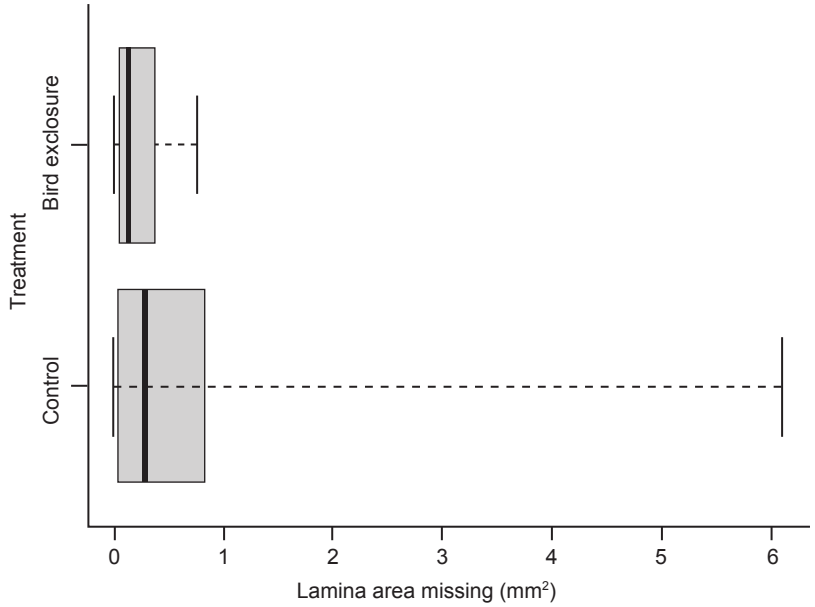

Figure 4. Herbivory rates of bird exclosure treatment and control groups.

adjacent forest remnants, such as spill-over of insect pests (Edwards *et al*., 2014). Insect species with high dispersal ability and little or no response to forest edge can disperse from the forest to adjacent oil palm plantations. For example, certain butterfly species can disperse from forest remnants to oil palm plantations (Lucey & Hill, 2012). In this study, forest patches may be the source habitat of oil palm insect pests. We also found an indication that the understorey of the oil palm smallholding is also the source of insect pests. The herbivory rates of oil palm smallholding which had high understorey coverage, such as sampling unit 8, was higher than smallholding that had low coverage, such as sampling unit 11. However, we did not measure the understorey coverage. Further study is needed to examine this relationship.

CONCLUSION

Our study investigated the role of bird exclosure treatments in mitigating herbivory rates on oil palm seedlings in independent smallholdings. Although we initially observed a reduction in herbivory rates associated with gleaning, sallying, omnivorous and large body size birds, our subsequent analysis did not reveal a statistically significant difference between the bird exclosure treatment and the control group.

These findings are consistent with previous research in similar oil palm smallholdings, which also failed to identify a significant impact of bird exclosure on herbivory rates. Moreover, local farmers reported that insect pests were not a significant concern in their smallholdings, suggesting that the ecosystem services provided by gleaning, sallying, omnivorous and large birds may be comparable to any potential disservices originating from adjacent forest remnants.

The study highlights the complexity of ecological interactions in agricultural landscapes. While the presence of gleaning, sallying, omnivorous and large body size birds may provide natural pest control benefits, other factors such as habitat connectivity and the specific pest species involved, can influence the effectiveness of this service. Further investigations into the dynamics of bird-insect-plant interactions in different contexts are warranted to better understand and harness the potential of birds as agents of pest management in agricultural settings.

ACKNOWLEDGEMENT

This study was funded by Universitas Indonesia Hibah PUTI Q2 (Grant number NKB-1297/UN2. RST/HKP.05.00/2022). We thank Nurcahyo Edi Sarwono and Pariman who helped us during the fieldwork. We also thank two anonymous reviewers who provided valuable comments to our previous manuscript.

REFERENCES

Abidin, C. M. R. Z., Hamid, N. H., & Noor, H. M. (2014). Observations of the diet of Black-winged Kite *Elanus caeruleus* in the oil-palm plantations of the Sahabat area, Sabah, Borneo, Malaysia. *BirdingASIA*, *22*, 55–57.

Basri, M. W., Norman, K., & Hamdan, A. B. (1995). Natural enemies of the bagworm, *Metisa plana* Walker (Lepidoptera: Psychidae) and their impact on host population regulation. *Crop Protection*, *14*(8), 637–645. https://doi.org/10.1016/0261-2194(95)00053-4

Bibby, C., Jones, M., & Marsden, S. (1998). *Expedition field techniques: Birds surveys.* Expedition Advisory Centre Royal Geographical Society.

Carlson, K. M., Curran, L. M., Ratnasari, D., Pittman, A. M., Soares-Filho, B. S., Asner, G. P., Trigg, S. N., Gaveau, D. A., Lawrence, D., & Rodrigues, H. O. (2012). Committed carbon emissions, deforestation, and community land conversion from oil palm plantation expansion in West Kalimantan, Indonesia. *Proceedings of the National Academy of Sciences*, *109*(19), 7559–7564. https://doi.org/10.1073/pnas.1200452109

Chenon, R. D. D., & Agus, S. (2006). Ecological observations on diurnal birds in Indonesian oil palm plantations. *Journal of Oil Palm Research*, *(Special Issue)*, 122–143.

Cornell Lab of Ornithology. (2022). *Birds of the World*. Retrieved August 10, 2023, from https://birdsoftheworld.org/bow/home

Denmead, L. H., Darras, K., Clough, Y., Diaz, P., Grass, I., Hoffmann, M. P., Nurdiansyah, F., Fardiansah, R., & Tscharntke, T. (2017). The role of ants, birds and bats for ecosystem functions and yield in oil palm plantations. *Ecology*, *98*(7), 1945–1956. https://doi.org/10.1002/ecy.1882

Edwards, F. A., Edwards, D. P., Sloan, S., & Hamer, K. C. (2014). Sustainable management in crop monocultures: The impact of retaining forest on oil palm yield. *PLoS ONE*, *9*(3), e91695. https://doi.org/10.1371/journal.pone.0091695

Gray, C. L., & Lewis, O. T. (2014). Do riparian forest fragments provide ecosystem services or disservices in surrounding oil palm plantations? *Basic and Applied Ecology*, *15*(8), 693–700. https://doi.org/10.1016/j.baae.2014.09.009

Kamarudin, N., & Wahid, M. B. (2010). Interactions of the bagworm, *Pteroma pendula* (Lepidoptera: Psychidae), and its natural enemies in an oil palm plantation in Perak. *Journal of Oil Palm Research*, *22*(1), 758–764.

Keddy, P. A. (1992). Assembly and response rules: Two goals for predictive community ecology. *Journal of Vegetation Science*, *3*(2), 157–164. https://doi.org/10.2307/3235676

Knudson, C. (2022). *Generalized Linear Mixed Models via Monte Carlo likelihood approximation [R package GLMM version 1.4.4]. Retrieved September 26, 2023 from* https://CRAN.R-project.org/package=glmm

Koh, L. P. (2008). Birds defend oil palms from herbivorous insects. *Ecological Applications*, *18*(4), 821–825. https://doi.org/10.1890/07-1650.1

Lucey, J. M., & Hill, J. K. (2012). Spillover of insects from rain forest into adjacent oil palm plantations. *Biotropica*, *44*(3), 368–377. https://doi.org/10.1111/j.1744-7429.2011.00824.x

Luck, G. W., Lavorel, S., McIntyre, S., & Lumb, K. (2012). Improving the application of vertebrate trait-based frameworks to the study of ecosystem services. *Journal of Animal Ecology*, *81*(5), 1065–1076. https://doi.org/10.1111/j.1365-2656.2012.01974.x

Murphy, D. J. (2007). Future prospects for oil palm in the 21st century: Biological and related challenges. *European Journal of Lipid Science and Technology*, *109*(4), 296–306. https://doi.org/10.1002/ejlt.200600229

Philpott, S. M., Soong, O., Lowenstein, J. H., Pulido, A. L., Lopez, D. T., Flynn, D. F. B., & DeClerck, F. (2009). Functional richness and ecosystem services: bird predation on arthropods in tropical agroecosystems. *Ecological Applications*, *19*(7), 1858–1867. https://doi.org/10.1890/08-1928.1

Puan, C. L., Goldizen, A. W., Zakaria, M., Hafidzi, M. N., & Baxter, G. S. (2011). Absence of differential predation on rats by Malaysian barn owls in oil palm plantations. *Journal of Raptor Research*, *45*(1), 71–78. https://doi.org/10.3356/jrr-10-18.1

R Core Team (2022). *R: A language and environment for statistical computing*. R Foundation for Statistical Computing. Retrieved January 30, 2023, from https://www.r-project.org/

Rasband, W. S. (2018). *ImageJ version 1.52a*. Retrieved September 5, 2019, from https://imagej.nih.gov/ij/

Remsen, J. V., & Krobinson, S. (1990). A classification scheme for foraging behavior of birds in terrestrial habitats. *Studies in Avian Biology*, *13*, 144–160.

Sekercioglu, C. H. (2012). Bird functional diversity and ecosystem services in tropical forests, agroforests and agricultural areas. *Journal of Ornithology*, *153*(S1), 153–161. https://doi.org/10.1007/s10336-012-0869-4

Sheil, D., Casson, A., Meijaard, E., van Noordwijk, M., Gaskell, J., Sunderland-Groves, J., Wertz, K., & Kanninen, M. (2009). *The impacts and opportunities of oil palm in Southeast Asia: What do we know and what do we need to know?* (Occasional paper no. 51). CIFOR.

Silmi, M., Mislan, Anggara, S., & Dahlen, B. (2013). Using leopard cats (*Prionailurus bengalensis*) as biological pest control of rats in a palm oil plantation. *Journal of Indonesian Natural History, 1*(1), 31–36.

Soliman, T., Lim, F. K. S., Lee, J. S. H., & Carrasco, L. R. (2016). Closing oil palm yield gaps among Indonesian smallholders through industry schemes, pruning, weeding and improved seeds. *Royal Society Open Science*, *3*(8), 160292. https://doi.org/10.1098/rsos.160292

Stibig, H., Achard, F., Carboni, S., Raši, R., & Miettinen, J. (2014). Change in tropical forest cover of Southeast Asia from 1990 to 2010. *Biogeosciences*, *11*(2), 247–258. https://doi.org/10.5194/bg-11-247-2014

Van Bodegom, P. M., & Price, T. (2015). A traits-based approach to quantifying ecosystem services. In J. A. Bauma & P. J. H. van Beukering (Eds.), *Ecosystem services: From concept to practice* (pp. 40–64). Cambridge University Press.

Whelan, C. J., Şekercioğlu, Ç. H., & Wenny, D. G. (2015). Why birds matter: From economic ornithology to ecosystem services. *Journal of Ornithology*, *156*(S1), 227–238. https://doi.org/10.1007/s10336-015-1229-y

Woittiez, L. S., Van Wijk, M. T., Slingerland, M., Van Noordwijk, M., & Giller, K. E. (2017). Yield gaps in oil palm: A quantitative review of contributing factors. *European Journal of Agronomy*, *83*, 57–77. https://doi.org/10.1016/j.eja.2016.11.002

Wood, B. J., & Fee, C. G. (2003). A critical review of the development of rat control in Malaysian agriculture since the 1960s. *Crop Protection*, *22*(3), 445–461. https://doi.org/10.1016/s0261-2194(02)00207-7

JOURNAL OF OIL PALM RESEARCH

GUIDE FOR AUTHORS

(for more details, kindly visit http://jopr.mpob.gov.my)

Type of Articles

1. **Regular Article**
   Full-length original empirical investigations, consisting of introduction, materials and methods, results and discussion, conclusions. Original work must provide references and an explanation on research findings that contain new and significant findings. Conclusion should be brief and focus on the research output, should not be in point form. These papers should not exceed 6,000 words of text (including tables, figures and references) and generally not more than a total of 10 figures and tables. After peer-review, the article word count limit can be extended to a maximum of 8,000 words to better address the reviewers' and editors' comments. Any additional figures or tables can be included in the supplementary data. Please note that papers submitted to JOPR will be sent back to authors because of poor figure resolution or exceeding the number of figures permitted.

2. **Short Communication**
   Significant new information to readers of the Journal in a short but complete form. Preferably not exceeding 3,000 words (including tables, figures and references), and is intended for rapid publication. They are not intended for publishing preliminary results or to be a reduced version of regular article.

3. **Review Article**
   Critical evaluation of materials about current research that have already been published by organising, integrating, and evaluating previously published materials. Re-analyses as meta-analysis and systemic reviews are encouraged. Review articles provide systemic overview, evaluation and interpretation of research in a given field. They should not exceed 12,000 words (excluding references only) and should contain no more than a total of 20 figures and tables. Any additional figures or tables can be included in the supplementary data. Please note that papers submitted to JOPR will be sent back to authors because of poor figure resolution or exceeding the number of figures permitted. The same information should not be repeated in a figure and a table.

Language

Please write your text in good English (US or UK). We do not accept mixture of US and UK English in one manuscript. All spelling must be checked carefully.

JOPR's Template

JOPR's template, which is a standard format that facilitates the manuscript writing and copyediting process. This template is created to provide a detail and clear house style of JOPR. The template is drafted according to JOPR's house style, but in standard word version format. When writing a paper, authors need to format their papers to fit into the journal's house style. To make this easier, Word templates are available for many of other established journals, ready for them to download and apply to their research paper format. It is crucial for author to write a research paper while considering formatting. Each journal has its own guidelines for formatting; hence, the template defines how an article will look when it is published online or in print.

JOPR's Aims & Scope

This is established to provide a detail and clear aims and scope for author reference. Authors should declare in the cover letter how the research fits the aims and scope of JOPR.

JOPR's House Style

A detail listing of JOPR's house style for authors and a checklist to facilitate the copyediting process and standardise the copyediting process. The JOPR's house style remains the same and is drafted into a detail version for author's reference.

Manuscript Submission

- Manuscripts should be submitted via: https://www2.cloud.editorialmanager.com/jopres/
- JOPR does not permit dual submission, publication and/or any archive platform (preprint) in violation of journal ethical practices.

For more details and to download the JOPR's House Style and Template, kindly visit http://jopr.mpob.gov.my

Contents of the Coming Issue
Journal of Oil Palm Research
Vol. 37 (4) December 2025*

Note: * Subject to change.